[redacted]

UNCLASSIFIED

CR-112090
8 MAY 1972

C72 71757

CLASSIFICATION CHANGE
To UNCLASSIFIED
By authority of DS ...
Changed by ... Date 2/8/79
Classified Document Master Control Station, NASA
Scientific and Technical Information Facility

STUDY OF THE APPLICATION OF ADVANCED TECHNOLOGIES TO LONG-RANGE TRANSPORT AIRCRAFT [U]

VOLUME I
TECHNOLOGY APPLICATIONS

[redacted]

[redacted]

[redacted]

(NASA-CR-112090) STUDY OF THE APPLICATION OF ADVANCED TECHNOLOGIES TO LONG-RANGE TRANSPORT AIRCRAFT. VOLUME 1: TECHNOLOGY APPLICATIONS (U) (General Dynamics/Fort Worth) 8 May 1972 414 p GP-4 CSCL 01C F3/02 71757

Prepared Under Contract No. NAS1-10702 by

GENERAL DYNAMICS
Convair Aerospace Division
Fort Worth Operation

For NATIONAL AERONAUTICS AND SPACE ADMINISTRATION

UNCLASSIFIED

[redacted] Control No. FW/72/89/14-1

(NASA-CR-112090) STUDY OF THE APPLICATION OF ADVANCED TECHNOLOGIES TO LONG-RANGE TRANSPORT AIRPORT. VOLUME 1: TECHNOLOGY APPLICATIONS (General Dynamics/Fort Worth) 422 p

N79-75317

Unclas
00/05 13997

CR-112090
8 May 1972

STUDY OF THE APPLICATION OF ADVANCED TECHNOLOGIES TO LONG-RANGE TRANSPORT AIRCRAFT

[U]

VOLUME I

TECHNOLOGY APPLICATIONS

Prepared Under Contract No. NAS1-10702 by

GENERAL DYNAMICS
Convair Aerospace Division
Fort Worth Operation

for

NATIONAL AERONAUTICS AND SPACE ADMINISTRATION

426

ABSTRACT

The economic impact of applying various technologies to two selected transport aircraft configurations is evaluated. One configuration has a design cruise Mach number of 0.98; the other, 0.90M. Both transports carry 40,000 lb (18,140 kg) of passenger payload (195 mixed class) over a design range of 3000 n.mi (5560 km). This payload/range combination was chosen to match a predicted airline requirement during the 1980's. The 0.98M transport embodies a supercritical wing and area-ruled fuselage, but the 0.90M airplane, having a less-swept supercritical wing, has a conventional constant-diameter fuselage arrangement. Other technologies evaluated on each of these transports include filamentary composite materials (graphite/epoxy), active control systems, relaxed static stability, and advanced propulsion systems with greatly reduced noise and pollutant levels. The economic payoff (or penalty) of individual and collective applications of the technologies is shown, together with a technical assessment of their suitability and scope. Also, the 0.90M and 0.98M cruise transports are compared with a conventional 1970 technology transport having identical payload/range capability.

PRECEDING PAGE BLANK NOT FILMED

TABLE OF CONTENTS

Preceding page blank

TABLE OF CONTENTS (Cont'd)

TABLE OF CONTENTS (Cont'd)

TABLE OF CONTENTS (Cont'd)

TABLE OF CONTENTS (Cont'd)

TABLE OF CONTENTS (Cont'd)

TABLE OF CONTENTS (Cont'd)

TABLE OF CONTENTS (Cont'd)

LIST OF SYMBOLS

$\overline{A}$	ratio of root mean square incremental load
A_i	inlet reference area
A_o	freestream area of the captured engine airflow
A_{th}	inlet throat area
ACS	active flight control system
AR	aspect ratio
a	crack length or half crack length
a_c	critical crack length
a_n	normal acceleration
ac	aerodynamic center
B_N	maximum nacelle breadth
b	scale parameter m probability density distribution of root mean square environmental velocity
b'	structural span
BPR	engine by-pass ratio
$\overline{c}$	wing mean geometric chord
cg	center of gravity location
C_D	drag coefficient
C_L	lift coefficient
$C_{m\delta_h}$	pitching moment coefficient due to horizontal tail deflection
C_{pi}	retardation parameter of i^{th} load
C_V	nozzle velocity coefficient

CET	combustor exit temperature
D	fuselage diameter
D_n	maximum nacelle depth
d_i	diameter at A_i
DOC	direct operating cost
E_1	extensional modulus of high modulus material
E_2	extensional modulus of low modulus material
EPNdB	units of effective perceived noise level
F_{tu}	ultimate tensile stress
F_{ty}	yield tensile stress
FAR	Federal Aviation Regulation
FPR	fan pressure ratio
FSS	flutter suppression control system
F_H	horizontal tail balancing load
F_V	vertical tail load
g	acceleration of gravity at nominal surface of earth
H	fuselage height
h	wing bending displacement
IOC	indirect operating cost
KEAS	knots equivalent air speed
K_C	fracture toughness or plain stress intensity factor

K_{IC}	plain strain fracture toughness
K_{Q1}	critical stress intensity factor for high modulus material
K_{Q2}	critical stress intensity factor for low modulus material
L	aerodynamic lift, or spectral shaping parameter in power spectral density function, or longitudinal, or one half crack length
L_t	length of structure over which a load is assumed to act
LT	long transverse
l/d	nacelle fineness ratio
L/D	lift to drag ratio
M	Mach number
M_C	cruise Mach number
M_D	dive Mach number
N	cycles or number of load cycles to failure
N_o	average number of cycles of specified response per second
N(y)	average number of cycles of specified response per second exceeding y
N_x	in plane load
n	normal load factor or number of load cycles
P	proportion of total time in atmospheric turbulence environment
p	pressure

LIST OF SYMBOLS (Cont'd)

PSF	pounds per square foot
P_{T_o}	free-stream total pressure
P_{T2}	compressor face total pressure
R	stress ratio or load cycling rate
r	hole radius
ROI	discounted cash flow return on investment
RDT&E	research, development, test, and evaluation
RSS	reduced (longitudinal) static stability
S	area
S_{HT}	horizontal tail area
S_N	nacelle cowl surface area
S_{PYL}	pylon planform area
S_{VT}	vertical tail area
S_W	theoretical wing area
S_{WETT}	fuselage wetted area
S_{max}	maximum stress
SM	static margin, distance from center of gravity to aerodynamic center
sfc	specific fuel consumption $W_F \div T\text{-}DD$
T	maximum operating temperature
T-DD	installed net propulsive force compatible with aerodynamic drag definition
T/W	S.L.S. thrust to takeoff weight ratio

LIST OF SYMBOLS (Cont'd)

t	time
t/c	wing thickness to chord ratio
U_{de}	derived gust velocity
U_σ	true gust velocity
V	velocity
V_A	design maneuver speed
V_B	design speed for maximum gust intensity
V_C	design cruise speed
V_D	design dive speed
V_S	stalling speed or minimum steady flight speed at which airplane is controllable
V_{S1}	stalling speed or minimum steady flight speed obtained in a specified configuration
W	weight
w_1	distance between low modulus material strips
w_2	width of low modulus material strips
W_F	installed engine fuel flow rate
W_{DES}	flight design gross weight
W_{NC}	weight of nacelle contents (excluding nacelle structure)
y	any response parameter
δ	angular displacement
λ	planform taper ratio (tip chord/root chord)
Λ	sweep angle

LIST OF SYMBOLS (Cont'd)

ρ	mass density
Φ	power spectral density
σ	root mean square gust velocity
σ_c	stress corresponding to critical crack length
σ_{c1}	critical stress for high modulus material
σ_{c2}	critical stress for crack propogation in low modulus material
σ_1	stress in high modulus material or stress in 1st element
σ_2	stress in low modulus material or stress in 2nd element
σ_3	stress in 3rd element
$\Lambda c/2$	mid chord wing sweep
η	nondimensional wing spanwise position
α	angle of attack (in regard to flutter suppression local value at pertinent wing station)
γ	flight path angle
$(\dot{\ })$	dot over symbol - derivative with respect to time

SECTION 1

SUMMARY

The first phase of the study of the application of advanced technologies to long-range transports revealed that there is a substantial market from 1980 onwards for a medium sized transport that could carry about 40,000 lb (18,140 kg) of payload (about 195 passengers, mixed class) over trans-continental routes of up to 3000 n.mi (5560 km) equivalent stage distance. Such an airplane would replace such transports as the Boeing 727 and would be capable of operation from most domestic and international airports. The engines on this aircraft would permit noise levels 10 EPNdB below FAR Part 36 standards for a penalty in ROI of about 9 percent. Atmospheric pollution would also be reduced to the levels outlined in the NASA Statement of Work (L17-1533). With more advanced technology engines, and by about 1985, noise levels will be reduced 15 EPNdB below FAR Part 36. With the use of operational procedures such as engine oversizing for takeoff and two-segment approach paths for landing, noise levels could be 20 EPNdB below FAR Part 36, although sideline noise would not be reduced. These levels are indicated by -20/15 EPNdB on the fourth bar of Figure 1-1, which illustrates the economic impact of the various noise reductions.

Application of the new high-speed airfoils will improve profitability, particularly if cruise speed is set at about 0.90M, which may not require that the fuselage be area-ruled. The above-sized transport designed to this cruise Mach number would have an ROI about 15½ percent better than a similarly sized transport employing conventional 1970 technology airfoils and cruising at 0.82M. On the other hand, if the airplane is designed to cruise at the highest practicable Mach number of 0.98M, the ROI would be only about 1 percent better than a 1970 technology transport. The relative economics of the three transports are shown in Figure 1-2. A 15½ percent improvement in ROI is equivalent to an additional profit margin of $73M per year when applied to a fleet of 280 airplanes of the size selected. On the other hand, a 1 percent improvement in ROI for the M 0.98 configuration gives only $6M per year extra profit.

Various degrees of filamentary composite materials in the structure were considered, and the payoffs are shown in Figure 1-3. It is evident that a maximum use of composites

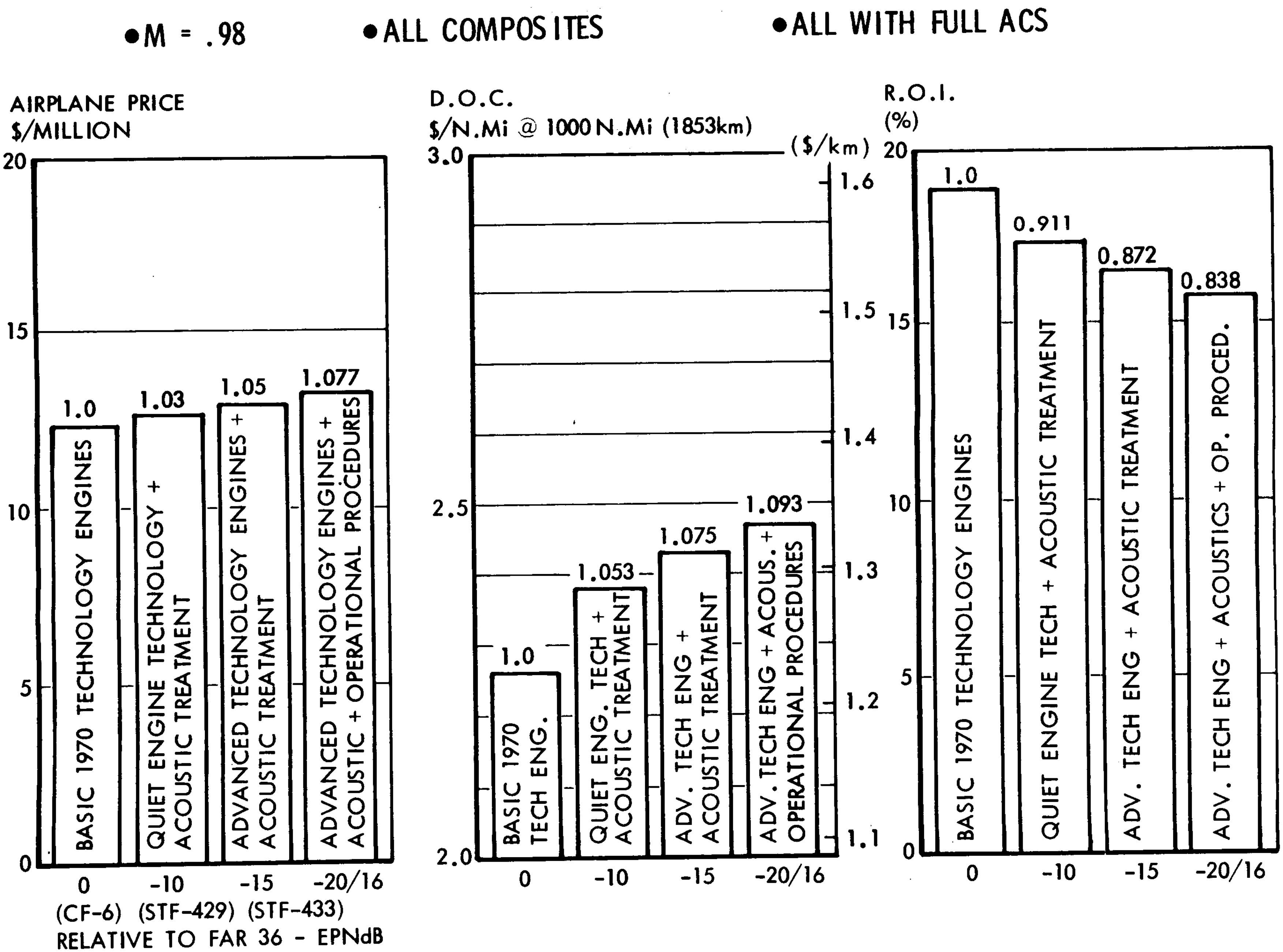

Figure 1-1 Economic Impact of Noise Reductions

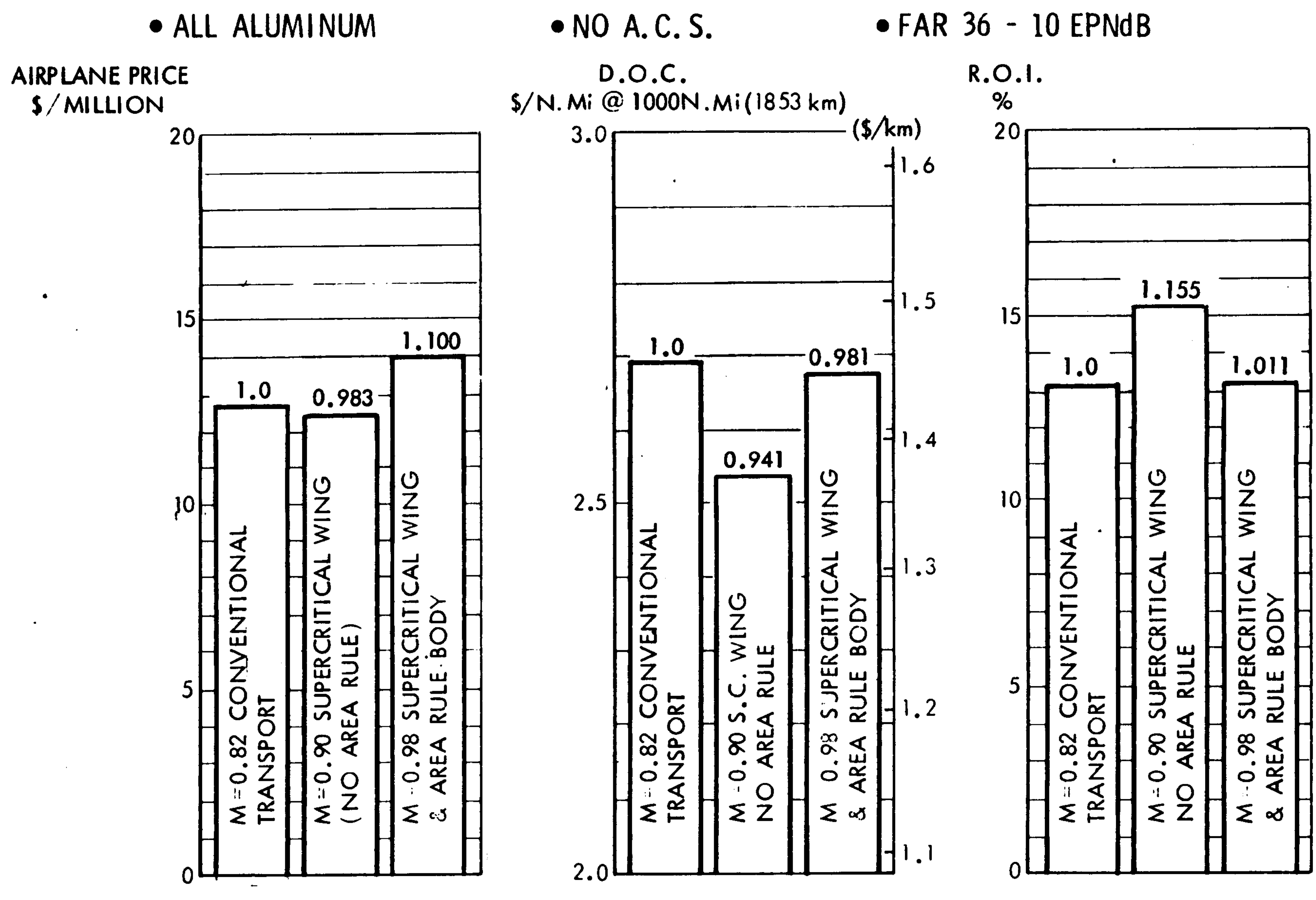

Figure 1-2 Economic Effects of Supercritical Technology

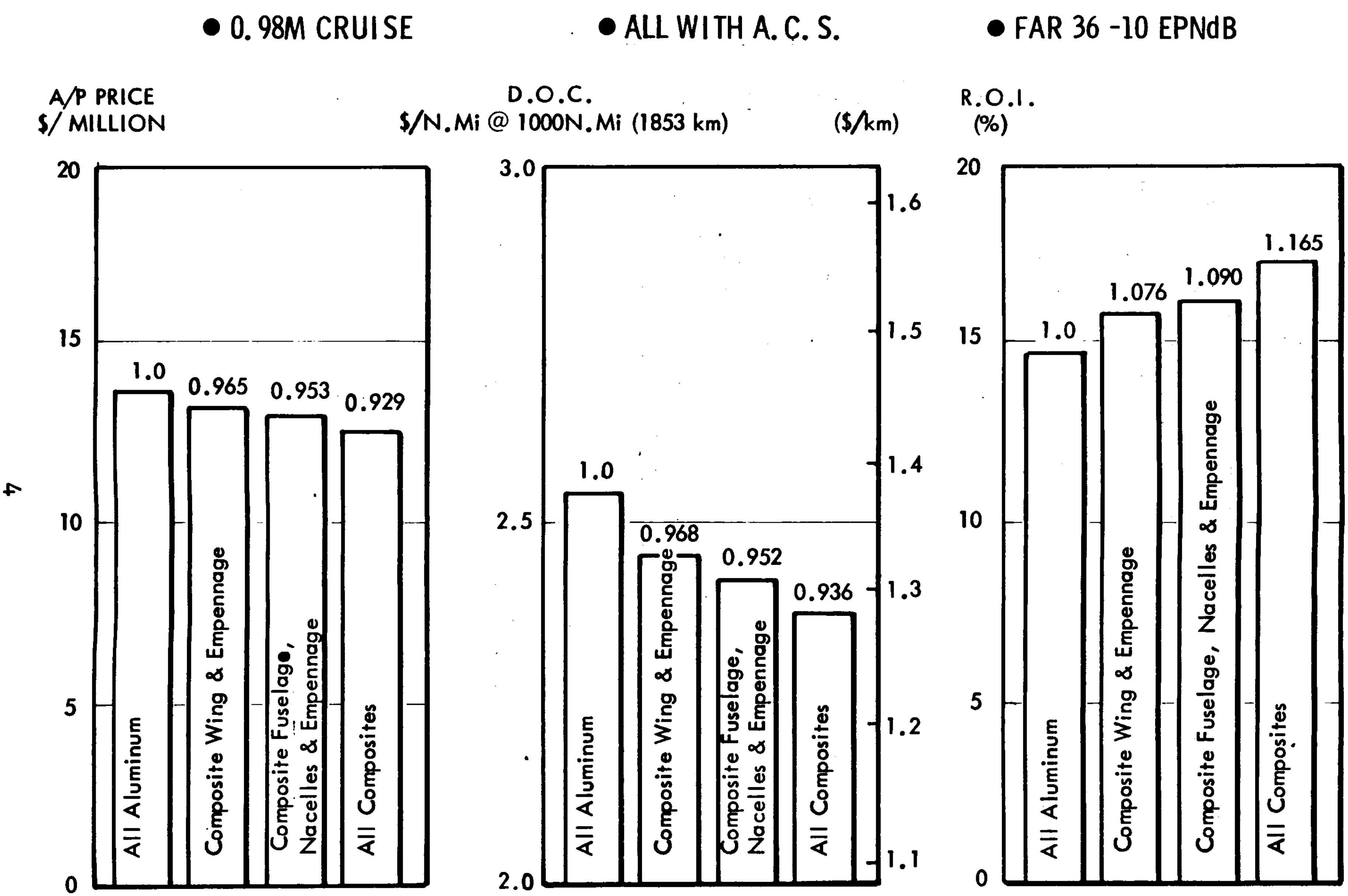

Figure 1-3 Economic Effects Of Applying Composites

throughout the structure should be the target, which will give improvement in ROI of up to 16½ percent. A significant result of the manufacturing cost study is that, with resizing of the lifting surfaces and engines with weight reductions, the airplane selling price and DOC can be reduced despite the higher materials cost.

The economic impact of employing an active control system is illustrated in Figure 1-4 for the 0.90M configuration and in Figure 1-5 for the 0.98M configuration. The influence of combining the ACS with the use of composites is also shown in each of the figures. It is seen that there is an improvement in ROI for a composite 0.98M transport of about 3.7 percent compared with a similar composite airplane not employing active control systems. The improvement appears to be somewhat less when active control systems are employed on a composite 0.90M transport. Caution should be exercised in the interpretation of the results when these technologies are combined, particularly those for the 0.90M configuration. The net weight savings of combining a full active control system with an all-composite structure were determined early in the study for the original high-performance 0.98M configuration of aspect ratio 6.4. These weight savings were then prorated to the selected configurations of Phase II, which had wings of aspect ratio 9.0 for the 0.90M transport and 8.0 for the 0.98M transport. Naturally, the weight savings should be greater with increased aspect ratio and, in consequence, the payoffs would be much better than that indicated in Figure 1-4 and slightly better than that shown in Figure 1-5. Additional study using the DAEAC computer facility on the selected configurations would reveal the correct magnitude of the expected weight savings and, in turn, the impact on the economics. When applied to aluminum airplanes, the effect of employing active control systems appears much greater. For the 0.98M transport, the improvement in ROI is 10.8 percent, and for the 0.90M airplane, ROI is 6.7 percent better.

The basic airplane is statically stable and a full active control system includes relaxing static stability to give essentially zero trim drag plus maneuver load and gust alleviation together with active flutter suppression. The individual economic effects of these systems when applied to aluminum airplanes is illustrated later in Figure 6.4-1.

Reducing fuel reserves from 1 hour holding plus 200 n.mi (370 km) diversion to 45 minutes holding and 150 n.mi (278 km)

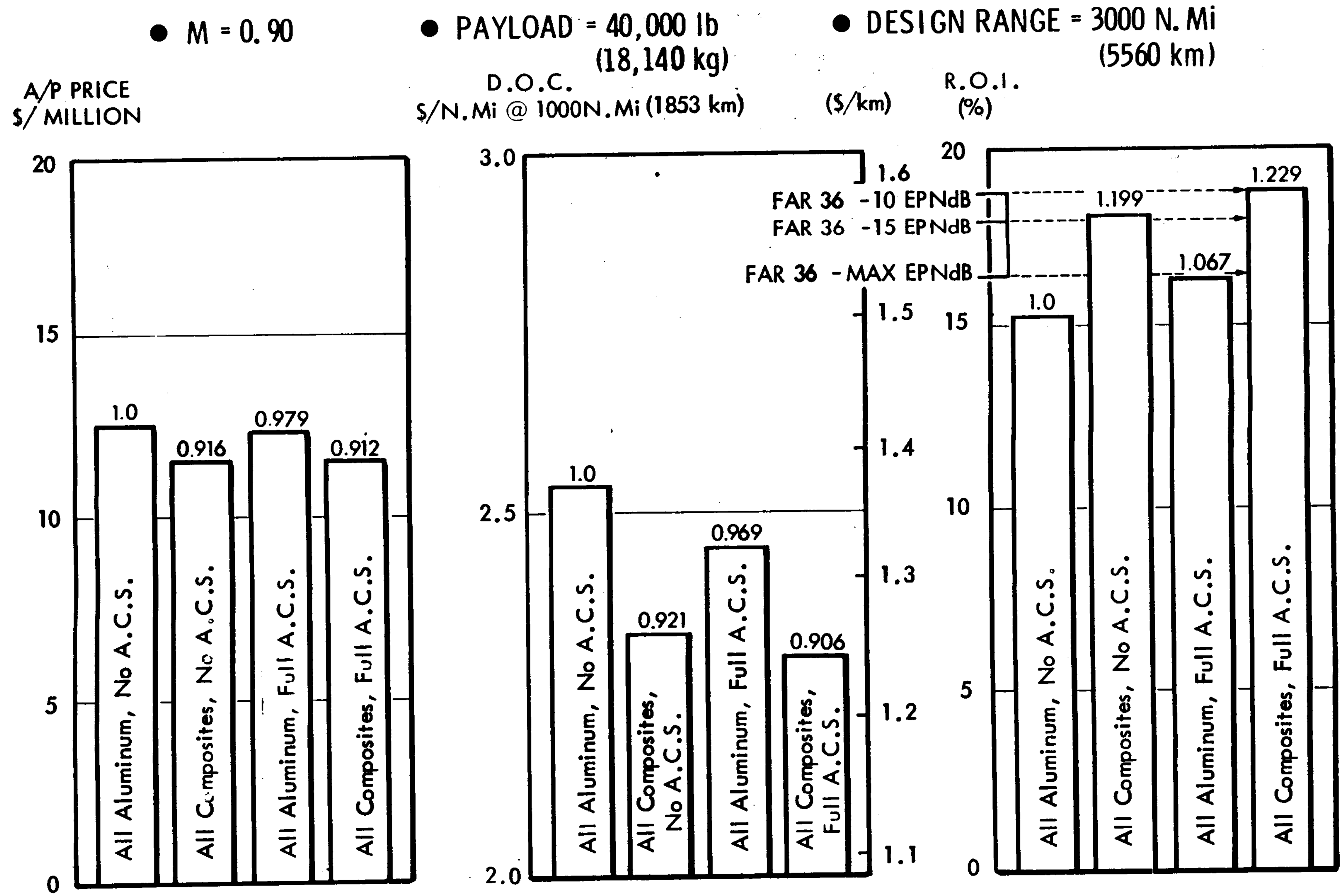

Figure 1-4 Economic Impact of Composites and Active Control Systems (M = 0.90)

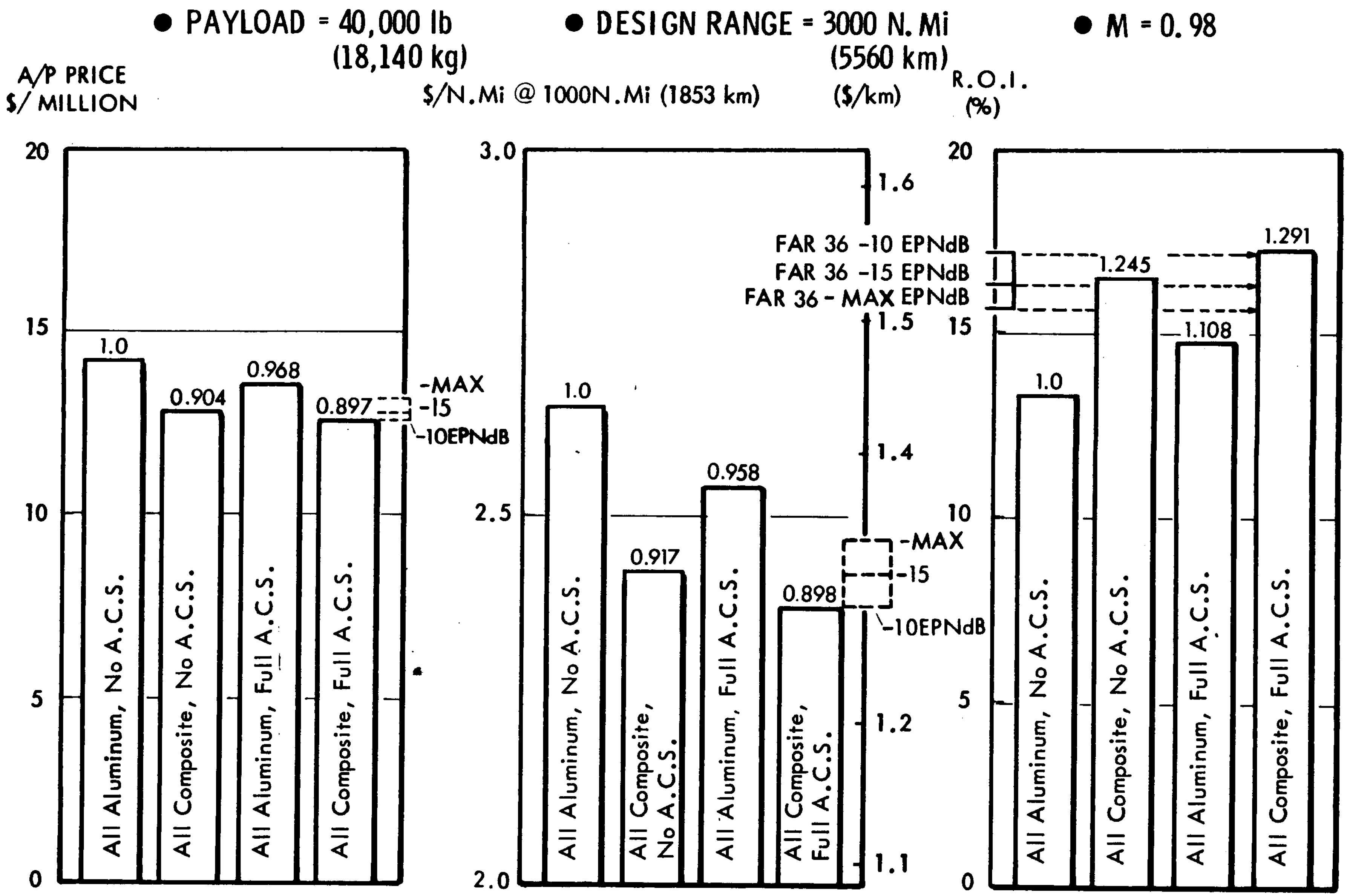

Figure 1-5 Economic Impact of Composites and Active Control Systems (M = 0.98)

diversion improves ROI by 5-3/4 percent (ROI increased from 18.06 to 19.10 percent) for a 0.90M transport. This improvement increases to 5.9 percent when reserves are reduced on a 0.98M transport.

Sensitivity of a 0.90M cruise transport to changes in structure weight, aerodynamic efficiency, airframe cost, engine cost, and propulsive efficiency is illustrated in Figure 1-6.

Since completing the study, certain aerodynamic and structural improvements seem possible with both the 0.98M and 0.90M configurations. The drag creep that seemed present in wind tunnel tests is markedly less in actual flight tests. Also, somewhat less wing sweep could have been tolerated. Another improvement would be to reduce the fineness ratio of the 0.98M area-ruled transport from about 9.9 to 8.5.

A summary of the economic improvements for applying the various technologies to 0.90M and 0.98M cruise transports is shown in Table 1-1. This summary indicates the additional profit earned per year when the technologies are applied to a fleet of 280 airplanes, each of 195 passenger capacity and operating over a typical domestic route structure.

Table 1-1

SUMMARY OF ECONOMIC IMPROVEMENTS

• PAYLOAD = 40,000 LB • DESIGN RANGE = 3000 N.MI. • FAR 36-10 EPNdB NOISE LEVEL

TECHNOLOGY	ΔPROFIT/YEAR ($ ÷ MILLION)			
	M = .90	M = .98	IMP M=.90*	IMP M=.98**
SUPERCRITICAL AERO TECHNOLOGY	73	6	103	59
COMPOSITES (41.4%)	108	124	108	124
ACTIVE CONTROL SYSTEMS	36	52	36	52
TOTAL	217	182	247	235
COMBINED TECHNOLOGIES	208	151	232	204

*10 Counts of Drag Creep Eliminated; Equivalent of 1° Less Sweep Allowed; (7 Abreast Seating)
**10 Counts of Drag Creep Eliminated; Equivalent of 2° Less Sweep Allowed; Body Fineness Ratio Reduced to 8.5 (8 Abreast Max. 6 Abreast Min.)

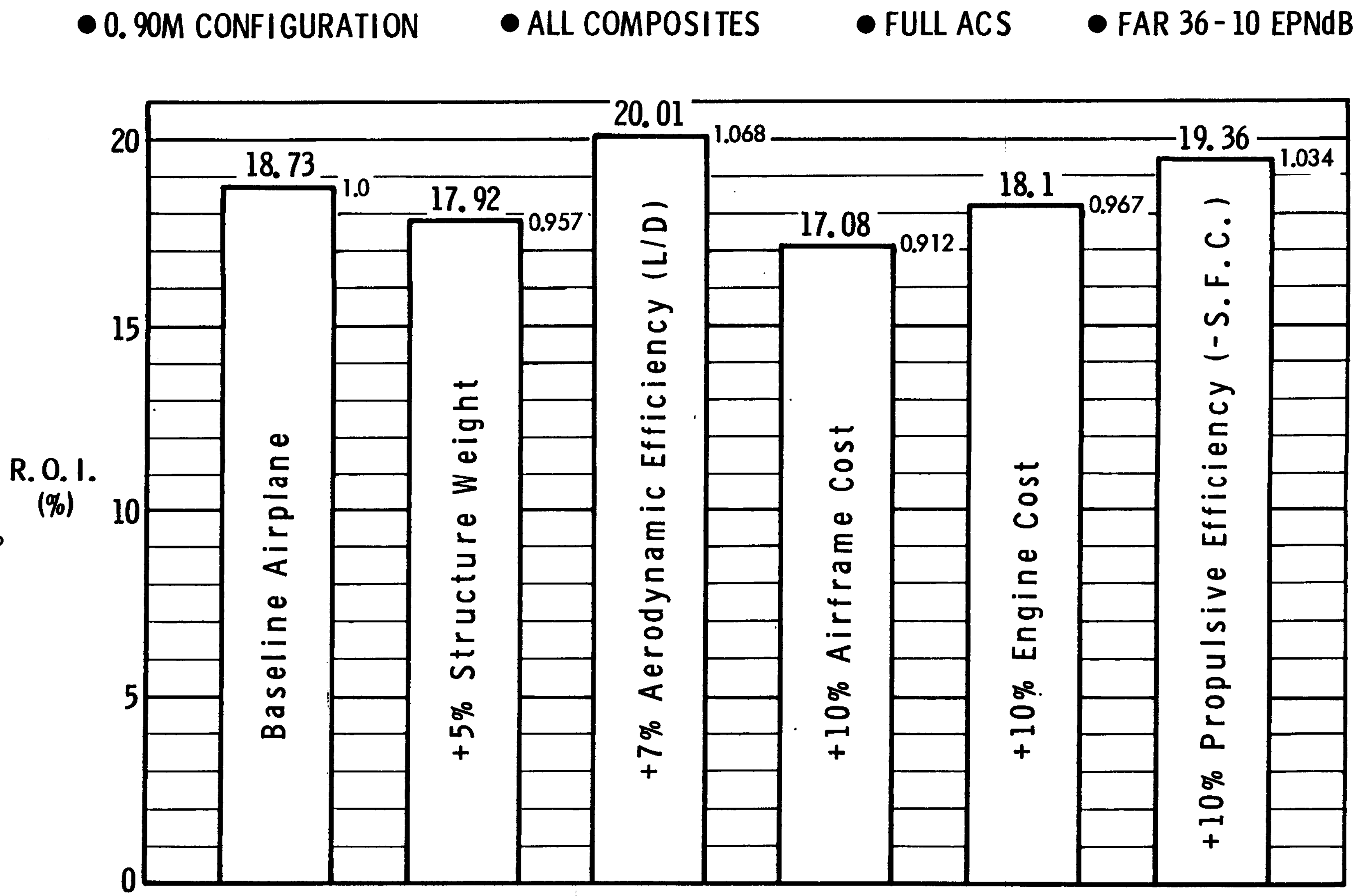

Figure 1-6 Sensitivity Summary

SECTION 2

INTRODUCTION

Since the advent of the swept-wing jet transport, most improvement in airline operating economics over the past decade have been achieved by advancements in propulsion technology. Within this time, fuel consumption has been reduced progressively with increases in the engine by-pass ratio. Starting with the pure jet of the early models through the JT-3D and JT-8D with modest by-pass ratios of around 1:1, the present turbofan engines, typified by the JT-9D and CF-6, have by-pass ratios of about 5:1. With the reductions in fuel consumption, the higher by-pass-ratio engines have also produced lower and lower noise levels. However, these improvements have now reached the point of diminishing returns, and it becomes necessary to look at developments in other areas in order that the downward trend in operating cost be maintained.

The new high-speed airfoils developed by Dr. R. T. Whitcomb and others over the last several years offer great possibilities for either improved productivity with increased cruise Mach number, or better aerodynamic efficiency at present-day cruise speeds, or combinations of both. Over the last six years considerable progress has also been made in the development of advanced materials, in particular the filamentary composites, which show great promise in providing a high strength-to-weight ratio, although at some increase in materials cost. Likewise, the use of control systems manipulated in such a fashion as to modify the airplane load distributions under maneuver and gust conditions seems to offer potential weight savings in the structure. These savings could be significant, particularly if the flutter problem resulting from reduced-strength structures is dealt with. In addition, community noise and atmospheric pollution have reached the point where something must be done to show the more discerning public that the airplane designer does care about improving the quality of life, especially around our major airports.

The study conducted by the Convair Aerospace Division of General Dynamics Corporation under NASA Contract NAS1-10702 of the application of advanced technologies to the design of long-range transports is thus timely and of great importance in charting a course of research and development which will insure that the next generation of U.S. commercial transports will be competitively superior in the world market. A summary of the various technologies to be applied during the study is shown in Figure 2-1.

During the first half of the contract period, which started in April 1971, the main emphasis was on a parametric study of three payloads, two design ranges, conventional and composite structures, all for two configurations. One configuration corresponded closely to the rear-engined trijet model with supercritical technology then being tested by Dr. R. T. Whitcomb of NASA, having a design cruise Mach number near unity. The other configuration was optional, and Convair's choice resulted from extensive analysis of cruise Mach number effects on economics. The study matrix is shown in Table 2-1. It was found that best return on investment (ROI) was achieved when the supercritical aerodynamic technology was applied to configurations cruising in the 0.92M range.

In addition to a study of the application of supercritical technology and its effects on economics, the Phase I tasks included a parametric study of the application of advanced filamentary composite materials to the wing and empennage of both configurations. Because of its obvious cost advantages, graphite-epoxy composite material was selected for these components.

Trade studies were also made during Phase I on selected configurations to show the potential economic gains of employing active control systems.

All the parametric data generated in Phase I are based on the use of scaled General Electric CF6-50C high-by-pass-ratio turbofan engines, with airplane noise levels to FAR Part 36 standards or better. The effect on economics of additional acoustic treatment to reduce noise levels to 10 EPNdB below FAR Part 36 was evaluated towards the end of Phase I.

In order to make a judgment as to the payoff expected from applying supercritical aerodynamics technology, a conventional 1970 technology transport was designed to form a baseline for comparison.

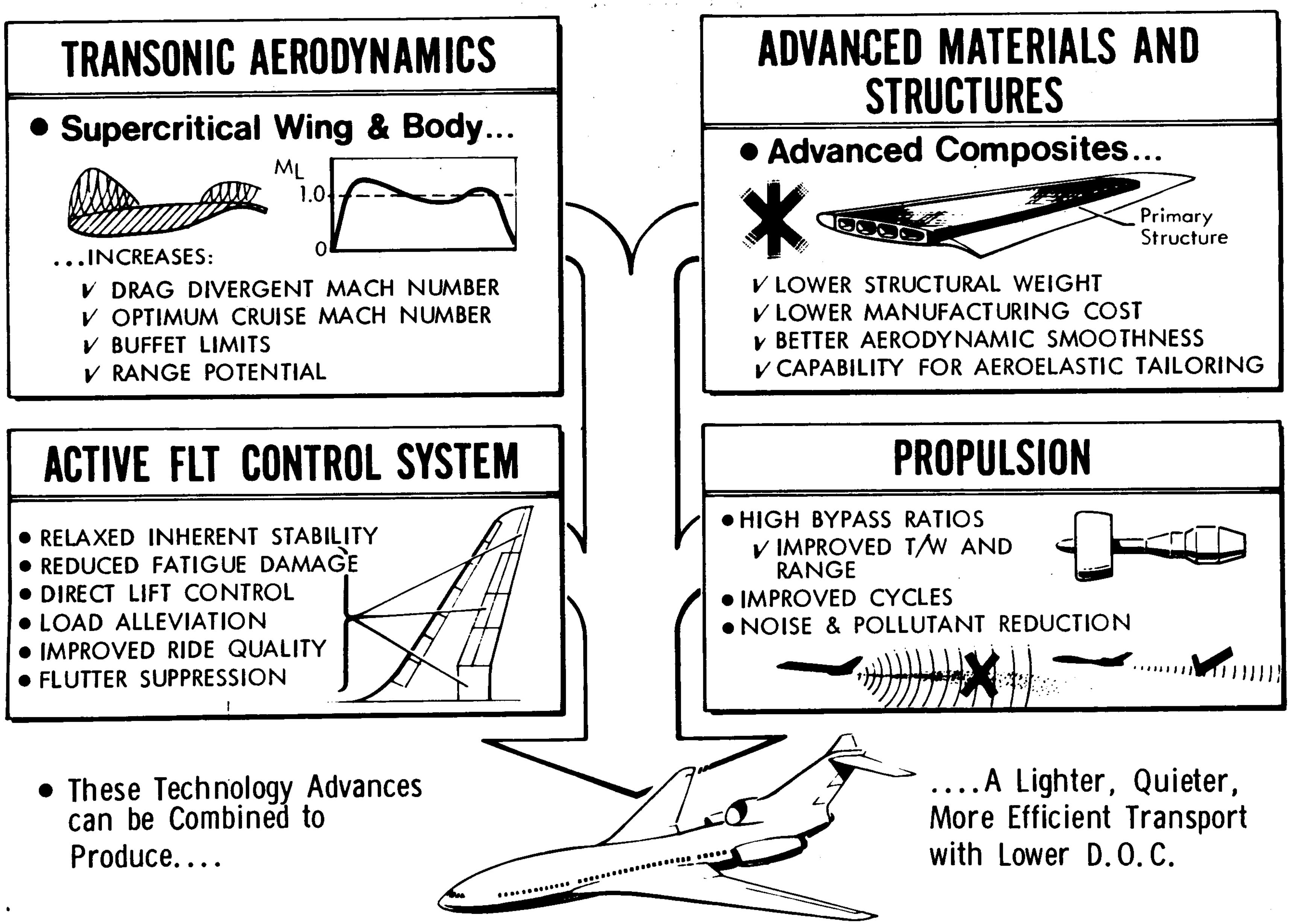

Figure 2-1 Summary of Advanced Technologies

Table 2-1 Study Configuration Matrix

AERODYNAMIC APPROACH	HIGH PERFORMANCE						ALTERNATE					
MACH NUMBER	≈ 1.0						$.85 < M < 1.0$					
PASSENGER PAYLOAD lb (kg)	○30K (13,600)	40K (18,140)	△80K (36,280)	○30K	40K	△80K	○30K	40K	△80K	○30K	40K	△80K
RANGE N.Mi. (km)	○3000 (5560)		△5500 (10,200)	○3000		△5500	○3000		△5500	○3000		△5500
STRUCTURAL CONCEPT	CONVENTIONAL			COMPOSITE WING & EMPENNAGE			CONVENTIONAL			COMPOSITE WING & EMPENNAGE		
NOISE LEVEL	FAR 36; ○△ FAR 36 MINUS 10 EPNdb; ○FAR 36 MINUS 20 EPNdb											
HI-LIFT SYSTEM	• DOUBLE SLOTTED FOWLER PLUS L.E. "VARICAM" KRUGER											
CRUISE ALTITUDE	≥40,000 FEET (12,200 m)											
CARGO	50% OF PASSENGER PAYLOAD											

- SINGLE DECK, ALL BELLY CARGO
- TWIN AISLE, WIDE BODIED FUSELAGES
- ALTERNATE CONFIGURATION: TWO WING MOUNTED ENGINES, ONE STRAIGHT THROUGH AT BASE OF VERTICAL STABILIZER. LOW TAILPLANE ON FUSELAGE
- SCALED CF-6-50C ENGINES (Phase I)

○; △; POINT DESIGNS ○PHASE II ONLY

Concurrently with the Phase I parametric study, a market analysis was carried out to determine the most suitable size (passenger payload) and the route structure (design range) over which the selected transport should operate for best profitability (ROI) and for meeting future airline needs in the 1980's. It was determined that a transport having a payload of 44,000 lb (20,000 kg) carried over a design range of 2800 n.mi (5170 km) would best suit those needs and provide a truly economic vehicle with good ROI. Subsequent refinement revealed that a payload of 40,000 lb (18,140 kg) and a design range of 3000 n.mi (5560 km) would be more appropriate, and these payload/range characteristics were carried over into the Phase II studies.

Choice of the cruise Mach number for selection of the alternate configuration was based on the data of Figure 2-2, although subsequent calculations showed that a more optimum cruise speed would have been somewhat lower.

Throughout the early parametric studies a minimum start-of-cruise altitude of 40,000 ft (12,200 m) was assumed to provide vertical separation from slower flying aircraft. This constraint proved costly because of the higher thrust levels required; in later Phase II studies, best economical cruise altitudes were used, consistent with the desire to operate from domestic airports, which also influenced installed thrust levels.

Following the Interim Oral Presentation (31 August 1971) a re-direction of the program was initiated, which affected the Convair Aerospace activities in Phase II as follows:

1. The Convair-selected (0.92M cruise-speed alternate configuration carrying a 44,000-lb (20,000 kg) payload for 2800 n.mi (5170 km) was replaced by a similar arrangement but with cruise at 0.90M while carrying a 40,000-lb (18,140 kg) payload for 3000 n.mi (5560 km).

2. The NASA high-performance near-sonic tri-jet configuration was dropped, and an arrangement with engines located similar to the McDonnell/Douglas DC-10 (with two engines underwing and one at the rear) was substituted, with cruise Mach number maintained at 0.98M while carrying a 40,000-lb (18,140 kg) payload for 3000 n.mi (5560 km).

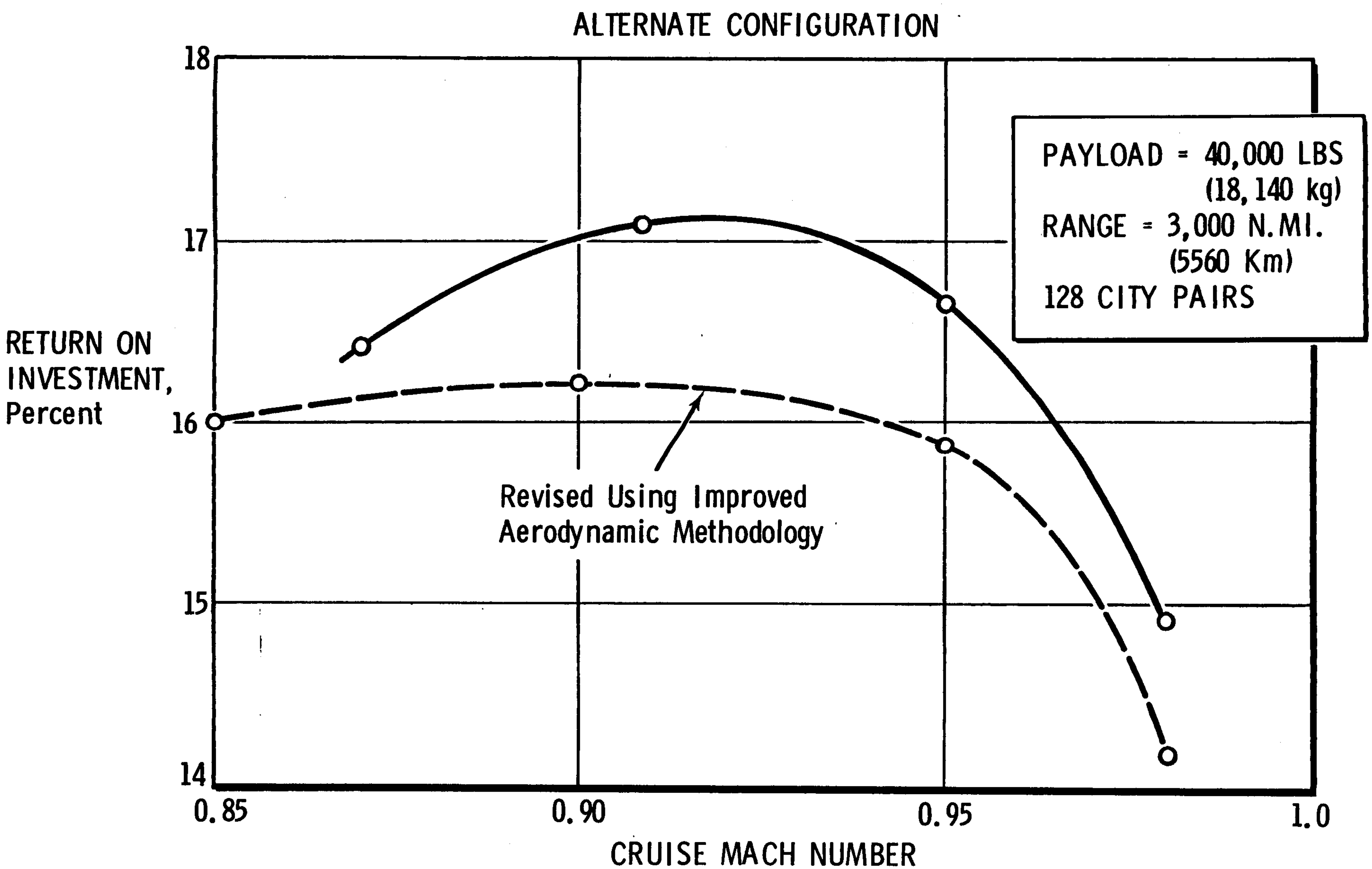

Figure 2-2 RETURN ON INVESTMENT Vs SPEED

3. Greater emphasis was placed on the application of composite materials to the structure, particularly stressing the manufacturing, tooling, and assembly costs compared to conventional light-alloy construction.

4. Noise levels were set at FAR Part 36 minus 10 EPNdB (1979 time frame without operational procedures), FAR Part 36 minus 15 EPNdB (1985 time frame without operational procedures), and a goal of FAR Part 36 minus 20 EPNdB (with operational procedures).

5. Emphasis was given to the economic benefits of employing active control systems.

6. Studies were included to determine the sensitivity to ROI of drag, weight, and cost (material, labor, etc.).

7. Effects of cruise altitude on economics was to be determined.

These re-directions, together with the other work outlined in the NASA Statement of Work (L17-1533), and in compliance with the schedule shown in Figure 2-3, are reported in the following sections of this Volume I.

In Volume II the state-of-readiness of the various technologies studied is outlined, and R&D programs are recommended that are designed to drive out the problems and reduce the risks to a degree where development of the next generation of advanced transports can be pursued with confidence.

Measurement values contained in this report are in both customary and SI units with the former stated first and the latter in parentheses. The principal measurements and calculations have been made in the customary system of units.

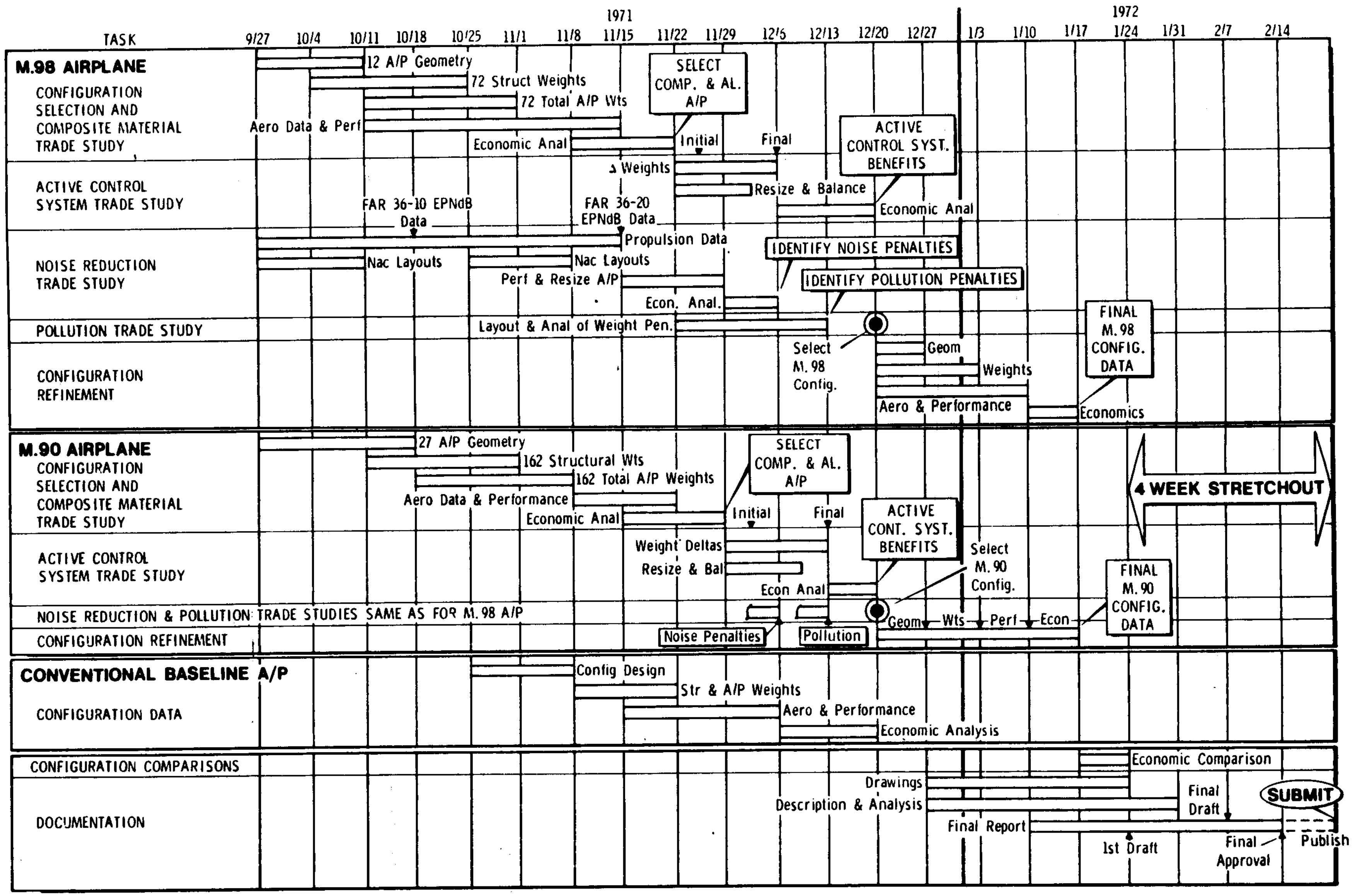

Figure 2-3 Phase II Schedule

SECTION 3

AIRPLANE DESCRIPTION AND OPERATION

In this section, the features of the two selected transport aircraft configurations embodying advanced technology (Mach .98 and Mach .90 cruise speeds) and the conventional aircraft configuration (Mach .82 cruise speed) used as a baseline for comparison in the study are described. Both advanced aircraft incorporate the maximum of composite materials, a full active control system, supercritical aerodynamics, and low-noise advanced-technology-propulsion engines. In order that the three aircraft could be compared easily, some performance characteristics and certain aircraft features were maintained common. Each aircraft is designed to carry a 40,000-lb (18,140-kg) payload (195 passengers) over a 3000-n.mi (5560-km) range. In addition, each aircraft employs a wide-body twin-aisle fuselage and a low wing. Engine location, landing gear arrangement, and internal equipment locations are the same, as near as possible, on all airplanes. The general features of the aircraft are compared in Table 3.0-1.

3.1 AIRCRAFT GENERAL ARRANGEMENT

3.1.1 Mach .98 Configuration

A general arrangement of the Mach .98 configuration is presented in Figure 3.1-1. The fuselage is area-ruled, and the wing, empennage, and engines are arranged to achieve the optimum cross-sectional area distribution for an aircraft cruising at Mach .98 airspeed. Maximum fuselage diameter is 18 ft, 11 in. (5.77 m). This allows seven-abreast seating in the coach section and the carriage of standard LD-3 containers in the cargo bay. The necked-down mid-section has a minimum diameter of 13 ft, 7 in. (4.14 m) and provides five-abreast seating.

Propulsion is by three scaled P&W STF-429 engines, two mounted beneath the wing on pylons and the third mounted above the fuselage in the base of the vertical tail. Each engine has a thrust of 26,480 lb (117,783 N).

Table 3.0-1 General Aircraft Features

FEATURE	ADVANCED TECHNOLOGY AIRCRAFT		CONVENTIONAL AIRCRAFT
Cruise Speed - M	.98	.90	.82
Range - n. mi	3000	3000	3000
(km)	(5560)	(5560)	(5560)
Engine Thrust, Each-lb	26,480	22,400	26,760
(N)	(117,783)	(99,700)	(119,028)
Wing			
Area - ft^2	2282	1970	2540
(m^2)	(212)	(183)	(236)
Aspect Ratio	8.0	9.0	6.8
Sweep - deg	40 @ c/2	36 @ c/2	35 @ c/4
Taper Ratio	.3874	.3874	.300
Overall Dimensions			
Length - ft & in.	193 & 7	172 & 2	169 & 8
(m)	(59.0)	(52.48)	(51.71)
Height - ft & in.	51 & 1.5	47 & 7	47 & 3
(m)	(15.58)	(14.50)	(14.40)
Span - ft & in.	141 & 9	139 & 10	131 & 5
(m)	(43.21)	(42.62)	(40.06)
Weight			
Structure -lb	75,222	62,980	94,260
(kg)	(34,114)	(28,562)	(42,748)
Sys & Equip - lb	42,353	41,658	42,080
(kg)	(19,208)	(18,893)	(19,084)
Propulsion - lb	19,189	15,933	19,850
(kg)	(8702)	(7226)	(9,002)
Useful Load - lb	7364	7364	7364
(kg)	(3340)	(3340)	(3340)
BOW - lb	144,128	127,935	163,554
(kg)	(65,364)	(58,021)	(74,174)
Payload - lb	40,000	40,000	40,000
(kg)	(18,140)	(18,140)	(18,140)
Water Inj Fluid - lb	960	810	965
(kg)	(435)	(367)	(438)
Fuel - lb	88,752	78,687	100,281
(kg)	(40,251)	(35,686)	(45,479)
Gross Weight - lb	273,840	247,432	304,800
(kg)	(124,190)	(112,214)	(138,231)

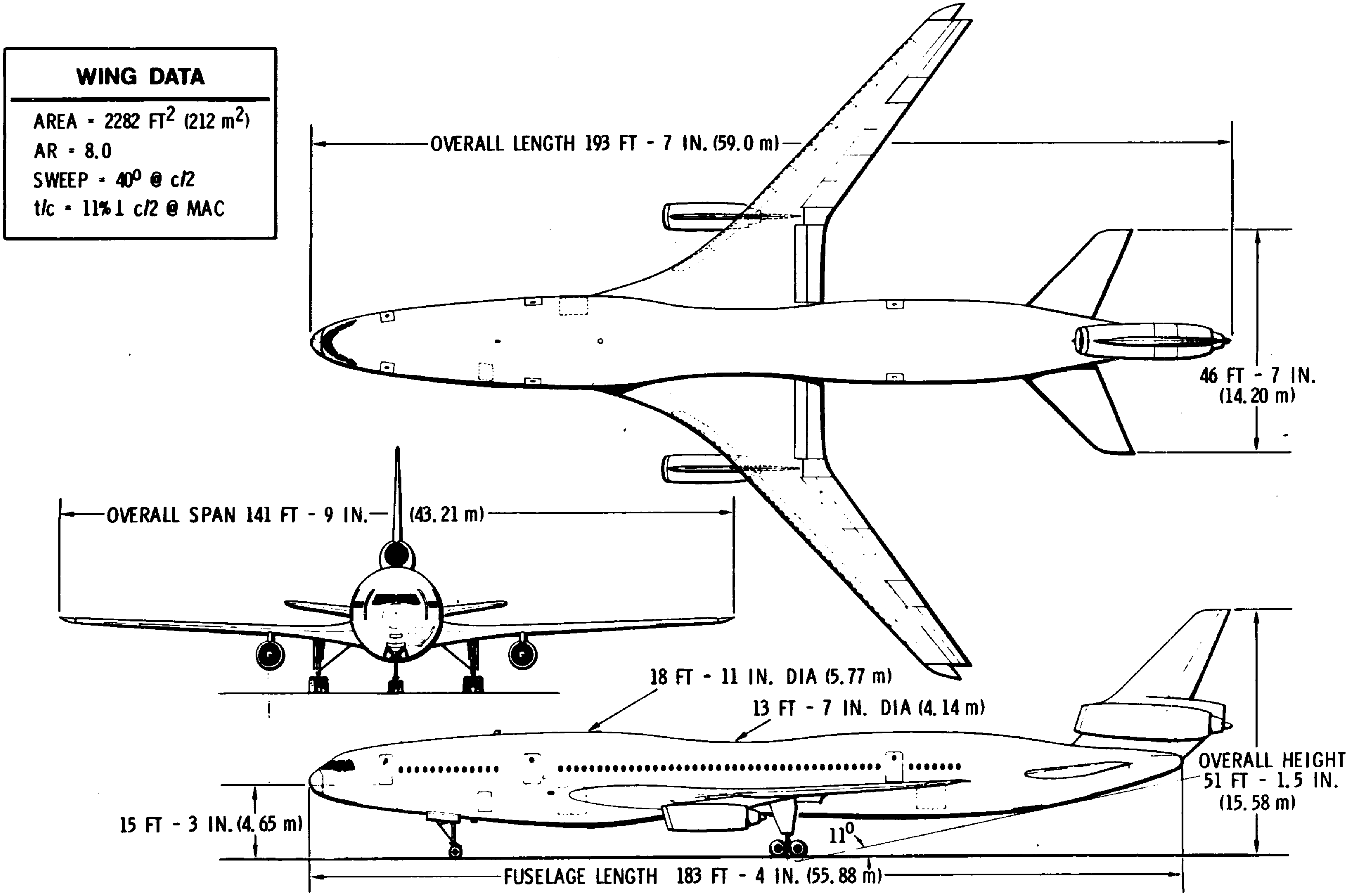

Figure 3.1-1 General Arrangement, Mach = .98 Configuration

The supercritical wing has an 8.0 aspect ratio and is swept at the mid-chord to 40 deg. The t/c at right angles to the mid-chord measured at the mean chord location is 11.0 percent.

The landing gear arrangement is conventional, with four-wheel trucks on the main landing gear and dual wheels on the nose gear. The main gear retracts inboard; the nose gear, forward. Tires are sized to require no greater pavement thickness than that approved by the Airport Operators Council and outlined in Department of Transportation Document AC/5320-6A dated 1 April 1970.

High lift is obtained by inboard and mid-span double-slotted Fowler flaps, simple outboard flaps, and Kruger-type "Varicam" leading-edge slats.

The advanced flight control system employed in the selected configurations provides not only three-axis control but also dynamic and static stability augmentation, active flutter suppression, maneuver load control, and gust alleviation. Lateral control is provided by an all-speed, mid-span aileron and wing-mounted spoilers. The all-speed aileron is also used for lateral trim and Automatic Flight Control System (AFCS) functions. The spoilers are also utilized as ground-roll brakes. Directional control is provided by large upper and lower rudders. Yaw damping and automatic turn coordination (high-lift configuration only) commands are supplied to both rudders. The horizontal stabilizer is used for longitudinal control, trim, static and dynamic stability augmentation, and AFCS functions. Longitudinal control in the landing approach is enhanced by use of spoilers in a Direct Lift Control (DLC) role. A small, outboard, trailing-edge surface and a very small surface located outboard of the wing tip are used for active flutter suppression.

Overall dimensions of the aircraft are: length, 193 ft, 7 in. (59 m); height, 51 ft, 1.5 in. (15.58 m); span, 141 ft, 9.0 in. (43.21 m). The passenger entrance is 15 ft, 3 in. (4.65 m) above the ground. Height above ground is dictated by takeoff angle requirements. Detailed data and dimensions are given in Figure 3.1-1.

3.1.2 Mach .90 Configuration

A general arrangement of the Mach .90 configuration is presented in Figure 3.1-2. The fuselage has a conventional constant-diameter section (i.e., non-area ruled); the wing has a mid-chord sweep of 36 deg. and an aspect ratio of 9.0. The t/c at right angles to the mid-chord measured at the mean chord location is 14.15 percent. The fuselage has a diameter of 216 in. (5.49 m) and is sized to accommodate the combination of seven-abreast coach seating and the standard LD-3 cargo bay containers.

The three scaled P&W STF-429 engines each have a thrust of 22,400 lb (99,700 N). Engine location is similar to the Mach .98 configuration, the major installation difference being the shape of the inlet.

Landing gear and flight control system arrangements are also similar to the Mach .98 configuration.

Overall dimensions of this airplane are: length, 172 ft, 2 in. (52.48 m); height, 47 ft, 7 in. (14.50 m); span, 139 ft, 10 in. (42.62 m). The passenger entrance is 13 ft, 0 in. (3.96 m) above ground. Ground height of this configuration is also dictated by takeoff angle. Detailed data and dimensions are given in Figure 3.1-2.

3.1.3 Baseline Conventional Configuration

The general arrangement of the baseline conventional aircraft is presented in Figure 3.1-3. The fuselage of the conventional aircraft is identical to that of the Mach .90 airplane.

Wing and tail surfaces have basically the same sweep, taper ratio, and aspect ratio as the DC-10. Areas have been scaled down, however, to correspond to the smaller aircraft size.

The baseline airplane utilizes conventional aerodynamics, flight controls, and structural materials.

Propulsion is by the same type of engine (i.e., scaled P&W STF-429) as used on the advanced technology configurations to assure comparable noise and pollution levels. Individual engine thrust is 26,760 lb (119,028 N).

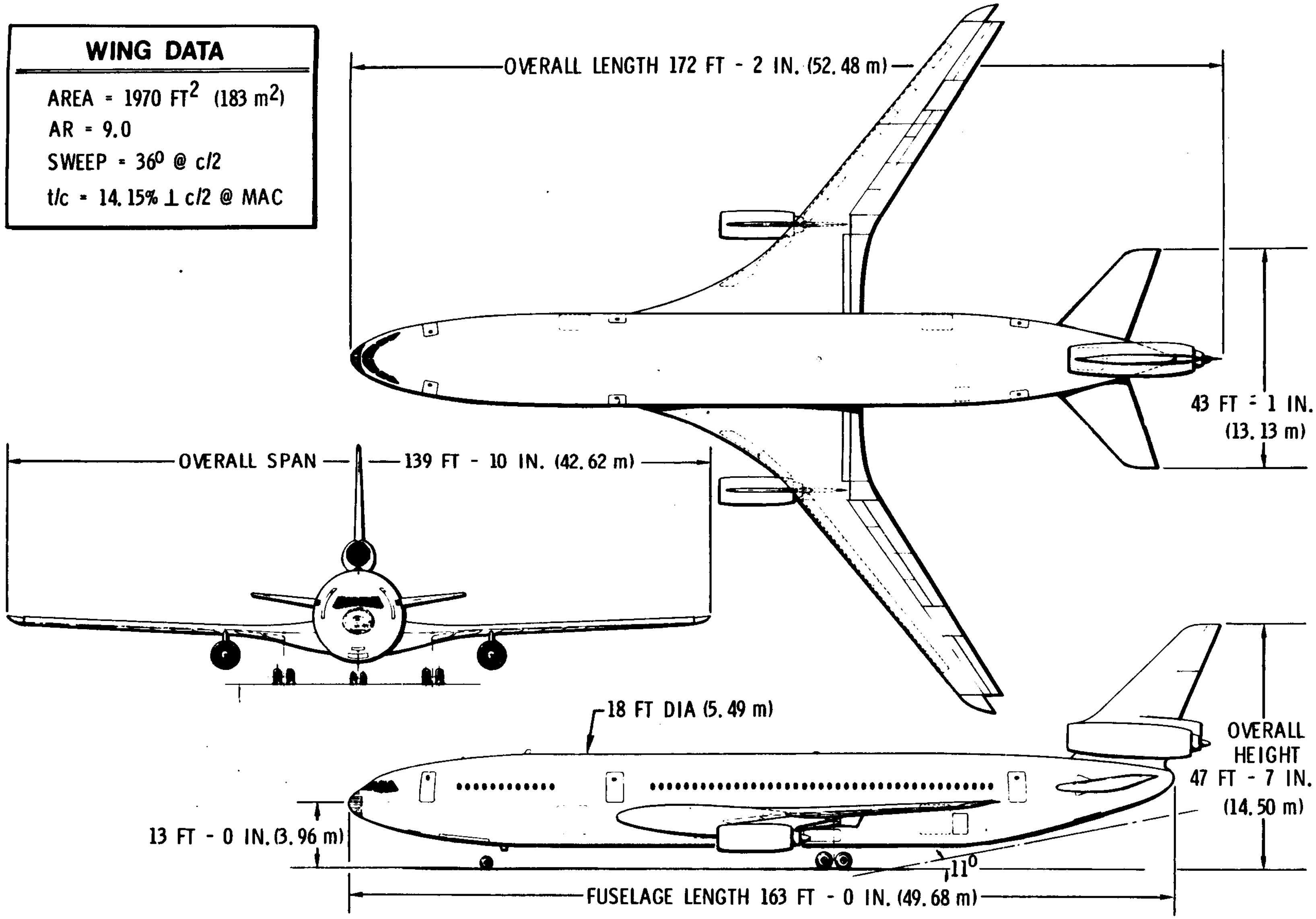

Figure 3.1-2 General Arrangement, Mach = .90 Configuration

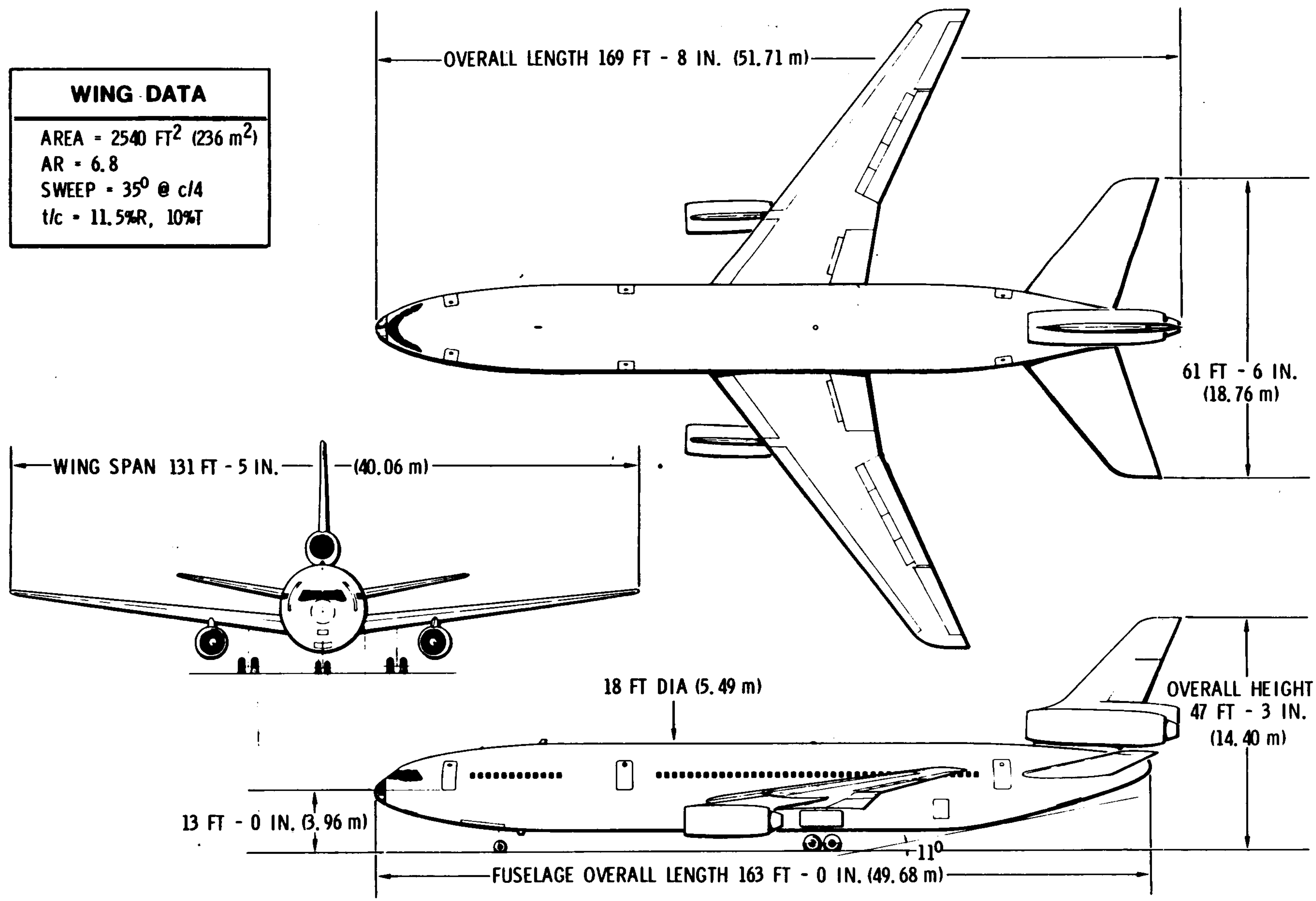

Figure 3.1-3 General Arrangement, Conventional Mach = .82 Configuration

Landing gear arrangement is the same as that used on the advanced technology configurations.

Overall dimensions are: length, 169 ft, 8 in. (51.71 m); height, 47 ft, 3 in. (14.40 m); span, 131 ft, 5.0 in. (40.06 m). The passenger door is 13 ft, 0 in. (3.96 m) above the ground. Engine lip clearance dictates the ground height.

Detailed dimensions are given in Figure 3.1-3.

3.2 AIRCRAFT INTERIOR ARRANGEMENT

The interior arrangements of the Mach .98 and Mach .90 advanced aircraft are presented in Figures 3.2-1 and 3.2-2, respectively. The interior of the baseline conventional aircraft is similar to the Mach .90 configuration.

Basically, the interior arrangements of all three aircraft are similar. Each fuselage is divided into conventional upper and lower compartments; the upper containing the passengers and crew; the lower, cargo and aircraft systems. The galley is located in the upper passenger compartment to provide maximum cargo volume below.

The upper compartment is conventionally arranged: flight deck forward, first class section next, galley, and a coach section continuing to the rear of the aircraft.

The area in the nose and immediately forward of the nose landing gear bay contains the avionics equipment. The area to either side of the nose gear bay is reserved for electrical distribution equipment.

Space for crossover routing is provided just forward of the wing box and below the passenger floor. The main landing gear is located immediately aft of the wing box.

Air conditioning equipment is located in the right- and left-hand wing gloves. The Auxiliary Power Unit is located in the tail section.

3.2.1 Cabin Compartment

The cabin compartment provides accommodations for 195 passengers (30 first class, 165 coach). Both the first-class and the coach-class compartments use twin aisles, each having a minimum width of 20 in. (50.8 cm) in first class and 19 in. (48.3 cm) in coach.

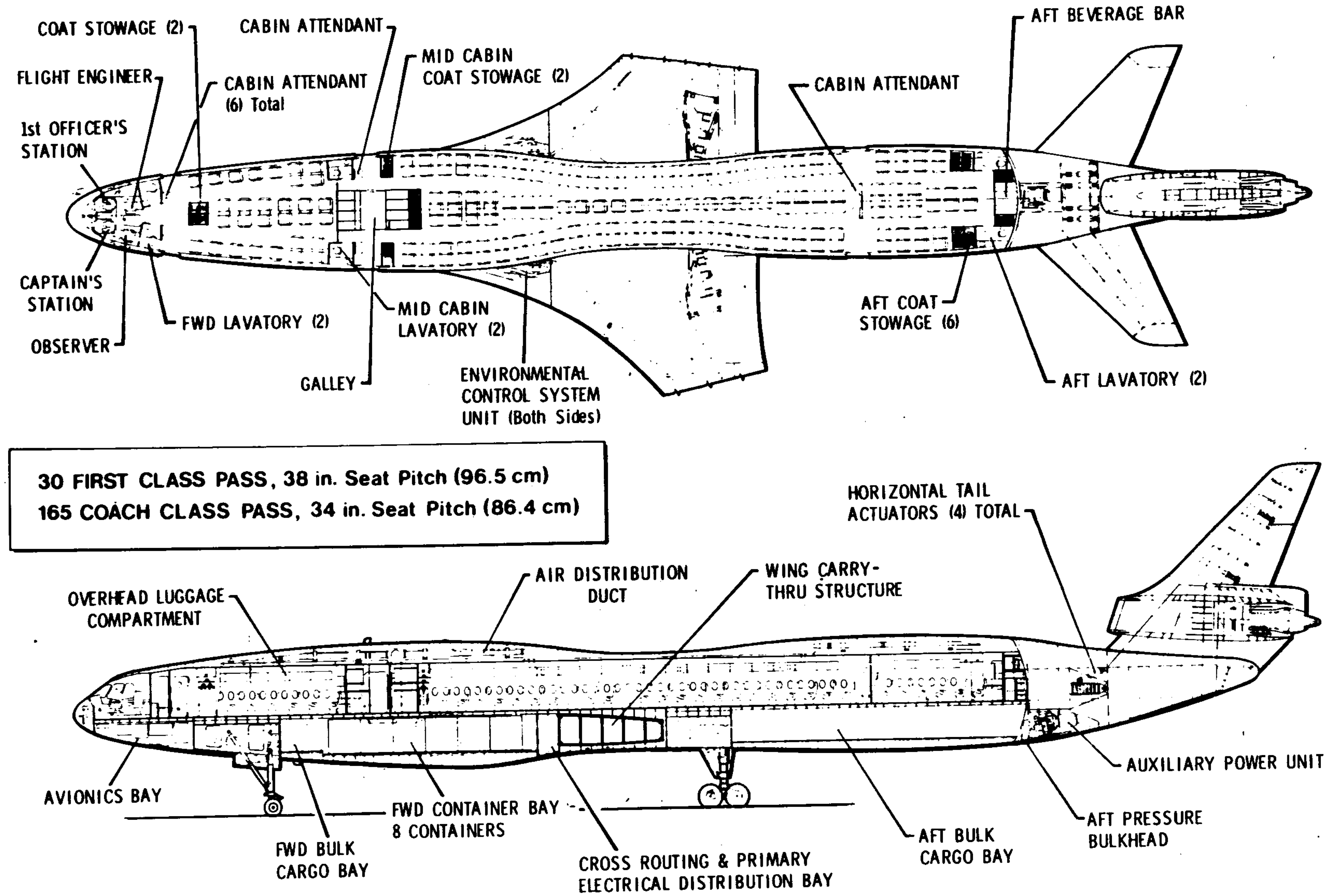

Figure 3.2-1 Interior Arrangement, Mach = .98 Configuration

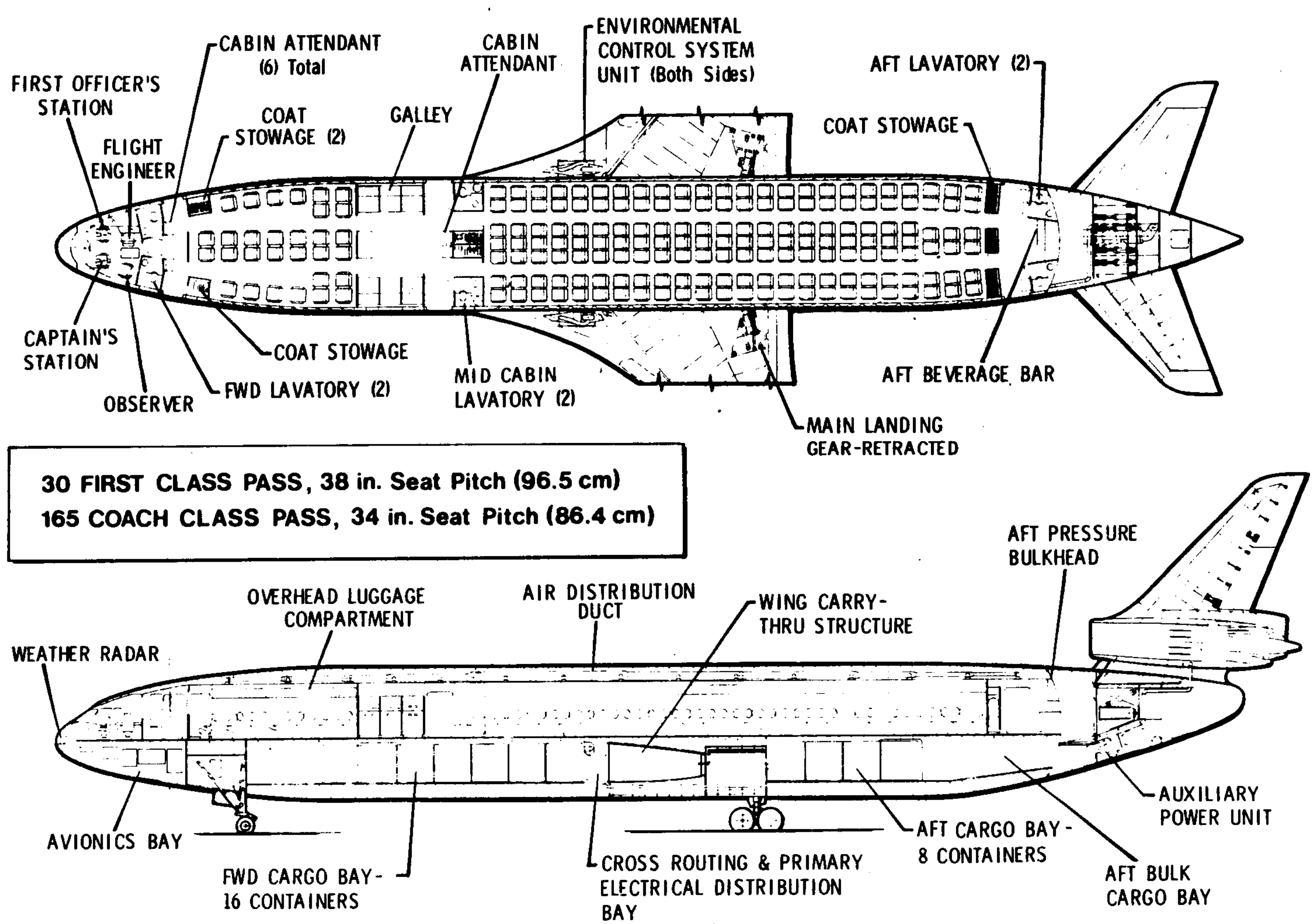

Figure 3.2-2 Interior Arrangement, Mach = .90 Configuration

Seating is maximum six abreast in first class and seven abreast in the coach section. First-class seats measure 20 in. (50.8 cm) between armrests. Armrests are 4 in. (10.2 cm) wide between seats and 3 in. (7.6 cm) at the end of rows. Coach-class seats measure 18.5 in. (47 cm) between armrests. Coach armrests are 3 in. (7.6 cm) between seats and 2 in. (5.1 cm) at the row ends. Seat dimensions and aisle widths are established as a result of contact with various airlines.

Windows are 10 in. (25.4 cm) wide and 14 in. (35.6 cm) high at 20-in. (50.8-cm) pitch.

Stowage areas are conveniently located throughout the passenger cabin, providing room for coats and other passenger items plus ample space for miscellaneous flight and emergency equipment.

Service utilities provide all passengers with seat-back oxygen modules, oxygen mask stowage, overhead reading lights, and individual air outlets. Contained in each seat arm is a light switch and a cabin-attendant call switch. Overhead enclosures provide stowage for blankets, pillows, and passenger personal effects. Additional storage is available under each passenger seat.

Each of the six cabin attendant seats is located adjacent to one of the passenger doors or emergency exits.

Food and beverage is supplied from one central galley located on the passenger deck between the first- and coach-class sections. Space is available for serving one meal to each of the passengers and crew. An additional beverage bar is located in the rear of the coach section to reduce congestion at the central galley and to increase the efficiency of the beverage service.

The galley is serviced by loading the galley modules through the service doors adjacent to the galley.

Six lavatories are distributed throughout the cabin compartment, two in first class, two in the forward end of the coach section, and two at the rear of the coach section.

Four Type A passenger doors (42 x 76 in.) (106.8 x 193 cm) and two Type I passenger doors (32 x 76 in.) (81.3 x 193 cm) are distributed along the fuselage length. Inflatable emergency evacuation slides are installed in each of these doors. The two forward Type I doors are fitted with single-track slides. The four Type A doors are fitted with double-track slides. A plan view of the Mach .98 aircraft with slides deployed is shown in Figure 3.2-3. Combination slide/rafts may be installed in place of the slides for overwater aircraft operation.

3.2.2 Baggage Compartment

The two baggage compartments located in the lower fuselage are both Class D as defined by FAR 25. The baggage compartment in the Mach .98 configuration will accommodate a combination of bulk and standard LD-3 containers in the forward area and bulk-only in the aft area. The cylindrical fuselages of the Mach .90 and conventional aircraft, however, allow the loading of standard LD-3 containers in both the forward and aft baggage compartments. Containers are loaded through 72-in.-wide by 66-in.-high (182.9 x 167.6 cm) doors on the right side of the airplane. Additional cargo doors are provided for bulk cargo loading. This allows for simultaneous loading of containerized and bulk cargo. The total capacity of the two selected configurations is summarized in Table 3.2-1.

Sills of all loading doors are flush with the internal flooring to provide easy cargo loading. The floors in the compartments handling containers incorporate a powered system for moving the containers longitudinally within the compartment and laterally in or out the door.

3.2.3 Flight Deck

The flight deck shown for each aircraft is a conventional commercial aircraft arrangement, providing normal seating for captain, first officer, flight engineer, and observer. Sufficient room is available in the flight compartment to accommodate an additional observer on a fold-down seat. The spaciousness of the flight deck arrangement shown allows for the required volume of controls, panel space, crew baggage, coats, briefcases, manuals, etc.

3.2.4 Landing Gear

The landing gear arrangements are conventional, with four-wheel trucks on the main landing gear and dual-wheels on the nose landing gear. The main landing gear retracts inboard and is stowed in a well beneath the cabin floor just

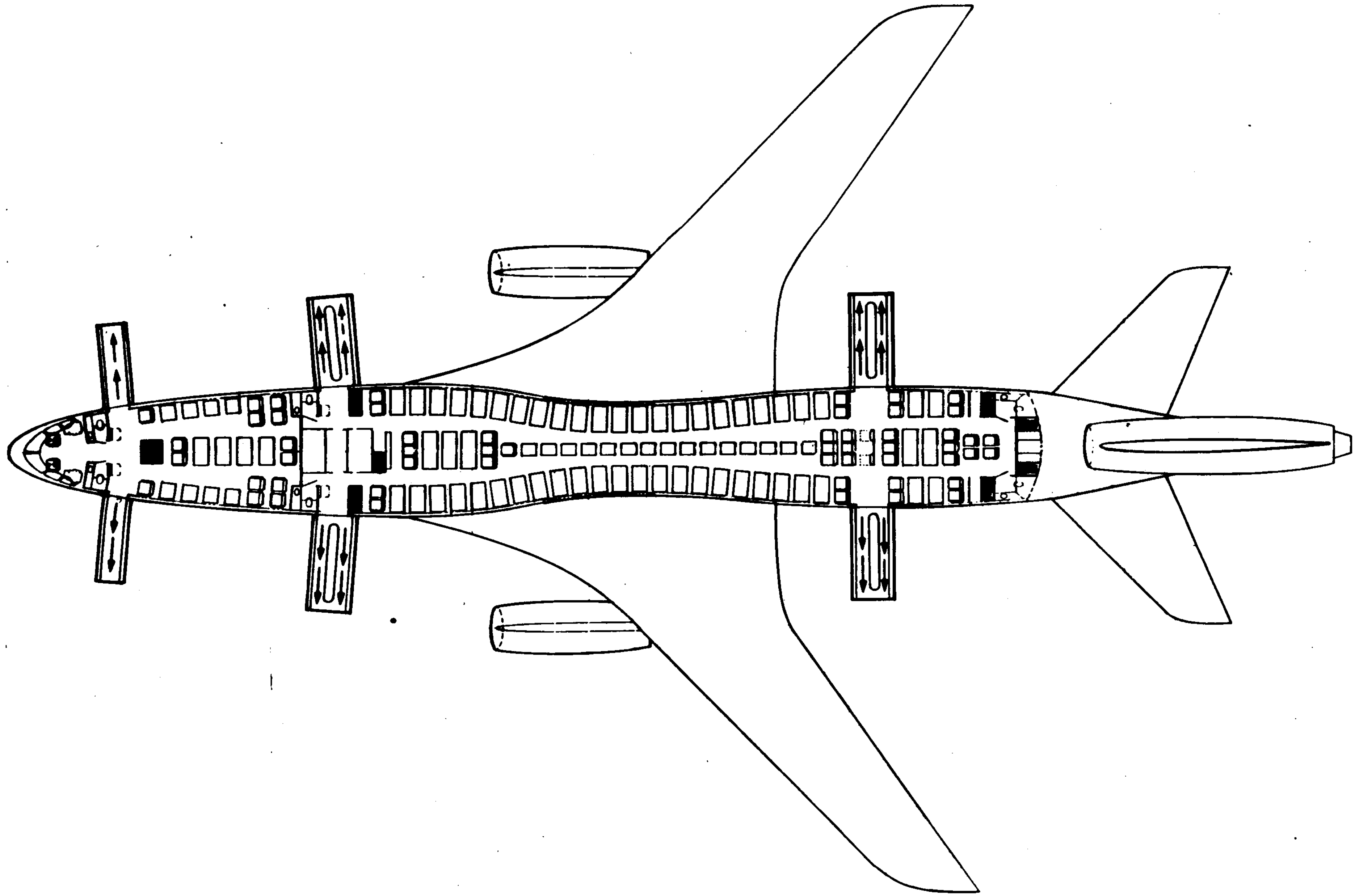

Figure 3.2-3 Emergency Evacuation Slide Arrangement

Table 3.2-1 Baggage and Cargo Capacity

COMPARTMENT	VOLUME - ft^3 (m^3)	
	MAX. CONTAINERS	ALL BULK
MACH .98 AIRPLANE		
• Forward Compartment		
• 8 Half-Width Containers	1264 (35.8)	
and Bulk	940 (26.6)	
Or		
• Bulk Only		2524 (71.5)
• Aft Compartment		
• Bulk Only	2357 (66.8)	2357 (66.8)
TOTALS	4561 (129.2)	4881 (138.3)
MACH .90 AIRPLANE		
• Forward Compartment		
• 16 Half-Width Containers	2528 (71.6)	
and Bulk	298 (8.4)	
Or		
• Bulk Only		3183 (90.1)
• Aft Compartment		
• 8 Half-Width Containers	1264 (35.8)	
and Bulk	921 (26.1)	
Or		
• Bulk Only		2556 (72.4)
TOTALS	5011 (141.9)	5739 (162.5)

aft of the wing rear spar. The nose landing gear retracts forward on the aircraft centerline. Tire and wheel sizes are as follows:

Landing Gear	M = 0.98 Configuration	M = 0.90 Configuration	Conventional M = 0.82 Configuration
Main Wheels in. (mm)	43 x 17-17 (8) (1092x432-432)	40 x 16-16 (8) (1016x406-406)	43 x 17-17 (8) (1092x432-432)
Tire Pressure psi (kg/sq cm)	162 (11.4)	161 (11.3)	157 (11.0)
Nose Wheels in. (mm)	33 x 13-13 (2) (838x330-330)	30 x 12-12 (2) (762x305-305)	33 x 13-13 (2) (838x330-330)

Tires have been sized to require no greater pavement thickness than that approved by the Airport Operators Council and outlined in Reference 3-1.

SECTION 4

ROUTE ANALYSIS

The economic evaluation of the many advanced transport configurations has been accomplished in the context of commercial usage by a major domestic airline. All direct comparisons have been made by simulating operation over identical routes. The route analysis is essentially an examination of that route structure and the passenger demand.

A route structure covering inter-city distances of 1000 to 5000 n.mi (1853 to 9265 km) was required to support Phase I of the study. Furthermore, a realistic definition of the optimum design range required that the distribution of city-pair passenger traffic, by inter-city distance, correspond closely to the existing market. The bulk of the required data was taken from Reference 4-1. For the year 1968, the top 100 city-pairs were ranked by both number of passengers and number of passenger-miles originated. Because of the long-range nature of the study, ranking by passenger-miles was selected. Eliminating city-pairs separated by less than 1000 n.mi (1853 km) left a group of 60 U.S. domestic routes ranging in distance to 4500 n.mi (8340 km).

A different procedure was required to estimate an international travel market. Reference 4-2 served as the basis for this expansion. Through a tedious perusal of this volume, a list of those markets having over 30 flights per week was compiled. These markets were ranked by flight volume and passenger volume and then calibrated by 1970 North Atlantic traffic data published by Ray and Ray (Av. Week, Reference 4-3). This procedure added 27 international routes varying from 2600 to 4800 n.mi (4820 to 8895 km).

The next step was to project the above traffic volume to the year 1985. Further statistics by Ray and Ray established the growth in domestic traffic between 1968 and 1970 at 14 percent. Historical traffic data from 1950 on is provided in Reference 4-1. From these data, the annual rate of increase in the number of passengers carried by U.S. domestic airlines was seen to approximate 10 percent. In light of the present economic situation and the prospect of decreased growth in the air travel market, an annual growth rate of 8 percent was used to project the 1985 market. Over a period of 15 years, however, this rate still accounts for a trebling of the current market. Since it was desired that the resultant market represent that of a single major trunk airline, it was presumed that such an airline would capture 1/3 of the domestic traffic and 1/2 of the international traffic on each route. The result of all these calculations is the daily traffic distribution shown in Figure 4.0-1. The distinctive peak at 2200 n.mi (4075 km) represents the east-west market; that at 3200 n.mi (5930 km), the North Atlantic routes. From this figure it would seem that 3000 n.mi (5560 km) is an excessive design range for the advanced transport; however, at least 15 percent must be added to these geographical distances to specify a design range because of prevailing winds affecting the east-west direction. Thus the 3000-n.mi (5560 km) design range specified for Phase II of this study is a logical range to cover the majority of the domestic routes, including mainland-Hawaii.

For Phase II, the selected markets were restricted to domestic routes of less than 3000 n.mi (5560 km), actually truncating at about 2350 n.mi (4355 km). To compensate for the reduced sample, major city-pairs down to 150 n.mi (280 km) were added. Particularly important additions were New York-Chicago, New York-Miami, and Los Angeles-San Francisco, the last being the single largest market in the United States. Data for these additional routes came from the previously mentioned tables of Reference 4-1. By combining the rankings based on passengers and on passenger-miles, a set of the top 128 U.S. domestic city-pairs was obtained.

The realism of the new route structure was enhanced by use of the data of Reference 4-4. Each of the 128 city-pair schedules was analyzed to determine the number of airlines servicing that market and the representative market share of an "average" truck airline. In some instances, this share is 70 to 80 percent, whereas in others, such as Los Angeles-San Francisco, it drops to only 10 percent because of the large number of competing airlines. The respective shares thus defined were applied to the total projected 1985 traffic, giving the distribution shown in Figure 4.0-2.

The route structure of this "cream of the crop" market is illustrated geographically in Figure 4.0-3. These selected markets do not represent the routes of any one typical

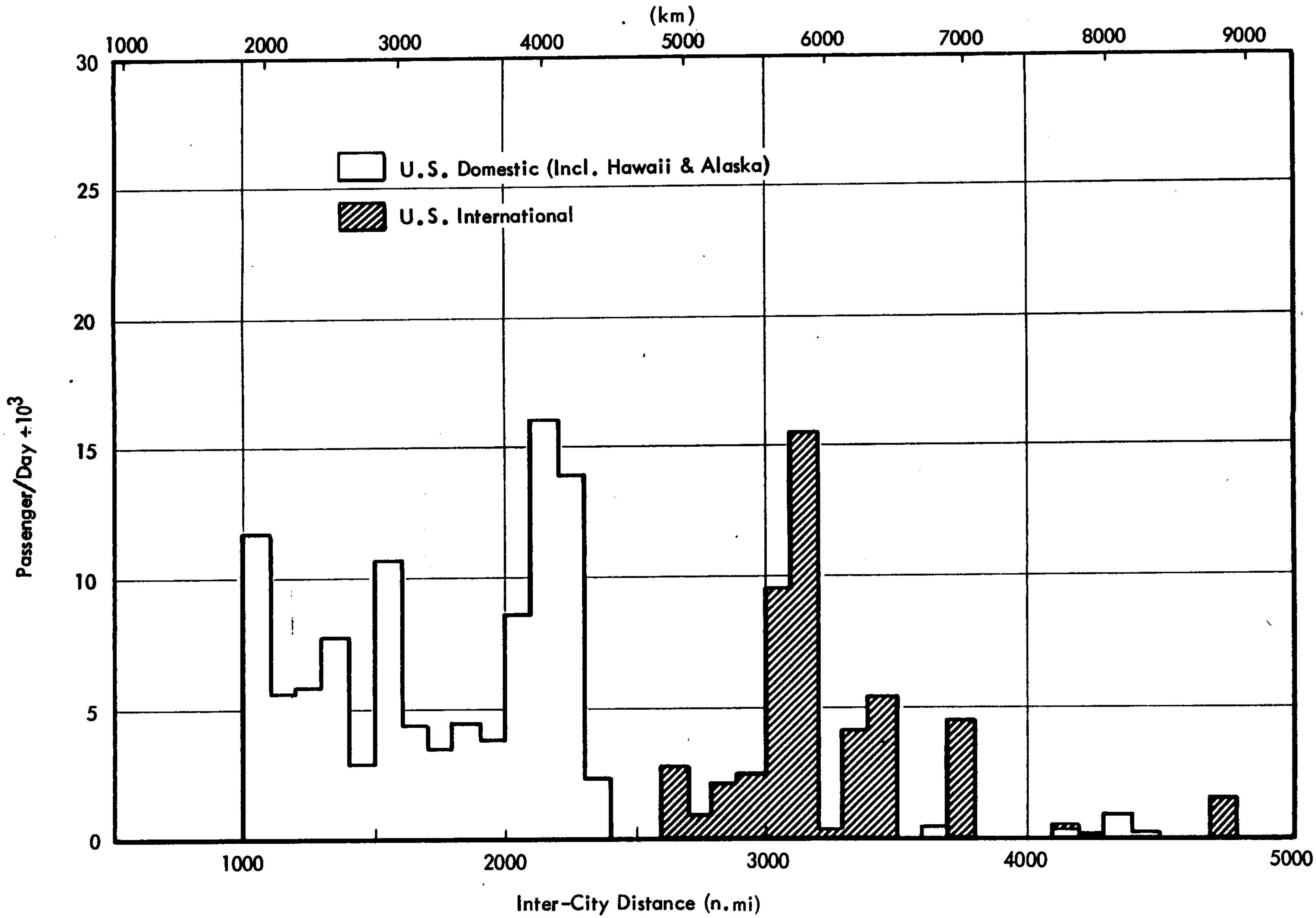

Figure 4.0-1 Projected Distribution of 1985 U. S. Domestic and International Airline Passenger Traffic, 1000-5000 n. mi

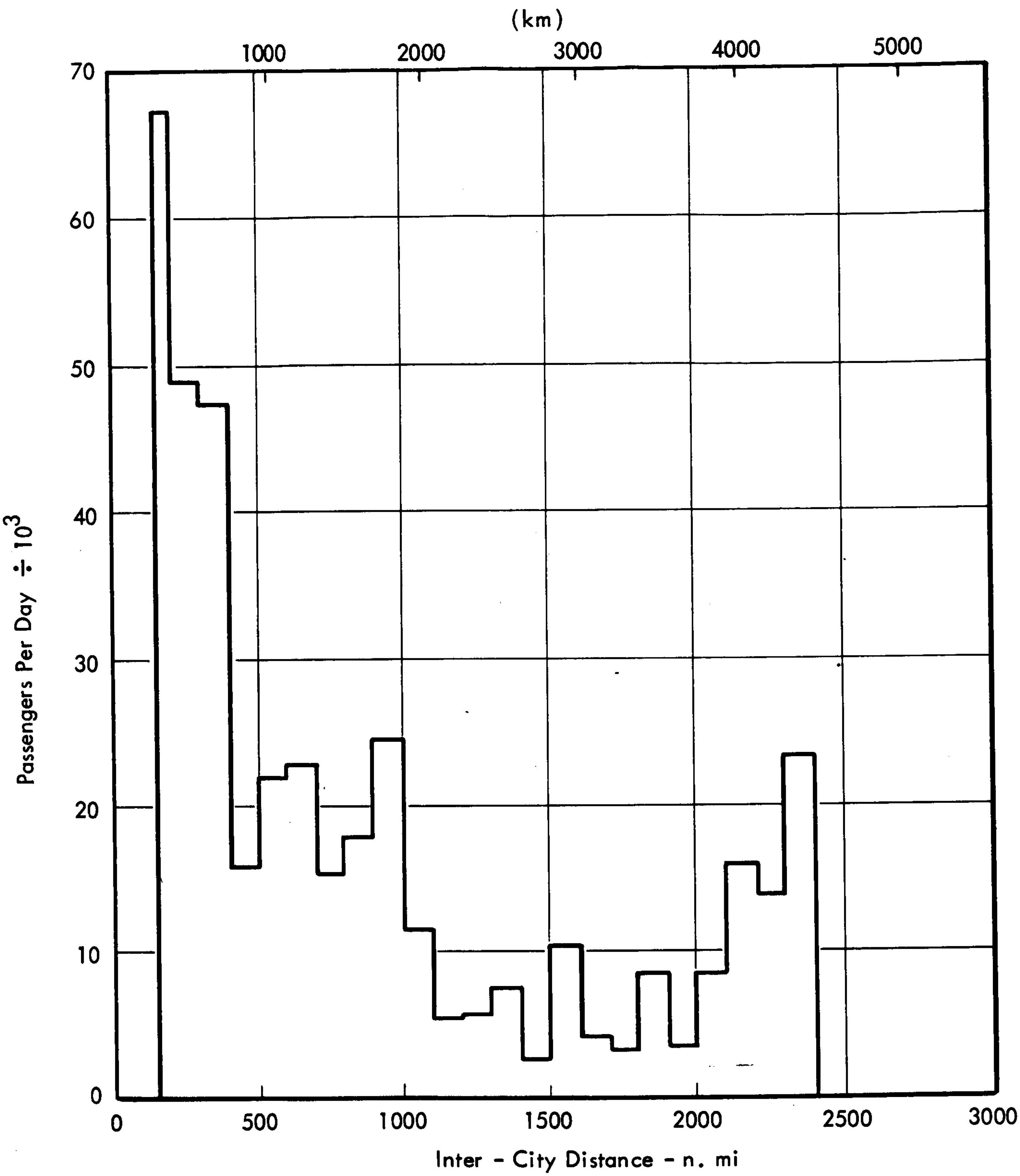

Figure 4.0-2 Projected Distribution of 1985 U. S. Domestic Airline Passenger Traffic, 150-3000 n. mi

1 Boston	8 Rochester	15 Detroit	22 Norfolk	29 Houston	36 Sacramento	43 Anchorage
2 Hartford	9 Buffalo	16 Indianapolis	23 Charlotte	30 Dallas	37 San Francisco	44 Lihue
3 New York	10 Pittsburgh	17 Chicago	24 Atlanta	31 San Antonio	38 Los Angeles	45 Honolulu
4 Philadelphia	11 Cleveland	18 Milwaukee	25 Tampa	32 Denver	39 San Diego	46 Hilo
5 Baltimore	12 Columbus	19 minneapolis	26 West Palm Beach	33 Phoenix	40 Spokane	
6 Washington	13 Dayton	20 St. Louis	27 Miami	34 Las Vegas	41 Seattle	
7 Syracuse	14 Cincinnati	21 Kansas City	28 New Orleans	35 Reno	42 Portland	

Figure 4.0-3 Selected Airline Route Structure, Top 128 U. S. Domestic City-Pairs

airline, but rather the best of all the major carriers. Likewise, the economic return over this set of routes will be higher than any one airline could ever hope to achieve. For the purpose of evaluating an airplane design, however, they are realistic, since a given airplane will be sold to several airline customers and the distribution of traffic over these routes, since it is based on actual statistics, gives a true evaluation of the worth of one design over another.

SECTION 5

PERFORMANCE ANALYSIS

Performance studies were conducted to select optimum commercial transport configurations having cruise speeds of .90 and .98M, a 3000-n.mi (5560 km) range, and a 40,000-lb (18,140 kg) payload. Analyses were also conducted to determine the impact of the following advanced technologies on airplane size and economics:

composite materials
active control systems
reduced noise and pollutant levels

The performance characteristics of the selected .90M and .98M designs are shown together with range/payload effects, speed and cruise altitude effects, and FAR field lengths with associated effects of temperature and airport elevations. Trade studies are also presented showing the effects of L/D, dry weight changes, initial cruise altitude, and field length requirements. The configuration selection process is summarized, including the effects of the various technologies on geometry optimization.

The above range and payload were selected on the basis of maximum return on investment during Phase I of the subject studies. A comprehensive matrix of parametric configurations were analyzed covering ranges from 2800 n.mi (5186 km) to 5500 n.mi (10,190 km) and payloads of 30,000 lb (13,608 kg), 40,000 lb (18,140 kg), and 80,000 lb (36,290 kg). The Phase I analysis is not described in this report, but the data were presented in Convair's Interim Oral Presentation and Documentation.

5.1 PERFORMANCE SUMMARY

The selected .98M and .90M airplanes utilize the advanced technologies selected by Convair that have the maximum payoff in return on investment. The major advanced technologies selected are a supercritical wing, an active control system, and maximum utilization of composite materials. The characteristics of the optimum airplane for each design Mach number are given in Table 5.1-1. The range payload capabilities of the selected configurations are shown in Figure 5.1-1.

Table 5.1-1 SELECTED CONFIGURATION CHARACTERISTICS
(3) PRATT & WHITNEY STF 429 ENGINES

	M = .90 Design	M = .98 Design
Takeoff Gross Weight lb (kg)	247432 (112214)	273840 (124190)
Basic Operating Weight lb (kg)	127935 (58021)	144128 (65364)
Wing Area ft^2 (m^2)	1970 (183)	2282 (212)
S.L.S. Thrust (1 Engine) lb (N)	22400 (99640)	26480 (117790)
Thrust/Weight Ratio	.272	.290
Aspect Ratio	9.0	8.0
Sweep (Half-Chord) deg	36	40
Thickness Ratio (Perpendicular to Half-Chord @ M.A.C.)	.1415	.1100
Range With 60,000 lb (27216 kg) Payload n.mi (km)	1880 (3481)	2020 (3740)
FAR Takeoff Field Length 90°F @ 1000 ft (305 m) (305.2°K) ft (m)	7900 (2410)	8300 (2531)
FAR Landing Field Length 90°F @ 1000 ft (305 m) (305.2°K) ft (m)	7100 (2164)	6800 (2073)
Noise Level - EPNdB	FAR36 -10	FAR36 -10
Approach Speed - Knots (km/hr) @M=.90, Landing Wt = 207840 lb (94276 kg)	144.5 (267.8)	
@M=.98, Landing Wt = 230025 lb (104339 kg)		144.5 (267.8)

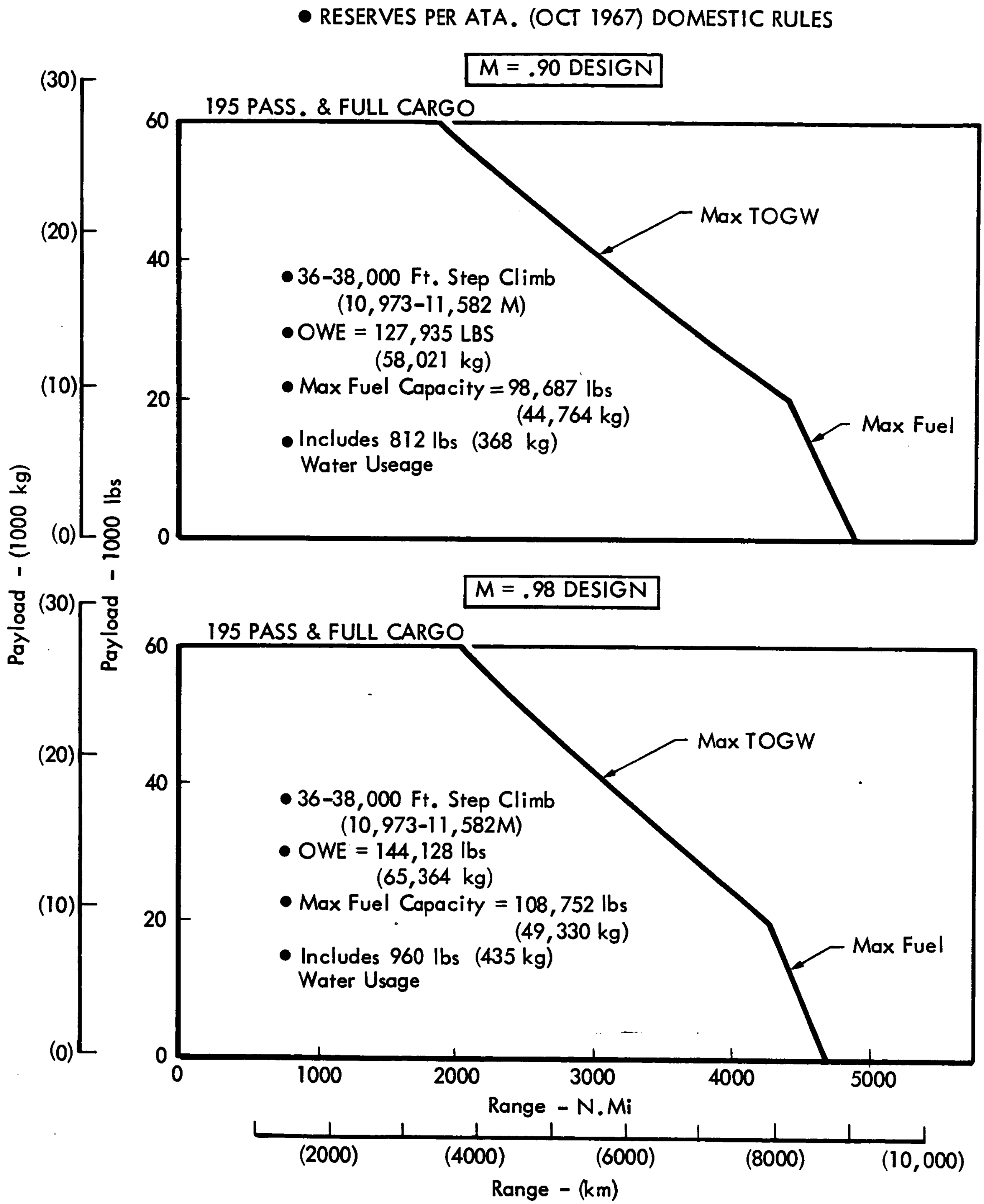

Figure 5.1-1 Range Payload Capability

A summary of the airplanes developed for the technology evaluation is shown in Tables 5.1-2 and -3. These tables also include a conventional-wing, 0.82M, aluminum transport for comparison purposes. The final selection of the incorporated technologies was based on the economic analysis (Return on Investment) as discussed in Section 6.

5.2 SELECTED CONFIGURATION PERFORMANCE

The performance capabilities of the selected .90M and .98M configurations are presented in this section. Included are the range/payload capabilities with the effect of off-design cruise speed, cruise altitude, and takeoff weight. FAR field lengths for takeoff and landing are also shown and incorporate the effects of ambient temperature, field elevation, and takeoff weight.

5.2.1 Range/Payload Capabilities

The range/payload capabilities of both configurations are shown in Figure 5.2-1. This figure also shows the effects of takeoff gross weight on range and payload capabilities. The maximum passenger load plus cargo range is 1880 n.mi (3481 km) for the .90M airplane and 2020 n.mi (3740 km) for the .98M design.

Payload/range trades for off-design cruise speeds are shown in Figure 5.2-2 and for off-design cruise altitudes in Figure 5.2-3. These effects are summarized as a function of cruise speed and altitude in Figure 5.2-4.

Typical range profiles at the design payload/range condition are shown in Figures 5.2-5 and 5.2-6. The tables give the time, fuel used, and range for each segment of the route flown.

5.2.2 FAR Takeoff Field Length

Takeoff field length variation with gross weight, ambient temperature, and field elevation for each design is shown in Figure 5.2-7. These takeoff field lengths are compatible with those of domestic airports currently in use.

It may be noted that the takeoff field length for both airplanes is very nearly the same. This is due to the

Table 5.1-2 EFFECT OF TECHNOLOGY APPLICATION

M = .98 Design

	M=.82 Aluminum*	Aluminum SCW**	Aluminum SCW+ACS***	Composite SCW	Composite SCW+ACS	Composite SCW+ACS -15EPNDB	Composite SCW+ACS +MAX EPNDB
Takeoff Gross Weight lb (kg)	317400 (143970)	322200 (146122)	308400 (139863)	278400 (126258)	273840 (124190)	279000 (126531)	282600 (128163)
Basic Operating Weight lb (kg)	172052 (78028)	182392 (82717)	171968 (77990)	147374 (66836)	144128 (65364)	147307 (66806)	152769 (69283)
Wing Area ft^2 (m^2)	2645 (245.7)	2685 (249.4)	2570 (238.8)	2320 (215.5)	2282 (212.0)	2325 (216.0)	2355 (218.8)
Aspect Ratio	6.8	7.5	7.5	8.0	8.0	8.0	8.0
Sweep (Half-Chord) deg	31.75	40	40	40	40	40	40
Thickness Ratio (Perpendicular to Half-Chord @ M.A.C.)	.1000	.1100	.1100	.1100	.1100	.1100	.1100
FAR 36 Noi e Level EPNDB(Critical Condition)	-10	-10	-10	-10	-10	-15	-15****
Engines (3) Pratt & Whitney	STF429	STF429	STF429	STF429	STF429	STF429	STF429
S.L.S. Thrust (1 Engine) lb (n)	32160 (143055)	29800 (132557)	28880 (128465)	26760 (119034)	26480 (117789)	26800 (119212)	31440 (139852)
Thrust/Weight Ratio	.304	.277	.281	.288	.290	.288	.334

*Conventional Aluminum Transport, Standard Airfoil Section
**SCW = Supercritical Wing
***ACS = Active Control Systems
****Maximum Community Noise Reduction (See Section 10.0); No Sideline Reduction

Table 5.1-3 EFFECT OF TECHNOLOGY APPLICATION

M = .90 Design

	M=.82 Aluminum*	Aluminum SCW**	Aluminum SCW+ACS***	Composite SCW	Composite SCW+ACS	Composite SCW+ACS -15 EPNDB	Composite SCW+ACS +MAX EPNDB
Takeoff Gross Weight lb (kg)	317400 (143970)	285740 (129588)	276948 (125600)	249944 (113353)	247432 (112214)	251830 (114208)	263760 (119619)
Basic Operating Weight lb (kg)	172052 (78028)	155835 (70674)	149097 (67618)	130375 (59127)	127935 (58021)	130250 (59070)	139580 (63302)
Wing Area ft^2 (m^2)	2645 (245.7)	2275 (211.4)	2205 (204.9)	1990 (184.9)	1970 (183.0)	2005 (186.3)	2100 (195.1)
Aspect Ratio	6.8	8.5	8.5	9.0	9.0	9.0	9.0
Sweep (Half-Chord) deg	31.75	36	36	36	36	36	36
Thickness Ratio (Perpendicular to Half-Chord @ M.A.C.)	.1000	.1415	.1515	.1515	.1415	.1415	.1415
FAR 36 Noise Level EPNDB (Critical Condition)	-10	-10	-10	-10	-10	-15	-15****
Engines (3) Pratt & Whitney	STF429	STF429	STF429	STF429	STF429	STF433	STF433
S.L.S. Thrust (1 Engine) lb (n)	32160 (143055)	25040 (111383)	24500 (108981)	22600 (100530)	22400 (99640	22720 (101064)	28960 (128821)
Thrust/Weight Ratio	.304	.263	.265	.271	.272	.271	.329

*Conventional Aluminum Transport, Standard Airfoil Section

**SCW = Supercritical Wing

***ACS = Active Control Systems

****Maximum Community Noise Reduction (See Section 10.0); No Sideline Reduction

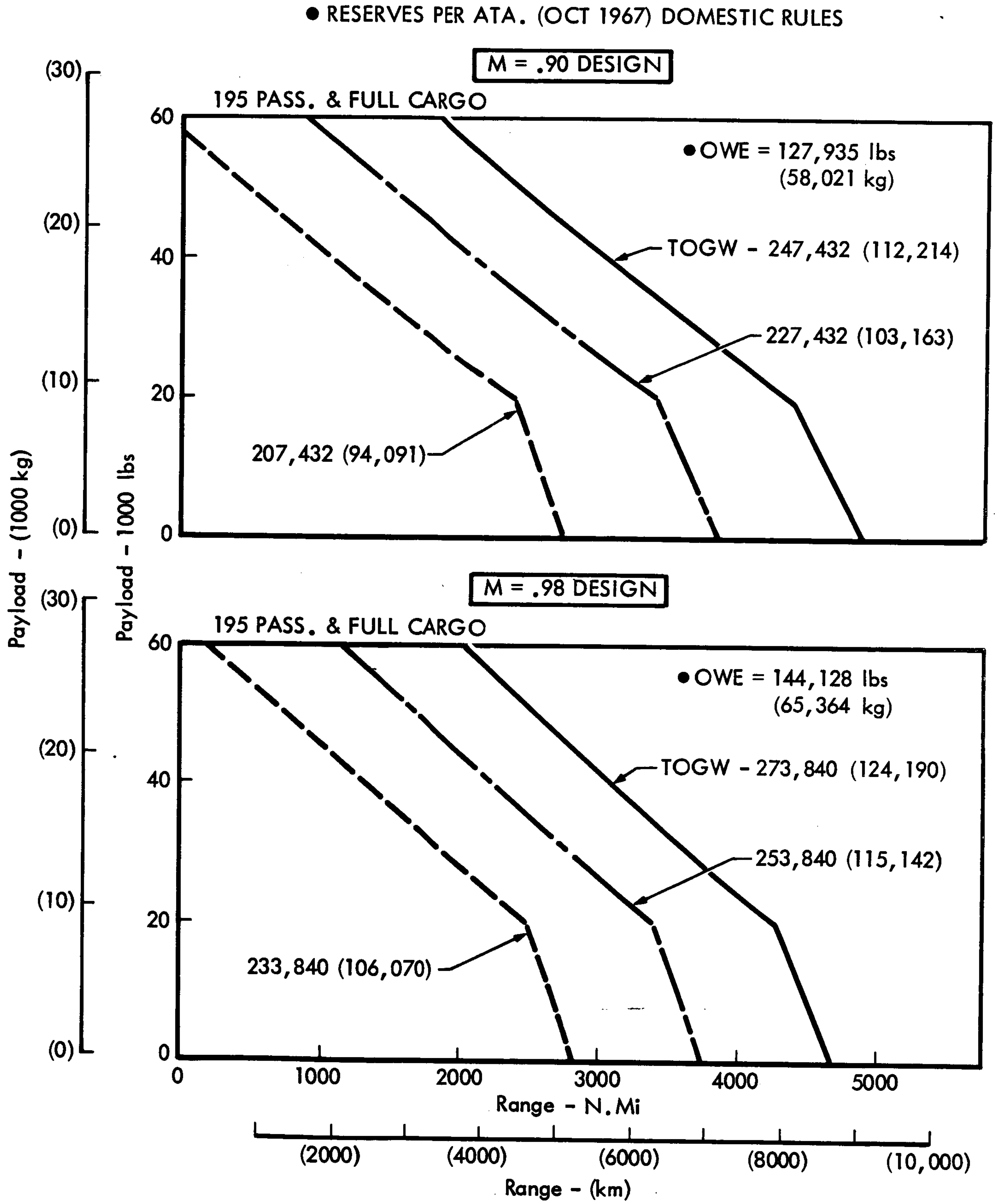

Figure 5.2-1 Effect of TOGW On Range/Payload

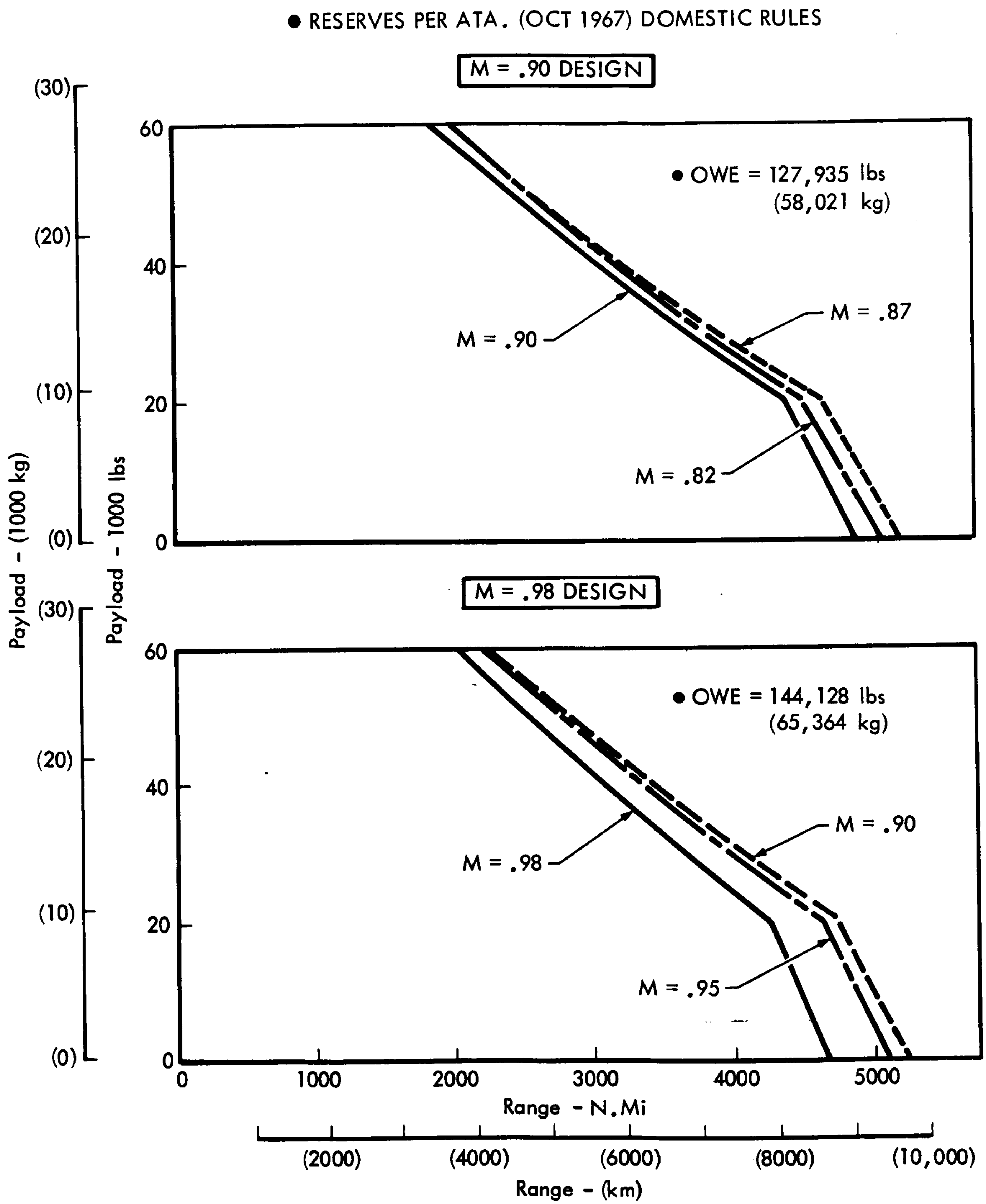

Figure 5.2-2 Effect of Cruise Mach On Payload/Range

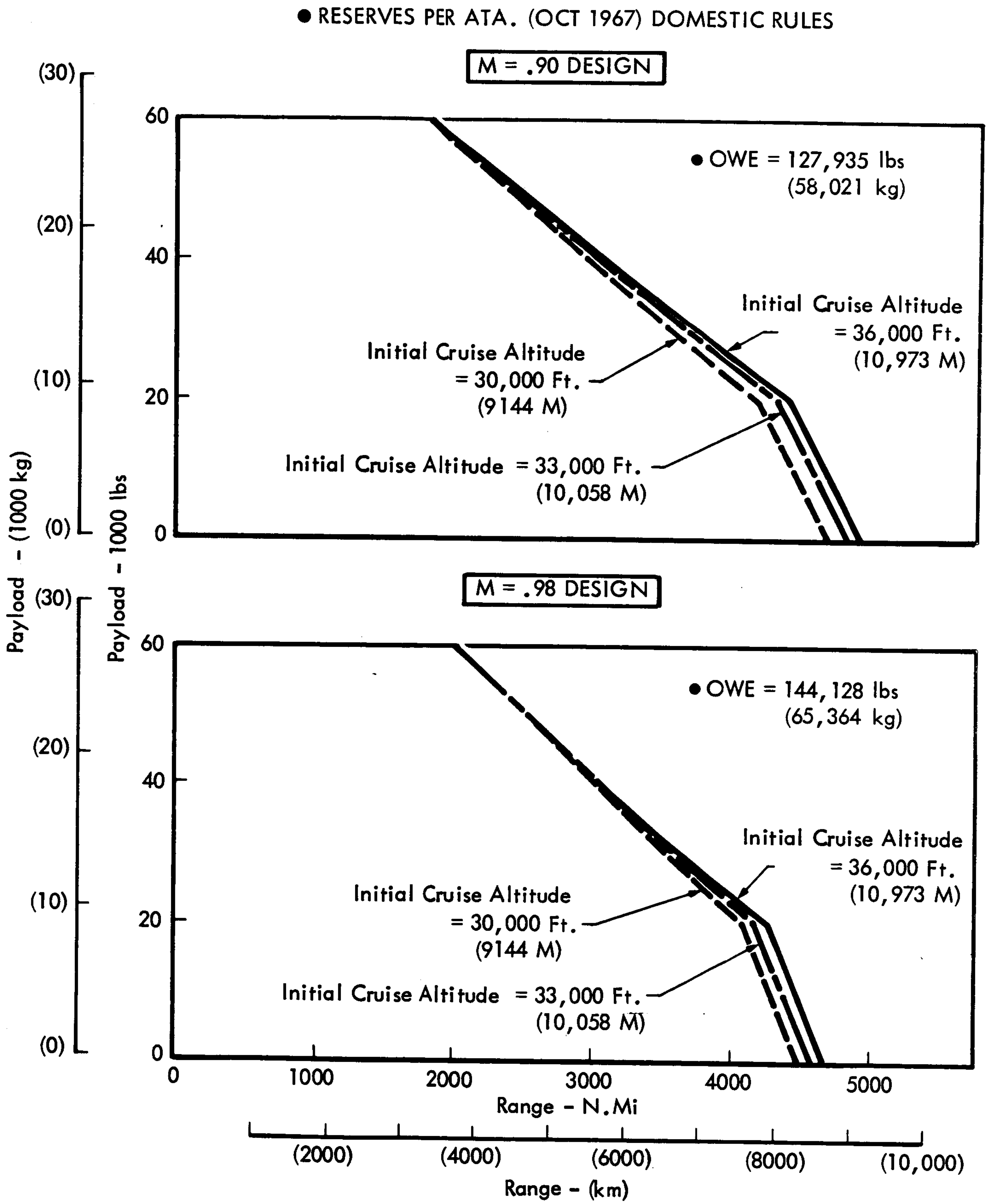

Figure 5.2-3 Effect of Cruise Altitude On Range/Payload

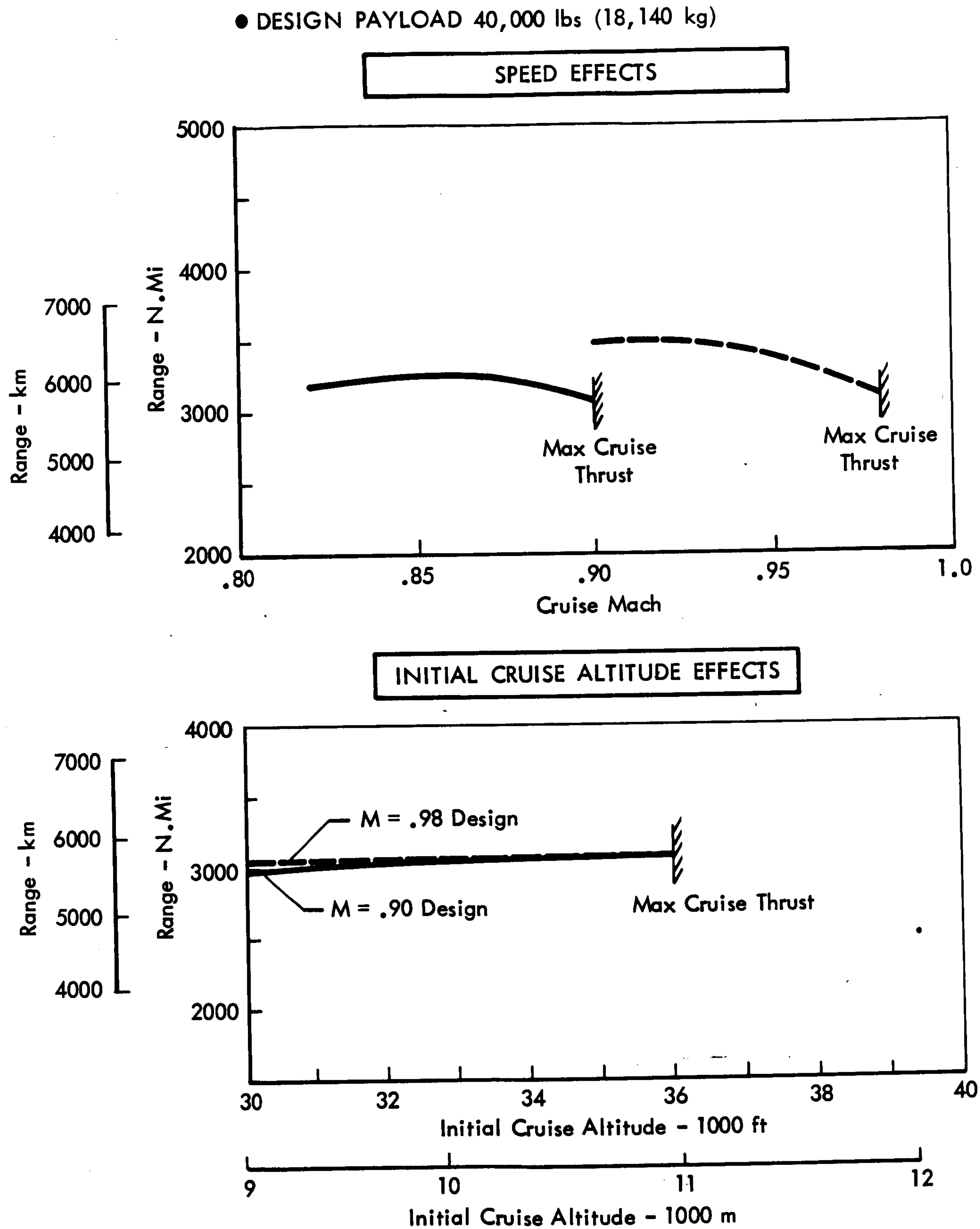

Figure 5.2-4 Off Design Cruise Speed & Altitude Effects

Taxi Weight = 247,432 lb (112,214 kg)
B.R.G.W. = 247,064 lb (112,068 kg)
O.E.W. = 127,935 lb (58,021 kg)
Payload = 40,000 lb (18,140 kg)
Fuel Capacity = 78,687 lb (35,686 kg)
Engine = P&W STF 429
Type of Cruise = Long Range Cruise
Temperature = Std Day
Block Time = 6.3 Hrs
Block Fuel = 63,557 lb (28,829 kg)
Water = 812 lb (369 kg)

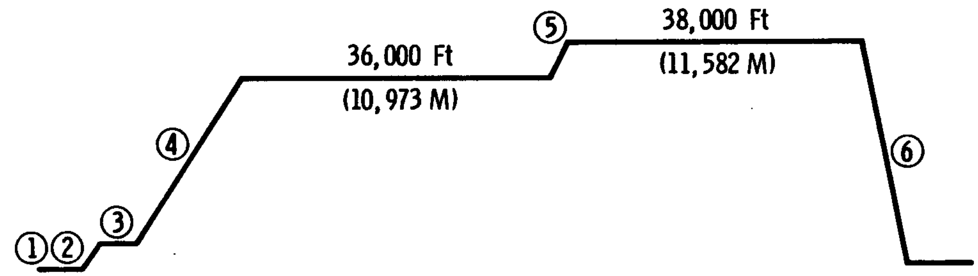

	FUEL BURNED (Lbs) (kg)	FUEL REMAINING (Lbs) (kg)	WEIGHT AT END OF OPERATION (Lbs) (kg)	SPEED (Mach)	TIME (Hrs)	DISTANCE (N.Mi.) (km)
1 Taxi Out (14 Min.)	368 (167)	78,319 (35,525)	247,064 (112,068)	0	.23	0
2 Takeoff (S.L. to 35 Ft) (S.L. to 11M)	674 (306)	77,645 (35,220)	245,985 (111,579)	.25	.02	1 (2)
3 Climb to 1500 Ft (457M) and Accel to 250 KEAS (463 km/hr EAS)	960 (435)	76,685 (34,784)	244,620 (110,960)	.25	.04	3 (6)
4 Climb to Cruise Altitude	11,140 (5,053)	65,545 (29,731)	233,480 (105,907)	.25/.90	.66	321 (595)
5 Cruise	50,020 (22,689)	15,525 (7,042)	183,460 (83,217)		5.23	2,657 (4,920)
6 Descend to Airport	395 (179)	15,130 (6,863	183,065 (83,038)	.90/.25	.22	88 (163)
Total Mission	63,557 (28,829)				6.30	3,070 (5,686)
7. Reserves						
A. Fuel Allowance (1 Hour at End Cruise Weight and Fuel Flow)	6,560 (2,976)	8,570 (3,887)	176,505 (80,063)			
B. Alternate [Missed Approach, Climb from 1500 Ft. (457M), Cruise, Descent to 1500 Ft. (457M)]	8,570 (3,887)	0	167,935 (76,175)			
Total Reserves	15,130 (6,863)					
Total Fuel	78,687 (35,686)					

Figure 5.2-5 Sample Mission Summary M = .90

Taxi Weight = 273,840 lb (124,190 kg)
B.R.G.W. = 273,472 lb (124,047 kg)
O.E.W. = 144,128 lb (65,364 kg)
Payload = 40,000 lb (18,140 kg)
Fuel Capacity = 88,752 lb (40,251 kg)
Engine = P&W STF 429
Type of Cruise = Long Range Cruise
Temperature = Std Day
Block Time = 5.94 Hrs
Block Fuel = 71,252 lb (32,320 kg)
Water = 960 lb (435 kg)

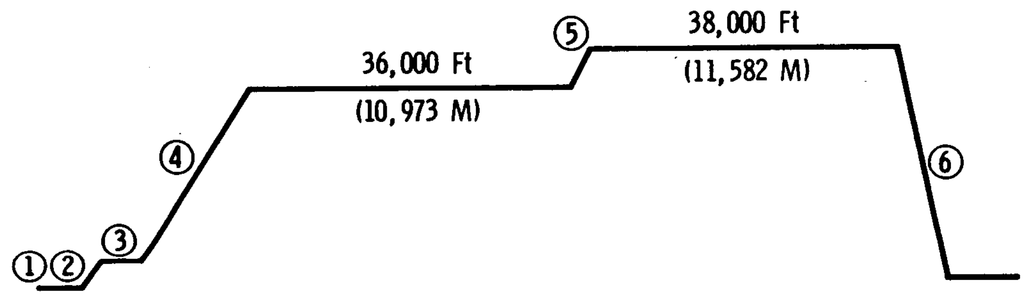

	FUEL BURNED (Lbs) (kg)	FUEL REMAINING (Lbs) (kg)	WEIGHT AT END OF OPERATION (Lbs) (kg)	SPEED (Mach)	TIME (Hrs)	DISTANCE (N.Mi.)
① Taxi Out (14 Min.)	368 (167)	88,384 (40,091)	273,472 (124,047)	0	.23	0
② Takeoff (S.L. to 35 Ft.) (S.L. to 11M)	842 (382)	87,542 (39,709)	272,150 (123,447)	.25	.02	1 (2)
③ Climb to 1500 Ft (457M) and Accel to 250 KEAS (463 km/hr EAS)	750 (340)	86,792 (39,369)	270,920 (122,889)	.25	.04	3 (6)
④ Climb to Cruise Altitude	10,870 (4,931)	75,922 (34,438)	260,050 (117,959)	.25/.98	.53	275 (510)
⑤ Cruise	57,972 (26,296)	17,950 (8,142)	202,078 (91,663)	.98	4.89	2,725 (5,046)
⑥ Descent to Airport	450 (204)	17,500 (7,938)	201,628 (91,458)	.98/.25	.23	86 (159)
Total Mission	71,252 (32,320)				5.94	3,090 (5,723)
7. Reserves						
A. Fuel Allowance (1 Hour at End Cruise Weight and Fuel Flow)	7,150 (3,243)	10,350 (4,695)	194,478 (88,215)			
B. Alternate (Missed Approach, Climb from 1500 Ft (457M), Cruise, Descent to 1500 Ft) (457M)	10,359 (4,695)	0	184,128 (83,520)			
Total Reserves	17,500 (7,938)					
Total Fuel	88,752 (40,251)					

Figure 5.2-6 Sample Mission Summary M = .98

● FAR BALANCED FIELD LENGTH PER FAR 25.113 & .111

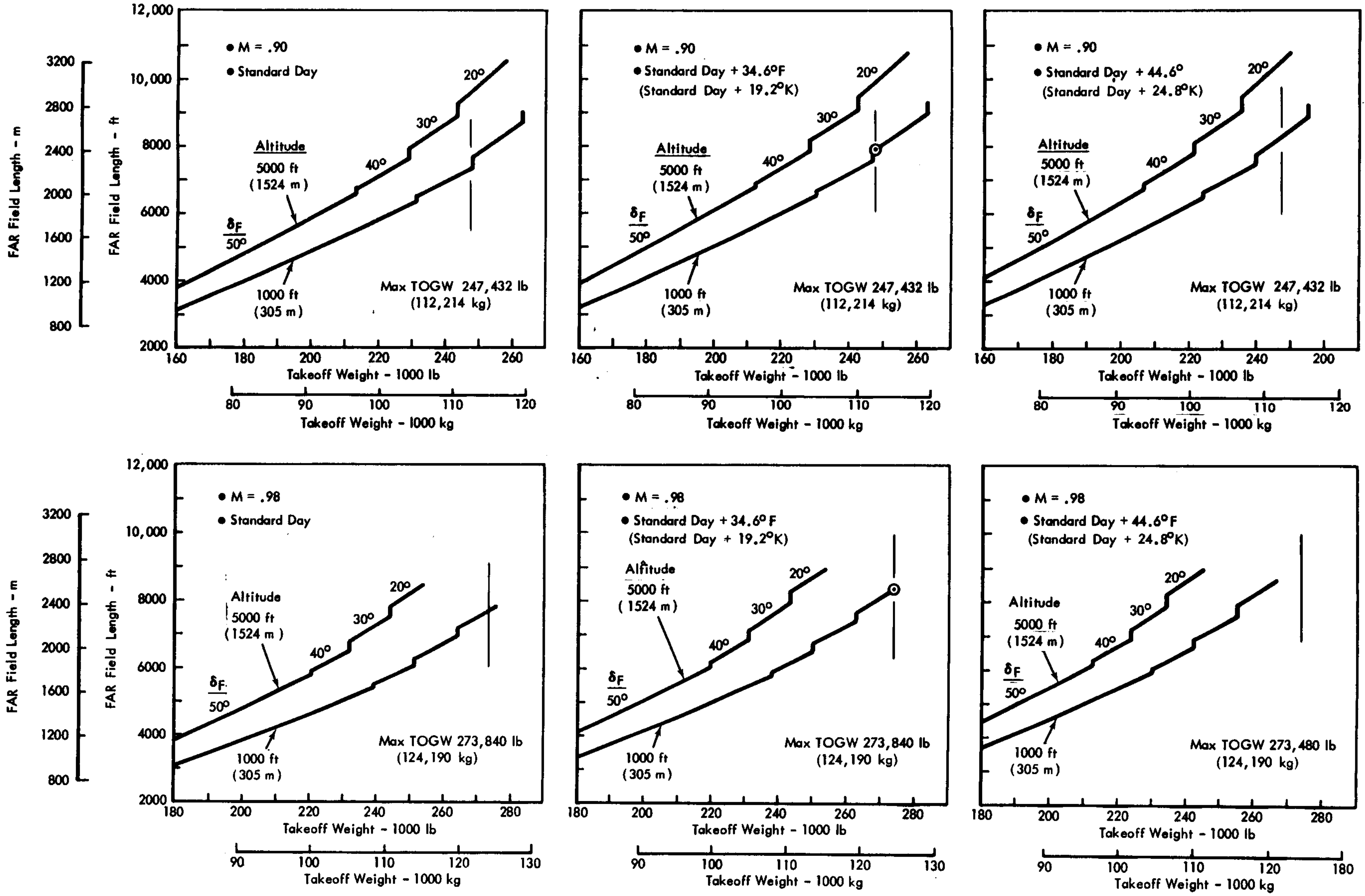

Figure 5.2-7 FAR Takeoff Field Lengths

higher L/D and C_{LMAX} of the .90M design being offset by the higher T/W (.290 vs .272) of the .98M design.

5.2.3 FAR Landing Field Length

Landing field length variation with landing weight and field elevation is shown in Figure 5.2-8 for both configurations. The approach speed is identical for each airplane, as shown in the upper portion of the figure. This was accomplished by setting the wing loading of the M=.90 design slightly higher than that of the M=.98 design to offset the higher C_{LMAX}. The difference in landing distance occurs in the ground roll portion where differences in weight, drag, and lift affect the braking characteristics.

5.3 SELECTED CONFIGURATION LIFT AND DRAG CHARACTERISTICS

5.3.1 Cruise Polars

Cruise drag polars for the selected configurations are shown in Figure 5.3-1. These cruise lift and drag characteristics are based on the wind tunnel results obtained on the Langley High Performance Configuration. These estimates were made in accordance with the guidelines suggested by Dr. R. T. Whitcomb for Phase II of the subject study.

5.3.2 Low Speed Lift and Drag Characteristics

The low-speed lift and drag characteristics for the selected configurations are presented in Figure 5.3-2 and 5.3-3 for flap deflections from 20 to 50 degrees. These predictions were made with a General Dynamics procedure that was found to give good agreement with the three-dimensional wind tunnel test results for the F-8 supercritical configuration. The increase in C_{LMAX} for the .90M design results from the increased thickness ratio and reduced sweep associated with the reduction in design Mach number.

5.4 PERFORMANCE TRADES

Trade data showing sensitivity of the airplane size to various design parameters such as L/D, dry weight, design cruise altitude, FAR field lengths, and reserve fuel requirements are given in this section.

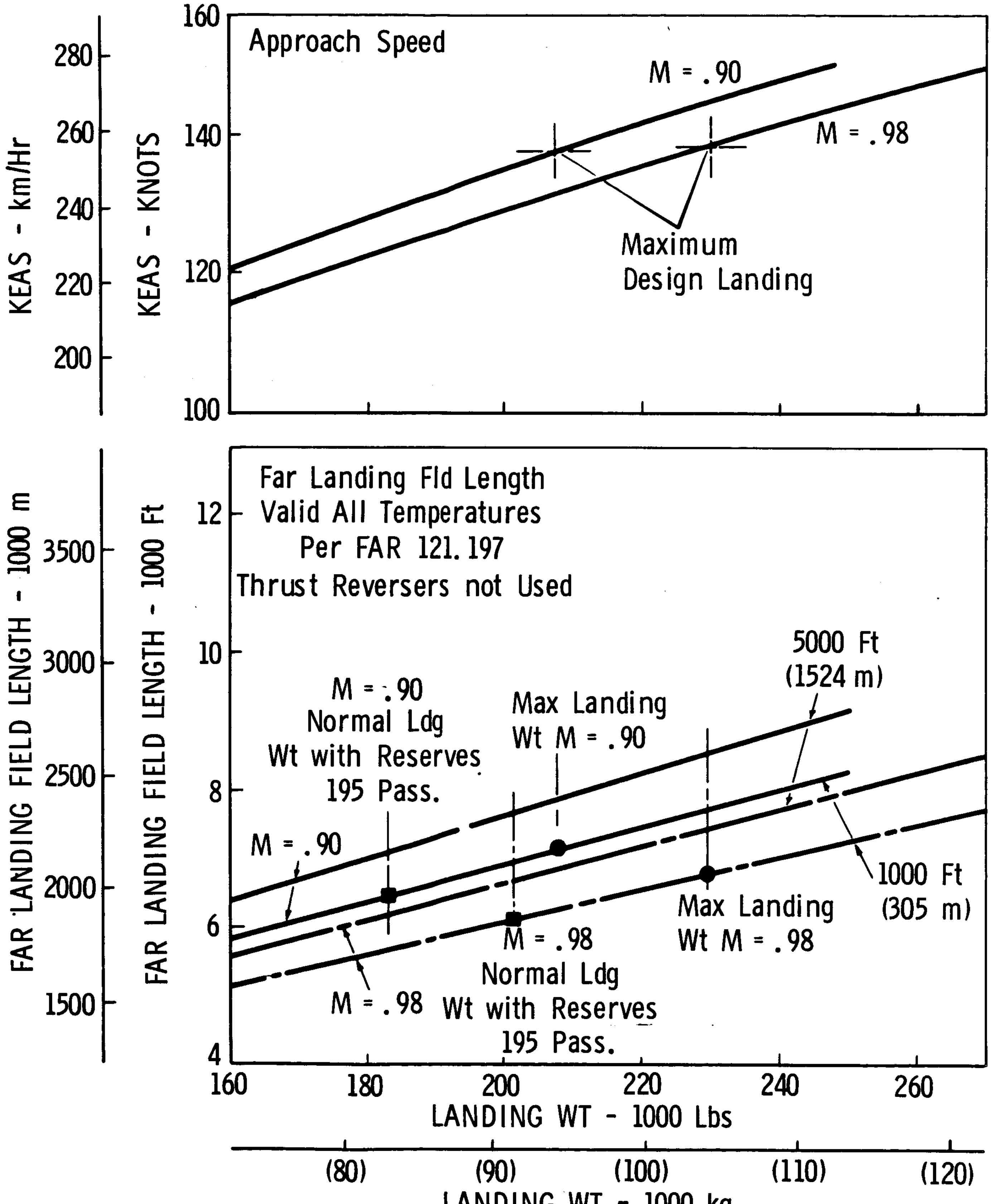

Figure 5.2-8 Far Landing Field Lengths

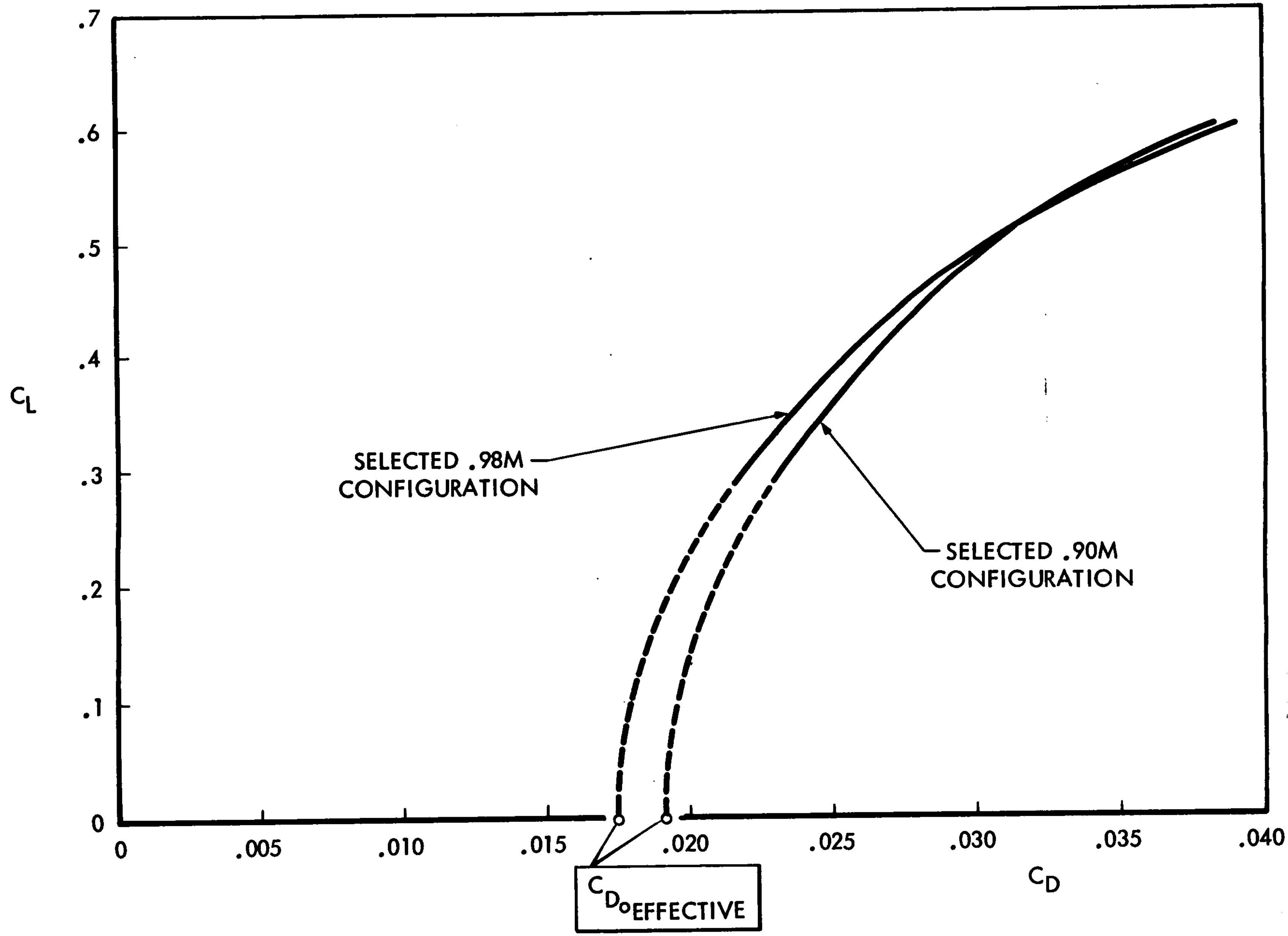

(c) Figure 5.3-1 Selected Configuration Design Mach Number Drag Polars (u)

[redacted]

• $AR = 8.0$ • $\Lambda_{LE} = 44.33°$ • $\delta_{SLAT} = 50°$ • GEAR UP

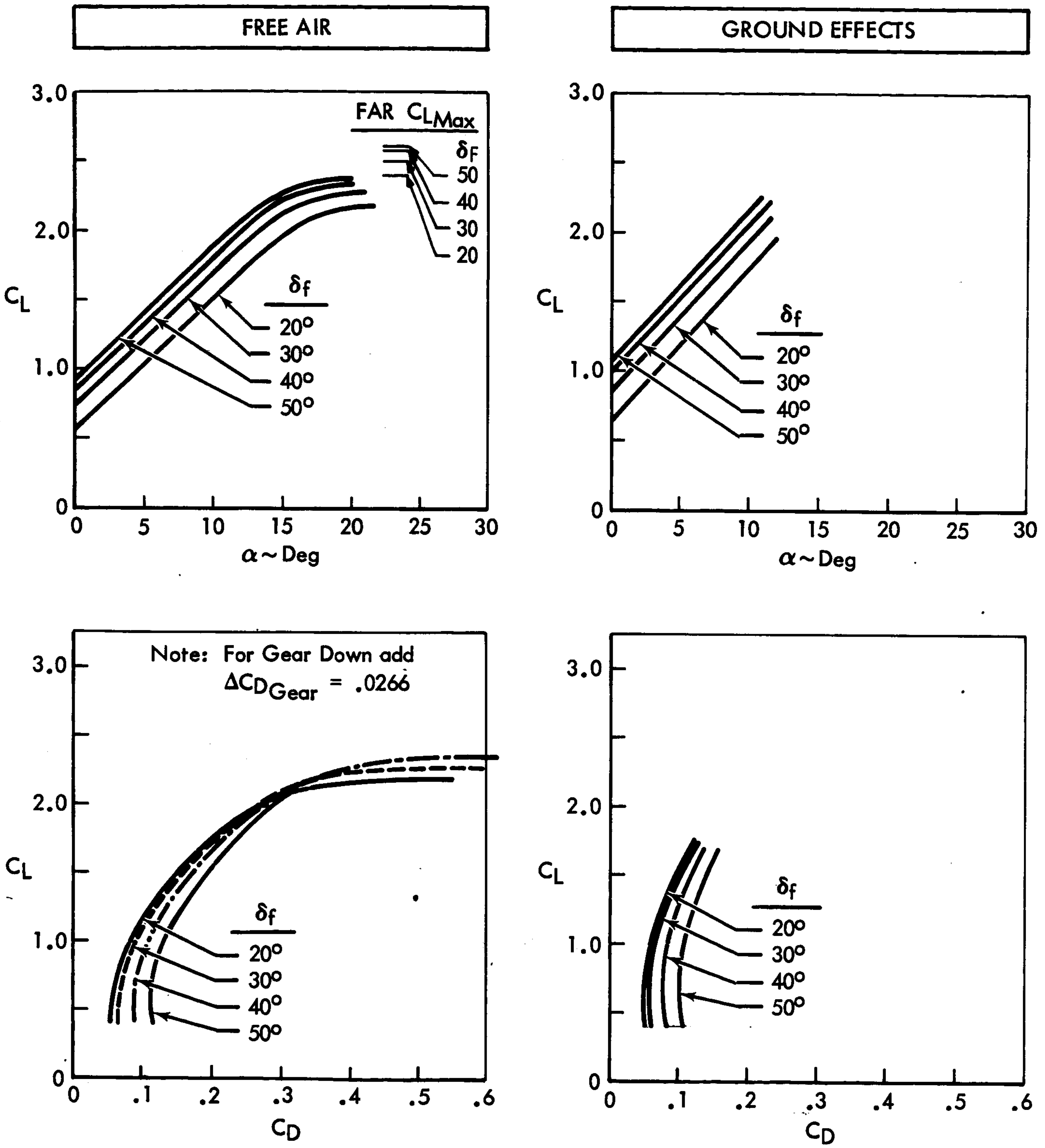

(c) Figure 5.3-2 Low Speed Lift & Drag Characteristics;
M = .98 Configuration (u)

[redacted]

[redacted]

• $AR = 9.0$ • $\Lambda_{LE} = 39.6°$ • $\delta_{SLAT} = 50°$ • GEAR UP

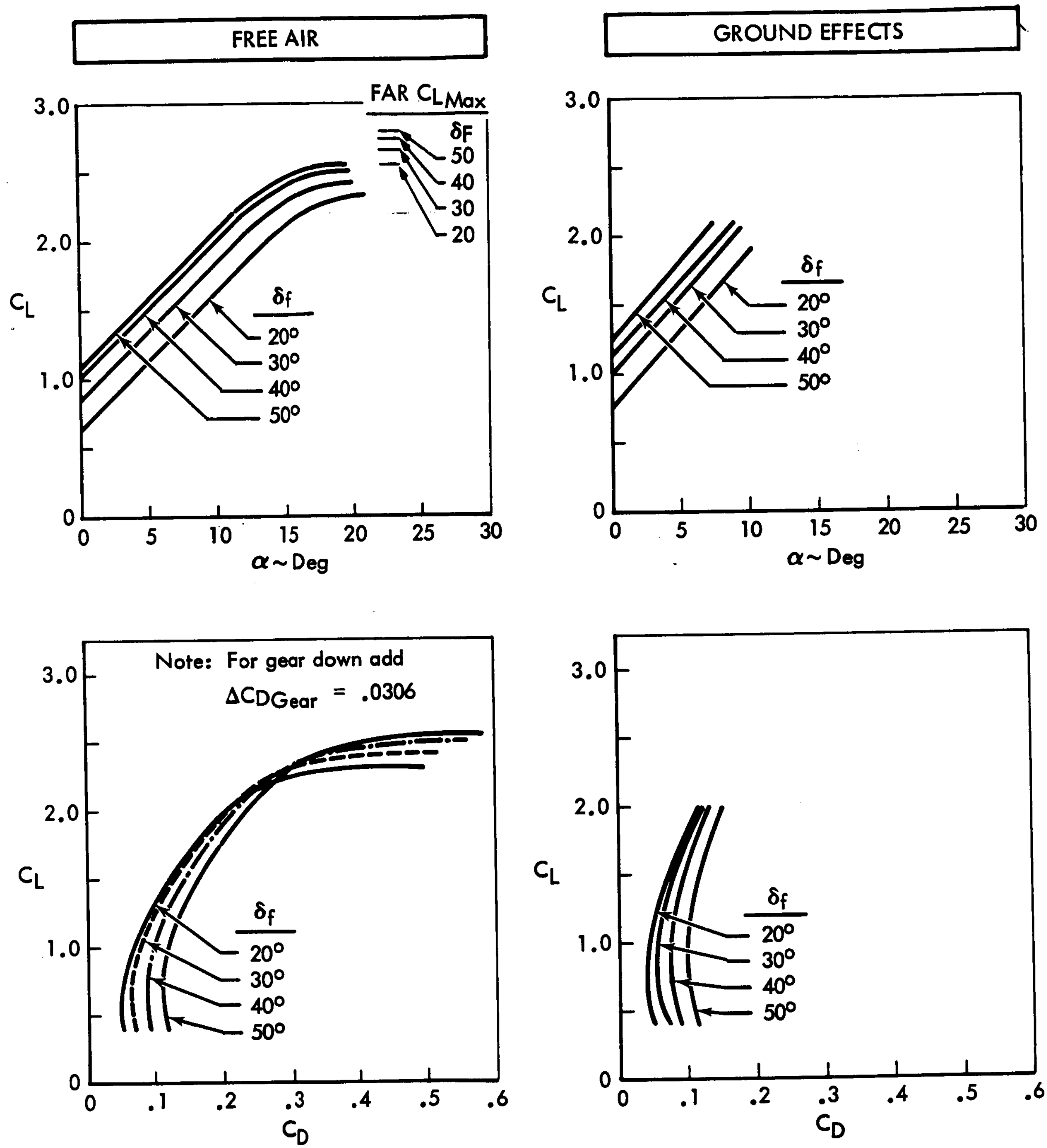

(c) Figure 5.3-3 Low Speed Lift & Drag Characteristics; M = .90 Configuration (u)

[redacted]

5.4.1 Effect of L/D and Dry Weight

The impact of L/D and dry-weight variations on airplane size are shown in Figure 5.4-1 for both airplane designs. These data were used in the analysis of Section 6, where the economic impact is shown. In each case the airplanes were resized to maintain the design payload/range.

5.4.2 Design Cruise Altitude Effect

The effect of designing the airplanes for higher initial cruise altitudes is shown in Figure 5.4-2. In order to achieve these higher cruise altitudes, oversized engines were utilized since early parametric studies showed that a wing loading of about 120 psf (5744 N/m^2) was optimum for altitudes in the range of these studies. The Return on Investment penalty for an initial cruise altitude of 40,000 ft (12,192 m) is a 7.4 percent reduction in ROI for the .90M design and 4.4 percent for the .98M design.

5.4.3 FAR Field-Length Trades

Increased engine sizes were also utilized to reduce field lengths. The effects of increased T/W on takeoff field length are shown in Figure 5.4-3 along with the airplane size required for the design payload/range capability. The corresponding penalty on Return on Investment as a function of the increased thrust levels is also shown in Figure 5.4-3.

The increased engine sizes have a beneficial effect on the takeoff noise level measured at the three-and-one-half-mile point. This noise level is decreased primarily due to the shorter takeoff distance and the higher climb-path capability. The noise levels, climb paths, and cutback thrust levels associated with these increased engine sizes are shown in Figure 5.4-4. A more complete noise level discussion is given in Section 10.

5.4.4 Reserve Fuel Trades

For the time period in which the advanced transport will be placed in commercial service, it is feasible to predict that improved ground control systems, better automatic landing systems, and an increased number of airports may reduce the reserve requirements from those currently in use. The maximum reduction could be as much as 25 percent.

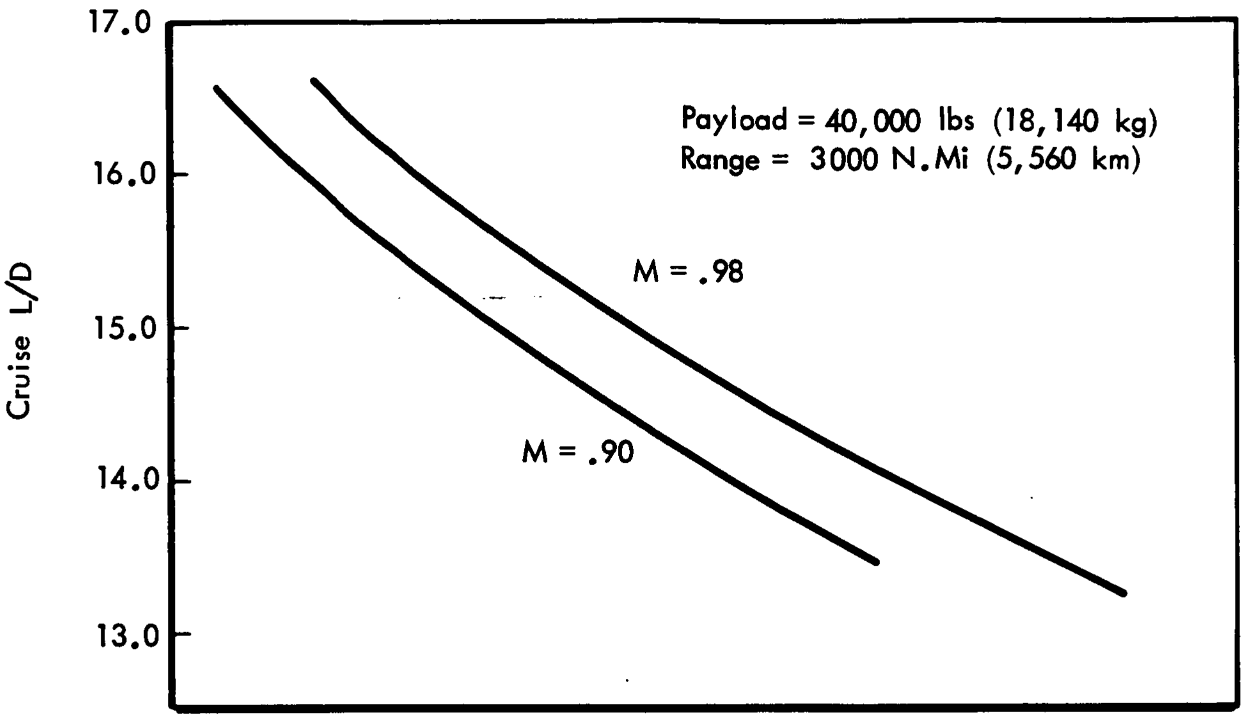

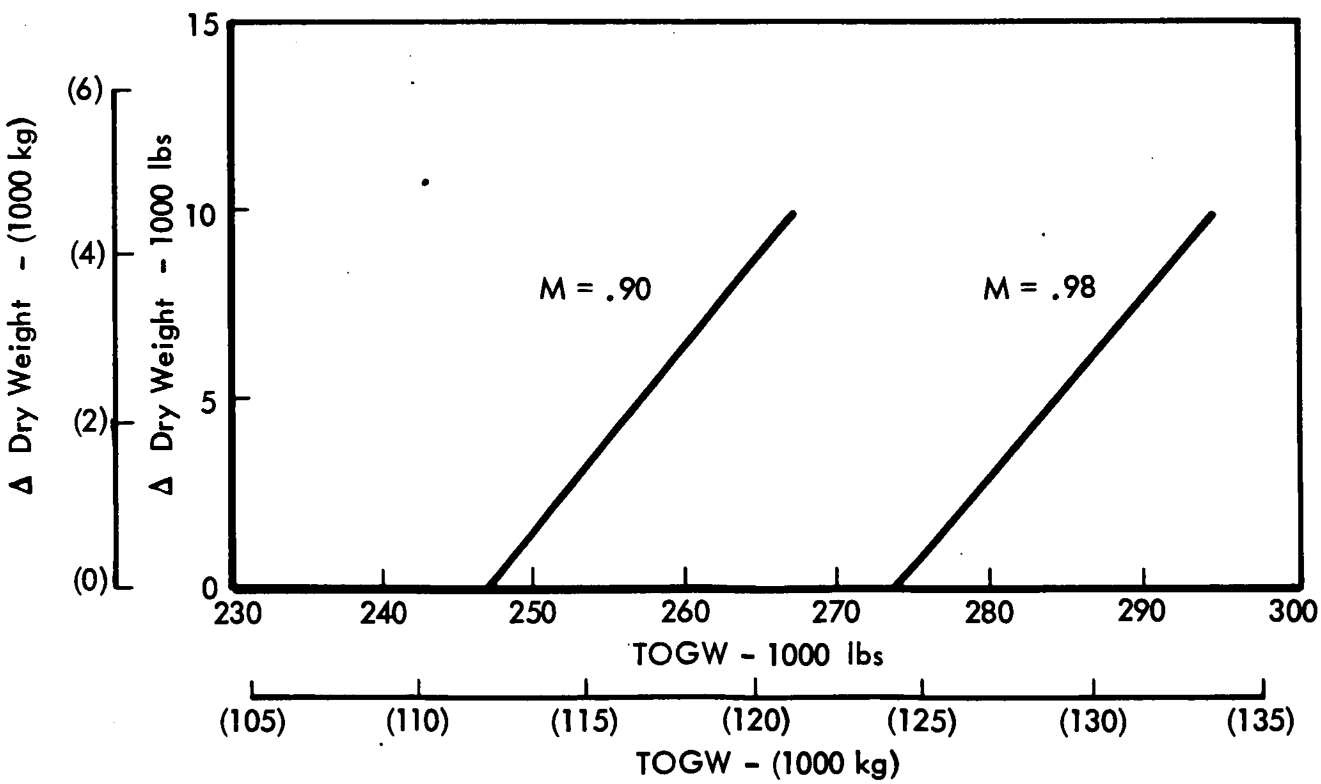

Figure 5.4-1 Effect of L/D & Dry Weight On Airplane Size

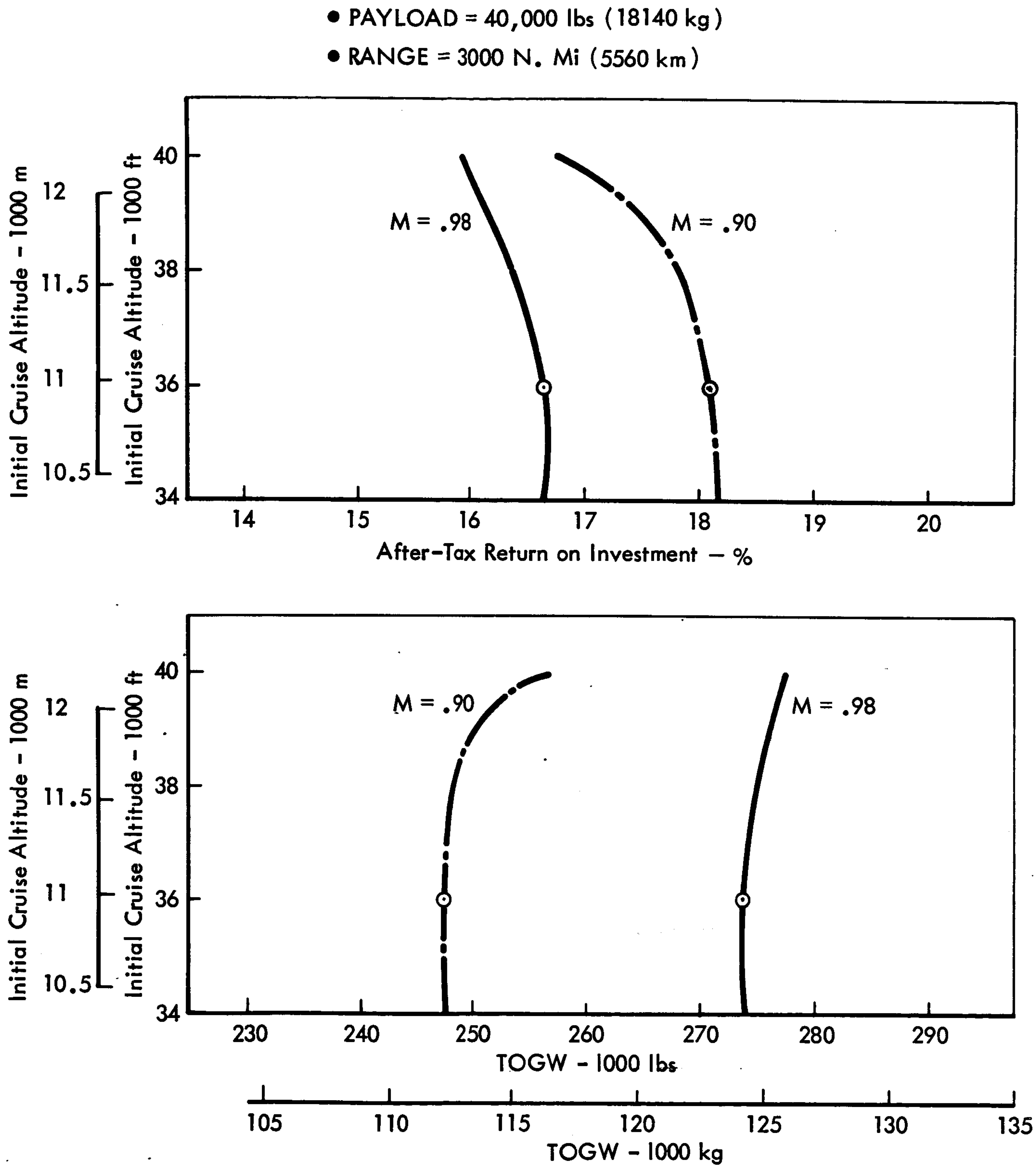

Figure 5.4-2 Effect of Design Cruise Altitude

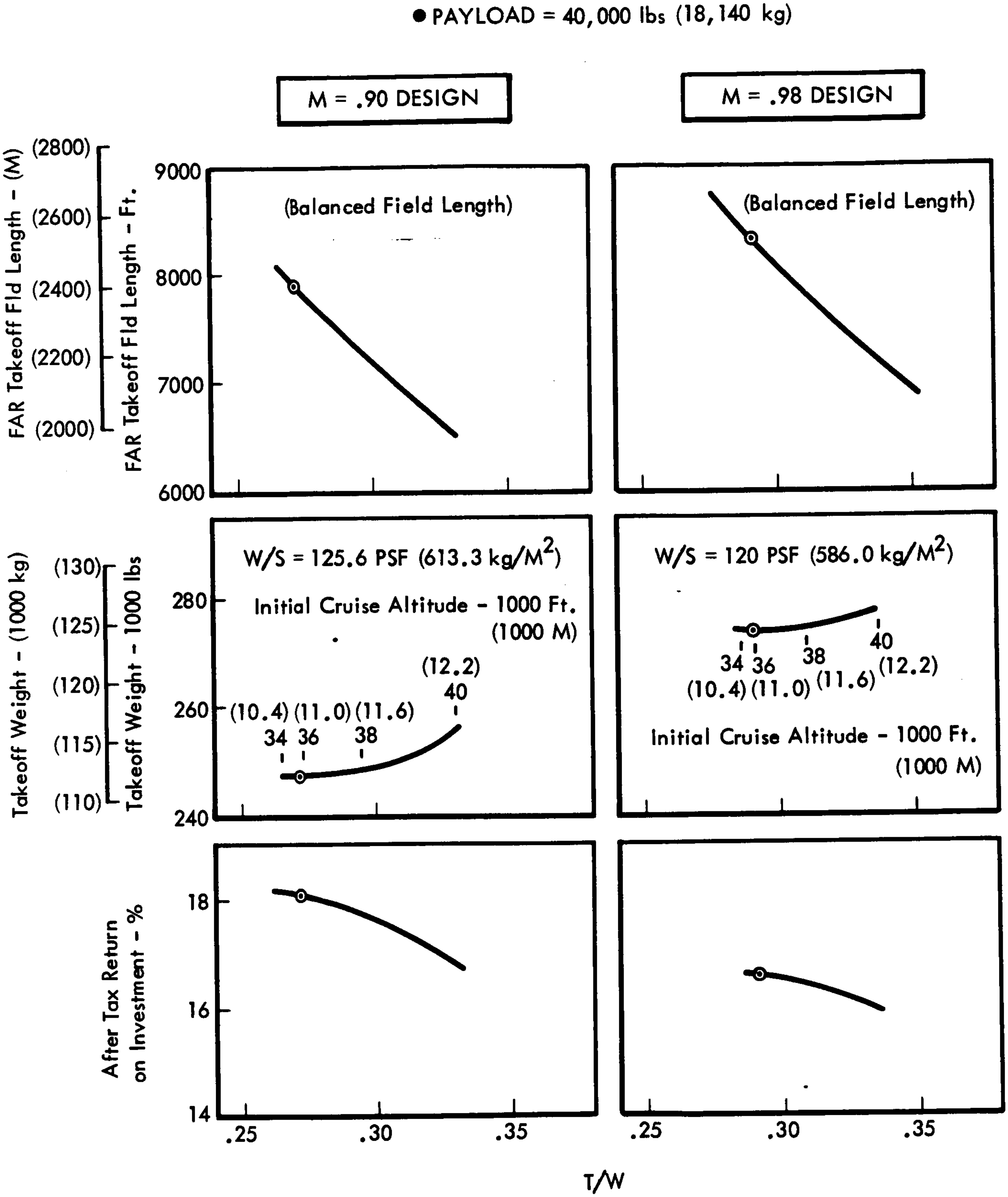

Figure 5.4-3 Effects of Larger Engines

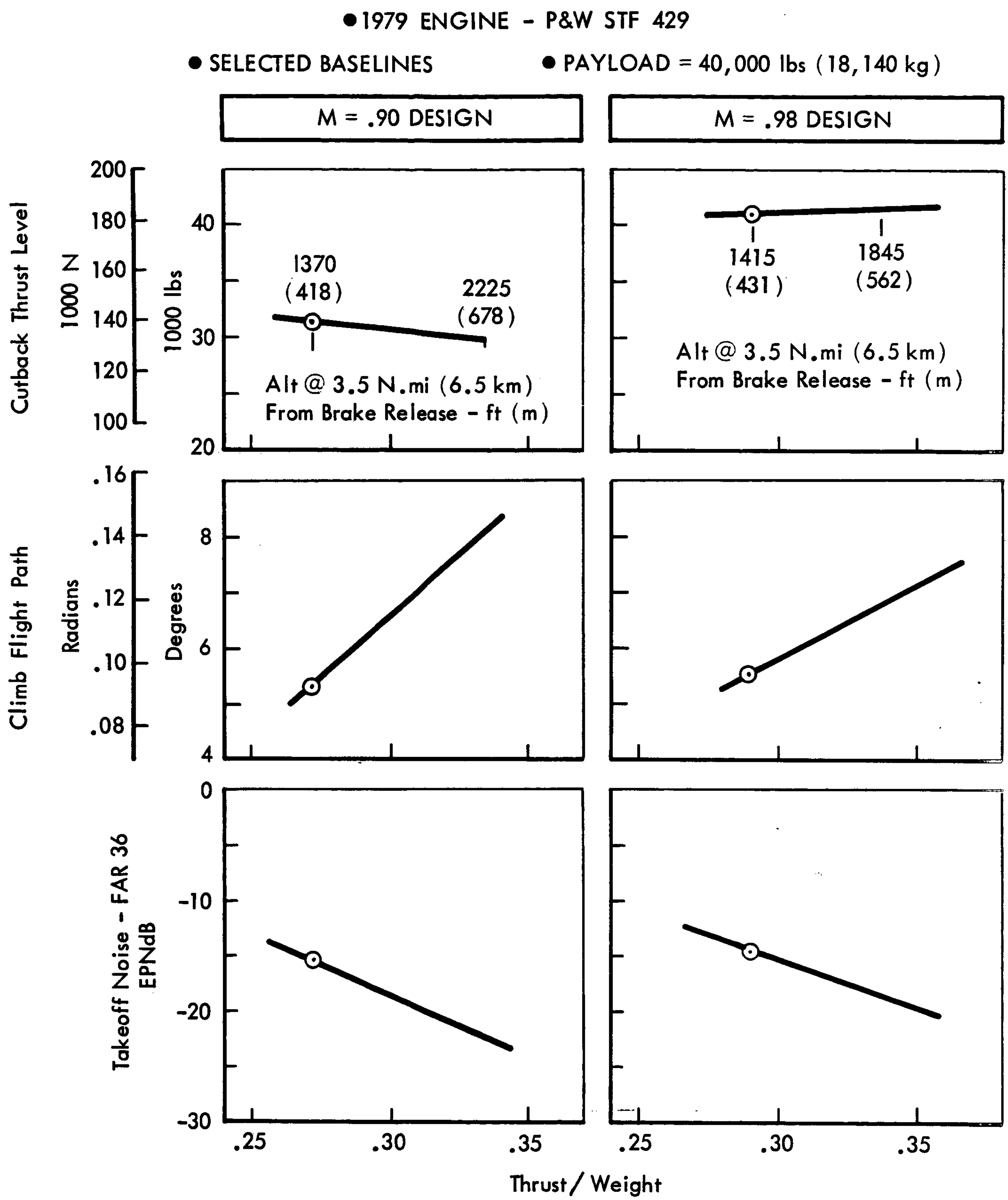

Figure 5.4-4 Effect of Increased Thrust Level on Noise

Such a reduction of the requirements used in this study (fuel for one hour at end cruise weight and fuel flow, plus fuel for missed approach, climbout, and cruise to an alternate airport 200 n.mi (370 km) away) would be reserves for 45 minutes plus missed approach, climb, and cruise a distance of 150 n.mi (278 km). This effect on airplane size, fuel, and cost is shown in Table 5.4-1.

5.5 CONFIGURATION SELECTION

The rationale and data used in the selection of optimum wing geometry, wing loading, and cruise altitude for each design speed is given in this section. In addition, the data generated for use in selection of advanced technology application and for final selected configuration sizing are shown.

Wing geometry was optimized using scalable GE CF 6 engines with a FAR 36 noise-level capability. This was done because the advanced technology engine data would not be available until late in the study period. The advanced technology engines (P&W STF 429 and P&W STF 433) were used in the final sizing and advanced technology application studies.

5.5.1 Selection Rationale

The rationale and steps used for optimization and selection of the final ATT configurations are shown in Figure 5.5-1. The requirements from the revised statement of work are shown along with the variables considered for optimization in the study. Each selection was made on the basis of maximum return on investment for both aluminum and composite wings. The selection process used is summarized in the steps in the lower portion of Figure 5.5-1.

5.5.2 Wing Geometry Selection

Optimum wing geometry was selected for both aluminum and composite wing airplanes. A preliminary wing loading (W/S) was selected to be used in parametric studies. A range of aspect ratios for each cruise speed and a wing sweep/thickness variation for the M=.90 design were selected for optimization procedures. From these data, airplanes were sized and optimum wing geometry and cruise altitudes were selected based on maximum return on investment. This optimum geometry was then utilized to assess the impact of the advanced technologies and select the promising technology payoffs.

Table 5.4-1 RESERVE EFFECTS ON ECONOMICS

	M=.90 DESIGN		M=.98 DESIGN	
RESERVES FOR:	1 HR CRUISE + 200 N.MI (370 km)	45 MIN CRUISE + 150 N.MI (278 km)	1 HR CRUISE + 200 N.MI (370 km)	45 MIN CRUISE + 150 N.MI (278 km)
TOGW, lb (kg)	247,432 (112,214)	241,152 (109,387)	273,840 (124,214)	266,400 (120,839)
ENGINE SIZE	.560	.552	.662	.652
T/W	.272	.275	.290	.294
DIRECT OPERATING COST, \$/A/C n.mi (\$/A/C km)	2.328 (1.256)	2.276 (1.228)	2.402 (1.296)	2.352 (1.269)
AIRPLANE COST, \$ X 10^6	11.88	11.424	13.08	12.544
AFTER TAX RETURN ON INVESTMENT	18.06	19.10	16.64	17.62

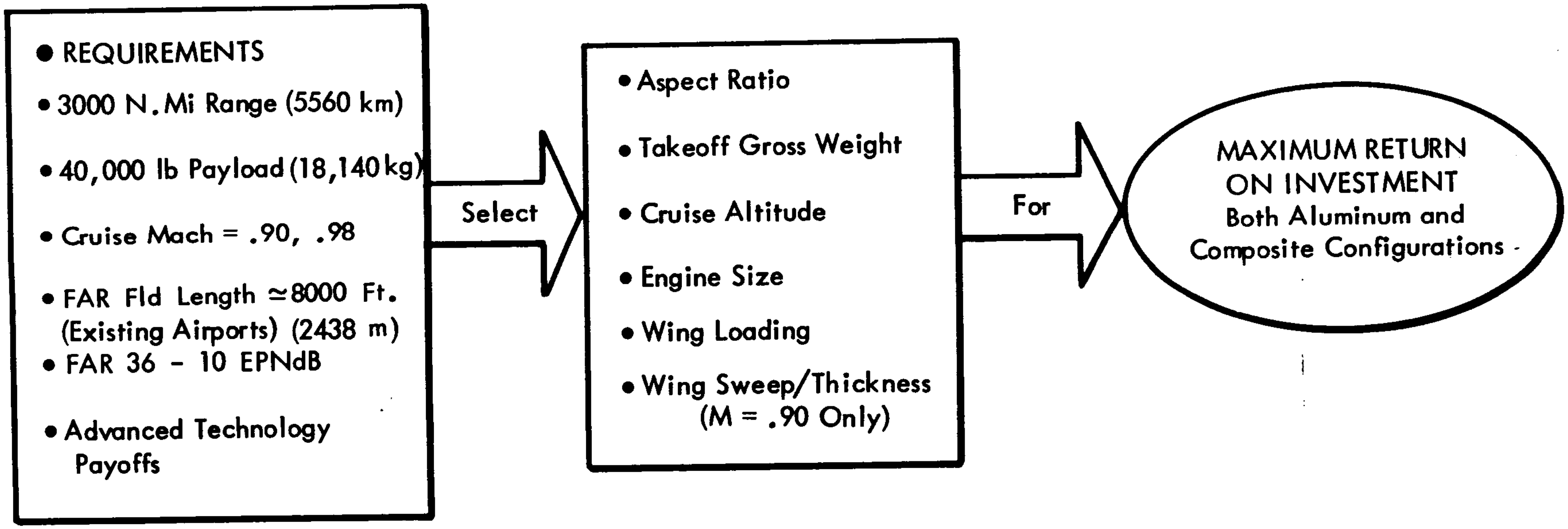

- SELECT OPTIMUM WING GEOMETRY
  (Æ) (Λ/t/c M = .90 Only) (W/S)
- ADVANCED TECHNOLOGY EVALUATION
- FINAL SELECTED CONFIGURATION SIZING

Figure 5.5-1 Selection Rationale

5.5.2.1 Range of Parametric Variations

A preliminary analysis was made using the NASA 0.98M High-Performance Configuration to select a wing loading to be used in the parametric studies. The selection of 120 psf (5744 N/m^2) was made on the basis of minimum airplane gross weight. This study is illustrated in Figure 5.5-2. A check of wing loading effects on ROI was also made after selection of optimum wing geometry.

The wing sweep/thickness distribution of the NASA High-Performance Configuration was used for the .98M design. This wing has a 40^o mid-chord sweep and a thickness ratio of 11 percent perpendicular to the reference sweep line at the mean aerodynamic chord.

Three sweep/thickness ratio combinations were selected for optimization on the .90M design. Each combination gives the design cruise Mach number of .90. These values were selected from the variation shown in Figure 5.5-3. This curve was obtained using infinite-span sweep theory adjusted to give a variation which satisfies both two-dimensional test results and the three-dimensional test results for the Langley High-Performance Configuration.

Aspect ratios from 6.4 to 9.0 were chosen as a range broad enough to optimize ROI.

5.5.2.2 Geometry Selection

Geometry selection was accomplished in two steps. Airplanes were sized for the required range at three cruise altitudes for each combination of wing geometry. With these airplanes, a cost analysis was then made to determine maximum return on investment as a function of wing geometry and cruise altitude.

The rules for range computation used for this study are those specified in the Air Transport Association of America Engineering and Maintenance Memorandum 67-81 dated October 26, 1967 and revised by memorandum 68-4 dated January 18, 1968. These rules are as follows:

Warm up and taxi allowance	Fuel for 14 min @ idle power
Takeoff allowance	1 min @ T.O. power
Climb with max climb power	As required

● NASA HIGH PERFORMANCE CONFIGURATION

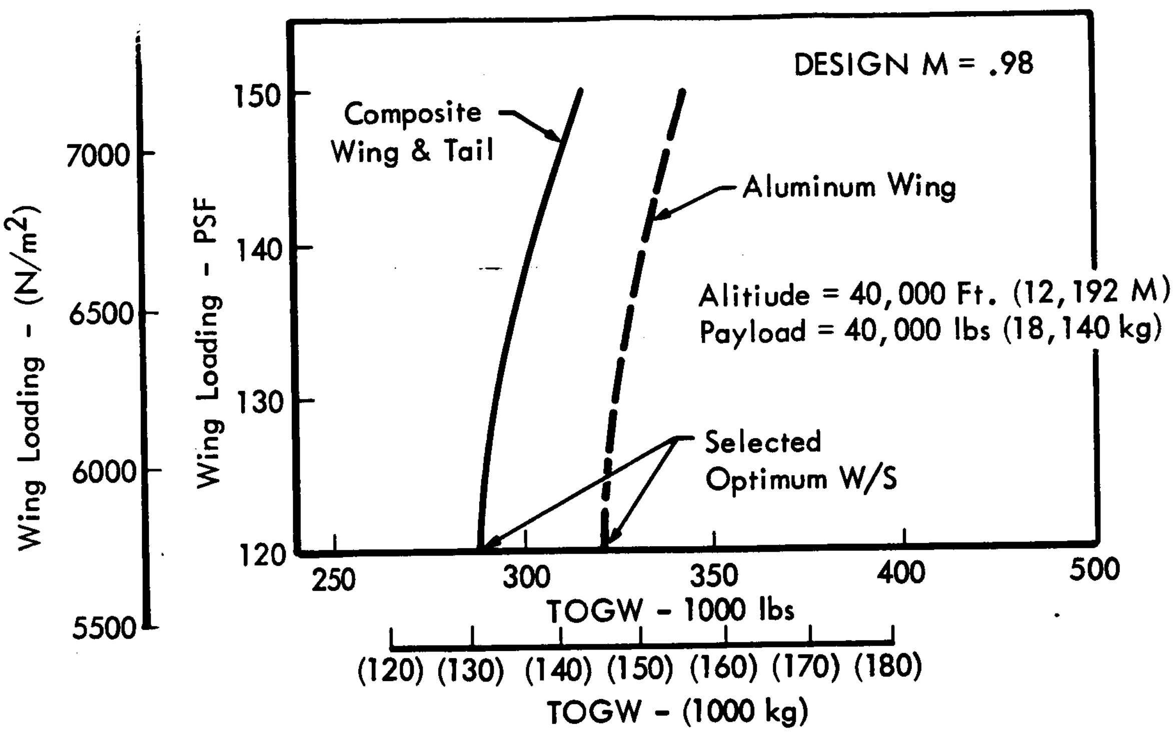

Figure 5.5-2 Effects of Wing Loading

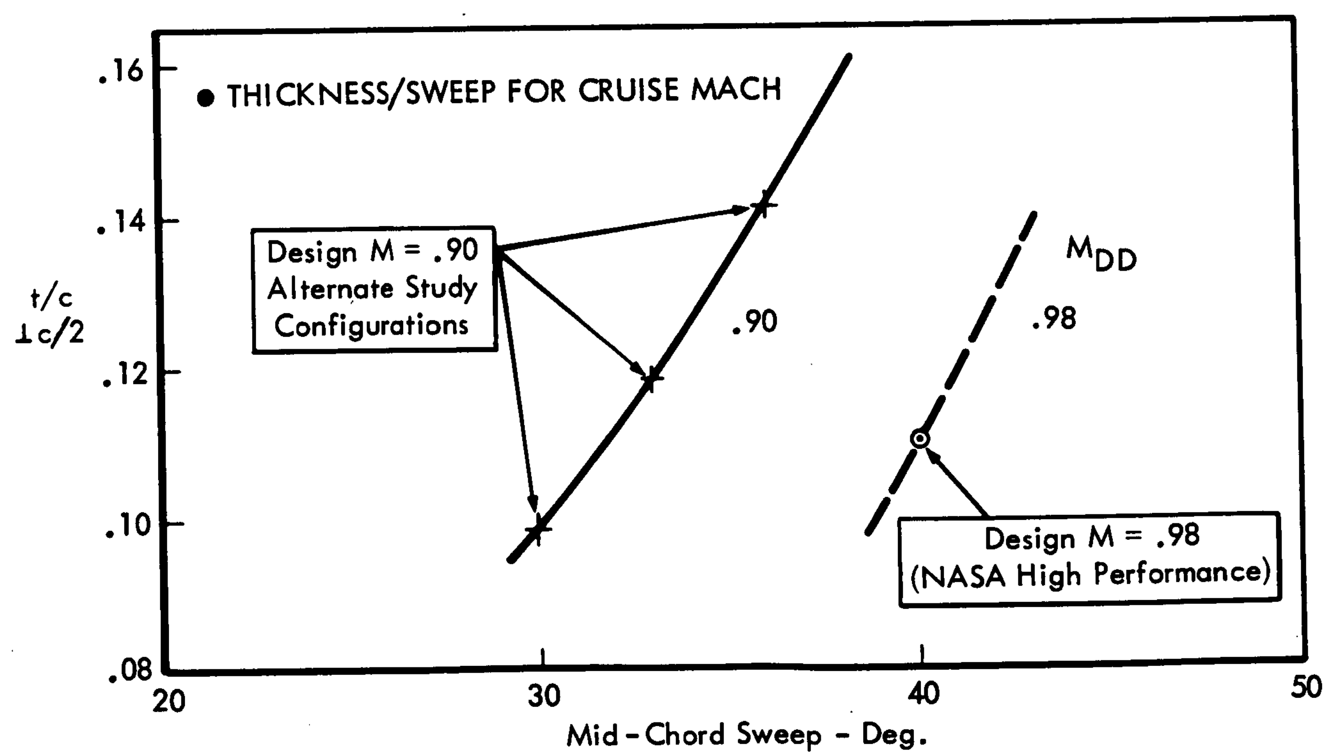

(c) Figure 5.5-3 Variation of Wing Sweep/Thickness For Cruise (u)

Step climb cruise (normal cruise power)	As required
Maneuver allowance	6 min @ cruise power
Descent	As required
Reserves	(a) Fuel for 1 hr at end of cruise wt and fuel flow (b) plus fuel for a missed approach, climb, and cruise to alternate airport.

M=.98 Aspect Ratio Selection

Airplane sizing effects are shown in Figure 5.5-4 for the .98M airplanes. Tables 5.5-1 through 5.5-3 present the pertinent data required for cost analysis. The results of the cost analysis are presented in Figure 5.5-5, showing the variation of return on investment with aspect ratio and cruise altitude. As may be noted, the optimum aspect ratio is slightly higher than the selected values. The slightly lower values of aspect ratio were selected since no appreciable change in ROI was indicated, and the structural and flutter problems associated with higher aspect ratios would be minimized. No constraint is placed on airplanes at this time for FAR field-length requirements since the bypass ratio of the new engines would change, hence affecting the thrust lapse rate and the field-length capabilities. This constraint was to be analyzed in the final airplane selection.

M=.90 Geometry Selection

The M=.90 optimum geometry selection included wing sweep/thickness in addition to aspect ratio selection. The first selection was for sweep/thickness. Airplanes with the nominal aspect ratio of 7.8 were sized for a variation of sweep/thickness giving a drag divergence Mach number of .90. The variations of airplane size and ROI are given in Figure 5.5-6 and the associated cost data in Tables 5.5-4 through 5.5-6. As may be seen in Figure 5.5-6, the return on investment increased with increasing sweep up to the maximum allowable thickness of the wing at the root chord. This thickness is set by the space between the floor of the passenger compartment and the lower fuselage contour. This results in a maximum thickness/sweep combination of .1415 t/c at a mid-chord sweep of 36° as about the maximum for the wing areas under consideration.

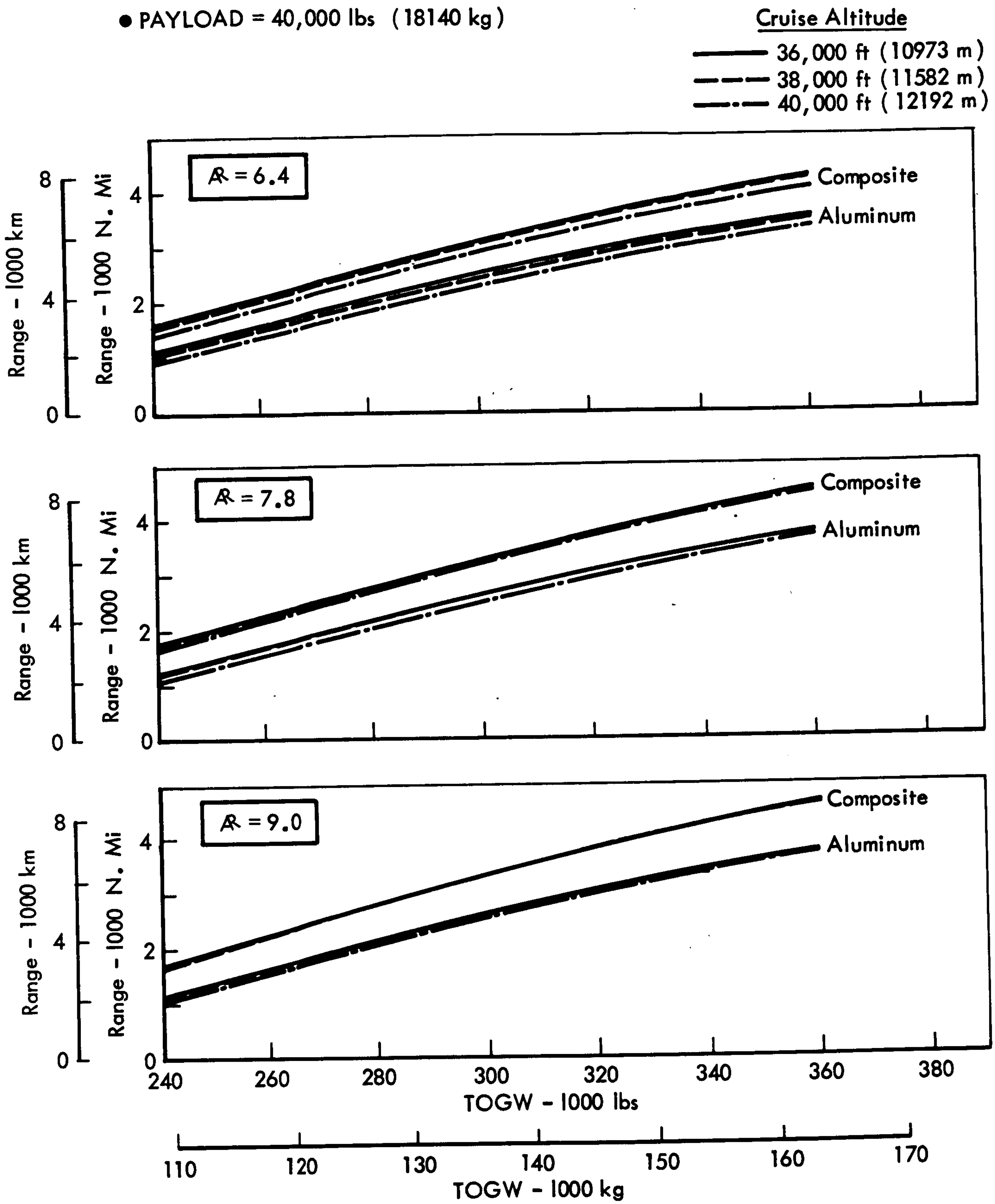

Figure 5.5-4 M = .98 Airplane Sizing

Table 5.5-1 COST ANALYSIS DATA FOR ASPECT RATIO SELECTION: M=.98, AR=6.4

- PAYLOAD = 40,000 lb (18,140 kg)
- RANGE = 3,000 n.mi (5,560 km)
- $\Lambda \frac{c}{2}$ = 40°
- t/c = .11

	COMPOSITE			ALUMINUM		
CRUISE ALT, ft (m)	36,000 (10,973)	38,000 (11,582)	40,000 (12,192)	36,000 (10,973)	38,000 (11,582)	40,000 (12,192)
SREF, ft^2 (m^2)	2,460 (228.5)	2,480 (230.4)	2,530 (235.0)	2,700 (250.8)	2,735 (254.1)	2,802 (260.3)
TOGW, lb (kg)	295,200 (133,903)	297,600 (134,991)	303,600 (137,713)	324,000 (146,966)	328,200 (148,872)	336,240 (152,518)
BOW, lb (kg)	159,400 (72,304)	162,500 (73,710)	168,400 (76,386)	181,450 (82,306)	185,800 (84,279)	193,150 (87,613)
USEFUL LOAD, lb (kg)	7,364 (3,340)	7,364 (3,340)	7,364 (3,340)	7,364 (3,340)	7,364 (3,340)	7,364 (3,340)
FUEL, lb (kg) TOTAL	95,800 (43,455)	95,100 (43,137)	95,200 (43,183)	102,550 (46,517)	102,440 (46,467)	103,090 (46,762)
TAXI & T.O. FUEL	1,360 (616.9)	1,460 (662.3)	1,640 (743.9)	1,450 (657.7)	1,565 (709.9)	1,770 (802.9)
CLIMB	9,820 (4,454)	9,800 (4,445)	9,550 (4,332)	10,750 (4,876)	10,740 (4,872)	10,490 (4,758)
CRUISE	65,400 (29,665)	64,610 (29,307)	64,540 (29,275)	69,510 (31,530)	69,165 (31,373)	69,520 (31,534)
DESCENT	720 (327)	770 (349)	860 (390)	780 (354)	850 (386)	980 (445)
RESERVES	18,500 (8,392)	18,460 (8,373)	18,610 (8,441)	20,060 (9,099)	20,080 (9,108)	20,330 (9,222)
BLOCK	77,300 (35,063)	76,640 (34,764)	76,590 (34,741)	82,490 (37,417)	82,320 (37,340)	82,760 (37,540)
ENGINE SCALE	.689	.738	.830	.736	.793	.897
T/W	.357	.3794	.4183	.3476	.3697	.4082
DISTANCE n.mi (km) CLIMB	196 (363)	192 (356)	174 (322)	200 (370)	196 (363)	177 (328)
DESCENT	106 (196)	110 (204)	114 (211)	109 (202)	114 (211)	119 (220)
TIME CLIMB, min	24	24	21	25	24	22
DESCENT, min	16	16	17	16	17	17
BLOCK, hr	5.95	5.95	5.95	5.96	5.96	5.95

Table 5.5-2 COST ANALYSIS DATA FOR ASPECT RATIO SELECTION: MACH .98, AR 7.8

●PAYLOAD = 40,000 lb (18,140 kg) ●RANGE = 3,000 n.mi (5,560 km) ● $\Lambda_{\frac{C}{2}}$ = 40° ●t/c = .11

	COMPOSITE			ALUMINUM		
CRUISE ALT, ft (m)	36,000 (10,973)	38,000 (11,582)	40,000 (12,192)	36,000 (10,973)	38,000 (11,582)	40,000 (12,192)
SREF, ft^2 (m^2)	2,403 (223.2)	2,408 (223.7)	2,431 (225.8)	2,642 (245.4)	2,652 (246.4)	2,692 (250.1)
TOGW, lb (kg)	288,360 (130,800)	288,960 (131,072)	291,720 (132,324)	317,040 (143,809)	318,240 (144,354)	323,040 (146,531)
BOW, lb (kg)	157.750 (71,555)	159,800 (72,485)	164,150 (74,458)	180,250 (81,761)	182,900 (82,963)	188,500 (85,504)
USEFUL LOAD, lb (kg)	7,364 (3,340)	7,364 (3,340)	7,364 (3,340)	7,364 (3,340)	7,364 (3,340)	7,364 (3,340)
FUEL, lb (kg) TOTAL	90,610 (41,101)	89,160 (40,443)	87,570 (39,722)	96,790 (43,904)	95,340 (43,246)	94,540 (42,883)
TAXI & T.O. FUEL	1,260 (571.5)	1,335 (605.6)	1,475 (669.1)	1,350 (612.4)	1,435 (650.9)	1,590 (721.2)
CLIMB	9,970 (4,522)	9,910 (4,495)	9,550 (4,332)	10,900 (4,944)	10,850 (4,922)	10,500 (4,763)
CRUISE	61,140 (27,733)	59,825 (27,137)	58,475 (26,524)	64,750 (29,371)	63,395 (28,756)	62,730 (28,454)
DESCENT	690 (313)	740 (336)	820 (372)	760 (345)	820 (372)	920 (417)
RESERVES	17,550 (7,961)	17,350 (7,870)	17,250 (7,825)	19,030 (8,632)	18,840 (8,546)	18,800 (8,528)
BLOCK	73,060 (33,140)	71,810 (32,573)	70,320 (31,897)	77,760 (35,272)	76,500 (34,700)	75,740 (34,356)
ENGINE SCALE	.640	.677	.748	.684	.727	.806
T/W	.3396	.3585	.3923	.3301	.3495	.3817
DISTANCE n.mi (km) CLIMB	215 (398)	214 (396)	195 (361)	220 (407)	218 (404)	198 (367)
DESCENT	109 (202)	113 (209)	119 (220)	113 (209)	118 (219)	123 (228)
TIME CLIMB, min	26	26	24	27	27	24
DESCENT, min	17	17	18	17	17	18
BLOCK, hr	5.97	5.97	5.97	5.97	5.96	5.95

Table 5.5-3 COST ANALYSIS DATA FOR ASPECT RATIO SELECTION: M=.98, AR=9.0

●PAYLOAD = 40,000 lb (18,140 kg) ●RANGE = 3,000 n.mi (5,560 km) ●$\Lambda_{\frac{c}{2}}$ = 40° ●t/c = .11

	COMPOSITE			ALUMINUM		
CRUISE ALT, ft (m)	36,000 (10,973)	38,000 (11,582)	40,000 (12,192)	36,000 (10,973)	38,000 (11,582)	40,000 (12,192)
SREF, ft^2 (m^2)	2,391 (222.1)	2,387 (221.8)	2,398 (222.8)	2,640 (245.3)	2,640 (245.3)	2,662 (247.3)
TOGW, lb (kg)	286,920 (130,147)	286,440 (129,929)	287,760 (130,530)	316,800 (143,700)	316,800 (143,700)	319,440 (144,898)
BOW, lb (kg)	158,650 (71,964)	160,100 (72,621)	163,500 (74,164)	182,400 (82,737)	184,150 (83,530)	188,600 (85,549)
USEFUL LOAD, lb (kg)	7,364 (3,340)	7,364 (3,340)	7,364 (3,340)	7,364 (3,340)	7,364 (3,340)	7,364 (3,340)
FUEL, lb (kg)						
TOTAL	88,270 (40,039)	86,340 (39,164)	84,260 (38,220)	94,400 (42,820)	92,650 (42,026)	90,840 (41,205)
TAXI & T.O. FUEL	1,220 (553.4)	1,280 (580.6)	1,400 (635.0)	1,305 (591.9)	1,370 (621.4)	1,510 (684.9)
CLIMB	10,160 (4,609)	10,190 (4,622)	9,680 (4,391)	11,180 (5,071)	11,180 (5,071)	10,650 (4,831)
CRUISE	59,080 (26,799)	57,320 (26,000)	55,770 (25,297)	62,565 (28,379)	61,030 (27,683)	59,710 (27,084)
DESCENT	700 (318)	720 (327)	820 (372)	750 (340)	770 (349)	870 (395)
RESERVES	17,110 (7,761)	16,830 (7,634)	16,590 (7,525)	18,600 (8,437)	18,300 (8,301)	18,100 (8,210)
BLOCK	71,160 (32,278)	69,510 (31,530)	67,670 (30,695)	75,800 (34,383)	74,350 (33,725)	72,740 (32,995)
ENGINE SCALE	.619	.648	.710	.661	.696	.765
T/W	.330	.346	.378	.319	.336	.336
DISTANCE n.mi (km)						
CLIMB	229 (424)	230 (426)	209 (387)	235 (435)	235 (435)	213 (394)
DESCENT	112 (207)	112 (207)	123 (228)	116 (215)	116 (215)	127 (235)
TIME						
CLIMB, min	28	28	25	29	29	26
DESCENT, min	17	17	18	18	18	19
BLOCK, hr	5.97	5.97	5.96	5.98	5.98	5.97

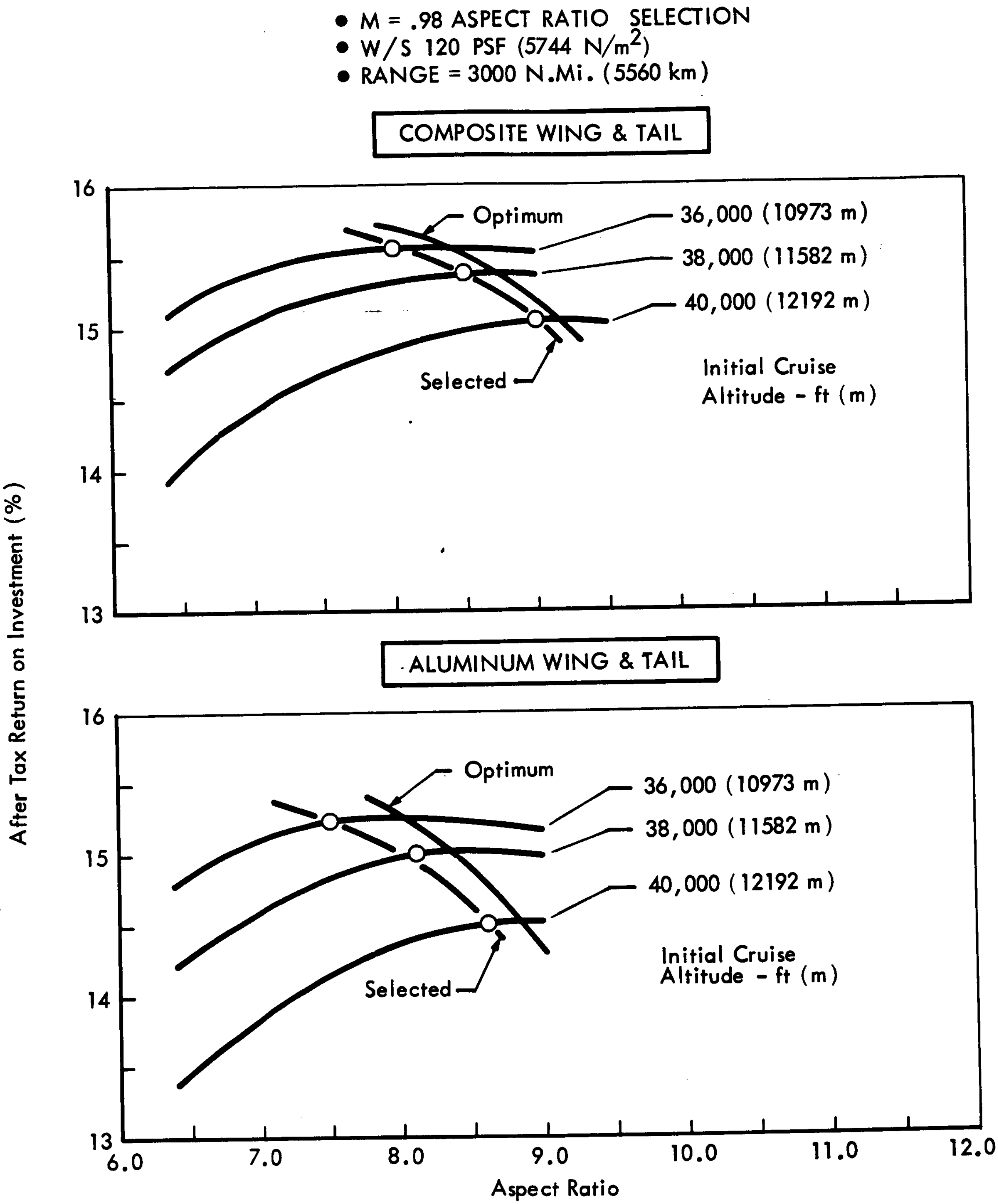

Figure 5.5-5 Effect of Aspect Ratio & Cruise Altitude on ROI (M = .98)

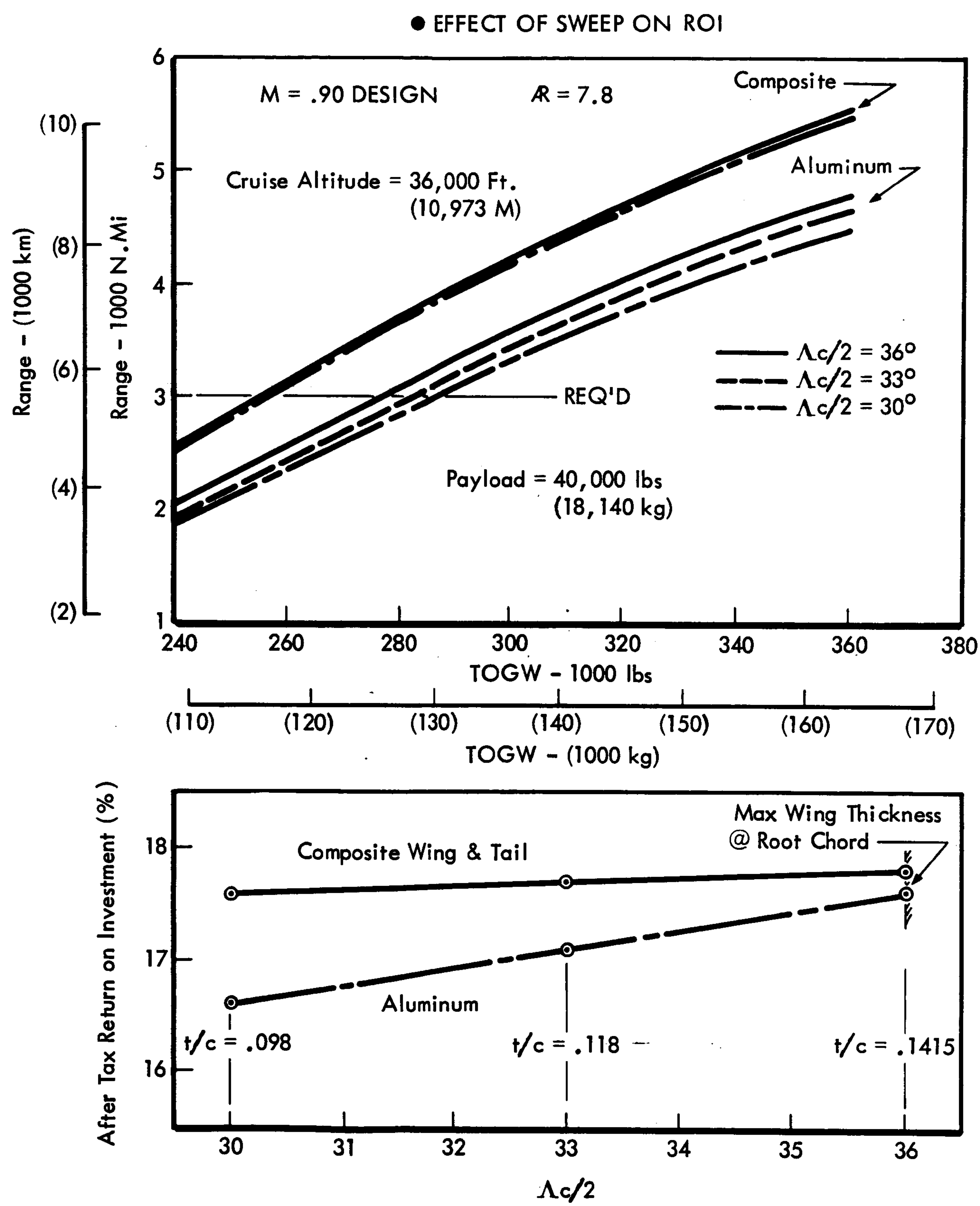

Figure 5.5-6 Effect of Sweep On R.O.I.

Table 5.5-4 COST ANALYSIS DATA FOR SWEEP SELECTION: M=.90, $\Lambda_{\frac{C}{2}}$ = 30°

●PAYLOAD = 40,000 lb (18,140 kg) ●RANGE = 3,000 n.mi (5,560 km) ●AR = 7.8 ●t/c - .098

	COMPOSITE			ALUMINUM		
CRUISE ALT, ft (m)	36,000 (10,973)	38,000 (11,582)	40,000 (12,192)	36,000 (10,973)	38,000 (11,582)	40,000 (12,192)
SREF, ft^2 (m^2)	2,145 (199.3)	2,170 (201.6)	2,233 (207.5)	2,384 (221.5)	2,418 (224.6)	2,503 (232.5)
TOGW, lb (kg)	257,400 (116,757)	260,400 (118,117)	267,960 (121,547)	286,080 (129,766)	290,160 (131,617)	300,360 (136,243)
BOW, lb (kg)	137,500 (62,370)	140,400 (63,685)	146,400 (66,407)	159,700 (72,440)	163,500 (74,164)	171,500 (77,792)
USEFUL LOAD, lb (kg)	7,364 (3,340)	7,364 (3,340)	7,364 (3,340)	7,364 (3,340)	7,364 (3,340)	7,364 (3,340)
FUEL, lb (kg) TOTAL	79,900 (36,243)	80,000 (36,288)	81,560 (36,996)	86,380 (39,182)	86,660 (39,309)	88,860 (40,307)
TAXI & T.O. FUEL	1,105 (501.2)	1,195 (542.1)	1,370 (621.4)	1,195 (542.1)	1,295 (587.4)	1,500 (680.4)
CLIMB	9,230 (4,187)	9,150 (4,150)	8,600 (3,901)	10,170 (4,613)	10,070 (4,568)	9,530 (4,323)
CRUISE	54,005 (24,497)	53,945 (24,469)	55,530 (25,188)	58,065 (26,338)	58,115 (26,361)	60,010 (27,221)
DESCENT	580 (263)	620 (281)	740 (336)	630 (286)	680 (308)	820 (372)
RESERVES	14,980 (6,795)	15,090 (6,845)	15,320 (6,949)	16,320 (7,403)	16,500 (7,484)	17,000 (7,711)
BLOCK	64,920 (29,448)	64,910 (29,443)	66,240 (30,046)	70,060 (31,779)	70,160 (31,825)	71,860 (32,596)
ENGINE SCALE	.560	.607	.696	.605	.657	.760
T/W	.333	.357	.397	.324	.346	.387
DISTANCE n.mi (km) CLIMB	226 (419)	217 (402)	186 (344)	230 (426)	220 (407)	189 (350)
DESCENT	102 (189)	105 (194)	112 (207)	108 (200)	110 (204)	116 (215)
TIME						
CLIMB, min	29	28	24	29	28	24
DESCENT, min	16	16	17	17	17	17
BLOCK, hr	6.42	6.42	6.42	6.42	6.42	6.42

Table 5.5-5 COST ANALYSIS DATA FOR SWEEP SELECTION: M=.90, $\Lambda_{\frac{c}{2}}$ = 33°

●PAYLOAD = 40,000 lb (18,140 lb) ●RANGE = 3,000 n.mi (5,560 km) ●AR = 7.8 ●t/c = .118

	COMPOSITE			ALUMINUM		
CRUISE ALT, ft (m)	36,000 (10,973)	38,000 (11,582)	40,000 (12,192)	36,000 (10,973)	38,000 (11,582)	40,000 (12,192)
SREF, ft^2 (m^2)	2,145 (199.3)	2,168 (201.4)	2,230 (207.2)	2,347 (218.0)	2,377 (220.8)	2,464 (228.9)
TOGW, lb (kg)	257,400 (116,757)	260,160 (118,009)	267,600 (121,383)	281,640 (127,752)	285,240 (129,385)	295,680 (134,120)
BOW, lb (kg)	136,800 (62,052)	139,600 (63,323)	145,600 (66,044)	155,700 (70,626)	159,100 (72,168)	167,200 (75,842)
USEFUL LOAD, lb (kg)	7,364 (3,340)	7,364 (3,340)	7,364 (3,340)	7,364 (3,340)	7,364 (3,340)	7,364 (3,340)
FUEL, lb (kg)						
TOTAL	80,600 (36,560)	80,560 (36,542)	82,000 (37,196)	85,940 (38,982)	86,140 (39,073)	88,480 (40,135)
TAXI & T.O. FUEL	1,110 (503.5)	1,200 (544.3)	1,375 (623.7)	1,180 (535.2)	1,280 (580.6)	1,485 (673.6)
CLIMB	9,470 (4,296)	9,310 (4,223)	8,660 (3,928)	10,270 (4,658)	10,090 (4,577)	9,430 (4,277)
CRUISE	54,430 (24,689)	54,300 (24,630)	55,805 (25,313)	57,700 (26,173)	57,760 (26,200)	59,925 (27,182)
DESCENT	570 (259)	620 (281)	740 (336)	610 (277)	670 (304)	800 (363)
RESERVES	15,020 (6,813)	15,130 (6,863)	15,420 (6,995)	16,180 (7,339)	16,340 (7,412)	16,840 (7,639)
BLOCK	65,580 (29,747)	65,430 (29,679)	66,580 (30,201)	69,760 (31,643)	69,800 (31,661)	71,640 (32,496)
ENGINE SCALE	.562	.608	.698	.599	.650	.754
T/W	.334	.358	.399	.325	.349	.390
DISTANCE n.mi (km)						
CLIMB	231 (428)	221 (409)	187 (346)	236 (437)	223 (413)	189 (350)
DESCENT	100 (185)	104 (193)	111 (206)	106 (196)	109 (202)	114 (211)
TIME						
CLIMB, min	29	28	24	30	28	24
DESCENT, min	16	16	17	17	17	18
BLOCK, hr	6.42	6.41	6.42	6.42	6.42	6.42

Table 5.5-6 COST ANALYSIS DATA FOR SWEEP SELECTION: M=.90, $\Lambda_{\frac{c}{2}} = 36^\circ$

●PAYLOAD = 40,000 lb (18,140 kg) ●RANGE = 3,000 n.mi (5,560 km) ●AR - 7.8 ●t/c = .1415

	COMPOSITE			ALUMINUM		
CRUISE ALT, ft (m)	36,000 (10,973)	38,000 (11,582)	40,000 (12,192)	36,000 (10,973)	38,000 (11,582)	40,000 (12,192)
SREF, ft^2 (m^2)	2,141 (198.9)	2,160 (200.7)	2,225 (206.7)	2,310 (214.6)	2,340 (217.4)	2,425 (225.3)
TOGW, lb (kg)	256,920 (116,539)	259,200 (117,573)	267,000 (121,111)	277,200 (125,738)	280,800 (127,371)	291,000 (131,998)
BOW, lb (kg)	136,100 (61,735)	138,600 (62,869)	144,800 (65,681)	151,800 (68,856)	155,300 (70,444)	163,200 (74,028)
USEFUL LOAD, lb (kg)	7,364 (3,340)	7,364 (3,340)	7,364 (3,340)	7,364 (3,340)	7,364 (3,340)	7,364 (3,340)
FUEL, lb (kg) TOTAL	80,820 (36,660)	80,600 (36,560)	82,520 (37,431)	85,400 (38,737)	85,500 (38,783)	87,800 (39,826)
TAXI & T.O. FUEL	1,110 (503.5)	1,197 (543.0)	1,384 (627.8)	1,170 (530.7)	1,270 (576.1)	1,479 (670.9)
CLIMB	9,470 (4,296)	9,280 (4,209)	8,580 (3,892)	10,150 (4,604)	9,950 (4,513)	9,280 (4,209)
CRUISE	54,620 (24,776)	54,413 (24,682)	56,556 (25,654)	57,460 (26,064)	57,400 (26,037)	59,631 (27,049)
DESCENT	570 (259)	620 (281)	640 (290)	620 (281)	760 (345)	790 (358)
RESERVES	15,050 (6,827)	15,090 (6,845)	15,360 (6,967)	16,000 (7,258)	16,120 (7,312)	16,620 (7,539)
BLOCK	65,770 (29,833)	65,510 (29,715)	67,160 (30,464)	69,400 (31,480)	69,380 (31,471)	71,180 (32,287)
ENGINE SCALE	.563	.607	.702	.594	.644	.750
T/W	.336	.358	.4023	.328	.3509	.3943
DISTANCE n.mi (km) CLIMB	232 (430)	222 (411)	185 (343)	235 (435)	224 (415)	187 (346)
DESCENT	102 (189)	104 (193)	106 (196)	104 (193)	106 (196)	108 (200)
TIME CLIMB, min	30	28	23.5	30	28.2	23.8
DESCENT, min	15	16	16	16	16	16
BLOCK, hr	6.41	6.42	6.42	6.42	6.42	6.42

The sweep of 36° $\Lambda_{c/2}$ was selected and airplanes sized for each aspect ratio. The sizing data for these airplanes are shown in Figure 5.5-7. The cost analysis data for each of these airplanes are given in Tables 5.5-6 through 5.5-8 and the resulting return on investment data in Figure 5.5-8.

5.5.3 Final Airplane Selections

With the optimum geometry selected, the next phase was twofold: to install the advanced technology engines and to select the advanced technologies to be incorporated in the final configuration.

5.5.3.1 Conventional Transport Sizing

For comparison purposes, a conventional aluminum wing transport was sized with the quiet 1979 engines. For simplicity, a scaled DC-10 type airplane was selected. The airplane was sized for a range of 3000 n.mi (5560 km) with a payload of 40,000 pounds (18,140 kg). Cost data is shown in Table 5.5-9.

5.5.3.2 Advanced Technology Application Effects

The impact of advanced technology applications on the design airplane characteristics is shown in Tables 5.5-10 and 5.5-11 for the Mach .98 and the Mach .90 airplanes, all having supercritical wings.

Progressing from left to right, the first airplane is an all aluminum airplane. Following in this order are an aluminum airplane with full active control system (ACS), maximum composite usage, and composite with ACS. Each of these airplanes have the 1979 engine (P&W STF429) and meet the FAR 36 -10 EPNdB noise levels. The next two airplanes are also composite with ACS but are sized with the 1985 engines (P&W STF433) to achieve the FAR 36 -15 EPNdB noise levels. The first of these airplanes achieves the -15 EPNdB noise level. The second one has oversized engines to achieve a maximum community noise abatement through shorter takeoff, steeper climbout, and two-segment-approach technique. The noise levels are discussed in Section 10.

The sizing curves for the technology trade airplanes are shown in Figure 5.5-9. Both selected configurations have full active control systems and maximum utilization of composites. This selection of advanced technology applications

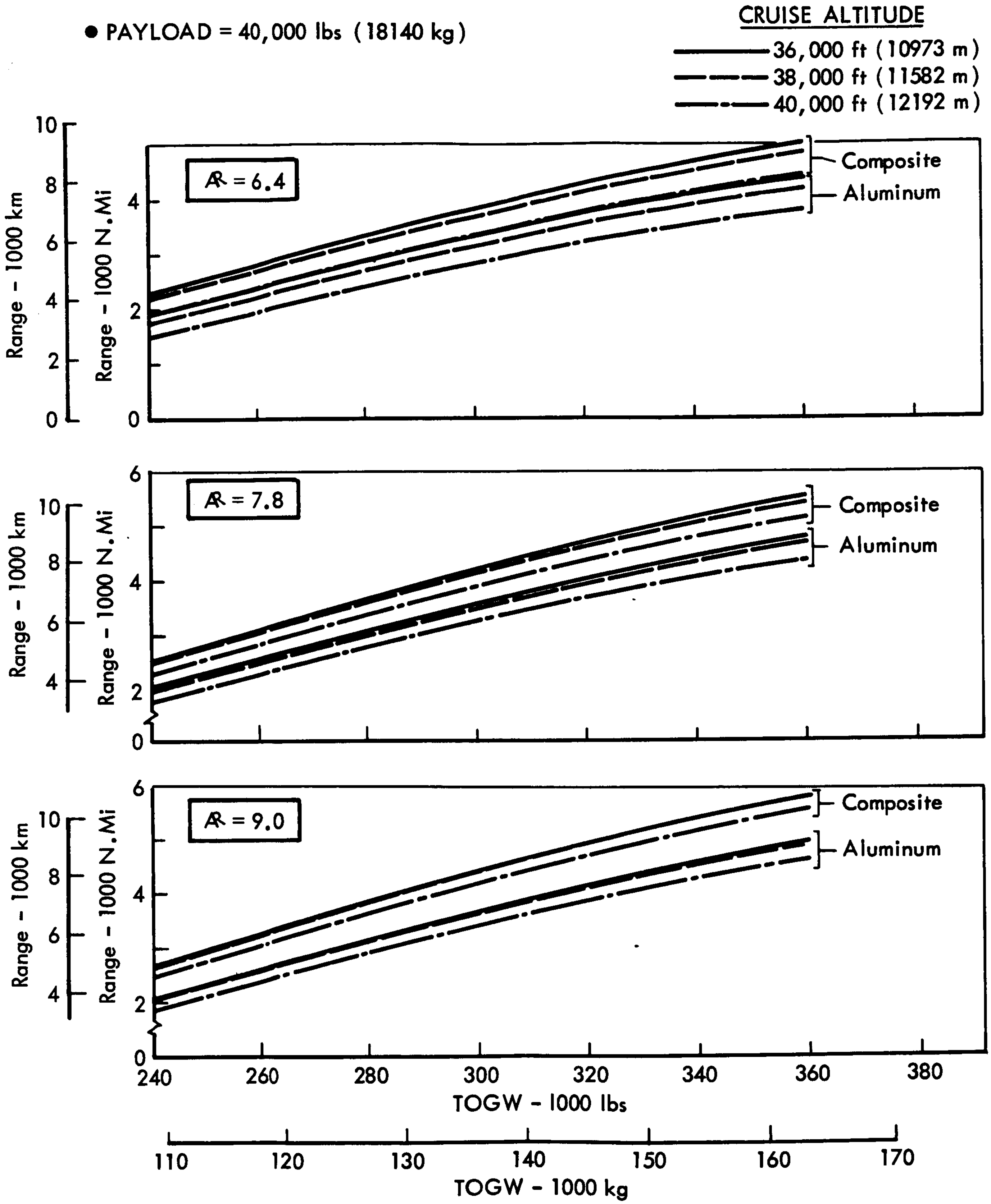

Figure 5.5-7 M = .90 Aspect Ratio Optimization Airplane Sizing

Table 5.5-7 COST ANALYSIS DATA FOR ASPECT RATIO SELECTION: M=.90, AR=6.4

●PAYLOAD = 40,000 lb (18,140 kg) ●RANGE = 3,000 n.mi (5,560 km) ●$\Lambda_{\frac{C}{2}} = 36^{o}$ ●t/c = .1415

	COMPOSITE			ALUMINUM		
CRUISE ALT, ft (m)	36,000 (10,973)	38,000 (11,582)	40,000 (12,192)	36,000 (10,973)	38,000 (11,582)	40,000 (12,192
SREF, ft^2 (m^2)	2,232 (207.4)	2,271 (211.0)	2,377 (220.8)	2,398 (222.8)	2,451 (227.7)	2,571 (238.9)
TOGW, lb (kg)	267,840 (121,492)	272,520 (123,615)	285,000 (129,276)	287,760 (130,528)	294,120 (133,413)	308,520 (139,945)
BOW, lb (kg)	140,500 (63,731)	144,200 (65,409)	153,000 (69,401)	155,600 (70,580)	160,500 (72,803)	171,100 (77,611)
USEFUL LOAD, lb (kg)	7,364 (3,340)	7,364 (3,340)	7,364 (3,340)	7,364 (3,340)	7,364 (3,340)	7,364 (3,340)
FUEL, lb (kg) TOTAL	87,340 (39,617)	88,320 (40,062)	92,000 (41,731)	92,160 (41,804)	93,620 (42,466)	97,420 (44,190)
TAXI & T.O. FUEL	1,225 (555.7)	1,345 (610.1)	1,595 (723.5)	1,295 (587.4)	1,430 (648.6)	1,700 (771.1)
CLIMB	9,240 (4,191)	9,120 (4,137)	8,670 (3,933)	9,870 (4,477)	9,780 (4,436)	9,300 (4,218)
CRUISE	60,065 (27,245)	60,775 (27,568)	63,805 (28,942)	63,135 (28,638)	64,170 (29,108)	67,160 (30,464)
DESCENT	610 (277)	680 (308)	780 (354)	660 (299)	730 (331)	860 (390)
RESERVES	16,200 (7,348)	16,400 (7,439)	17,150 (7,779)	17,200 (7,802)	17,510 (7,943)	18,400 (8,346)
BLOCK	71,140 (32,269)	71,920 (32,623)	74,850 (33,952)	74,960 (34,002)	76,110 (34,523)	79,020 (35,843)
ENGINE SCALE	.622	.683	.809	.656	.724	.862
T/W	.356	.383	.434	.350	.377	.427
DISTANCE n.mi (km) CLIMB	203 (376)	192 (356)	160 (296)	205 (380)	194 (359)	161 (298)
DESCENT	99 (183)	102 (189)	104 (193)	101 (187)	104 (193)	106 (196)
TIME CLIMB, min	26	25	21	26	25	21
DESCENT, min	15	16	16	16	16	16
BLOCK, hr	6.41	6.42	6.42	6.42	6.42	6.41

Table 5.5-8 COST ANALYSIS DATA FOR ASPECT RATIO SELECTION: M=.90, AR=9.0

●PAYLOAD = 40,000 lb (18,140 kg) ●RANGE = 3,000 n.mi (5,560 km) ●$\Lambda \frac{c}{2}$ = 36° ●t/c = .1415

	COMPOSITE			ALUMINUM		
CRUISE ALT, ft (m)	36,000 (10,973)	38,000 (11,582)	40,000 (12,192)	36,000 (10,973)	38,000 (11,582)	40,000 (12,192)
SREF, ft^2 (m^2)	2,100 (195.1)	2,110 (196.0)	2,152 (199.9)	2,290 (212.7)	2,304 (214.0)	2,363 (219.5)
TOGW, lb (kg)	252,000 (114,307)	253,200 (114,852)	258,240 (117,138)	274,800 (124,649)	276,480 (125,411)	283,560 (128,623)
BOW, lb (kg)	134,500 (61,009)	136,500 (61,916)	141,400 (64,139)	152,300 (69,083)	154,700 (70,172)	160,800 (72,939)
USEFUL LOAD, lb (kg)	7,364 (3,340)	7,364 (3,340)	7,364 (3,340)	7,364 (3,340)	7,364 (3,340)	7,364 (3,340)
FUEL, lb (kg)						
TOTAL	77,500 (35,154)	76,700 (34,791)	76,840 (34,855)	82,500 (37,422)	81,780 (37,095)	82,760 (37,540)
TAXI & T.O. FUEL	1,055 (478.5)	1,125 (510.3)	1,278 (579.7)	1,120 (508.0)	1,197 (543.0)	1,364 (618.7)
CLIMB	9,720 (4,409)	9,550 (4,332)	8,680 (3,937)	10,550 (4,785)	10,320 (4,681)	9,400 (4,264)
CRUISE	51,695 (23,449)	51,005 (23,136)	51,842 (23,516)	54,740 (24,830)	53,953 (24,473)	55,666 (25,250)
DESCENT	550 (249)	580 (263)	620 (281)	610 (277)	720 (327)	770 (349)
RESERVES	14,480 (6,568)	14,440 (6,550)	14,420 (6,541)	15,480 (7,022)	15,590 (7,072)	15,560 (7,058)
BLOCK	63,020 (28,586)	62,260 (28,241)	62,420 (28,314)	67,020 (30,400)	66,190 (30,024)	67,200 (30,482)
ENGINE SCALE	.535	.5705	.648	.567	.607	.6915
T/W	.325	.3447	.3839	.3155	.3359	.3731
DISTANCE n.mi (km)						
CLIMB	252 (467)	242 (448)	203 (376)	257 (476)	246 (456)	205 (380)
DESCENT	103 (191)	106 (196)	108 (200)	107 (198)	108 (200)	109 (202)
TIME						
CLIMB, min	32	31	26	33	31	26
DESCENT, min	15	16	16	16	17	17
BLOCK, hr	6.40	6.42	6.42	6.42	6.42	6.42

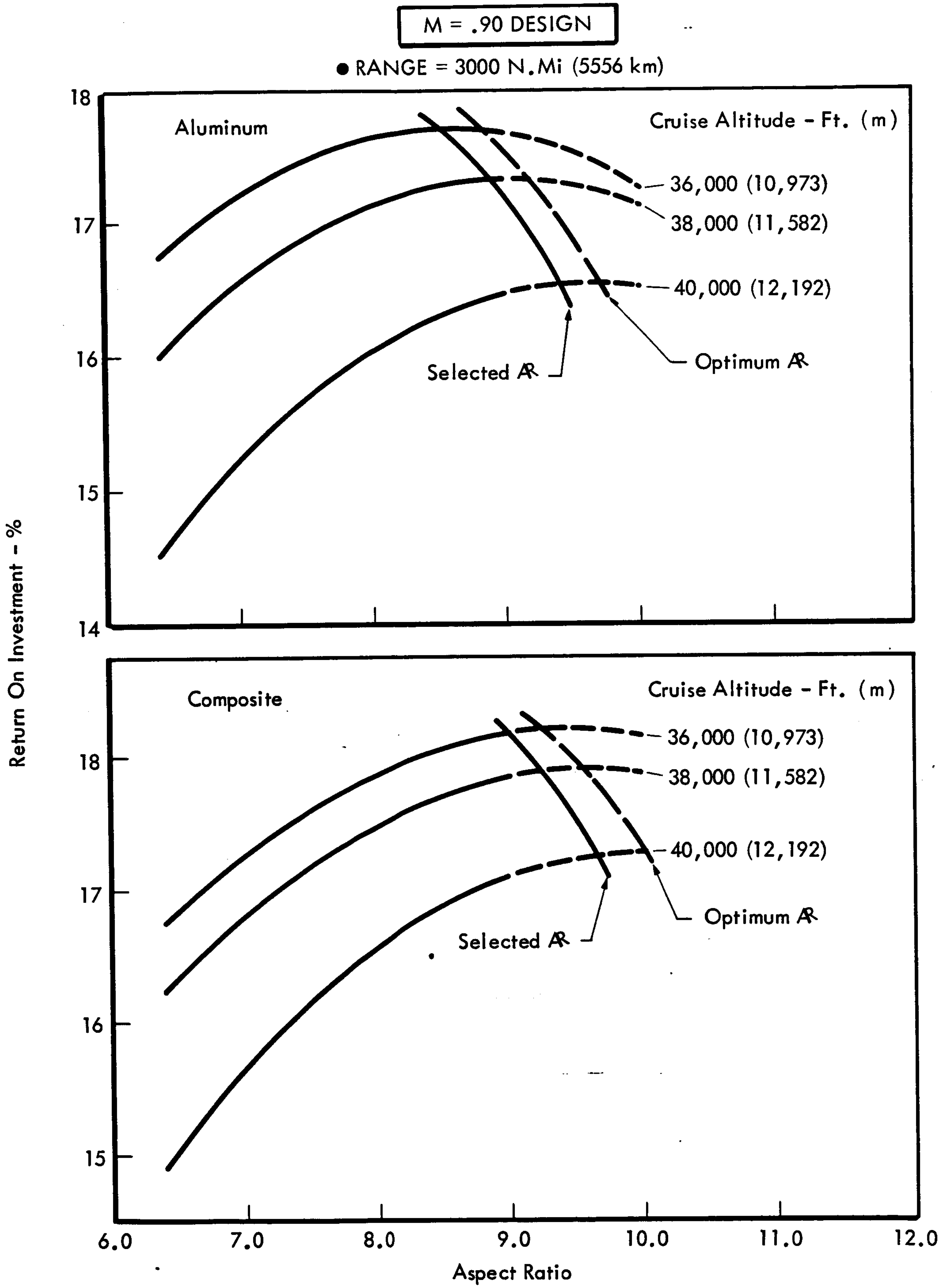

Figure 5.5-8 Effect of AR and Cruise Altitude On R.O.I.

C2

Table 5.5-9 CONVENTIONAL M=.82 TRANSPORT

●PAYLOAD = 40,000 lb (18,140 kg) ●RANGE = 3,000 n.mi (5,560 km) ●$\Lambda \frac{C}{2}$ = 31.75°

●AR = 6.8 ●t/c = .10

NOISE LEVEL	FAR 36	FAR 36 -10 EPNDB
CRUISE ALT, ft (m)	33,000 (10,058)	33,000 (10,058)
SREF, ft^2 (m^2)	2,485 (230.9)	2,540 (236.0)
TOGW, lb (kg)	298,200 (135,264)	304,800 (138,231)
BOW, lb (kg)	162,144 (73,549)	163,554 (74,174)
USEFUL LOAD, lb (kg)	7,364 (3,340)	7,364 (3,340)
WATER, lb (kg)	0 (0)	970 (440)
FUEL, lb (kg)		
TOTAL	96,055 (43,571)	100,281 (45,479)
TAXI & T.O. FUEL	1,170 (531)	1,264 (573)
CLIMB	11,040 (5,008)	11,500 (5,216)
CRUISE	66,265 (30,058)	68,327 (30,993)
DESCENT	560 (254)	490 (222)
RESERVES	17,020 (7,720)	18,700 (8,482)
BLOCK	79,035 (35,850)	81,581 (37,005)
ENGINE	GE-CF6	P&W429
ENGINE SCALE	.585	.669
T/W	.30	.263
DISTANCE, n.mi (km)		
CLIMB	230 (426)	240 (444)
DESCENT	92 (170)	75 (139)
TIME		
CLIMB, min	31	22
DESCENT, min	15	12
BLOCK, hr	6.92	6.92

Table 5.5-10 COST ANALYSIS DATA FOR TECHNOLOGY STUDIES: M=.98

●PAYLOAD = 40,000 lb (18,140 kg) ●RANGE = 3,000 n.mi (5,560 km) ●$\Lambda\frac{c}{2}$ = 40° ●t/c = .11 ●SUPERCRITICAL WING

*FAR36-15 EPNDB NOISE LEVEL **FAR36-MAX EPNDB NOISE LEVEL (SEE SECTION 10)

	ALUM	ALUM + ACS	COMP	COMP + ACS	COMP + ACS*	COMP + ACS**
CRUISE ALT, ft (m)	36,000 (10,973)	36,000 (10,973)	36,000 (10,973)	36,000 (10,973)	36,000 (10,973)	40,000 (12,192)
AR	7.5	7.5	8.0	8.0	8.0	8.0
SREF, ft^2 (m^2)	2,685 (249.4)	2,570 (238.8)	2,320 (215.5)	2,282 (212.0)	2,325 (216.0)	2,355 (218.8)
TOGW, lb (kg)	322,200 (146,122)	308,400 (139,863)	278,400 (126,258)	273,840 (124,190)	279,000 (126,531)	282,600 (128,163)
BOW, lb (kg)	182,392 (82,717)	171,968 (77,990)	147,374 (66,836)	144,128 (65,364)	147,307 (66,806)	152,769 (69,283)
USEFUL LOAD, lb (kg)	7,364 (3,340)	7,364 (3,340)	7,364 (3,340)	7,364 (3,340)	7,364 (3,340)	7,364 (3,340)
WATER, lb (kg)	1,080 (490)	1,035 (469)	965 (438)	960 (435)	1,020 (463)	1,190 (540)
FUEL, lb (kg) TOTAL	98,728 (44,775)	95,397 (43,264)	90,061 (40,844)	88,752 (40,251)	90,673 (41,122)	88,641 (40,200)
TAXI & T.O. FUEL	1,363 (618)	1,321 (599)	1,224 (555)	1,210 (549)	1,270 (576)	1,486 (674)
CLIMB	12,360 (5,606)	11,930 (5,411)	12,000 (5,443)	11,620 (5,271)	12,170 (5,521)	10,700 (4,854)
CRUISE	64,740 (29,366)	61,886 (28,071)	58,677 (26,616)	57,972 (26,296)	59,103 (26,809)	58,215 (26,046)
DESCENT	515 (234)	510 (231)	450 (204)	450 (204)	480 (218)	540 (245)
RESERVES	19,750 (8,959)	19,750 (8,959)	17,710 (8,033)	17,500 (7,938)	17,650 (8,006)	17,700 (8,029)
BLOCK	78,978 (35,824)	75,647 (34,313)	72,351 (32,818)	71,252 (32,320)	73,023 (33,123)	70,941 (32,179)
ENGINE	STF429	STF429	STF429	STF429	STF433	STF433
ENGINE SCALE	.745	.722	.669	.662	.670	.786
T/W	.277	.281	.288	.290	.288	.334
DISTANCE n.mi (km) CLIMB	250 (463)	250 (463)	280 (519)	275 (510)	282 (522)	234 (433)
DESCENT	95 (176)	95 (176)	85 (157)	86 (159)	86 (159)	90 (167)
TIME CLIMB, min	34	34	35	34	34	27
DESCENT, min	14	14	13	14	14	14
BLOCK, hr	5.94	5.94	5.94	5.94	5.94	5.94

Table 5.5-11 COST ANALYSIS DATA FOR TECHNOLOGY STUDIES: M=.90

•PAYLOAD = 40,000 lb (18,140 kg) •RANGE = 3,000 n.mi (5,560 km) •$\Lambda \frac{c}{2}$ = 36° •t/c = .1415

•SUPERCRITICAL WING

*FAR36-15 EPNDB NOISE LEVEL **FAR36-MAX EPNDB NOISE LEVEL (SEE SECTION 10)

	ALUM	ALUM + ACS	COMP	COMP + ACS	COMP + ACS*	COMP + ACS**
CRUISE ALT, ft (m)	36,000 (10,973)	36,000 (10,973)	36,000 (10,973)	36,000 (10,973)	36,000 (10,973)	40,000 (12,192)
AR	8.5	8.5	9.0	9.0	9.0	9.0
SREF, ft^2 (m^2)	2,275 (211.4)	2,205 (204.9)	1,990 (184.9)	1,970 (183.0)	2,005 (186.3)	2,100 (195.1)
TOGW, lb (kg)	285,740 (129,588	276,948 (125,600)	249,944 (113,353)	247,432 (112,214)	251,830 (114,208)	263,760 (119,619)
BOW, lb (kg)	155,835 (70,674)	149,097 (67,618)	130,375 (59,127)	127,935 (58,021)	130,250 (59,070)	139,580 (63,302)
USEFUL LOAD, lb (kg)	7,364 (3,340)	7,364 (3,340)	7,364 (3,340)	7,364 (3,340)	7,364 (3,340)	7,364 (3,340)
WATER, lb (kg)	910 (413)	895 (406)	820 (372)	810 (367)	870 (395)	1,100 (499)
FUEL, lb (kg) TOTAL	88,995 (40,361)	86,956 (39,436)	78,749 (35,714)	78,687 (35,686)	80,710 (36,603)	83,080 (37,678)
TAXI & T.O. FUEL	1,145 (519.4)	1,120 (508.0)	1,034 (469.0)	1,040 (471.7)	1,075 (487.6)	1,370 (621.4)
CLIMB	13,400 (6,078)	13,050 (5,919)	12,200 (5,534)	12,100 (5,489)	12,270 (5,566)	9,630 (4,368)
CRUISE	56,910 (25,814)	55,666 (25,250)	49,915 (22,641)	50,022 (22,690)	51,765 (23,481)	55,720 (25,275)
DESCENT	440 (200)	430 (195)	400 (181)	395 (179)	400 (181)	510 (231)
RESERVES	17,100 (7,757)	16,690 (7,571)	15,200 (6,895)	15,130 (6,863)	15,200 (6,895)	15,850 (7,190)
BLOCK	71,895 (32,612)	70,266 (31,873)	63,549 (28,826)	63,557 (28,829)	65,510 (29,715)	67,230 (30,496)
ENGINE	STF429	STF429	STF429	STF429	STF433	STF433
ENGINE SCALE	.626	.6125	.565	.560	.568	.724
T/W	.263	.265	.271	.272	.271	.329
DISTANCE n.mi (km) CLIMB	326 (604)	326 (604)	332 (615)	321 (615)	332 (615)	204 (378)
DESCENT	92 (170)	91 (169)	91 (169)	91 (169)	91 (169)	96 (178)
TIME CLIMB, min	42	42	42	42	42	26
DESCENT, min	13.5	13.7	14.0	13.0	13.0	15.0
BLOCK, hr	6.42	6.42	6.42	6.42	6.42	6.42

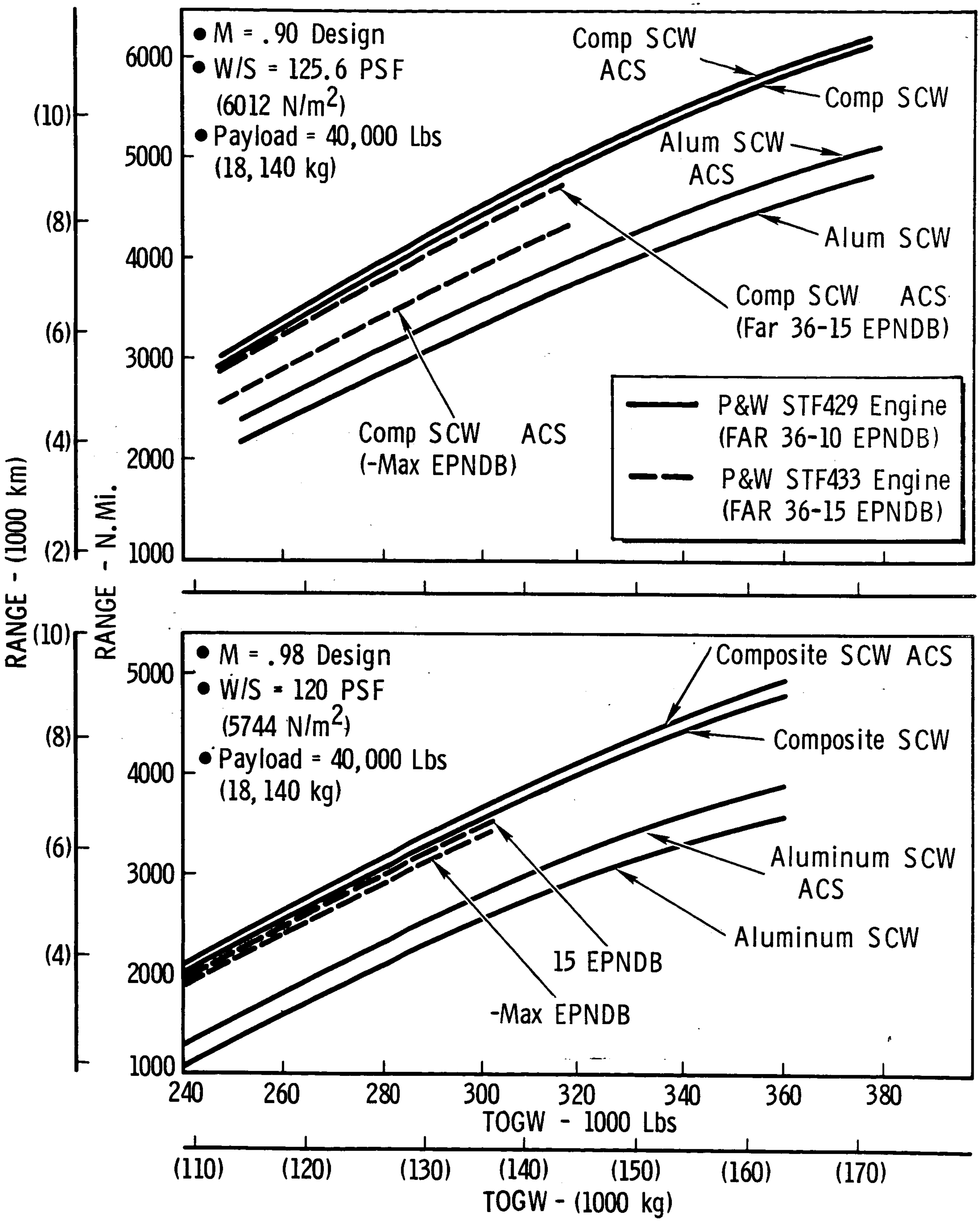

Figure 5.5-9 Technology Application Study Sizing Data

is discussed in the summary section and the cost analysis of these airplanes given in Section 6.

5.5.4 Selected Airplane Sizing

Final sizing of the selected configurations was made to include the effects of FAR field-length requirements, climb gradients, and other cruise impacts. The growth curves for these airplanes with engines sized for several cruise altitudes are shown in Figure 5.5-10, and data for the cost analysis of the airplanes sized for 3000 n.mi (4828 km) are shown in Tables 5.5-12 and -13. FAR field lengths for each of these airplanes are shown in Figure 5.5-11.

Cost variations with initial cruise altitude are presented in Figures 5.5-12 and -13 for the selected configurations. It may be noted that the .98M airplane ROI peaks near an altitude of 36,000 ft (10,973 m), hence the selection of that initial cruise altitude. ROI for the .90M airplane continues to increase with reduced altitude; however, 36,000 ft (10,973 m) was selected in order to maintain the T/W levels compatible with achieving takeoff field lengths near those of the .98M airplane. Finally, the wing loading of the .90M configuration was increased to 125.6 psf (6012 N/m^2) to obtain the same approach speed as the .98M design. It is seen that this change in wing loading has very little effect on ROI except, perhaps, at the very lowest initial cruise altitude.

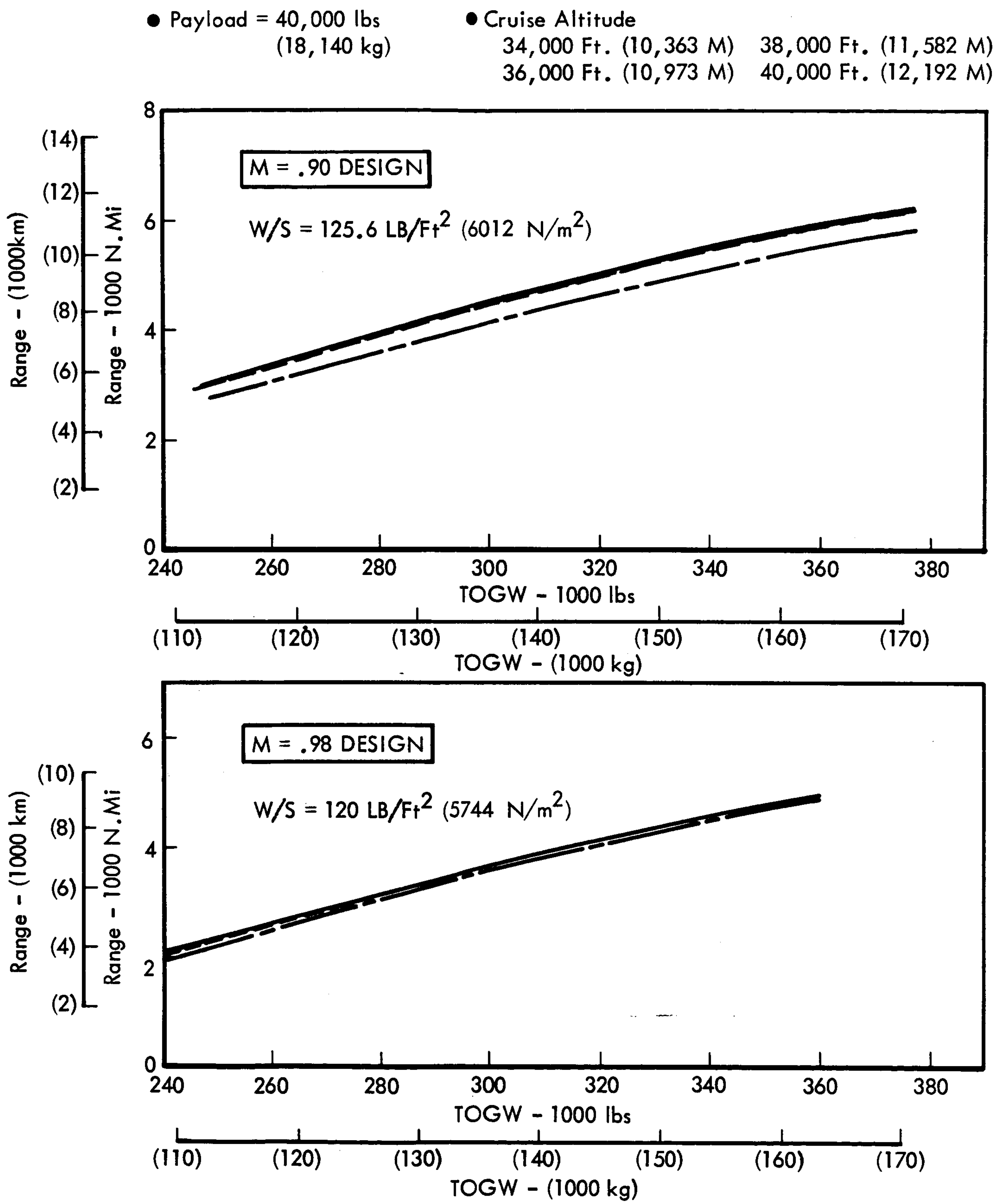

Figure 5.5-10 Selected Airplane Sizing

Table 5.5-12 COST ANALYSIS DATA FOR SELECTED AIRPLANES: M=.98

- PAYLOAD = 40,000 lb (18,140 kg)
- RANGE = 3,000 n.mi (5,560 km)
- $\Lambda_{\frac{c}{2}} = 40^{\circ}$
- t/c = .11
- W/S = 120 lb/ft^2 (6744 N/m^2)
- AR = 8.0

CRUISE ALT, ft (m)	34,000 (10,363)	36,000 (10,973)	38,000 (11,582)	40,000 (12,192)
SREF, ft^2 (m^2)	2,284 (212.2)	2,282 (212.0)	2,290 (212.7)	2,312 (214.8)
TOGW, lb (kg)	274,080 (124,323)	273,840 (124,214)	274,800 (124,649)	277,440 (125,847)
BOW, lb (kg)	144,250 (65,432)	144,128 (65,376)	146,650 (66,520)	150,050 (68,063)
USEFUL LOAD, lb (kg)	7,364 (3,340)	7,364 (3,340)	7,364 (3,340)	7,364 (3,340)
WATER, lb (kg)	945 (429)	960 (435)	1,025 (465)	1,125 (510)
FUEL, lb (kg)				
TOTAL	88,885 (40,318)	88,752 (40,258)	87,125 (39,520)	86,265 (39,130)
TAXI & T.O. FUEL	1,190 (540)	1,210 (549)	1,290 (585)	1,415 (642)
CLIMB	11,800 (5,352)	11,620 (5,271)	11,040 (5,008)	10,390 (4,713)
CRUISE	57,845 (26,238)	57,972 (26,296)	56,925 (25,821)	56,370 (25,569)
DESCENT	450 (204)	450 (204)	470 (213)	520 (236)
RESERVES	17,600 (7,983)	17,500 (7,938)	17,400 (7,893)	17,570 (7,970)
BLOCK	71,285 (32,335)	71,252 (32,320)	69,725 (31,627)	68,695 (31,160)
ENGINE SCALE	.652	.662	.707	.776
T/W	.285	.290	.309	.336
DISTANCE, n.mi (km)				
CLIMB	273 (506)	275 (510)	252 (467)	223 (413)
DESCENT	89 (165)	86 (159)	88 (163)	89 (165)
TIME				
CLIMB, min	34.3	33.9	30.9	27.3
DESCENT, min	13.5	13.5	13.5	13.5
BLOCK, hr	5.93	5.96	5.96	5.95

Table 5.5-13 COST ANALYSIS DATA FOR SELECTED AIRPLANES: M=.90

●PAYLOAD = 40,000 lb (18,140 kg) ●RANGE = 3,000 n.mi (5,560 km) ●AR = 9.0

●$\Lambda \frac{c}{2}$ = 36° ●t/c = .1415 ●W/S = 125.6 lb/ft^2 (6012 N/m^2)

CRUISE ALT, ft (m)	34,000 (10,363)	36,000 (10,973)	38,000 (11,582)	40,000 (12,192)
SREF, ft^2 (m^2)	1,970 (183.0)	1,970 (183.0)	1,975 (183.5)	2,045 (190.0)
TOGW, lb (kg)	247,432 (112,214)	247,432 (112,214)	248,060 (112,520)	256,852 (116,508)
BOW, lb (kg)	127,400 (57,789)	127,935 (58,021)	130,000 (58,968)	135,900 (61,644)
USEFUL LOAD, lb (kg)	7,364 (3,340)	7,364 (3,340)	7,364 (3,340)	7,364 (3,340)
WATER, lb (kg)	793 (360)	812 (368)	883 (401)	1,022 (464)
FUEL, lb (kg) TOTAL	79,239 (35,943)	78,687 (35,686)	77,177 (35,007)	79,930 (36,256)
TAXI & T.O. FUEL	1,015 (460)	1,040 (472)	1,130 (513)	1,320 (599)
CLIMB	12,150 (5,511)	12,100 (5,489)	10,450 (4,740)	9,100 (4,128)
CRUISE	50,724 (23,008)	50,022 (22,690)	50,067 (22,710)	53,310 (24,181)
DESCENT	370 (168)	395 (179)	430 (195)	500 (227)
RESERVES	14,980 (6,795)	15,130 (6,863)	15,100 (6,849)	15,700 (7,122)
BLOCK	64,259 (29,148)	63,557 (28,829)	62,077 (28,158)	64,230 (29,135)
ENGINE SCALE	.547	.560	.609	.711
T/W	.265	.272	.295	.339
DISTANCE n.mi (km) CLIMB	331 (613)	321 (595)	268 (496)	204 (378)
DESCENT	85 (157)	91 (169)	95 (176)	96 (178)
TIME CLIMB, min	43	42	35	26
DESCENT, min	13	13	14	15
BLOCK, hr	6.43	6.42	6.42	6.42

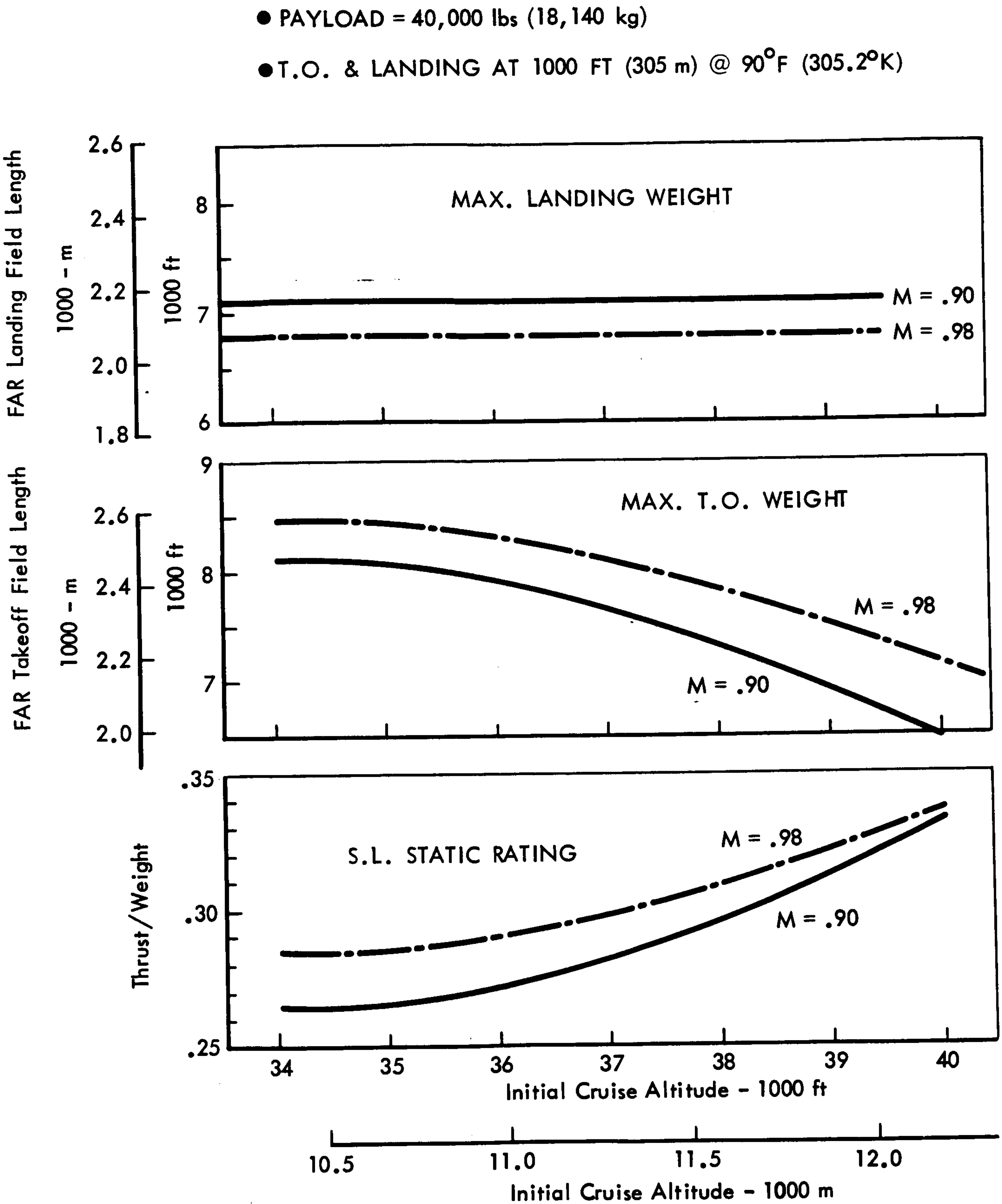

Figure 5.5-11 Critical Sizing Effects

- CRUISE M = .98
- W/S = 120 PSF (5744 N/m^2)
- (3) P&W 429 Engine
- Maximum Composite Usage
- Range = 3000 N.Mi. (5560 km)
- $\Lambda_{c/2} = 40^0$
- $t/c \perp c/2 = .11$
- FAR 36-10 EPNDB Noise Level
- Full Active Control System
- Payload = 40,000 Lbs (18,140 kg)
- AR = 8.0

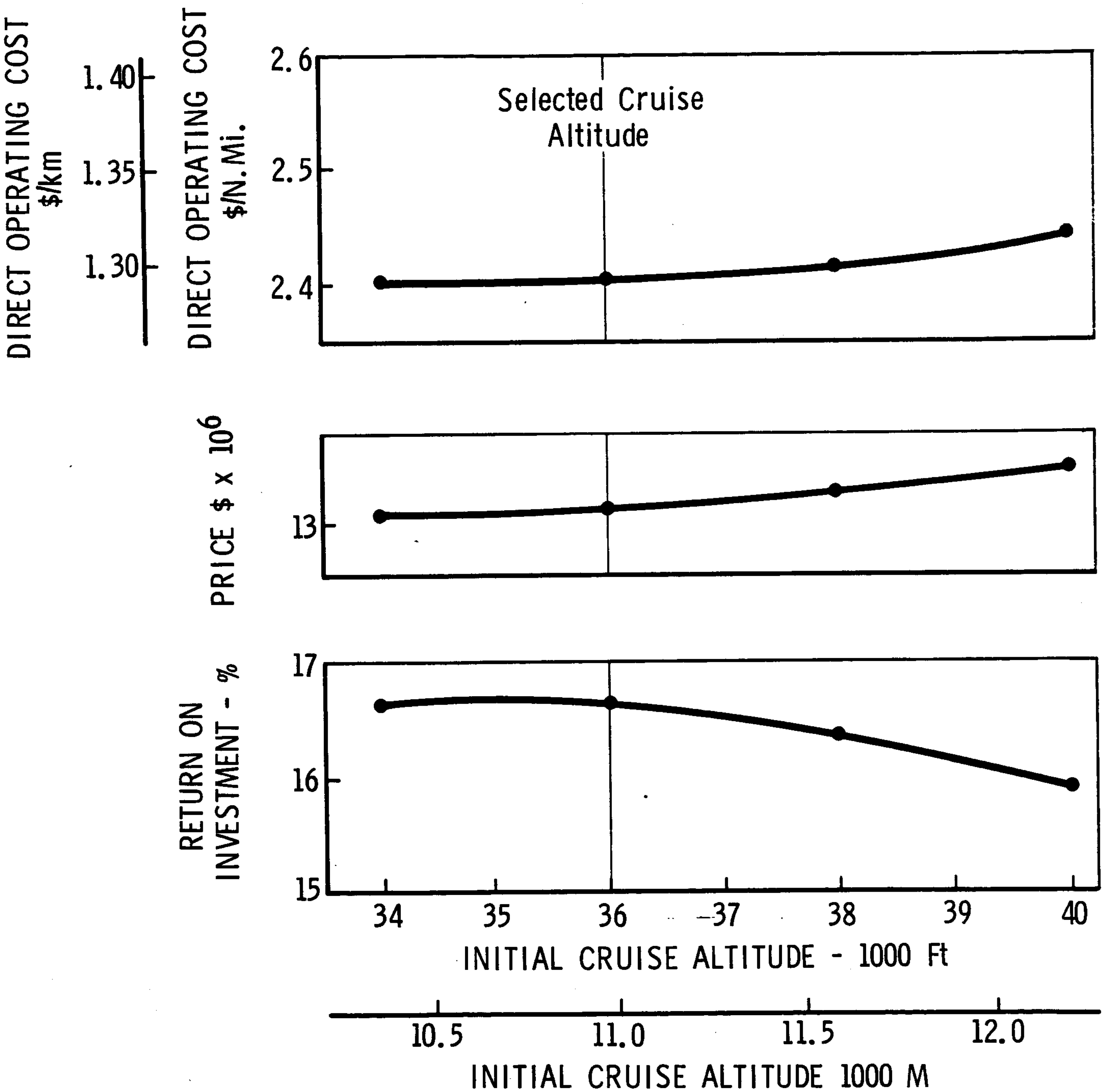

Figure 5.5-12 Final Configuration Selection, M = .98

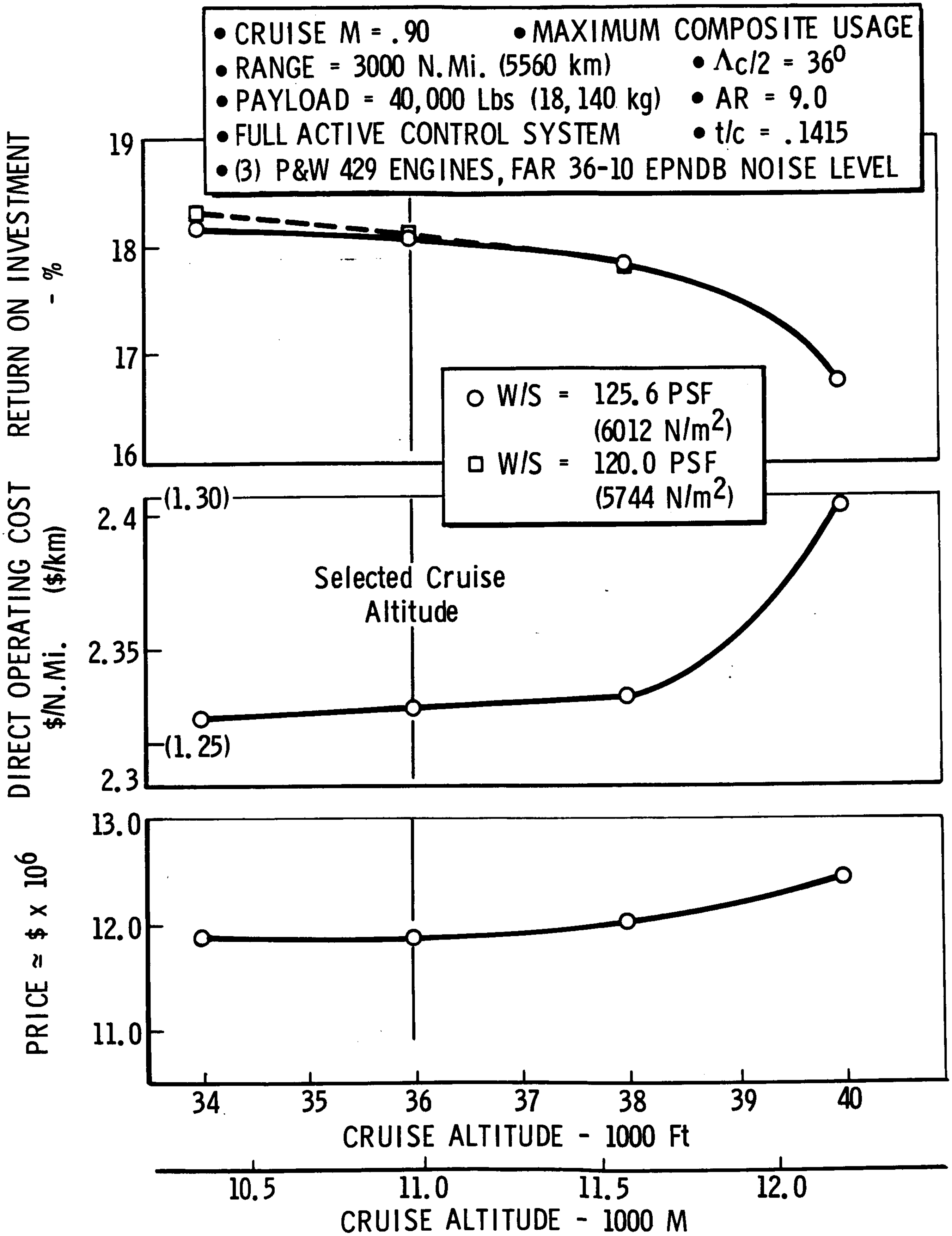

Figure 5.5-13 Final Configuration Selection, M = .90

SECTION 6

ECONOMIC ANALYSIS

The principal objectives of the economic analysis activities were (1) to evaluate the individual and collective benefits of the various technological advances studied in the program and (2) to relate the economics of aircraft incorporating desirable technologies to current production transports and other transports likely to be operational in the 1980-1985 time period. To accomplish these, a set of parametric cost equations was developed to generate flyaway costs. Candidate designs were then exercised against the route structure and traffic projection (see Section 4) to develop direct operating costs, indirect operating costs, and return on investment. Flow of the evaluation process is shown on Figure 6.0-1.

6.1 INITIAL STUDY COST BASIS

For the purpose of evaluating the many design configurations of potential interest, a preliminary economic analysis procedure was used. This initial procedure considers the whole airframe as a unit and uses a single cost-estimating equation which essentially represents the solid line seen in Figure 6.1-1. A series of data points representing subsonic aircraft are shown, and commercial subsonic airframe costs are believed to fall in this region but are adjusted upward from 1967 dollars due to inflation. A word of caution is indicated for projecting costs of heavy airframes (above 250,000 lb) (113,380 kg). Because of increasing design-for-low weight problems the cost projections will probably curve upward from the straight-line projection.

Aircraft production costs for a given quantity to be produced (250 in this study) are predicted by use of a standard cost-quantity analysis. These projections, as well as other cost analysis methods, are discussed in Reference 6-1, submitted as a part of this study.

In the study, considerable effort was directed toward the influence on cost of design choices. These included area ruling, supercritical wing, active control system, use of composite material, and others. In the initial cost analysis, the cost increment associated with each of these design choices was handled as a unique problem. The results

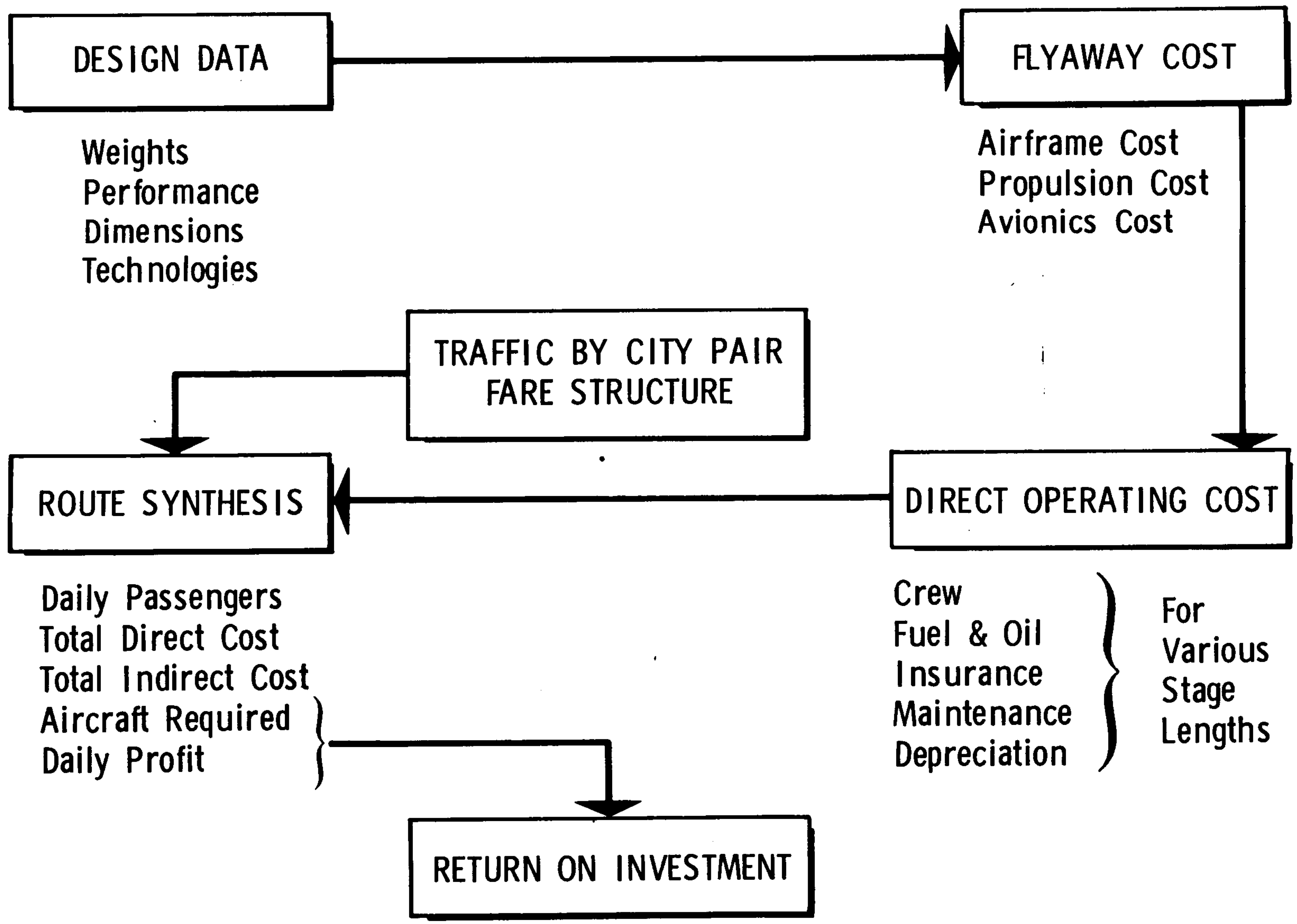

Figure 6.0-1 Flow of the Evaluation Process

B

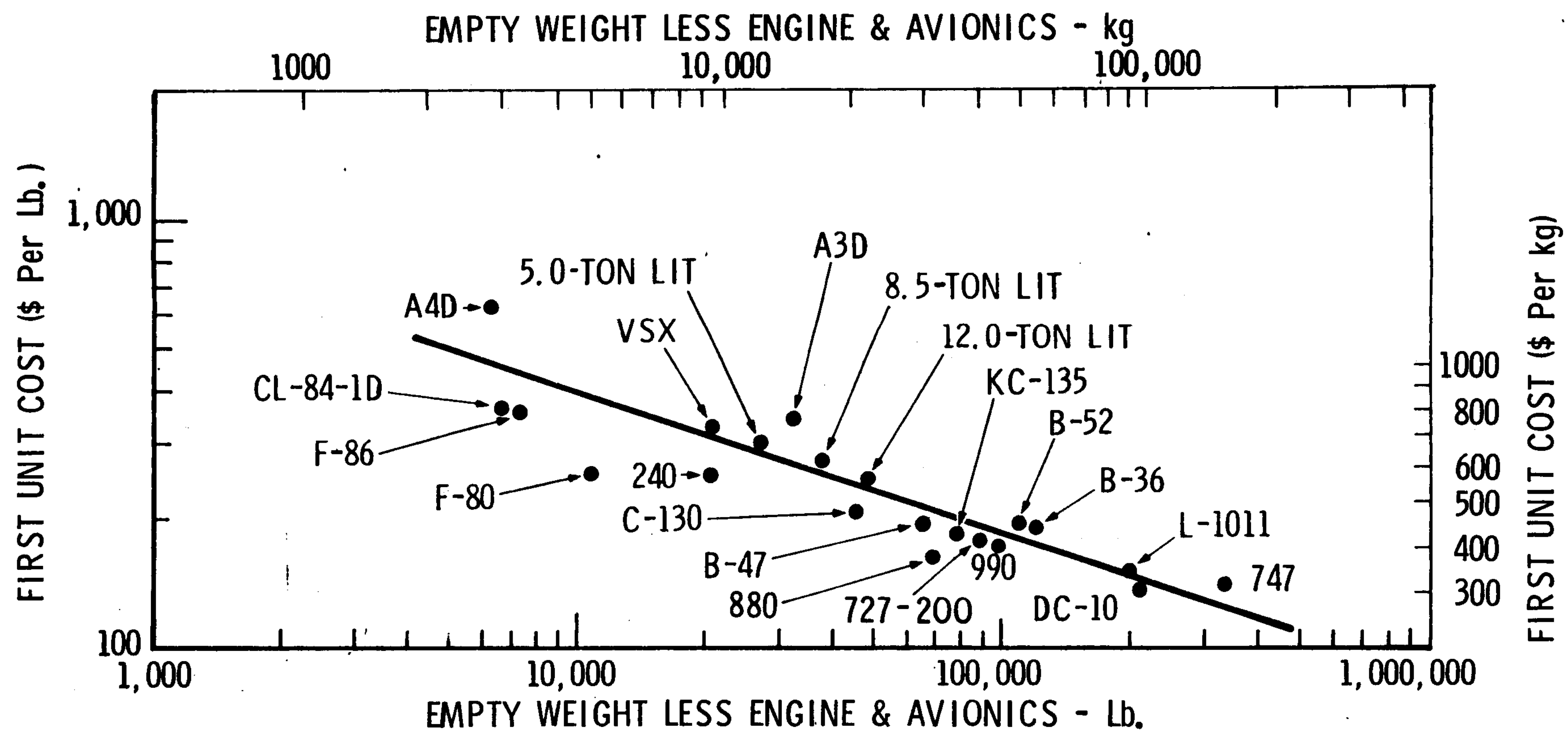

Figure 6.1-1 Subsonic Aircraft Airframe First Unit Cost Per Pound (1970 Dollars)

showed that, in the case of the area-ruled fuselage and the supercritical wing, there was a weight increase commensurate with the expected cost increase so that the effect was taken care of by the airframe cost prediction formula. In the case of the active control system, however, it was necessary to provide a cost increment for the electronics and extra sensing and control items required. This was based upon engineering judgment initially, which was later verified when detailed item-by-item component studies could be made. A $200,000 average cost figure was used.

Assessment of the impact of costs due to the application of composite material was a much more complicated task. However, the initial cost adjustment was simplified for tradeoff study purposes. After review of available cost data, costs of composite structure were adjusted upward from the standard prediction by an amount equal to $30.00 per pound ($66.00 per kg) of actual composite used. This increment later proved correct for the wing structure but excessive for the fuselage when using a substantial proportion of machine lay-up. An overview of graphite composite cost considerations is shown in Figure 6.1-2. Further analysis of graphite composite structure costs is given in Section 6.6.

6.2 PHASE I CONFIGURATION SELECTION

For the high-performance Mach .98 configuration, range and payload for best return on investment were sought. For the alternate configuration, a systematic variation of speed was introduced to examine return on investment as a function of Mach number. The flow of configuration selection is depicted in Figure 6.2-1. Each "X" in the various matrices represents a different airplane. A circled "X" denotes a configuration combination specifically called out in the statement of work.

Highest return on investment, calculated for airplanes flying the route structure described in Section 4, serves as the evaluation criterion for configuration selection. Direct operating cost, while serving to differentiate between airplanes of similar technology, is a less sensitive measure of economic worth than ROI, since an aircraft of low DOC, but relatively high unit flyaway cost may have a lower ROI than a less expensive design having a higher DOC.

• BASIC MATERIAL	• QUOTES FROM 3 VENDORS TYPICALLY \$30/LB (\$66/kg) FOR PRE-PREGS IN THE 1975-1980 PERIOD
• TECHNOLOGY BASE	• F-5 FUSELAGE (in assembly) • F-111 PIVOT FAIRING (in Production) • F-111 FUSELAGE SECTION (Tested) • ATLAS OV-1 ADAPTER (in test) • VS (X) WING BOX (Tested) • TAPE LAYING MACHINE
• LABOR COSTS	• HAND LAY-UP - Equal or Higher Manhours for Similar Components in Aluminum • MAJOR ASSEMBLIES INCORPORATING MACHINE LAY-UP - Wing - Labor Penalty = 21% in ATT Size Wing (Equal Area, Resized = +7%) - Fuselage - Labor = 96% of Aluminum
• TOOLING COSTS	• 70% OF THOSE FOR ALUMINUM. Less if Rate Tooling Reqd.
• DESIGN COST	• INITIALLY SAME AS ALUMINUM (Fewer Parts to Draw but More Learning) LATER WILL BE LOWER WITH EDUCATION

Figure 6.1-2 Cost Basis for Graphite/Epoxy Composites

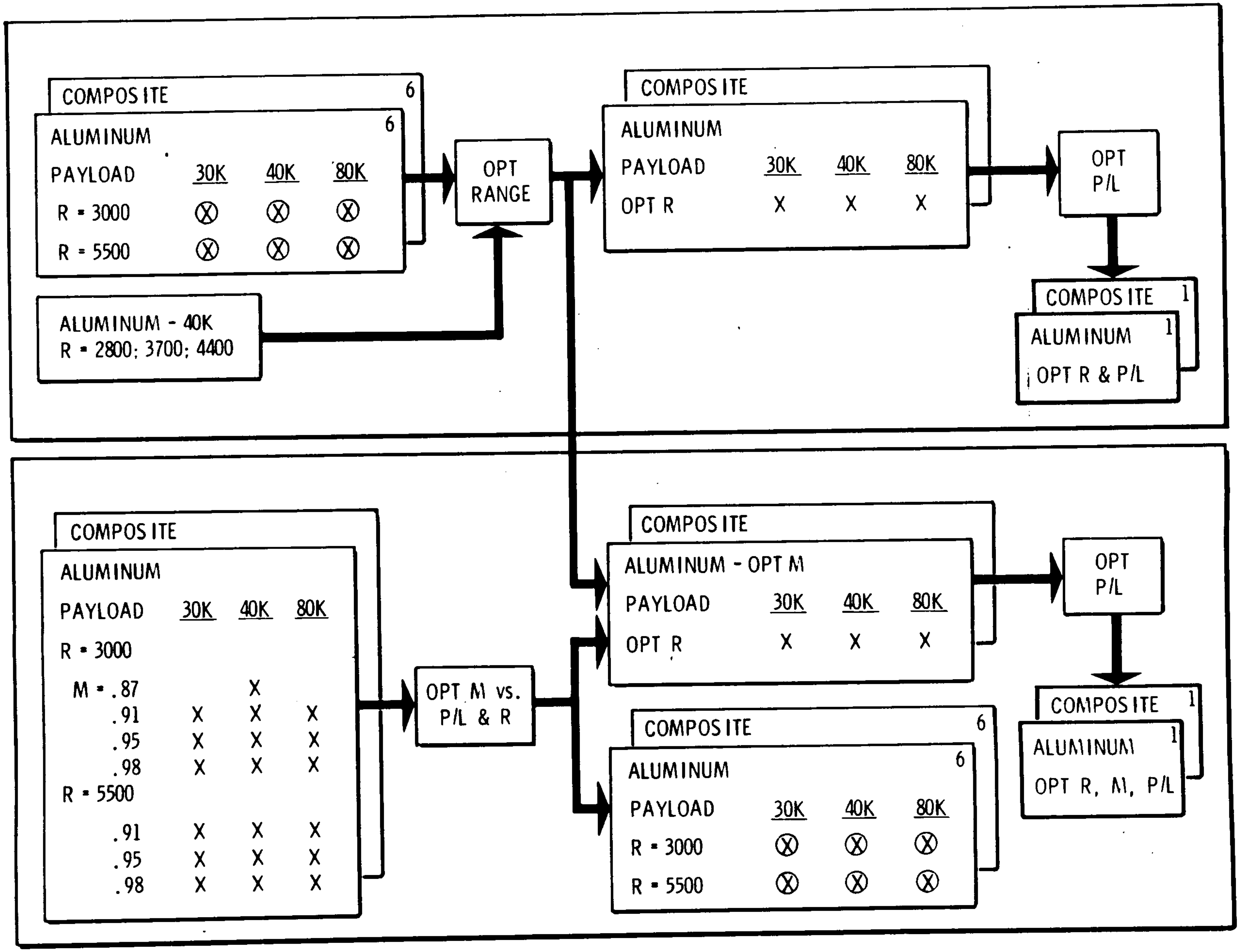

Figure 6.2-1 Phase I Configuration Selection Logic

6.2.1 Design Range

Design range was systematically varied from transcontinental capability to trans-Atlantic capability (3700 n.mi)(6860 km), from U.S. to interior European capability (4400 n.mi)(8150 km), and finally, from western U.S. to European capability (5500 n.mi)(10,180 km). The longer-range aircraft were of course able to serve progressively more city-pairs, but the larger size required to achieve the longer range induced higher operating costs and investment base for the more numerous routes through transcontinental capability. Accordingly, return on investment drops sharply with design range (Figure 6.2-2). If an aircraft specifically suited to long-range flights were chosen and its application restricted to those routes (similar to the use of the DC-8-62) an excellent ROI would result for the long-range airplane, but the market would be fairly limited (i.e., not attractive enough to induce near-term development of a new transport).

6.2.2 Design Payload

Having selected transcontinental design range, it is now possible to address payload sizing. The significant assumptions here are market share (assumed to be one-third at this point) and schedule frequency -- assumed to be 4 flights per day per carrier for the top 56 U.S. city-pairs from 1000 n.mi to 3000 n.mi (1850 to 5560 km) stage length. As seen on Figure 6.2-3, return on investment is quite flat in the region from 195 passengers to about 250 passengers. Both above 250 and below 195, ROI drops fairly sharply on a fleet-wide basis. Here, the economies of scale are balanced (the 390-seat airplane has a seat-mile-DOC 15 percent below the 195-seat configuration) against the ability to handle passenger demand in usable-size packages.

6.2.3 Design Speed -- Alternate Configuration

New technology can emphasize either performance or a reduction in the size of an aircraft with given capability to seek operating cost reductions. Faster aircraft can generate more seat miles per day but, being larger, will be most costly. Aircraft were synthesized for speeds of Mach .87, .91, .95, and .98 to systematically explore the effects of speed, productivity, and cost. The major elements of cost are defined in Table 6.2-1 along with the cost per element for each of the four Mach Numbers. Flyaway costs

- TRAFFIC BASE (1980)
  - 60 Domestic City-Pairs (Min. 4 Flt/Day)
  - 27 International City-Pairs (Min. 1Flt/Day)
- 40,000 Lb PAYLOAD ALUMINUM AIRPLANE (18,140 kg)

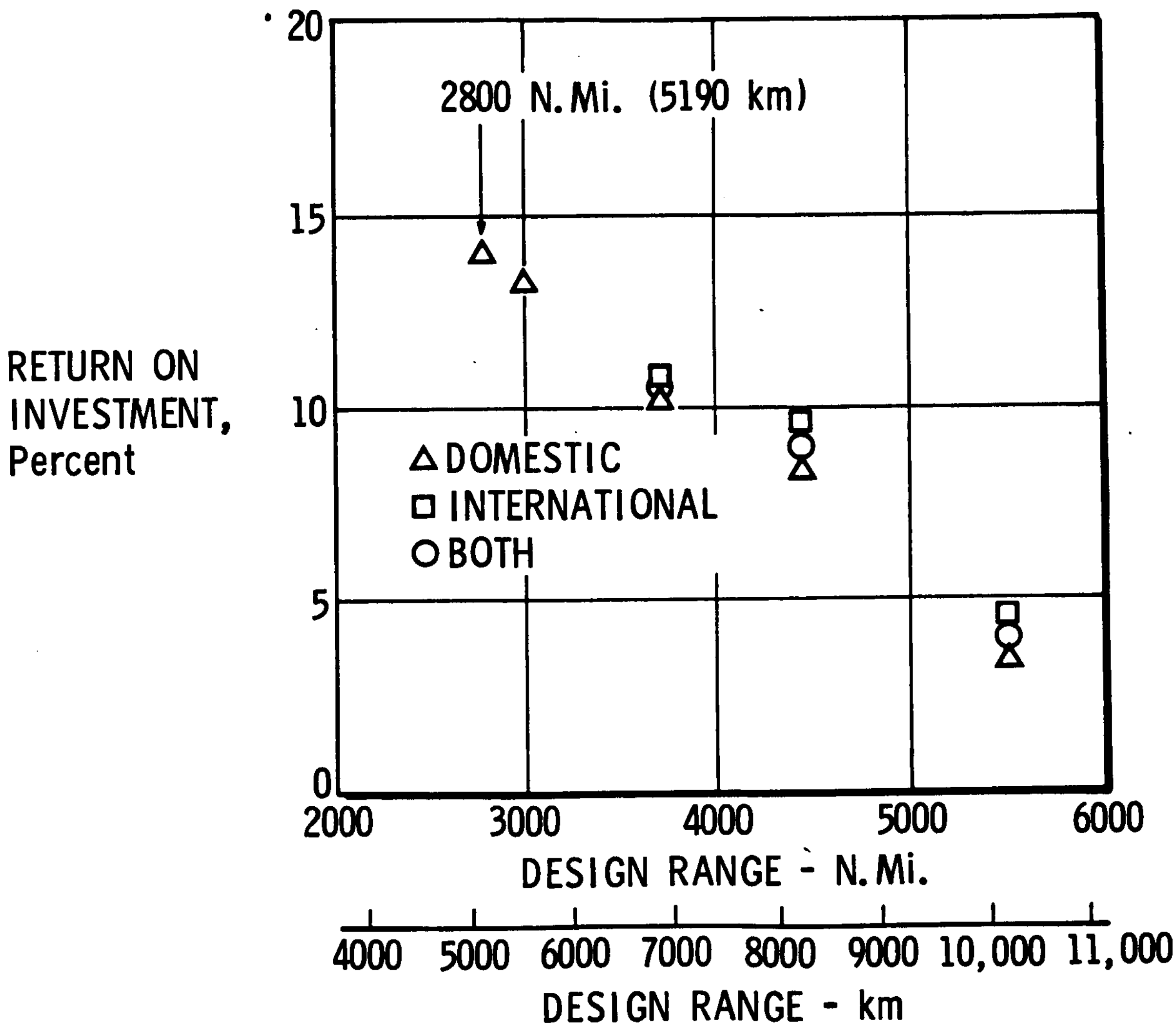

Figure 6.2-2 Design Range Selection, High-Performance Configuration

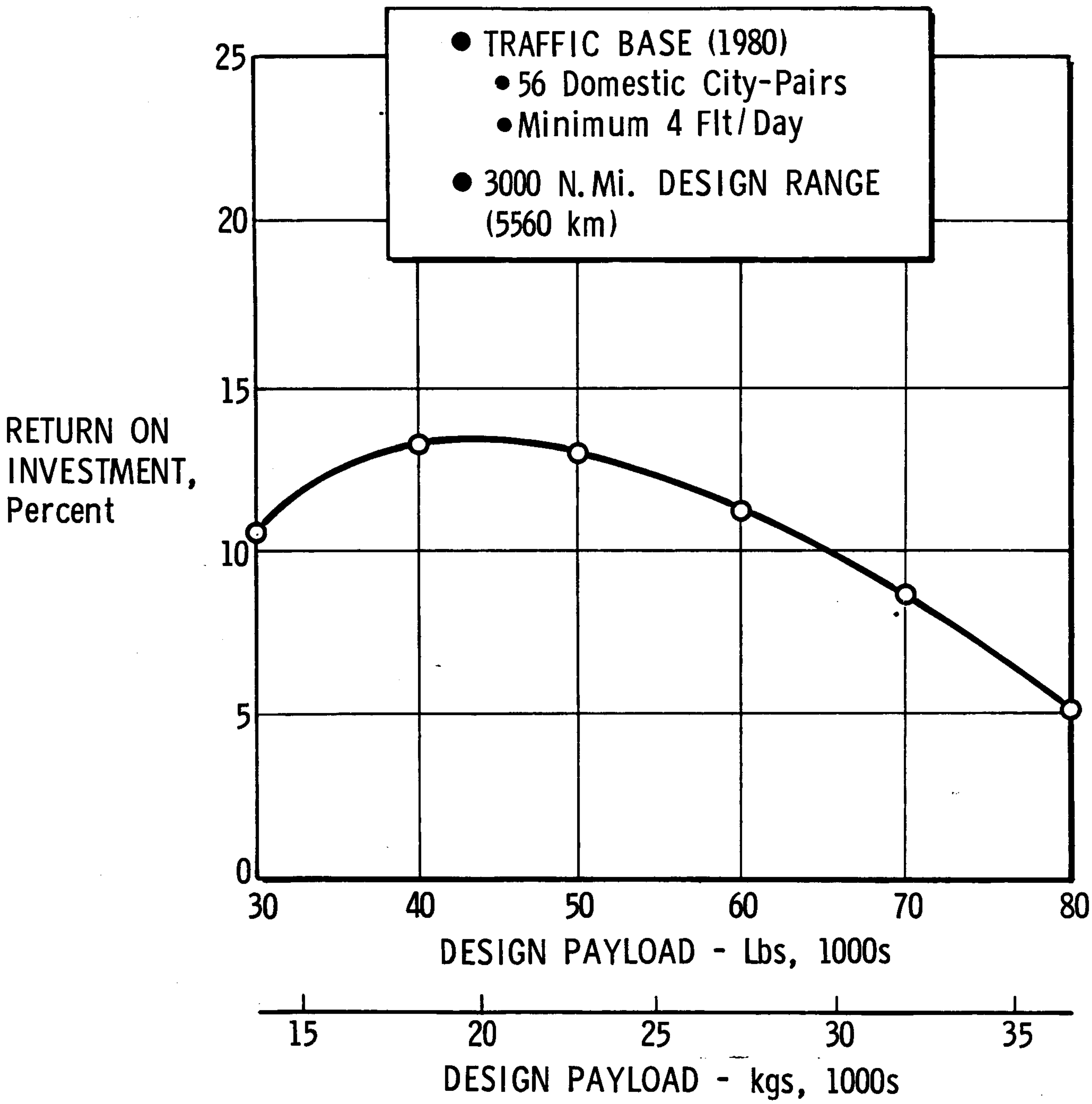

Figure 6.2-3 Design Payload Selection, High-Performance Configuration

Table 6.2-1 Selection of Alternate Configuration Speed

● 40,000-Lb PAYLOAD (18,140 kg) ● 3000-N.Mi. RANGE (5560 km) ● D.O.C. @ 1000 N. Mi. (1853 km)

DESIGN MACH NUMBER	0.87	0.91	0.95	0.98
FLEET SIZE	299.0	277.1	270.4	267.1
FLYAWAY COST ($M)	11.69	12.12	12.56	13.36
EACH ENGINE COST ($M)	0.706	0.721	0.738	0.784
INVESTMENT TOTAL ($B)	4.15	3.98	4.02	4.21
CREW ($/N.Mi.)	0.4426	0.4293	0.4162	0.4134
($/km)	(0.2388)	(0.2317)	(0.2246)	(0.2231)
FUEL & OIL ($/N.Mi.)	0.4484	0.4584	0.4777	0.5280
($/km)	(0.2420)	(0.2474)	(0.2578)	(0.2849)
INSURANCE ($/N.Mi)	0.1486	0.1499	0.1509	0.1586
($/km)	(0.0802)	(0.0809)	(0.0814)	(0.0856)
MAINTENANCE ($/N.Mi)	0.7825	0.7898	0.7976	0.8451
($/km)	(0.4222)	(0.4262)	(0.4304)	(0.4560)
DEPRECIATION ($/N.Mi.)	0.5718	0.5762	0.5800	0.6095
($/km)	(0.3086)	(0.3109)	(0.3130)	(0.3289)
D.O.C. ($/N.Mi.)	2.3938	2.4036	2.4225	2.5547
($/km)	(1.2917)	(1.2970)	(1.3072)	(1.3785)
R.O.I.	16.5%	17.1%	16.7%	14.9%

increase systematically with speed, and the increase is steeper at higher speeds. Fleet size reductions counter this increase in unit costs up to about Mach .93. This is reflected in the total investment (includes spares), which is seen to be very flat between Mach .91 and Mach .95.

All elements of DOC except crew cost increase with speed; crew costs decrease, reflecting the greater route miles covered per hour of duty time.

When operating costs and investment requirements are combined with passenger demand and fares to develop ROI, ROI increases to a peak near Mach .90-.92 and falls rapidly above Mach .95 (Figure 6.2-4). In the speed regime below the peak, productivity increases at a greater rate than direct operating cost. Investment base, measured by flyaway costs and fleet size, decreases sufficiently in this region to offset the increasing direct operating cost.

6.2.4 Selected Configuration

The aircraft selected after the mid-term review with NASA carried a 40,000-lb (18,140 kg) payload for a design range of 3000 n.mi (5560 km) and at design speeds of Mach .98 and .90.

6.3 COST METHODOLOGY

The aerodynamic optimization of both the Mach .90 and Mach .98 airplanes is discussed in Section 5 of this volume. In the following discussion, the general methodology used to support those studies is described.

For each family of airplanes a definition was provided in terms of weight, thrust, block fuel, block time, and unique technology features. The aircraft thus defined were individually costed, and direct operating cost and return on investment data were then generated. For example, in the case of the aspect-ratio selection, a family of aircraft ranging from aspect ratio 5 through 9 was studied to develop flyaway costs, direct operating costs, and return on investment as a systematic function of aspect ratio. Figure 6.3-1 illustrates the approach for a typical configuration. Similarly, for initial cruise altitude and wing sweep, aircraft were evaluated economically. In all cases, the aircraft selected in the aerodynamic optimization process were those which yielded highest return on investment. This did not

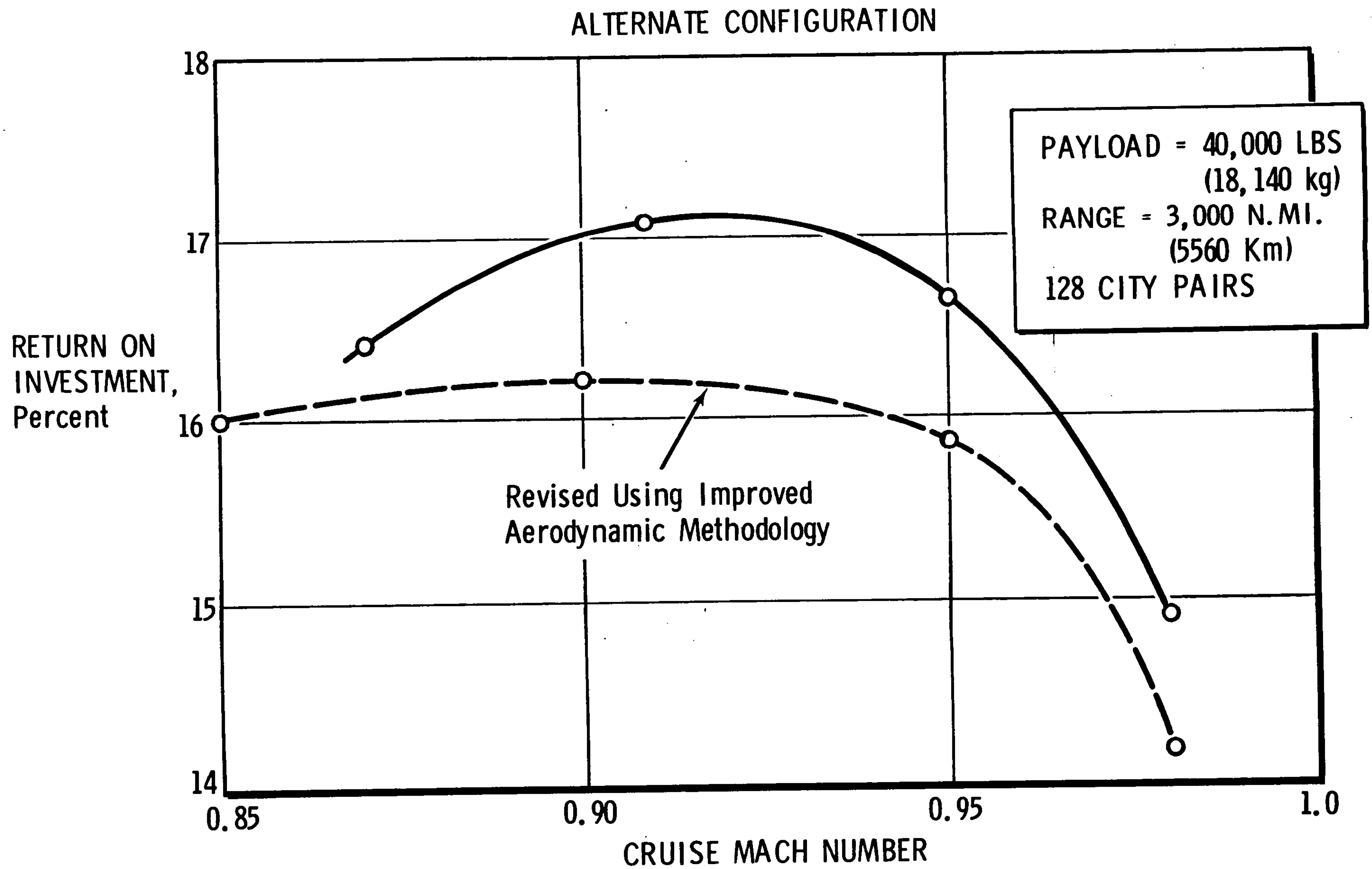

Figure 6.2-4 RETURN ON INVESTMENT Vs SPEED

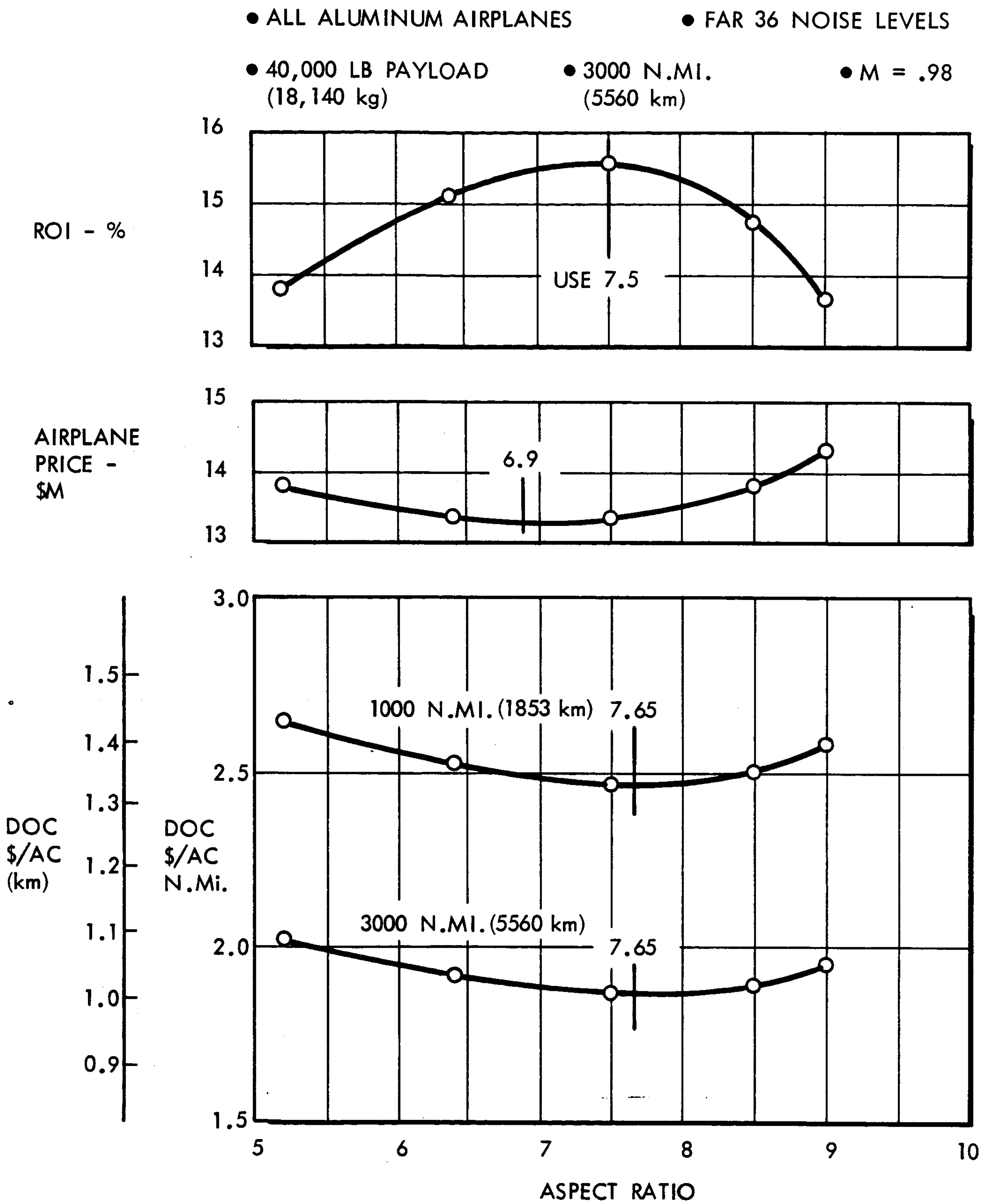

Figure 6.3-1 Aspect Ratio Selection

always correspond with minimum direct operating cost since in some cases the impact of flyaway cost on return on investment is enough to drive the ROI optimum slightly away from the DOC optimum. This is shown on Figure 6.3-1, where the minimum-cost airplane is at aspect ratio 6.9 and, because of better fuel economy, DOC is lowest at aspect ratio 7.65. ROI, being influenced both by flyaway cost and DOC, is highest at an aspect ratio of 7.5.

6.4 TECHNOLOGY EVALUATION

6.4.1 Degree of Composite Usage

As shown in Table 6.4-1, a family of aircraft having different degrees of composite application were studied. The initial baseline is the all-aluminum aircraft with a flyaway cost of $13.76M and a return on investment of 14.78 percent. Applying composites to the wing and tail results in both a reduced flyaway cost and an increased return on investment. Alternatively, applying composites to the fuselage, nacelle, and tail while retaining an aluminum wing results in an even greater decrease in flyaway cost and increase in return on investment. This is the result of two primary factors. First, the aircraft size is reduced significantly through application of composites and, second, in the case of the fuselage, the labor cost of the composites is somewhat below that for a comparably sized aluminum fuselage, thus resulting in a cost which decreases faster per pound of composite applied in the fuselage relevant to the wing. This happens even though the absolute weight savings is less per pound of composites used.

In the case of an all-composite airplane, further reductions in flyaway cost and direct operating cost occur, with the result that return on investment is increased significantly. For aircraft which fly as often as commercial transports, the saving of weight through application of composites continues to offer a major economic advantage.

6.4.2 Degree of Active Control System Usage

A family of aircraft was examined to determine the specific effects of incorporating various degrees of active control systems. The baseline high-performance aluminum configuration was sized with adequate tail volume for static stability. This results in 7 counts of trim drag when shifts in aerodynamic center and the center of gravity are

Table 6.4-1 Degree of Composite Application

- 0.98M CONFIGURATION
- ACTIVE CONTROL SYSTEM
- FAR 36-10 dB

Parameter	Aluminum	Composite Wing & Tail	Composite Fuselage, Nacelle and Tail	All Composite
Flyaway Cost ($M)	13.67	13.20	13.02	12.68
Direct Operating Cost ($/N.Mi.) ($/km)	2.539 (1.575)	2.455 (1.528)	2.417 (1.502)	2.376 (1.475)
Return On Investment (%)	14.78	15.90	16.11	17.22

considered. As shown in Figure 6.4-1, the ROI for this configuration is 13.78 percent. With the airplane redesigned to incorporate a stability augmentation system, drag is reduced, tail size decreased, and ROI is raised to 14.33 percent (1.040 times baseline). Adding maneuver load and gust alleviation saves enough structure weight to more than offset the added cost of this system, and ROI is increased to 1.087 times the baseline. Incorporating flutter suppression further raises the ROI to 1.115 times that of the baseline. This is accomplished by further reductions in structure weight and re-sizing of the airplane for constant range and payload.

6.4.3 Noise Reduction

As shown on Figure 6.4-2, incorporating noise reduction into an aircraft which just meets FAR Part 36 results in decreased ROI. The first increment (10 dB) below FAR Part 36 is achieved by going from a 1970 technology engine to a 1979 technology engine (P&W STF-429). This engine is slightly heavier, slightly more costly, and slightly less efficient than the less-quiet 1970 technology engine typified by the CF6 or JT9D engines. These changes in weight, cost, and fuel efficiency directly reflect into the lower ROI. Similarly, by going to 15 dB below FAR Part 36 with the 1985 technology engine (P&W STF-433), return on investment is further eroded. Taking this latter configuration and increasing aircraft thrust-to-weight in order to achieve noise reduction by being at a higher altitude over the takeoff and approach measuring points will achieve a further reduction. This increased thrust-to-weight ratio causes the aircraft to grow in size and results in the ROI degradation shown between the last two bars of Figure 6.4-2.

6.4.4 Aerodynamic Technology Evaluation

To serve as a standard of comparison with the Mach .90 and Mach .98 airplanes, a conventional aircraft of equivalent range and payload was sized. This conventional aircraft could be considered typical of DC-10 and B747 technology. The relative return on investment of the conventional airplane, the M .90 airplane, and the M .98 airplane is shown in Figure 6.4-3. These aircraft are all-aluminum designs which meet FAR Part 36 minus 10 EPNdB noise levels. This is done for the purpose of illustrating the isolated effect of aerodynamic technology. The major conclusion drawn from this evaluation is that through advanced aerodynamic

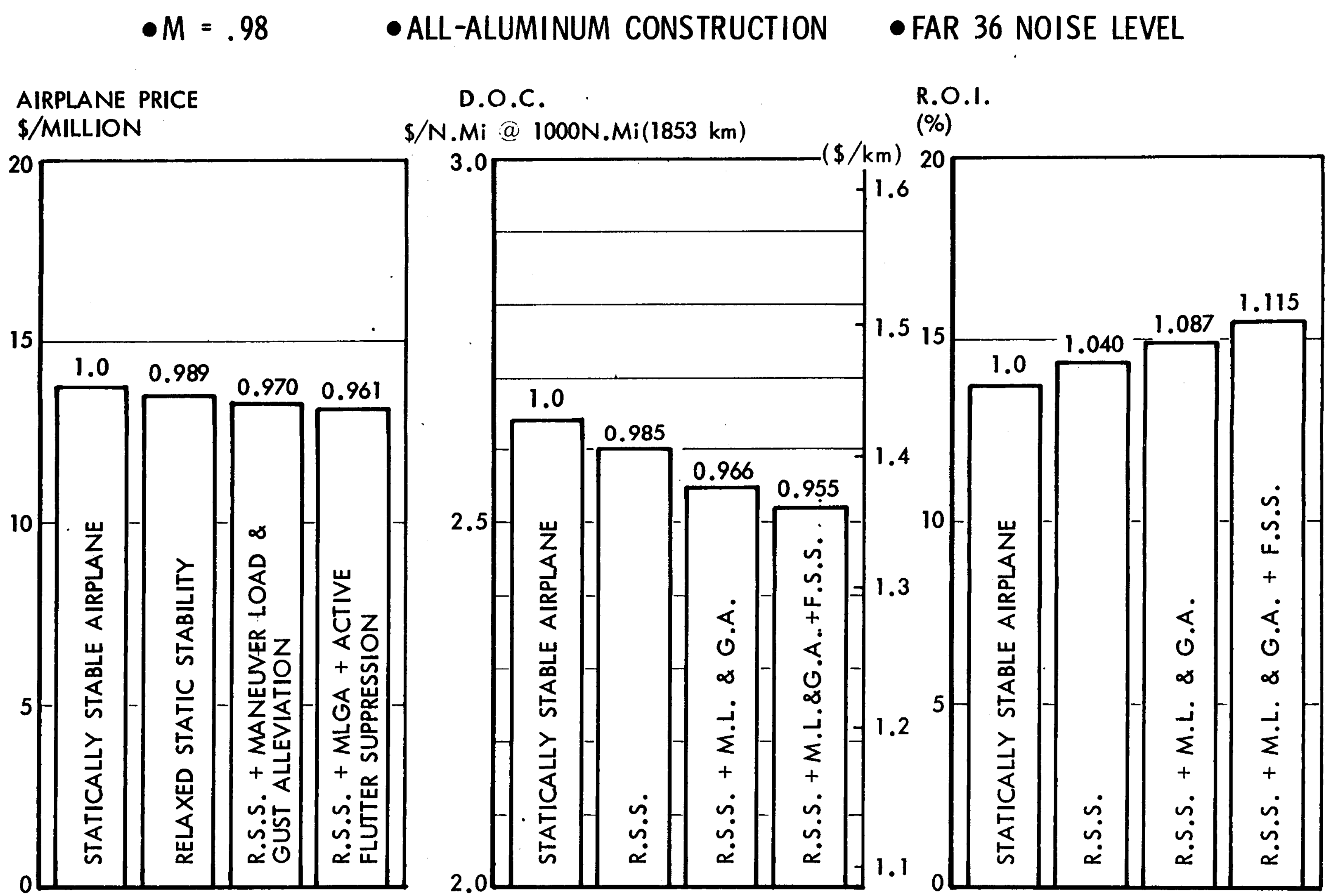

Figure 6.4-1 Economic Benefits of Active Control Systems

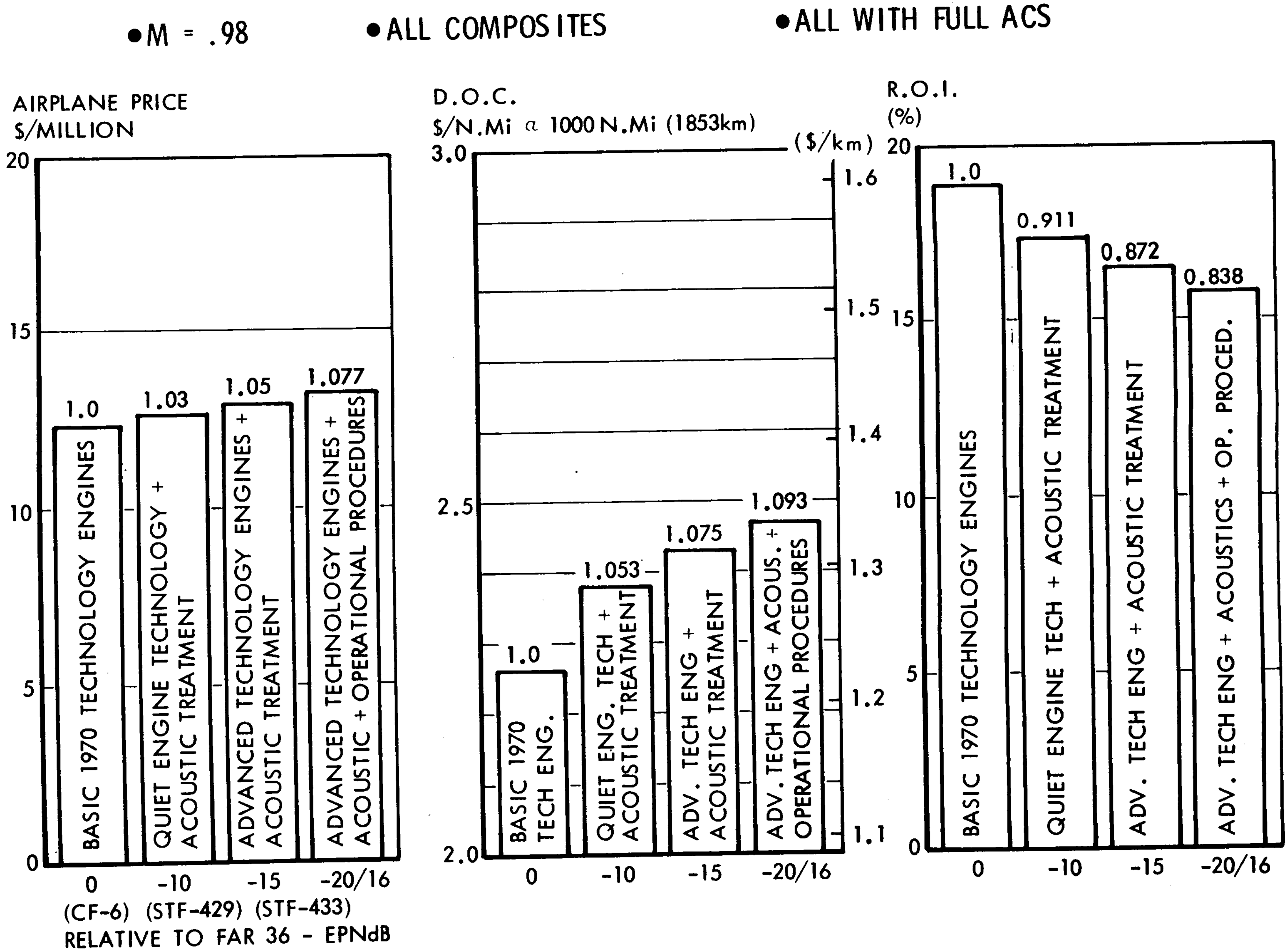

Figure 6.4-2 Economic Impact of Noise Reductions

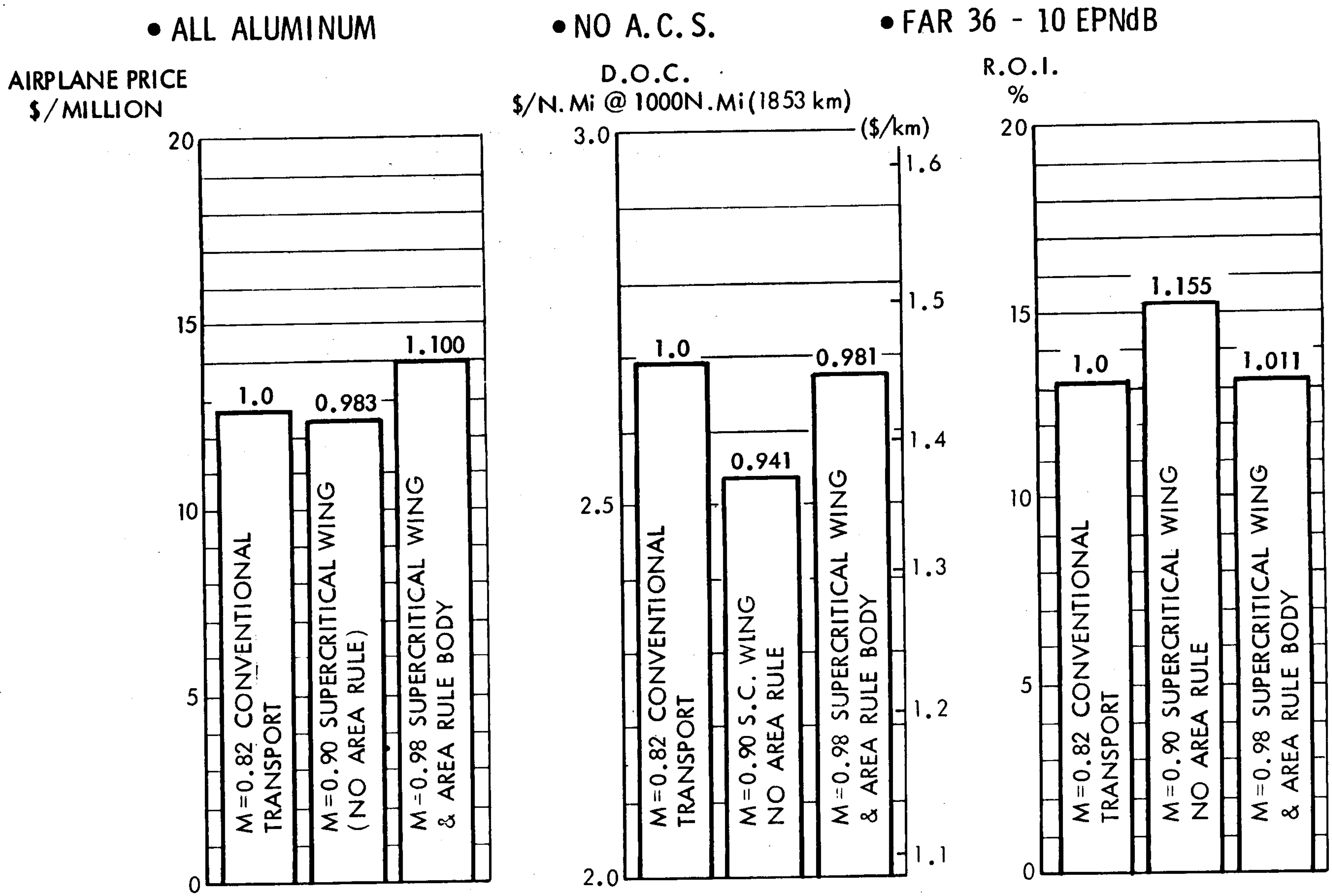

Figure 6.4-3 Economic Effects of Supercritical Technology

technology it is possible to achieve a dramatic increase in ROI at a modest increase in speed (Mach .90) or a modest increase in ROI with a major increase in speed (Mach .98).

6.5 COST OF SELECTED AIRPLANES

Cost analyses for two selected aircraft have been prepared in greater detail than the cost analyses used in the aircraft design selection process. The analysis procedures used for the Mach .98 aircraft will be discussed. The same calculation forms and the same procedures were used on the analysis of the Mach .90 aircraft. All costs are based upon 1970 dollars.

The analyses are presented in Tables 6.5-1 through 6.5-6, three pages for each aircraft. The first page shows a cost breakdown of the aircraft structure and subsystems. The analysis procedures are explained later. The next page examines the research and development costs to be expected for design, development, testing, and technical data. The third page sums the figures from the other pages and adds costs for production-sustaining engineering, production-rate tooling, tooling maintenance, production technical data, and warranty expense.

The analysis is started by completing the first-unit cost form. This form contains a listing of the structural parts and subsystems to be assembled into a whole airplane. An estimate of the first-unit cost is obtained for each structural assembly or subsystem listed. To aid in making this estimate, the weight of the subsystem is provided and a plot of available cost data as a function of weight is used. Data plots and cost estimating relationships for most of the subsystems have been published in Reference 6-1, which has been submitted as part of the ATT study contract.

Since the two final aircraft selected both use composite material designs, the four structural elements (wing, tail, fuselage, and nacelles) are estimated by other analysis methods. A cost comparison study was undertaken by the industrial estimating department at the Fort Worth operation of General Dynamics. Composite structure cost data for that study have been used to establish values for the unit cost analysis of the .98M and .90M airplanes. First-unit structure costs entered in the form are based upon these results adjusted for weight differences.

Table 6.5-1

ATT .98 MACH COMPOSITE AC

FIRST UNIT COST ANALYSIS

Item	Weight	First Unit Cost	Learning Percentage	# AC = 250 Cumulative Factor	# AC = 250 Total $ (Millions)
Wing	26,300	3.06	.85	88.8	$272.
Tail	5,150	1.02	.85	88.8	91.
Fuselage	28,075	3.53	.85	88.8	313.
Landing Gear	12,545	.98	.83	76.8	75.
Flight Controls	4,210	1.08	.87	102.6	111.
Nacelles	4,470	.91	.85	88.8	81.
Total Structure Wt	80,750				
Water Injection System	265	.08	.85	88.8	8.
Fuel System	1,525	.37	.83	76.8	28.
Engine Controls	195	.05	.85	88.8	4.
Starting	140	.04	.85	88.8	4.
Reversers	2,105	.46	.87	102.6	48.
Total Propulsion Assoc Wt	4,230				
Hydraulics	1,960	.48	.87	102.6	49.
Instruments	1,740	1.05	.90	126.9	133.
Electrical	3,217	.84	.87	102.6	86.
Furnishings	23,169	1.73	.85	88.8	154.
Air Conditioning & Anti-Ice	3,990	.56	.85	88.8	50.
Auxiliary Gear	45	.01	.85	88.8	1.
APU	908	.20	.87	102.6	21.
Total Subsystem Wt	35,029				
Subtotal Costs		16.45			
Factory Assembly .125 × Total		2.06	.81	66.2	136.
Mission Equip Assembly .04 × Avionics		.04	.81	66.2	3.
Factory Acceptance .04 × Total		.76	.81	66.2	50.
Engines (P&W-STF-429)	14,959	2.51	1.00	250.0	628.
Avionics		.91	.97	205.0	187.
Total Cost		$22.74			$2,533.

Table 6.5-2

NON-RECURRING -- RDT&E

ATT .98 Mach Composite A/C

Precontract Gov't. Funded Studies	Not App.
Airframe Design	
$194\ (119{,}000 \times 1.3\ \text{lb.})^{.82}\ (M = .98/.9)^{1.15} = 3{,}870{,}000$ hrs	
3,870,000 hrs x $20.00/hr =	$ 77,300,000
Air Vehicle Integration	
Airframe Design $77,300,000 x .35 =	27,050,000
Integration Engr. Hours = 3,870,000 Design Hrs. x .35 = 1,360,000 Hrs.	
Propulsion Development	0
Avionics Development	0
Development Shop & Material Support	
$20.50 x (3,870,000 Design Hrs. + 1,360,000 Integr. Hrs.) =	107,200,000
Basic Tooling	
(Factor Value 40 x 1.35) x 119,000 lbs. Airframe Wt. ($16.70) =	107,400,000
AGE Development & Procurement for R&D	
10% x Flt. Test Recurring Prod. $35,000,000 =	3,500,000
Training Equipment Development & Procurement for R&D	0
Test Aircraft & Refurbishment (1 1/2 AC equivalent)	34,100,000
Flight Test Operations	
$0.137\ (119{,}000 \times 1.3\ \text{lbs})^{.93}\ (750\ \text{knots})^{.98}\ (3\ A/C)^{1.32}$	
= 9170 x 650 x 4.26 =	25,400,000
Technical Data	
0.018 x (Design + Integration + AGE + Training + Test + Recurring R&D A/C) =	5,150,000
Total (excluding Tooling)	279,700,000

Table 6.5-3

ATT .98 COMPOSITE AC

	Investment (Millions)
Shop, QC, & Material Cost for 250 AC. (From First Unit Analysis Sheet)	$2533.0M
Sustaining Engineering = Initial Engr. $(\#AC)^{.2}$ - Initial Engr.	
= 104.35 (3.01) - 104.35 =	197.65
Rate Tooling for 6/Mo. = 0.15 (Basic Tooling) =	16.14
Tool Maintenance = (Basic + Rate) (Delivery Months) (.009)	
= (107.4 + 16.14 (50) (.009) =	50.9
Technical Data -- Manuals, Service Engineering	43.7
Warranty Expense 3 %	105.0
Basic Tooling (From Non-recurring page)	107.4
Non-Recurring R&D	279.7
Total Program	$3333.49M

Total Cumulative Average Cost Per Aircraft

$$= \frac{\text{Total Program}}{250} = \qquad \$\ 13.33\text{M}$$

Table 6.5-4

ATT .90 MACH COMPOSITE AC

FIRST UNIT COST ANALYSIS

Item	Weight	First Unit Cost	Learning Percentage	# AC = 250	
				Cumulative Factor	Total $ (Millions)
Wing	20,070	2.48	.85	88.8	$220.
Tail	4,450	.90	.85	88.8	80.
Fuselage	24,870	3.26	.75	88.8	289.
Landing Gear	11,393	.87	.83	76.8	67.
Flight Controls	3,830	1.03	.87	102.6	106.
Nacelles	3,410	.69	.75	88.8	61.
Total Structure Wt	68,023				
Water Injection System	230	.07	.85	88.8	6.
Fuel System	1,325	.33	.83	76.8	25.
Engine Controls	195	.05	.85	88.8	4.
Starting	140	.04	.85	88.8	4.
Reversers	1,780	.39	.87	102.6	41.
Total Propulsion Assoc Wt	3,670				
Hydraulics	1,750	.44	.87	102.6	45.
Instruments	1,740	1.05	.90	167.4	130.
Electrical	3,217	.84	.87	102.6	86.
Furnishings	23,167	1.73	.85	88.8	154.
Air Conditioning & Anti-Ice	3,990	.56	.85	88.8	50.
Auxiliary Gear	45	.01	.85	88.8	1.
APU	908	.20	.87	102.6	21.
Total Subsystem Wt	34,817				
Subtotal Costs		14.94			
Factory Assembly .125 × Total		1.87	.81	66.2	124.
Mission Equip Assembly .04 × Avionics		.04	.81	66.2	3.
Factory Acceptance .04 × Total		.64	.81	66.2	42.
Engines (P&W-STF-429)	12,263	2.29	1.00	250.0	573.
Avionics		.91	.97	205.0	187.
Total Cost		$20.69			$2,319.

Table 6.5-5

NON-RECURRING -- RDT&E

ATT .90 Mach Composite AC

Precontract Gov't. Funded Studies	Not App.
Airframe Design	
$194\ (105,620 \times 1.3\ \text{lb.})^{.82}\ (M = .9/.9)^{1.15} = 3,220,000$ hrs	
3,220,000 hrs x $20.00/hr =	$ 64,400,000
Air Vehicle Integration	
Airframe Design $64,400,000 x .35 =	22,500,000
Integration Engr. Hours = 3,220,000 Design Hrs. x .35	
= 1,130,000 hrs.	
Propulsion Development	0
Avionics Development	0
Development Shop & Material Support	
$20.50 x (3,220,000 Design Hrs. + 1,130,000 Integr. Hrs.) =	89,000,000
Basic Tooling	
(Factor Value 40 x 1.35) x 105,600 lbs. Airframe Wt. ($16.70) =	95,300,000
AGE Development & Procurement for R&D	
10% x Flt. Test Recurring Prod. $32,000,000 =	3,200,000
Training Equipment Development & Procurement for R&D	0
Test Aircraft & Refurbishment (1 1/2 1st AC equivalent)	31,100,000
Flight Test Operations	
$0.137\ (105,600 \times 1.3\ \text{lbs.})^{.93}\ (680\ \text{knots})^{.98}\ (3\ A/C)^{1.32}$	
= 8230 x 600 x 4.26 =	21,100,000
Technical Data	
0.018 x (Design + Integration + AGE + Training + Test + Recurring R&D A/C) =	4,160,000
Total (excluding Tooling)	235,460,000

Table 6.5-6

ATT .90 COMPOSITE AC

	Investment (Millions)
Shop, QC & Material Cost for 250 AC (From First Unit Analysis Sheet)	\$2319.0M
Sustaining Engineering = Initial Engr $(\#AC)^{.2}$ - Initial Engr.	
= 86.9 (3.01) - 86.9 =	174.1
Rate Tooling for 6/Mo. = 0.15 (Basic Tooling) =	14.3
Tool Maintenance = (Basic + Rate) (Delivery Months) (.009)	
= (95.3 + 14.3) (50) (.009) =	49.4
Technical Data -- Manuals, Service Engineering =	
(Shop + Sustaining Engr.) x .016 =	40.0
Warranty Expense 3% of total	94.5
Basic Tooling (From Non-recurring page)	95.3
Non-recurring R&D	235.5
Total Program	\$3022.1M
Total Cumulative Average Cost Per Aircraft	
$= \frac{\text{Total Program}}{250} =$	\$ 12.09M

When this predesign method of estimating is used, it is desirable to investigate design features of the structure assemblies or subsystems that will have unusual cost impact. In most cases the analyst will want to adjust chart values to account for unusual features.

The ATT flight control system does have unusual attributes, therefore requiring a more detailed look at design features to determine cost deltas to add to chart values since the charts reflect conventional designs. The ATT designs considered are unique in two respects. First, conventional aircraft are designed to be stable in the pitch mode at cruise speeds without a control system input, whereas ATT uses stability augmentation. Second, there are the additional active control system features on ATT. Figure 6.5-1 shows cost deltas over and above costs associated with weight deltas for these unique ATT control system features. The figure shows $100,000 as the first cost delta in going from the conventional flight control system to the augmented stability system. This cost delta was arrived at by study of the following electronic design differences.

Design delta reverting to a conventional balance basic mechanical flight control system:

1. Delete quad rudder pedal position sensors.
2. Replace quad control column and control wheel position sensors with dual sensors.
3. Delete one Air Data Computer.
4. Delete one digital flight control computer. Two remaining computers can be of reduced computing capacity.
5. Replace quad 2-axis accelerometer package with dual.
6. Replace quad 3-axis gyro package with dual.
7. Delete quad engine control servo units.
8. Add control cables from control columns and rudder pedals to surface actuators.
9. Add dual yaw damper servo.

	Straight Mechanical System (880 or DC-10 Type)	Augmented Stability (ATT Baseline)	Augmented Stability Maneuver & Gust Alleviation & Flutter Suppression (ACS)
WEIGHT	3810 lb (1730 kg)	3850 lb (1750 kg)	4210 lb (1910 kg)
Δ COST PER AIRCRAFT	$100,000 +Weight Effect		$135,000 +Weight Effect

Figure 6.5-1 Control System Cost Differences

10. Add dual roll and yaw parallel autopilot servos.

11. Add controller from throttles to engines.

12. Add artificial feel package (Q-Pots).

The cost delta in going from the augmented stability design to the augmented stability plus ACS was found to be $135,000, based upon study of the electrical design differences. The trade-off cost delta used was a cumulative average of $200,000, but it was found that $70,000 of this was attributable to increased complexity in the wing by reason of the extra control surfaces required which are part of the wing structure.

Design delta reverting to the augmented stability system from the ACS plus augmented stability system:

1. Delete flutter suppression surface and dual actuators (both sides).

2. Delete outboard trailing edge surface and dual actuators (both sides). These become a plain flap.

3. Delete flutter sensors

   a. 4 gyros per side (8 total).

   b. 4 accelerometers per side (8 total).

4. Reduce flight control computer computation requirements.

The remainder of the subsystem first-unit costs have been discussed in Reference 6-1. Engine costs have been derived from parametric data supplied by Pratt & Whitney for the ATT study. These are the quiet (P&W STF-429)-type engines designed to meet FAR Part 36 minus 10 EPNdB requirements.

Avionics system costs are based upon a review of the avionics equipment list plus an allowance for interconnecting cabling, equipment mounting, antennae installations, etc. This allowance is proportionally greater where the system considers parallel circuit redundancy for reliability improvement.

The avionics complement includes a dual set of communications and beacon equipment, a dual set of navigation equipment for U.S. operations, a triple set of inertial navigation equipment for international operations plus weather radar, and a complete flight data recording system. The cost of these avionics items plus cabling and installation is estimated to average $748,000 for 250 shipsets, with a first unit cost of $910,000.

The column of values on the right side of the first unit analysis form shows costs for the 250 production units considered for the study. Cost-quantity improvement-curve values are shown in the column under "learning." Cost-quantity values have been selected for each subsystem. As a general rule the larger the percentage of purchased parts in the subsystem the higher the cost-quantity percentage, which results in less cost reduction with quantity.

The next analysis sheet, entitled "Non-Recurring—RDT&E," predicts costs for a number of development categories. The initial engineering equation, the engineering integration, and the basic tooling equation have each been discussed in the referenced report. The initial engineering equation, when used to obtain a composite aircraft design estimate, requires an adjustment to the weight input. The present thinking is that the composite aircraft design task will be the same as for an equivalent aluminum aircraft. This assumes that suitable prototype design experience will have been achieved by the time an ATT program is undertaken. To obtain equivalent weight, a 1.3 factor is used under the 0.82 exponent.

The manufacturing development shop and material support to engineering cost is estimated by multiplying design and integration hours by $17.50 for aluminum aircraft or $20.50 for composite designs. The test aircraft and refurbishment cost estimate is based upon standard commercial flight test program practice,which ends up with one aircraft unsaleable and refurbishment costs such as test instrumentation removal and repair for delivery equal to the cost of one-half an aircraft. Flight test operations cost is estimated by use of an equation developed by Rand Corporation and is in agreement with Convair commercial experience.

The "Investment" cost summary page brings together program costs computed on the other pages and introduces additional ones associated with production and delivery. Equations for these costs are shown with the calculations.

The effect of quantity of aircraft purchased upon the cost per aircraft is illustrated in Figure 6.5-2. This figure shows two major effects which contribute to the lowering of per aircraft cost as a function of quantity delivered. One effect is the production cost-quantity cost reduction shown by the triangular segment in the center of the figure. The second effect is the proration of the development and tooling cost shown by the curved triangular segment at the top of the figure. The shaded area in the upper left corner indicates tooling and production support costs which would not be incurred if it were known in advance that only a few aircraft would be produced. In the figure the topmost line, as perhaps modified by the shaded area, indicates the declining cost per aircraft as delivery quantity increases.

One aspect of cost not mentioned is concerned with the capital facilities and equipment required for extensive composite manufacture. A listing of capital equipment and facilities improvements has been prepared and is presented in Table 6.5-7. This list represents about the level of capital equipment and facilities needed by a manufacturer to undertake the manufacture of 250 transport aircraft designed from composite materials. Most of the capital is required for tape-laying machinery, which would be of new design. In general, the tape-laying equipment is expected to be considerably larger than any currently existing.

The $15.25M outlay indicated in the table would represent an initial increase in overhead burden of between 1 and 2 percent on an ATT size program. This outlay would represent an overhead burden increase over the aluminum fabrication case only in facilities where the aluminum fabricating machinery already existed in adequate quantity to support an ATT program. Despite the initial small increase in burden rate due to composite manufacturing start-up, the relative machine cost burden for a shop emphasizing graphite composite manufacture is expected to decrease in time compared to an aluminum fabricating shop. This is so since, if one started with no equipment and bought either composite application equipment or aluminum fabricating equipment for a plant meeting fixed aircraft production requirements, the composite equipment investment would be less.

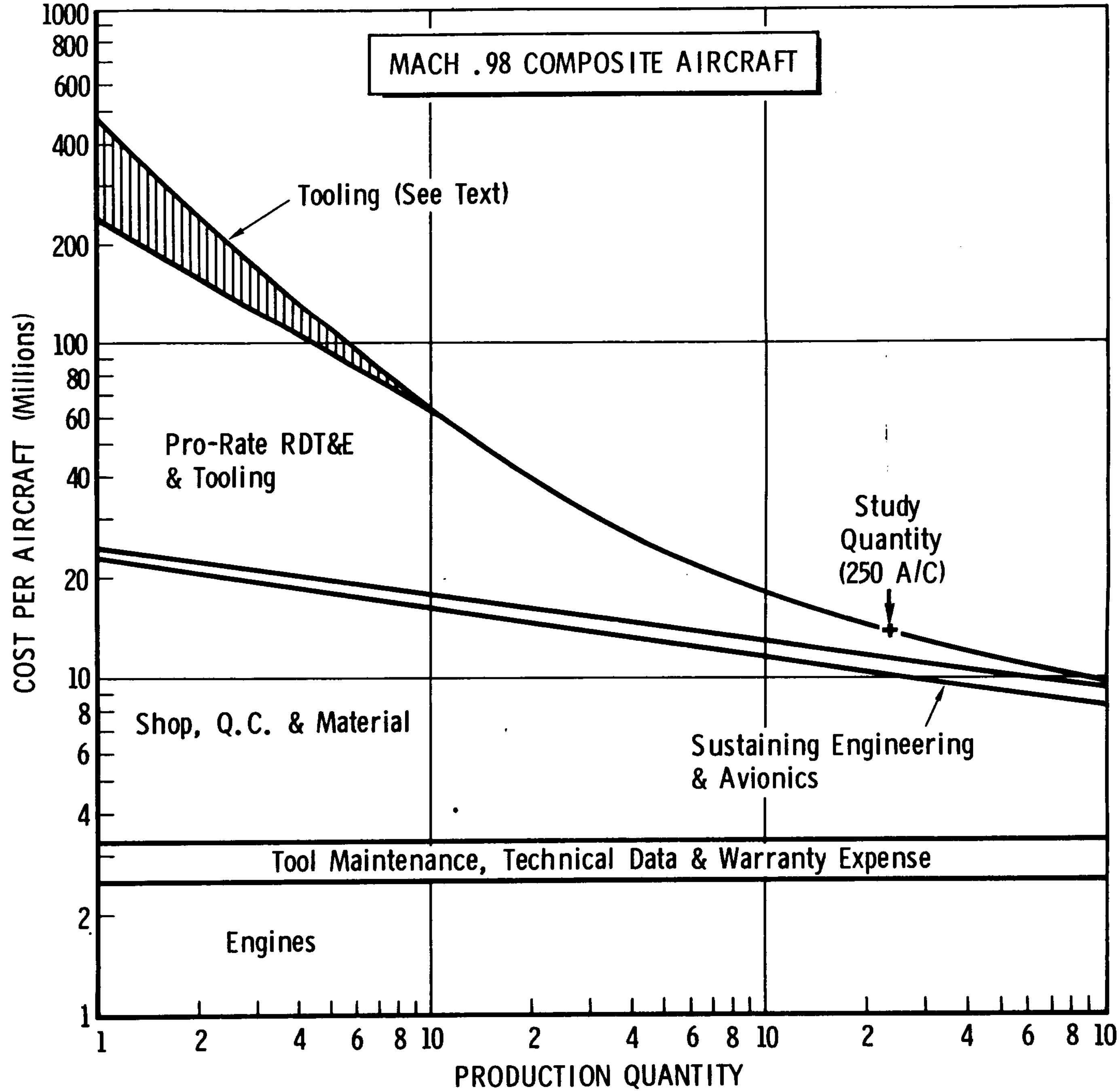

Figure 6.5-2 Effect of Production Quantity on Airplane Cost

Table 6.5-7

GRAPHITE COMPOSITE MANUFACTURING FACILITIES LISTING

	Quantity	Cost
A. Fuselage		
1. Tape Laying Machine, 24' (7.3 m) Gantry	6	$ 2,570,700
2. Tape Laying Machine, Gantry, 3' x 130' (0.91m x 39.6m)	2	465,400
3. Tape Laying Machine, Gantry, 8' x 30' (2.44m x 9.13m)	2	587,300
4. Tube Wrapping Machine	4	146,470
5. HOBE Saw, Band, 36" (0.91m) with Collection System	2	36,500
6. Core Sander, 36" (0.91m)	2	118,100
7. Forming Roll, 10 Stage	3	89,950
8. Vacuum Curing System	-	42,000
B. Wing		
1. Tape Laying Machine, Moving Column, 18' (5.49m) Wide	12	5,140,200
2. Tape Laying Machine, 8' (2.44m) Gantry	3	778,250
3. Tape Laying Machine, Gantry, 8' x 30' (2.44m x 9.13m)	2	587,300
4. Vacuum Curing System	-	42,000
5. Curing Oven, $250^{o}F \pm 15$, ($394.1^{o}K \pm 8.3^{o}$) 6' x 25' x 100' (1.83m x 7.62m x 30.48m)	3	697,825
C. Inspection		
1. Strip Slicing Machine	1	12,000
2. Infrared Scanning System	2	75,850
3. In Motion Radiography Sys.	4	461,500
4. Ultrasonic System, 10 Chan.	4	778,900
5. Other Inspection Equipment	-	200,000
D. General		
1. Plaster Mixer	2	44,300
2. Support Equipment & Installations	-	1,275,000
E. Utilities		
1. Steam lines, Filtered Air, etc.	-	1,100,000
Total		$15,249,545

6.6 SENSITIVITY ANALYSIS

The selected high-performance and alternate configurations were analyzed to determine economic sensitivity to technical and cost changes. The systematic variations made to the selected baseline designs are summarized in Table 6.6-1. Where technical changes occur, the resulting aircraft are resized to retain equal range and payload. For example, an increase in drag will induce a larger engine size, increased fuel load, and concomitant changes in supporting systems. These in turn affect flyaway costs as aircraft definition changes. Fuel requirements, weights, and hardware costs influence direct operating costs and, similarly, return on investment is driven by investment and operating costs.

The sensitivities are essentially linear within the credible ranges -- as illustrated by relative impact of the changes shown in Figure 6.6-1. The amount of variation shown represents a "reasonably credible" variation in the independent parameters. Each analyst can by linear interpolation or extrapolation establish sensitivity of ROI to his own credible variation as long as it is reasonably close to the ranges examined.

No attempt was made to re-optimize wing geometry for the range of variations examined.

For the Mach .90 configuration, ROI can be changed one point (18.73 percent to 17.73 percent) by 4300 pounds (1950 kg) of structural weight, 14 counts of drag (L/D average 14.22 to 13.45), 7 percent in airframe cost, or 20 percent in engine cost. Results are fairly similar on the Mach .98 configuration, except that it is slightly more sensitive to aerodynamic efficiency. Doubling the basic cost of composite raw material from $30 per pound ($66 per kg) to $60 per pound ($132 per kg) would increase airframe cost 10 percent.

Propulsive efficiency changes also have an effect on system economics. A 10-percent change in specific fuel consumption gives a 3.4-percent change in ROI. However, SFC has fairly narrow limits and, as such, should not greatly influence total performance uncertainty.

Table 6.6-1 Sensitivity Summary

.90 CONFIGURATION	FLYAWAY ($M)	D.O.C. $/N.MI. ($/km)	R.O.I. (%)
BASELINE (COMPOSITE & ACS)	11.518	2.299 (1.241)	18.73
+5000 Pounds STRUCTURE (+2270 kg)	11.979	2.364 (1.276)	17.56
+10,000 Pounds STRUCTURE (+4540 kg)	12.450	2.432 (1.312)	16.44
-.002 C_D	11.228	2.205 (1.190)	20.01
+.002 C_D	11.872	2.404 (1.297)	17.33
+ 10% AIRFRAME COST	12.339	2.357 (1.272)	17.32
- 10% AIRFRAME COST	10.698	2.241 (1.209)	20.32
+ 10% ENGINE COST	11.750	2.332 (1.258)	18.12
- 10% ENGINE COST	11.287	2.266 (1.223)	19.36
.98 CONFIGURATION			
BASELINE (COMPOSITE & ACS)	12.677	2.376 (1.282)	17.22
+5000 Pounds STRUCTURE (+2270 kg)	13.158	2.443 (1.318)	16.14
+10,000 Pounds STRUCTURE (+4540 kg)	13.651	2.510 (1.354)	15.12
-.002 C_D	12.172	2.253 (1.216)	18.93
+.002 C_D	13.201	2.501 (1.350)	15.60

• 0.90M CONFIGURATION • ALL COMPOSITES • FULL ACS • FAR36-10 EPNdB

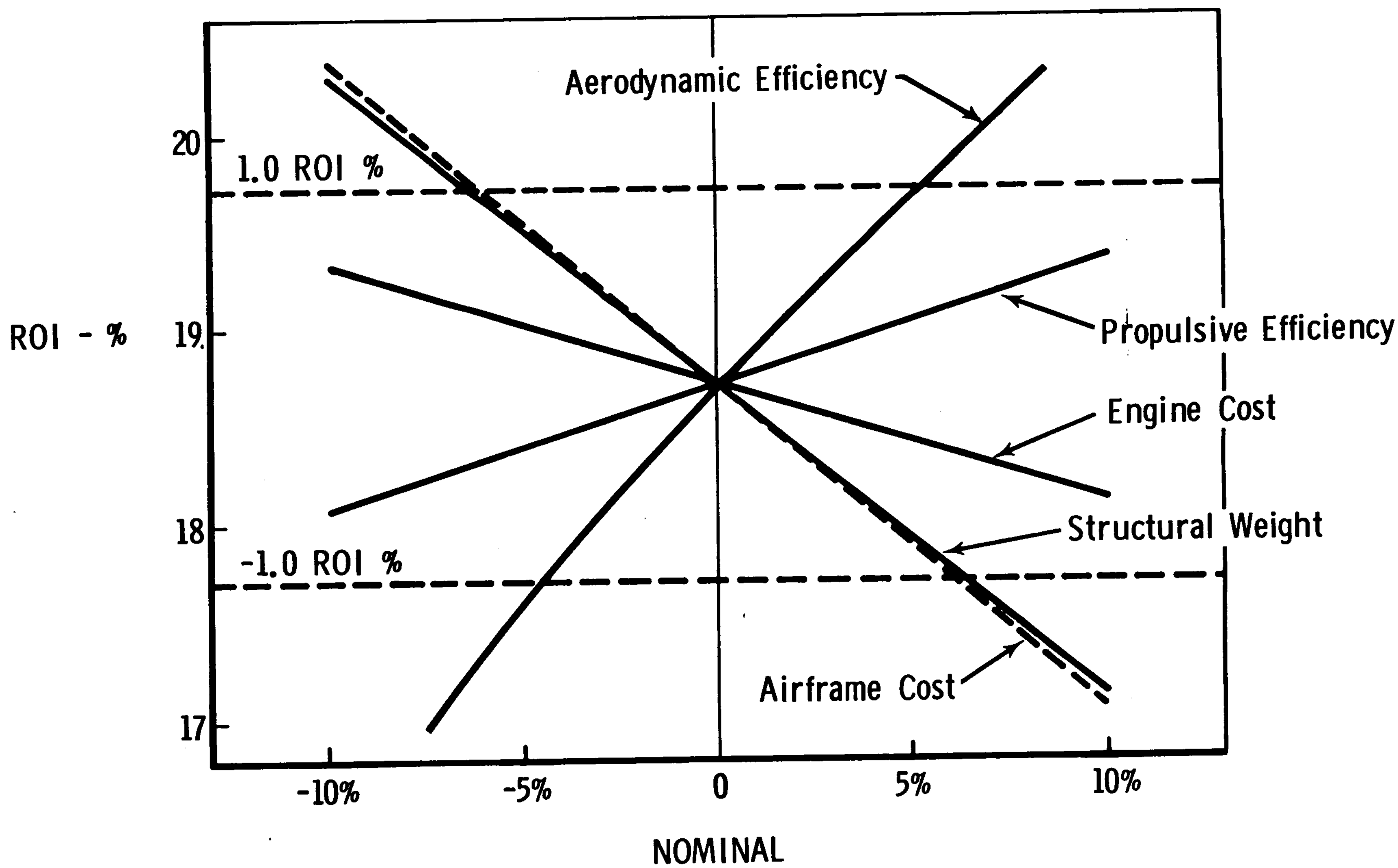

Figure 6.6-1 ECONOMIC SENSITIVITY

After system sensitivity to the major parameters is reviewed and a judgment as to the uncertainty in each parameter is made, it is possible to assess the relative contribution to program uncertainty of each parameter. Those parameters which combine a high degree of sensitivity and uncertainty are natural targets for technology programs that should be able to reduce significantly the uncertainty in system ROI.

A case can thus be built for a full-scale demonstrator to improve prediction of aerodynamic efficiency and to better estimate the structural costs and weights of a large-scale composite structure. If technical uncertainty (or risk) is to be reduced to the point where a firm contract between a manufacturer and an airline is possible, a vigorous technology program must be pursued.

6.7 COMPETITIVE AIRPLANE ANALYSIS

The selected advanced designs have been compared against existing aircraft and those currently on order. A comparison on the basis of seat-mile direct operating cost is shown in Figure 6.7-1. Three technology families are apparent -- supersonic (Anglo-French Concorde), conventional first-generation turbofans, and second-generation wide-body turbofans.

Computed DOC for the Concorde is based on a flyaway cost of $30M. It is clearly shown to be suitable only for premium fare markets. The Soviet IL-62 M200 has a competitive edge against the Boeing 707 only because of a quoted cost of $7M. This is believed to be unrealistically low (should be about $10M). Based on the data of Reference 6-2, the structural and aerodynamic efficiency of the IL-62M200 are somewhat less than the Boeing 707. Accordingly, at a realistic price its DOC should be higher.

Within the wide-bodied, second-generation turbofan class the most striking difference is that of range -- the shorter-range aircraft (A-300B and DC-10-10) are significantly cheaper to operate at their design range than the B747 or DC-10-30. For this analysis the DC-10-10 and L-1011-1 are considered to be interchangeable. As between the DC-10-10 and DC-10-30, this is almost entirely a range difference, as the passenger cabin volumes are equal. At transcontinental ranges the Mach .98 ATT is directly competitive with the wide-bodied transports, and the Mach .90

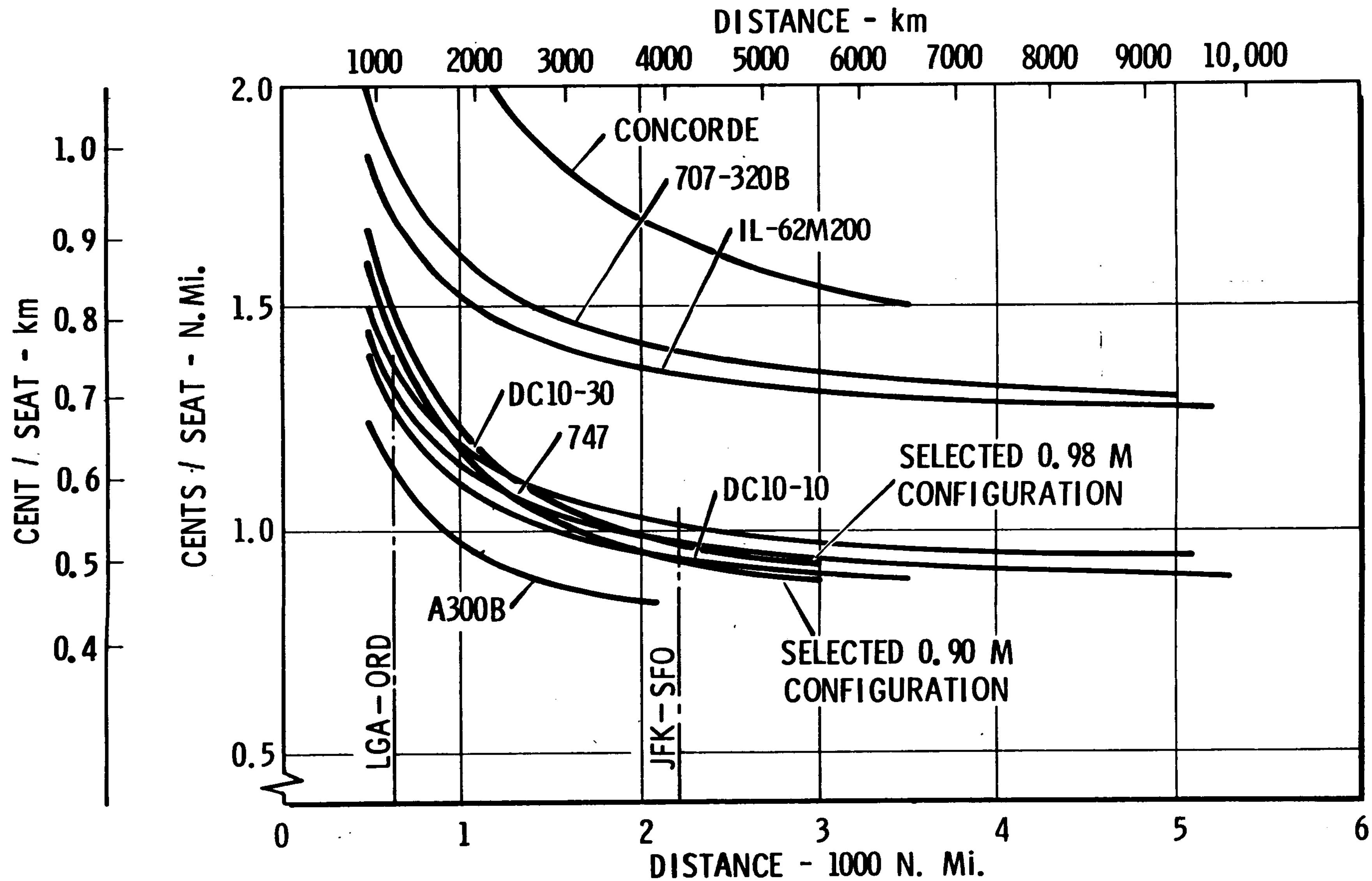

Figure 6.7-1 Comparative Direct Operating Costs

ATT is superior. The relatively steep slope of the DOC-versus-distance curve for the ATT's reflect increased speed. On shorter routes, the faster airplanes cannot utilize their speed advantage.

Seating for this comparison is based on wide-body improved-comfort standards (relative to B707 and DC-8). This amounts to 350 seats in a B747, 270 in a DC-10, and 195 in ATT. With its shorter design range and eloser seat pitch, the twin-engined A-300B airbus, is very economical. Perhaps the greatest lesson here is that the economics of scale can easily be lost even on a seat-mile basis if an extreme-range configuration is desired. This also points out the economics possible within a technology family by tailoring range and payload, as in the case of the DC-8-60 family or the DC-10 family. The effects of range and size scaling are discussed in detail in Reference 6-3.

DOC is an abstract measure of an airplane's economic efficiency. To reduce the analysis to more concrete terms, return on investment data were computed for the route structure described in Section 4. Plotting return on investment for individual city pairs as a function of intercity distance results in an envelope curve which defines the upper and lower ROI's at each distance (Figure 6.7-2). For 1970 traffic, this was done for a B737, B727, and DC-10. Because it is possible to achieve a better load factor with the smaller aircraft, its ROI is consistently best on average out to its range limit. The larger aircraft has a much wider range of values, better on the highest traffic routes and worse on the poorer routes. For the city pairs considered, and these are all relative high-traffic city pairs, the best mix is to use DC-10's at the longer ranges and high-density routes and to assign B737's or B727's as appropriate to the less dense routes.

Note that this does not prevent losses in the short-range market. With the fare structure used (\$7.00 + \$0.056/st.mi)(\$7.00 + \$0.0348/km), there is no way to make a profit at realistic load factors on short flights. Matching aircraft to the traffic will, however, serve to strongly limit losses. For the markets considered, there were <u>no</u> city pairs on which four-engined aircraft were best.

Progressing to 1985 traffic, the picture changes significantly, as shown on Figure 6.7-3. Traffic has now built up to a point (3 times 1970) where the B737 has a

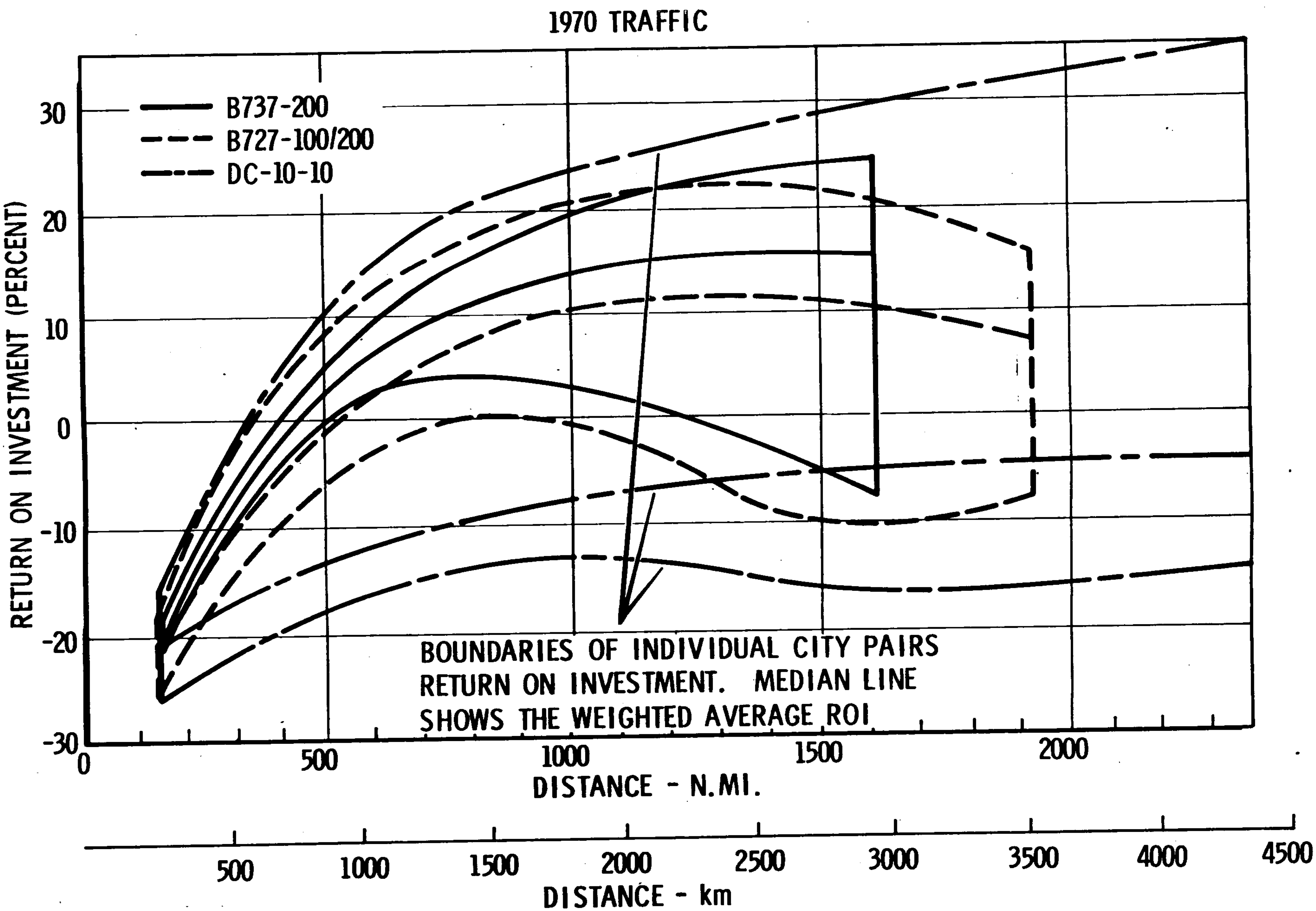

Figure 6.7-2 Comparison of Current Transports

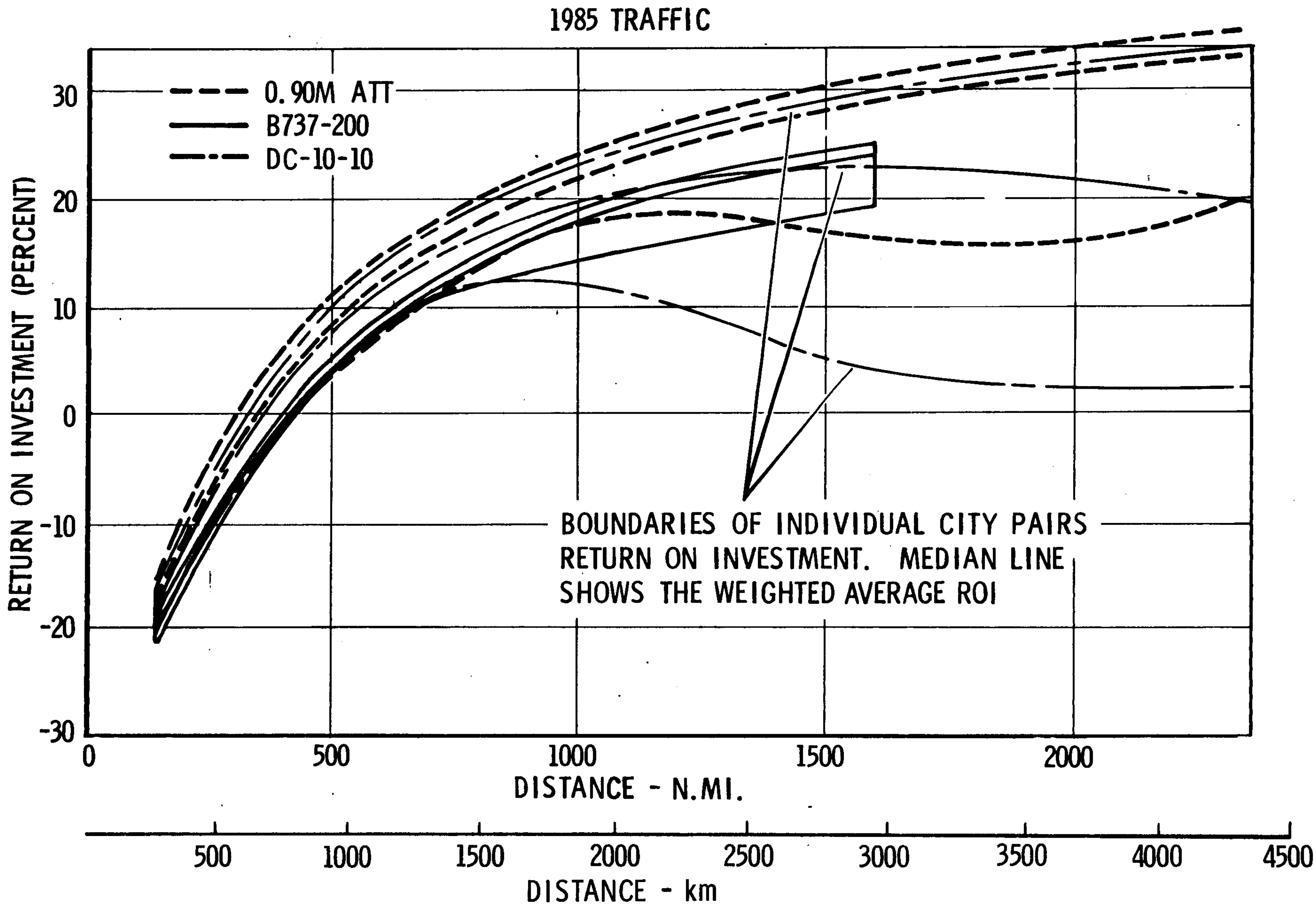

Figure 6.7-3 Comparison of Future Transports

very narrow spread. This is because, for all city pairs, there is now adequate traffic to develop good load factors. Similarly, there are no city pairs beyond 400 n.mi (741 km) where the DC-10 loses money.

At this time period, almost any advanced configuration studied under the current contract can be considered available. The most economical aircraft considered (the Mach .90 composite transport with active control system) is found to be equal to the DC-10-10 in the densest markets and significantly superior to it for the longer-range, less-dense markets. The B737 remains as an economical airplane for medium-range, low-density routes and for short routes. There is no incentive to apply ATT (as sized) to routes under 300 n.mi (556 km).

For 1985, on the high-traffic city pairs examined, the B727 has dropped out as a viable competitor. The major markets are thus expected to be served by wide-bodied trijets (particularly where their size acts to help relieve traffic congestion), a 195-passenger ATT, and a small, short-range twin jet for medium-density routes below about 500 n.mi (927 km) where congestion is not a major problem.

With this assignment logic, the U.S. domestic market for 1985 is estimated to require 600 advanced technology transports of 195 seats and transcontinental range.

Daily system costs for a fleet of airplanes serving the top 128 U.S. domestic city pairs are shown in Table 6.7-1. The traffic served is 48.5 billion passenger miles per year. In 1985, this market share for the hypothetical airline is roughly 15 percent of estimated total domestic traffic. (In terms of today's traffic, the 267 high-performance or 280 alternate-speed airplanes could serve 45 percent of total domestic needs at a load factor of 55 percent. This is done simply as an illustration, since packaging this many people into aircraft this large at today's traffic levels is clearly unrealistic.)

As shown in Table 6.7-1, system-wide indirect costs are about 95 percent of direct costs. This is for a system average passenger trip length of 950 statute miles. Relative to current experience, the advanced transports save more in direct operating cost items such as fuel and maintenance, the technically related items, than in the indirect functions which are passenger related. Accordingly, the

Table 6.7-1

SYSTEM DAILY OPERATING COST SUMMARY

Operation	Mach .98 Final (267 Aircraft)	Mach .90 Final (280 Aircraft)	Remarks
Aircraft Servicing	$517,000	$465,000	f(Gross Weight)
Passenger Service	548,000	548,000	Same pass.
Reservations and Sales	994,000	994,000	Same pass.
Stewardess Cost	255,000	269,000	f(Block Time)
Food	256,000	270,000	f(Block Time)
General and Admin.	236,000	230,000	-
IOC	2,806,000	2,776,000	
DOC	3,005,000	2,899,000	
TOC	5,811,000	5,676,000	
Income	8,429,000	8,429,000	
Gross Profit	2,618,000	2,853,000	
ROI	17.22%	18.73%	

ratio of indirect cost to direct cost is higher for a high-technology transport.

A comparison of the Mach .98 and .90 designs shows a significant difference only in the aircraft servicing account. In spite of the difference in fleet size, each fleet makes the same number of aircraft departures per day, and since aircraft servicing is computed as a function of gross weight, there is a benefit to the smaller, Mach .90 airplane.

E

SECTION 7

STRUCTURAL SYSTEM

DESCRIPTION AND ANALYSIS

7.1 GENERAL

The most significant structural feature in the selected configuration is the maximum use of advanced filamentary graphite composites in the fuselage, nacelles, and lifting surfaces. Such wide-spread use of composites is justified by the results of the Economics Analysis (Section 6). A detailed study of light alloy vs composites for use in this airframe application was made to evaluate weight and cost ratios. The pertinent aspects of this study are the primary content of Section 15. A summary of the most important material selections and applications used in the selected aircraft configurations is presented in Table 7.1-1. The maximum application of composites projected a weight savings of 25 percent on the wing and horizontal tail, 20 percent on the fuselage and vertical tail structure, and 10 percent on nacelle structure, where the respective components are the same size. Absolute maximum weight savings were traded in favor of design simplicity and producibility where such a choice was possible and cost effective.

Although the advantages of composite strength/stiffness characteristics are generally well established and understood, the projected all-out use of composites in an airframe application usually elicits comments and questions about their acceptability as regards fatigue, fracture, and various environmental factors. Section 15, Materials Selection Analysis, contains discussions pertinent to these items.

Sufficient research and prototype experience have been accumulated to justify the decision to commit primary composite structural applications to the F-14 and F-15 tail surfaces. Stiffness (flutter)-critical horizontal tails are being flight tested on an F-111 for service-life experience, and numerous full and fractional scaled laboratory test specimens of wings and fuselages have been or are being constructed and evaluated. Therefore, composite materials are destined to be used in complete airframe

TABLE 7.1-1 SUMMARY OF MATERIAL SELECTIONS AND APPLICATIONS

Component	Type Of Construction	Materials & Application
Wing		
Structural Box		
covering	sandwich	graphite-compsite facings with aluminum honeycomb core
spars	sandwich	graphite-composite channel facings with aluminum honeycomb core
ribs	stiffened sheet	graphite-composite sheet with fiberglass-composite stiffeners
fuel blkhds	sandwich	graphite-composite facings with aluminum honeycomb core
Flaps & Ailerons		
covering	sandwich	graphite-composite facings with aluminum honeycomb core
spars and ribs	stiffened sheet	graphite-composite sheet with fiberglass-composite stiffeners
Vanes		
covering	sandwich	graphite-composite facings with fiberglass or multi-flex honeycomb core
spar	sheet	graphite-composite hat-section
Spoilers & Air Deflection Doors	full depth sandwich	graphite-composite facings with full depth aluminum honeycomb core
L.E. Slats		
basic surface	sheet	membrane of fiberglass reinforced spanwise with graphite-composite laminates
slat nose	wrap-around sandwich	graphite-composite outerfacing, fiberglass inner facing with fiber-glass or multi-flex honeycomb core
ribs	machined	aluminum forging 7075-T73

TABLE 7.1-1 (Continued)

Component	Type Of Construction	Materials & Application
Wing (Continued)		
Fixed Secondary Structure		
fixed leading edge, tip & fairings	sandwich	graphite-compsite facings with aluminum honeycomb core
under struct.	stiffened sheet	graphite-composite laminated sheet with fiberglass stiffening
Misc. Fittings		
flap tracks	machined	D6ac forged steel
support fittings and hinges	machined	machined forgings - aluminum, 7075-T73 or X7050-T73 - steel, D6ac depending on stress level
Fuselage		
external shell	sandwich	graphite-composite laminated facing with fiberglass honeycomb core
frames	formed sheet	fiberglass hat sections with graph-hite reinforcing plies added to cap
window doublers	sheet	graphite-composite laminated sheet
cabin floor beams	formed sheet	graphite-composite formed channels with fiberglass stiffeners
panels	sandwich	graphite-composite facings with either aluminum honeycomb core or edge-grain balsa wood core
cargo floor	sandwich	graphite-composite facings with aluminum honeycomb core

TABLE 7.1-1 (Continued)

Component	Type Of Construction	Materials & Applications
Horizontal Tail		
Secondary Struct. (L.E.,T.E. & Tip)		
covering	sandwich	graphite-composite facings with aluminum honeycomb core
sub-structure	stiffened sheet	graphite-composite laminated sheet with fiberglass stiffeners
Support and Actuation		
fittings	machined	7075-T73 or X7050-T73 aluminum forgings
Vertical Tail		
Structural Box		
covering	sandwich	graphite-composite facings with aluminum honeycomb core
spars	sandwich	graphite-composite channel facing with aluminum honeycomb core
ribs	stiffened sheet	graphite-composite laminated sheet with fiberglass stiffeners
Rudder		
covering	sandwich	graphite-composite facings with aluminum honeycomb core
spar	stiffened sheet	graphite-composite laminated sheet with fiberglass stiffeners
Secondary Struct. L.E. and Tip covering	sandwich	graphite-composite-facings with aluminum core

TABLE 7.1-1 (Continued)

Component	Type Of Construction	Materials & Application
Fuselage (Continued)		
Internal Pressure bulkheads	Sandwich with stiffeners	graphite-composite facings with aluminum honeycomb core and fiberglass/graphite composite formed hat section stiffeners
pressure seal webs	sandwich with stiffeners	graphite-composite facings with aluminum honeycomb core and fiberglass/graphite-composite formed hat section stiffeners
landing gear wheel well shear webs	sandwich with stiffeners	graphite-composite facings with aluminum honeycomb core and graphite-composite hat sections stiffeners
aft pressure blkhd.	stiffened sheet	graphite-composite web with graphite-composite stiffeners
door structure (cabin & cargo)		
covering	sheet	graphite-composite laminate
framing	formed sheet	7475-T761 aluminum built-up framing
fuselage frames (wing to fuselage attachment)	machined	D6ac steel forgings-built-up
<u>Horizontal Tail Structural Box</u>		
covering	sandwich	graphite-composite facings with aluminum honeycomb core
spars	sandwich	graphite-composite facings with aluminum honeycomb core
ribs	stiffened sheet	graphite-composite laminated sheet with fiberglass stiffeners.

TABLE 7.1-1 (Continued)

Component	Type Of Construction	Materials & Applications
Vertical Tail		
sub-struct.	stiffened sheet	graphite-composite laminated sheet with fiberglass stiffeners
Support and Actuation		
fittings	machined	7075-T73 or X7050-T73 aluminum forgings
Nacelle & Pylon		
Nose Cowl		
translating cowl & radial frames	sheet	graphite-composite laminated inner and outer skin and formed radial frames
fixed cowl & inlet		
covering	sheet	graphite-composite laminate inner and outer skins
frames & longerons	formed and machined	7075-T76 aluminum and graphite-composite laminated formed sheet
accoustical treatment		
cowl inner wall	sandwich and sheet	aluminum honeycomb core with perforated aluminum cover skin
splitters & support vanes	sandwich and sheet	aluminum honeycomb core with perforated aluminum cover skin
Fan Cowl		
panels	sheet	graphite-composite sheet
framing	sheet	7475-T761 aluminum

TABLE 7.1-1 (Continued)

Component	Type Of Construction	Materials & Applications
<u>Nacelle & Pylon</u>		
<u>Fan Duct Cowl</u>		
inner panels	sandwich	perforated titanium inner skin titanium honeycomb core and solid titanium outer skin - all welded
outer panels	sandwich	graphite-composite facings with aluminum core
outer framing and support structure	formed sheet	7475-T761 aluminum
<u>Landing Gear</u>		
basic elements	machined	300M alloy steel forging
wheels	machined	aluminum alloy forging
<u>Landing Gear Doors</u>	sandwich	graphite-composite facings with aluminum honeycomb core and wet layup fiberglass edge members

applications; it simply remains for the detailed research to be completed (as described in Volume II) in order that adequate answers be provided to outstanding questions.

The composite airframe components that make up the selected configurations are described in the following subsections.

7.2 WING

Wing structure consists of a continuous structural box from tip to tip, leading-edge and trailing-edge movable control surfaces, and fixed wing secondary structure. Wing structural arrangements for the M .98 and M .90 configurations are shown in Figures 7.2-1 and -2, respectively.

7.2.1 Effect of Advanced Aerodynamic Technology

The outstanding feature of the wing structure for both the M .98 and M .90 configuration is the significantly expanded root chord provided by the supercritical wing. Departure from conventional straight-line elements in the spanwise direction influences the selection of wing structural materials and manufacturing methods. In the consideration of aluminum plank skins, the double curvature of the wing contour requires expensive forming processes to shape the skin planks. Even considering aluminum sandwich panels, expensive stretch form tools must be created to shape the aluminum facings. On the other hand, composite skin facings, which are laid up in the uncured condition, are pliable enough to drape to shape, and the only tooling required is an inexpensive plaster or composite mold. This feature significantly reduces the cost of fabrication of the wing primary structure.

Beside the material selection impact, the expanded root section significantly reduces the internal loads because of the greater wing thickness. This results in a stiffer, lighter-weight structure and reduced skin-thickness requirements, thus making sandwich skins more attractive and efficient.

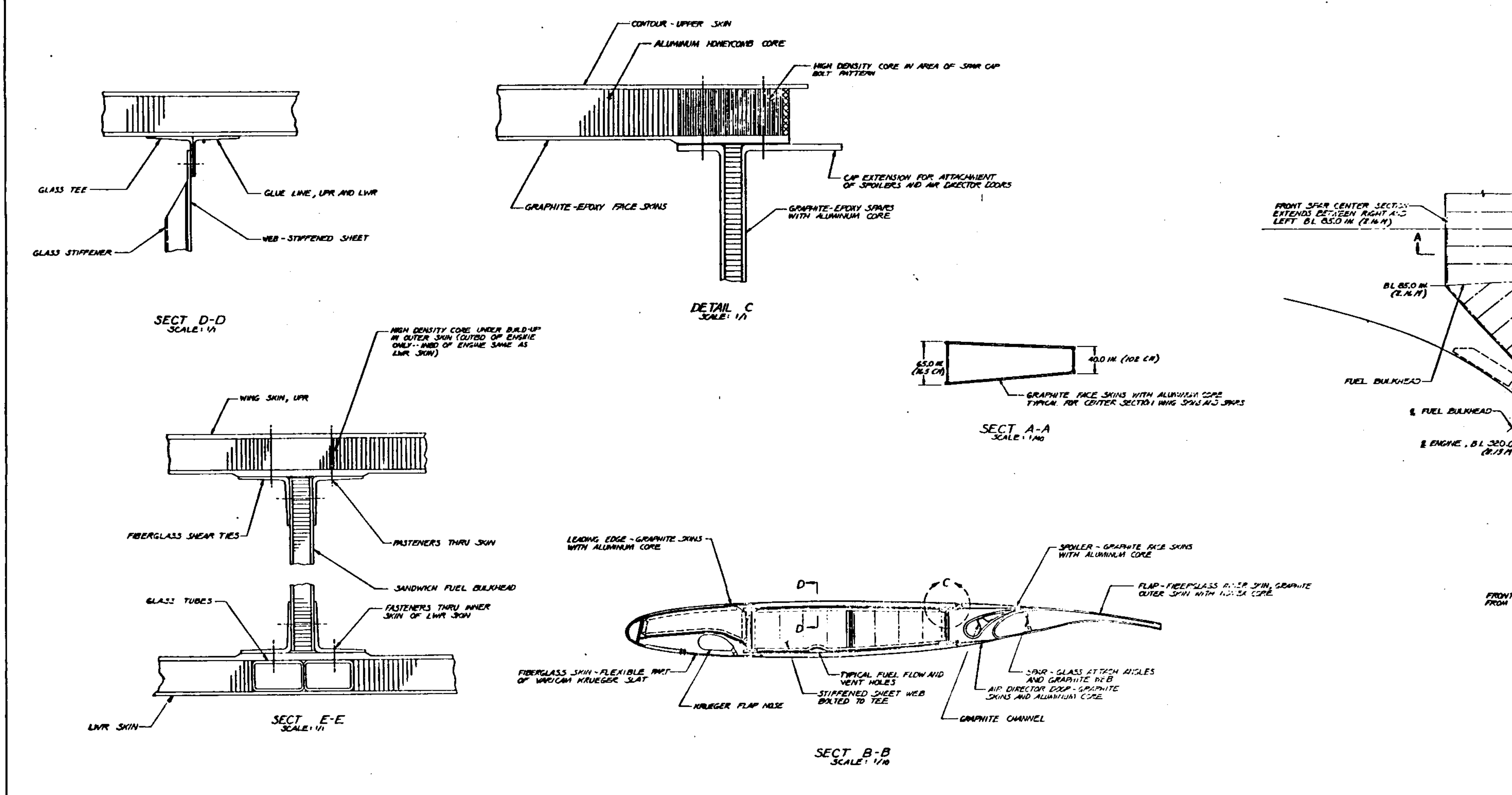
GLASS TEE
GLUE LINE, UPR AND LWR
WEB - STIFFENED SHEET
GLASS STIFFENER
SECT D-D
SCALE: 1/1
CONTOUR - UPPER SKIN
ALUMINUM HONEYCOMB CORE
HIGH DENSITY CORE IN AREA OF SPAR CAP BOLT PATTERN
CAP EXTENSION FOR ATTACHMENT OF SPOILERS AND AIR DIRECTOR DOORS
GRAPHITE-EPOXY FACE SKINS
GRAPHITE-EPOXY SPARS WITH ALUMINUM CORE
DETAIL C
SCALE: 1/1
HIGH DENSITY CORE UNDER BUILD-UP IN OUTER SKIN (OUTBD OF ENGINE ONLY -- INBD OF ENGINE SAME AS LWR SKIN)
WING SKIN, UPR
FIBERGLASS SHEAR TIES
FASTENERS THRU SKIN
SANDWICH FUEL BULKHEAD
GLASS TUBES
FASTENERS THRU INNER SKIN OF LWR SKIN
LWR SKIN
SECT E-E
SCALE: 1/1
65.0 IN (165 CM)
40.0 IN (102 CM)
GRAPHITE FACE SKINS WITH ALUMINUM CORE TYPICAL FOR CENTER SECTION WING SKINS AND SPARS
SECT A-A
SCALE: 1/40
LEADING EDGE - GRAPHITE SKINS WITH ALUMINUM CORE
FIBERGLASS SKIN - FLEXIBLE PART OF VARICAM KRUEGER SLAT
KRUEGER FLAP NOSE
TYPICAL FUEL FLOW AND VENT HOLES
STIFFENED SHEET WEB BOLTED TO TEE
GRAPHITE CHANNEL
AIR DIRECTOR DOOR - GRAPHITE SKINS AND ALUMINUM CORE
SPAR - GLASS ATTACH ANGLES AND GRAPHITE WEB
SPOILER - GRAPHITE FACE SKINS WITH ALUMINUM CORE
D
C
SECT B-B
SCALE: 1/10
FRONT SPAR CENTER SECTION EXTENDS BETWEEN RIGHT AND LEFT BL 85.0 IN (2.16 M)
A
BL 85.0 IN (2.16 M)
FUEL BULKHEAD
℄ FUEL BULKHEAD
℄ ENGINE, BL 320.0 IN (8.13 M)

Figur

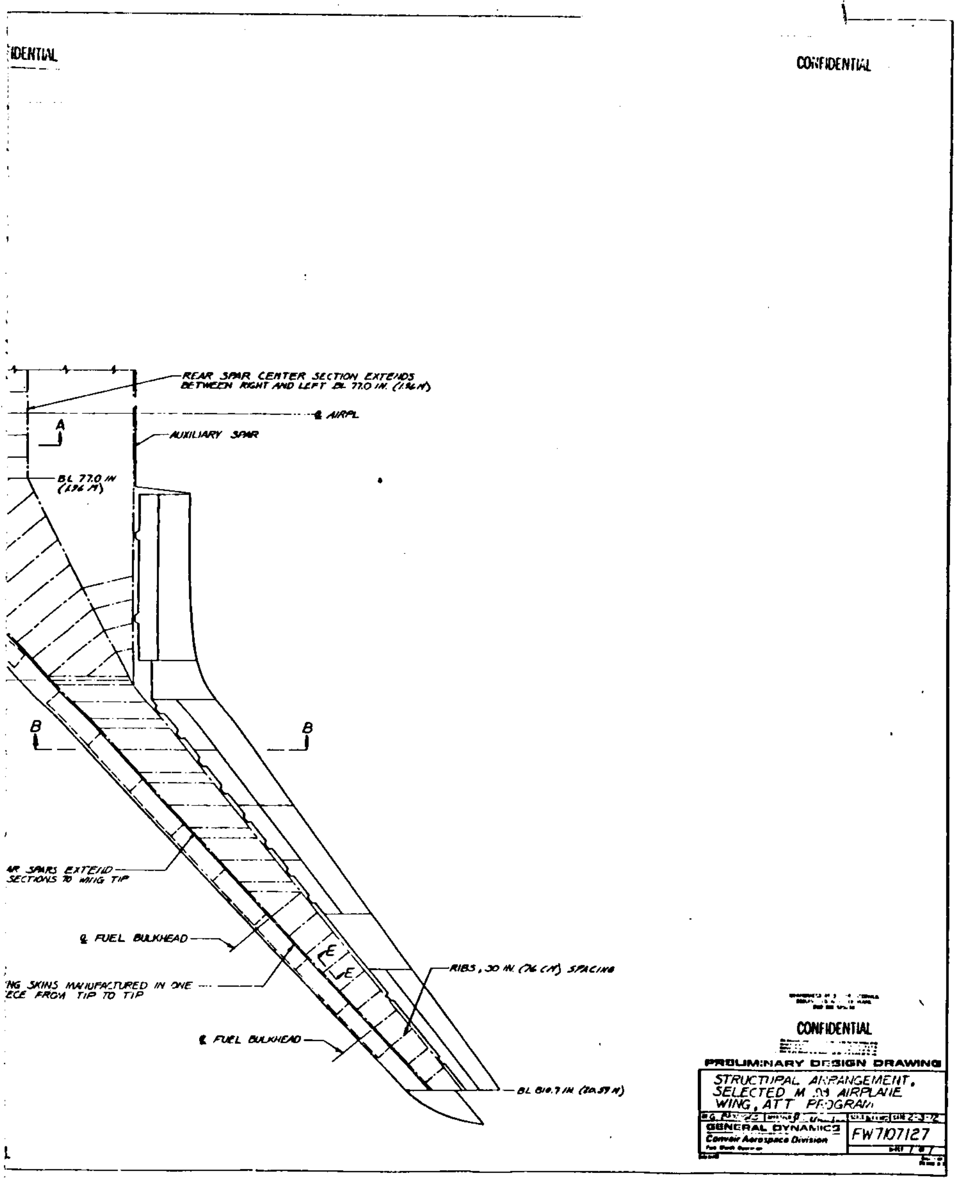

.2-1 Mach 0.98 Wing Structural Arrangement FW7107127

Preceding page blank

CONFIDENTIAL

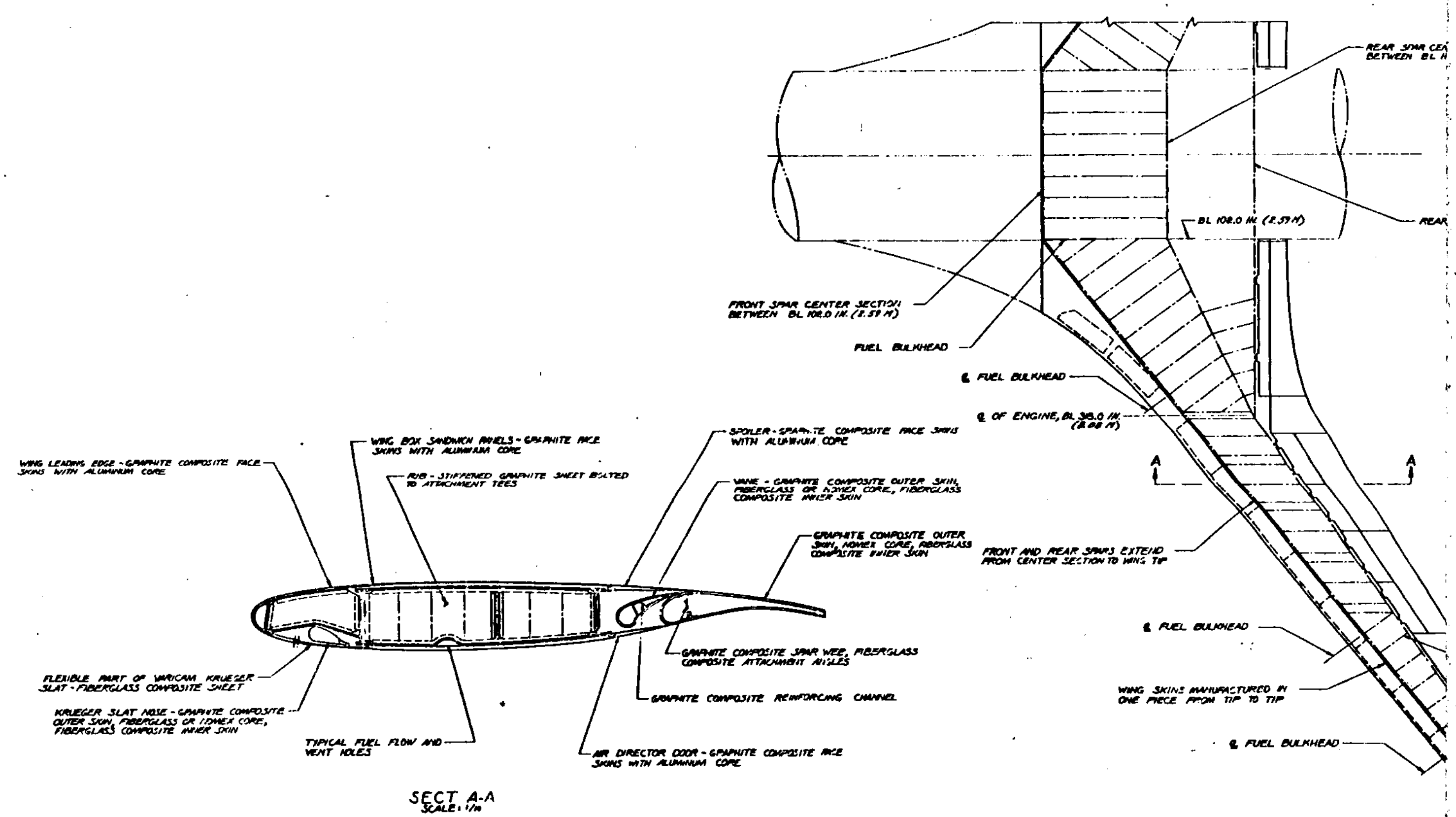

CONFIDENTIAL

Figure 7.2-2 Mach 0.90 Wing Structu

148 - a

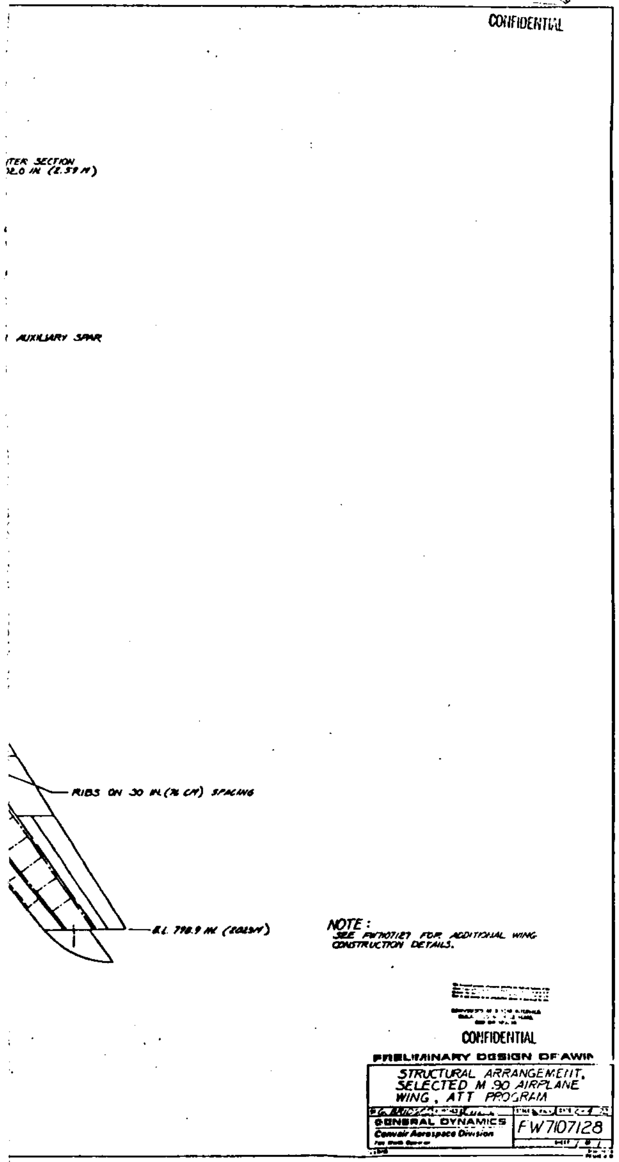

ral Arrangement FW7107128

Preceding page blank

7.2.2 Primary Structure

The primary structural box consists of upper and lower sandwich skins, two sandwich spars, and ribs placed at appropriate spanwise positions. Wing skins are of honeycomb sandwich construction with graphite composite facings and aluminum honeycomb core. Skins are manufactured in one piece, tip to tip and front spar to rear spar. The outer facing is of constant thickness with a minimum number of buildups so that the honeycomb core can be of constant thickness. The majority of the buildups and skin-thickness variations are incorporated in the inner facing away from the core. The result is a one-piece continuous skin with no splices. Both skins are mechanically attached to the spars. Manufacturing and cost considerations lead to the conclusion that a sandwich skin is better than the sheet-stringer approach, although the shifting of the effective bending material away from the extreme edge results in additional weight. In addition, fabrication cost considerations lead to a desire for a constant-thickness core and constant-thickness external facing in the sandwich. This feature is desirable even though the use of a variable-thickness outer skin is more efficient. The assembly difficulties of the ribs and fuel bulkheads mating with the spanwise stiffeners also suggest the sandwich skin approach.

Continuous wing skin, in addition to manufacturing and cost advantages, also offers structural endurance and possible failure safety in the wing fuselage intersection design. The continuous skin provides the load path for the bending moment, so that only the vertical and horizontal shear and torsional moment require a fuselage reaction.

Two spars form the front and rear boundaries of the wing box. The front spar is located at the 15% theoretical root chord and 28% tip chord, while the rear spar is at the 60% chord line outboard of the expanded root and forward of the main landing gear bay inboard. The spars are made in three sections. Left and right segments extend from the wing-fuselage intersection to the wing tip. The front spar is straight, while the rear spar has a large radius bend beginning near the engine centerline. Spars are made of two graphite-composite channels back to back with aluminum honeycomb core between them. The core is constant thickness, and all thickness variations are away from the

F

core. Access doors for wing assembly, maintenance, and inspection purposes are located in the front spar.

Ribs are located at approximately 30-in. (76 cm) intervals and normal to the 60% chord line except in the areas of the internal flap-actuation mechanism, where they are streamwise. Ribs are graphite-composite sheet with fiberglass composite stiffeners. They are mechanically fastened on the bottom to fiberglass tees bonded to the lower skin and spars and on the top through the upper surface skins.

The fuel pressure bulkheads are sandwich panels with graphite-composite face skins and aluminum honeycomb core. The fuel bulkheads are mechanically attached to fiberglass angles that are bolt-bonded to the spars and skins.

Structural design criteria for transport airframes are currently being evaluated with respect to the capabilities and requirements of advanced composite materials. The design approach expected to be postulated will replace fail-safe requirements as defined for conventional materials with reliability goals for pristine and flawed materials and structures. The design of the ATT wing will reflect the structural design criteria established for advanced composite materials; however, those criteria are not available at this time, and the damage-tolerant features of the wing design are discussed without references to specific requirements.

Low-modulus crack-arrestment strips will be incorporated in the composite wing skins (reference Subsection 15.2.2) to perform much the same crack-stopping function as do stringers in light-alloy two-spar transport wings. Also low-modulus laminates will be used where mechanical fasteners are employed so as to provide the necessary toughness or ductility needed around fasteners to provide long service life and prevent crack nucleation. The leading-edge D section also has significant shear capability, which will come into play in the event of any front-spar web failure. Finally, the employment of sandwich skins and spars affords redundant load-path capability, since load paths exist through either skin panel facing. Detailed design, analysis, and development testing is required to demonstrate specific damage-tolerant capabilities. These are beyond the scope of this study. However, it is believed that the design concepts enumerated in combination with the observed excellent fatigue characteristics of composites provide good opportunities for effective and reliable design.

7.2.3 Wing Control-Surface Structure

Control surfaces consist of trailing-edge flaps, vanes, ailerons, and spoilers, and leading-edge variable-cambered slats.

The flaps and aileron segments are sandwich skin construction with graphite-composite facings and aluminum honeycomb core. The single front spar and chordwise ribs are graphite-composite sheet with fiberglass shear ties to the sandwich skins. A fiberglass closure channel forms the blunt trailing edge typical of the supercritical airfoil.

Vane skins are of sandwich construction with graphite-composite face skins and fiberglass or multi-flex honeycomb core. A graphite-composite hat section channel forms the understructure of the vane. The feet of the channel are bonded to the lower skin and the top is bonded to the upper skin. The trailing edge is constructed of fiberglass and is mechanically attached to the other portion of the vane. All end closure members are graphite-composite sheet stiffened as required with fiberglass.

Spoiler segments are of full-depth bonded honeycomb sandwich. Sandwich facings are graphite-composite laminates, and the core and support fittings are aluminum. The same type of construction is true for the air-deflection doors.

Flap tracks and highly stressed fittings are steel or titanium. Aileron support fittings, spoiler hinges, actuator attach fittings, and others which are less highly stressed are aluminum.

Leading-edge "varicam" slats consist of a membrane sheet member forming the undersurface of the wing in the stowed position, a stiff nose piece, and a linkage that actuates the slat and also deforms it to the required shape. The membrane sheet is fabricated of fiberglass reinforced in the spanwise direction with graphite-composite laminates. The slat nose is made of wrap-around sandwich construction, with an inner skin of fiberglass, a fiberglass or multi-flex honeycomb core, and an outer skin of graphite composite. A metal piano hinge fitting attaching the nose segment to the sheet skin is bonded with the sandwich structure as an integral part of the nose. The mechanical linkage and the supporting ribs located in the fixed leading edge are machined aluminum forgings.

7.2.4 Fixed Secondary Structure

The fixed leading edges, tip, and fairing structure is generally graphite-composite laminate or sandwich structure of graphite-composite facings and aluminum honeycomb core. Under structure is graphite-composite laminated sheet with fiberglass stiffening. The components are permanently assembled by bonding and riveting but are installed on the wing with mechanical fasteners so they may be removed and replaced if damaged.

7.3 FUSELAGE

The fuselage structure consists of three principal components. These are (1) the nose structure containing the flight deck and electronics bay, (2) the main cabin area consisting of the passenger compartment, cargo compartment, and wheel wells, and (3) the tail structure consisting of the empennage support structure and auxiliary power unit bay. The fuselage structural arrangements for the M .98 and M .90 configurations are shown in Figures 7.3-1 and -2, respectively. The primary difference between the two fuselages is shown in the length difference and the fact that the M .98 fuselage is area-ruled while the M .90 fuselage is of constant diameter and is shorter. The materials and methods of construction are the same for both configurations.

7.3.1 External Shell Structure

The external shell structure is fabricated from 1-in. (.025 m) minimum honeycomb core and graphite-composite laminated facings. The core is filled with foam for sound suppression and thermal insulation, while the composite facing laminates are thickness controlled and directionally tailored for optimum structural efficiency. The shell structure is designed to be manufactured in three sections, each the full length of the cabin and about 120° (2.1 rad) of the circumference. Frames are hat-shaped sections, of fiberglass fabric with graphite reinforcing plies added to the cap. The ring frame segments are bonded to the skin panels prior to final assembly. The bond attachment at approximately every fourth frame and in other local areas is reinforced

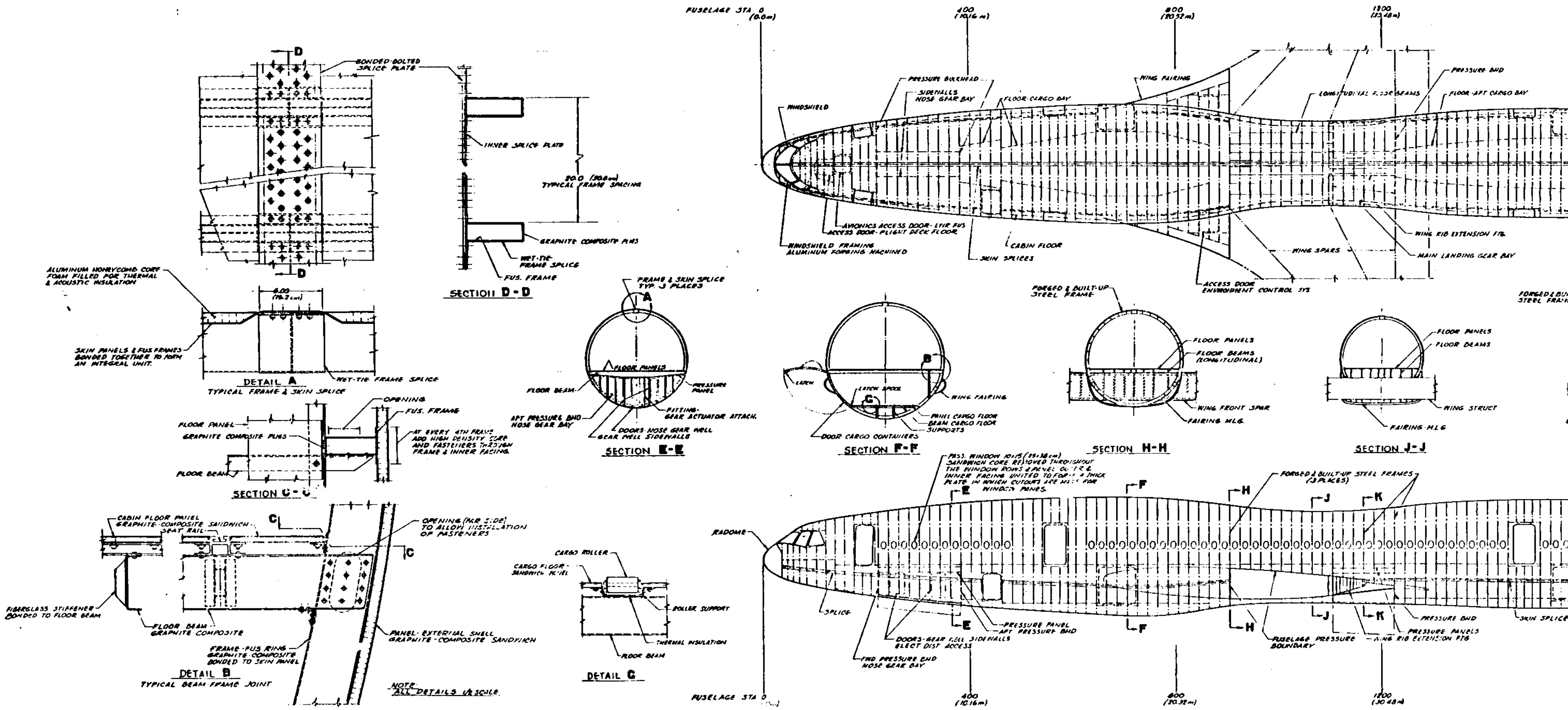

Figure 7

154-a

154-B

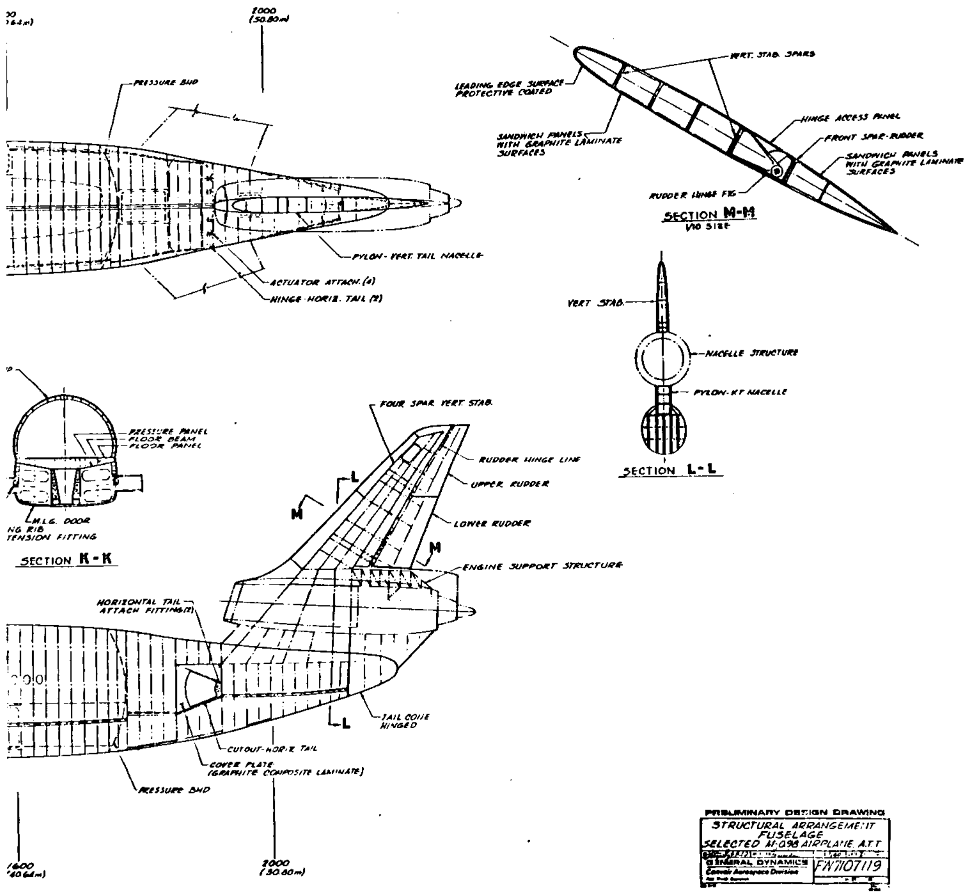

3-1 Mach 0.98 Fuselage Structural Arrangement FW7107119

Preceding page blank

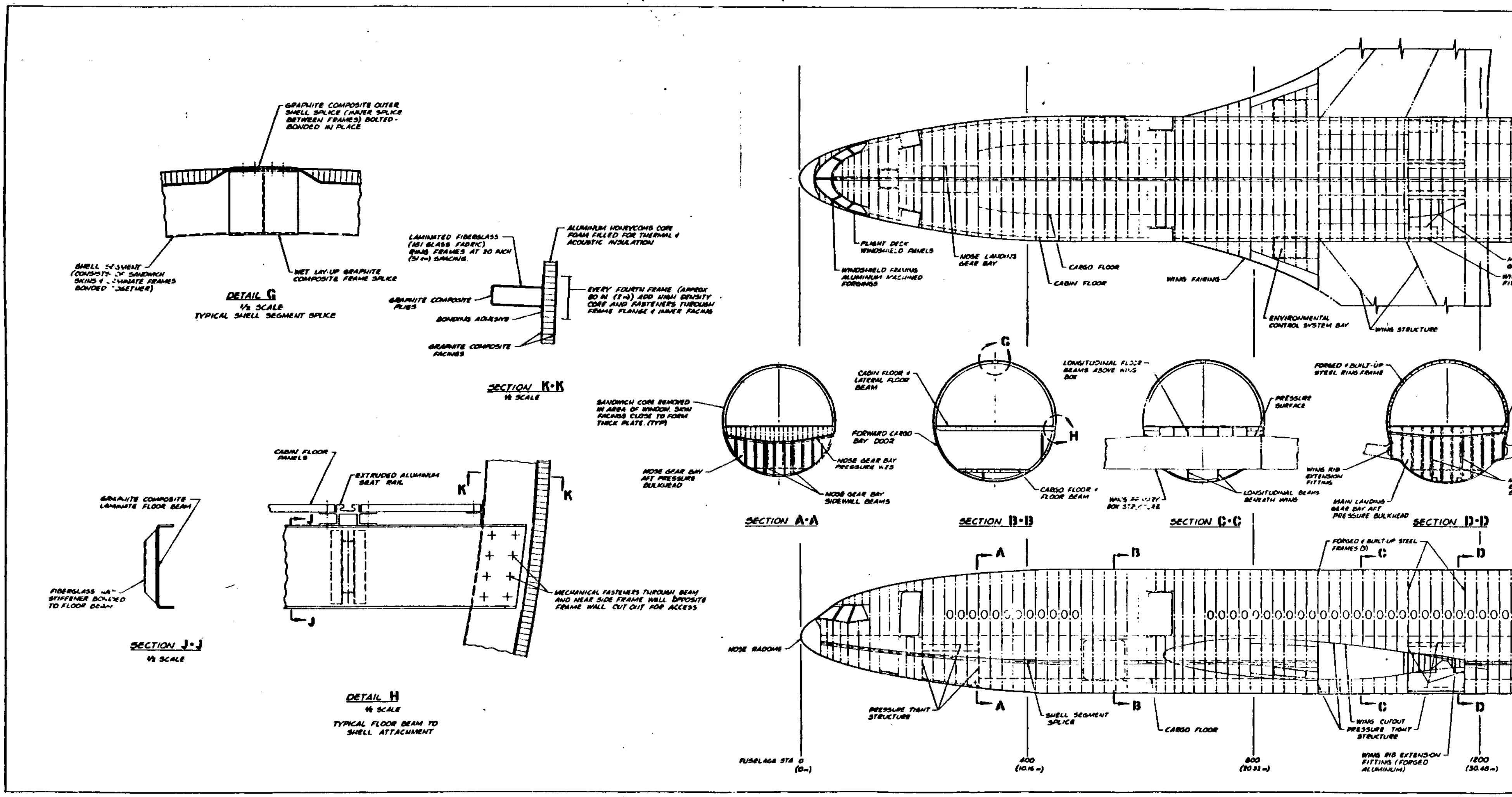

Fig

156-a

156-B

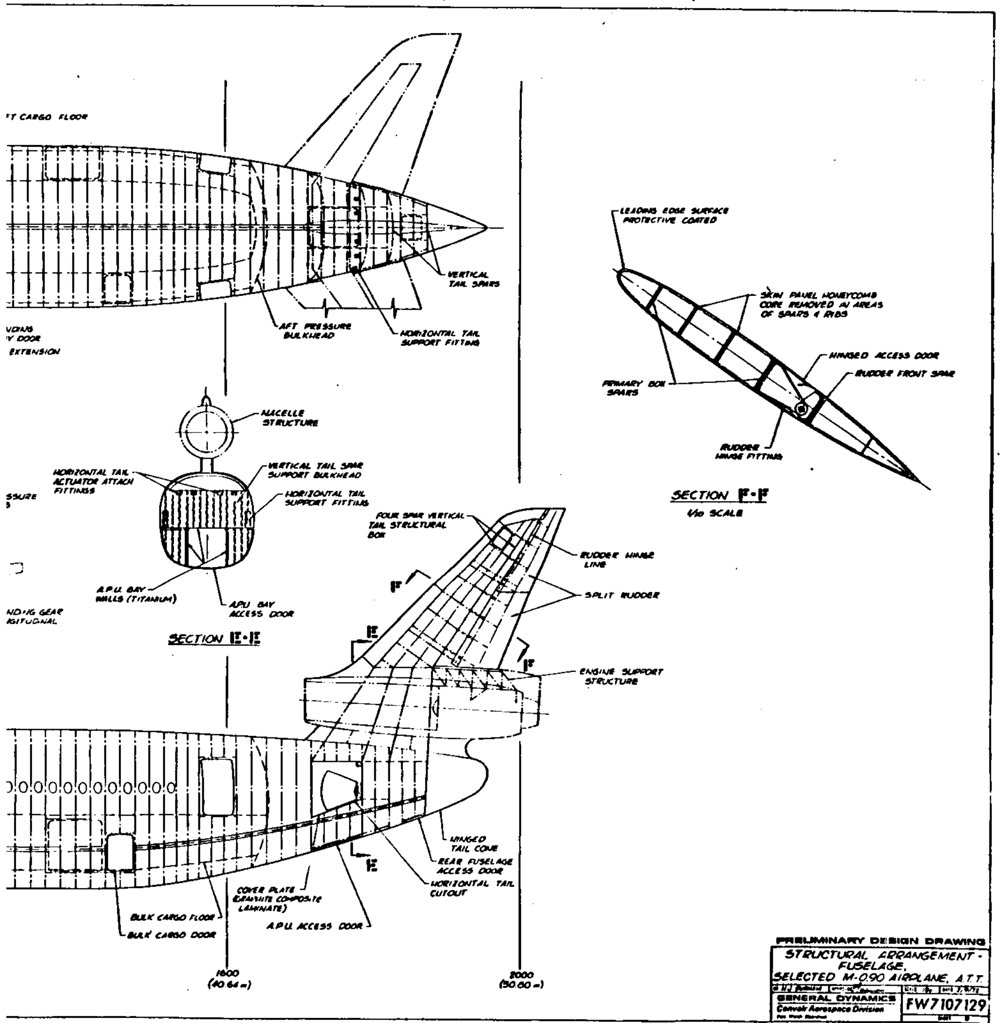

'e 7.3-2 Mach 0.90 Fuselage Structural Arrangement FW7107129

Preceding page blank

with fasteners through the frame flange and inner-skin face for added strength. The shell subassemblies are joined at final assembly by splicing at the upper centerline and at 60° (1.05 rad) from the lower centerline. External and internal skin splices are bonded in place and reinforced with mechanical fasteners in double shear. Frame segments are spliced using a bonded wet layup graphite-composite splice.

The core in the upper two fuselage panels is omitted in the window belt area. Appreciably thicker basic skin laminate is required in this area due to the large number of cutouts for windows. A composite doubler, added around each window cutout, is elliptically shaped for minimum stress buildup. Conventional window pan assemblies are riveted or bonded to the skin in the conventional manner.

7.3.2 Internal Fuselage Structure

Cabin floor beams are attached to each ring frame forward and aft of the wing. These are formed graphite-composite laminate channels stiffened with fiberglass hat stiffeners bonded to the beam. Cargo floor beams are fabricated essentially the same.

Above the wing center section, longitudinal floor beams are substituted for the tranverse beams, which would cause unnecessarily high stresses under high wing deflections.

Cabin floor panels are of sandwich construction, using graphite-composite facings and either aluminum honeycomb or edge-grain balsa wood core depending upon the floor usage. Floor panels are installed between seat tracks with loose-fitting fasteners for ease of removal. Cargo floor panels are permanently installed graphite-composite sandwich panels between the roller support rails.

Internal pressure bulkheads are located beneath the cabin floor at each end of the nose wheel bay and at each end of the main wheel bay. These bulkheads are of sandwich design, using graphite-composite facings and aluminum core. Hat-section fiberglass and graphite-composite stiffeners are bonded to the bulkhead for pressure load transfer. Above each landing gear well, beneath the cabin floor, are the pressure seal webs. These too, are graphite-composite sandwich, using the same fabrication methods. Longitudinal shear webs, forming the sides of the nose wheel bay, separate the landing gear from the electrical system equipment and transfer the gear loads to the skins and pressure bulkheads. Between the main landing gear wheels, running longitudinally between the pressure bulkheads, are shear webs which transfer landing gear door loads and also provide a path for bending loads from the aft fuselage to the wing. These shear webs are fabricated of graphite-composite sandwich stiffened with graphite-composite hat sections bonded to the webs.

The aft pressure bulkhead is a membrane type graphite-composite web which is radially stiffened. It is installed as a single piece on final assembly.

7.3.3 Door Structure

The cabin passenger doors are conventional type with graphite-composite skins and metal framing. The doors are of the inward/outward opening plug type. Each door has emergency equipment installed in it and is electrically powered during normal operation and/or pneumatically operated in emergency.

Cargo doors are conventional in design and are hinged along the upper surface and open outwards. Latches along the lower surface provide hoop-tension continuity when the doors are closed and locked. The hoop-tension door design, through its good structural continuity of the fuselage, results in a minimum weight, reliable installation. The doors are electrically operated.

7.3.4 Wing-Fuselage Attachment

Wing-to-fuselage attachment is accomplished through three primary frames and a drag angle along the upper surface of the wing. Metal forged and built-up frames replace the composite frames at the forward spar, just aft of the aft box spar and at the auxiliary spar behind the main wheel well. The front spar frame is attached directly to the front spar web while the other two frames are attached to a wing rib extension fitting running between the box aft spar and the auxiliary spar. Wing torsion and shear loads, landing gear side loads, and inboard flap loads are transferred through these members. Wing drag loads are transferred from the wing upper surface to the fuselage shell structure through a titanium drag angle.

7.4 HORIZONTAL TAIL

The horizontal tail is a one-piece all-movable tailplane hinged at the aft edge of the center box and actuated by four hydraulic actuators mounted above the box. The horizontal tail structure consists of the primary structural box and secondary structure composed of the leading edge, trailing edge, and tip. The horizontal tail structure is shown in Figure 7.4-1 for the M .98 and Figure 7.4-2 for the M .90 configuration. Except for minor size and sweep differences, the two structures are identical; therefore only the M .98 structure is described.

7.4.1 Primary Structural Box

The primary structural box is a one-piece section from tip to tip, consisting of a front spar at the 37.0% chord line, a rear spar at the 61.5% chord line, upper and lower skins, and multiple ribs. The front and rear spars are fabricated of sandwich construction with graphite-composite facings and aluminum honeycomb core. Each spar is broken at the fuselage intersection point. The upper and lower skins are also sandwich construction; however, these components are fabricated in one piece, tip to tip, consisting of graphite-composite laminated facings with aluminum honeycomb core. The facing laminate orientation and thickness are tailored to provide optimum load capacity. The box ribs are of laminated graphite-composite with bonded fiberglass stiffening. The lower skins and spars are attached by non-expanded shank rivets, while the ribs are bonded in. The removable upper skin is then mechanically attached to the box.

7.4.2 Secondary Structure

Horizontal tail secondary structure consists generally of graphite-composite laminated understructure with bonded sandwich skin panels of graphite-composite facings and aluminum core. Intermediate spars are located on the 8.0% and 80.0% chord lines. Leading-edge segments and tips are interchangeable and are easily removed and replaced.

7.4.3 Support and Actuation

The horizontal tail is supported at each side of the aft fuselage by a clevis joint. The single lug of each joint is attached to the tail structural box, while the double-lug fitting is attached to the fuselage bulkhead. The single lug contains the bearing insert and is composed of two laminates of metal for fail safety. A rib is located in the structural box forward of and in line with each support fitting.

The actuator fittings are forged aluminum fittings bolted to the upper surface of the center box. As in the hinge fittings, the actuator fittings are backed up by a center box rib. The redundant actuators are sized and located for fail safety.

7.5 VERTICAL TAIL

The vertical tail structure contains a fixed multi-spar primary box supporting both a rudder and the tail-mounted engine. Fixed-secondary-structure leading-edge, tip, and trailing-edge access panels complete the vertical tail structure. The structural arrangements of the vertical tails may be seen on the fuselage structural arrangements (Figures 7.2-1 and -2). Since both structures are similar, only the M .98 is described.

7.5.1 Primary Structural Box

The primary structural box is a four-spar box between the 15.0% and the 55.0% chord lines. The spars transfer all bending loads to bulkheads in the aft fuselage; around the engine nacelle, the spars split and form rings around the inlet structure. There are four spars for added fail safety. The primary box skins are sandwich panels that transfer air loads to the spar caps. Ribs are located to support the spars and break up the skin panels.

As in the wing spars, the primary box spars are formed of back-to-back graphite-composite laminated channels separated by aluminum honeycomb core. The double webs of the sandwich-type spars provide individual fail safety. The box sandwich skins are fabricated of graphite-composite facings separated by aluminum honeycomb core. The core is eliminated in the areas of the spars and ribs to facilitate attachment. Access to the rudder actuator and linkage is through the skins. Rib segments are stiffened sheet webs formed of graphite-composite laminations stiffened by fiberglass hats bonded to the webs.

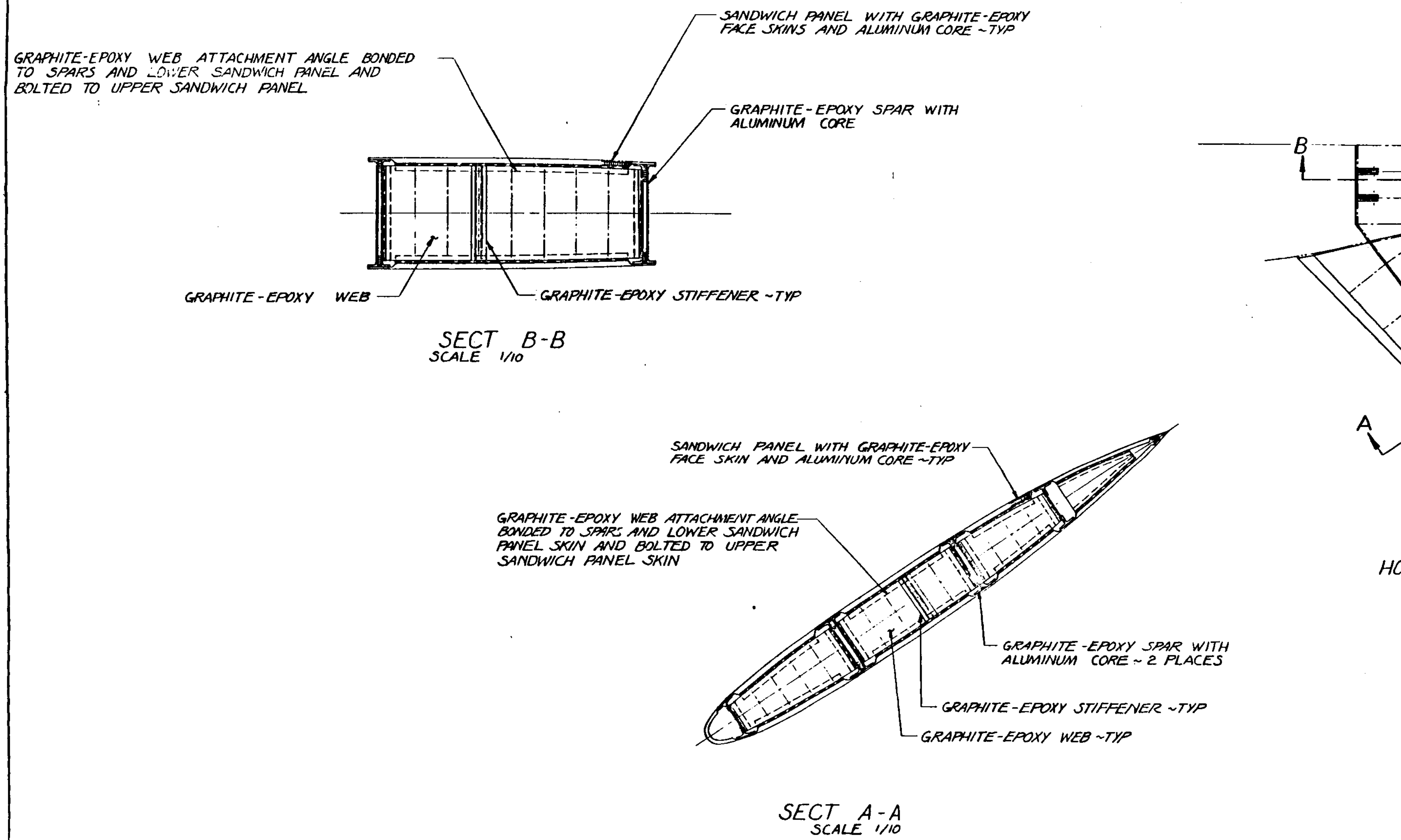

162-a

162-B

Figure 7.4-1

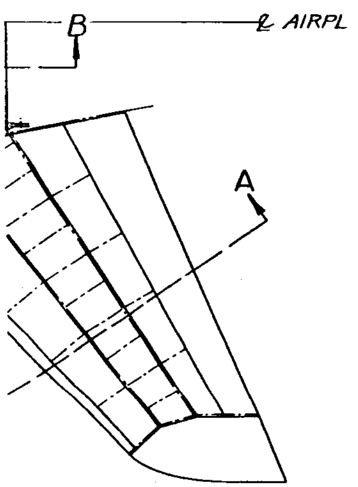

'IZONTAL TAIL PLAN VIEW
SCALE 1/40

PRELIMINARY DESIGN DRAWING

STRUCTURAL ARRANGEMENT,
HORIZONTAL TAIL, M .98, ATT PROGRAM

G. BRIDGES	APPROVED	SCALE NOTED	DATE 1-25-72
GENERAL DYNAMICS Convair Aerospace Division Fort Worth Operation		FW7107124	
		SHEET 1 OF 1	

Preceding page blank

Mach 0. 98 Horizontal Tail Structural Arrangement FW7107124

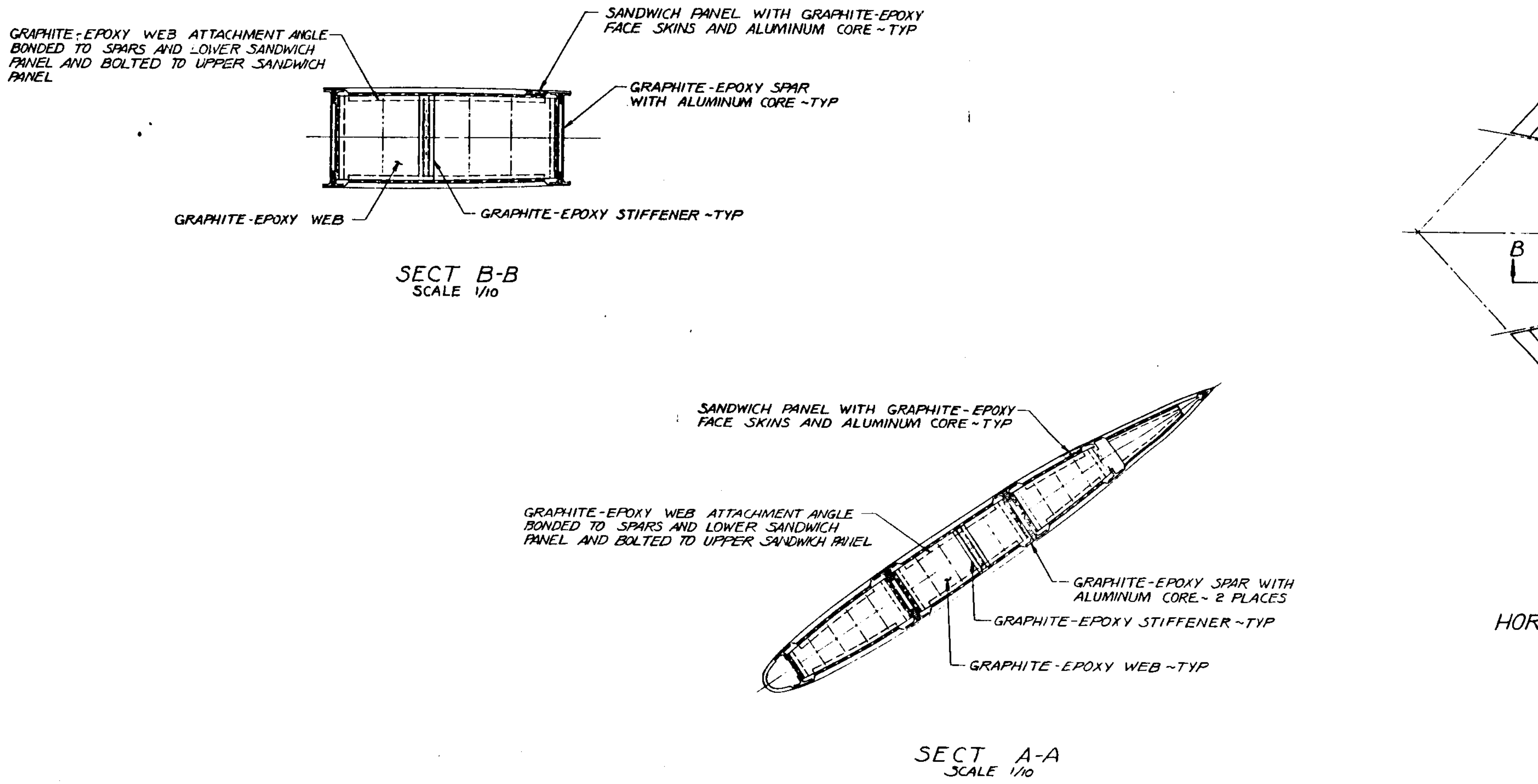
GRAPHITE-EPOXY WEB ATTACHMENT ANGLE BONDED TO SPARS AND LOWER SANDWICH PANEL AND BOLTED TO UPPER SANDWICH PANEL
SANDWICH PANEL WITH GRAPHITE-EPOXY FACE SKINS AND ALUMINUM CORE ~ TYP
GRAPHITE-EPOXY SPAR WITH ALUMINUM CORE ~ TYP
GRAPHITE-EPOXY WEB
GRAPHITE-EPOXY STIFFENER ~ TYP
SECT B-B
SCALE 1/10
SANDWICH PANEL WITH GRAPHITE-EPOXY FACE SKINS AND ALUMINUM CORE ~ TYP
GRAPHITE-EPOXY WEB ATTACHMENT ANGLE BONDED TO SPARS AND LOWER SANDWICH PANEL AND BOLTED TO UPPER SANDWICH PANEL
GRAPHITE-EPOXY SPAR WITH ALUMINUM CORE ~ 2 PLACES
GRAPHITE-EPOXY STIFFENER ~ TYP
GRAPHITE-EPOXY WEB ~ TYP
SECT A-A
SCALE 1/10
B

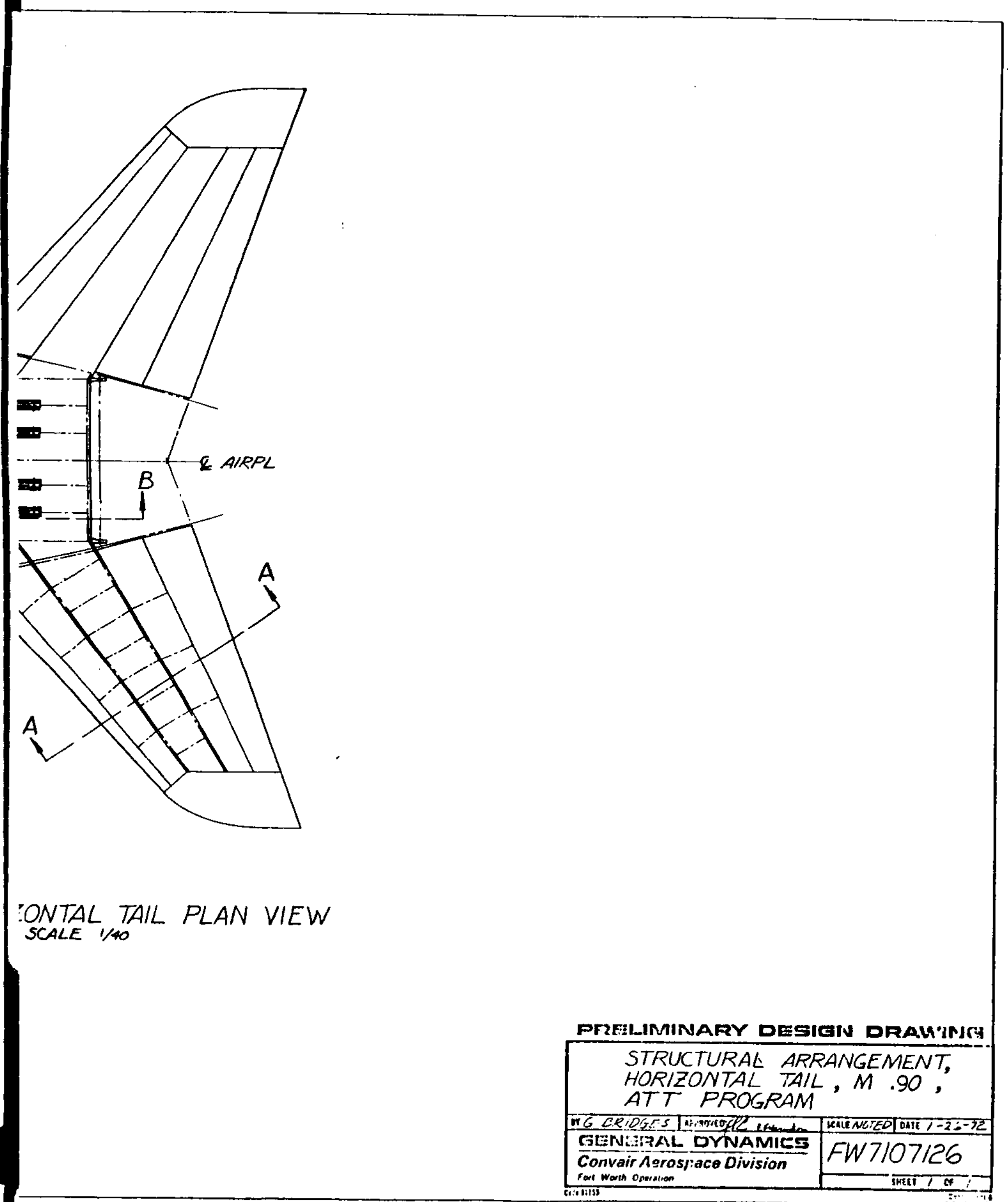

e 7.4-2 Mach 0.90 Horizontal Tail Structural Arrangement FW7107126

Preceding page blank

7.5.2 Secondary Structure

The rudder consists of two sections, from the 68% chord line aft, each acting independently for fail safety. The rudder fiberglass-composite substructure consists of a single spar with chordwise formed ribs terminating on the aft closing channel. The skins are bonded sandwich panels with graphite-composite facings, aluminum core, and fiberglass wet layup edge members at the substructure intersection. The rudder segments are supported from the aft spar by forged aluminum hinge fittings at five places for each rudder segment. Access doors between the rear spar and rudder are hinged from the rear spar for quick, easy access. These doors are sandwich panel construction, using graphite-composite facings and aluminum honeycomb core.

The fixed leading edge segments and tip are of similar construction to the wing and horizontal tail leading edge and tip structure. These removable, replaceable segments have chordwise formed ribs covered by bonded sandwich skins. The segments are assembled by bonding and riveting and installed with mechanical fasteners.

7.6 NACELLE AND PYLON

The M .98 and M .90 engine nacelles consist of two wing mounted units and one unit mounted in the vertical tail. Each nacelle is made up of a nose cowl assembly, fan cowl, and fan duct cowl assembly. The wing mounted engines are supported by a pylon cantilevered forward and below the wing while the tail mounted engine is supported by a beam extending aft of the vertical tail structural box.

7.6.1 Nose Cowl Structure

The nose cowl consists of a translating leading edge (for M .98 nacelle only), fixed cowl, inlet duct, built-in pylon disconnect, and the noise treatment secondary structure. The cowl leading edge translates on six shafts through long ball bearing bushings located in the fixed cowl structure. No actuators are required as lip suction extends the leading edge when auxiliary air is required. Spring closing is required to assure that the leading edge has moved back at speeds greater than M .4 and to eliminate leading-edge chatter. Anti-icing is provided to both the translating leading edge and the fixed-cowl leading edge. The leading-edge structure consists of graphite-composite inner and outer skins and radial frames of laminated sheet. The forward portion of the pylon is integrally built into the fixed cowl to provide adequate structure to support the cowl from the pylon and disconnect. The fixed cowl and inlet consists of graphite-composite formed frames and aluminum machined frames, machined longerons, and graphite-composite sandwich inner and outer skin panels.

The inlet duct wall surface is acoustically treated with porous filamentary composite material. Further noise attenuation is provided by two concentric splitters that are 1 in. (.025 m) thick for a length of 36 in. (.91 m). These splitters, supported by three radial vanes, are also acoustically treated with porous filamentary composite materials.

7.6.2 Fan Cowl Structure

The fan cowl is a wrap-around cowl access door over the engine and is supported by aluminum frames attached to the nose cowl and the engine fan section. The cowl has four hinges, equally spaced over 58 inches (1.47 m), which are attached to hinge fittings on the pylon. Four cowl latches at the lower centerline complete the attachment. The cowl skin is constructed of aluminum framing and graphite-composite skin panels.

7.6.3 Fan Duct Cowl Structure

The fan duct cowl structure consists of two integrated doors, one on each side of the engine, that contain the thrust reverser, the outer structure, the fan duct, and noise attenuation treatment. These doors, when opened, expose the entire engine and the engine/airplane accessories. The doors are constructed of half-round frames and longerons and skin panels. The inner structure consists of a fan duct, noise-treated surfaces, and splitters. The bottom portion has a smooth "canoe" shape surface which houses the engine/airplane accessories.

Door framing and supporting structure are constructed of aluminum. The core panels must withstand the high temperatures of the engine; therefore, these panels are constructed of welded titanium honeycomb with the facing on the fan-duct side perforated for acoustic treatment. The splitters and external fan-duct skins are sandwich with perforated aluminum skin on the duct surfaces and graphite-composite structural skins. Outside sandwich skin panel is of graphite-composite facings with aluminum honeycomb core.

7.6.4 Pylon Structure

The nacelle pylon structure consists of front and rear spars, internal ribs, and external skins. The pylons are attached to the nacelle and engine by drag angles at the skin intersections and with fittings at the main nacelle frames and at the engine mounts. The attachment to the wing structure is accomplished by spar attach fittings at the wing front and rear spars and by drag angles attaching the pylon skin to the wing skin and ribs.

The front and rear pylon spars are sandwich construction, using graphite-composite facings and aluminum core. Internal ribs and frames are graphite-composite laminates with fiberglass stiffening. Pylon side skins, leading edges, and trailing-edge fairing panels are of bonded sandwich, using graphite-composite facings and aluminum honeycomb core. Fittings and engine-mount structure are fabricated from machined forgings of aluminum or steel, as dictated by the stress level and temperature requirements.

7.7 LANDING GEAR

The landing gear is basically conventional, with four-wheel trucks on the main landing gear and dual wheels on the nose landing gear. The main landing gear retracts inboard, and is stowed in a well beneath the cabin floor just aft of the wing rear spar. The nose landing gear retracts forward. Hydraulic power is used for normal actuation, but both gears will lower by gravity in emergency.

7.7.1 Gear Design and Materials

The landing gear has been designed to permit the airplane to operate at maximum gross weight from any airfield that can accommodate current wide bodied and other DC-8/B707 Class Aircraft. This is accomplished by a wide spacing of the main gear wheels and by selection of large tires with moderate inflation pressure.

For the M .98 airplane, the main gear shock strut has a piston diameter of 9.0 inches (.23 m) and a 23.0-inch (.58 m) total stroke. The nose landing gear shock strut is 5.8 inches (.15 m) in diameter and the total stroke is 17.0 inches (.43 m).

For the M .90 airplane, the main gear shock strut has a piston diameter of 8.6 inches (.22 m) and a 23.0-inch (.58 m) total stroke. The nose landing gear shock strut is 5.5 inches (.14 m) in diameter and the total stroke is 17.0 inches (.43 m). Both nose and main gear units are conventional oleo-pneumatic design.

The basic elements of the landing gear are fabricated from 300M alloy steel forgings, fully machined to eliminate surface decarbonization. This alloy is characterized by excellent fracture toughness, fatigue strength, and resistance to hydrogen embrittlement and stress corrosion. The heat treat range is 280-300,000 psi ($1.93\text{-}2.06 \times 10^9$ N/m^2) ultimate tensile strength.

7.7.2 Tires, Wheels, and Brakes

For the M .98 configuration, 43x17-17 tires are selected for the main landing gear and 33x13-13 tires for the nose landing gear. At maximum gross weight, these tires require an inflation pressure of 153 psi (1.05×10^6 N/m^2) and 139 psi($.96 \times 10^6$ N/m^2), respectively. Similarly the M .90 configurations has 40x16-16 main gear tires and 30x12-12 nose gear tires with max gross weight pressures of 154 psi (1.06×10^6 N/m^2) and 161 psi (1.11×10^6 N/m^2), respectively. These larger tires permit a lower inflation pressure, resulting in more landings per tire change and contribute to better braking performance and reduced field length requirements.

Both the nose and main landing gear wheels are conventional in design and construction and are fabricated from aluminum alloy forgings.

The multiple-disk brakes employ granulated graphite pads and are designed with sufficient energy capacity to permit a rejected take-off stop with the brakes already hot from previous usage. A fully proportional, pressure modulating,anti-skid control system is installed in each of the two brake hydraulic systems to provide maximum brake performance with minimum tire wear.

7.7.3 Landing Gear Doors

Two doors on each side close the openings in the wing and fuselage when the main landing gear is retracted. The outboard doors are connected directly to the shock struts by a simple link. The inboard doors are actuated by separate hydraulic cylinders.

The nose wheel well is enclosed by two pairs of clamshell doors. The aft doors are connected directly to the shock strut by simple mechanical links. The forward doors are actuated by the motion of the upper drag brace links through a mechanical linkage. These doors return to the closed position when the landing gear is extended.

All landing gear doors are fabricated from bonded sandwich panels, using graphite-composite facings and aluminum honeycomb core. Edge members are wet layup fiberglass over beveled core edges. Link and mechanism fittings are machined aluminum.

7.7.4 Steering and Towing

Nose wheel steering is accomplished by means of two actuating cylinders connected to the axle through the torque links and a rotating collar at the lower end of the strut barrel. Each cylinder receives pressure independently from one of two separate hydraulic systems. Maximum steering angle is 78 degrees (1.4 rad) to either side of center.

Towing can be accomplished from either the forward or the aft side of the nose landing gear.

SECTION 8

HIGH-LIFT SYSTEM DESCRIPTION

The high-lift system (Figure 8.0-1) incorporates essentially full-span leading-edge slats and trailing-edge flaps. The devices are interrupted only by the engine pylon at the leading edge and by the all-speed aileron at the trailing edge.

The slats outboard of the engine pylon are of the variable-camber Kruger type, divided into eight equal sections with a span-to-chord ratio of approximately 4.0. Short slat spans reduce induced stresses due to wing bending and provide a means of optimizing slat deployment angles along the wing span. The wing lower-surface leading-edge skin is extended to form the slats. A linkage mechanism bends the skin to make it aerodynamically more effective.

The compound curvature of the wing leading edge inboard of the engine does not lend itself to the variable-camber concept. Hence, the two slat sections inboard of the engines are of the simple Kruger type.

The inboard and midspan trailing-edge flaps are of the double-slotted Fowler type. These flaps are divided into three sections and form a continuous trailing edge except where interrupted by the all-speed aileron. The outboard flaps, of the simple hinged type, are divided into two sections.

A ground spoiler located forward of the inboard flap is provided for lift dumping during ground roll.

The concept of a buried flap-actuation system (Figure 8.0-2) was generated to avoid the use of large external fairings on the supercritical wing. In this concept, all of the desired aerodynamic features are retained. The large constant-chord leading-edge slats fold into the lower wing surfaces so that no surface roughness occurs on the wing nose or upper contour. The large double-slotted Fowler flaps have optimum air gaps at both the takeoff and the landing deflection. No external fairings are required.

The above system is expected to provide maximum lift coefficients (FAR rules) of 2.61 for the .98M design and

CONFIDENTIAL

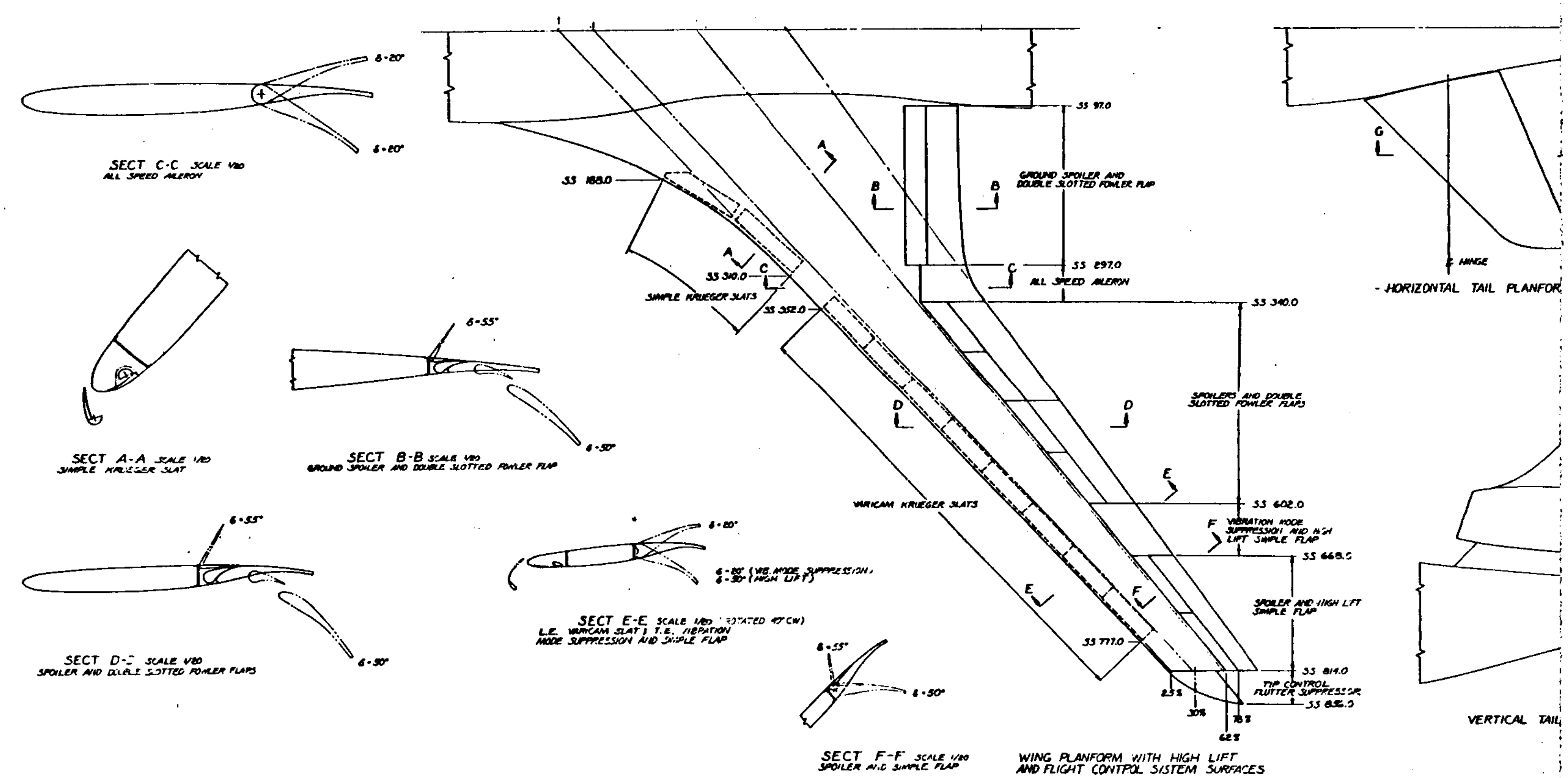

CONFIDENTIAL

Figure 8.0-1 High Lift and Fli

172-a

172-B

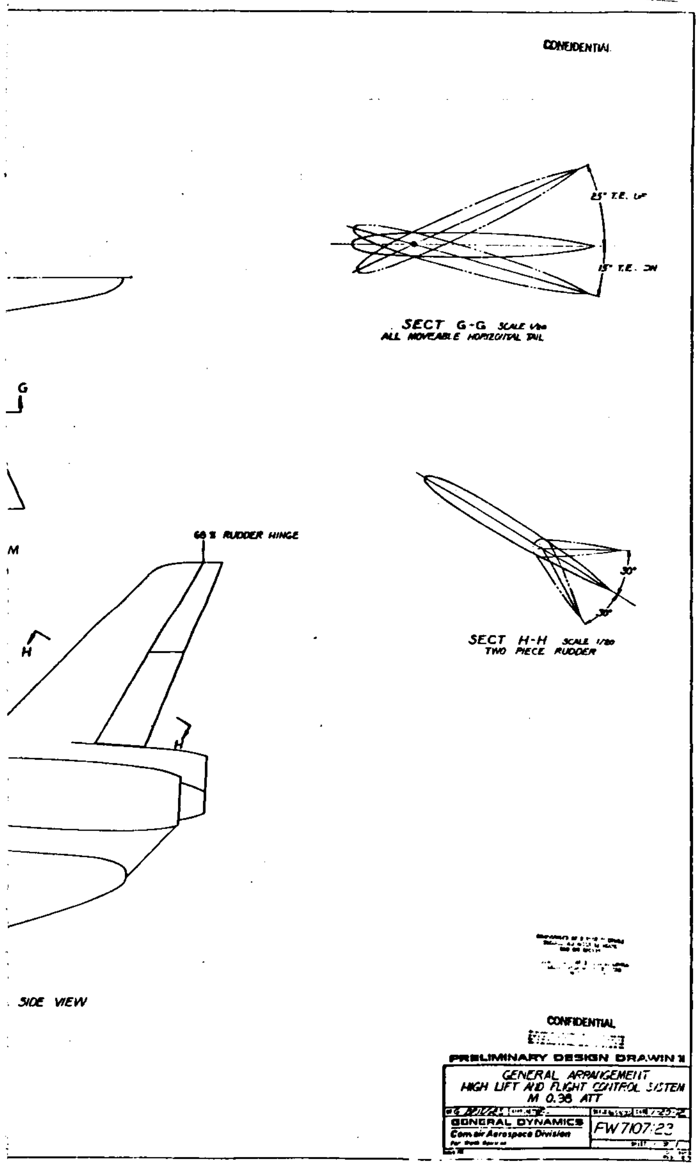

ght Control System FW7107123

172 -C

Preceding page blank

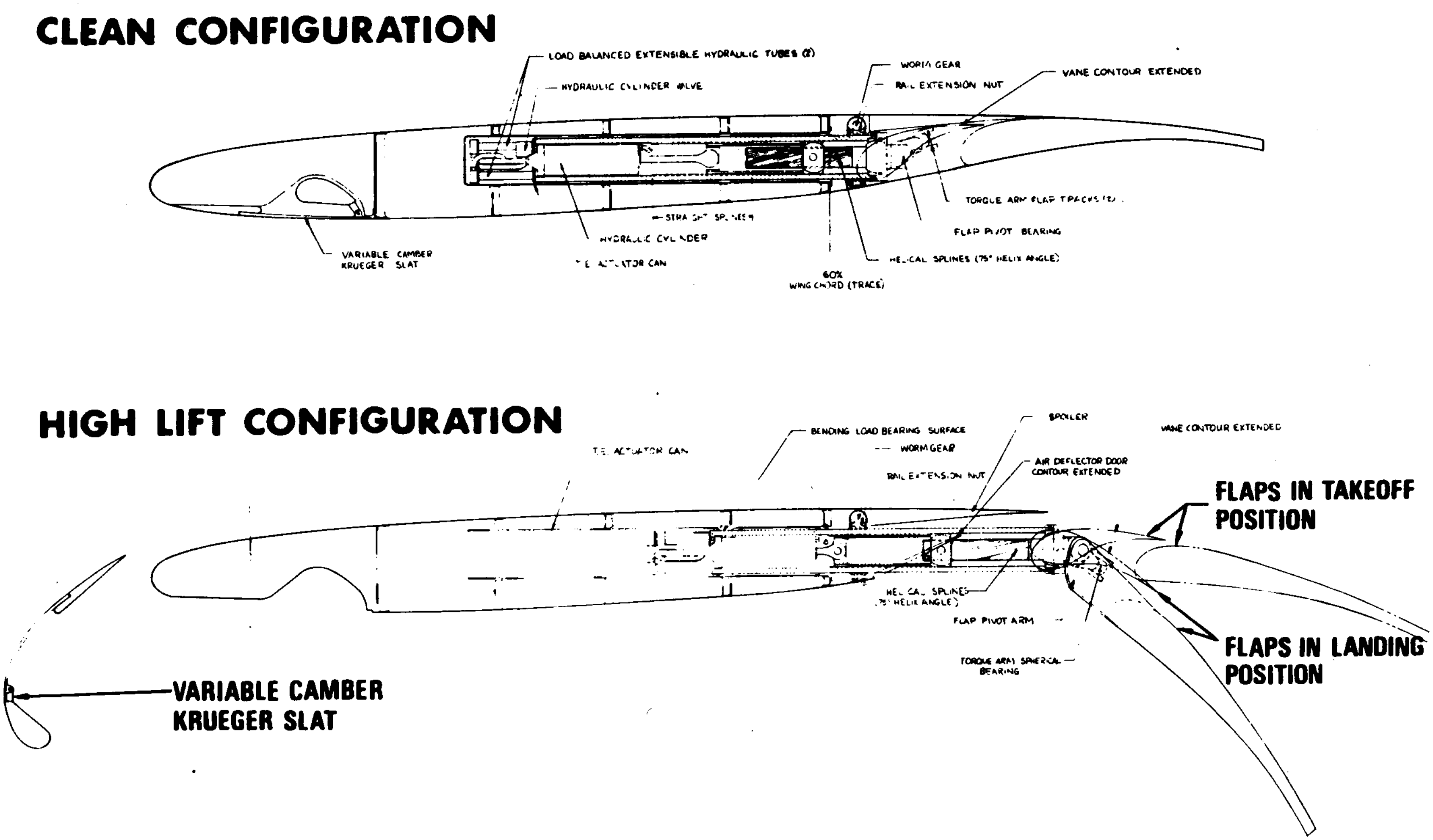

(c)Figure 8.0-2 Buried-Flap Actuation System (u)

2.80 for the .90M design. The larger value for the .90M design results from increased wing thickness ratio and reduced sweep. These levels of lift are representative of what would be expected for a comparable system on a conventional airfoil. Test results reported in LWP 990 and preliminary two-dimensional results indicate that a supercritical airfoil with a high-lift system has aerodynamic characteristics quite similar to those of a conventional airfoil with a comparable system.

SECTION 9

CONTROL OF FLIGHT

DESCRIPTION AND AERO

ANALYSIS

9.1 INTRODUCTION

This section contains a description of the various aspects of advanced flight controls considered in the ATT system study. Specific items include aerodynamic stability and control, key handling qualities characteristics, flight controls with emphasis placed on several advanced technology concepts, and avionics in terms of functional usage as well as general implementation/installation aspects. During the initial phase of the study, the stability and control effort was concentrated on two main tasks: (1) support of the configuration selection process and (2) a detailed analysis/simulation of active flight controls on a baseline NASA configuration. In this time period, avionics work was focused upon requirement analysis and review of current and developmental equipment. In the remainder of the study, the promising active control features were applied to the selected configurations, and checks were conducted on the most significant items of handling qualities. As a result of NASA redirection at the study mid-point, the flight controls and handling qualities effort was shifted to the Convair Aerospace-derived configurations. The avionics system was definitized in terms of overall organization, suitable component items, and implementation.

9.2 ACTIVE FLIGHT CONTROLS EVALUATION

The following subsections contain the most significant results obtained in the evaluation of various active control system (ACS) concepts on the NASA baseline configuration (Figure 9.2-1). In several instances, key data are also presented for a representative final 0.98 Mach number configuration (Figure 9.2-2).

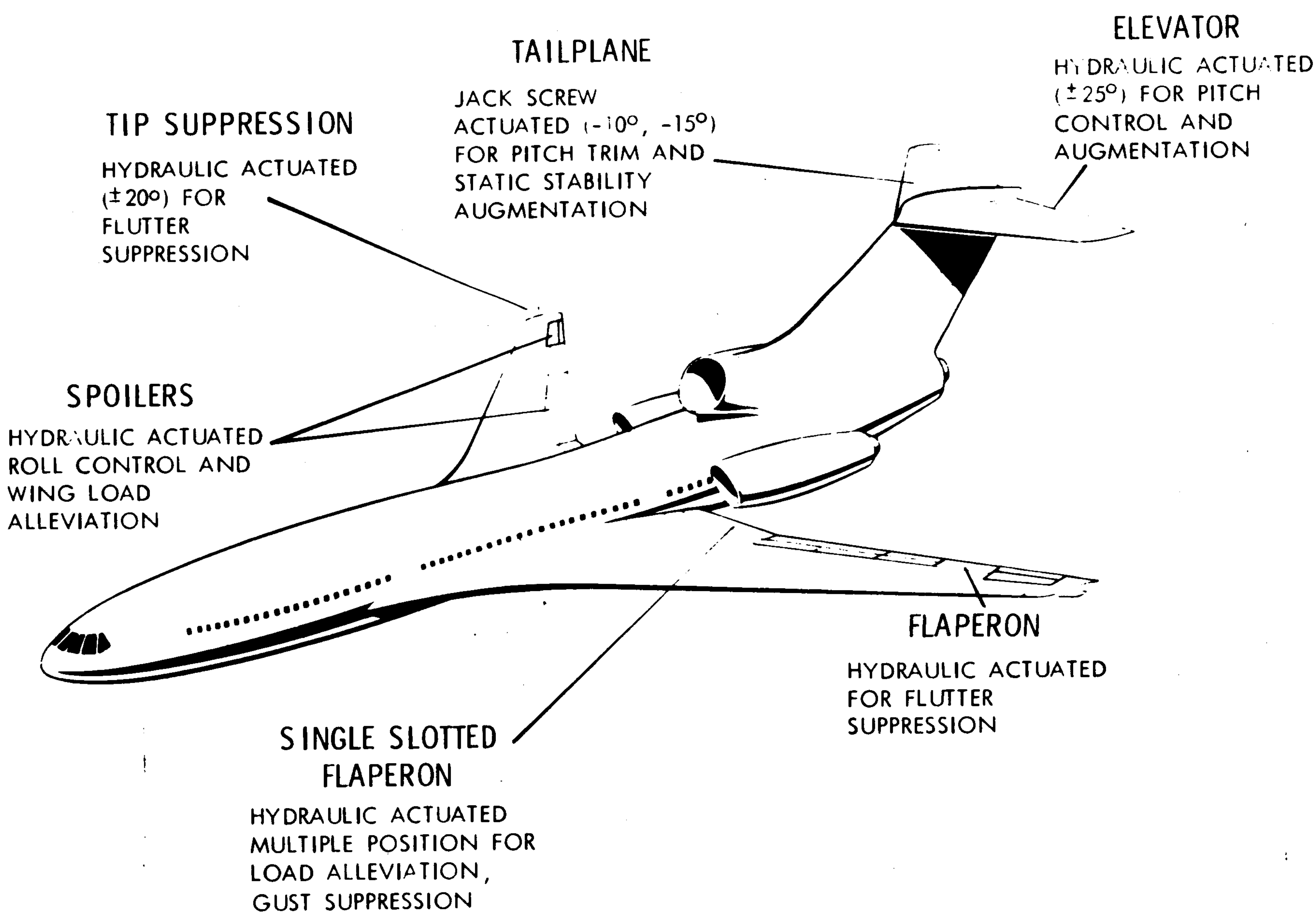

Figure 9.2-1 ACS Features on NASA Baseline Configuration

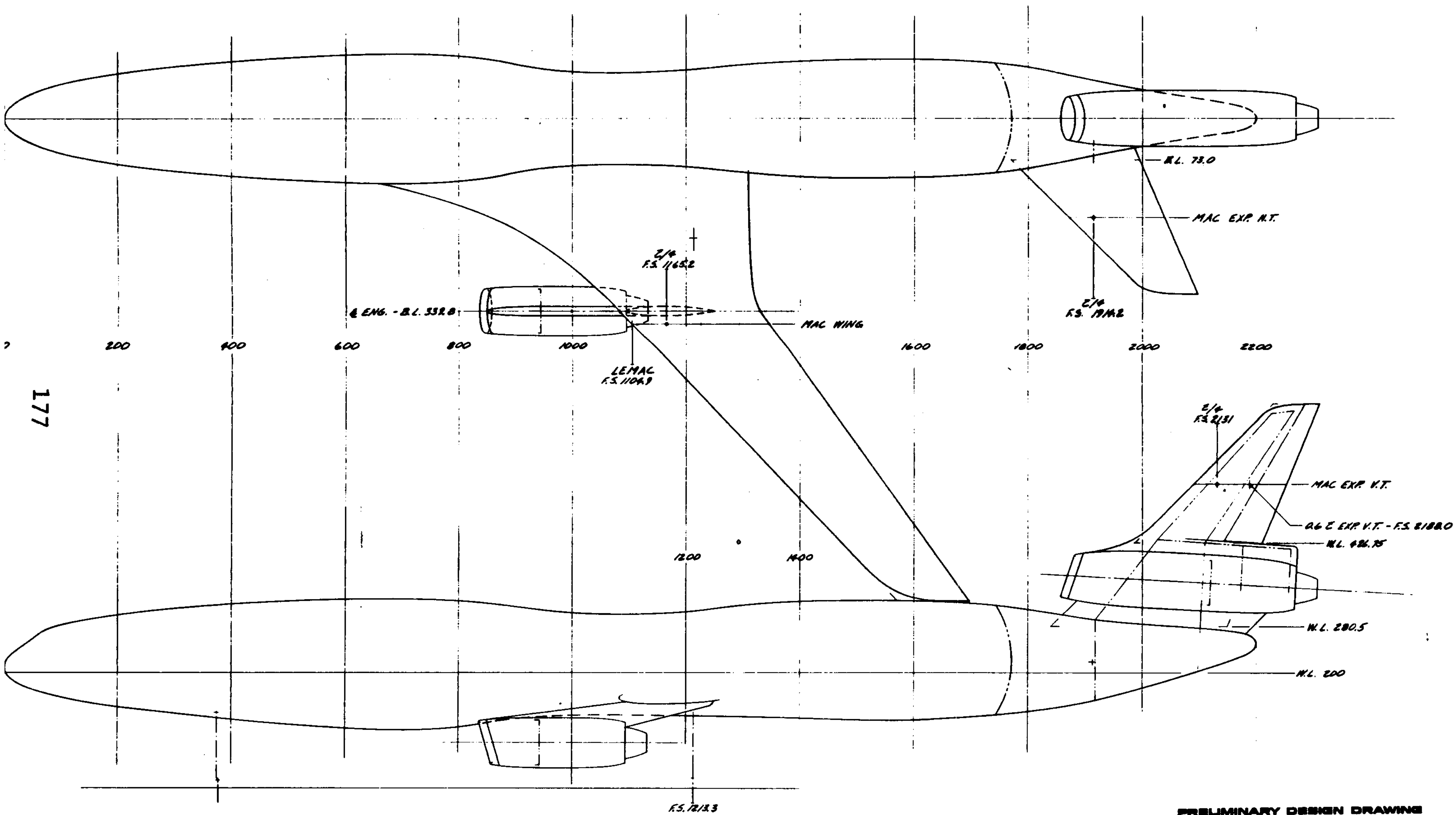

Figure 9.2-2 Mach 0.98 Configuration for Control of Flight Analysis

9.2.1 Active Flutter Suppression

The improvements in the damping of flutter mode response obtainable with various active suppression concepts are illustrated in Figures 9.2-3 through 9.2-5. These results have been obtained from a Direct Analogy Electronic Analog Computer (DAEAC) simulation of the flexible NASA baseline configuration, together with an Electronic Differential Analyzer (EDA) representation of the salient control system characteristics. The structural simulation is that of a wing of composite materials designed to the reduced loads afforded via maneuver load alleviation. Figures 9.2-3 and 9.2-4 illustrate that the Nissim concept (Reference 9-1) of applying a combination of feedback signals to both trailing-edge and leading-edge controls results in the largest improvements in flutter mode damping. A basic limitation in suppressing flutter of the reduced-loads wing is that, as feedback gain is increased to stabilize the 3-cps mode, a 6-cps mode is destabilized. A revised wing structural arrangement which incorporates increased torsional stiffening will reduce the dominance of the 6-cps mode so that the critical flutter case may be stabilized by a single control surface (Figure 9.2-4).

The data presented in Figures 9.2-3 and 9.2-4 are based upon feeding back idealized response signals, i.e., position and velocity structural responses in bending and torsion. The results of a brief study on approximating such signals via a normal accelerometer with signal compensation are illustrated in Figure 9.2-5. Note that significant degradation was experienced in the simulation of present-day compensation hardware. Since both 3-cps and 6-cps modes are important in suppressing flutter, in the future a more sophisticated compensation network exhibiting minimum phase shift in this frequency range is expected to result in materially enhanced flutter suppression. Another plausable approach would be to perform more sophisticated mathematical operations upon the feedback signals by use of a digital flight control computer.

Weight savings are presented in Figure 9.2-6 for the case of three control arrangements capable of providing significant flutter suppression. Note that the weight saving possible with an outboard aileron is almost twice that of a small all-movable tip control. It is significant that about three-fourths of the control system weight increase is due to increased hydraulic flow rate requirements. Thus,

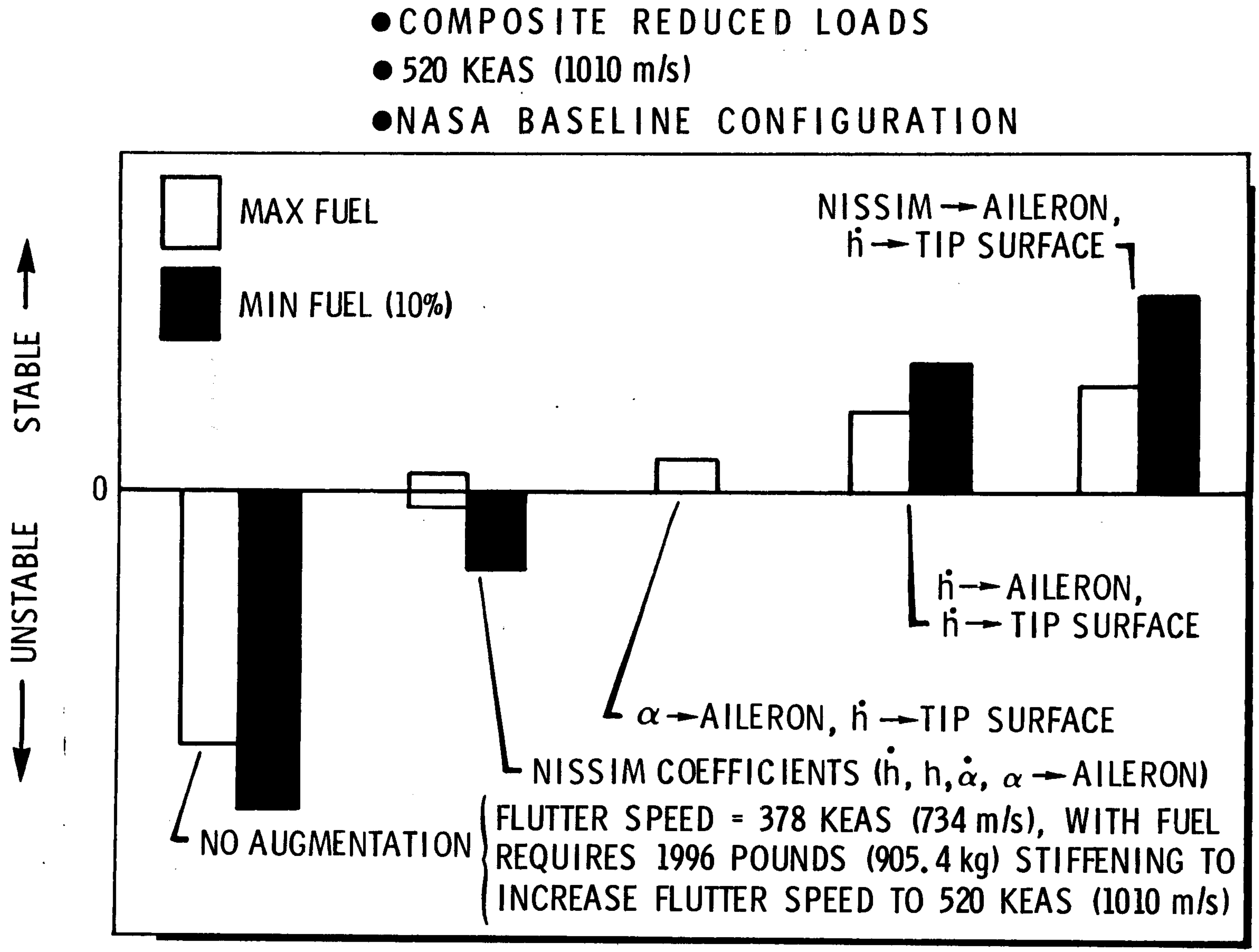

Figure 9.2-3 Flutter Suppression - Reduced Design Loads Wing

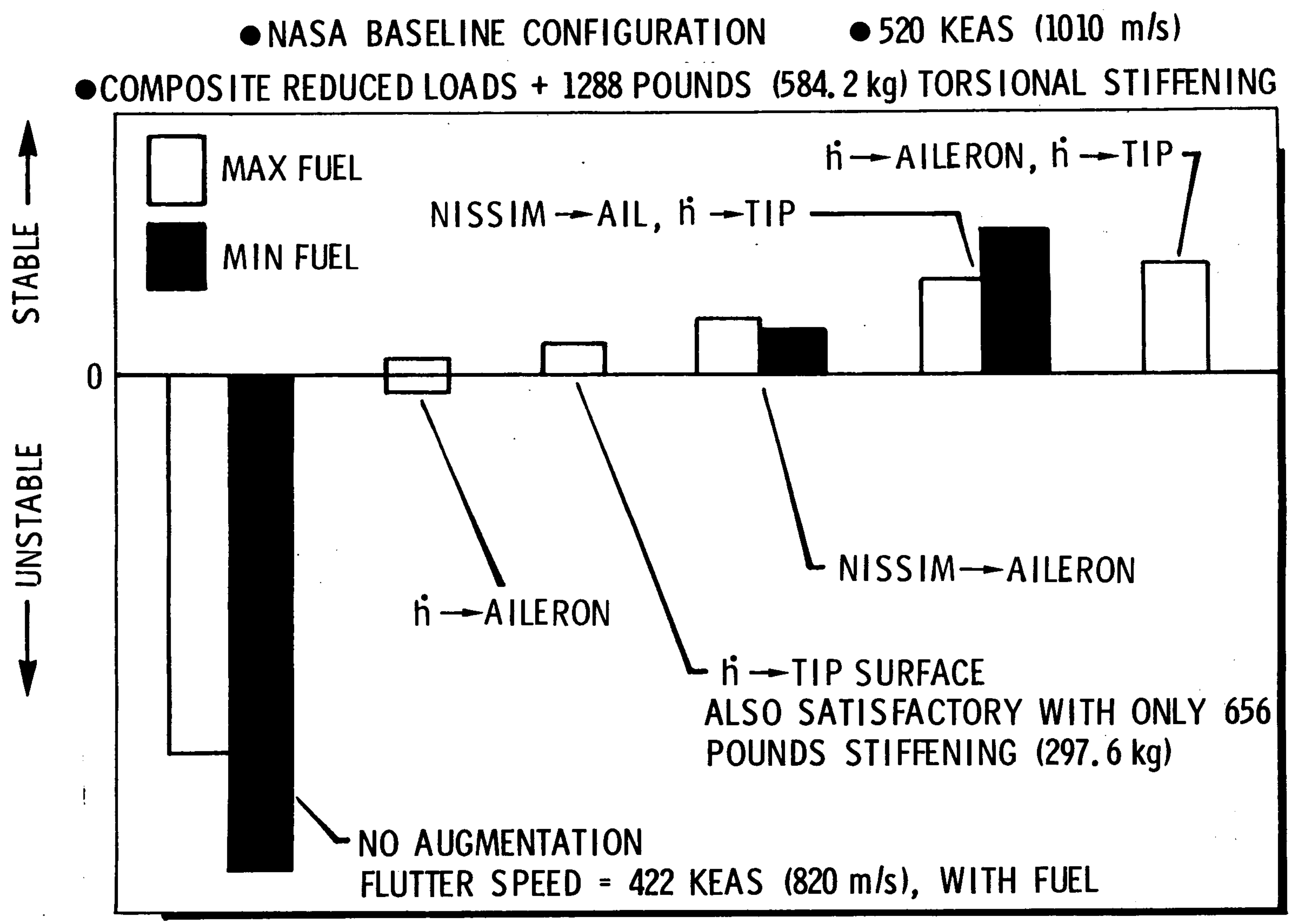

Figure 9.2-4 Flutter Suppression - Wing with Torsional Stiffening

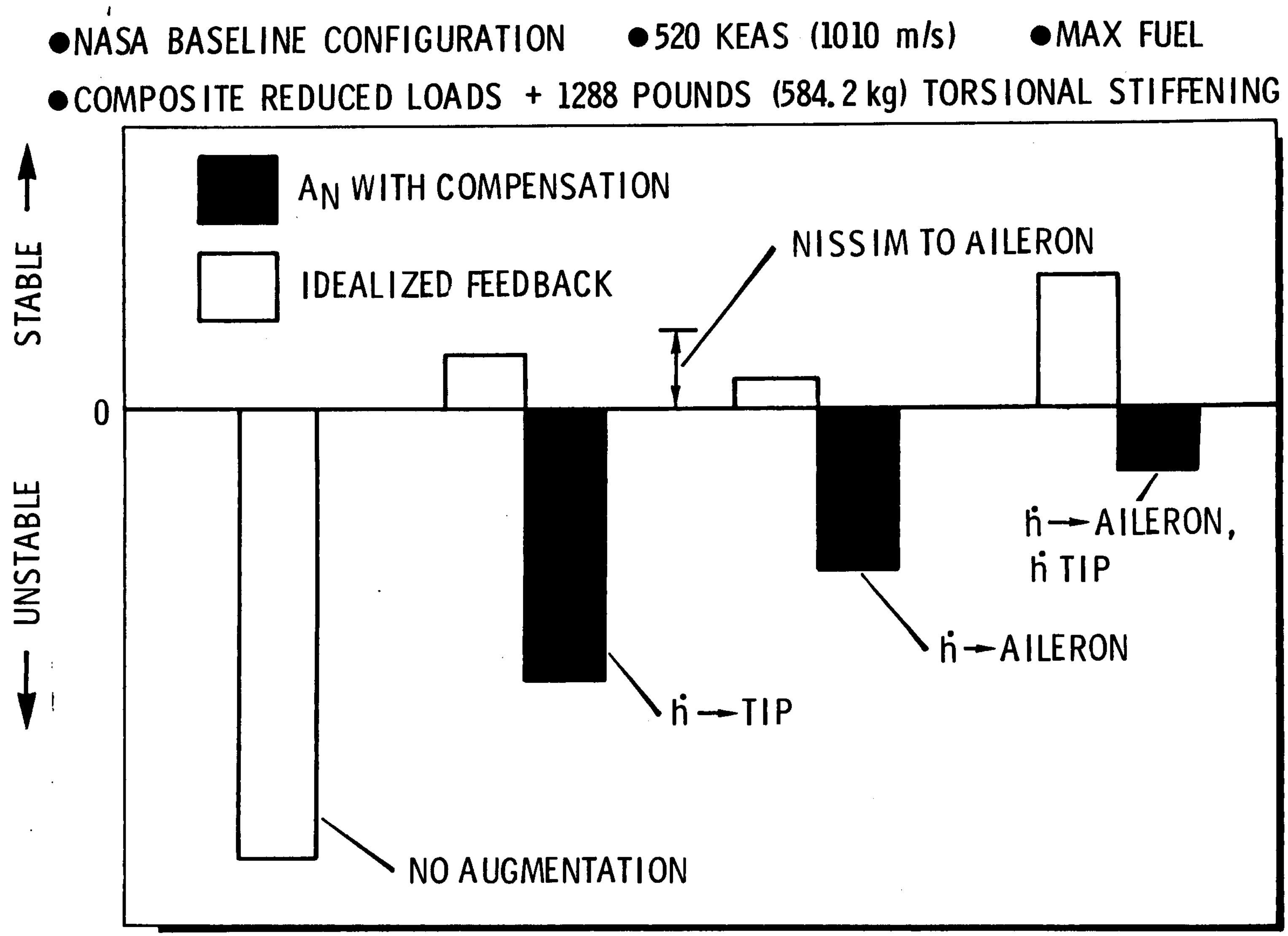

Figure 9.2-5 Flutter Suppression - Current Technology Implementation

• NASA BASELINE CONFIGURATION • REDUCED LOADS
• COMPOSITE MATERIALS • 520 KEAS (1010 M/S)

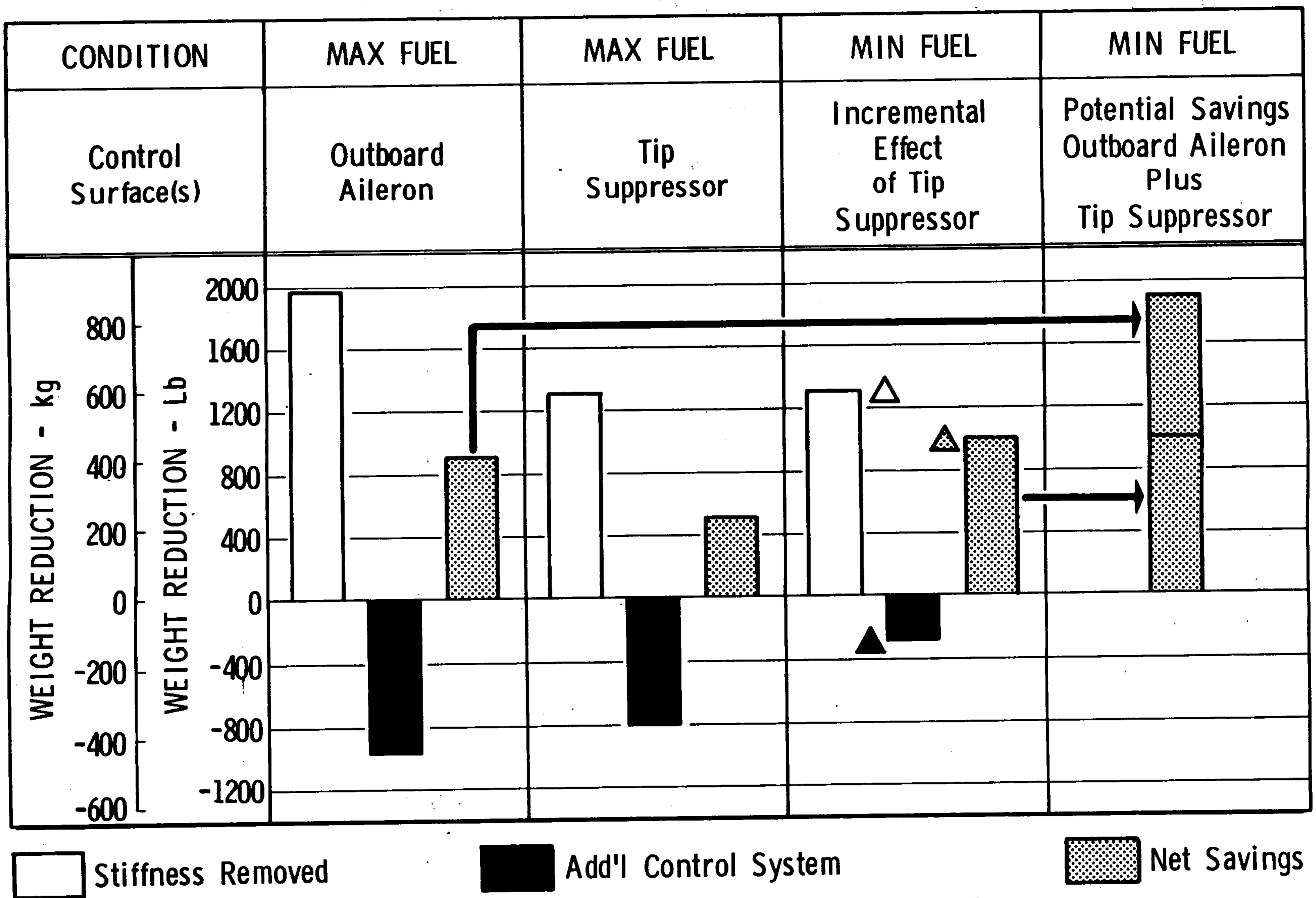

Figure 9.2-6 Active Flutter Suppression Weight Savings

significant additional savings would accrue from any obtainable reductions in hinge moments and/or required deflection rates.

The brief evaluation of flutter suppression at the more critical minimum wing-fuel condition revealed additional potential savings. In this case, 1288 pounds (584 kg) of additional torsional stiffening is required to exclude flutter in combination with the aileron control. However, the usage of both the tip (leading edge) and trailing-edge controls results in flutter-free characteristics with the minimum weight structural arrangement. This finding is considered to be a substantiation of the basic Nissim flutter suppression concept. However, it should be pointed out that the full potential of the Nissim concept could not be evaluated in the present study as a result of a lack of detailed aerodynamic data on supercritical wings with leading-edge controls. Further work along this line should be accomplished when the necessary control characteristics have been established.

9.2.2 Maneuver and Gust Load Alleviation

The data in Figures 9.2-7 and 9.2-8 illustrate the weight savings obtainable through the use of an inboard flaperon and/or an outboard spoiler to reduce wing design loads. The payoff is essentially due to the outboard spoiler, but the development risk is associated with providing an inboard trailing-edge control capable of functioning both as a high-speed flaperon and a low-speed double-slotted fowler flap. A comparison of the data in Figures 9.2-7 and 9.2-8 reveals that the saving for a composite wing is much less than that for an aluminum wing with the same reduction in design load.

The term "wing design load control" has been applied to the data in Figures 9.2-7 and 9.2-8 in that the indicated structural weight savings are based upon a slight reduction of the outboard wing gust-induced loads as well as the wing bending moment caused by 2.5-g maneuver loads.

The benefits of alleviating the response to large discrete gust inputs are illustrated in Figure 9.2-9. These data, based upon a normal acceleration feedback to the inboard flaperon, reveal a twenty to twenty-five percent reduction in peak g's at the center of gravity. Since gust-induced loads are critical on the forward fuselage, some

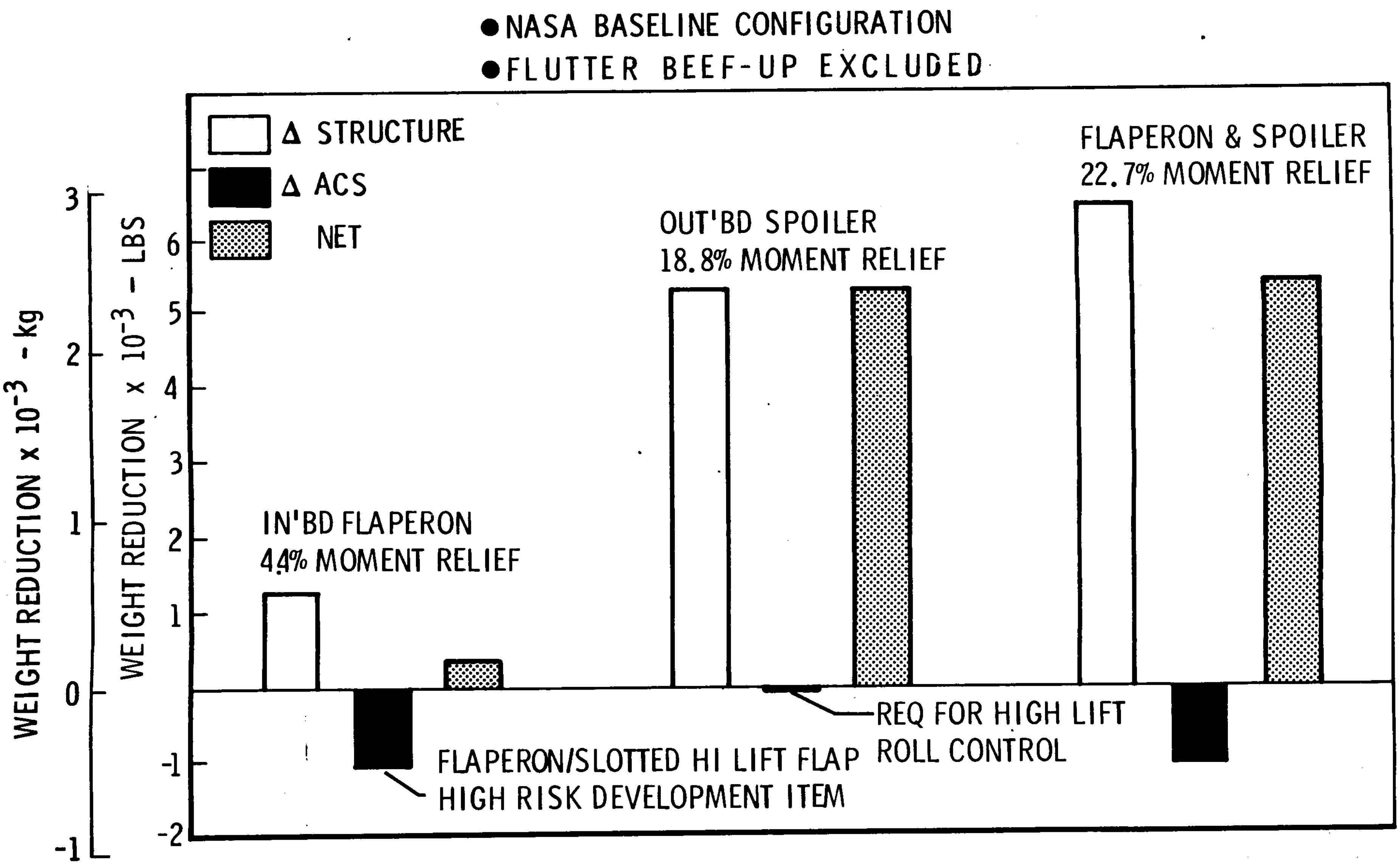

Figure 9.2-7 Wing Design Load Control - Aluminum Structure

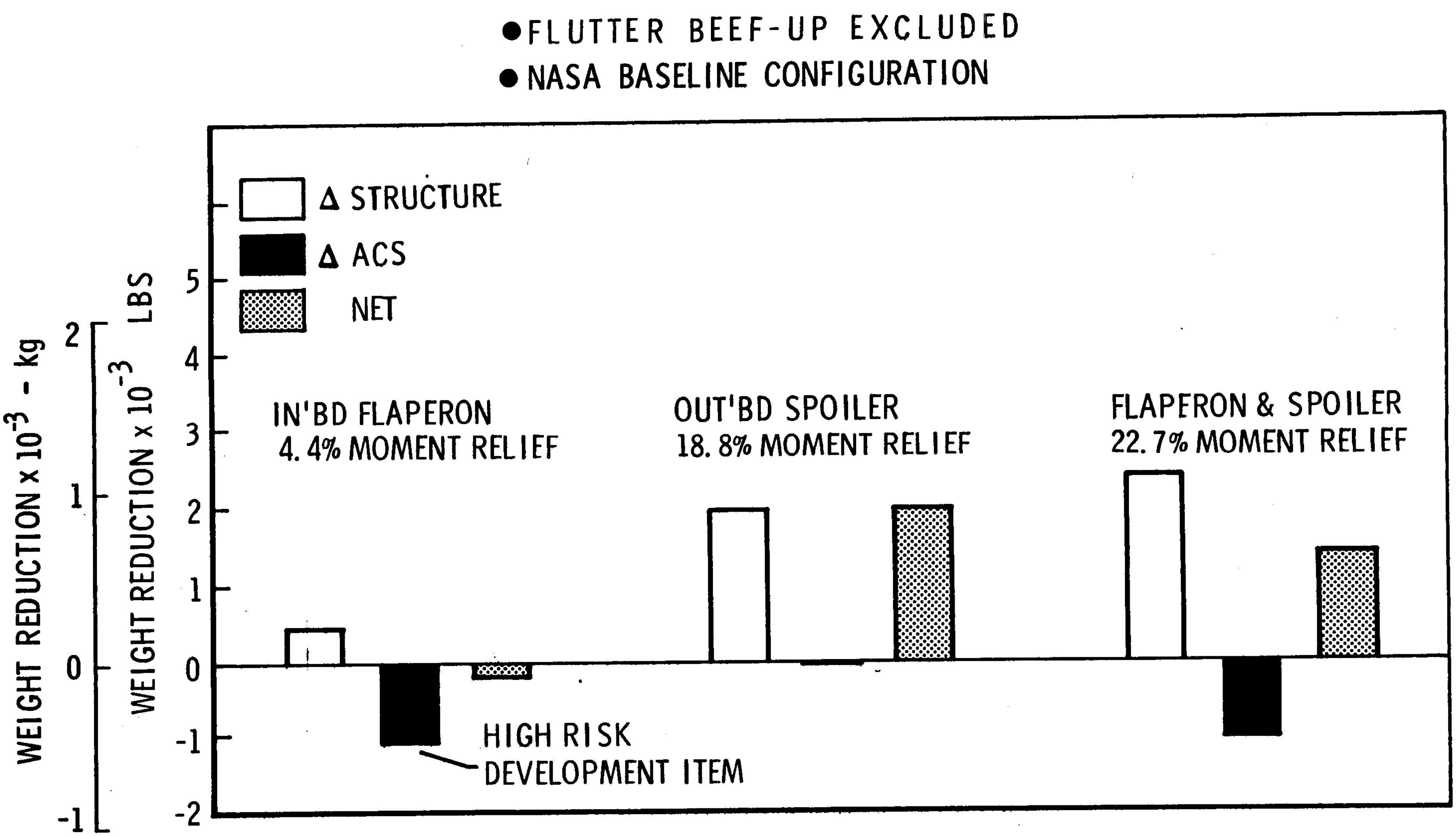

Figure 9.2-8 Wing Design Load Control - Composite Structure

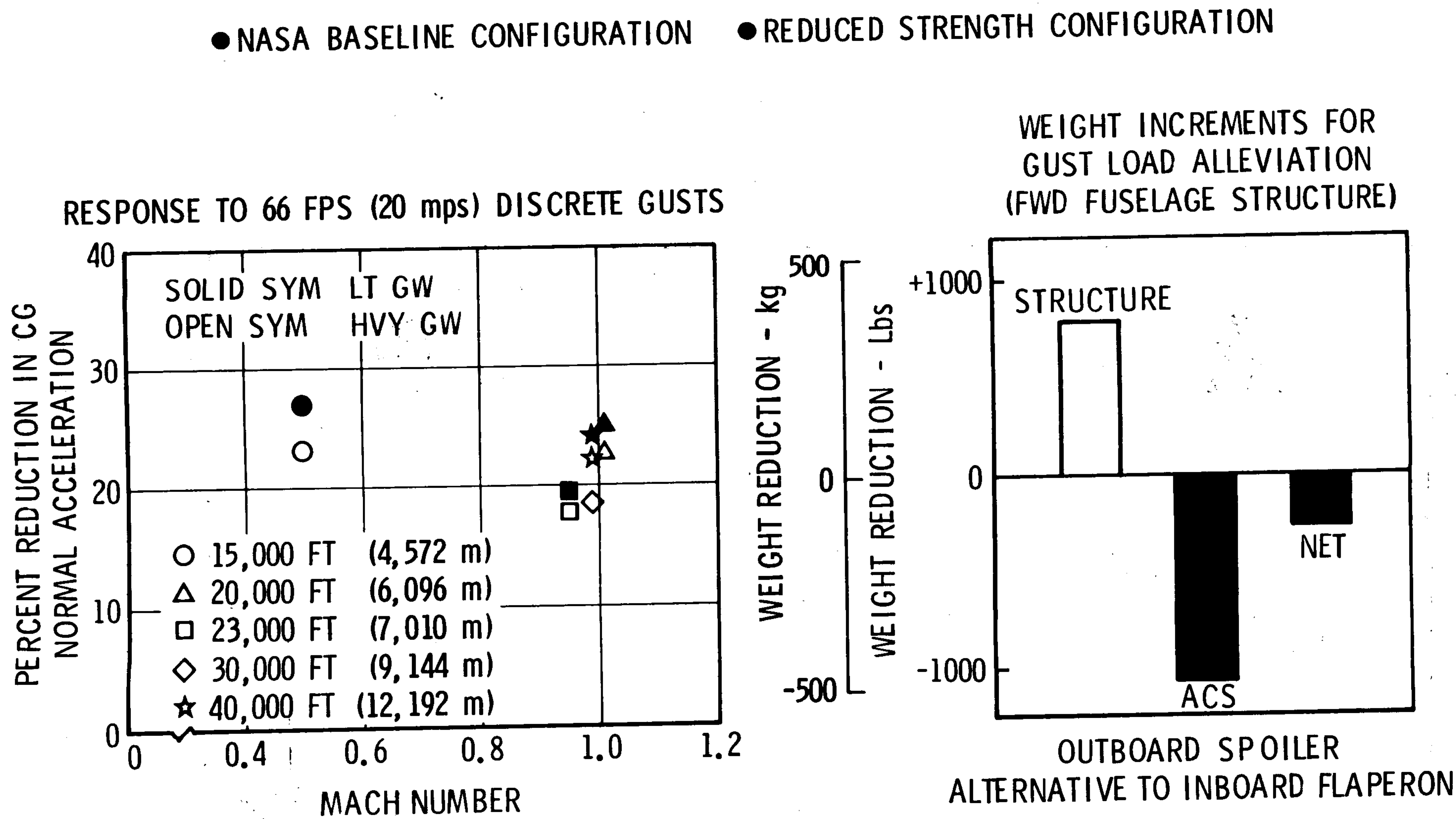

Figure 9.2-9 Benefits of Gust Load Alleviation

structural weight reductions are obtainable; however, this is not sufficient to offset the increase in control system weight. A better alternative would be to attenuate only the peak positive-g response by symmetrical outboard spoiler deflection. Such an arrangement is in good accord with the preferred wing design load control functional implementation.

9.2.3 Relaxed Aerodynamic Stability

Results of the relaxed longitudinal stability evaluation on the NASA baseline configuration are illustrated in Figure 9.2-10. Data on flexible aerodynamic center location in the left portion of the figure illustrate that a configuration balance to ensure a minimum of zero static margin at the extreme condition (limit dive speed, sea-level altitude) will result in a static margin of 27.5 percent MAC at the cruise condition. Data in the right portion of the figure illustrate that such a conventional balance corresponds to 7 counts of trim drag at a cruise C_L of 0.4. This trim drag may be essentially negated by static stability augmentation via the flight control system implementation.

The initial evaluation of relaxed aerodynamic stability, as discussed above, did not include horizontal tail size as a variable. However, this variable is included in the more complete analysis performed with the representative Phase II configuration shown in Figure 9.2-2. The results of this study are summarized in Figure 9.2-11. The forward and aft center-of-gravity limits are presented in Figure 9.2-11 as a function of horizontal tail volume coefficient, i.e., the moment area of the all-movable longitudinal control surface non-dimensionalized by the product of wing reference area and MAC.

The balance characteristics shown in Figure 9.2-11 must be considered somewhat tentative in that experimental high-lift aerodynamics are not yet available for the Convair Aerospace selected configurations. For the purposes of this evaluation, high-lift longitudinal aerodynamic characteristics have been estimated upon the basis of wind tunnel data obtained with NASA configurations of ATT and F8-1 prototype models. Ground effect increments were estimated upon the basis of standard practices in the case of lift coefficient and of general trends for vehicles of similar geometry in the case of pitching moment coefficients.

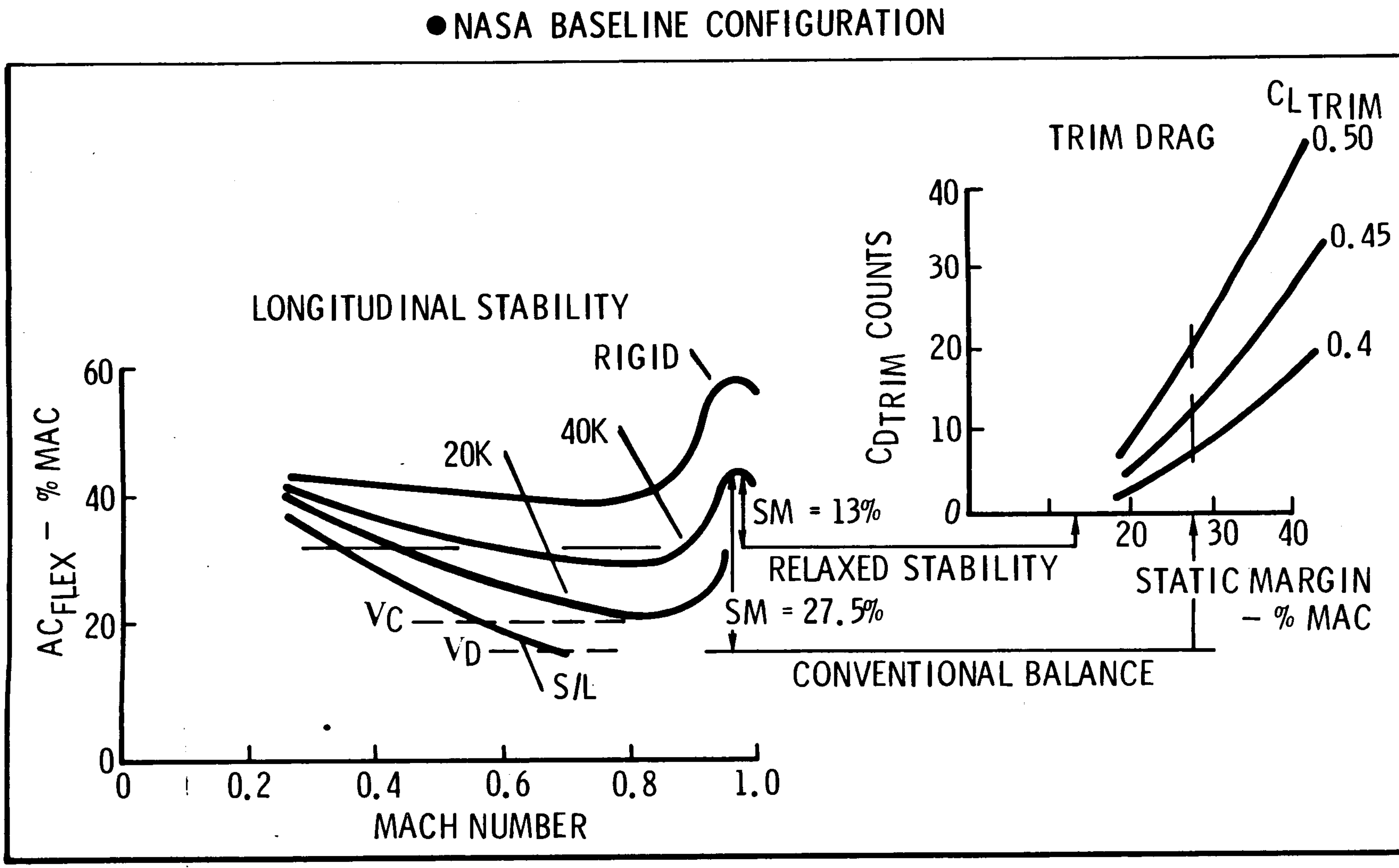

(c) Figure 9.2-10 Stability Effects on Trim Drag - NASA Baseline Configuration (u)

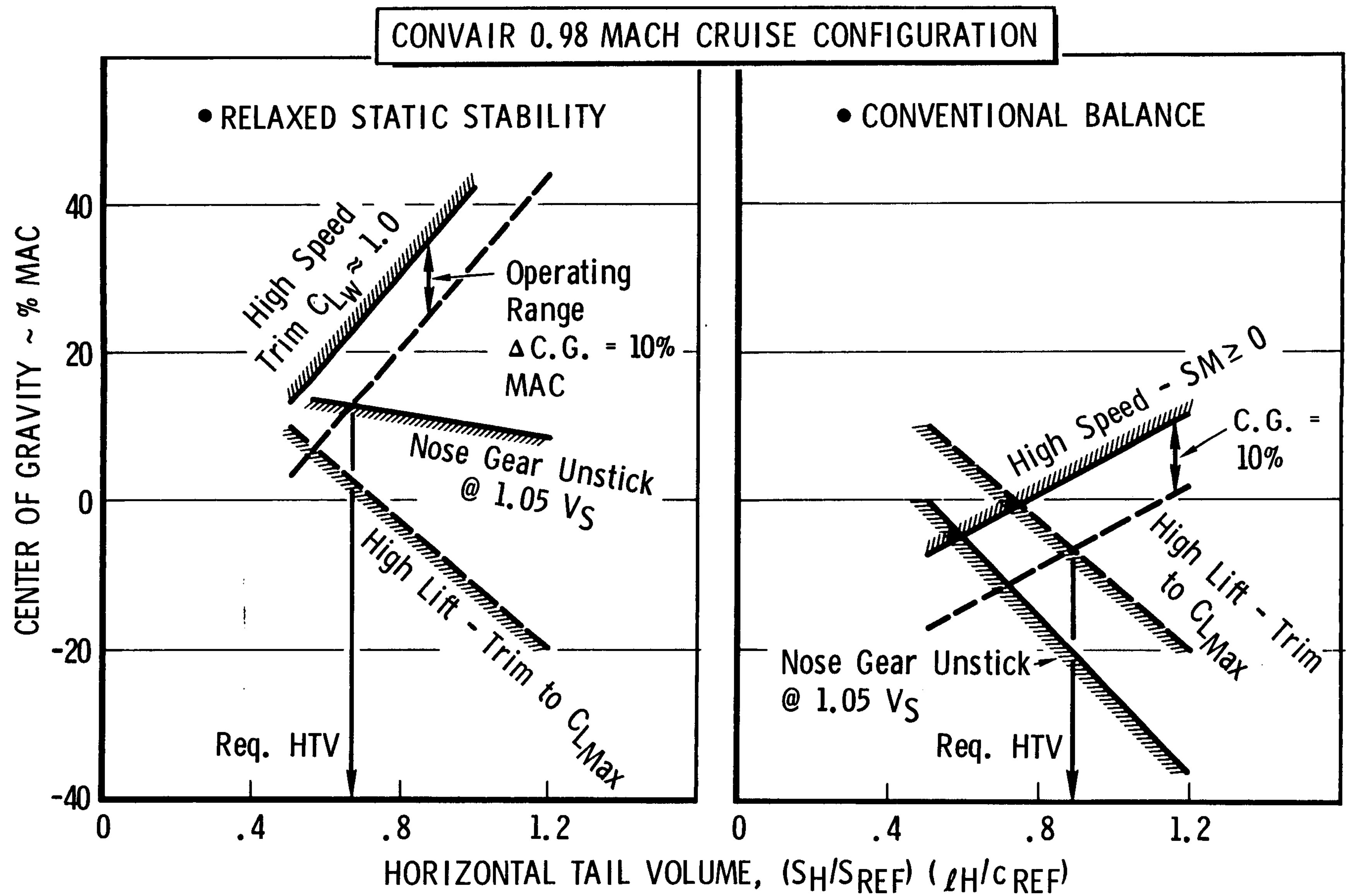

Figure 9.2-11 Balance Characteristics - All Movable Horizontal Tail

Limits are shown for two cases. In the case of conventional balance, the aft limit is selected to have the static margin be at least positive within the dive speed envelope. In the case of relaxed aerodynamic stability, the aft limit is based upon the ability to trim the clean configuration to a wing-body lift coefficient of 1.0 (taking into consideration the nonlinearities in pitching moment with lift coefficient evident in the ATT Parametric Wind Tunnel Program data). In this latter case, a maximum horizontal tail deflection of +15 degrees is employed to afford ample control power reserve (approximately 40 percent) to handle the dynamic aspects of critical upset disturbances. Both of the normal low-speed control requirements, (1) trim to $C_{L_{max}}$ in the takeoff and landing configurations in free air and (2) noise gear unstick at 105 percent stall speed, are presented in regard to the forward center-of-gravity limits. In all cases, the main landing gear location is varied as a function of the aft center-of-gravity limit so as to meet standard tip-back constraints. The required horizontal tail volumes and the corresponding center-of-gravity limits are shown in Figure 9.2-11 on the basis of operational forward-to-aft center-of-gravity range of ten-percent MAC. Note that these results carry the implication that a twenty-five-percent reduction in horizontal tail area may be obtained by employing relaxed longitudinal aerodynamic stability concepts.

Effects of horizontal tail volume on the cruise drag contribution of the horizontal tail are illustrated in Figure 9.2-12 for the case of conventional balance. The trim drag component may be reduced to zero by increasing tail volume, but the total horizontal tail drag at cruise remains essentially constant because of increases in skin friction drag in proportion to horizontal tail wetted area.

The major impact of balance concept upon vehicle characteristics may be summarized in terms of the changes in structural weight and drag at the trimmed cruise condition. Application of the data presented in Figures 9.2-11 and 9.2-12 to the final selected 0.98 Mach cruise configuration yield the following savings as a result of relaxed static stability:

1. Reduced Structural Weight 690 lb (313 kg)

2. Decreased Drag at Cruise 7 counts.

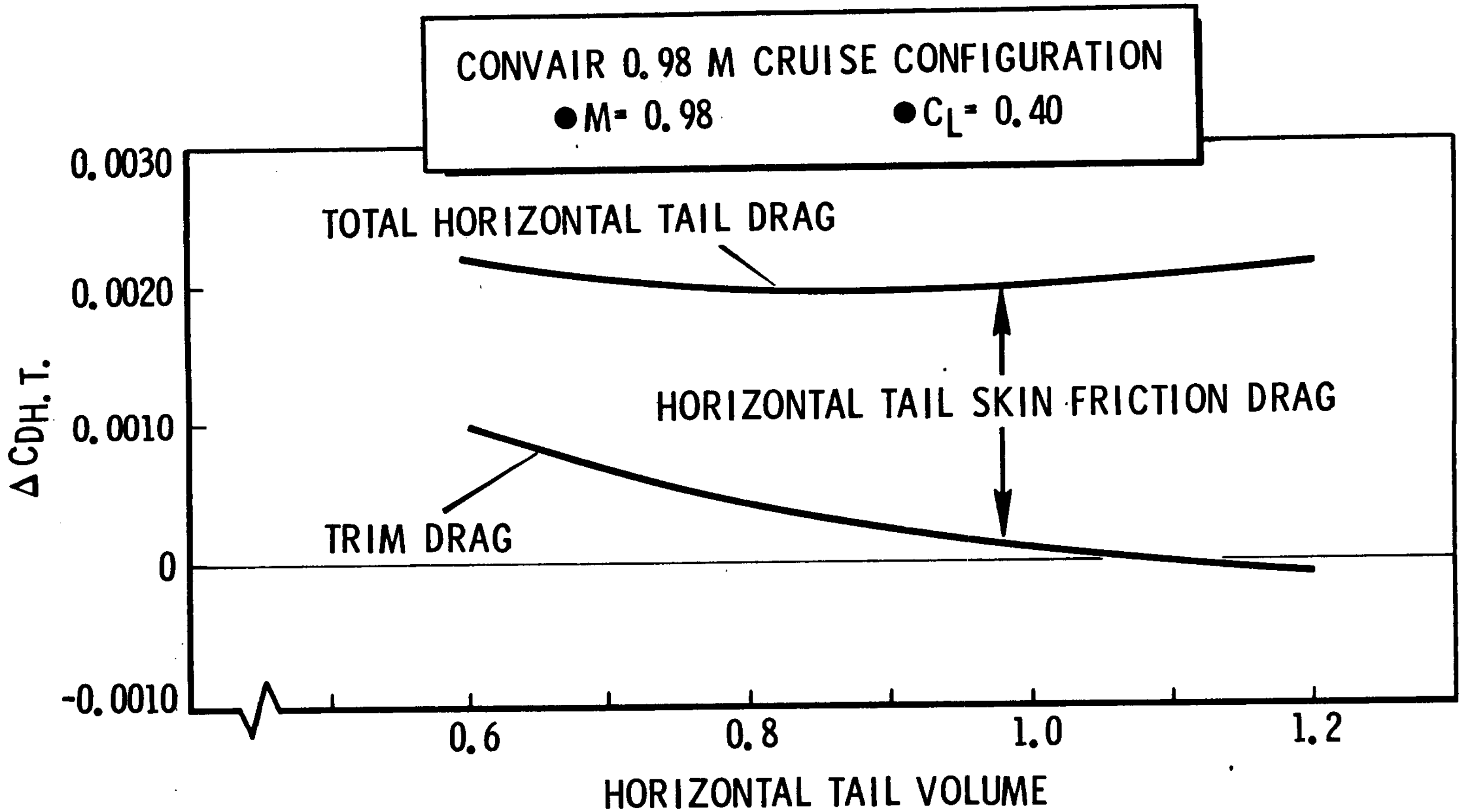

(c) Figure 9.2-12 Drag Effects of Horizontal Tail - Conventional Balance (u)

[redacted]

In view of the fact that the longitudinal control requirements have significant impacts on configuration operating characteristics through structural weight and cruise drag effects, further benefits may be obtained by incorporating a geared trailing-edge control on the all-movable horizontal tail (such as that employed on the Lockheed L-1011). Balance characteristics of such a configuration, with a 0.3c full span trailing edge control geared 1:1 to the all-movable horizontal tail, are given in Figure 9.2-13. Note that the addition of the geared trailing edge enables further substantial horizontal tail area reductions (nearly 20 percent) from the values previously given for an all-movable horizontal tail (Figure 9.2-11).

Throughout the ATT configuration selection studies, a horizontal tail volume coefficient of 0.60 has been used in sizing horizontal tails on Convair Aerospace configurations designed to relaxed aerodynamic stability levels. The data presented in Figures 9.2-11 and 9.2-13 are considered to represent a firm substantiation of this guideline, particularly in view of the tentative nature of the pertinent high-lift aerodynamic characteristics.

Additional information on the payoffs of relaxed aerodynamic stability is presented in Section 6 in terms of economic characteristics.

9.2.4 Other Benefits of Active Flight Controls

Several other advanced flight control concepts, in addition to those discussed above, may be beneficially applied to the ATT configurations. Although the benefits are not presently quantitatively assessable in terms of mission performance and economic improvements, several significant concepts are discussed, i.e., improved path control, reduced fatigue damage, improved ride quality, and safety-of-flight under upset conditions.

9.2.4.1 Improved Path Control

A considerable number of engineering efforts (References 9-2 through 9-11) have demonstrated by flight evaluations, ground-based simulations, and detailed studies that flight path control during landing approach may be significantly enhanced by the use of Direct Lift Control (DLC). Indications are that the benefits of DLC, in conjunction with

[redacted]

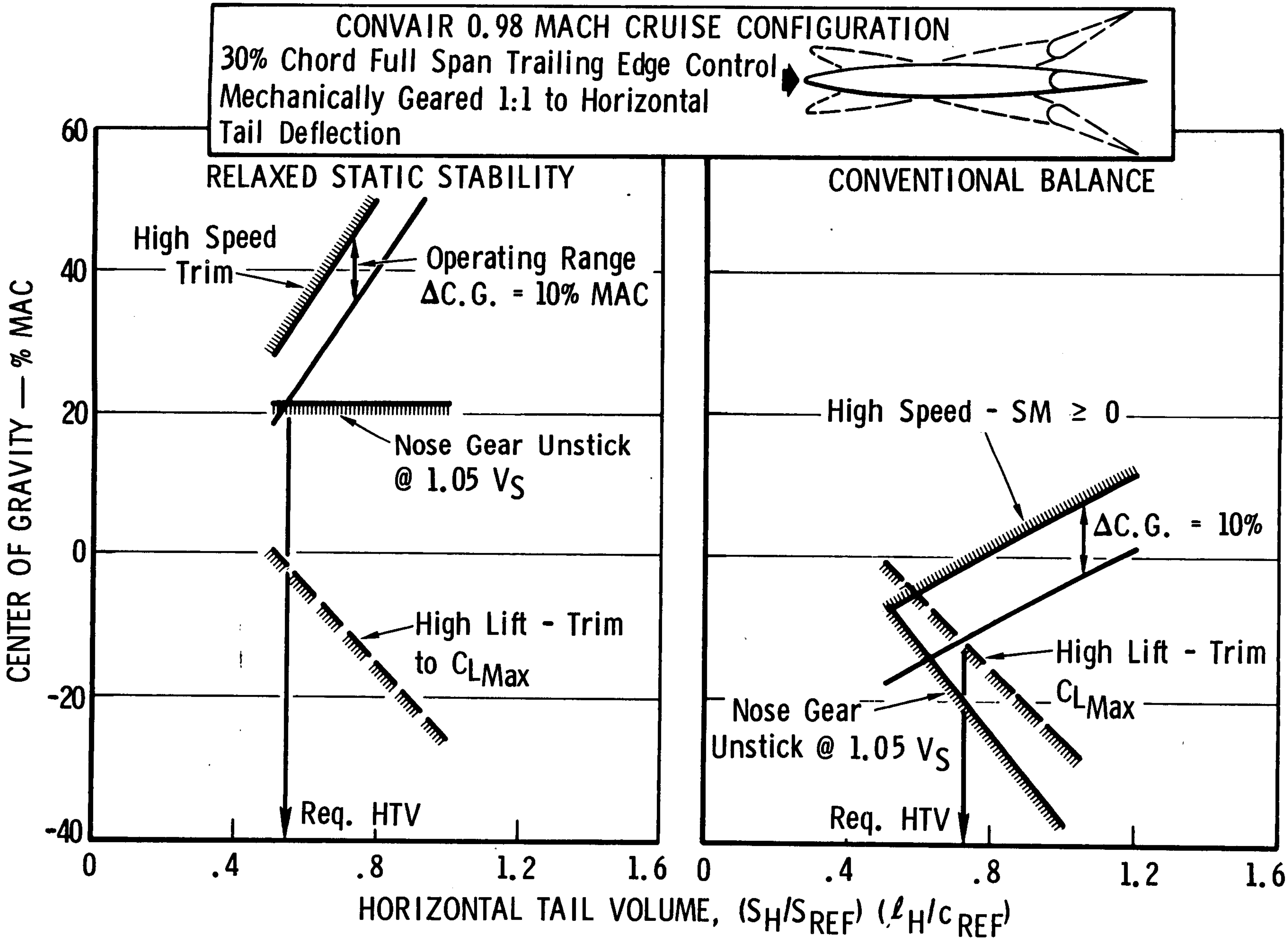

Figure 9.2-13 Balance Characteristics - All Movable Horizontal Tail Plus Geared Trailing Edge

automatic landing systems, will be as large if not larger than those already identified for manual landing approaches. On the ATT configurations, implementation is obtained by symmetrical deflection of the inboard spoilers about a 10-degree biased position with pitching moment compensation via horizontal tail deflection. In addition, the auto-throttle function will be available during manual, auto-pilot, and automatic landing operation to provide improved speed control. Further information on the flight controls implementation may be found in Subsection 9.5.

Consideration of the application of DLC to a large transport vehicle reveals that several significant benefits may accrue. The greatest of these is in providing an aircraft with a control system which cannot induce stalling but at the same time will enable the pilot to utilize practically all the available C_L range of the configuration. In view of such new vehicle usage, present airworthiness concepts should be reappraised to define the applicable low-speed safety rules. An overall assessment of DLC concepts, given by Pinsker in Reference 9-10, indicates that a crucial consideration is the effective point of application of the net lift produced by DLC. In a practical implementation, the pitching moment produced by the chosen direct-lift surface would be altered by automatic deflection of the basic pitch control surface to obtain an effective DLC center of pressure at the desired point. The work of Pinsker suggests that such a DLC effective center of pressure should be ahead of the aerodynamic center by a distance equal to or greater than the maneuver margin, the so-called "ideal point" being a distance just equal to the maneuver margin. When the DLC lift acts at this "ideal point," total lift change will be proportional to control application with no aircraft response in pitch angle. This type of control would be ideal for the automatic control of vertical velocity and height above runway during Automatic Landing Operation. If the DLC center of pressure acts ahead of this "ideal point," DLC action will be amplified by favorable aircraft incidence response. This type of application would be beneficial during manual pilot control since the net result would be to correct the sluggish response of large vehicles at flight conditions of low dynamic pressure. Note that these considerations carry the implication that different values of pitching-moment compensation should be employed in the separate cases of manual and automatic flight-path control.

On the premise that DLC allows substantial improvements in precision control during approach and landing, the following benefits are anticipated for the use of DLC:

1. Reduced vertical velocity at touchdown will enable relief in undercarriage design requirements with attendant savings in landing gear weight.

2. In conjunction with item 1, a softer oleo suspension may be utilized to reduce dynamic taxi loads and thereby extend fatigue life.

3. Items 1 and 2 may be traded off against a steeper landing approach flight path to reduce fly-over noise and increase obstacle clearance.

4. Increased precision control of touchdown point would yield better runway utilization and enhance safety under wet or icy runway conditions.

5. The operating margins above stall speed during approach for landing may possibly be reduced through the use of DLC in conjunction with an auto-stall-avoidance system so as to achieve improvements in landing performance.

6. Improved control system performance characteristics under manual and automatic control will enable use of higher feedback gains and result in much tighter system dynamics.

The future control system technology programs recommended in Volume II include a possible DLC systems application study for ATT-type configurations in which the above anticipated benefits would be evaluated.

9.2.4.2 Fatigue Damage Effects of ACS

Fatigue damage calculations were performed to determine the effects of a maneuver- and gust-load-alleviating active control system (ACS) on transport aircraft service life. Three airplane configurations were analyzed; namely, (1) 100-percent strength without ACS, (2) 100-percent strength with ACS, and (3) reduced strength with ACS. Damage was calculated at the following four control points:

Wing at Span Station η = 0.187

Wing at Span Station η = 0.702

Fuselage at Station 957 inches (24.2 m)

Fuselage at Station 1196 inches (30.4 m).

The fatigue damage caused by gust, maneuver, and ground-air-ground cycle, including landing impact, is summarized for each control point in Table 9.2-1. All values are presented as fractions of damage calculated for the 100-percent strength without ACS configuration. Thus the effect of ACS can readily be seen.

Results of the analysis are summarized as follows:

1. Gust and Maneuver Load Alleviation ACS applied to an aircraft that was designed to be satisfactory without ACS significantly reduces fatigue damage caused by gust, maneuver, and ground-air-ground cycles. The reduced ground-air-ground cycle damage is attributable to the ACS action in moderating the highest peak load per flight.

2. Gust and Maneuver Load Alleviation ACS applied to an aircraft optimumly designed for the reduced loads reduces the damage caused by gust and maneuver by approximately 40 to 70 percent in terms of the control points studied. However, the Ground-Air-Ground damage increased from 10 to 30 percent of the baseline configuration. This effect is reasonable because the one-g operating stresses are generally higher for the ACS <u>optimum</u> designed airplane than for the baseline airplane when both are designed to the same limit maneuver and gust environment.

9.2.4.3 <u>Improved Ride Quality</u>

The effects of employing a normal acceleration feedback to the inboard flaperon of the NASA baseline configuration are illustrated in Figure 9.2-14. Such a gust-alleviation function results in significant reductions in RMS gust response all along the fuselage; however, the unalleviated response characteristics are by themselves suitably small.

Table 9.2-1

FATIGUE DAMAGE RESULTS

Control Point	Relative* Fatigue Damage Study Configuration 100% Strength without ACS	100% Strength with ACS	Reduced Strength with ACS
Wing @ $\eta = 0.187$			
Gust	1.00	.39	.65
Maneuver	1.00	.09	.64
G.A.G.	1.00	.65	1.10
Wing @ $\eta = 0.702$			
Gust	1.00	.25	.55
Maneuver	1.00	.50	.50
G.A.G.	1.00	.90	1.16
Fuselage Sta 957 (24.2 m)			
Gust	1.00	.37	.49
Maneuver	1.00	.42	.58
G.A.G.	1.00	.82	1.08
Fuselage Sta 1196 (30.4 m)			
Gust	1.00	.29	.42
Maneuver	1.00	.13	.27
G.A.G.	1.00	.75	1.29

* Data normalized on 100% strength without ACS configuration.

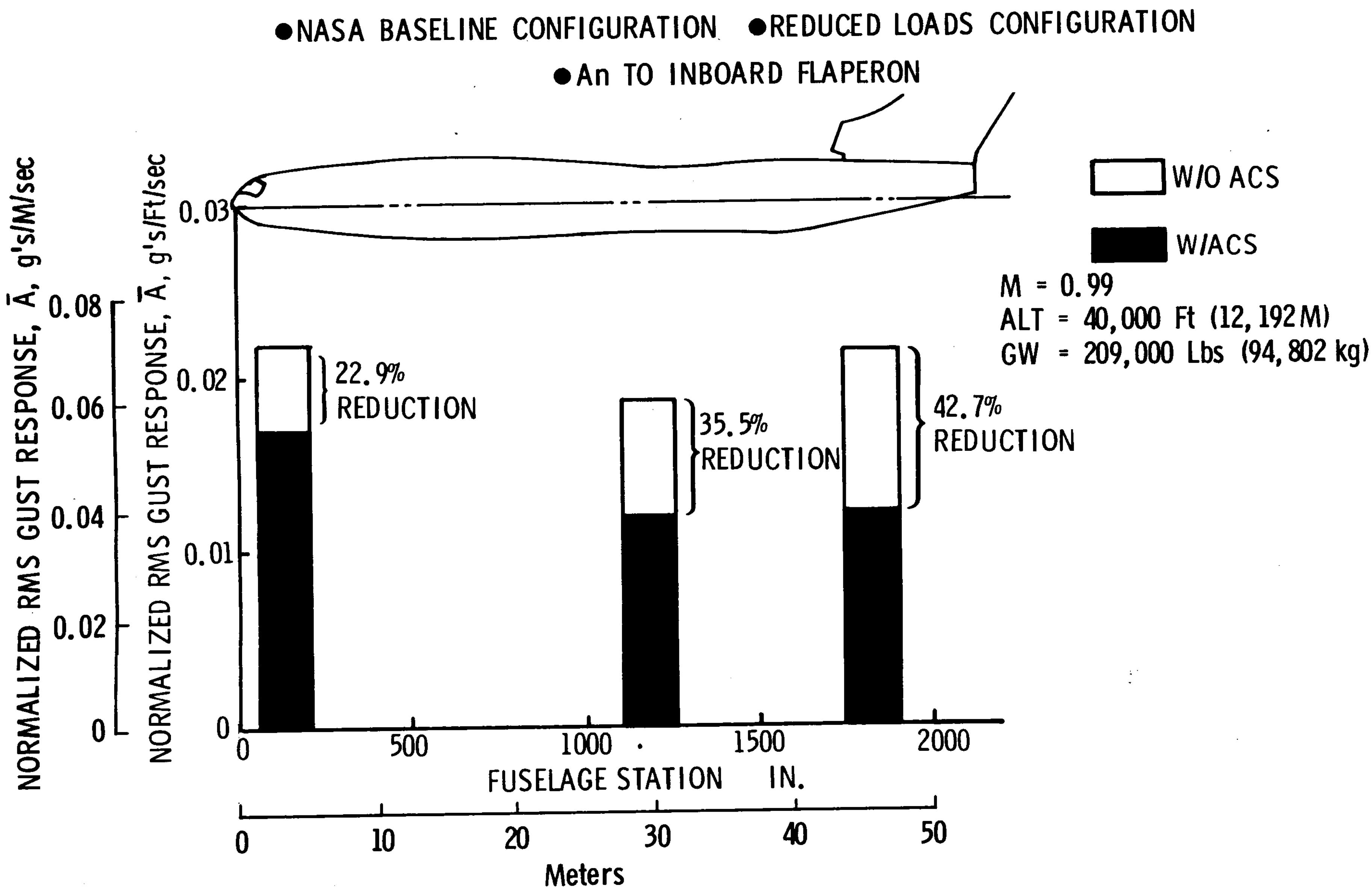

Figure 9.2-14 Ride Quality Benefits of Gust Alleviation

Such a gust alleviation implementation has not been included on the final Convair configurations because of a conflict in implementing the inboard trailing edge as both a high-speed flaperon and a low-speed double-slotted flap. If such an implementation could be devised, a significant weight penalty would be imposed by the high-speed hinge-moment characteristics. On the selected Convair configurations, some ride-quality improvement will be obtained via gust-load alleviation in that the outboard spoiler will minimize the peak positive normal accelerations induced by large discrete gusts.

9.2.4.4 Safety of Flight in Turbulence and Critical Upsets

The employment of the relaxed aerodynamic stability concept results in placement of additional emphasis on the ability to control extreme upset conditions. One such critical situation is control of the response to large discrete gust inputs at conditions characterized by longitudinal aerodynamic instability. The flight conditions of interest occur at the low-altitude, high-speed and dive-speed limits since aeroelastic losses dominate in the reduction of static longitudinal stability. Since the FAR Part 25 design discrete gust magnitudes are 50 feet per second (15.2 meters per second) at the high-speed, low-altitude limit and only 25 feet per second (7.6 meters per second) at the corresponding dive-speed limit, discrete gust response at the high-speed limit poses the more difficult control problem.

Typical time history response data for such a case are presented in Figure 9.2-15. The period of the gust input used to calculate these data is somewhat longer than the FAR standard. This longer period of gust waveform was employed in order to tune the input to the longitudinal short-period response and thereby consider the largest transient condition possible with the given peak value of gust velocity. Note that both with and without Maneuver Load Control (MLC) via wing tip spoilers, the transients are quite mild and only small control-surface deflections are needed to rapidly stabilize the aircraft response.

9.2.5 Active Controls Payoffs - NASA Baseline Configuration

Payoffs on the application of selected active control features are shown in Figure 9.2-16 in terms of the

CONVAIR 0.98M ACS CONFIGURATION
H.T.V. = 0.60
• MACH = 0.70, H = 10K FT (3048 METERS) • GW = 320,000 LBS (145,150 KG)
STATIC MARGIN = -24.7% MAC

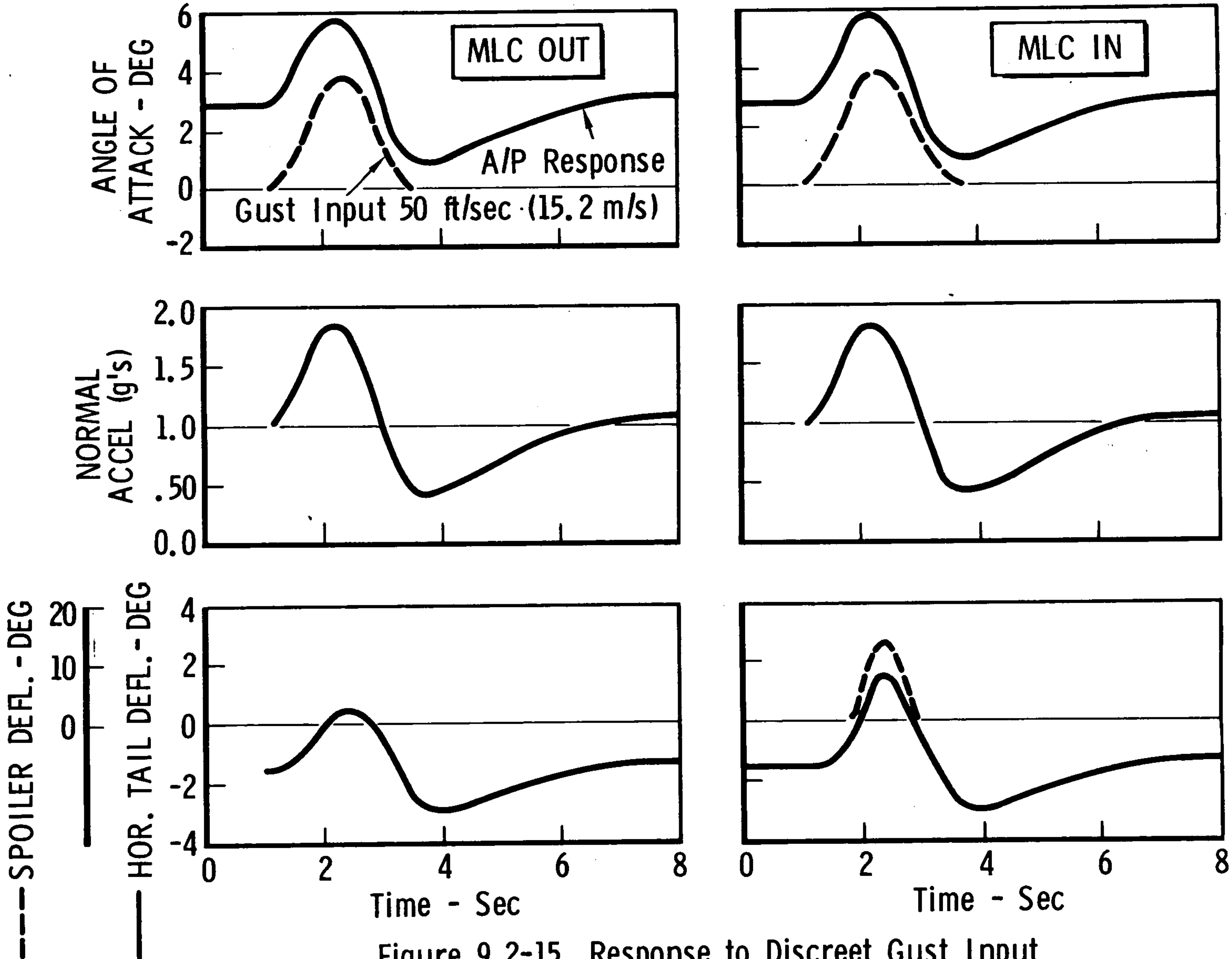

Figure 9.2-15 Response to Discreet Gust Input

NASA BASELINE 0.98 MACH CRUISE CONFIGURATIONS SIZED FOR CONSTANT PERFORMANCE
Range 3000 N.Mi. (5560 Kilometers)
Payload 40,000 lb (18,140 Kilograms)

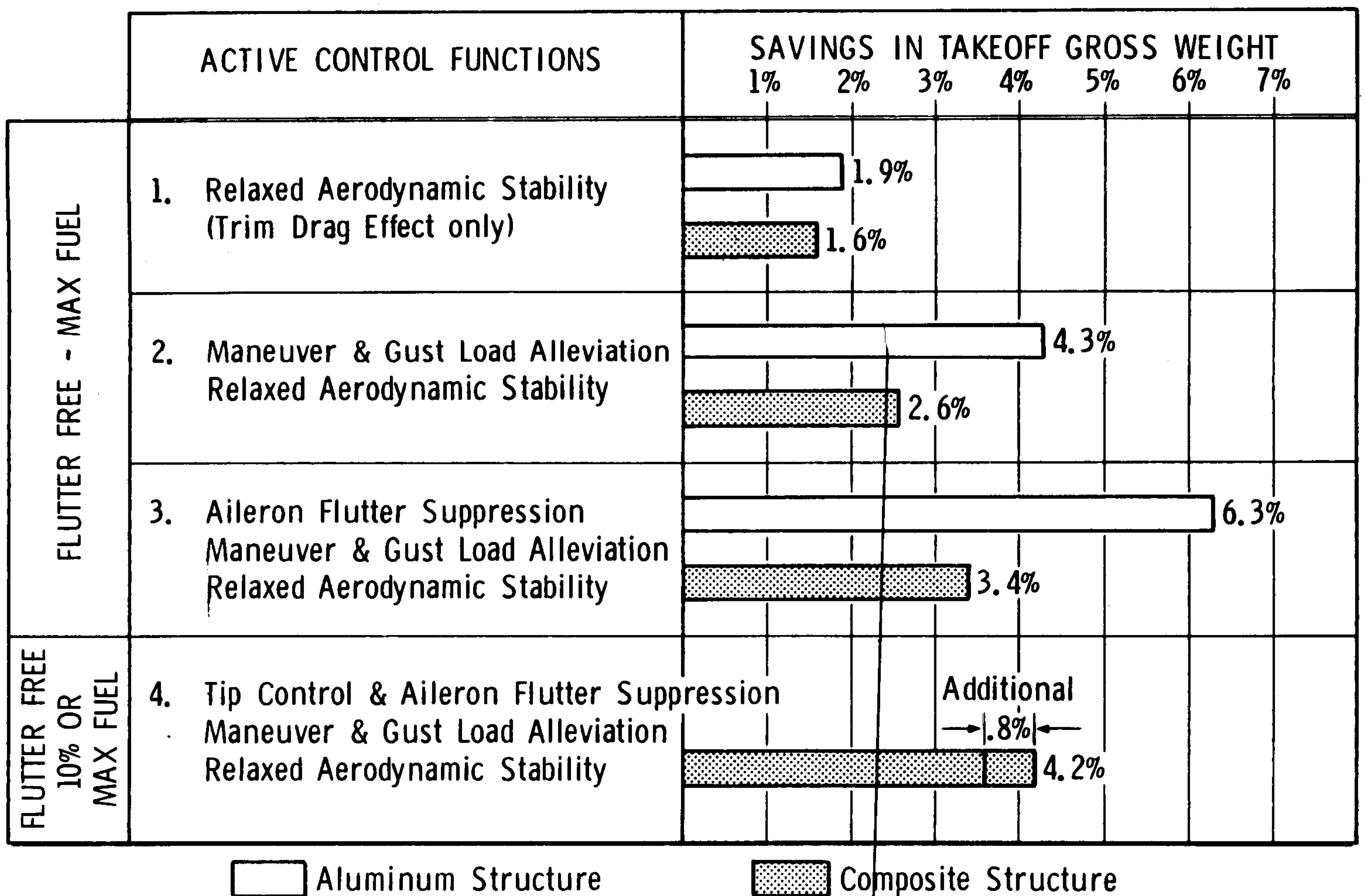

Figure 9.2-16 Active Flight Controls Payoffs: NASA Baseline Configuration

obtainable reductions in takeoff gross weight when the configuration is resized to maintain constant performance. Note that the savings are significantly less if the wing and empennage are fabricated of composite materials rather than aluminum. The baseline used in establishing the incremental effects is a configuration with the trim drag of conventional balance and a structural arrangement for 100-percent design maneuver and gust loads. A common ground rule is that all configurations are flutter free. For the most part, the flutter constraint is based upon a maximum wing fuel condition since this was the primary case considered in the flutter investigation. Where available, data are also presented for a low fuel condition that was found to be more critical in flutter.

The benefits of relaxed aerodynamic stability reflect only the elimination of cruise trim drag since horizontal tail size was not varied in this evaluation. Comparable additional savings are obtained by maneuver and gust-load alleviation via symmetrical outboard spoiler deflection. In Case 2, some torsional stiffening is added as wing bending material is decreased so that the reduced design load configuration remains flutter free. Additional weight savings accrue when flutter suppression via the small outboard aileron is included (Case 3). Prevention of flutter at the 10-percent wing fuel loading via combined use of aileron and tip flutter suppressors offers additional payoff in the only case of this type investigated.

9.3 AERODYNAMIC STABILITY AND CONTROL

9.3.1 Longitudinal Characteristics

Longitudinal stability and control effectiveness data on a representative final configuration are given in Figure 9.3-1 to illustrate both the Mach number and aeroleastic effects. Excellent control effectiveness is evident throughout the flight envelope to beyond limit dive speeds. In the case of aerodynamic-center position, two factors result in considerably forward locations. Large aeroelastic effects are associated with the selected wing planform and minimum weight structural arrangement. Also, the rigid aerodynamic-center location is in itself quite far forward due to two geometric features. The highly swept wing-strake with blended fuselage juncture yields quite-far-forward wing-body values. Unpublished results of the ATT Parametric Wind Tunnel Program indicate that the horizontal tail is located

[redacted]

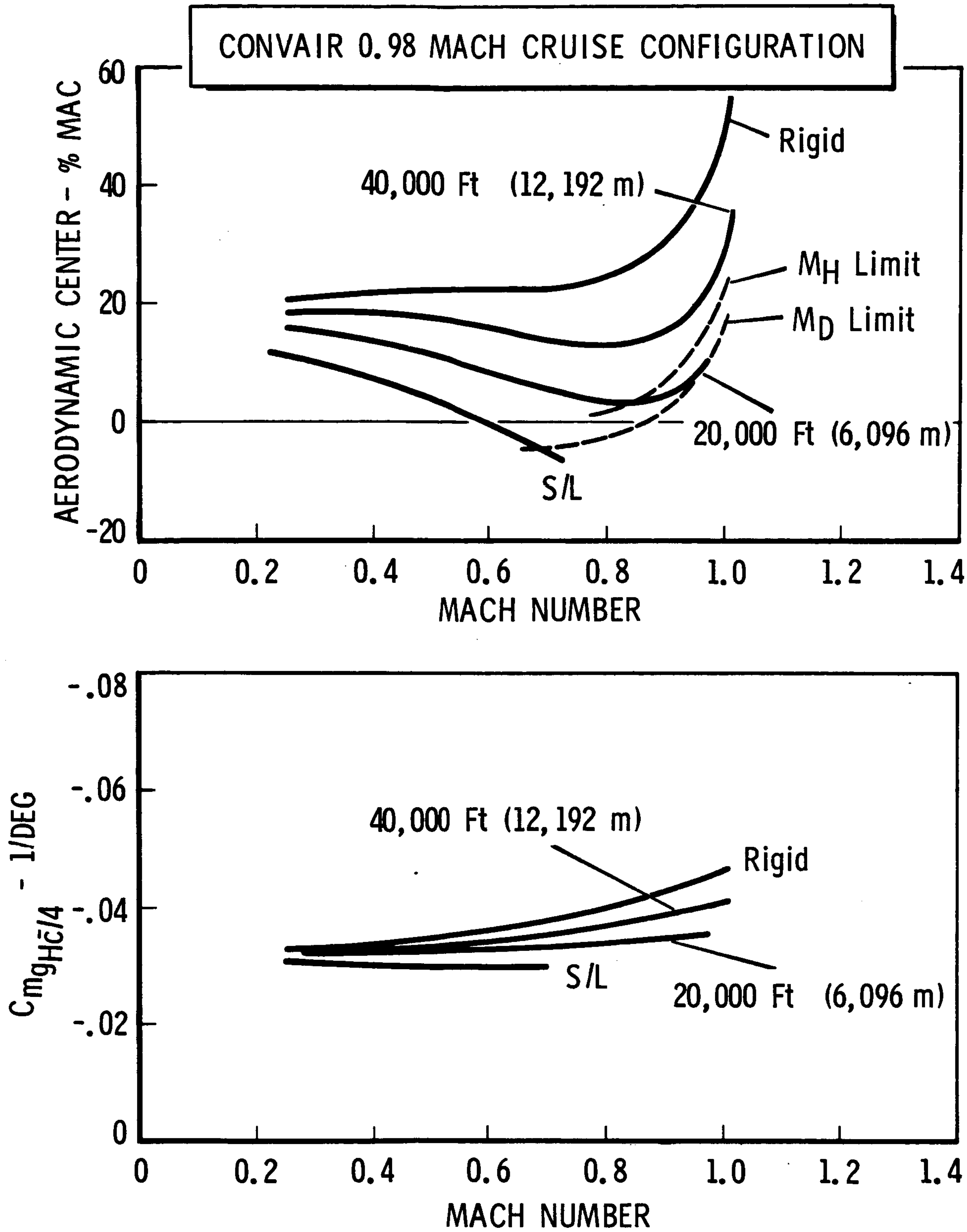

(c)Figure 9.3-1 Longitudinal Aerodynamic Stability and Control Effectiveness (u)

[redacted]

[redacted]

in region of high downwash, as discussed in Reference 9-12; thus the horizontal tail contribution to longitudinal stability is significantly less than normal.

The variation in aerodynamic static margin during a typical flight profile is given in Figure 9.3-2. The configuration balance of this data meets the two basic requirements: (1) that trim drag at cruise be essentially zero and (2) that the vehicle be completely controllable in the event of an extreme upset at the most critical flight condition. (See Sections 9.2.3 and 9.2.4.4 for additional discussion.) The data in this figure illustrate that, for most of the normal operation, small to moderate values of positive static margin will occur; only during brief transient conditions will it be necessary to rely on the artificial static stability afforded by the advanced flight control system.

9.3.2 Lateral-Directional Considerations

The primary impact of the lateral-directional aerodynamic characteristics upon overall configuration arrangement is in the selection of suitable vertical tail geometry. Initial checks accomplished to support parametric configuration layouts lead to the general conclusion that engine-out directional control during takeoff is the critical item on configurations with two wing-mounted and one centerline flow-through nacelles, as in Figure 9.2-2. Accordingly, on such configurations, the exposed vertical tail is sized to enable directional control of one engine out at the stall speed in the takeoff configuration. A specific layout guideline in terms of tail volume has been employed for the moment area of that part of the vertical tail flapped by the rudder as a function of the thrust-to-weight ratio and spanwise location of the wing-mounted engines.

9.4 HANDLING QUALITIES

9.4.1 Longitudinal Dynamics

The short-period dynamics associated with the aerodynamic characteristics reviewed previously in Section 9.3.1 are illustrated in Figure 9.4-1. Characteristics at a wide range of flight conditions are given for the NASA baseline configuration since much of the flight control formulation was accomplished on this arrangement. The results of key checks on a representative final arrangement are also

[redacted]

CONVAIR 0.98 MACH CRUISE CONFIGURATION

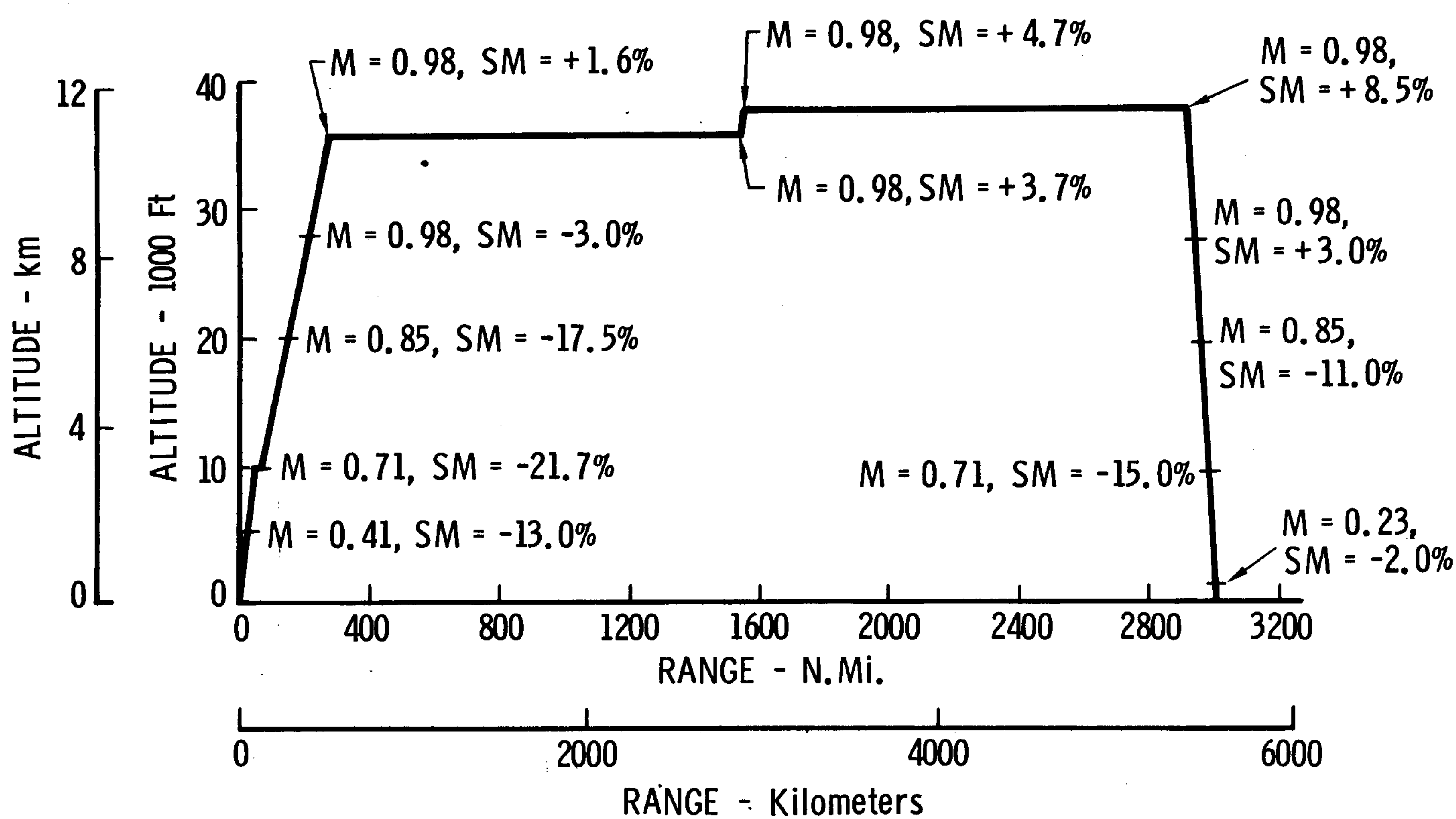

Figure 9.3-2 Variation of Aerodynamic Static Margin During Typical Flight Profile

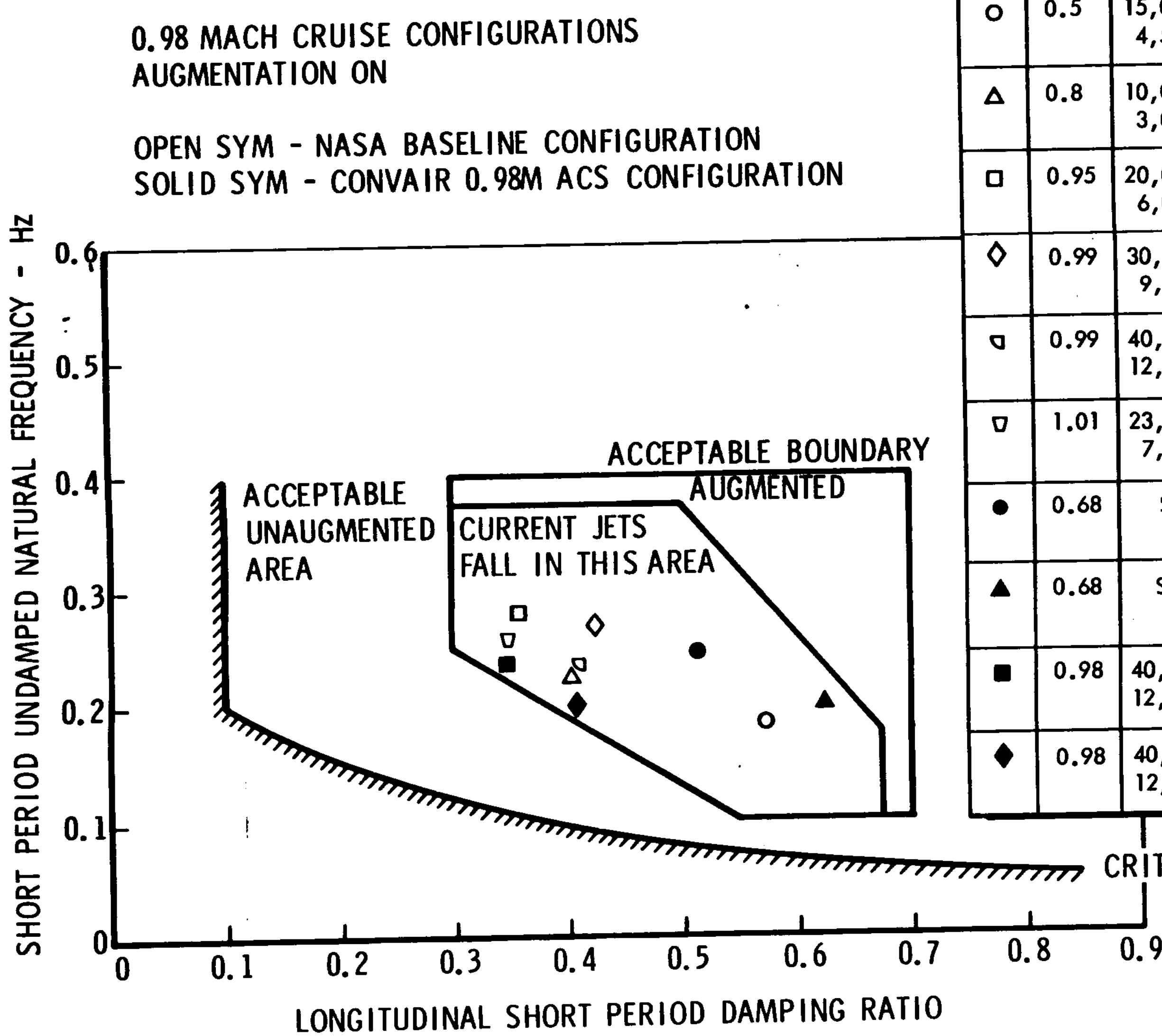

SYM	MACH	ALT	GW	SM
○	0.5	15,000 Ft 4,572 M	385,500 Lb 174,860 kg	2%
△	0.8	10,000 Ft 3,048 M	385,500 Lb 174,860 kg	-11%
□	0.95	20,000 Ft 6,096 M	385,500 Lb 174,860 kg	6.3%
◇	0.99	30,000 Ft 9,144 M	385,500 Lb 174,860 kg	11.9%
▽	0.99	40,000 Ft 12,192 M	385,500 Lb 174,860 kg	17%
▽	1.01	23,000 Ft 7,010 M	385,500 Lb 174,860 kg	5.2%
●	0.68	S.L.	320,000 Lb 145,150 kg	-14.7%
▲	0.68	S.L.	320,000 Lb 145,150 kg	-24.7%
■	0.98	40,000 Ft 12,192 M	320,000 Lb 145,150 kg	14.1%
◆	0.98	40,000 Ft 12,192 M	320,000 Lb 145,150 kg	4.1%

Figure 9.4-1 Longitudinal Short Period Characteristics

presented to verify control system adequacy on the final configurations over a wide range of positive and negative static margins.

9.4.2 Recovery from Upset

Peak transient response to large discrete gusts at the flight conditions of maximum static instability were presented previously in Figure 9.2-15 for a flight condition of large aerodynamic instability. These data illustrate that the longitudinal control power and control system implementation are adequate to handle this most critical upset condition. As noted previously, no objectional variations in control power occur due to either Mach number or aeroelastic effects within the dive-speed envelope (see Figure 9.3-1). Since both the trim and longitudinal control function are implemented via the all-movable horizontal tail, no conflict between trim and control will occur, and ample control is provided for all other types of upsets such as center-of-gravity shifts and overspeed conditions.

9.4.3 Low-Speed Control Requirements

The critical longitudinal control requirement for takeoff and landing operations is the ability to rotate to takeoff attitude prior to the attainment of the desired lift-off speed. As presented previously, Figure 9.2-11 illustrates the corresponding forward center-of-gravity limits based upon the ability to accomplish nose-gear unstick at 105-percent stall speed in the takeoff configuration. Note that the use of the relaxed static stability concept enables the attainment of a suitable center-of-gravity operating range with a smaller size horizontal tail. Use of the above discussed control criteria results in considerable excess in trim capability for all conditions up through stall on those configurations balanced to relaxed static stability concepts. As discussed in Subsection 9.2.3, the forward center-of-gravity limit on configurations with conventional longitudinal balance is set by the ability to trim to $C_{L_{max}}$ in the takeoff and landing configurations in free air. Deep stall avoidance is not anticipated to be a significant handling qualities factor on the Convair selected configurations since use of a low horizontal tail position is expected to result in nose-down pitching moment trends at and above stall.

No difficulty is anticipated in low-speed directional control since vertical tail size is based upon control of engine-out yawing moments at speed down to stall in the takeoff configuration. On the Convair configurations, directional control requirements for crosswind landings are significantly less than the requirements imposed by engine-out conditions.

9.5 FLIGHT CONTROL SYSTEM

Several sources of information were utilized to determine the flight control requirements for the next generation of commercial transport aircraft, to determine the optimum implementation of these requirements, and to assess the readiness of the required technology. Major vendors of commercial flight control hardware were contacted and, although no funding was available for them to perform any new studies, they did supply valuable commentary and literature. The following companies which supply flight control or air data hardware were contacted:

Bendix Corporation
General Electric Corporation
Honeywell, Inc.
Sperry Rand Corporation
Lear Siegler, Inc.
Airesearch Manufacturing Company

Bendix and Lear Siegler visited Fort Worth for discussions. Bendix, Sperry, Lear Siegler, Honeywell, and Airesearch submitted pertinent literature. Additionally, Bendix and Sperry submitted written comments. Verbal discussions were held with all of the vendors contacted. The unfunded support provided by these companies is greatly appreciated.

In assessing the state of readiness of the desired technology, current and projected programs were analyzed. Not only commercial research and development programs such as those sponsored by NASA, FAA, and individual companies were considered, but also the large number of military programs that can also lead to the development of the required technology were reviewed. Convair study programs concerning fly-by-wire flight controls and multiplexing have provided an awareness of the benefits of these techniques.

Discussions were also held with airline operators concerning some of the newer concepts being considered. However, technical and economic considerations only influenced the recommended flight control system features and implementation since the state of readiness of certain technologies is easier to predict than is their acceptability to airline operators, pilots, or the FAA.

9.5.1 System Modes and Functions

The results of the active control system study described in Section 9.2 reveal that several advanced control concepts may be applied to transport aircraft of the future with significant economic benefits. Advanced control concepts which are included in the Convair configurations are as follows:

1. Maneuver Load Control - Wing-tip spoilers deflected symmetrically during maneuvers to reduce wing-root bending moments.

2. Active Flutter Suppression - Wing flutter mode damped by employment of small, outboard, trailing edge surface, and a tip flutter suppression surface located outboard and forward on the wing tip.

3. Static Stability Augmentation - Feedbacks to the horizontal tail utilized to augment both angle-of-attack and speed stability.

4. Direct Lift Control - Biased wing spoilers used to improve flight-path control during the landing approach.

The evaluation of the full-time gust-alleviation system indicated that the improvements in ride qualities and fatigue life did not justify the incorporation of this feature. However, the recommended implementation of the Maneuver Load Control feature is such that it provides attenuation of large-amplitude positive gusts.

The primary flight controls provide three-axis control and trim. Dynamic stability augmentation is included in the pitch and yaw axes. Automatic turn coordination is provided in the landing approach configuration.

Although an extensive assessment of the autopilot requirements was not made, it is felt that features available in the most recent vintage of commercial transports (DC-10, L-1011) are adequate for the 1975-1985 time frame with the exception that a Category III automatic landing capability will be both desirable and available. The following autopilot/flight director system modes are available on the L-1011 and are recommended for the Convair designs:

1. Attitude Hold
2. Heading Hold
3. Control-Wheel Steering
4. Altitude Select
5. Vertical Speed Hold and Select
6. Localizer
7. Heading Select
8. Altitude Hold
9. Mach Hold
10. IAS Hold
11. VOR and Area Nav.
12. Approach
13. Approach/Land.

An automatic throttle system is also a feature of the proposed flight control system. This system is an airspeed command system except during final approach, when it will revert to angle-of-attack control. The auto-throttle may be used for manual approaches but will also be compatible with the auto-land system.

9.5.2 Basic Flight Control Implementation

9.5.2.1 Implementation Philosophy

After surveying the current state of flight control technology and projecting forward to the 1975-1985 time frame based on current and proposed research programs, Convair envisions some rather drastic changes in flight control implementation philosophy. It is the opinion of Convair, and also of those vendors of flight control hardware which were contacted, that flight control equipment for the 1975-1985 time period will be digital in concept and design. Honeywell and possibly others have determined the computational requirements for the digital implementation of the outer loops of a fighter aircraft Automatic Flight Control System, an Automatic Throttle Control System, a Stall Warning System, and Built-in Test Equipment for all of the above. The implementation of the above computations did not tax a 1968-vintage (HDC-201) airborne digital computer. With the significant increase in computational speed obtained recently (Honeywell claims a 3-to-1 speed increase from the HDC-201 and the 1970-model HDC-301) and the projection of further speed increases, it seems reasonable to assume that the 1975-1985 computers could also handle the primary control and inter-loop computations as well as those required by the Active Control System.

Convair is proposing dedicated computers for the flight control computations and separate dedicated computers for the air data computations. Some people feel that the trend is to one centralized "super computer" to perform all on-board computations. The question of having a "super computer" as opposed to smaller, dedicated computers was not specifically posed to the flight control vendors, but Bendix did furnish an opinion that the trend would not be to the large centralized computer.

The Convair-recommended flight control implementation departs significantly from that employed in present day commercial transports in that it is completely fly-by-wire with no mechanical backup. There are many factors which affected the decision to recommend the electro-hydraulic flight control system. Extensive company studies were conducted in support of the Advanced Manned Strategic Aircraft (AMSA) program. During the AMSA Task 14C, a fly-by-wire system was designed for the AMSA aircraft (forerunner of the B-1). A quad electronic voter was designed, built and tested. Results of this program may be obtained from Reference 9-13. Much work has been done in the area of fly-by-wire systems, and flight demonstration programs are currently in progress. Fly-by-wire is not a new or radical concept. The A3J (now RA-5) of the 1950s had a fly-by-wire flight control system with manual backup. The spoiler control system incorporated in the F-111 is completely fly-by-wire. Another factor which influenced the decision to recommend the fly-by-wire approach is the high reliability requirements of some of the desirable active control system features. The reliability of the static stability augmentation feature for instance must equal that of the primary flight controls. Since the electrical reliability must be provided, it seems logical to utilize the same equipment for the primary flight controls.

9.5.2.2 Longitudinal Flight Control System

Primary pitch control is achieved by controlling the horizontal stabilizer. Fore and aft control column position is sensed by redundant electrical transducers. The outputs of these transducers are voted and transmitted to the three digital flight control computers. In a similar manner the computers receive signals from the redundant pitch rate, angle-of-attack, normal acceleration, and air data sensors. Command and stability augmentation commands are computed and transmitted to the two dual tandem hydraulic horizontal stabilizer actuators. Performance and failure monitoring is accomplished within the flight control computers. The horizontal stabilizer actuators are supplied from four hydraulic systems and are sized such that 100 percent of design hinge moment is available after loss of one hydraulic system. Adequate control power is available after loss of two systems to control the aircraft and land safely.

Direct Lift Control (DLC) is provided when the flaps are extended to the landing position and power is retarded to approach power. The two mid-span spoilers on each wing are biased to the 10-degree position and then modulated symmetrically by control-column position. The DLC spoilers are retracted near stall angle of attack to provide additional stall margin.

Maneuver Load Control (MLC) is accomplished by symmetrical deflection of the tip spoilers. MLC spoiler commands are computed in the flight control computers from normal acceleration and air data inputs. The MLC computation is such that commands are supplied to the spoilers only above 1.5-g normal acceleration. When the spoilers are employed in a MLC or DLC role, a spoiler/stabilizer interconnect provides compensation for spoiler pitching moment.

9.5.2.3 Lateral Flight Control System

Lateral control is achieved by controlling two large spoilers on each wing and an all-speed, mid-span aileron. Control-wheel rotation is sensed by redundant electrical sensors and transmitted to the flight control computers. Surface commands are computed and transmitted to the electrical-input control-surface actuators. Each lateral control surface is powered by a dual tandem hydraulic actuator. Four hydraulic systems are employed such that at least two control surfaces on each wing are available for lateral control after loss of two hydraulic systems.

9.5.2.4 Directional Flight Control System

Two large rudders located on the trailing edge of the vertical fin are used for directional control and stability augmentation. Rudder pedal position is sensed by redundant electrical transducers and transmitted to the flight control computers. The computers also receive signals from redundant yaw rate, angle-of-attack, and aileron-position sensors for computation of stability augmentation and automatic turn coordination commands. Total rudder commands are transmitted to the upper and lower rudder surface actuators. Each rudder is powered by a dual tandem hydraulic actuator. Four hydraulic systems are utilized to insure that adequate directional control is available for landing after loss of two systems.

9.5.2.5 Active Flutter Suppression

Active flutter suppression is accomplished by modulating a small, outboard, trailing-edge surface and a small flutter-suppression surface located forward and outboard of the wing tip. The location of these surfaces as well as other control surfaces referred to in this section are shown in Figure 9.5-1. Linear accelerometers and angular rate gyros are located in the tip section of the wing to provide the feedback signals for the active flutter-suppression system. The sensor signals are transmitted to the flight control computers, where the flutter suppression surface commands are generated. These commands are transmitted back to the wing tip section where they are used to drive the flutter-suppression system actuators.

CONVAIR ACS CONFIGURATIONS

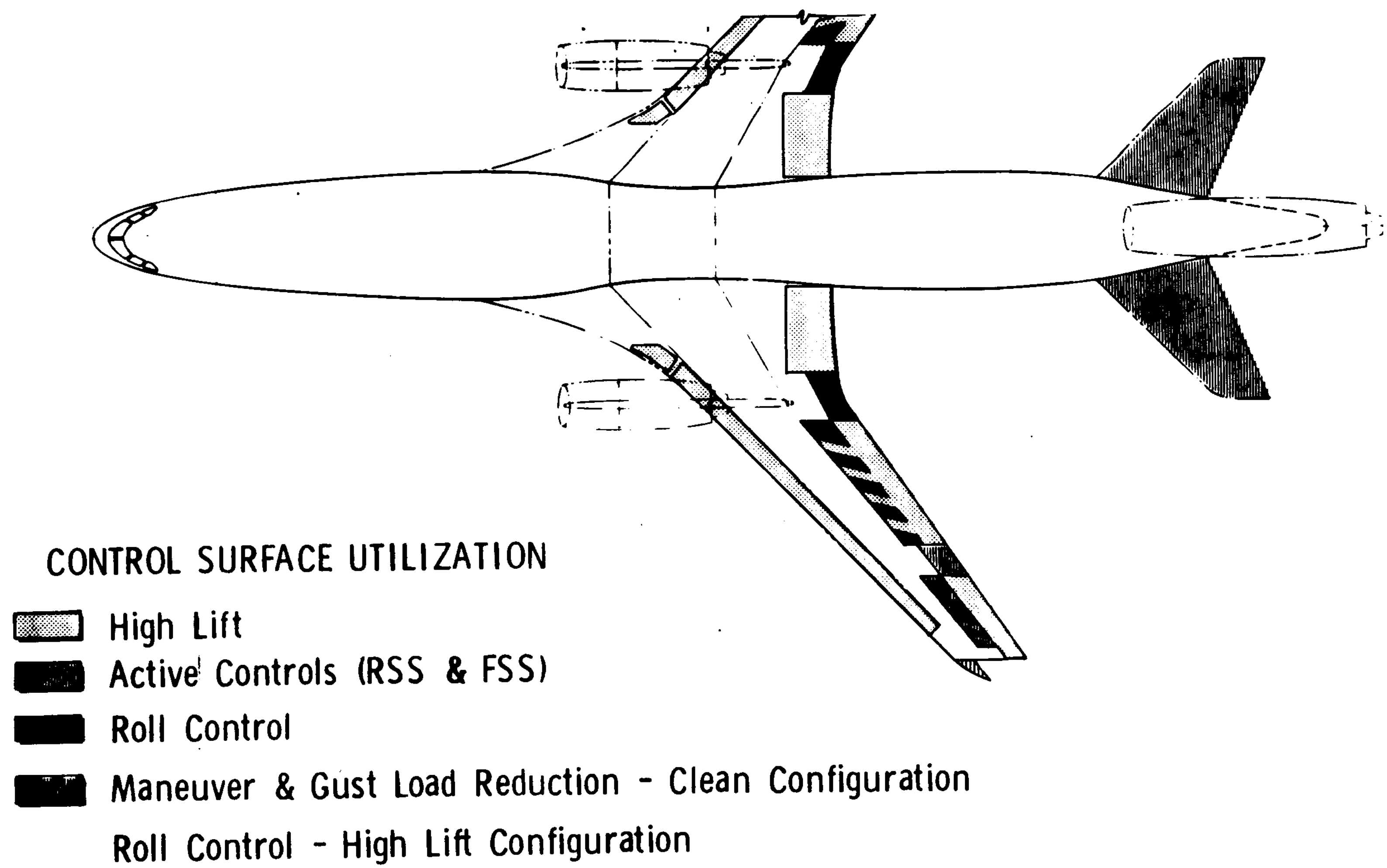

Figure 9.5-1 Flight Control Surface - ACS Configurations

9.5.2.6 Equipment Location and Data Transmission

The general location of flight control electrical equipment is shown in Figure 9.5-2. The flight control computers are located in the forward avionics bay. Multiplexing techniques are utilized throughout for transmission of flight control signals. This concept is a logical complement to any digital flight control system. It makes possible the time sharing of certain equipment such as voters, allows more accurate failure isolation, and provides growth potential for additional signals. In a hybrid system such as the one proposed, the multiplex encoder performs the function which would otherwise be performed by an analog/digital converter. Multiplexing can also be a weight saver in large aircraft because many signals may be transmitted over a single, shielded, twisted pair rather than over long runs of many-cabled harnesses.

Multiplex transmitter/receiver units are located in the forward avionics bay, central fuselage area, inboard and outboard sections of each wing, and the aft fuselage area. The inputs and outputs of these units are indicated in Figure 9.5-2.

9.5.3 Redundancy and Monitoring

The primary flight control and essential augmentation functions are operational after a second similar failure. It is expected that this level of redundancy will be required to insure safety even considering expected improvements in reliability in the next several years. To insure no degradation after two electrical failures, those units and components which require branch-comparison-type monitors must employ quad redundancy. These include control position sensors, rate gyros, accelerometers. The flight control computers, which can be programmed for self-test, can provide two-fail-operational performance with only three units. Changing the level of redundancy poses no problem. A typical quad-to-triplex conversion scheme is shown in Figure 9.5-3. Non-critical flight control functions, such as autopilot, are single-fail operational.

All performance assessment will be accomplished in the flight control computers. Failure monitoring will also be performed in the computers except for the sensors which are monitored by the branch comparison method. Indications of flight control system status will be provided to the pilot.

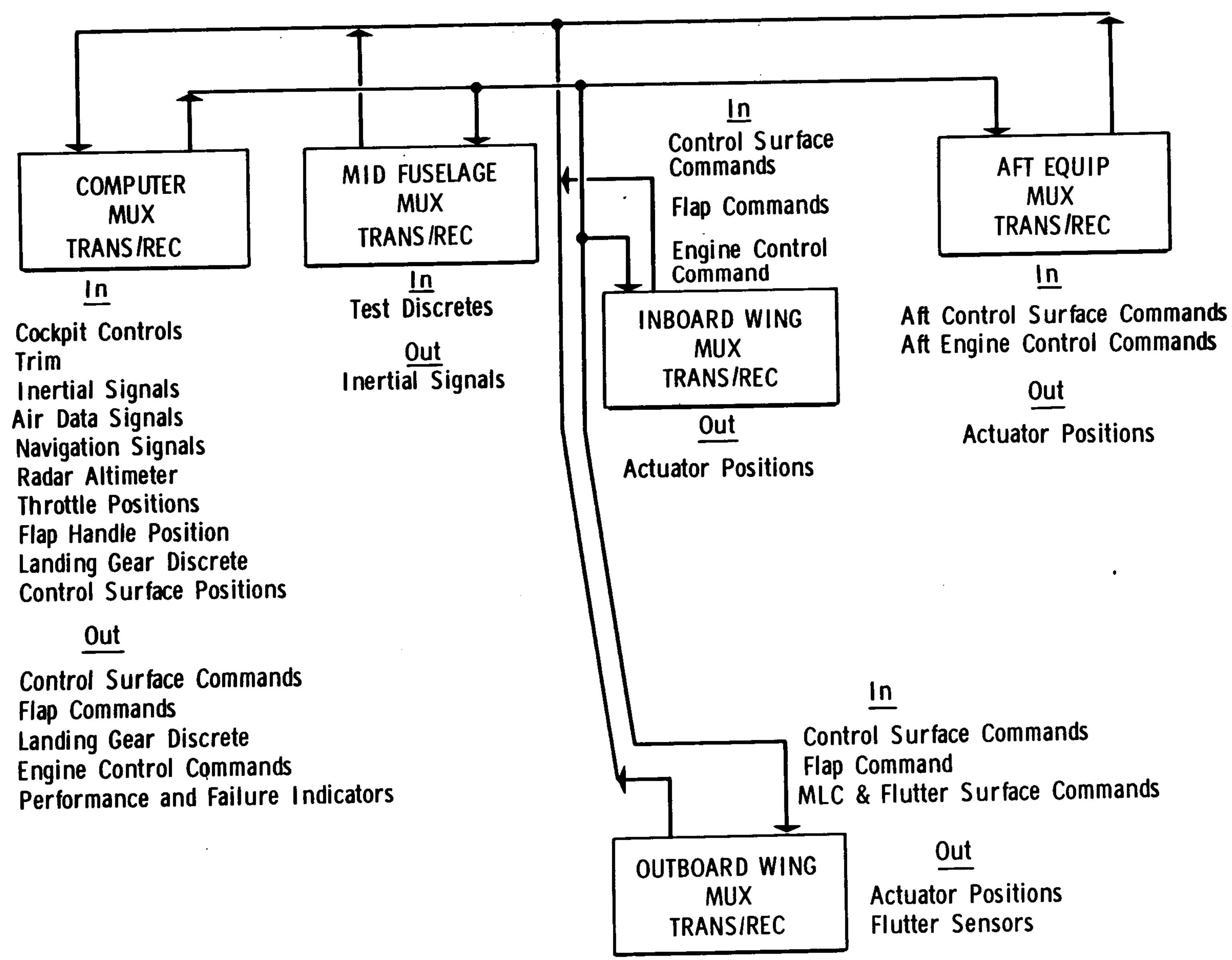

Figure 9.5-2 Flight Control System Electrical Equipment

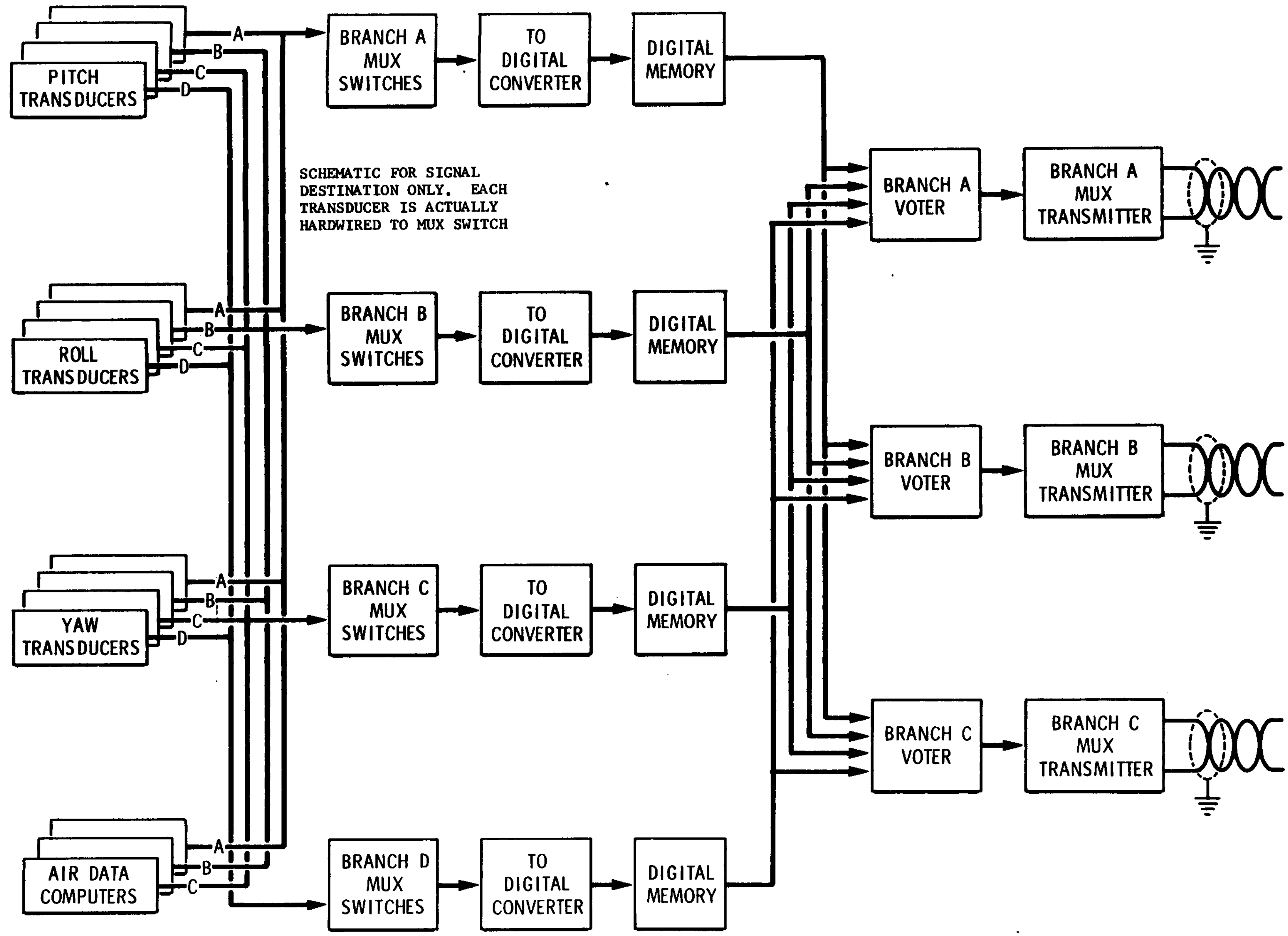

Figure 9.5-3 Typical Quad to Triplex FCS Signal Conversion

Hydraulic redundancy has been discussed in the previous section (Section 9.5.2) and will not be reiterated except to note that the aircraft can be safely controlled and landed after loss of any two systems.

9.6 AVIONICS

9.6.1 Avionics Systems

The development of avionics systems for commercial aircraft is continuously undergoing an evolutionary trend toward automated operation and modularized design. Many functions have been incorporated into these systems, and for the 1975-1985 ATT time span it is anticipated that a fully integrated avionics system concept will be employed. The ATT avionics study has been oriented toward defining the functions which will likely be employed and examining equipment developmental status and availability for accomplishing these functions.

Emphasis was on defining and examining the functions required to provide the ATT aircraft with the following features and operational capabilities:

1. The ability to negotiate the growing congested terminal areas in adverse weather conditions while retaining the benefits realized from the advanced technology aerodynamic improvements.

2. Navigational and guidance capabilities for precise world-wide operation.

3. Flight management capability coupled with displays to enable the crew to better manage the total aircraft operation.

4. Onboard data recording and equipment monitoring capability for improved maintenance management.

During the study, a letter of inquiry was sent to a broad spectrum of avionic equipment manufacturers for the purpose of obtaining an industry-wide equipment availability and status evaluation. The results of this survey and a comprehensive literature survey together with related

Convair Aerospace Division avionics system experience were utilized to describe the avionics functions envisioned for the ATT aircraft and arrive at a possible avionic equipment configuration layout.

9.6.1.1 General Avionics Functional Description

The major functions envisioned for incorporation into the ATT avionics system are summarized in Table 9.6-1. Terminal-area operation represents the most critical operational phase for commercial aircraft in the present-day operating environment. For the ATT aircraft, terminal-area operation becomes especially critical since the anticipated increase in aircraft operating performance speed could be entirely negated by the inability to efficiently negotiate terminal-area traffic patterns and land in adverse weather conditions. The capability to perform four-dimensional area navigation and Category III(a) and III(b) all-weather automatic landing are functions which are believed to be necessary for inclusion in the ATT avionics system. Four-dimensional navigation techniques will enable the aircraft to utilize preprogrammed curved-path approaches and computed arrival touchdown times to enable air traffic controllers to optimally slot aircraft precisely into a landing pattern in spite of approach speed variations. The in-development microwave-scanning-beam approach and landing aid will be utilized to control the aircraft during final approach and landing. The avionics system operating in conjunction with the new microwave-scanning-beam system and properly interfaced with the aircraft flight control system and autothrottle will accomplish Category III landings and grossly decrease the need for go-around in adverse weather conditions.

Enroute navigation with associated guidance (steering) functions can be accomplished by defining two options for the ATT aircraft, depending on the planned operational area. For domestic stateside operation, VOR/DME information optimally combined with airspeed can adequately satisfy the enroute navigation requirements and orient the aircraft properly in the terminal approach pattern. Additional improvements in positional accuracy are expected by DME triangulation techniques currently being developed. Intercontinental flights will likely employ duplicate or triplicate inertial navigation systems to provide self-contained navigational data in overwater and primitive land-based nav-aid areas. Integrating these inertial systems with the world-wide Omega system planned for completion in 1974 would

Table 9.6-1 Major Avionics Systems Functions

FUNCTIONS	FEATURES	DEVELOPMENTAL STATUS
ADVANCED AREA NAVIGATION	• Flight Direction from Departure to Destination • Improved Terminal Area Operations • Instrument Approaches to Austere Airports • Vertical & 4-Dimensional Guidance Capability	• Two Dimensional Systems in Use • Sensors Available to Give 4-D Guidance Capability
ALL WEATHER AUTOMATIC LANDING	• Provide Category III (a) and III (b) Landing Capability • Alleviate Terminal Area Noise with Steep Glide Slope Angle Approach	• Concept Demonstrated with Conventional ILS • Micro-Wave Scanning Beam System Under Development
FLIGHT MANAGEMENT	• Provide Fuel/Energy Management • Landing and Takeoff Performance Monitoring • Automatic Flight Plan Execution	• Employed in Varying Degrees on Present Commercial Aircraft • Concept should be Expanded to Include Increased No. of Functions
ONBOARD DATA RECORDING AND ACQUISITION	• Provides Permament Record of Inflight System Performance • Provides Aircraft Crew Performance Data	• Concept Well-Developed for Onboard Use • Data Link and Integration with Ground Systems Requires Development

provide the ATT with navigational capability to operate in much narrower airlanes than the present 160-n.mi-wide Atlantic corridor. This type of Omega/inertial system will have a continuously bounded positional accuracy of less than 2 n.mi (3.7 km).

Flight management deals with inflight-initiated procedural conduct of the flight crew with airplane systems control and its bearing on the resultant flight path and operating envelope relative to established safe and efficient practices. Heretofore, most of the disciplines associated with flight management have been performed manually by aircraft pilot or crew or, at best, by isolated system aids. The ATT flight management system would integrate these functions into an orderly system of automatic computer solutions and displays, thus unburdening the flight crew to make timely decisions required for optimum mission accomplishment. The primary flight management activities address themselves to (1) assurance that the airplane systems are, at all times, operated within existing "safety-of-flight" limitations and (2) the efficient use of onboard fuel reserves through the optimum employment of the advanced aerodynamic design features. In an advanced-design airplane such as the ATT whose inherent versatility involves wide variations in speed and altitude, much of the work load associated with flight management would be relegated to special-purpose digital-computer computations.

Incorporating onboard data recording and monitoring equipment into the ATT aircraft will provide the user airline with the capability to obtain expanded flight data to support long-term trend analysis for improved maintenance management, identify and catalog inflight system performance and failures to expedite service by ground maintenance crews, and generate historical data files on aircraft crew performance. The onboard digital computer in conjunction with appropriate system monitor sensors and data recorders comprises the recognized tool for maintenance data monitoring and manipulation. The onboard data system would be designed to provide a building-block capability that can be structured to meet the data recording and processing needs of the airline purchaser. The two cost-savings areas which are presently utilizing onboard data monitoring and recording are engine-trend analysis and aircraft crew performance. It is anticipated that the engine analysis will eventually change the engine maintenance concept from scheduled to on-condition maintenance and prevent catastrophic failures. Aircraft crew performance data will provide the airline training department with up-to-date information on crew proficiency such that training can be concentrated in areas where it is most needed. Data monitoring and recording hardware will also include acquisition and signal conditioning systems for detection and recording of mechanical, pneumatic, hydraulic, electrical, and electronics systems malfunction and degradation.

9.6.1.2 Advanced Area Navigation

The crowded conditions in the current air-traffic routes have produced a crisis in the free-world air transportation system. Commercial aviation activity is expected to at least double by 1980; thus the present crisis will likely become more acute if positive action is not completed to better control, schedule, and increase terminal-area traffic. Primary improvements to alleviate the situation are expected to come from improvements in the ground-based Air Traffic Control System as described in the Report of Department of Transportation Air Traffic Control Advisory Committee, December 1969. However, it is believed by Convair that implementation of advanced area navigation equipment onboard the aircraft could favorably complement and simplify the ground-based ATC equipment requirements. Area navigation systems have been successfully designed and tested which utilize either VOR/DME or inertial navigation data to provide four principal operational features. These features are: (1) direct flight from departure to destination, (2) terminal area operation along multiple prescribed flight paths, (3) instrument approaches down to certain minimums at airports with no landing aids, and (4) vertical guidance capability. These systems also provide for reductions in the communications work load of both the air traffic controller and the aircraft pilot, since the system can provide continuous positional data to the aircraft crew and enable the ground-based radar controllers to monitor rather than direct flight approaches.

Present operational area-navigation systems suffer from inaccuracies in the basic data being employed to generate the aircraft guidance signals. These inaccuracies prevent the aircraft from being operated within an accurately defined airspace without the assistance of the ground-based air traffic controller. New methods of utilizing and processing the available data promise to significantly improve the accuracy of the aircraft navigation data. Two methods of providing this upgraded accuracy are currently in development and should be available for ATT application. For aircraft which do not have inertial equipment onboard (i.e., those employed in domestic stateside operations), advanced statistical filtering methods are being developed for combining VOR/DME data, airspeed,and magnetic heading to yield accurate navigational information. A variation of this approach is to employ a continuous triangulation computation using only DME data to provide the navigation data. In DME coverage areas which have at least two-station coverage, the resulting positional error from this approach is estimated to be less than 500 ft (151 m). Aircraft which have inertial equipment can also use VOR/DME and DME triangulation data to optimally update all navigation system parameters and provide bounded position accuracy.

Associated with achieving improved accuracy in the navigation system is the development of guidance techniques for precisely controlling the positioning and timing of the aircraft. These techniques have been referred to as "Four-Dimensional Guidance" and involve the integration of the aircraft navigation system with automatic flight controls and automatic throttle control. Four-dimensional guidance techniques automatically provide three-dimensional aircraft spatial position at particular times along a specified flight path. By employing the four-dimensional guidance system in commercial aircraft, precise pre-programmed terminal approaches could be accurately achieved,thus facilitating tight aircraft scheduling and use of flight paths least disturbing to the residents below. Systems which utilize inertial systems aided by DME/DME data can be expected to achieve the desired two-mile (3.7 km) aircraft spacing and five-second one-sigma timing error at the final terminal approach gate.

The results of previous FAA area navigation evaluation programs have shown the feasibility of utilizing DME/DME-aided inertial systems for the primary data reference. These studies also revealed the need for development of procedures and display of navigation information in the terminal area. Moving map displays are being developed and utilized for this purpose; however, it is anticipated that additional display developments will be needed to fully utilize the potential of the four-dimensional guidance concept and handle the all-weather landing system requirements.

9.6.1.3 Automatic Landing System

Recent activity in the development of automated landing systems and landing aids will most likely make all-weather automatic landing systems a reality on the ATT aircraft. Aircraft systems are presently undergoing tests which are designed to accomplish Category IIIA minimum weather operations, utilizing the currently employed ILS equipment. A scanning-beam microwave landing system to replace the present ILS system is currently in the Contract Definition phase. This system design is to be based on the recommendations of RTCA Special Committee 117. This system will be designed to facilitate full-scale, all-weather automatic landings and multiple closely-spaced runway operations. The development of this microwave system must be closely followed by the ATT avionic and flight control system designers to enable incorporation of all-weather Category IIIA and B automatic landing capability into production aircraft.

Another more sophisticated approach to the automatic landing design problem is to employ an inertial system to generate aircraft attitude, velocity, and position information for use in generating guidance signals to the automatic flight control system. Ground-based terminal navigation system signals (ILS, microwave, etc.) would be combined with the inertial system parameters via optimal filtering techniques to improve and bound the inherent drift and to bias inertial system errors. The basic objective of the system would be to cause the aircraft to precisely follow a preprogrammed reference flight path to touchdown. This concept has been discussed extensively by the M.I.T. Instrumentation Laboratory and is diagrammed in Figure 9.6-1. The desirability of employing this type of landing system stems from the signal characteristics of the inertial and ILS systems. Inertial signals are characterized by low noise levels at high frequencies and are very accurate for short periods of time. However, gyro drift error creates errors in the inertial system outputs which generally increase in amplitude with time. ILS system signals, in general, provide reliable, accurate position signals; however, these signals are corrupted by high-frequency noise. Combining the inertial system and ILS signals provides an overall integrated sensor signal which combines the accurate low-frequency ILS signals with the wide noise-free dynamic range of the inertial signals. Resultant improvements in the vertical-and lateral-position flight control systems

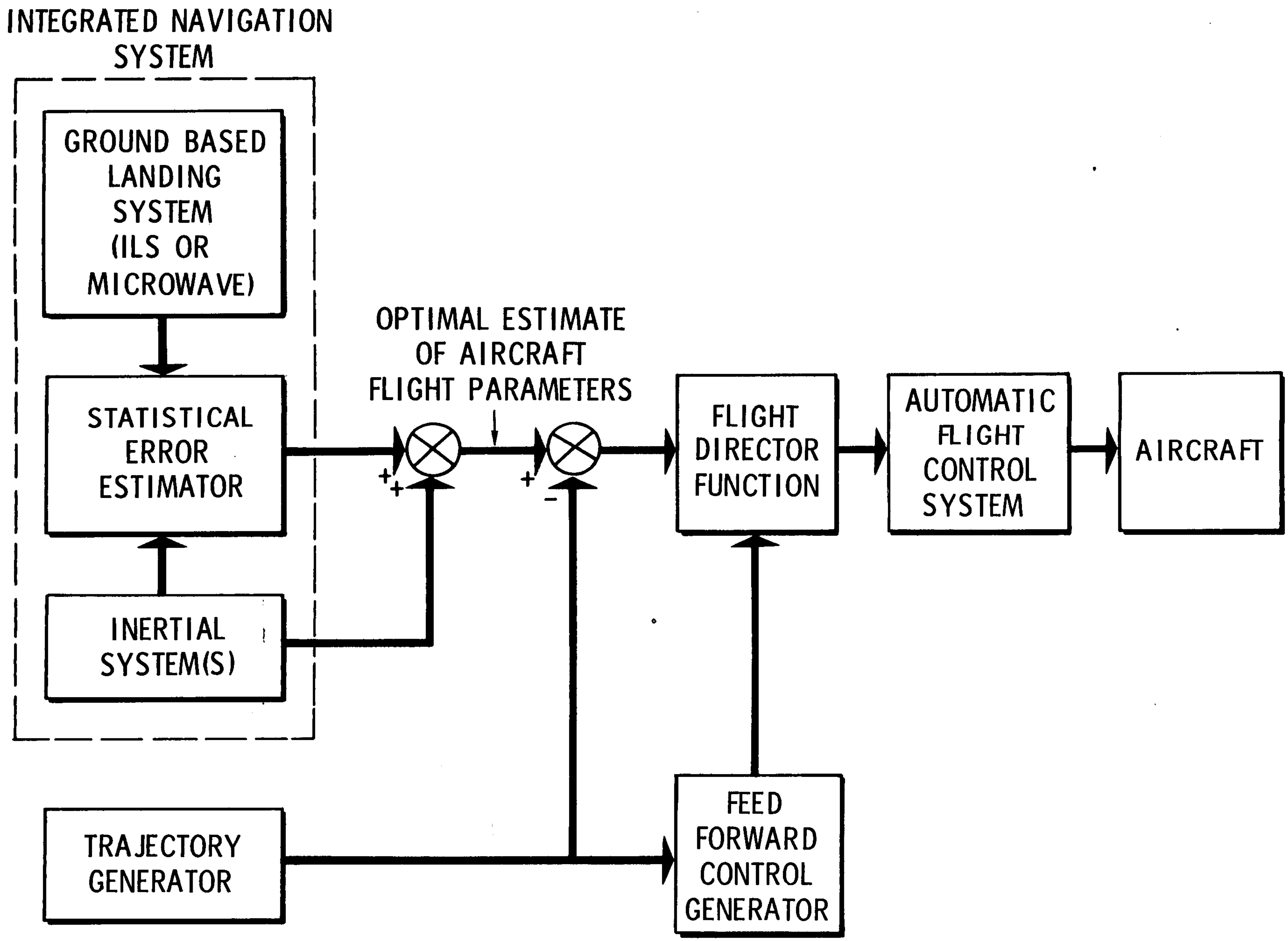

Figure 9.6-1 Integrated Inertial/ILS Automatic Landing System

provide a landing system that is able to successfully perform over a much broader range of atmospheric turbulence and windshear than is possible with the conventional open-loop ILS or microwave landing systems.

The integrated inertial/ILS landing-system approach should be incorporated into the ATT avionics system for the aircraft which will be employed for transoceanic operations. As discussed in the previous section, these systems will likely incorporate a statistical estimation technique such as Kalman filtering to combine Omega, VOR/DME, and/or DME/DME information with inertial data during the entire flight. This updating process will make it possible to accurately position the aircraft in the terminal control area and allow a smooth transition from area navigation to ILS beam capture and initiation of the automatic landing phase. This type of system implementation would alleviate the problems presently encountered during this transition period and tremendously aid the ground controller in scheduling traffic in crowded airspaces.

9.6.1.4 Flight Management System and Displays

With the employment of extensively automated avionics systems on the ATT aircraft, it will be imperative that comprehensive flight management functions and appropriate displays be included in the system. This flight management system will decrease the crew work load and provide efficient methods of manually entering inputs to edit the system's operation and instigate changes of operational modes. Numerous functions can be incorporated into a flight management system and should be planned during the early design stages of the aircraft's overall systems definition. Typical functions which can be included in a flight management system are: (1) fuel/energy management coupled with route optimization, (2) performance monitoring on landing and takeoff, and (3) automatic flight plan execution from takeoff to landing.

The primary purpose of the fuel/energy management function is to provide the crew with a realistic and current estimate of mission constraints imposed by fuel reserve limitations. These constraints are affected by both aircraft configuration and flight conditions such as Mach number, flight altitude, winds, etc. Specific definition of the operational characteristics of the ATT aircraft will be determined during the development phase of the design.

With these characteristics, fuel/energy management computations can be made to estimate fuel range and fuel time remaining based on current flight conditions or based on optimum flight conditions which are determined by the flight management system and constrained by ATC requirements. Continuous fuel monitoring will be accomplished on all flights to assure the safe arrival of the aircraft at its destination and that adequate reserves are available for alternate destinations. The system would include the capability to perform computations to assist the crew in evaluation of the range and fuel consumption effects of crew or ground-controller selected flight parameter changes.

The performance monitoring function would be included in the flight management system to assess the total state of the aircraft and its systems primarily during the takeoff, automatic landing, and other critical phases of operation. The performance monitor will assist the pilot in making decisions during these operations and would be designed to substantially reduce risk without imposing unacceptable economic penalties in the number of aborted landings and takeoffs. Performance criteria would be developed in the design of the monitor. During operation, the monitor would use onboard observables to compute values for these performance criteria and employ these values to formulate a performance assessment of aircraft controllability, status of the takeoff or landing, and the degree of safety to which the operation is being accomplished. The performance monitor function is specifically related to assuring the safety of the automatic operations which are envisioned for the ATT aircraft systems.

Another function which could be incorporated into the ATT flight management system is the ability to automatically execute the preprogrammed flight plan from takeoff to landing. Storage units associated with the computer complex will have the ability to provide on-board bulk storage of all navigation information required for the route structure of a given airline. Using this information, appropriately modified by the pilot to reflect particular flight conditions and restrictions, the flight management system would automatically optimize and execute the flight plan unless interrupted by the pilot.

Implementation of the above flight management function requires that a control and display unit be specifically designed to give the pilot a concise, clear picture of overall system and aircraft performance. As described in Reference 9-14, much development and design work has been accomplished on this type of display. Current versions of these types of control and display units employ a CRT to provide a flexible display of numerals, letters, and symbols. By time-sharing the labeling of a few pushbuttons and using a single key set for all manual entries, an integrated unit can be achieved in a minimum of panel area. The design philosophy in developing the display system is to create a compatible interface between a highly automated avionics system and the pilot's manual intervention and monitoring of these processes. A paging index concept is utilized to display the information to the pilot. These callable pages contain flight plan data such as designated airways, way-points, and latitude/longitude for various flight segments, assigned altitude, etc. Other types of information planned for the paging system include flight progress data giving the current flight leg waypoints, estimated time of arrival, fuel reserves for present and alternate flight plans, navigation sensors presently in use, and data pertaining to flight plan revisions.

9.6.1.5 Onboard Data Recording and Monitoring System

Data recording and computerized airborne integrated data systems (AIDS) have been designed and are currently being utilized on the B747, DC-10, and L-1011 aircraft. These systems make it possible to selectively keep a running record of aircraft performance throughout the flight regime. This record provides the airlines with a computerized data file for long-term trend analysis to facilitate system failure predictions and also provide historical data files on aircraft crew performance. Many varied designs and applications for AIDS system exists since the user airlines usually structure their system requirements around fleet size, maintenance concepts, route structures, and ground-based computer capabilities. Basic AIDS systems are designed to provide interface wiring and space provisions per ARINC 563 to facilitate future expansion as required by the airline customer.

The AIDS is usually configured to monitor propulsion, avionics, and airframe system parameters. The two cost saving areas which are presently being extensively studied for full-scale usage of AIDS data are engine analysis and aircraft crew performance. Engine analysis, as described in Reference 9-15, falls within three categories: (1) limit evaluation, (2) trend analysis, and (3) thermodynamic model analysis. Limit evaluations compare engine performance data values with predetermined limits. When these limits are exceeded, the indication is that the component involved has deteriorated and should be repaired or replaced. The trend analysis objective is the prediction of the future wear and failure behavior of specific system components such that a near real-time status record of equipments can be maintained. The thermodynamic model analysis uses current and past engine data to compute thermodynamic efficiencies, nozzle area coefficients, and combustor-hardware pressure loss coefficients to hopefully ascertain a direct measurement of engine health.

Crew performance analysis consists of evaluation of flight parameters recorded by AIDS to determine adherence or departure from established procedures by the crew. A typical crew proficiency program would divide the flight into segments to permit analysis of the important phases of the flight (i.e., approach and landing) with editing of less critical flight phases. This crew performance data provide the airline training departments with up-to-date information on their crews such that crew training can be concentrated in areas where it is most needed. Optional AIDS hardware includes data acquisition and signal conditioning systems for detection and recording of mechanical, pneumatic, and hydraulic system malfunction and degradation.

9.6.1.6 Equipment Implementation and Availability

During the ATT avionics study, a large number of avionics equipment manufacturers were contacted for the purpose of obtaining a commercial equipment availability and developmental status evaluation. The results of this survey were used to formulate configurations of equipments which could be utilized for implementing the ATT avionic system functions. These equipment configurations have been grouped into the following categories:

I. Standard Equipment - Includes basic communications, radio navigation, and other equipments to be installed on all aircraft.

II. Self-Contained Navigation Equipment - Includes area navigation capability for both Continental U.S. and International operations.

III. Data Acquisition System - Includes capability for inflight data recording and acquisition.

IV. Microwave Landing System - Provides accurate groundbased reference signals to accomplish Category III(a) and III(b) automatic landings.

Equipments in each of these groups are given in Tables 9.6-2 through 9.6-5 together with physical data, candidate system identification, and developmental status. As denoted in the tables, equipment is available for accomplishing most of the avionics functions envisioned for the ATT aircraft. The major exceptions are the groundbased microwave landing system required to provide accurate and reliable reference signals for accomplishing all-weather automatic landings and the onboard collision avoidance system. However, equipment for both these systems is in the development stage at this time and should be available for use in conjunction with the ATT aircraft.

The concept which is employed to integrate these various sensor, display, and control systems appears to be the major area of required technological development with regard to implementing the ATT avionics system. Recent developments in the design of the multiprocessor digital computers should be explored for potential application in integrating the ATT avionics system. Although complex, the multiprocessor computer will process features such as automatic fault diagnosis and correction to achieve high reliabilities and fail-soft capabilities. It is believed as the avionics, flight controls, and onboard data processing become more digitally oriented and automated, the use of the multiprocessor computer to accomplish all computations onboard the aircraft will become attractive from both design and economical considerations.

Table 9.6-2

ATT AVIONICS LIST
(STANDARD)

Functional Item per Shipset	Physical Data	Candidate Systems	Status
(2) VHF Communication Transmitter/ Receivers 720/1440 Channels	28 Volt 20 lb (9.1 kg) 1/2 ATR Short ea.	Collins 681M-2D Bendix RTA-42 King KTR 9100	In Current Quantity Production
(2) VHF VOR/LOC/ILS Navigation Receivers 200 Channels	28 Volt 20 lb (9.1 kg) 1/2 ATR Short ea.	Collins 51RV-2B Bendix RNA-26C RCA AVN-210	↓
(2) UHF DME Navigation Receivers 200 Channels	28 Volt 15 lb (6.8 kg) 1/2 ATR Short ea.	Collins 860E-3 King KDM 7000 RCA AVQ-85	↓
(2) UHF L Band ATC Transponders 4096 Codes	115 Volt 15 lb (6.8 kg) 3/8 ATR Short ea.	Collins 621A-6 King KXP750A Wilcox 1014A	↓
(2) LF ADF Receivers (Non Directional Beacons)	28 Volt 20 lb (9.1 kg)	Bendix DFA-73 King KDF 8000 Collins DF 206	↓
(2) UHF Radar (Radio) Altimeters	28 Volt 18 lb (8.2 kg) 1/2 ATR Short ea.	Litton Ind. 506 Bendix ALA-51 Collins AL-101	↓
(2) VHF Marker	28 Volt 1/4 ATR Short ea.	Bendix MKA-28C Collins 5126	↓
(1) Weather Radar System	1 ATR plus Dual Cockpit Display Indicators 14x6.25x6.25 in. (34.6x15.9x15.9 cm) 495VA at 115 VAC (400 cps)- 27 W. at 27.5 VDC; 108 lb (49 kg)	Bendix RCA	↓
(1) Collision Avoidance System	Unknown	McDonnell Douglas (Tentative)	In flight test-subject to selected system

Table 9.6-3

ATT AVIONICS LIST
(SELF-CONTAINED NAVIGATION EQUIPMENT)

Functional Item per Shipset	Physical Data	Candidate Systems	Status
Continental U.S. Operations			
(2) Navigation (Area) Digital Computer Units	115 VAC, 355 W. 50 lb (22.6 kg) 1 ATR Long ea.	Collins C-8564-1 Delco Magic 362	In Current Quantity Production
(2) Flight Data Storage Units	115 VAC, 22 W. 5 lb (2.3 kg) 5.75x4.09x6.5 in. (14.8x10.4x16.5 cm)	Collins 8847A-1 Delco	↓
(2) Flight Data Display Unit	115 VAC, 115 W. 20.5 lb (9.3 kg) 5.75x7.5x16 in. (14.8x19.0x40.6 cm)	Collins 813H-1 Delco	↓
(2) Navigation Interface Unit (Coupler)	115 VAC, 165 W. 14.5 lb (6.6 kg) 1/2 ATR Long	Collins 599V-2 Delco	↓
International and Remote Area Operations			
(3) Inertial Control Units	115 VAC 4.5 lb (2.0 kg) 5.75x3.38x5 in. (14.8x8.6x12.7 cm)	Collins 5140-7 Delco Litton	↓
(3) Inertial Navigation Units	115 VAC, 251 W. 41 lb (18.6 kg) 1 ATR Long	Kearfott 345E-1 Litton LTN-58 Delco C-IV	↓
(3) Battery Units	--- 20 lb (9.1 kg) ½ ATR Short	Kearfott 652U-1 Litton Delco	↓

Table 9.6-4

ATT AVIONICS LIST
(DATA ACQUISITION SYSTEM)

Functional Item per Shipset	Physical Data	Candidate Systems	Status
(1) Flight Data Entry Panel	5 Watts 3 lb (1.4 kg) 9x6x6 in. (22.9x15.2x15.2 cm)	Garrett/ AiResearch	In Current Quantity Production
(1) Flight Data Acquisition Unit	115 VAC 43 Watts 18 lb (8.2 kg) 1/2 ATR	Garrett/ AiResearch	
(1) Digital Flight Data Recorder	115 VAC 40 Watts 20 lb (9.1 kg) 1/2 ATR	Sundstrand Data Control, Inc.	
(1) Digital Management Unit	115 VAC 30 Watts 17 lb (7.7 kg) 1/2 ATR	Garrett/ AiResearch	
(1) Cockpit Voice Recorder	115 Volts 42 Watts 24 lb (10.9 kg) 1/2 ATR	Sundstrand Data Control, Inc.	
(1) Crash Recorder	30 Watts 15 lb (6.8 kg) 1/4 ATR	Sundstrand Data Control, Inc.	

Table 9.6-5

ATT AVIONICS LIST
(MICROWAVE LANDING SYSTEM)

Functional Item per Shipset	Physical Data	Development Status
(2) Transmitter-Receiver-Decoder	80 Watts 20 lb (9.1 kg) 7x5x24 in. (17.8x12.7x61 cm)	Phase I Contract Definition Technical Approach Contracts have been made to the following companies:
(2) Control & Display Unit	10 Watts 4 lb (1.8 kg) 6x5x6 in. (15.2x12.7x15.2 cm)	1. Cutler-Hammer, Inc. AIL Division 2. Bendix Communication Division
(2) Antenna C-Band	5 Watts 2 lb (0.9 kg) 3x3x4 in. (7.6x7.6x10.1 cm)	3. Texas Instruments, Inc. 4. Hazeltine Corporation
(2) Antenna K_u-Band	5 Watts 2 lb (0.9 kg) 3x3x4 in. (7.6x7.6x10.1 cm)	5. Raytheon Company 6. ITT Gilfillan. These contracts are sponsored by the Department of Transportation, FAA

9.6.2 Avionics Installation

9.6.2.1 General

The avionics installation configuration for the ATT shown in Figure 9.6-2 is typical of each of the aircraft presented in this study. Therefore, the following discussion is common to any single configuration. As subsequently shown, the antenna arrangement, the external lighting arrangement, and wiring-harness routing provisions are also common to any configuration.

The foremost objective in the area of avionics installation during this study has been to ensure that the configuration included herein is compatible with current and projected airline practices. In order to become thoroughly familiar with requirements and problems pertaining to this objective, engineering design personnel observed a number of in-service airliners at Love Field, Dallas, Texas, during high activity gate turnaround time. Airline personnel, including flight line mechanics, avionics maintenance shop employees, and flight engineers, were personally interviewed for their comments and recommendations pertaining to installations in future aircraft.

Flight line gate maintenance is recognized as a most formidable task, considering that one man has the assigned responsibility for servicing all avionics and electrical equipment requiring attention during turnaround time. During the normal 30-minute scheduled stop, less than 20 minutes is available for a flight line mechanic to accomplish his work. On occasion, this task includes the diagnosis of an equipment problem and the removal and replacement of a faulty line replaceable unit (LRU) or multiple LRU's.

The designs of numerous commercial aircraft (DC-8, DC-9, DC-10, B707, B727, B747), as well as actual aircraft observed, were studied in order to assess their avionic and electrical requirements. These data, correlated with ATT variations, served as a guide for the ATT configuration.

9.6.2.2 Installation Design

Convenient access to the avionics for maintenance and unit replacement is considered a mandatory requirement and is a feature of the installation arrangement presented in this study. Growth capability in terms of additional space is also included in the generous size of the dedicated avionics compartment. Future modifications and additions can be more easily accomplished as a result of the type of design provisions included for equipment racks.

Layout drawings were prepared and evaluated in order to establish installation concepts for avionic and electrical equipment, antennas, exterior lights, and routing provisions. Since specific sizes and shapes have not been assigned for all system components, the layouts are general in nature but are representative of real requirements. Data generated on the layouts are reflected into the aircraft configuration design and assure proper space allocation for the various aircraft systems.

The major portion of the avionics equipment is located in a single pressurized avionics bay below the crew compartment. A quick-opening access door is provided in the lower skin of the aircraft. Another hinged access door is provided in the lower skin of the aircraft. Another hinged access door is provided in the floor of the crew compartment. The equipment LRUs will be installed in racks which provide generous growth space and wiring accessibility. Maximum use will be made of rear mounted rack and panel connectors to expedite LRU replacement.

9.6.2.3 Antennas

The ATT antenna configuration will make maximum use of the off-the-shelf designs, when possible, which are compatible with functional and aerodynamic considerations. Antennas will generally be replaceable from outside the aircraft, and appropriate means for disconnecting transmission lines will be incorporated into the installation design.

Each ATT antenna location was selected to provide the proper field-of-view to optimize the intended function of the associated equipment. An example is the collision avoidance antennas, which are located to optimize forward coverage, where a collision situation is most likely to occur, but which will still provide omnidirectional coverage to detect all collision situations. Figure 9.6-2 shows the various antenna locations. Table 9.6-6 lists the antennas by equipment function and gives the coverage of each. Standard "off-the-shelf" antennas can be used throughout, with the possible exception of the VOR antenna. The VOR

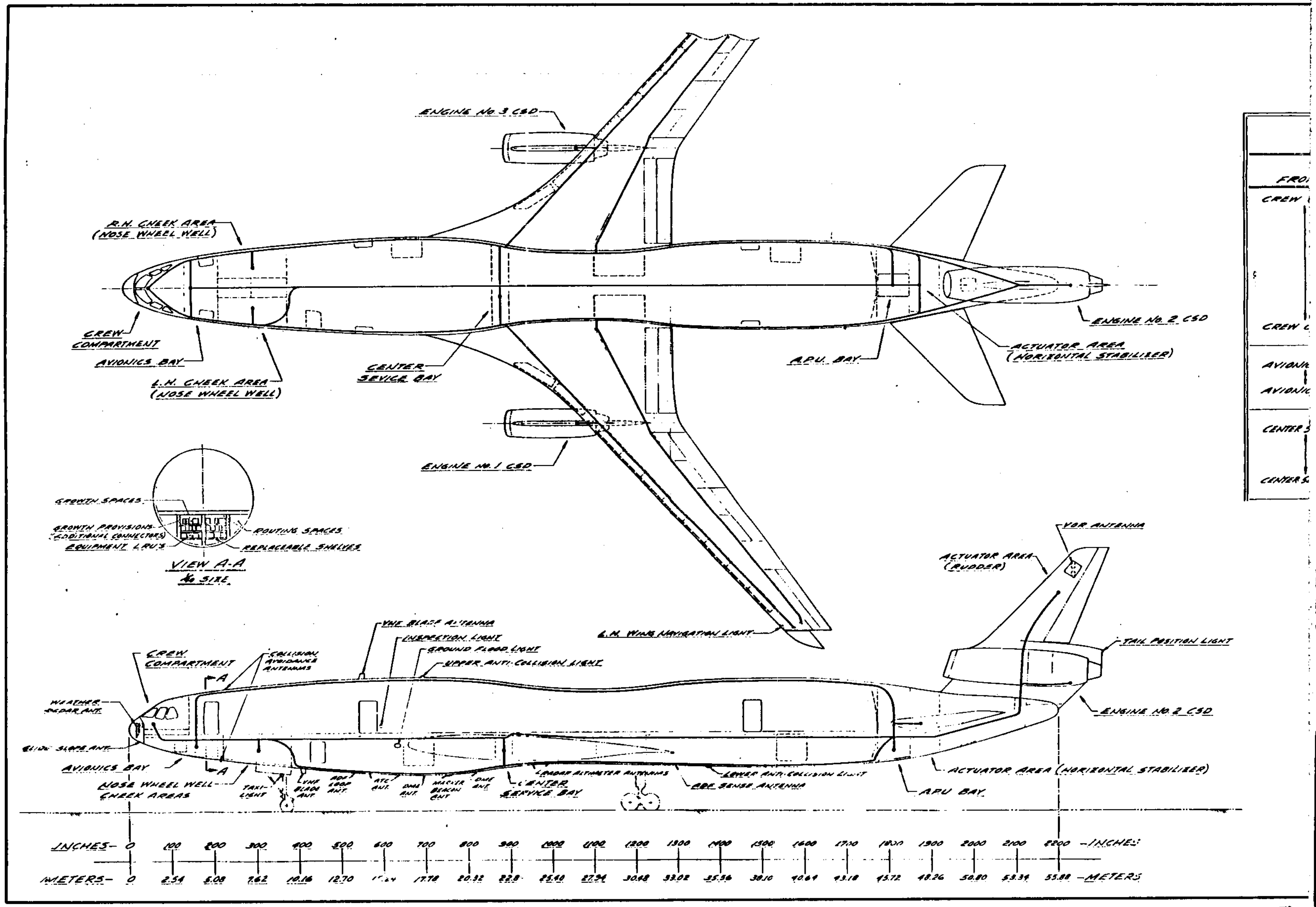

ENGINE No. 3 CSD
R.H. CHEEK AREA (NOSE WHEEL WELL)
CREW COMPARTMENT
AVIONICS BAY
L.H. CHEEK AREA (NOSE WHEEL WELL)
CENTER SEVICE BAY
ENGINE No. 1 CSD
ENGINE No. 2 CSD
ACTUATOR AREA (HORIZONTAL STABILIZER)
A.P.U. BAY
GROWTH SPACES
GROWTH PROVISIONS (ADDITIONAL CONNECTORS)
EQUIPMENT LRU'S
ROUTING SPACES
REPLACEABLE SHELVES
VIEW A-A
VOR ANTENNA
ACTUATOR AREA (RUDDER)
L.H. WING NAVIGATION LIGHT
VHF BLADE ANTENNA
INSPECTION LIGHT
GROUND FLOOD LIGHT
UPPER ANTI-COLLISION LIGHT
COLLISION AVOIDANCE ANTENNAS
TAIL POSITION LIGHT
WEATHER RADAR ANT.
GLIDE SLOPE ANT.
NOSE WHEEL WELL-CHEEK AREAS
TAXI LIGHT
CENTER SERVICE BAY
LOWER ANTI-COLLISION LIGHT
ADF SENSE ANTENNA
APU BAY
INCHES- 0 100 200 300 400 500 600 700 800 900 1000 1100 1200 1300 1400 1500 1600 1700 1800 1900 2000 2100 2200 -INCHES
METERS- 0 2.54 5.08 7.62 10.16 12.70 17.78 20.32 22.8 25.40 27.94 30.48 33.02 35.56 38.10 40.64 43.18 45.72 48.26 50.80 53.34 55.88 -METERS
FRO
CREW
AVIONI
CENTER

238-a

238-B

WIRE ROUTING DISTANCES

...M	TO	ROUTING PATH: L.H. SIDE FEET	L.H. SIDE METERS	R.H. SIDE FEET	R.H. SIDE METERS	TOP FEET	TOP METERS	BOTTOM FEET	BOTTOM METERS
...COMPT.	AVIONICS BAY	~	~	~	~	~	~	10	3.05
	NOSE WHEEL CHEEKS	22	6.71	22	6.71	~	~	~	~
	CENTER SERIKE BAY	80	24.38	80	24.38	~	~	88	26.82
	WING TIP (FWD SPAR)	155	47.24	155	47.24	~	~	~	~
	WING TIP (AFT SPAR)	165	50.29	165	50.29	~	~	~	~
	APU BAY	~	~	160	48.77	170	51.82	165	50.29
	RUDDER ACTUATORS	205	62.48	205	62.48	200	60.96	210	64.01
	HORIZONTAL TAIL ACTUATORS	165	50.29	165	50.29	170	51.82	170	51.82
	ENGINE No 1 CSD	112	34.14	~	~	~	~	~	~
	ENGINE No. 2 CSD	190	57.91	190	57.91	185	56.39	195	59.44
...OMPT.	ENGINE No. 3 CSD	~	~	112	34.14	~	~	~	~
...S BAY	NOSE WHEEL CHEEKS	13	3.96	13	3.96	~	~	~	~
	CENTER SERVICE BAY	76	23.16	76	23.16	~	~	78	23.74
...S BAY	APU BAY	~	~	150	45.72	160	48.77	155	47.24
...ERVICE BAY	NOSE WHEEL CHEEKS	62	18.90	62	18.90	~	~	58	17.68
	ENGINE No. 1 CSD	46	14.02	~	~	~	~	~	~
	ENGINE No. 2 CSD	130	39.62	130	39.62	~	~	132	40.23
	ENGINE No 3 CSD	~	~	46	14.02	~	~	~	~
...ERVICE BAY	APU BAY	~	~	92	28.04	~	~	84	25.60

PRELIMINARY DESIGN DRAWING

EQUIPMENT ARRANGEMENT, AVIONICS & ELECTRICAL, ATT

GENERAL DYNAMICS
Convair Aerospace Division

FW7107132

...re 9.6-2 Avionics and Electrical Equipment Arrangement

Preceding page blank

Table 9.6-6

ATT ANTENNA COVERAGE

Antenna	Location	Coverage
Glide Slope	Nose Radome	Forward Hemisphere
Collision Avoidance	Top & Bottom Forward Fuselage	Omnidirectional, Optimized Forward Coverage
VHF	Top & Bottom Fuselage	Omnidirectional Above and Below Horizon
ADF	Bottom Fuselage	Omnidirectional, Optimized for Lower Hemisphere
ATC	Bottom Fuselage	Omnidirectional
DME	Bottom Fuselage	Omnidirectional
Marker Beacon	Bottom Fuselage	Lower Hemisphere
Radar Altimeter	Bottom Fuselage	Down $\pm$ 45^{o} Cone
VOR	Both Sides of Vertical Stab.	Omnidirectional Horizon Coverage

antenna may, however, be an existing design with a slight modification to fit the aircraft contour.

9.6.2.4 Lighting

The exterior lighting system will be designed in accordance with FAA specifications for Commercial Transports. Installations will be governed by the high degree of maintainability desired. Sufficient slack in wiring harnesses will be provided at light positions to facilitate servicing and repair. Lights and wiring in areas subject to environmental exposure will be suitably protected against dirt, oil, corrosion, etc.

The magnitude of the aircraft lighting requirements (both internal and external) for airline service make reliability and maintainability a prime concern to maintenance personnel. Installation of such devices as ballasts will be designed to be readily replaceable. Wherever possible, connectors will be incorporated into the design to avoid the time-consuming operation of disconnecting several individual wires and also to prevent the possibility of incorrect reconnections.

To reduce spare-part requirements, components performing the same function will, where possible, be packaged into a common LRU. When left-hand and right-hand installations are required, common items will be configured to be interchangeable. A minimum number of different types of lights will be used, particularly small lights in localized areas. Use of this approach will be of benefit in such areas as the instrument panels, where delays can occur in bulb replacement when an identifying number is indistinguishable. Particular emphasis will be placed on component labeling to assure individual identification and also to identify the related units they affect or control.

9.6.2.5 Wiring and Routing

Wiring requirements set forth by the FAA and ARINC (References 9-16, -17, and -18) have been evaluated and followed in establishing the wiring and routing concepts for the ATT. Incorporation of standardized practices in this design area will assure maximum flexibility in selecting future avionic systems and vendors. Information taken from an AFFDL report (Reference 9-19) was utilized for guidance in formulating the routing concept depicted in Figure 9.6-2.

The table shown on the drawing represents the approximate routing distances between the various aircraft equipment areas and unit locations.

Emphasis will be given to the critical wiring requirements peculiar to the flight control system. Multiple routing paths for redundant functions will be provided with appropriate separation of one from the other and from the routing provisions for other systems. Suitable protection will also be provided through use of conduit, barriers, etc. in areas susceptible to possible damage. Special consideration will be given to using wiring troughs that will enable the spreading of wires to simplify the task of identification and tracing.

The primary means of access to the routing paths will be restricted to areas within the aircraft. Use of this approach not only avoids undesirable access penetrations in the graphite composite skins of the aircraft but also expedites maintenance through eliminating the need for work stands required in many areas for external access. Another inherent advantage of internal access that facilitates servicing is the nature of aircraft structure, which permits inside panels to be more easily removed than the more highly stressed outside skin panels.

SECTION 10

PROPULSION SYSTEM DESCRIPTION

The Pratt & Whitney STF-429 engine was selected for point design evaluation studies basically because of better data availability than for the General Electric ATT No. 1 engine. It is a twin-spool, unaugmented turbofan designed to operate with separate, fixed, primary and fan exhaust nozzles. The performance data for this engine are based on a 1975 level of technology, i.e., certification should be accomplished by 1979. Noise levels for the STF-429 with acoustic treatment are estimated to be at least 10 EPNdB less than FAR Part 36 requirements at sideline, takeoff, and approach conditions. Acoustic treatment required to meet the minus 10 EPNdB noise level is described in Section 10.3 of this report. Exhaust pollutants will be held within the statement of work specified values, and are described in Section 10.5 of this report.

Data were also supplied by Pratt & Whitney for the STF-433 engine, which incorporates more advanced technology such that the engine should be certifiable by 1985. This engine, with the same acoustic treatment as employed in the STF-429 engine design, exhibits noise levels 15 EPNdB less than FAR Part 36 requirements. Its design incorporates advanced levels of combustor exit temperature (CET).

10.1 PROPULSION INSTALLATION

10.1.1 Nacelle Description

The three STF-429 engines are each mounted in typical nacelles. One nacelle is pylon-mounted from each wing and one is mounted in a nacelle structurally integral with the vertical tail. All of the nacelles are of round cross section throughout, and no curves or bends are utilized in any inlet or exhaust ducts.

The nacelles for the .98 design Mach number airplane differ somewhat from those of the .90 design Mach number airplane because of the different engine scale required and because of the different aerodynamic requirements of the inlet region. The differing aerodynamic requirements are explained in Section 10.2 of this report and the engine scale factors are given in Section 10.4. Figure 10.1-1 shows the features of the .98 design Mach number nacelles, and Figure 10.1-2 shows the .90 design Mach number nacelles. Engine buildup is common to all three nacelles.

The air induction system is described in Section 10.2; the acoustical treatment system, in Section 10.3.

10.1.2 Engine Description

Engine installation drawings were not provided by the engine study contractors. An outline dimensional tabulation and appropriate scaling data were provided, however. From this information, an engine outline was constructed; the resulting engine outline and engine installation are shown in Figure 10.1-1.

The engine accessory section location, also shown in Figure 10.1-1, is appropriate for all of the nacelles. The engine and aircraft accessories are mounted to separate gear boxes. The engine gear box is located just to the rear of the fan exit plane so that the engine accessories are arranged in a circular arc around the core engine. The aircraft accessories gear box is located below the core engine, housed in a strut vane in the fan duct. This system has space provisions for one 120-kVA alternator and two 60-gpm (229 l/m) hydraulic pumps.

The whole accessory section is isolated by a firewall barrier designed to resist 3000°F (1923°K) for 15 minutes and is ventilated with fan discharge air.

The engine access doors are hinged from the pylon and, when opened, provide access to the entire accessories section for inspection, maintenance, or servicing. A complete description of engine access and maintenance is given in Section 16.5, Engine Maintenance.

10.1.3 Engine Starting System

A low-pressure pneumatic starting system using conventional air turbine starters is provided. The engines can be started from the onboard auxiliary power unit, from external ground power carts, or through the cross bleed system utilizing bleed air from an operating engine. A schematic of this system is presented in Figure 10.1-3.

10.2 NACELLE AERODYNAMICS

The basic objective in specifying nacelle lines for the ATT airplane is to provide nacelle envelopes that will add minimal drag to the airplane, particularly at the cruise Mach numbers, and that will provide adequate pressure recovery at takeoff and cruise. Also, the inlet and fan discharge ducts must provide enough noise damping to enable the engine to meet the stringent noise levels specified for the ATT.

In order to meet these demands, a nacelle with high critical Mach number (having zero, or very low, drag rise to Mach .98) is required. This requires that the inlet be sized and the nacelle proportioned so that spillage drag is avoided. A compromise in takeoff pressure recovery results from sizing the inlets for low spillage at the cruise condition.

10.2.1 Design Approach and Selected Nacelle Geometry Mach .98 Design

The primary design requirement is to keep the nacelle drag divergence Mach number less than the cruise Mach number. The design cruise Mach number for the high-performance airplane is .98. (This cruise Mach number results in a more difficult design task than the cruise Mach number of .90 selected for the alternate design.) NASA-Langley, as reported in Reference 10-1, has accomplished a drag divergence Mach number of 1.0 for a nacelle mounted on the aft portion of an ATT fuselage. In a wing-mounted nacelle installation for a similar vehicle, a drag rise of about 12 counts is incurred with nacelles which, when isolated from the airplane, have a drag rise of only 4 counts (Reference 10-2). Further development will undoubtedly reduce the interference drag of the wing-mounted nacelles. The aforementioned results of transonic nacelle tests by NASA represent the virtual extent of available data for this type of nacelle, and so, in selecting nacelle geometry, heavy reliance was placed on these nacelles and their associated data.

Because of the fact that, below drag rise, friction drag comprises 85 to 90 percent of the total nacelle drag, it is important to keep the wetted area, and hence the length of the nacelle, to a minimum. On the other hand, to achieve a high drag divergence Mach number at transonic

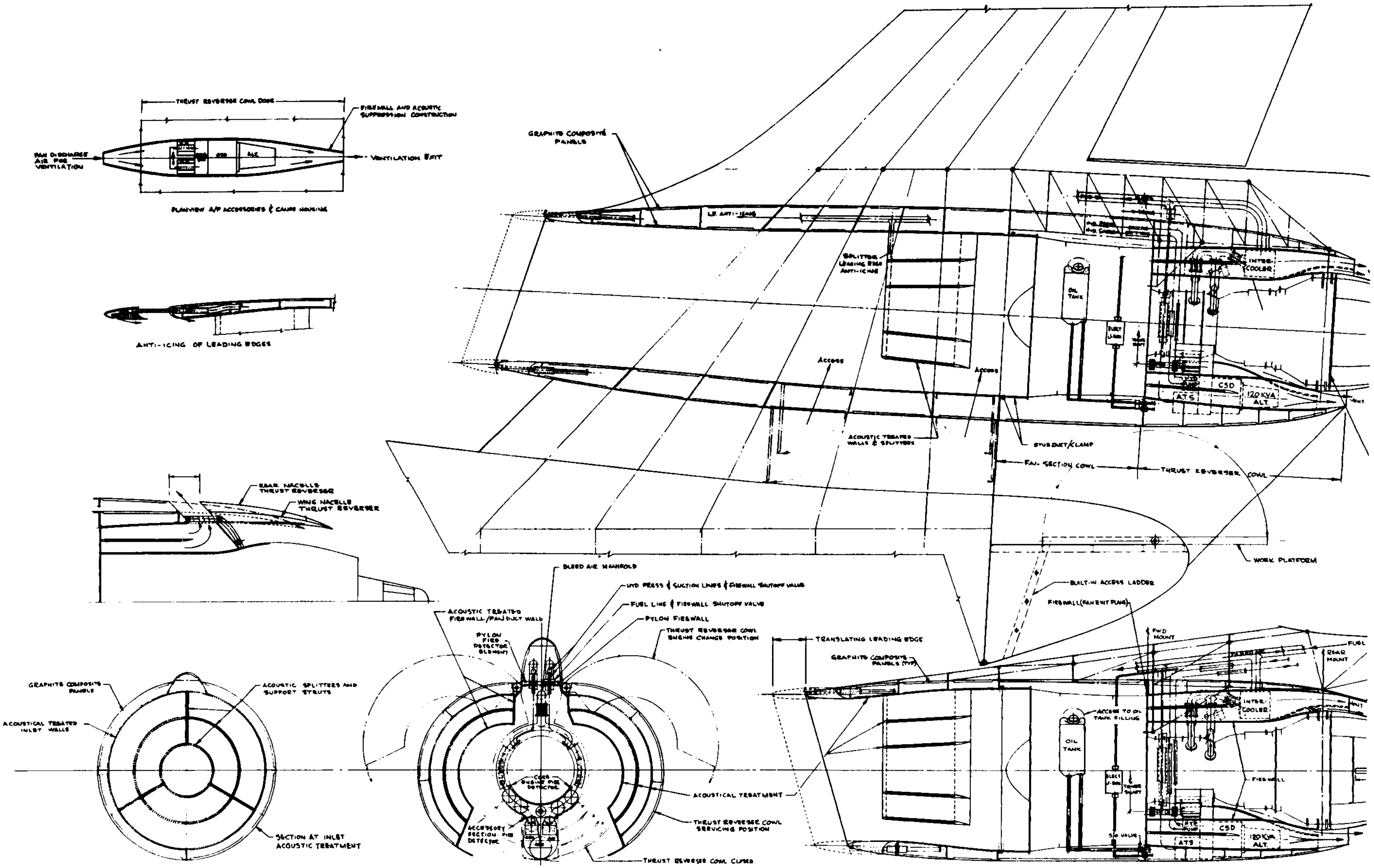

Figure 10.1-1 ATT Propulsion

246-A

246-B

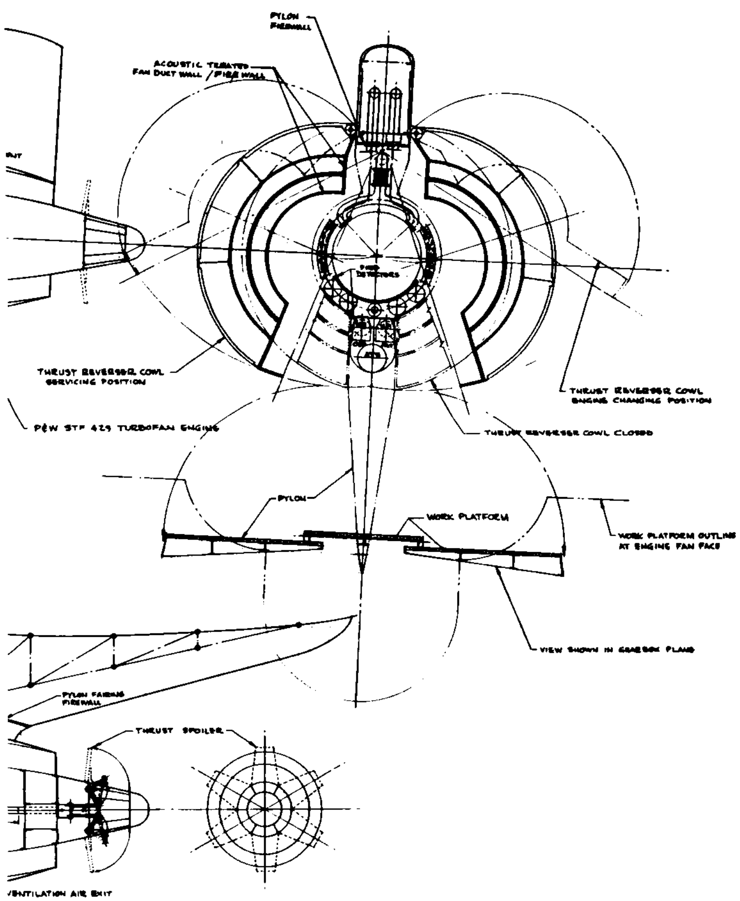

Installations, Mach 0.98 Wing/Tail Mounted Nacelles
FW7107125

Preceding page blank

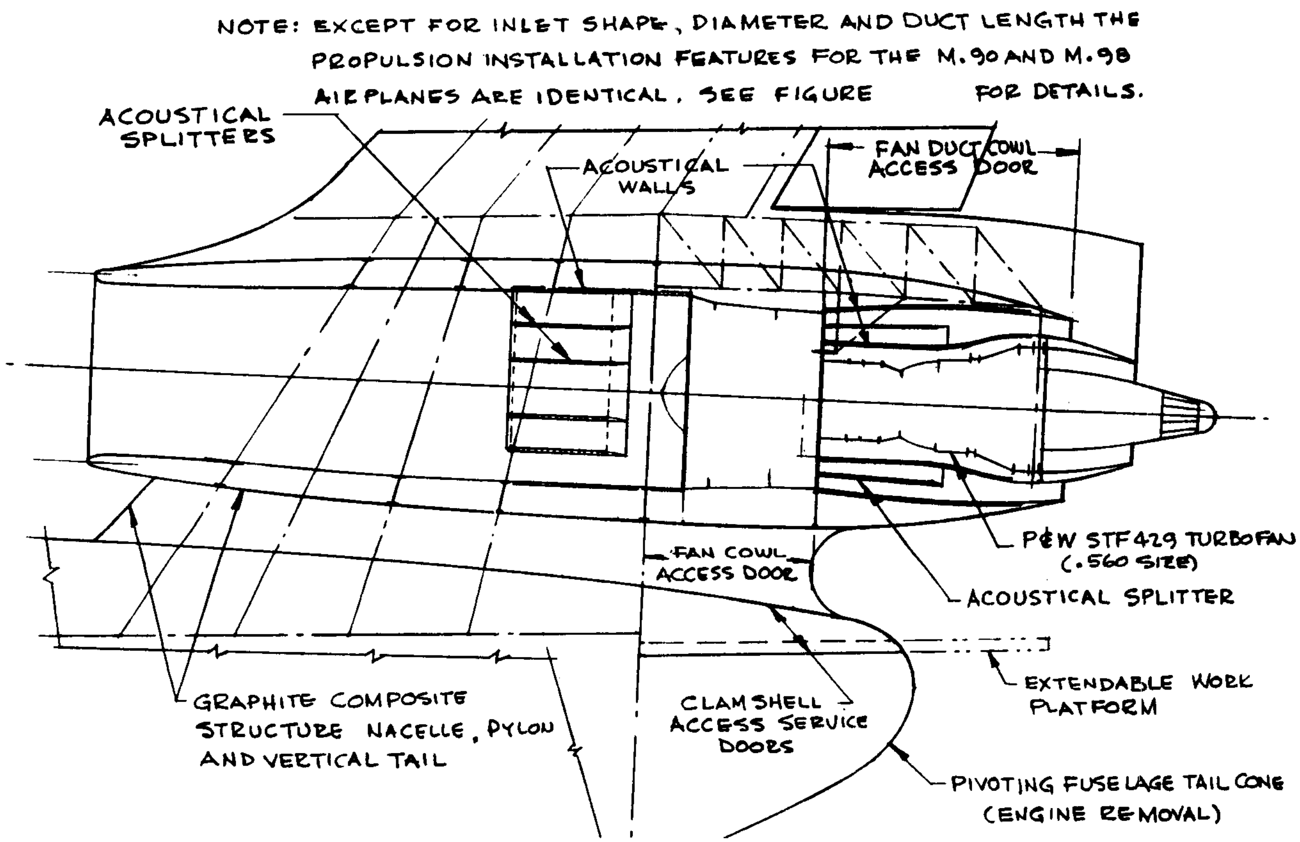

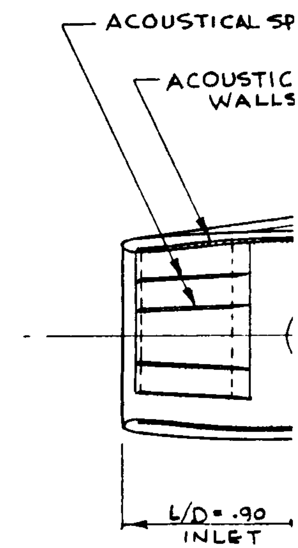

Figure 10.1-2 ATT Pr

258-A

244-A

FOR INLET SHAPE, DIAMETER AND DUCT LENGTH THE
SION INSTALLATION FEATURES OF THE M.90 AND M.98
NES ARE IDENTICAL. SEE FIGURE FOR DETAILS.

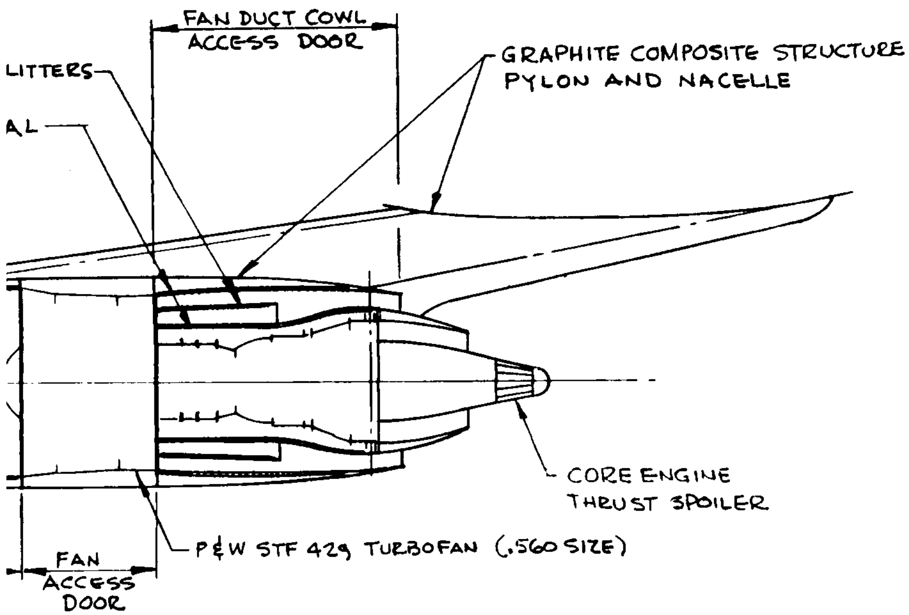

pulsion Installations, Mach 0. 90 Wing/Tail Mounted Nacelles
No Number

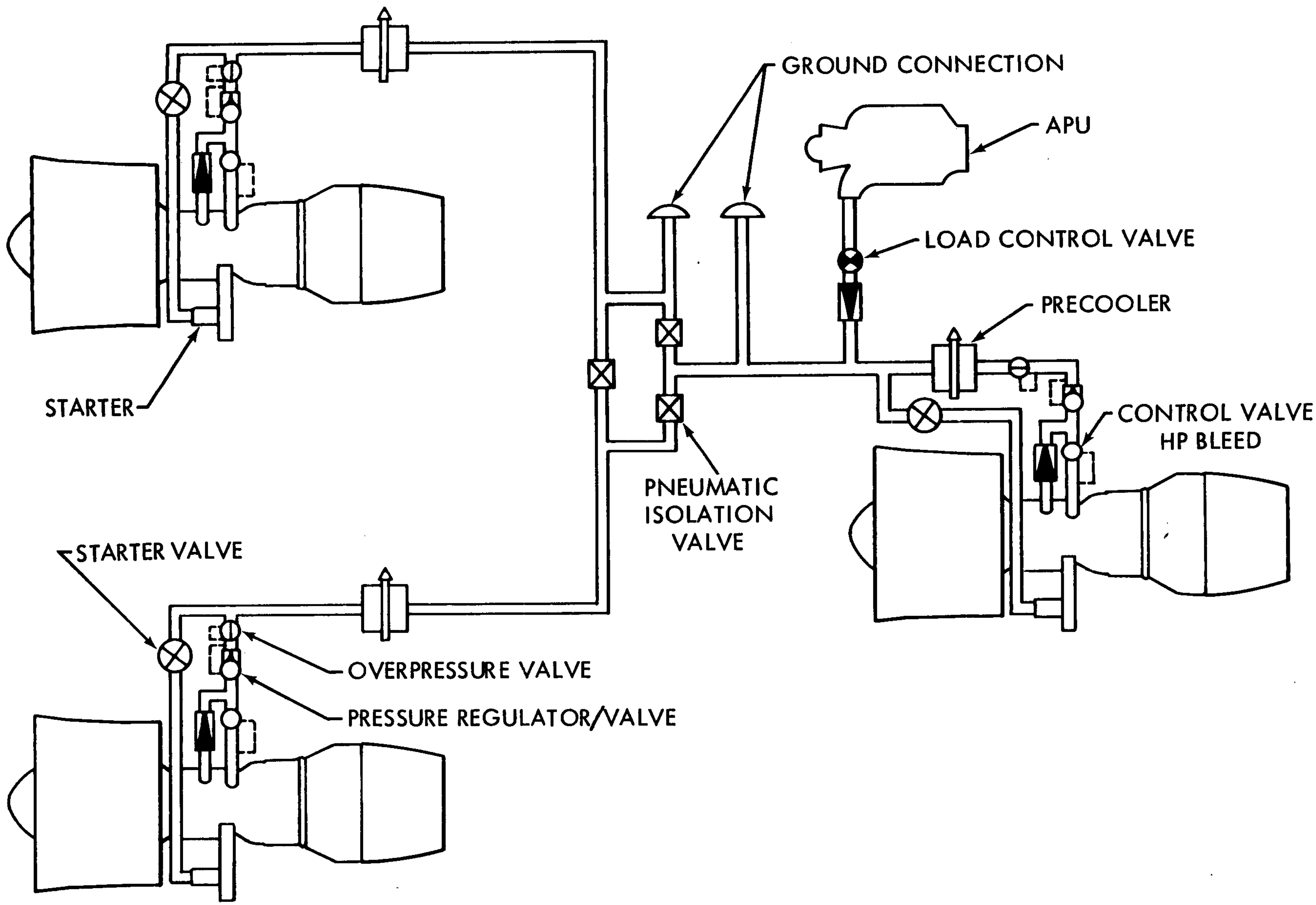

Figure 10.1-3 Starter System Schematic

cruise speeds, it is necessary to provide larger nacelle fineness ratios than are required on conventional subsonic nacelles in order to avoid high local slopes and velocities that would tend to create shock formation and drag rise.

The General Dynamics Mach .98 nacelle is shown in Figure 10.1-1.

Forebody - The General Dynamics nacelle forebody has an l_i/d_n of 1.0, based on the shortest length of the canted lip. Total nacelle l_n/d_n is 2.9 for the fan (outer) cowl. It is felt that these proportions are sufficiently close to that of the NASA force model nacelles to have similar drag characteristics.

The nacelle inlet lip is canted at 16 degrees with the vertical to facilitate area-ruling the nacelle/airplane combination. The l_i/d_n of the longest portion of the lip is 1.24. The aforementioned nacelle lengths apply to the wing-mounted nacelles. The l_i/d_n for the longer vertical-tail-mounted nacelle is 2.33, which is more favorable for critical Mach number.

The inlet cowl external proportions developed by NACA during early 1-series cowl tests (Reference 10-3) are marginal for the Mach .90 design cowl, and are not applicable quantitatively to Mach .98 nacelles. Further development will be required to avoid drag rise in nacelles cruising at Mach .98 while operating at a capture-area ratio in the vicinity of .80 to .85. However, the recent NASA nacelle tests provide valuable information that may be used to initiate the design of a transonic nacelle. With these data as a guide, the inlet diameter ratio of the nacelles was based on considerations of cruise spillage drag, takeoff pressure recovery, and nacelle structural thickness.

The diameter of the streamtube of incoming airflow is computed at maximum cruise power since most operation will occur near this power setting. Cruise airflow is expected to be within about 2 percent of maximum cruise airflow. The operating capture-area ratio, and the amount of airflow spillage are then determined by inlet size, which is made as large as possible to benefit pressure recovery without realizing spillage drag. Figure 10.2-1 shows the effect of inlet capture-area ratio on takeoff pressure recovery and spillage drag for the P&W STF-429 engine nacelle.

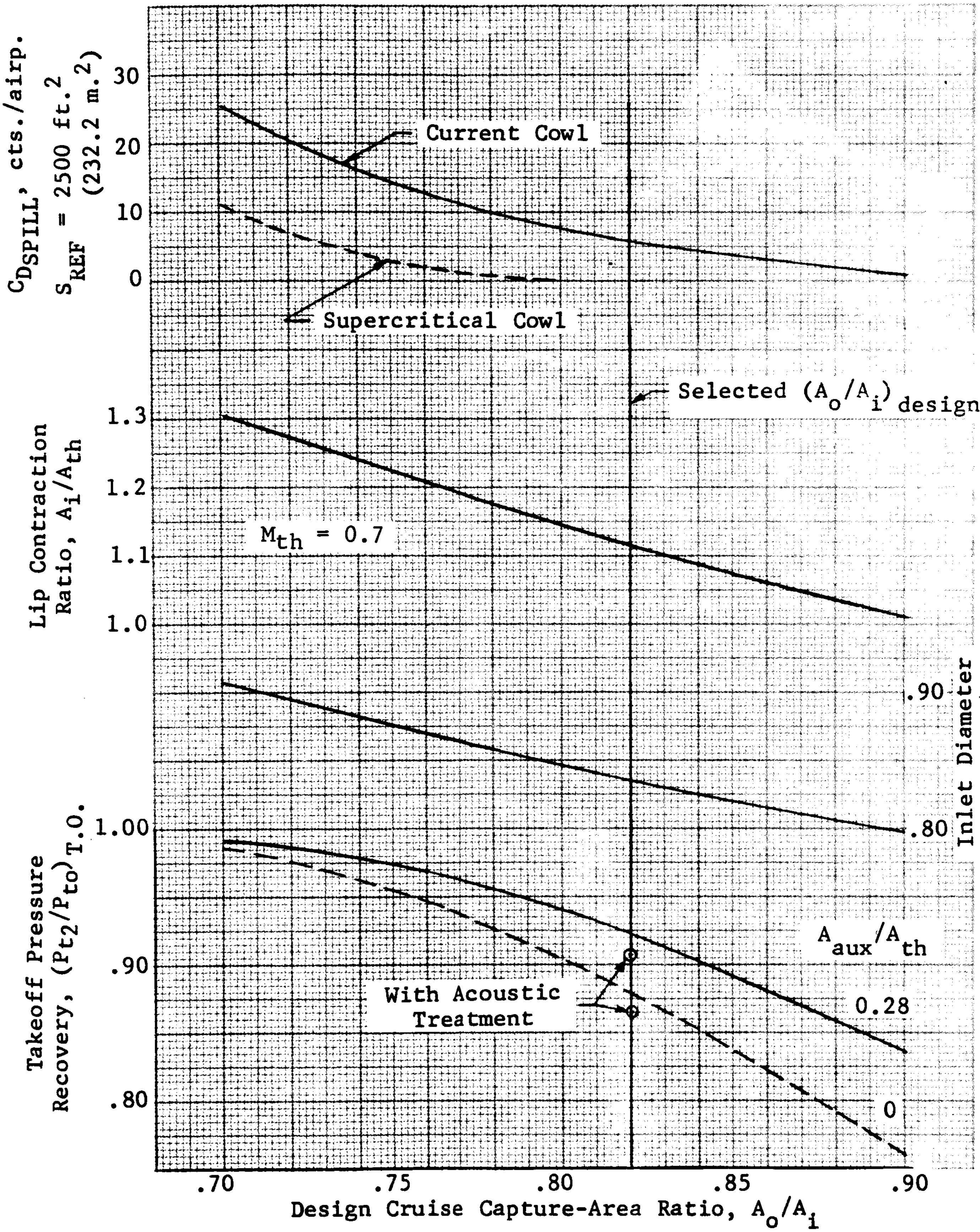

Figure 10.2-1 Mach 0.98 Inlet Design Parameters - P&W STF 429 Engine

It can be seen from Figure 10.2-1 that takeoff pressure recovery at reasonable values of spillage drag (5 counts or less for conventional cowls) is quite low (approximately 0.88). The strong effect of a low contraction ratio (1.11) on takeoff pressure recovery produces the low recovery even though the airflow per unit of throat area results in a throat Mach number of only 0.63. It is believed that a pressure recovery of at least 0.90 is required for adequate engine/inlet compatibility and engine operation. The only means of improving takeoff pressure recovery without increasing spillage drag is to augment the inlet flow area for takeoff and low-speed operation. This can be done by the use of self-actuating blow-in doors or a translating cowl lip. A layout study was made to determine how much auxiliary area could reasonably be added by these methods. It was concluded that about 28 percent auxiliary flow area could be added. At present, the use of a translating cowl is considered preferable to the use of multiple blow-in doors because of the expected additional noise that may be generated in the segmented annulus of the blow-in doors. A design and cost study showed that the translating cowl should weigh about 33 percent less than the blow-in door cowl and should require about 15 percent less tooling and manufacturing cost. The feasibility of the self-actuating feature of the translating cowl has been demonstrated at static conditions, but the effect of flight speed on its operation has not.

In determining the effect of flow per unit area on pressure recovery, the auxiliary inlet area is simply added to the throat area of the basic inlet. With 28 percent auxiliary area, pressure recovery at takeoff is increased from 0.88 to 0.92, which is still somewhat marginal. If, during the development of a supercritical cowl, it can be shown that inlet area can be increased without incurring spillage drag, then a higher level of takeoff pressure recovery will be attainable.

Inlet area is 2743 sq in. (1.770 sq m) for the 0.662-scale P&W STF-429 engine. Inlet size, within the range of capture-area ratios shown, is not expected to affect inlet pressure recovery at cruise.

<u>Afterbody</u> - The fan cowl envelops about 86 percent of the nacelle length, terminating a little distance aft of the bulge at the maximum diameter of the engine turbine. The fan cowl extends far enough aft of this bulge to direct the

fan flow parallel to the external surface of the primary nozzle. This is considered to be the shortest possible fan cowl that will permit (1) adequate acoustic treatment, (2) adequate length for thrust reverser installation, and (3) proper direction of the fan exhaust. A full-length fan duct would be heavier, have more aft-facing projected area, and have a higher terminal slope. The aerodynamic performance of a full-length fan-duct nacelle would not likely be greatly different from the one adopted, but the weight would obviously be greater. Several studies made of nacelles at lower drag divergence Mach numbers have favored 3/4-length fan ducts (References 10-4 and 10-5), while one (Reference 10-6) concluded that the long duct is desirable from the standpoint of improved internal mixing efficiency of the exhaust flows. Since the STF-429 engine does not mix the fan and core exhaust flows, a long fan cowl is not required.

The length of the primary nozzle is that required to maintain a final chordal angle of 15 degrees. The diameter ratio of the fan cowl is 0.82, while that of the protruding portion of the primary nozzle is 0.57. Both exits are convergent plug nozzles. A comparison of the geometry of Convair nacelles for the Mach .98 airplane and the apparent best nacelles tested by NASA is given in Table 10.2-1.

Table 10.2-1

COMPARATIVE NACELLE GEOMETRY

Geometric Parameter	G.D. Wing-Mtd Nacelle	G.D. Tail-Mtd Nacelle	NASA N_{13} Nacelle (Wing Mtd) (Ref. 10-2)	NASA Nacelle (Aft-Mtd) (Ref. 10-1)
Forebody l_i/d_n	1.00-1.24	2.33-2.53	1.54	1.09-1.31
Afterbody l_e/d_n (fan cowl)	1.77	1.51	1.54	1.64
Forebody d_i/d_n	0.835	0.70	0.84	0.79
Afterbody d_e/d_n (fan cowl)	0.815	0.70	0.84	0.79
Afterbody Slope (fan cowl)	16°	26°	3.5°	10°
Forebody $(A_{proj}/A_{max})_i$	0.30	0.51	0.29	0.38
Afterbody $(A_{proj}/A_{max})_e$ (fan cowl)	0.34	0.74	0.29	0.38

10.2.2 Performance of Mach .98 Design Nacelle

10.2.2.1 Drag

Nacelle drag is comprised of (1) baseline external drag at an inlet capture-area ratio of unity and cruise nozzle pressure ratio, and (2) inlet spillage drag at capture-area ratios less than unity. The effect of nozzle pressure ratio on nacelle drag has been omitted in performance calculations for the ATT because of the relatively small portions of the flight at non-cruise flight speeds.

External drag of the nacelles at unity capture-area ratio and cruise Mach number is shown in Figure 10.2-2 as a function of STF-429 engine scale. This drag is obtained from the friction drag of a flat plate having a wetted area equal to the nacelle wetted area multiplied by a form factor of 1.15 to account for additional form drag and local velocity effects. This assumes that the nacelles can be designed to avoid shock losses and separation on the forebody. The flat-plate friction is based on the turbulent mean skin friction coefficient of Eckert. The resulting nacelle external drag is included as a part of the airplane drag polar.

Inlet spillage drag is the sum of additive drag and the change in nacelle drag resulting from operating the inlet at capture-area ratios less than 1.0. The additive drag is determined by computing the change in total momentum between the inlet and the freestream. The change in cowl drag was initially estimated by using General Dynamics test data from open-nose-inlet cowl models. At the design-point capture-area ratio of 0.82, this resulted in about 5 counts of spillage drag for the three inlets. This data was subsequently revised at the request of NASA to show zero spillage drag at capture-area ratios greater than 0.8 on the assumption that further development of a supercritical cowl would provide this improvement in performance.

The spillage drag used in airplane performance is shown in Figure 10.2-3 as a function of Mach number and capture-area ratio. Spillage drag is essentially zero at all cruise points since cruise airflows are within about 2 or 3 percent of maximum cruise airflow. Results from recent NASA-Langley inlet cowl tests show little or no spillage drag at capture-area ratios above 0.8 for most of the inlet configurations at Mach .98. The trend of spillage drag versus capture-area

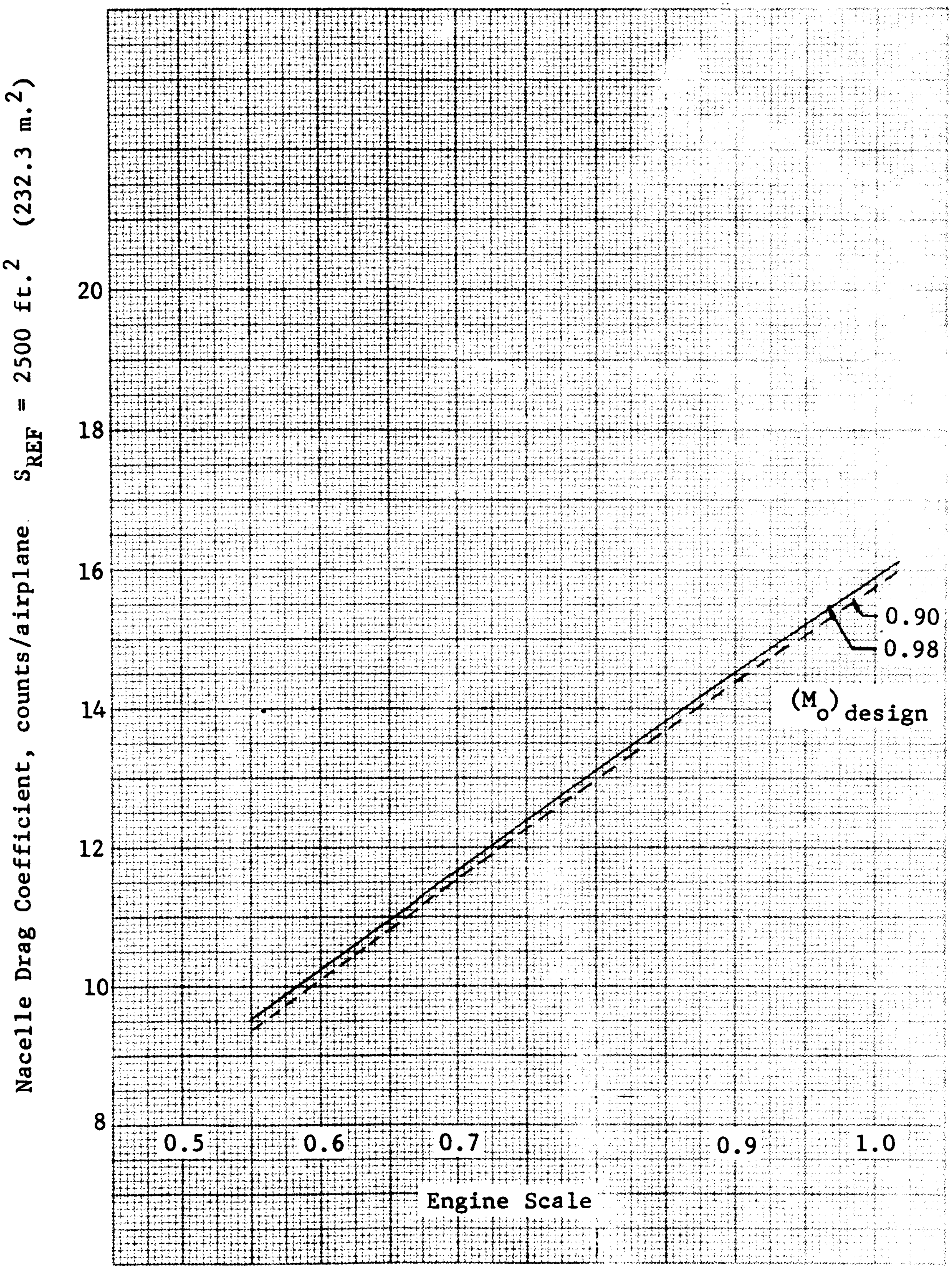

Figure 10.2-2 Nacelle External Drag; STF 429 Engine; A_o/A_i = 1.0

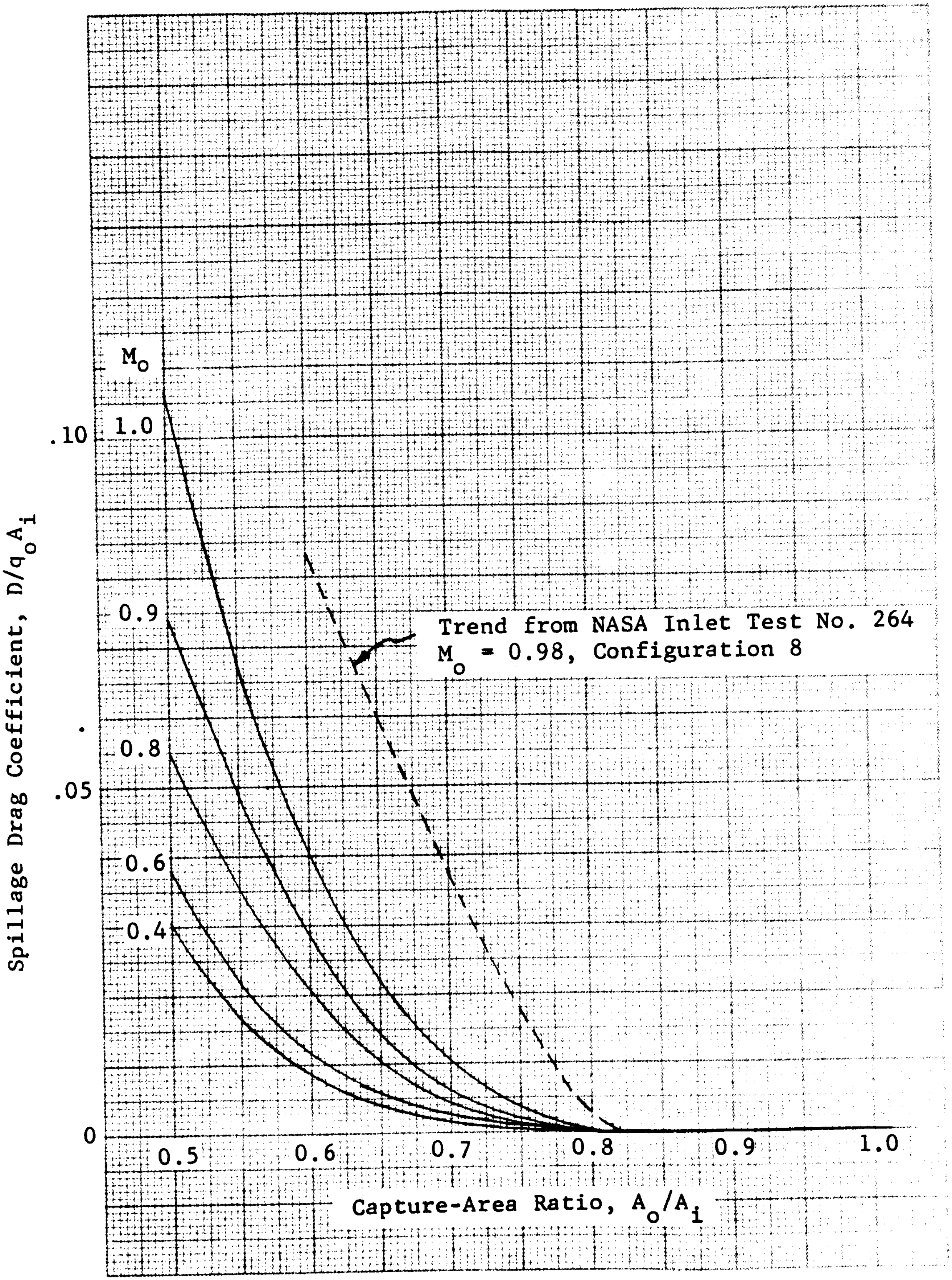

Figure 10.2-3 Inlet Spillage Drag; $(M_o)_{design} = 0.98$

ratio for the NASA cowl is somewhat steeper than the data used in the airplane performance studies. The NASA cowl tested, however, had NACA 1-series contours and was not presumed to achieve the ultimate drag divergence Mach number. Further development will probably reduce the minimum capture-area ratio for zero spillage drag.

10.2.2.2 Inlet Pressure Recovery

Inlet pressure recovery for the STF-429 engine inlet is shown in Figure 10.2-4 at takeoff, climb, and maximum cruise airflows. As previously stated, the engine airflows for all cruise power settings do not deviate significantly from the maximum cruise value. A pressure drop penalty for acoustic treatment of the inlet duct wall and two inlet splitters was supplied by P&WA. Convair's calculated pressure drop, which agreed very closely with the P&WA value, is included in the pressure recoveries shown in Figure 10.2-4. The penalty amounts to 1.4 percent at maximum airflow for the inlet splitter and wall treatment shown in Figures 10.1-1 and 10.1-2.

10.2.3 Alternate (Mach .90) Nacelle Design

The nacelles for the Mach .90 design airplane were designed in a manner similar to those for the Mach .98 airplanes with the following three exceptions:

(1) The lower cruise Mach number will allow operation to lower capture-area ratios without incurring spillage drag. Spillage drag characteristics, takeoff pressure recovery, lip contraction ratio, and inlet diameter ratio of the Mach .90 inlet used in engine and airplane performance are shown in Figure 10.2-5. Zero spillage drag was assumed at capture-area ratios greater than 0.7. The capability for achieving this level of spillage drag has been demonstrated on present-day conventional cowls. The design capture-area ratio selected for the Mach .90 nacelles is 0.77. This capture-area ratio was selected on the basis of providing a takeoff pressure recovery of 0.95, as shown in Figure 10.2-5. The lip contraction ratio is based on maintaining a throat Mach number of 0.7 at the design point, as is also true for the Mach .98 nacelle.

(2) Since the Mach .90 nacelle is designed to operate at a lower capture-area ratio than the Mach .98 nacelle, the inlet size per unit airflow is greater. Inlet area is

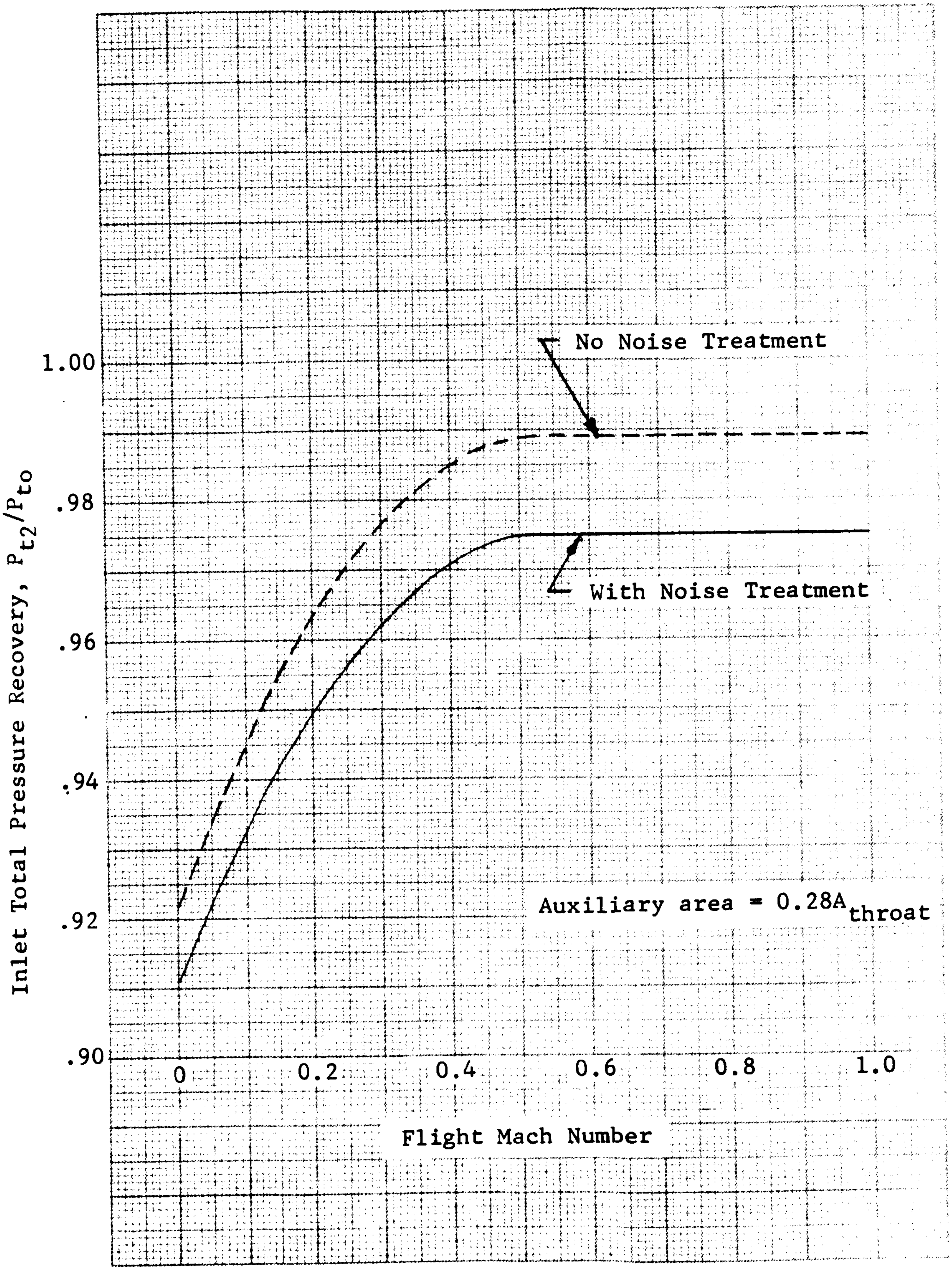

Figure 10.2-4 Inlet Pressure Recovery; STF 429 Engine; $(M_o)_{des.}$ = 0.98

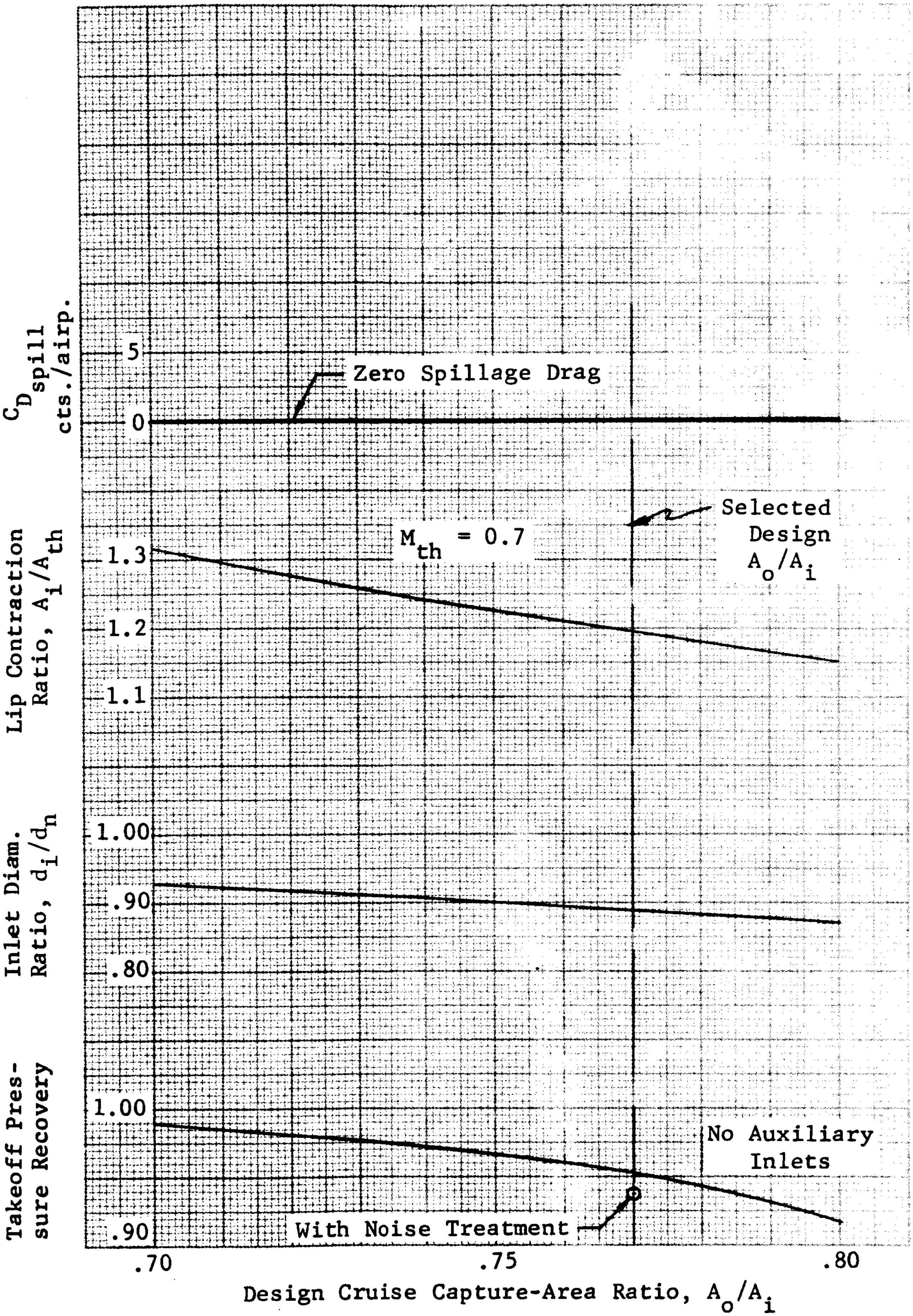

Figure 10.2-5 Mach 0.90 Inlet Design Parameters - STF 429 Engine

2546 sq in. (1.643 sq m). For a throat Mach number of 0.70 at cruise, the lip contraction ratio for the Mach .90 nacelle is 1.20 versus the 1.11 for the Mach .98 nacelle. Both the larger inlet area per unit airflow and the inlet contraction ratio improve takeoff pressure recovery, so that a recovery of 0.953 is attainable when noise treatment is not applied and without the use of any auxiliary inlet devices. The elimination of auxiliary inlet devices for takeoff is considered a major advantage of the Mach .90 design.

(3) The length of the Mach .90 nacelle is less than that of the Mach .98 design because the reduced drag divergence Mach number does not require a nacelle of as high a fineness ratio. Were it not for the length required to install acoustic treatment material in the inlet, the Mach .90 inlet l_i/d_n could be as low as 0.7. The length of the acoustic duct splitter rings require an increase in l_i/d_n to 0.9.

10.2.4 Performance of the Mach .90 Nacelle

10.2.4.1 Drag

External Drag - External drag of the Mach .90 nacelle is shown for cruise speed in Figure 10.2-2 as a function of engine scale for the P&W STF-429 engine. As in the case of the Mach .98 nacelle, the external drag is at unity capture-ratio and is based on flat-plate friction drag plus 15 percent form drag. The drag coefficient of the Mach .90 nacelle is only about 0.1 count less than that of the Mach .98 nacelle. While the Mach .90 nacelle is somewhat shorter and has less wetted area than the Mach .98 nacelle, the greater friction drag coefficient at the lower Reynolds number offsets this advantage.

Spillage Drag - Spillage drag used in performance calculations for the Mach .90 nacelle is given in Figure 10.2-6 as a function of capture-area ratio. At cruise speeds, the capture-area ratio is in the 0.75-to-0.77 range and, hence, the spillage drag is zero. For comparison, the spillage drag of the NASA inlet cowl Configuration 8 is also shown in Figure 10.2-6. For this cowl, spillage drag is zero at capture-area ratios above about 0.74 but rises rapidly at lower capture-area ratios. This data, as well as that from other sources, confirms the use of zero spillage drag in the cruise range of 0.75-to-0.77 capture-area ratio.

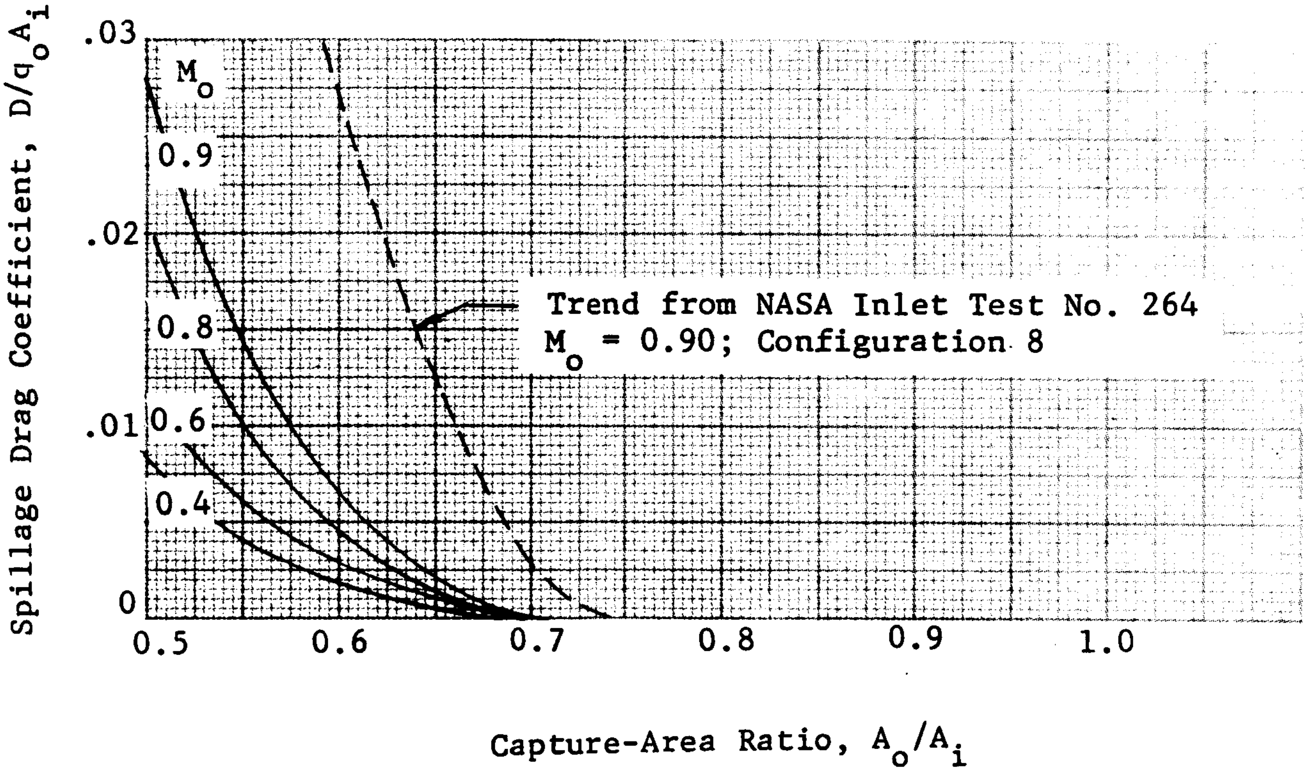

Figure 10.2-6 Inlet Spillage Drag; $(M_o)_{design} = 0.90$

10.2.4.2 Pressure Recovery

Pressure recovery for the Mach .90 nacelle is shown in Figure 10.2-7 as a function of flight Mach number.

10.3 ACOUSTIC NOISE

10.3.1 Noise Objectives

The noise objective for the P&WA STF-429 engine at each of the required measuring stations is FAR 36 minus 10 EPNdB. Comparisons between this objective and the estimated noise levels for various amounts of acoustic treatment applied to each airplane design are shown in Figure 10.3-1. Full duct-wall acoustic treatment plus two inlet splitters and one fan exhaust duct splitter are required to meet the noise level objective.

10.3.2 Nacelle Treatment Description

Details of the locations of the nacelle acoustic treatment are shown on the propulsion installation drawing, Figure 10.1-1. The treatment material is 1/2 in. (12.7 cm) thick on the walls and on each side of the splitters for attenuation in the predicted frequency range. The splitters provide acoustic paths with effective L/h ratios of approximately 5.0 in the inlet and 9.0 in the fan exhaust duct.

10.3.3 Effects of Special Operational Techniques

In hopes of reducing the community noise to as low a level as possible, various special operational techniques for takeoff and approach were investigated. These consisted of varying T/W and/or flight path angle during takeoff and using a two-segment approach for landing.

10.3.3.1 Takeoff

Figure 10.3-2 presents the results of a takeoff noise reduction study. These results show that the .98M airplane's noise level can be reduced by approximately 4.0 EPNdB by increasing T/W from .290 to .336. A 6.5-EPNdB reduction can be realized on the .90M airplane by increasing T/W from .272 to .339. The above reductions apply for single-stage takeoff flight paths. Further increases in T/W would cause the sideline noise to exceed FAR Part 36 minus 10 EPNdB and hence were not considered.

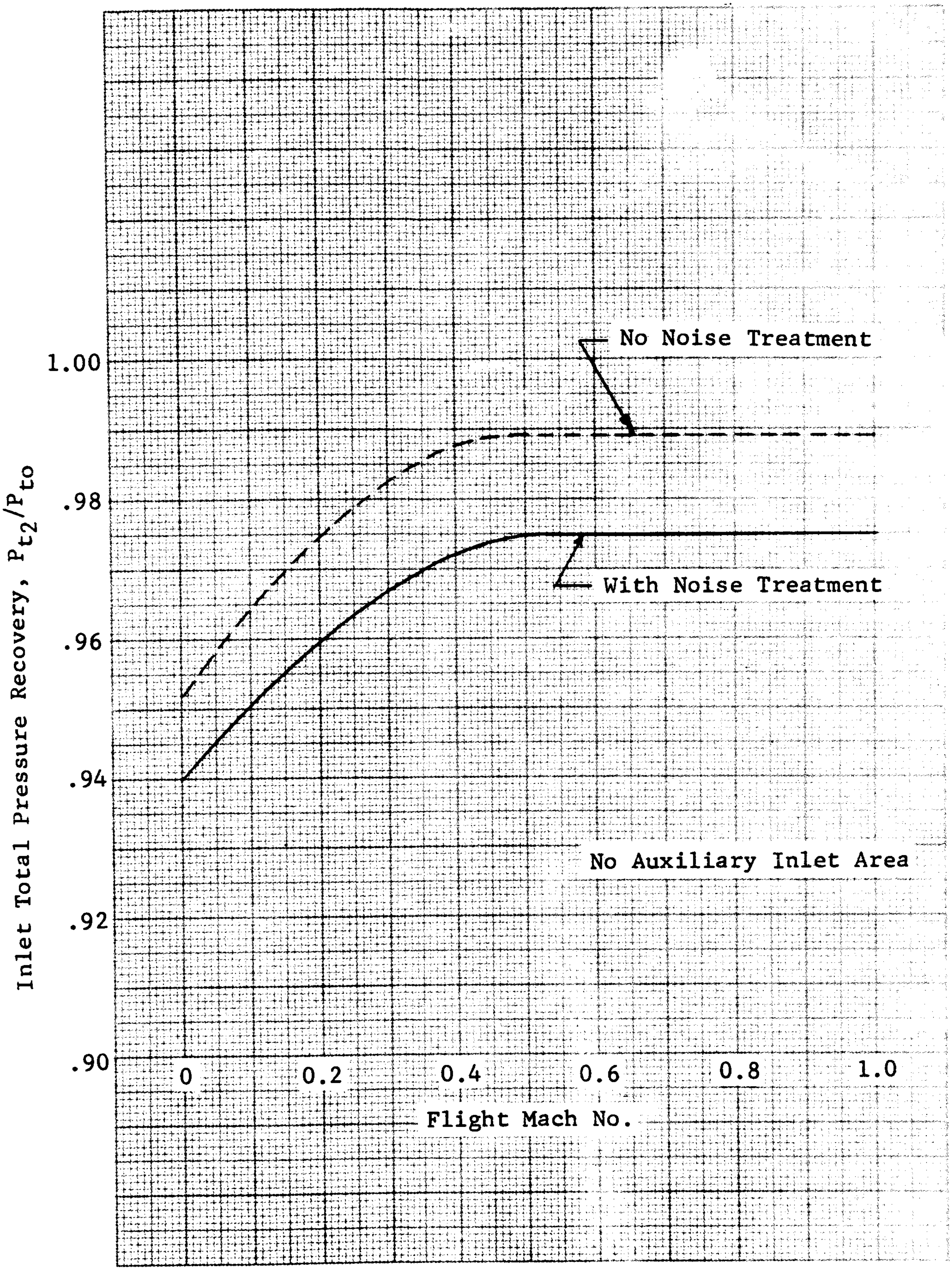

Figure 10.2-7 Inlet Pressure Recovery; STF 429 Engine; $(M_o)_{design} = 0.90$

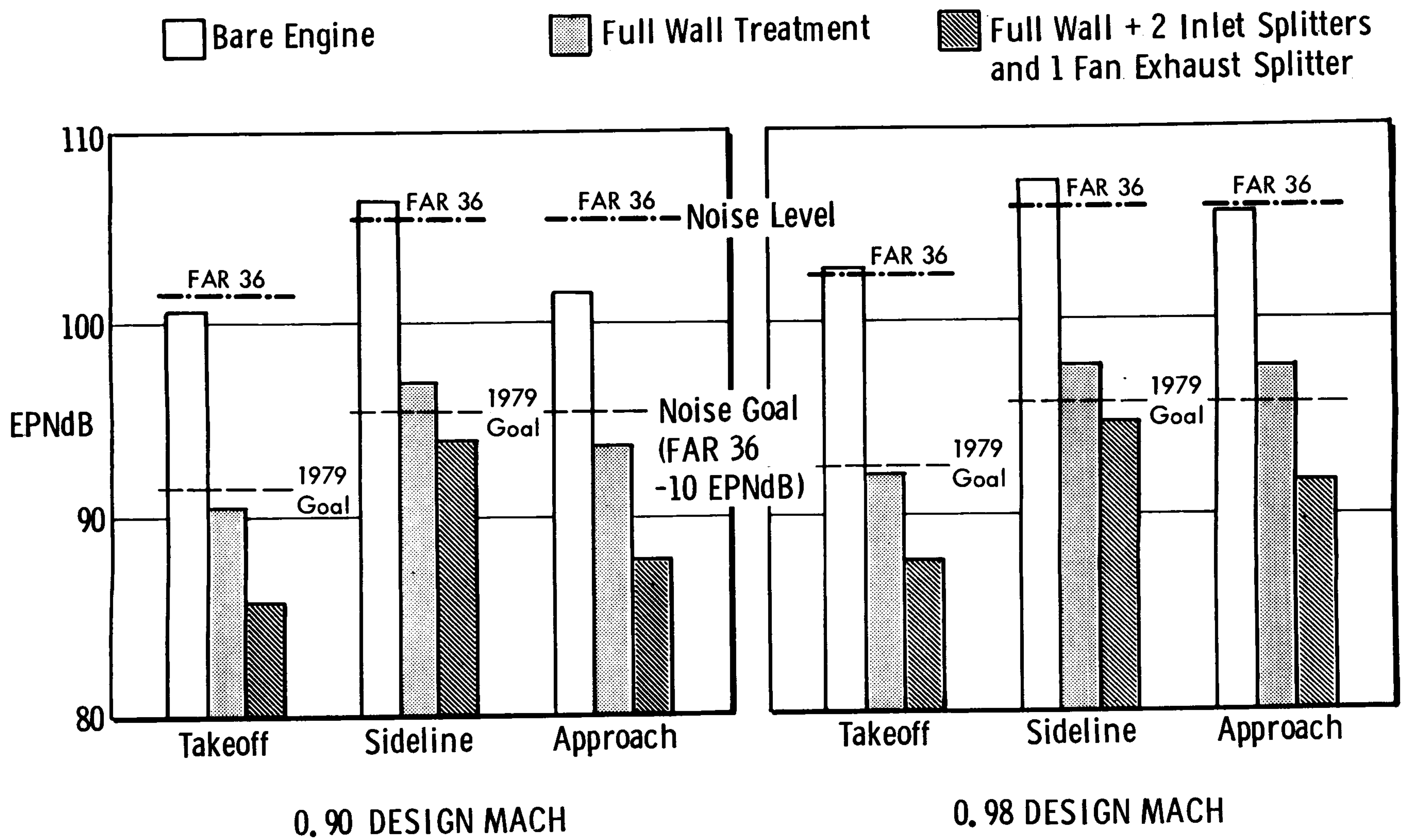

Figure 10.3-1 Noise Predictions for the STF 429 Engine for Each Airplane Design

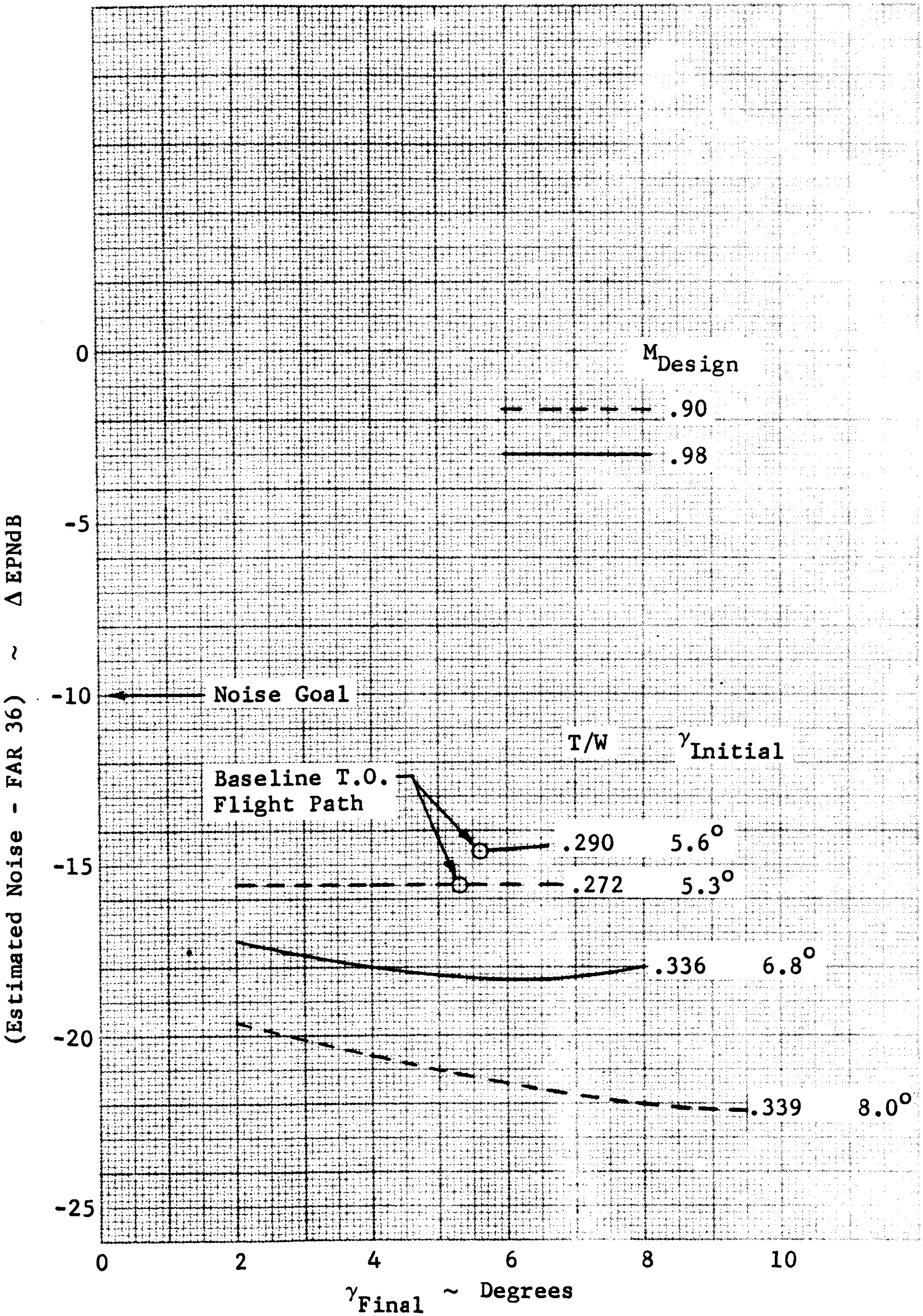

Figure 10.3-2 Takeoff Noise Variation With Flight Path Angle and T/W

10.3.3.2 Approach

The calculation of the noise improvement attainable by the use of a two-segment approach path would require knowledge of the airframe and engine dynamics as well as detailed noise characteristics of the engine. None of these was available, so actual noise reduction calculations were not attempted. The thrust required for a 6-degree glide slope is much less than for a 3-degree approach and, if a smooth transition from 6 to 3 degrees is in progress at the approach-noise measuring station, the noise is obviously going to be less than that of a single-segment 3-degree approach. Previous studies and even flight tests conducted by an airline crew have shown that a reduction of about 7 EPNdB can be realized by utilizing a two-segment 6-degree/ 3-degree rather than the usual single-segment 3-degree approach.

10.3.4 1985 Noise Projection

The Pratt & Whitney STF-433 engine was selected by P&WA on the basis that a 5-EPNdB noise improvement over the STF-429 could be attained, but with some system performance degradation. The resulting economic penalty can be determined by comparing the bar labeled -15 EPNdB and the bar labeled -10 EPNdB on Figure 6.4-2 in Section 6.4.

The engine's characteristics are such that a predicted noise level of FAR Part 36 minus 16 EPNdB is attained at the sideline condition, which is the critical condition. Even without special operating techniques, the community noise levels will be quite low. The noise at the approach is expected to be about 19 EPNdB below FAR Part 36, whereas the noise at the takeoff conditions will be about FAR Part 36 minus 20 EPNdB.

It appears certain that with the use of the special operating techniques described in Subsection 10.3.3 the community noise levels will be very low. EPNdB values which should be attainable are shown by Figure 10.3-3. Note that the noise in the immediate airport vicinity, the sideline condition, will still be about 15 EPNdB below the current FAR Part 36 requirements.

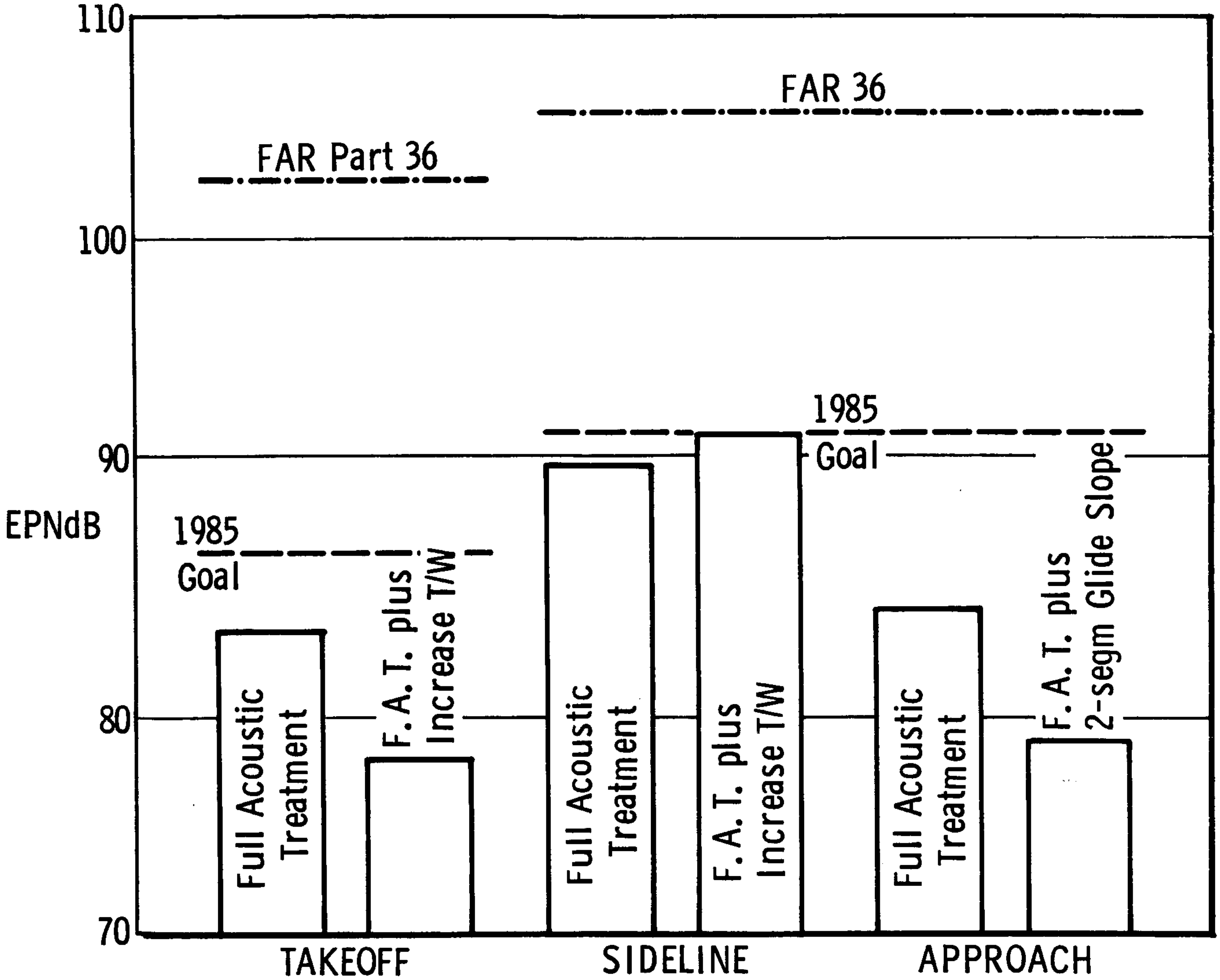

Figure 10.3-3 1985 Noise Projection - M = .98 Design

10.4 INSTALLED PROPULSION SYSTEM PERFORMANCE

Engine performance data supplied by the engine manufacturers were corrected for installation losses estimated for the ATT airplane. Corrections were made for inlet pressure recovery, inlet spillage drag, engine bleed, horsepower extraction, and noise-treatment installation effects. This resulted in an installed thrust-minus-delta-drag (T-DD). Inlet pressure recovery and spillage drag data employed are discussed in Section 10.2. Based on the design passenger capacity, engine bleed was estimated as 2 lb/sec (.906 kg/sec) per engine. These estimates for bleed and horsepower extraction were unchanged throughout the study. Corrections for pressure losses resulting from noise treatment were included in installed engine performance as applicable. Noise treatment data are further discussed in Section 10.3.

Installed propulsion system performance data were generated for several engines, including the General Electric CF6-50C, P&WA Parametric ATT Engines (five engines), GE ATT Engine No. 1, P&WA STF-429, and P&WA STF-433. Estimates of performance penalties for acoustic treatment were included in data for all engines except the CF6-50C, which was used as the baseline engine for Phase I studies. As stated earlier, corrections for bleed and power extractions were unchanged. Additional data for the STF-429 was supplied without corrections for noise treatment pressure drop to allow evaluation of the economic penalty for noise treatment.

10.4.1 Comparison of GE ATT Engine No. 1 and P&WA STF-429 Engines

The GE ATT Engine No. 1 and P&WA STF-429 engines were candidate engines for the ATT baseline configuration studies. These engines were selected by the Engine Design Study contractors and the contract monitor from NASA Lewis Research Center because they give good cruise installed performance and meet the noise limitation of FAR Part 36 minus 10 EPNdB. Convair's cycle selection studies agree well with the STF-429 selection. The Convair studies do not include mixed flow cycles, but the GE ATT Engine No. 1 cycle selection appears satisfactory also. The two engines were scaled to the same maximum cruise power T-DD at Mach .98, 36,089 ft (11,000 meters) for comparison, as shown in Figure 10.4-1. Both engines exhibit essentially the same cruise SFC's; however, the P&WA STF-429 engine has about 8 percent more takeoff T-DD. Physically the GE ATT Engine No. 1 is smaller in

Physical Characteristics

ENGINE	GEATT No. 1	P&WA STF 429
Weight* - lb (kg)	6230.0 (2825.9)	7000.0 (3175.2)
Length*-in. (m)	137.7 (3.498)	140.3 (3.44)
Diameter-in. (m)	74.8 (1.900)	78.0 (1.98)
Scale Factor	0.787	1.0

*Bare Engine

INSTALLED PERFORMANCE

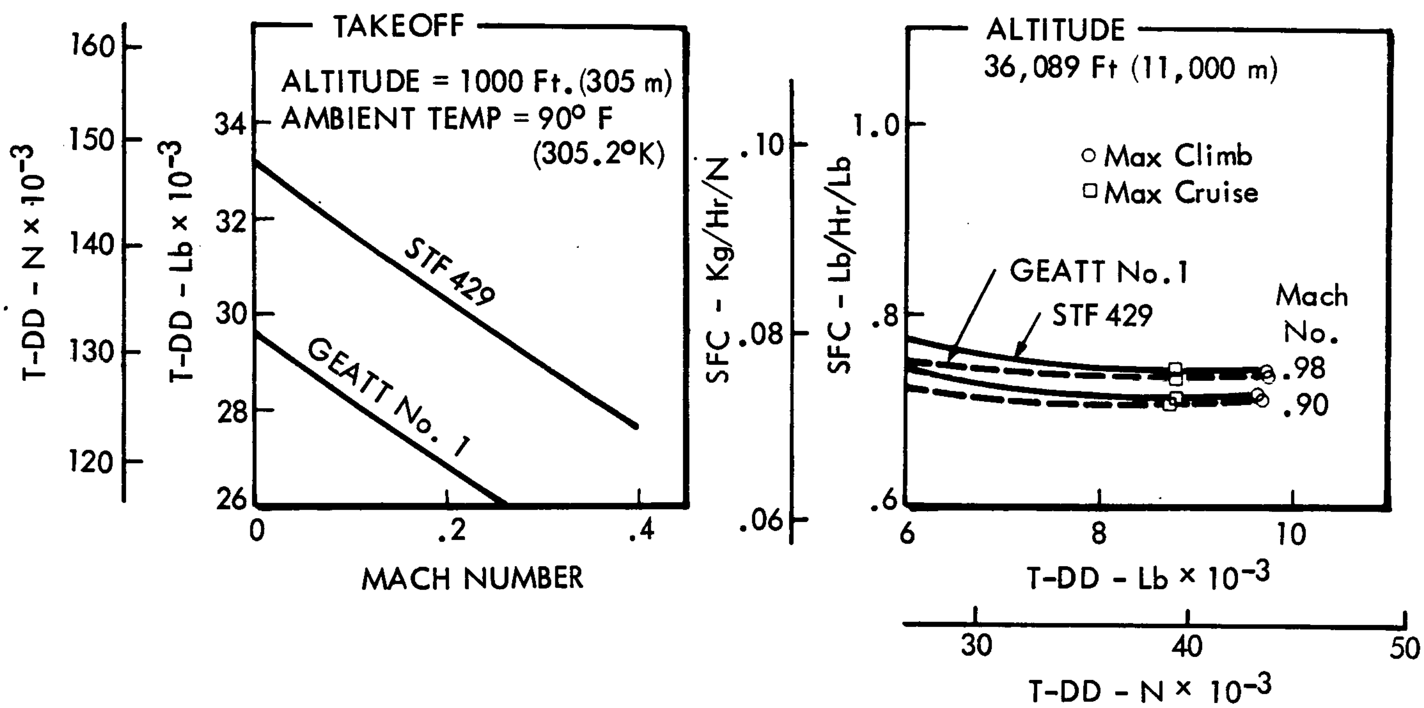

Scaled to T-DD @ M_0 = 0.98, 36,089 Ft (11,000 m) = 8800 Lb (39,140 N)

Figure 10.4-1 Comparison of the GEATT No. 1 and P&WA STF429 Engines diameter, lighter in weight, and longer than the P&WA engine. Based upon this comparison, there is no obvious reason for selection of one engine over the other. The P&WA engine was selected primarily because of data availability. Pratt & Whitney supplied a computer deck suitable for calculation of installed net thrust over the complete flight envelope. General Electric supplied only limited tabular data.

10.4.2 Installation Effects on Propulsion System Performance

The data in Figure 10.4-2 show the percentage change in net thrust resulting from corrections for the various installation parameters. At takeoff the inlet pressure recovery correction exhibits the largest difference in percentage change in net thrust for the various corrections for the two design-point airplanes. This increment is due to higher pressure recovery for the Mach .90 design at takeoff. The higher inlet total pressure recovery results from better matching of inlet size between takeoff and cruise flight conditions for the Mach .90 design. Both the Mach .90 and .98 design inlets were sized for cruise power airflows; consequently, the penalty at cruise for inlet pressure recovery is very close to the same for both designs. Engine bleed is a greater percentage penalty to thrust at cruise flight conditions than at takeoff because the constant bleed flow requirement is a greater percentage of engine core flow at cruise than at takeoff. Corrections for horsepower extraction are small at both takeoff and cruise flight conditions; however, they are included. Inlet and duct pressure loss due to splitters and wall treatment result in a penalty to net thrust at both takeoff and cruise of about 3 percent for noise treatment. A constant 0.985 nozzle velocity coefficient is assumed.

In order to reduce NO_X emissions at takeoff, combustor inlet water injections of 8120 lb/hr/engine (3680 kg/hr/engine) for the Mach .90 design and 9600 lb/hr/engine (4350 kg/hr/engine) for the Mach .98 design are used. This results in an increase of 3.4 percent in net thrust at takeoff. There is no water injection at cruise. The weight of equipment required to supply these water injection rates is 265 lb (120.2 kg) for the Mach .98 design and 230 lb (104.3 kg) for the Mach .90 design. This amount of dry weight has a negligible effect on DOC since the cost of the water is only about $4.00 per takeoff.

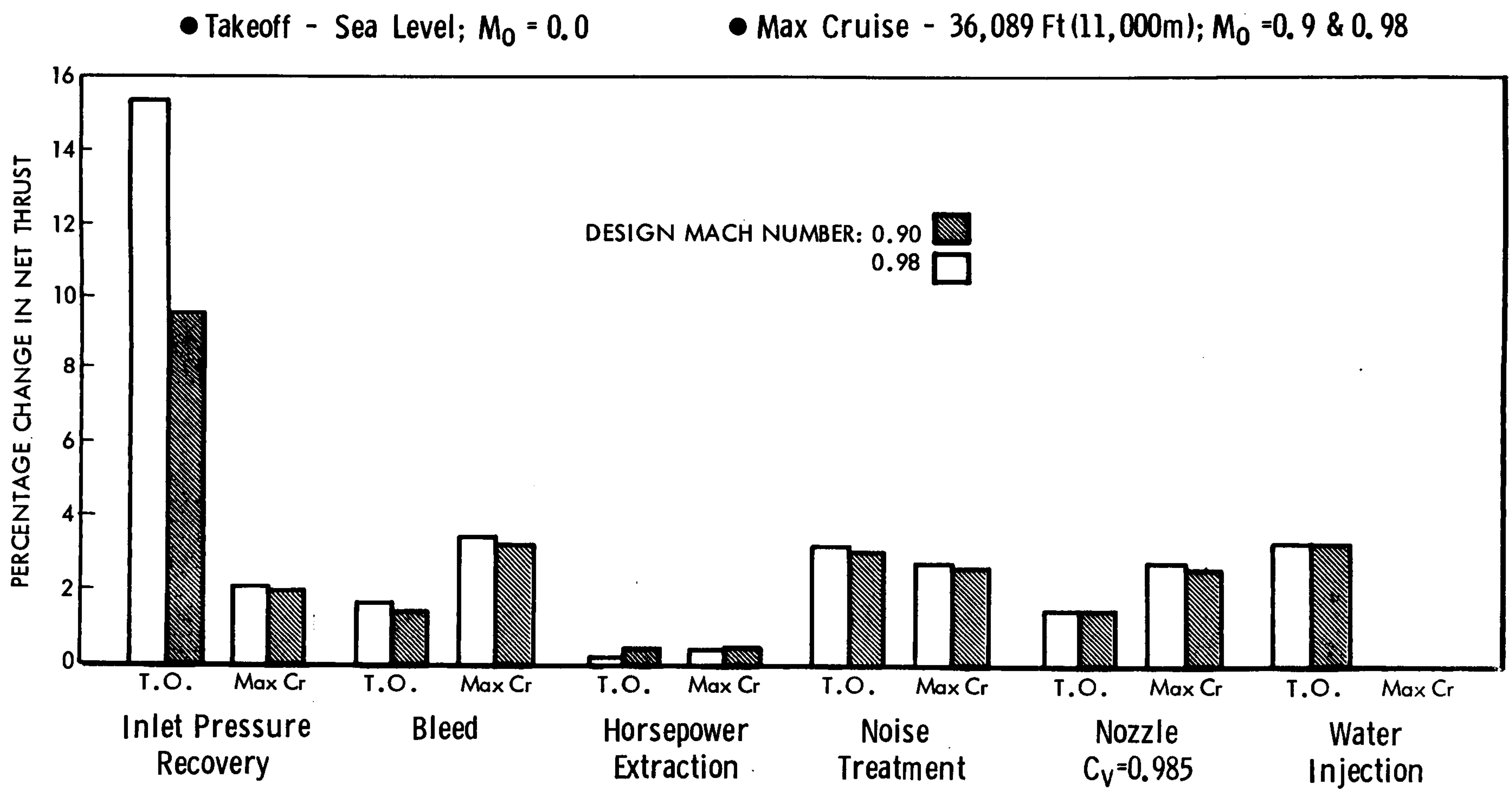

Figure 10.4-2 Installation Effects on Propulsion System Performance

10.4.3 Comparison of Engines Selected for the Mach .90 and .98 Designs

A comparison of the performance and physical characteristics of the P&WA STF-429 engine scaled for the Mach .90 and .98 designs is shown in Figure 10.4-3. The Mach .90 data are for a 0.56-scale engine; the Mach .98 data are for a 0.662-scale engine. Engine scale factor is defined as the thrust required per engine divided by the thrust available from a specific baseline engine size defined by P&WA. The scale factors are based on performance and economic analyses. Installation penalties are about the same at maximum cruise power for both cruise Mach designs, as shown in Figure 10.4-2; consequently, the SFC comparison typical of turbofan engines shows the Mach .90 cruise SFC to be 4 percent less than the Mach .98 cruise SFC.

10.4.4 Comparison of a 1979 Technology Engine with a 1985 Technology Engine

Figure 10.4-4 presents a comparison of P&WA's 1985 time-period engine (STF-433) with the 1979 time-period engine (STF-429). Both are 0.56-scale engines consistent with the STF-429 Mach .90 design scale factor. The STF-433 design is a 6.5-by-pass-ratio engine compared with the STF-429 4.5-by-pass-ratio engine. The objective of the STF-433 engine is to be 5 EPNdB quieter than the STF-429 technology engine and 15 EPNdB less than present FAR Part 36 noise requirements. Increased combustor exit temperature (CET) is a design feature of the STF-433 engine. However, the cycle compromises necessary to attain the lower noise causes the 1985 engine to exhibit 1-percent higher cruise SFC, 8-percent greater weight, 8-percent larger diameter, 1-percent lower climb power T-DD, and 4.5-percent less Mach 0.2, 90°F (305.3°K), 1000 ft (304.8 m) takeoff T-DD.

10.5 EXHAUST EMISSIONS

10.5.1 Emission Pollutant Limitations

A major objective of the Advanced Transport Technology evaluation is to demonstrate capability for much improved environmental factors. The noise factor has been previously discussed (Section 10.3). The other important environmental consideration is that of the atmosphere-polluting constituents of the exhaust gas; thus, very stringent emission pollutant limits are met by the ATT propulsion system. The

Physical Characteristics - Scaled STF429

	Mach Design = 0.90	Mach Design = 0.98
Weight - Lb (kg)	3535 (1602)	4430 (2008)
Length - in (m)	108 (2.74)	116.5 (2.96)
Diameter - in (m)	58.4 (1.482)	63.2 (1.602)
Scale Factor	.560	.662

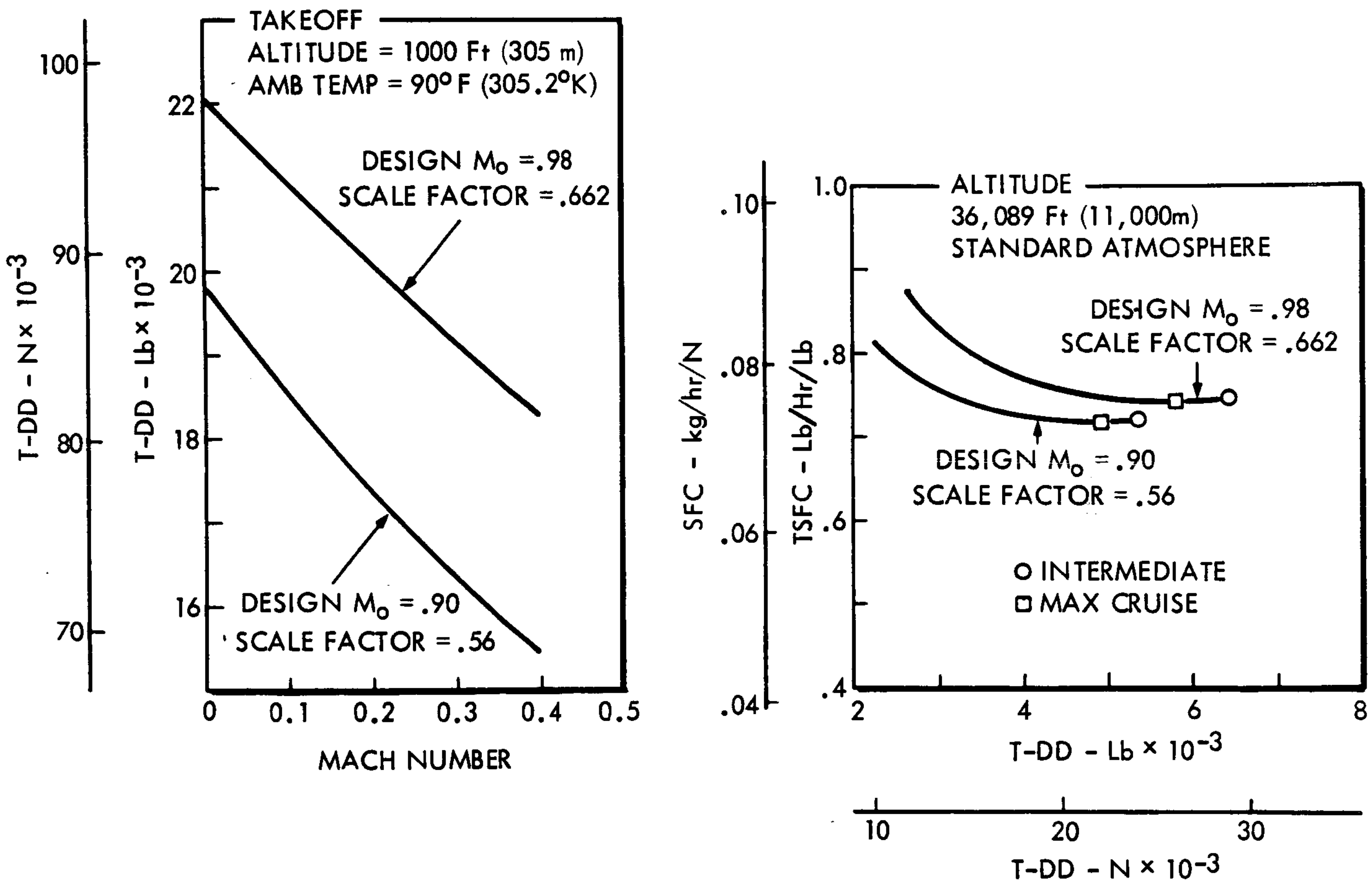

Figure 10.4-3 Comparison of Engines Selected for the Mach 0.90 and Mach 0.98 Design

Physical Characteristics - Scale Factor = .56

ENGINE	STF433 (1985)	STF429 (1979)
BPR	6.5	4.5
OPR	25	25
FPR	1.92	2.03
Fan Tip Diam in.	62.8 (1.597m)	58.4 (1.482m)
Weight	3840 (1740kg)	3535 (1602kg)
ΔEPNdB	-15	-10

Installed Performance Characteristics - Scale Factor = .56

Takeoff T-DD

$M_o = 0.2$ Alt = 1000 Ft (305m)
Ambient Temp = 90° F (305.2°K)

ENGINE	T-DD - Lb (N)
STF429	17,350 (77,180)
STF433	16,400 (72,950)

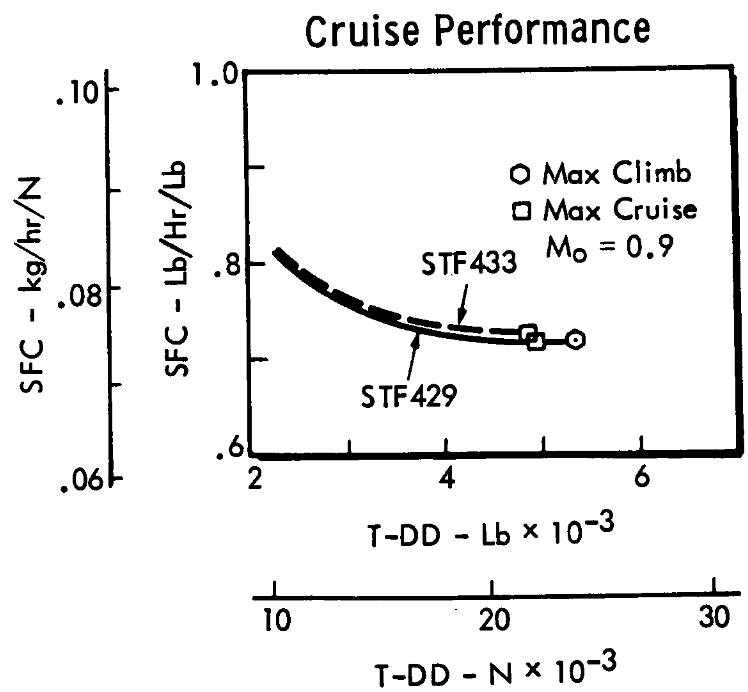

Figure 10.4-4 Comparison of a 1979 Technology Engine with a 1985 Technology Engine

total hydrocarbon emissions (H/C) are required to be below 8 lb per 1000 lb of fuel (8 kg per 1000 kg fuel); the carbon monoxide (CO), below 40 lb per 1000 lb fuel (40 kg per 1000 kg fuel); the nitrogen oxides (NO_X), below 3 lb per 1000 lb fuel (3 kg per 1000 kg fuel); and the smoke emissions to meet an SAE No. of 15.

10.5.2 Problem Discussion

The problems of attaining the emission limitations described above are grouped into two discrete engine operating regimes. The CO and H/C limitations are easily met in today's engines at medium and high power settings but may be exceeded at idle power settings. The NO_X and smoke limits are easily met at low power settings but present some difficulty at high power settings.

The STF-429 engine selected for the final aircraft designs meets all of the requirements, but requires water injection to avoid exceeding the NO_X limit.

The two engine study contractors use slightly different combustor design approaches to meet the smoke, CO, and H/C limits, but both require the use of water during takeoff to meet the NO_X requirement. The water consumption per engine required to avoid exceeding the limit is 8120 lb/hr/engine (3680 kg/hr/engine) for the .90 Mach number design.

The ATT engine burners using variable-geometry combustor domes or two-stage fuel injection for low power emission control and using pre-mixed fuel-air or carbureting combustors for high power emission control augmented with water injection to further reduce the NO_X are expected to meet levels shown by Figure 10.5-1.

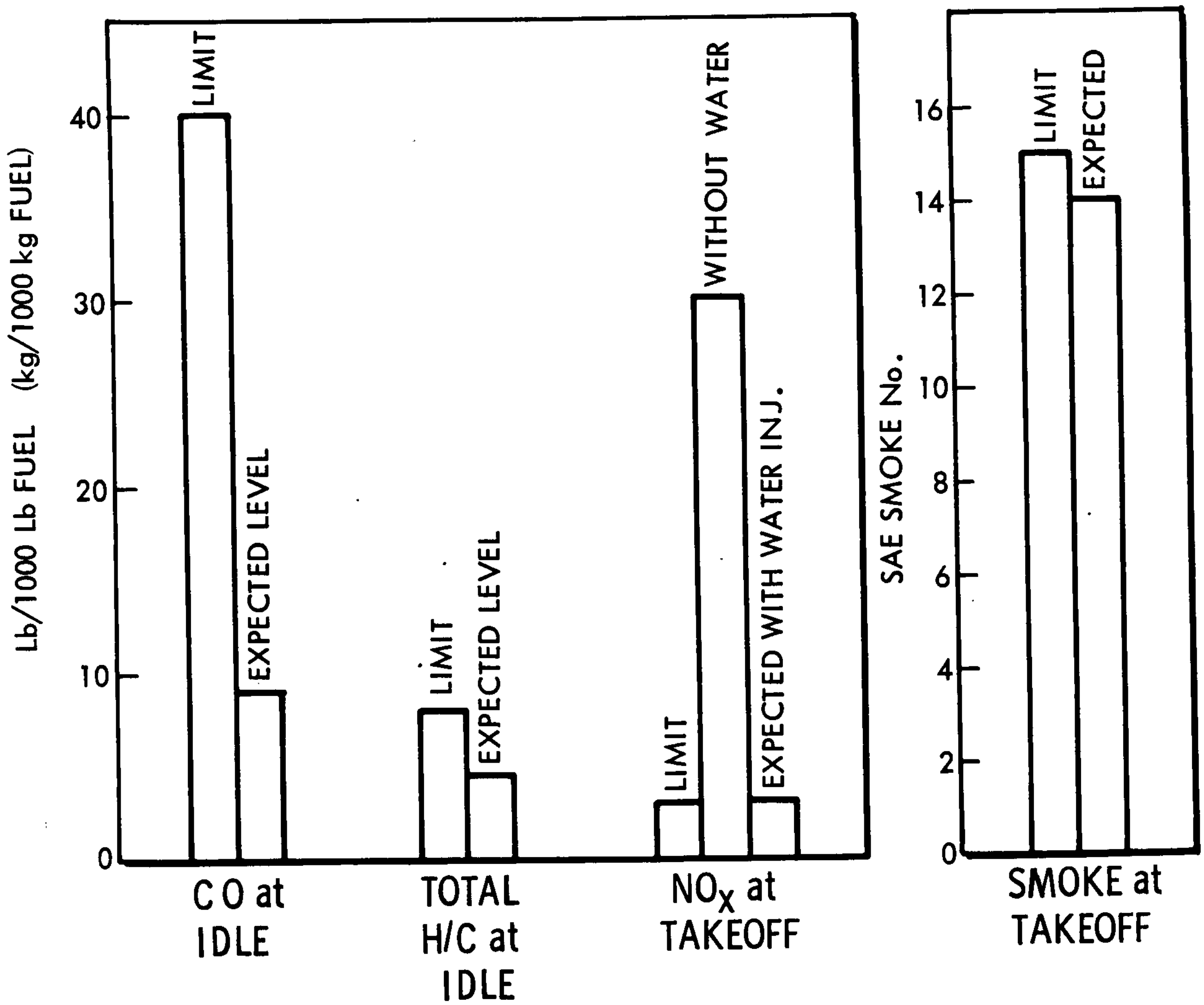

Figure 10.5-1 Improvement in Exhaust Emissions

SECTION 11

MAJOR SUBSYSTEM

DESCRIPTION

The program redirection prior to initiating the Phase II effort limited Convair's subsystem efforts to that just sufficient to allow reasonable subsystem weight, volume, and cost estimates. Convair's approach was to assimilate data from all of the new wide-body transports and to apply its statistical estimating techniques to arrive at the appropriate estimates. The resulting subsystems are described briefly in the following subsections.

11.1 ENVIRONMENTAL CONTROL SYSTEM

The environmental control system encompasses the following subsystems: (1) pneumatic, (2) cabin air conditioning and pressurization, (3) ice and rain protection, and (4) oxygen.

The air conditioning system derives its cooling from two independent bootstrap air-cycle refrigeration units. One unit is located in the inboard section of each wing leading-edge area, forward of the main spar. Zone temperature control, built-in test circuits for rapid, accurate fault isolation, and large access doors for easy servicing of the equipment are additional features of the system.

Each air conditioning unit is capable of maintaining a fully loaded cabin at a temperature less than 80°F (299.7°K) on the ground and below 75°F (296.9°K) above 10,000 feet (3048 m) during hot-day operation at all normal cruise and descent conditions. The two units provide a combined fresh air at 16 cfm (0.45 m^3/min) to the passenger compartment plus 400 cfm (11.328 m^3/min) to the cockpit. One unit is capable of providing full pressurization and ventilation in excess of FAR Part 25 requirements. Perimeter heating provided in cargo compartments insures warm walls and floors for all possible types of loading.

The anti-icing system provides for unrestricted flight through icing conditions as defined in FAR Part 25. The critical portion of the wing slats, the engine inlet cowls, and the inlet sound suppression splitters are thermally anti-iced with engine bleed air. Other-ice sensitive components such as the windshield and pitot tube are electrically anti-iced. Windshield rain removal is effected by electrically operated windshield wipers combined with a liquid rain repellant.

The integrated pneumatic system consists of an onboard auxiliary power unit (APU); the ducting and controls for the air conditioning, pressurization system, and anti-icing system; and engine cross-bleed starting ducts. Air is supplied to the pneumatic distribution manifolds from three functionally identical engine bleed systems. It is processed by the components shown in the schematic diagram of Figure 11.1-1.

In normal flight, bleed air is extracted from the compressor intermediate stage port and through the check valve to the pressure regulator, where its downstream pressure is limited to approximately 45 psig (31,000 N/m^2). Downstream of the regulator the air passes through the overpressure shutoff valve to the pre-cooler, where it is cooled by fan air to maintain a bleed manifold air inlet temperature of approximately 400°F (473°K).

The air conditioning system features two dual (redundant), three-wheel air-cycle systems located one on each side in the leading edge of the wing root. This area, because of its central location, provides a minimum length of air distribution ducting, convenience for ram air intake, and easy access through large nonstructural doors.

11.2 FUEL SYSTEM

The fuel is contained in integral tanks between the front and rear wing spars outboard of the fuselage. Solid enclosure ribs form the tank end-walls. The tanks are baffled to prevent excessive fuel shifting and to reserve the outboard-section fuel until the airplane gross weight is reduced by fuel usage. Tanks No. 1 and 3, the outboard wing tanks, normally serve the adjacent engine on that wing. Tank No. 2 is divided into two halves, located in the inboard wing section, one half in each wing. The two halves are gravity interconnected through open lines. This tank normally supplies the tail-mounted engine. Figure 11.2-1 is a schematic of the fuel system; Figure 11.2-2, of the vent system.

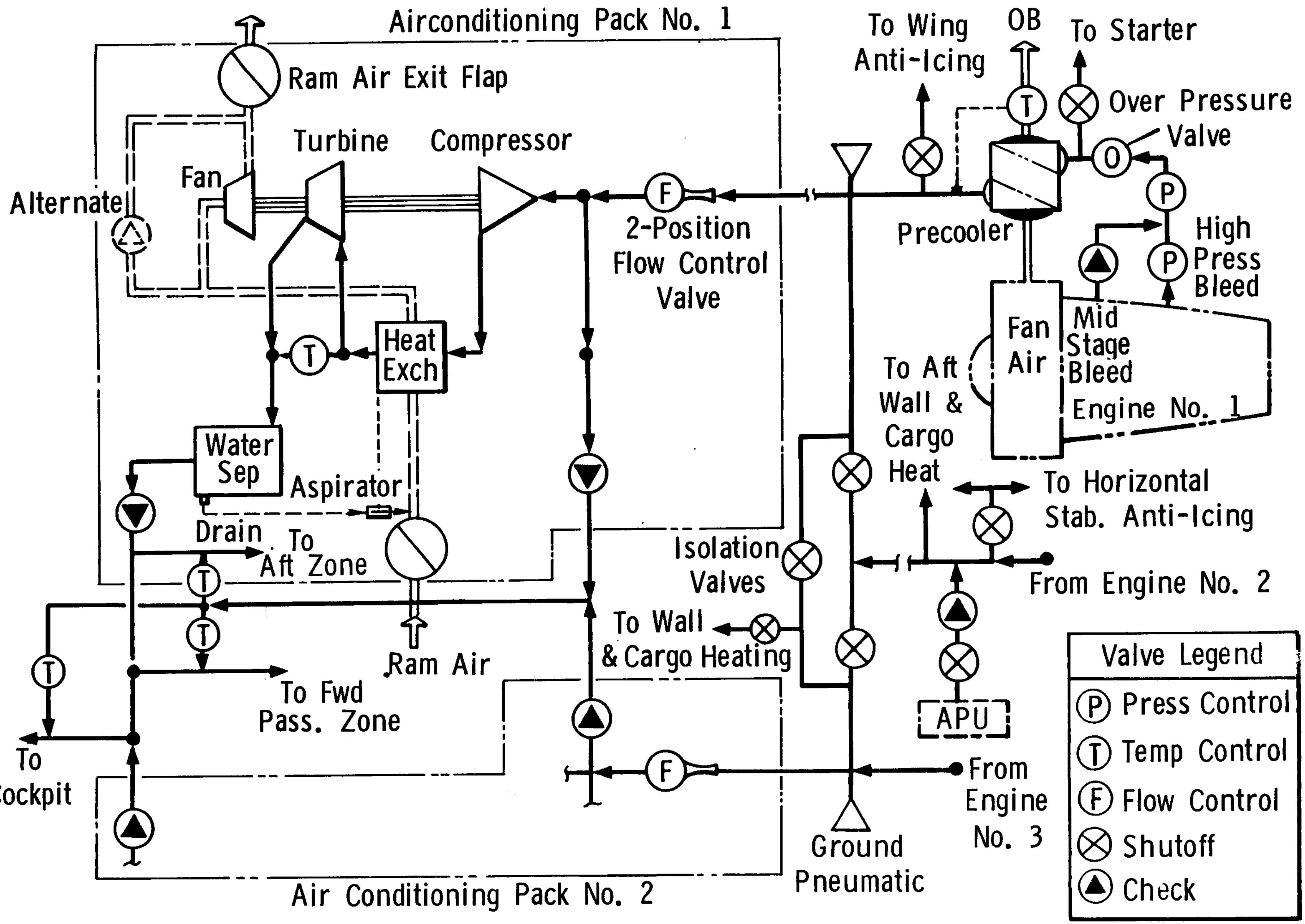

Figure 11.1-1 Environmental Control & Related Pneumatic System Schematic

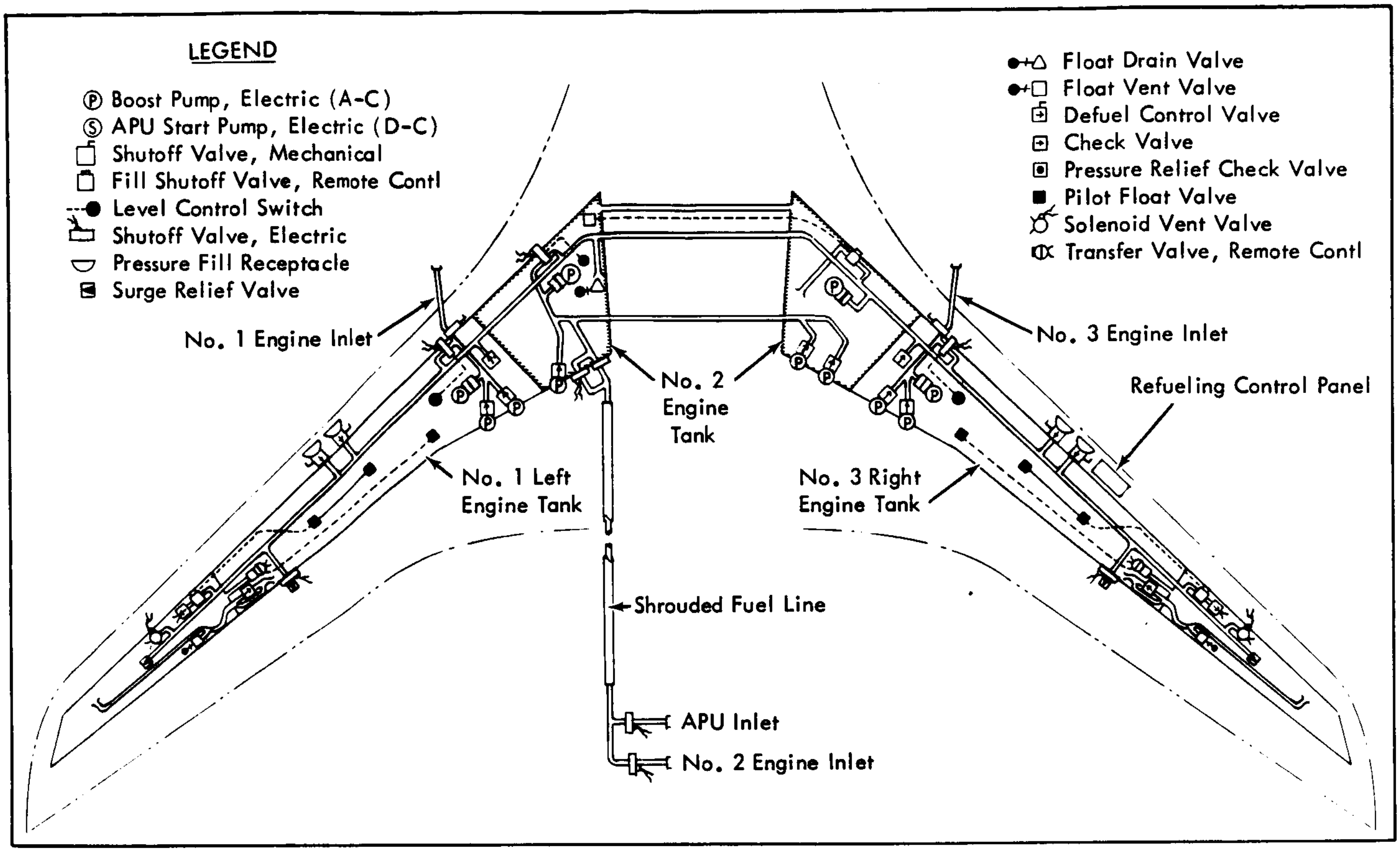

Figure 11.2-1 Fuel System Schematic

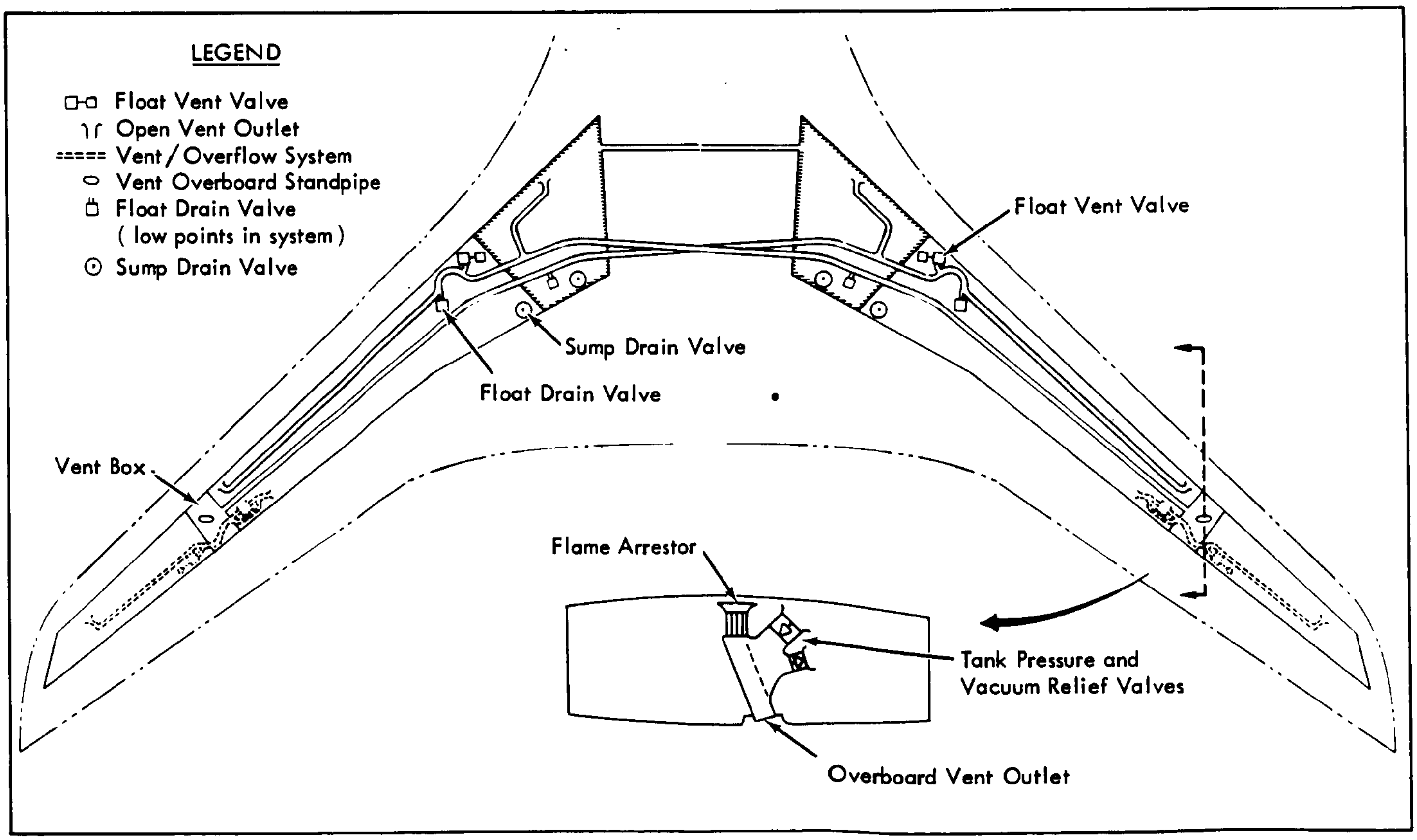

Figure 11.2-2 Vent Tank Schematic

Fuel is pumped from the tanks to each engine through separate lines. Fuel for the APU is taken from the No. 2 engine feed line. The fuel lines are aluminum alloy tubing within the tanks. Stainless steel tubing completely shrouded with vented and drainable tubing is used in all places where the feed lines pass through the pressurized area of the fuselage. Stainless-steel tubing or fire resistant hose is used elsewhere.

Multiple booster pumps are installed for redundancy. However, in the case of complete failure of the booster pumps, the engines will operate satisfactorily and maintain sustained flight on suction feed. Each pump is operated from a separate electric circuit so that the failure of one circuit will not affect another pump.

The airplane is normally fueled through two adjacent international standard pressure receptacles in the right wing. Two additional, identical receptacles are provided on the left wing to permit simultaneous filling of both sides of the airplane when desirable. A fueling control panel is located adjacent to the two refueling receptacles. The panel includes controls for automatic cut-off at preselected partial loads.

Defueling is accomplished by manually opening the fueling adaptor check valve. Defueling by suction at the fill adaptor removes up to 75 percent of the fuel at a rate of about 200 gallons per minute (756 liters/minute). With the cross feed valves open the tank booster pump will completely remove the fuel at a rate of about 650 gallons per minute (2460 liters/minute).

11.3 AUXILIARY POWER UNIT

11.3.1 General Description

An onboard auxiliary power unit (APU) is installed on the ATT as standard equipment. The unit is located in the aft fuselage section, where it is conveniently accessible. The primary function of the APU is to furnish power for the aircraft systems on the ground. The unit is also capable of continuous operation in flight to provide an auxiliary source of electrical power. A 90-kVA alternator identical to those on the main engine is driven by the APU. The hydraulic system can also be operated by the APU through an electrically driven hydraulic pump.

11.3.2 Installation Description

The APU is fundamentally another engine; so essentially the same design criteria are applied to its installation as to the installations of the main engines.

The APU compartment is ventilated and drained to prevent an accumulation of fluids. Air for operation of the unit is delivered through a sound-attenuated fireproof duct. A blower, mounted on the APU gear box, provides cooling air for the APU accessories, the APU oil cooler, and compartment ventilation. Air is delivered to the blower inlet by a short duct completely independent from the APU charge air. The duct is of fireproof material, and a check valve positively separates the APU compartment and the aft-fuselage cavity.

The APU exhaust system consists of a dual duct of fireproof materials. The outer shroud is titanium and separates the inner duct from the fuselage cavity. The inner duct is steel.

11.4 HYDRAULIC SYSTEM

The ATT is equipped with three separate, parallel, closed-circuit hydraulic systems, each supplied from two pumps located on the main engine accessory gear box. All of the systems are continuously operated, and each one supplies power to all of the primary flight control functions and the wheel brakes.

Hydraulic fluid at 3000 psi (2.06×10^6 N/m^2) is supplied through an all-metal piping system designed for essentially infinite service durability. Flexible-metal pipes, which in reality are low-stress hollow springs, replace hose fittings at the actuators. Steel or titanium is used for all lines within fire zones, and aluminum alloy tubing is utilized outside the fire zones.

The hydraulic circuit is designed so that a fuel-oil heat exchanger is not required. This is accomplished through the use of finned tubing, selection of reservoir location, and care in pipe routing to avoid areas of excessive heat.

11.5 ELECTRICAL POWER SYSTEM

The primary electrical power system is a three-generator system providing 115/200-V, 400-Hz alternating current. A fourth generator is provided on the APU which can replace any one of the three primary generators. A 28-V dc is derived from the ac system through transformer-rectifiers. All four generators are identical 90-kVA, three phase, brushless generators of the current state-of-the-art. Space on the engine-mounted accessories case is provided for 120-kVA generators.

The main-engine-mounted generators are driven through hydro-mechanical type constant speed drives of current design. These drives have proven to be highly reliable.

Emergency power is provided through a battery system for short-term electrical requirements and by an air-driven generator (ADG) for long-duration requirements.

The battery is kept in a fully charged condition by means of a battery charger from the ac system. The charger is capable of replacing a charge at the same rate that it is discharged to eliminate flight delays for battery charging.

Operation of the ADG deploy handle places the ADG in the air stream. When deployed it automatically comes up to speed and supplies 400 Hz ac power at 115/200-V.

SECTION 12

DESIGN CRITERIA

Design criteria are divided into two categories: (1) recommended changes to FAR Part 25 so that it adequately applies to a transport aircraft incorporating advanced technologies, and (2) specific structural design loads criteria used for the evaluation of selected aircraft.

12.1 FAR PART 25 STRUCTURAL DESIGN CRITERIA MODIFICATIONS RECOMMENDATIONS

Subpart C - Structure, and Subpart D - Design and Construction of FAR Part 25 have been examined with respect to their applicability and adequacy for application to advanced transport aircraft. The treatment of one aspect of the proposed modifications, the detailed structural design criteria unique to a composite-materials airframe, may appear too abbreviated. The rationale employed is that FAR Part 25 should provide the broad coverage on the use of composite materials, and to the same general depth, as it provided on metals usage. It remains for the detailed composites design criteria and practice to be assembled in a supplementary bulletin, as described in Volume II, for use by all concerned parties.

The recommended changes to FAR Part 25 are presented below in the following format: (1) the specific FAR Part 25 paragraph that is proposed for modification is identified, (2) the modification rationale is discussed, and (3) the paragraph modification is presented. This is the same format used in the Tentative Airworthiness Standards for Supersonic Transports (TASST), dated November 1, 1965. In fact, in the majority of instances, the modification material seen as applicable to the advanced transport is an editorialized version of the TASST.

12.1.1 FAR Part 25, Subpart C - Structure

12.1.1.1 <u>General</u>

<u>FAR 25.301 Loads</u>

<u>Discussion</u>

The advanced transport will operate at near-sonic speeds and, therefore, operate under a wider range of airplane stability than lower-speed transports. Since loads can be critically affected by stability and transonic speed, the design standards should highlight these areas and cover them specifically. In addition, since safety is dependent on the reliable operation of automatic devices, such as stability augmentation devices and automatic flight control systems, the effects of probable malfunctions need to be considered in the development of airplane design loads.

Recommended Standard

Add the following paragraphs to FAR 25.301:

(d) For advanced transport airplanes the stability of the airplane appropriate to each particular flight condition must be considered for all loading conditions. Conditions which are normal and reasonable deviations therefrom, within the prescribed design flight envelope, must be considered in the mission analysis which determines the appropriate airplane stability parameters.

(e) For advanced transport aircraft the loads must be determined within the design flight envelope, considering the effects of stability augmentation and automatic flight control systems, including probable failures and changes in systems characteristics which can be expected in service. All malfunctions and failures of these systems must be considered under FAR 25.671 and FAR 25.1309 within the normal flight envelope except those shown to be extremely improbable.

FAR 25.305 Strength and Deformation

Discussion

Power spectral gust design criteria have been under discussion between the FAA and industry for the past several years. In Amendment 25-23, the FAA adopted a requirement covering the assessment of the dynamic response of the airplane to continuous turbulence. During discussions with industry in June 1970, the AIA proposed criteria for compliance with the newly adopted rule under Amendment 15-23. The FAA believes that these criteria should be proposed as part of the rules rather than as an acceptable means of compliance and that the criteria should be modified to reflect at least the existing gust strength levels of presently certificated aircraft. Discussions that took place with industry were on the basis of a generally applicable requirement for all transport-type aircraft.

Recommended Standard

Amend 25.305 by adding a new paragraph (e) which states the following:

> 25.305(e) In complying with the provisions of paragraph (d), the continuous gust design criteria of Appendix G must be used in lieu of more rational analysis.

APPENDIX G

CONTINUOUS GUST DESIGN CRITERIA

The following gust loads requirements apply to mission analysis or design envelope analysis:

(a) The limit gust loads utilizing the continuous turbulence concept must be determined in accordance with the provisions of either Paragraph (b) or Paragraphs (c) and (d) below. For structural components stressed by both vertical and lateral components of turbulence, the resultant combined stress must be considered. The combined stress may be determined on the assumption that vertical and lateral components are uncorrelated.

(b) Design envelope analysis. The limit loads must be determined in accordance with the following:

(1) All critical altitudes, weights, and weight distributions, as specified in FAR 25.321(b), and all critical speeds within the ranges indicated in Paragraph (b)(3) below, must be considered.

(2) Values of $\bar{A}$ (ratio of root-mean-square incremental load to root-mean-square gust velocity) must be determined by dynamic analysis. The power-spectral density of the atmospheric turbulence must be as given by the equation,

$$\phi(\Omega) = \frac{\sigma^2 L}{\pi} \frac{1 + \frac{8}{3}(1.339\, L\Omega)^2}{\left[1 + (1.339\, L\Omega)^2\right]^{11/6}}$$

where

ϕ = power-spectral density, (ft/sec)^2/rad/ft (m/sec)^2/rad/m

σ = root-mean-square gust velocity, ft/sec (m/s)

Ω = reduced frequency, rad/ft (rad/m)

L = 2500 ft (762 m)

(3) The limit loads must be obtained by multiplying the $\bar{A}$ values given by the dynamic analysis by the following values of U_σ :

(i) At speed V_C: U_σ = 85 ft/sec (25.91 m/sec) true velocity on the interval 0 to 30,000 ft (9144 m) altitude and is linearly decreased to 30 ft/sec (9.14 m/sec) true at 80,000 ft (24,384 m) altitude.

(ii) At a speed V_B: U_σ is given by 1.32 times the values obtained under subparagraph (i) above.

(iii) At speed V_D: as given by 1/2 the values obtained under subparagraph (i) above.

(iv) At speeds between V_B and V_C, and between V_C and V_D: as given by linear interpolation.

(4) When a stability augmentation system is included in the analysis, the effect of system nonlinearities on loads at the limit load level must be realistically or conservatively accounted for.

(c) Mission Analysis. Limit loads must be determined in accordance with the following:

(1) The expected utilization of the airplane must be represented by one or more flight profiles in which the load distribution and the variation with time and speed, altitude, gross weight, and center-of-gravity position are defined. These profiles must be divided into mission segments, or blocks, for analysis, and average or effective values of the pertinent parameters defined for each segment.

(2) For each of the mission segments defined under Paragraph (c)(1), values of $\bar{A}$ and N_o must be determined by dynamic analysis. $\bar{A}$ is defined as the ratio of root-mean-square incremental load to root-mean-square gust velocity and N_o as the radius of gyration of the load power-spectral-density function about zero frequency. The power-spectral density of the atmospheric turbulence must be given by the equation in paragraph (b)(2).

(3) For each of the load and stress quantities selected, the frequency of exceedance must be determined as a function of load level by means of the equation

$$N(y) = \Sigma t N_o \left[P_1 \exp\left(-\frac{y-y_{1g}}{b_1\bar{A}}\right) + P_2 \exp\left(-\frac{y-y_{1g}}{b_2\bar{A}}\right) \right]$$

where

y = net value of the load or stress

y_{1g} = value of the load or stress in 1 g level flight

$N(y)$ = average number of exceedance of the indicated value of the load or stress in unit time

Σ = symbol denoting summation over all mission segments

$N_0, \bar{A}$ = parameters determined by dynamic analysis as defined in Paragraph (c)(2)

P_1, P_2, b_1, b_2 = parameters defining the probability distributions of root-mean-square gust velocity, to be read from Figures 1 and 2.

The limit gust loads must be read from frequency of exceedance curves at a frequency of exceedance of $2x10^{-5}$ exceedances per hour. Both positive and negative load directions must be considered in determination of the limit loads.

(4) If a stability augmentation system is utilized to reduce the gust loads, consideration must be given to the fraction of flight time that the system may be inoperative. The flight profiles of Paragraph (c)(1) must include flight with the system inoperative for this fraction of the flight time. When a stability augmentation system is included in the analysis, the effect of system non-linearities on loads at the limit load level must be realistically or conservatively accounted for.

(d) Supplementary design envelope analysis. In addition to the limit and fail-safe loads defined by Paragraph (c) above, limit and fail-safe loads must also be determined in accordance with Paragraph (b) above, modified as follows:

(1) In Paragraph (b)(3)(i), the value of U_σ = 85 ft/sec (25.91 m/sec) true is replaced by U_σ = 60 ft/sec (18.29 m/sec) true on the interval 0 to 30,000 ft (9144 m) altitude, and is linearly decreased to 25 ft/sec (7.62 m/sec) true at 80,000 ft (24,384 m) altitude.

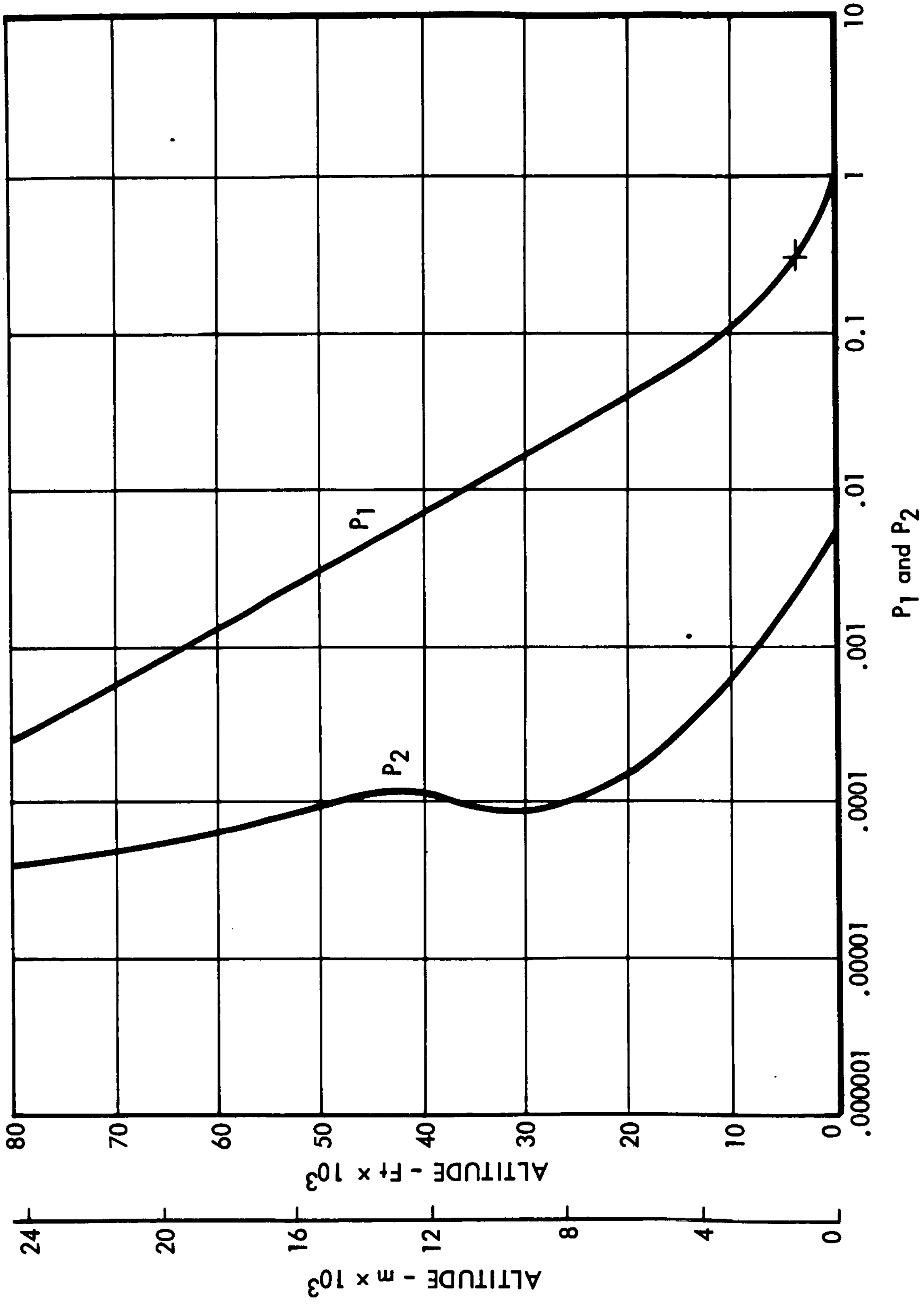

Figure 1 P_1 AND P_2 VALUES (FAA-ADS-53)

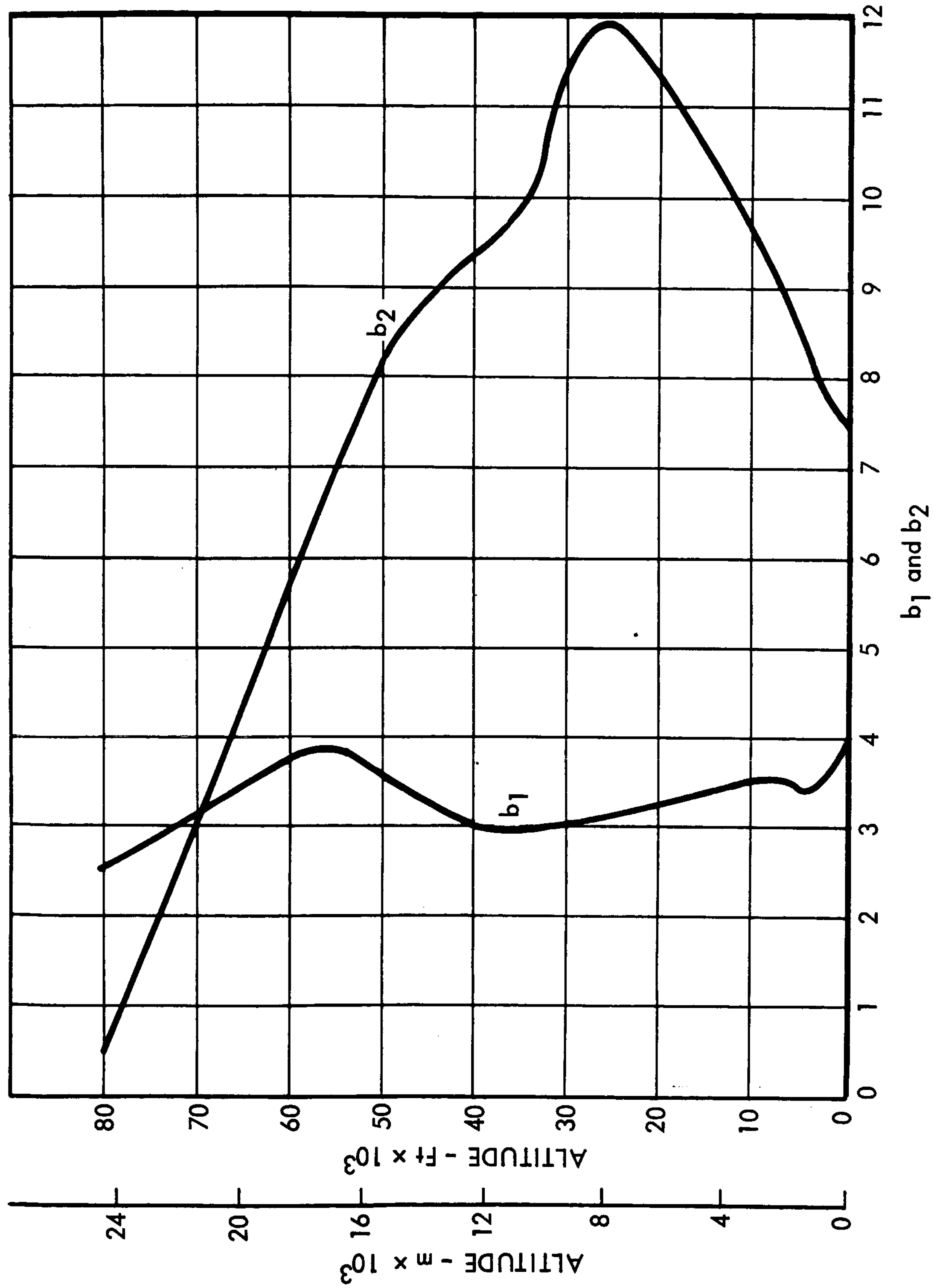

Figure 2 b_1 AND b_2 VALUES (FAA-ADS-53)

(2) In paragraph (b), the reference to Paragraph (b)(3)(i) through (b)(3)(iii) is to be understood as referring to the paragraph as modified by Paragraph (d)(1) above.

(e) Response to turbulence at pilot's station. Vertical and lateral acceleration environment at the pilot's station must be established for response to continuous turbulence at intensity levels encountered in normal operations (ref. 25.255). Adequacy for levels of turbulence encountered in normal operations shown by analysis may be established on the basis of comparison with airplanes which have acceptable service experience.

12.1.1.2 Flight Maneuver and Gust Conditions

FAR 25.331(a) Procedure

Discussion

Service experience on a number of jet-transport-category airplanes indicates that maneuvers within the design envelope, while in out-of-trim configurations, occur sufficiently often to warrant investigation of the airplane's maneuver stability and control characteristics in out-of-trim configurations. During flight tests and normal service, airplanes are maneuvered while the airplane is out-of-trim and the proposed amendment to 25.331(a)(4) would require the airplane to be designed structurally for the loads that result from maneuvers while in the out-of-trim configurations that may occur during the mistrim conditions specified in 25.144. The proposal reflects the reasoning used in the development of the special condition applied to several subsonic transport aircraft.

Recommended Standard

Add the following new sentence at the end of FAR 25.331(a)(4):

(4) .... "Maneuvers must consider the airplane in trimmed flight and for out-of-trim configurations which may occur during the mistrim conditions specified in 25.144."

FAR 25.335(b) Design Dive Speed, V_D

Discussion

The advanced transport design will be optimized for cruise at near sonic speed. This will entail use of advanced aerodynamic configurations, control systems, and engines. Response of the airplane to upset and atmospheric variations must be characterized by performance and stability investigations prior to establishing minimum margins between V_C/M_C and V_D/M_D on a rational basis. The Tentative Airworthiness Standards for Supersonic Transports recommends that the minimum margin of .05M be increased for speeds greater than .95 Mach number. It is therefore recommended that 25.335(b)(2) be modified as shown below until such time that investigations can be accomplished to establish the rationale for setting the minimum margin.

Recommended Standard

Change the sentence in FAR 25.335(b)(2) to the following: "However, the spread must not be less than 0.1 delta Mach number."

FAR 25.335(c) Design Maneuvering Speed, V_A, and FAR 25.335(d) Design Speed for Maximum Gust Intensity, V_B

Discussion

Providing minimum criteria for aircraft that do not have a definable stall is difficult. In some cases, wind tunnel data for advanced transport configurations exhibit lift variations at high angles of attack that characterize a non-definable stall. Therefore, the reference stall speeds that have been used in the past for determination of structural design criteria, may be inappropriate for advanced transport design. The Tentative Airworthiness Standards for Supersonic Transports presents an approach for establishing a "minimum operational speed" for configurations not having a definable stall. It is therefore proposed that a similar approach be taken to establish V_A and V_B for the advanced transport whenever definable stall is not exhibited. Where the left side of the V-n envelope is angle-of-attack limited rather than stall limited, suitable indication to the pilot should be provided.

Recommended Standard

Add a new subparagraph (iii) to FAR 25.335(c)(1):

(iii) For advanced transport configurations not having positive indications of stall, in lieu of the definition of V_S in subparagraph (ii), V_{S1} is defined as the minimum speed with flaps retracted as specified in those portions of FAR 25.201 which are applicable to advanced aircraft.

Add a new subparagraph (iii) to FAR 25.335(d)(1):

(iii) For advanced transport configurations not having positive indications of stall, in lieu of the definition of V_{S1} in subparagraph (ii), V_{S1} is defined as the minimum speed with flaps retracted at a particular weight under consideration as defined in those portions of FAR 25.201 which are applicable to advanced aircraft.

FAR 25.341 Gust Loads, and
FAR 25.351 Yawing Conditions

Discussion

The combination of a static-gust-load-formula approach with the dynamic continuous turbulence methods, which will be required under the item covering FAR 25.305, will yield a level of safety essential for successful advanced transport design.

Recommended Standard

At the end of FAR 25.341(c) add the phrase "(see FAR 25.305(d))."

At the end of FAR 25.351(b) add the phrase "(see FAR 25.305(d))."

FAR 25.349 Rolling Conditions

Discussion

Experience in the design of military aircraft, including bomber types, shows that it is possible to get peak roll acceleration during the recovery from rolling maneuvers, where, for a brief time, rolling moment due to roll rate (i.e., roll damping) is additive with that due to roll command for recovery. This condition can result in critical design loads for nacelle/engine installations located outboard under the wing. The Tentative Airworthiness Standards for Supersonic Transports provides criteria based on a rolling pullout-type maneuver. It is recommended that these criteria be included for design of advanced transport configurations.

Recommended Standard

Add the following to FAR 25.349(a):

(5) For advanced transport configurations, in lieu of subparagraphs (2), (3) and (4) of this paragraph, at speeds up to V_D/M_D, the cockpit lateral control is displaced to the maximum attainable by two equal-and-opposite 50-lb (222.41 N) forces applied at the rim of the control wheel. The rate of control force application and the surface deflection and rate need not be greater than permitted by the pilot and control system characteristics. For rolls with g-positive entry, the airplane will be assumed to be initially in a steady constant-altitude turn at a bank angle corresponding to a load factor of 2/3 n. The airplane will roll out of the turn and be assumed to be checked so as to limit the bank angle to a value equal and opposite to the initial angle. For rolls with zero-g entry, the initial attitude shall be wings level at zero-g entry, and action to check the roll will be assumed to occur at an angle of bank appropriate to the airplane-pilot response characteristics.

12.1.1.3 Ground Loads

FAR 25.491 Ground Loads, and
FAR 25.492 Response to Runway Roughness at Pilot's Station

Discussion

The FAA has recently required assessment of dynamic loads associated with runway roughness for large transport aircraft. A new rule is proposed, where previously these loads were handled by interpretation of the current rule. These loads are critical in parts of the structure and should be accounted for.

Recommended Standard

Revise FAR 25.491 to read as follows:

FAR 25.491 Taxi, Takeoff, and Landing Runs

An assessment of the dynamic taxi loads is required for the roughest runway-taxiway profiles to be encountered in operation using the most critical airplane configuration. Arbitrary, discrete, deterministic, and/or statistical methods may be used to accommodate both the discrete and random aspects of the profiles. Both symmetric and anti-symmetric responses will be considered.

Add new FAR 25.492 as follows:

FAR 25.492 Response to Runway Roughness at Pilot's Stations

The vertical and lateral acceleration response at the pilots' stations must be determined for runway-taxiway profiles expected in normal operations. The acceleration response must be such as to permit the pilots to read instruments, control the airplane, and perform other functions necessary for safe operations on the ground. Compliance may be demonstrated by comparing the response with that of airplanes which have had satisfactory service experience.

12.1.1.4 Fatigue Evaluation

FAR 25.571 Fatigue Evaluation of Flight Structure,
FAR 25.573 Fatigue Evaluation of Landing Gear, and
FAR 25.577 (New) Advanced (Near-Sonic) Transport Airplane Fatigue

Discussion

The Tentative Airworthiness Standards for Supersonic Transports, covering fatigue evaluations for supersonic aircraft, embodies criteria, including fail-safe residual strength requirements, which are also suited to structural reliability concepts for advanced near-sonic transports. Therefore, portions of the TASST discussion, modified slightly to delete reference to supersonic aircraft/operations, and the tentative standard are presented in the following paragraphs as discussion material and a proposed standard for advanced transport fatigue evaluations.

The exposure of the advanced near-sonic transport to a unique loading environment, new materials, new fabrication techniques, and new configurations will require consideration of these factors in evaluating the fatigue aspects of the advanced transport design.

The present fatigue requirements, FAR 25.571, provide for either a fail-safe or safe-life approach in establishing the fatigue strength of the flight structure. The fail-safe approach for the flight structure has been used in the design of the present jet transport fleet. This design concept in conjunction with inspection procedures has proven effective. The objective of the proposed advanced transport fatigue strength standards is to obtain the highest practicable level of safety compatible with current technology. It is believed that this objective can be achieved by the following:

1. Require that the primary structure be capable of supporting the expected repeated loads and design limit loads after fatigue failure or partial failure. The present fatigue requirements, FAR 25.571, do not specifically provide that the structure must support repeated loads after partial failure. The structure is, in fact, exposed to repeated loads after each partial failure until the failure is detected. Therefore, it is believed that the structure should be required to support such loads in lieu of assuming that residual static strength requirements will provide the needed strength. Also, it is believed the structure should remain capable of supporting limit loads after partial failure since they are the maximum loads expected in service and may be imposed, especially if the period between inspections is long or if the partial failure occurs in severe turbulence. Under the proposed standards, the fail-safe evaluation would involve a determination of

probable failure areas by fatigue tests except where analysis is considered reliable. The residual fatigue and required static strength would then be demonstrated with obvious partial failures in the probable failure areas and in other critical areas. The residual fatigue strength would have to be sufficient to provide assurance that the partial failure would be discovered during the inspection program. An obvious partial failure would usually consist of complete failure of one element but may involve partial failure of an element or complete failure of several elements, depending on the nature and location of the failure and the type of inspection contemplated, but in any case it must be obvious during the planned inspection. While the proposed standard does not include a dynamic magnification factor on fail-safe loads, it would require that the design limit be supported under realistic partial-failure conditions.

2. Provide that the landing gear be either a safe-life or fail-safe type of structure on the basis of practical considerations and that the gears are readily inspectable. Other requirements provide that the airplane must be capable of a wheels-up landing.

The flight structure loading conditions for fail-safe strength set forth in FAR 25.571(c) do not include such conditions as lateral gusts, maneuvers at V_A and V_D, rolling maneuvers, unsymmetrical gusts, negative maneuvers, gusts and maneuvers with zero wing fuel, dynamic yaw due to critical engine failure, engine torque and side loads, nor the more rational loading conditions for continuous turbulence and runway roughness specified in Sections 25.305 and 25.491. Further, the flap loading condition coverage is not specific. FAA Report FAA-ADS-53 indicates that lateral gusts exceed design limit strength more frequently than vertical gusts. A review of NASA jet VGH data and incident reports indicates that maneuvers at high and low speeds are as likely as at V_C. A review of the remaining conditions does not indicate that the proposed conditions are unreasonable nor sufficiently remote to eliminate. It should be noted that supplementary engine and control surface loads are largely covered by airplane loading conditions.

Landing and takeoff loading may be critical for portions of the structure, especially the fuselage. While failure under flight loading conditions is obviously catastrophic, failure during these high-speed ground conditions could also be catastrophic.

In view of the foregoing and because conditions other than those specified in 25.571(c) may be critical on an advanced aircraft, it is believed that the fail-safe static loading conditions should cover the proposed conditions.

It is the intent of the proposed standard to require substantiation of the fail-safe residual static strength for only the critical loading conditions, and the word "critical" has been inserted to emphasize this aspect.

Industry has contended that the residual static strength level specified in FAR 25 (80 percent limit load) is adequate. The FAA has made a study of the likelihood of fail-safe damage and fail-safe load (both 100 percent and 80 percent of design limit) occurring prior to detection by inspection. Copies of the study were provided at the October 8-10, 1968 FAA/Industry meeting. The results of this study indicate that both a fail-safe load level of limit load and a rigorous inspection program are needed. AIA contends that, based on the latest VGH jet data, the gust frequency data used in the FAA study is overly conservative. However, when maneuvers are added to the gust data, the total load factor exceedance curve corresponds to that used in the study. Further service experience indicates that structural failures are more prevalent under severe loading conditions in which frequent high loads could be expected. Consequently, it is believed that the study results are reasonable and that a residual static strength level of 100 percent limit load is necessary to assure the desired safety objective.

Recommended Standard

Add a new FAR 25.577 Advanced (Near-Sonic) Transport Airplane Fatigue

For advanced near-sonic transport airplanes the following standards apply in lieu of FAR 25.571 and FAR 25.573:

(a) Fatigue and Fail-Safe Characteristics. The strength and design of the primary structure must be adequate to insure that the catastrophic failure in the service environment under the expected repeated loads is extremely improbable.

(b) Fatigue Evaluation Procedures. It must be shown by analysis and repeated and static load tests that the primary structure, in conjunction with the inspection program established in accordance with 25.1529(h), meets the provisions of paragraph (a). The probable-failure locations must be determined by analysis, tests, or both. The loading spectra used in analysis and tests must be representative of critical types of operations. The effects of maneuvers, ground-air-ground cycles, gusts, landing and taxiing, and pressure cycles must be included in the spectra, if significant. All primary structure must be evaluated to show compliance with paragraph (a) in accordance with (1) below except as specified in (2) below.

(1) It must be shown that adequate residual strength is provided to assure that any partial failure will be detected before a hazardous condition develops. This involves showing that the structure remains capable of supporting the expected repeated loading spectrum and critical design limit loads for the following conditions without catastrophic results during the period after any fatigue failure or partial failure has progressed to obvious proportions and prior to detection by inspection:

(i) Maneuvering conditions of 25.331(b) and 25.331(c)(2).

(ii) Load factor conditions of 25.337.

(iii) Gust loads of 25.341 and 25.305(e).

(iv) High-lift-device loads of 25.345.

(v) Rolling conditions of 25.349.

(vi) Yawing conditions of 25.351.

(vii) Pressurized-cabin loads of 25.365.

(viii) Unsymmetrical loads due to engine failure of 25.367.

(ix) Speed-control-device loads of 25.373.

(x) Unsymmetrical loads of 25.427.

(xi) Special-devices loads of 25.459.

(xii) Landing conditions of 25.473.

(xiii) Takeoff run loads of 25.491.

(xiv) Braked roll loads of 25.493.

(xv) Any probable loading condition found to be appropriate to the configuration.

(2) The landing gear and attaching structures and other areas of the less critical primary structure, where it is shown that extreme design penalties would result, need not comply with subparagraph (1). This structure may be evaluated by showing that it is capable of supporting the expected repeated loading spectrum without failure.

12.1.2 FAR Part 25, Subpart D - Design and Construction

12.1.2.1 General

FAR 25.603 Materials and
FAR 25.605 Fabrication Methods

Discussion

The advanced transports will be affected by the longtime exposure to corrosive elements and errosive effects of rain. The structural materials used should be investigated for those environmental factors which affect the material characteristics.

Recommended Standard

Add the following to FAR 25.603:

(c) Be established to show that they maintain throughout their service life their design strength considering deterioration as a result of longtime exposure to the operating environment.

Add a new paragraph, FAR 25.605:

For airplanes using new fabrication methods and materials which are to be exposed to new critical environmental conditions for which adequate experience is not available, a fabrication test program is required to substantiate the fabrication methods to be used.

FAR 25.609 Protection of Structure

Discussion

Encounter with hail at high speeds is considered to be a hazard to safe flight of high-performance aircraft. In order that adequate levels of safety are assured, the strength and detail design of affected areas should be designed for hail and rain encounter. An objective requirement is considered appropriate.

Very limited test information is currently available. However, initial approaches have been proposed, and guidance to acceptable substantiation programs can be formulated.

A suggested approach in this country is to test affected structure for a nominal (1-in. (2.54 cm) diameter) size of hail to show no appreciable indentation and to substantiate that larger sizes (2-in. (5.08 cm) diameter) will produce no appreciable damage. With this approach, it is believed that the question of capability of the structure for encounter with relatively rare large hail or encounter at the relatively high speeds associated with cruise operations should be assessed by showing that limit tests result in adequate ultimate capability. Qualitative data have been presented by pilot groups to indicate that large-size-hail encounter is sufficiently probable to warrant assessment during design.

As test data become available, more specific test procedures should be developed.

Recommended Standard

Add the following to FAR 25.609(a):

(4) Rain erosion

Add a new paragraph to FAR 25.609 as follows:

(c) For advanced transport aircraft, the strength, detail design, and fabrication of fuselage, nose, and leading-edge structure, windshields, and radomes shall prevent extreme hazards to the airplane from hail encounter. For all speeds up to those associated with M_C at 40,000 ft (12,192 m), hail-impingement tests on representative structure should be made (1) to show that 1-in. (2.54 cm) diameter hail will result in no appreciable indentation, (2) to show that 2-in. (5.08 cm) diameter hail will produce no appreciable damage. Sufficient tests involving variations of hail size and speed of impact must be conducted to assure that (1) encounter of large-size hail, and (2) encounter of hail at higher speeds will not result in catastrophic structural failure.

FAR 25.629 Flutter, Deformation and Fail-Safe Criteria

Discussion

The current standards are not sufficiently objective and comprehensive to cover modern complex transports. The proposed standard reflects the objectives of the system failure criteria set forth in FAR 25.671, 25.672, and 25.1309, which were adopted under Amendment 25-23. In addition, failure criteria are proposed for flutter dampers consistent with the control system failure modes of 25.671.

Recommended Standard

Make the following changes:

1. In paragraph (d)(1), add the phrase "each of the following" after the last word of the paragraph.

2. In subparagraph (d)(1)(i), eliminate the semicolon and the word "and" at the end of the paragraph.

3. Change subparagraph (d)(1)(ii) to read as follows:

   (ii) Any other combination of failures not shown to be extremely improbable.

4. Substitute the following for subparagraphs (d)(4)(v) and (d)(4)(vi):

   (v) Failure of each principal structural element selected for compliance with 25.571(c). Safety following a failure may be substantiated by showing that losses in rigidity or changes in frequency, modal form, or damping are within the general parameter variations shown to be satisfactory in the flutter and divergence investigations.

   (vi) Any single or combination of failures, malfunctions, or disconnections in the flight control system considered under the requirements of 25.671, 25.672, and 25.1309 and any single failure in any flutter damper system and combinations of failures except those shown to be extremely improbable. Investigation of forced structural vibration, other than flutter, resulting from failures, malfunctions, or adverse conditions in the automatic flight control system may be limited to airspeeds up to V_C.

12.2 STRUCTURAL DESIGN CRITERIA

The definitions and general criteria used are consistent with FAR Part 25 but are much simplified in keeping with the preliminary design nature of the study. A summary follows.

A. Design Gross Weights

   1. Maximum Flight Gross Weight = Maximum Ramp Gross Weight

   2. Maximum Taxi and Ground Handling Gross Weight = Maximum Ramp Gross Weight

3. Minimum Flight Weight = Zero Fuel Gross Weight

4. Maximum Landing Gross Weight =

    a. 84 percent of Maximum Ramp Gross Weight for a 10-ft/sec (3.048 m/sec) descent rate.

    b. Maximum Ramp Gross Weight for a 6-ft/sec (1.829 m/sec) descent rate.

5. Calculate loads for the most critical weight distribution of either

    a. Design Passenger Payload, or

    b. Weight Limited Payload = 1.5 x Design Passenger Payload.

B. Design Speeds

The Mach-Altitude speed envelopes used as parameter boundaries in structural load calculations are shown in Figure 12.2-1. They are specifically applicable to the .98 M_C configuration. The $(V_D/M_D)-(V_C/M_C)$ speed increment is consistent with the recommended change to FAR 25.335(b) given in Subsection 12.1.1.2.

Stall Speed vs Wing Loading is defined in Figure 12.2-2 for flap deflection of zero, 20 degrees (.35 rad), and 50 degrees (.87 rad). Flap design speeds per FAR Part 25, Section 25.335(e), are based on this data.

C. Load Factor

a. Takeoff and Landing Configuration = 2.0-g limit

b. Cruise Configuration = 2.5-g limit

D. Gust

Gust loads are based on the most critical of

a. U_{de} = 50 ft/sec (15.15 m/sec) for discrete gust analysis

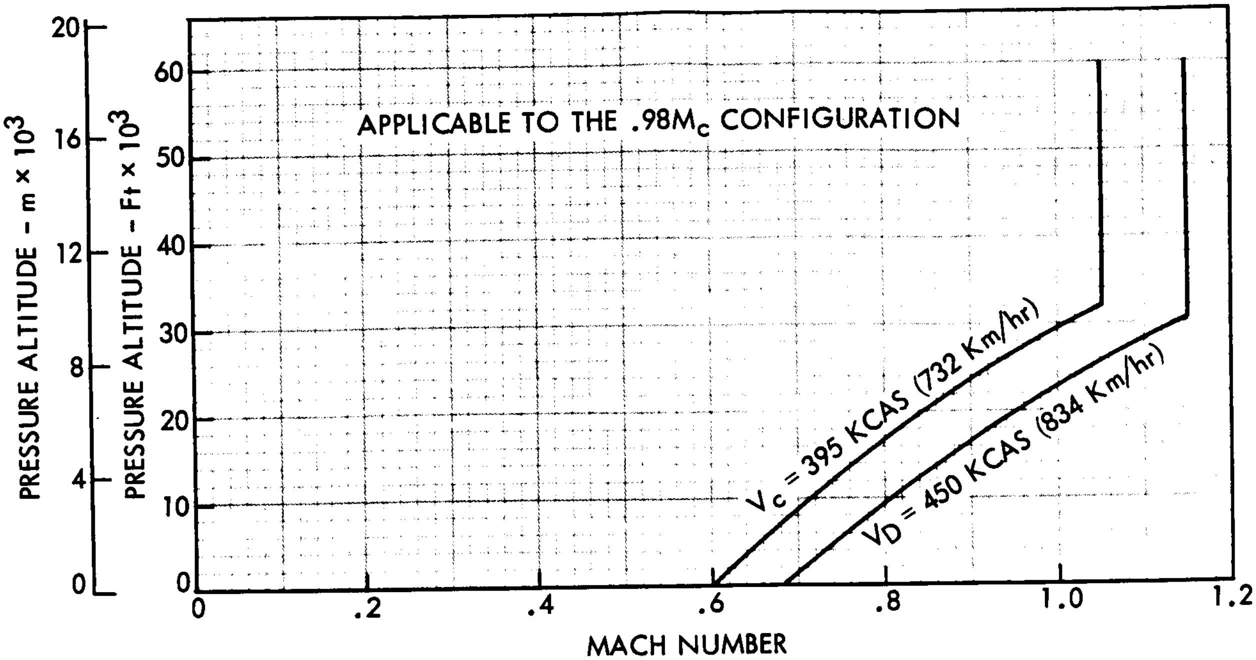

Figure 12.2-1 Structural Design Speeds

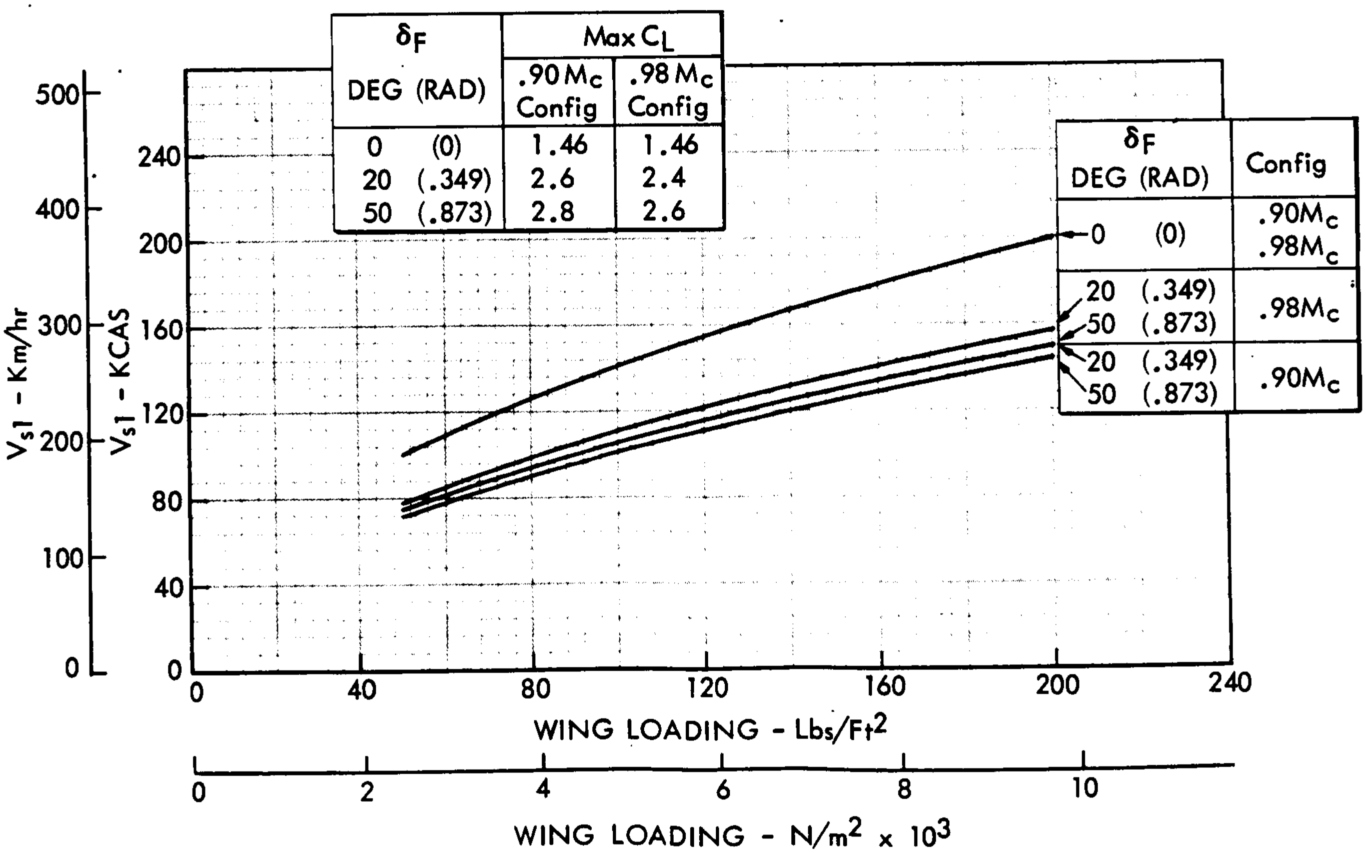

Figure 12.2-2 Preliminary Stall Speeds

b. U_σ = 85 ft/sec (25.9 m/sec) for design envelope analysis

E. Cabin Pressurization

Cabin pressure is based on the following Δp(cabin) schedule:

Altitude Range	Δp(cabin), psi (N/m^2) limit
Sea Level to 26,700 ft (8138 m)	14.7(10.135×10^4) - p(ambient)
Above 26,700 ft (8138 m)	9.64 (6.646×10^4)

where (1) Δp(cabin) = p(internal) - p(ambient)

(2) Maximum limit Δp(cabin) = 9.64 psi (6.646×10^4 N/m^2) based on maintaining the cabin at 6,000 ft (1829 m) altitude while flying at 45,000 ft (13,716 m).

F. Fail Safe

The minimum fail-safe requirement = 100 percent limit design load with an ultimate factor of safety of 1.0.

G. Fatigue

The Design Life and Usage Baseline Fatigue Criteria are presented in Figure 12.2-3. They are based on a 15-year service life with a scatter factor of 2 for fail-safe elements and 4 for non-fail-safe elements. As a result of the mid-term re-direction by NASA, only the Trans-Continental Route criteria are applicable to Phase II of the study.

The Fatigue Loads Spectra for Taxi, Climbout, Cruise, Descent, and Check Flight Operation are illustrated in Figure 12.2-4. Data were obtained from NASA documentation.

DESIGN LIFE / USAGE BASELINE

Trans-Continental Route

	FAIL-SAFE STRUCTURE	LDG GEAR & SUPPT STRUC.
• FLIGHT HOURS	120,000	
• LANDINGS	90,000	180,000
• FUSELAGE PRESSURIZATIONS	90,000	

FLIGHT LENGTH N. MI. (km)	% OF FLIGHTS
300 (556)	34
650 (1205)	47
2,000 (3706)	15
TRAINING	4
	100

Inter-Continental Route

	FAIL-SAFE STRUCTURE	LDG GEAR & SUPPT STRUC.
• FLIGHT HOURS	120,000	
• LANDINGS	40,000	80,000
• FUSELAGE PRESSURIZATIONS	40,000	

FLIGHT LENGTH N. MI. (km)	% OF FLIGHTS
750 (1390)	31
1,500 (2780)	25
2,400 (4448)	20
3,000 (5560)	14
4,000 (7413)	6
TRAINING	4
	100

LOAD SPECTRA

DATA ON	FROM	
• SYMMETRICAL MANEUVER LOAD FACTOR SPECTRA	NASA TN D-527	NASA TN D-4330
• LANDING SINK SPEED SPECTRUM	NASA TN D-899	NASA TN D-5601
• GROUND OPERATIONS LOAD FACTOR SPECTRA	NASA TN D-1392	NASA TN D-6124
• GUST LOAD FACTOR SPECTRA	NASA TN D-1483	NASA LWP-309
	NASA TN D-1801	

Figure 12.2-3 Fatigue Design Criteria

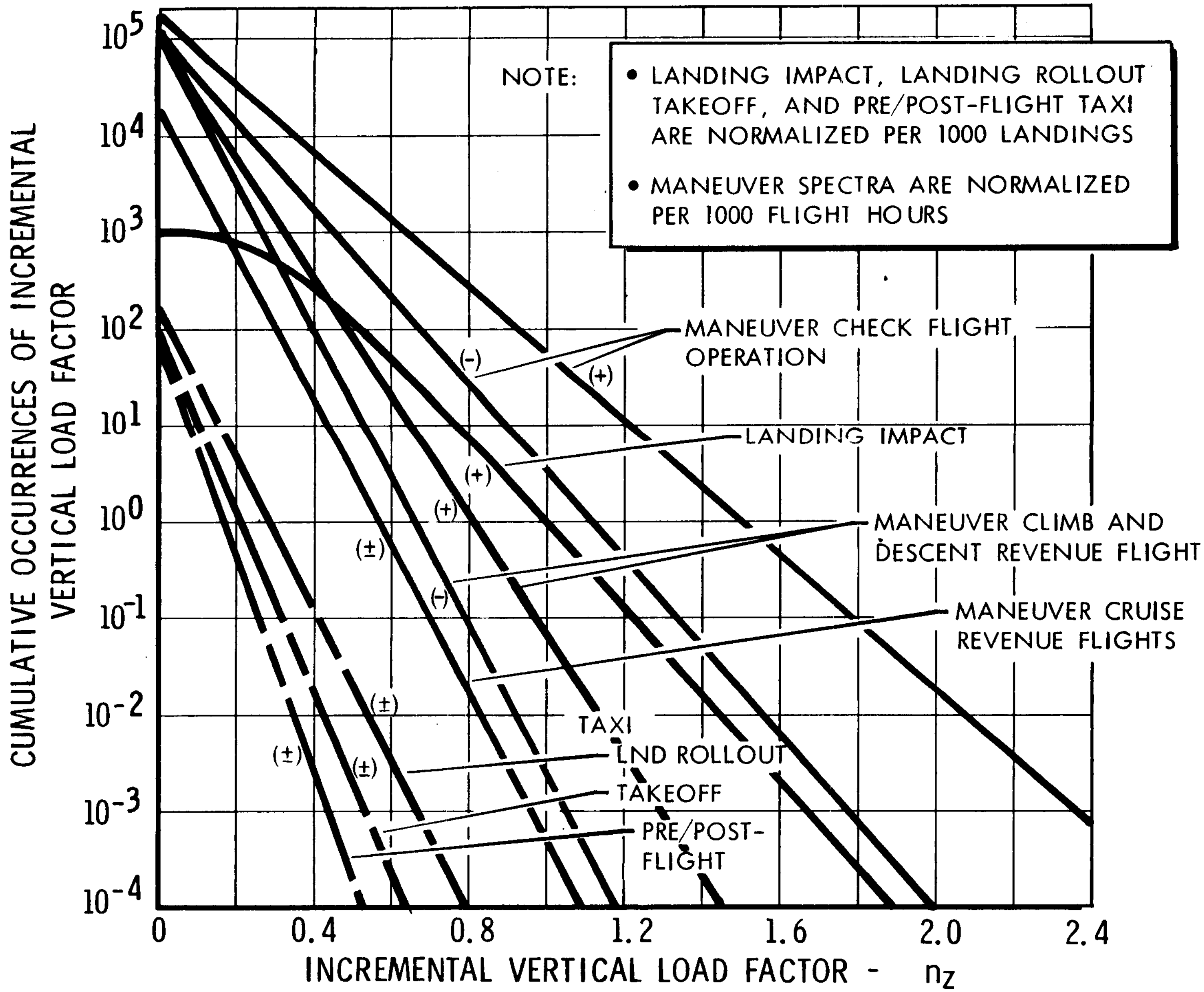

Figure 12.2-4 Fatigue Loads Spectra

H. Factors

Use approved handbook fitting factors for all structural connections.

The ultimate landing factor of safety = 1.5 times fitting factors.

SECTION 13

DESIGN LOADS ANALYSIS

Evaluation of the final transport configurations required the determination of airframe weight for many hundreds of airplane configurations. Not only did these weights need to be realistic but also did the weight differences between configurations need to be accurate so that the economic analysis would yield correct data. Although the weights calculation was necessarily a statistical-analytic process because of the large number of configurations exercised, considerable detailed structural analysis was performed that required definition of design loads. These analyses along with their purpose are summarized in Table 13.0-1.

Design loads in support of the structural analysis effort were developed through an unsophisticated methodology and engineering judgment. They were generally conservative rigid-airframe loads, compatible with the preliminary-design-type airframe definition and FAR Part 25. A description of methodology, component by component, is presented in the following subsections. Since detailed structural analyses of the final selected configuration were not performed, numerical loads values are not included.

13.1 WING

Critical design loads were determined from an examination of the following conditions:

1. Cruise Configuration Maneuver (2.5 g) at Ramp Gross Weight.

2. High-Lift Configuration Maneuver (2.0 g) at Ramp Gross Weight.

3. Cruise Configuration Gust at Ramp Gross Weight.

4. Cruise Configuration Gust at Zero Fuel Gross Weight.

Spanwise airload distributions due to angle of attack for Items 1, 2, and 4 were assumed to be elliptical. Incremental load factor was defined for gust for both tail on and tail off. The high-lift-configuration air-load distribution

Table 13.0-1

SUMMARY OF DETAILED STRUCTURAL ANALYSIS

Type	Purpose
1. Phase I Alternate Configuration Wing Optimization AR = 9.0, $\Lambda = 35^{o}$ (.61 rad)	. Detail stiffness data for flutter analysis check . Wing-box weight check with statistical-analytical method.
2. NASA HPC Wing Design	. Basic wing stiffness data for Active Control System (ACS) Study . Comparative light-alloy and composite construction member size.
3. NASA HPC Fuselage Data	. Basic fuselage stiffness data for ACS study . Comparative light-alloy and composite construction member size.
4. NASA HPC Horizontal Tail Design	. Basic stiffness data for ACS study
5. NASA HPC Vertical Tail Design	. Basic stiffness data for ACS study

was developed from NACA TN 3476 and had a center of pressure slightly outboard of the elliptical distributions.

A down-acting tail load of 0.1 nW, assumed necessary for balancing of airplane pitching moment, was also included as a contribution to the positive lift force acting on the wing (theoretical) to maintain net (balanced) overall airplane aerodynamic lift.

Wing structural and fuel inertia loads were applied in combination with the airload distributions.

13.2 FUSELAGE

For the Active Control System (ACS) study it was concluded that the 2.5-g balanced symmetric maneuver and a 1-g sideslip condition in combination with pressure produces the design fuselage loads. Gust loadings were determined to be non-critical with the ACS operative. Air loads on the fuselage itself were neglected.

Gust loads were critical for fuselage design for the airplane not employing ACS gust alleviation.

13.3 HORIZONTAL TAIL

The critical horizontal tail load condition was selected from a comparison of a 2.5-g balanced pull-up condition and an arbitrary asymmetric load at 1.0 g. A minus .1nW horizontal tail balance load and an elliptical spanwise load distribution were assumed.

13.4 VERTICAL TAIL

The vertical tail design shear load was assumed to be 0.25 times the ramp gross weight, which is slightly (about 10 percent) conservative compared with results based on the lateral gust load equation of FAR Part 25, Section 25.351. For the T-tail configuration, a uniform spanwise load distribution was assumed, to account for the horizontal tail endplate effect. In addition to the lateral load, a rolling moment due to asymmetric horizontal tail load was applied.

SECTION 14

WEIGHT ANALYSIS

Weight analysis and summaries are presented for the selected 0.90M and 0.98M configurations and the baseline (0.82M) conventional transport. Standard AN group weight coding has been utilized for component and subsystem weights, as specified in MIL-STD-254 (ASG), given in all tables, figures, and discussions in the following subsections.

14.1 WEIGHT SUMMARIES

A weight comparison summary is presented in Table 14.1-1 to identify the weight variations evolved from conventional aircraft into the 0.90M and 0.98M advanced technology aircraft. This summary reveals the individual weight effects of employing composite materials, supercritical aerodynamics, and active flight control systems. Component and subsystem breakdowns for these configurations are shown in Tables 14.1-2 through 14.1-6.

14.2 AIRFRAME

The process for obtaining structural weights for the various components of the ATT matrix of configurations was, first, to develop the weights for the conventional aircraft materials (light-alloy) and, then, to convert to composite (graphite) construction and, if required, adjust either or both for the added effects of an active control system. The procedures for calculating these weights are described in detail in the following paragraphs.

The basic aluminum (light-alloy) structural weights were calculated by a statistical-analytical procedure developed and continuously modified by Convair through research studies. The procedure in most part makes use of preliminary design aerodynamics, geometric parameters, and basic stress analyses. Because of the geometric extremes represented in some components of the advanced aircraft configurations, the stress analyses were used extensively to reinforce and refine the statistical-analytical results. In some instances, flutter and aeroelastic analyses were used to define the incremental wing weight necessary to meet the stiffness requirements. Table 14.2-1 shows, by

TABLE 14.1-1 WEIGHT SUMMARY COMPARISONS

DESCRIPTION	1 CONVENTIONAL AIRCRAFT	2 ADVANCED TECHNOLOGY AIRCRAFT	3	4	5	6	7	8	9
CRUISE MACH NUMBER	.82	.90	.90	.90	.90	.98	.98	.98	.98
MATERIALS	Aluminum	Aluminum	Aluminum	Composites	Composites	Aluminum	Aluminum	Composites	Composites
SUPERCRITICAL WING	No	Yes	Yes	Yes	Yes	Yes	Yes	Yes	Yes
AREA RULED FUSELAGE	No	No	No	No	No	Yes	Yes	Yes	Yes
ACTIVE CONTROL SYSTEM	None	None	Full	None	Full	None	Full	None	Full
WING AREA - FT.^{2} (M^2)	2,540 (236.0)	2,275 (211.3)	2,205 (104.8)	1,990 (184.9)	1,970 (183.0)	2,685 (249.4)	2,570 (238.8)	2,320 (215.5)	2,282 (212)
ENGINE SCALE	.669	.626	.6125	.565	.560	.745	.722	.669	.662
WEIGHT - LB. (KG)									
STRUCTURAL WEIGHT	94,260 (42,748)	88,510 (40,141)	81,670 (37,039)	65,820 (29,850)	62,980 (28,562)	110,200 (49,977)	99,790 (45,256)	79,120 (35,882)	75,222 (34,114)
PROPULSION SYSTEMS	19,850 (9,002)	18,326 (8,311)	17,780 (8,063)	16,255 (7,372)	15,933 (7,226)	22,330 (10,127)	21,541 (9,769)	19,345 (8,773)	19,189 (8,702)
EQUIPMENT	42,080 (19,084)	41,635 (18,882)	42,283 (19,176)	40,436 (18,565)	41,658 (18,893)	42,498 (19,273)	43,273 (19,625)	41,545 (18,841)	42,353 (19,208)
USEFUL LOAD	7,364 (3,340)	7,364 (3,340)	7,364 (3,340)	7,364 (3,340)	7,364 (3,340)	7,364 (3,340)	7,364 (3,340)	7,374 (3,340)	7,364 (3,340)
OPERATING WEIGHT	163,554 (74,174)	155,835 (70,674)	149,097 (67,618)	130,375 (59,127)	127,935 (58,021)	182,392 (82,717)	171,968 (77,990)	147,374 (66,836)	144,128 (65,364)
PAYLOAD	40,000 (18,140)	40,000 (18,140)	40,000 (18,140)	40,000 (18,140)	40,000 (18,140)	40,000 (18,140)	40,000 (18,140)	40,000 (18,140)	40,000 (18,140)
ZERO FUEL WEIGHT	203,554 (92,314)	195,835 (88,814)	189,097 (85,758)	170,375 (77,268)	167,935 (76,160)	222,392 (100,857)	211,968 (96,130)	187,374 (84,976)	184,128 (83,504)
WATER INJECTION FLUID	965 (438)	910 (413)	895 (406)	820 (372)	810 (367)	1080 (490)	1035 (469)	965 (438)	960 (435)
FUEL	100,281 (45,479)	88,995 (40,361)	86,956 (39,436)	78,749 (35,714)	78,687 (35,686)	98,728 (44,775)	95,397 (43,264)	90,061 (40,844)	88,752 (40,251)
GROSS WEIGHT	304,800 (138,231)	285,740 (129,588)	276,948 (125,600)	249,944 (113,353)	247,432 (112,214)	322,200 (146,122)	308,400 (139,863)	278,400 (126,258)	273,840 (124,190)

TABLE 14.1-2 CONVENTIONAL AIRCRAFT WEIGHT SUMMARY

(See Table 14.1-1, Column 1 for Aircraft Description)

COMPONENTS	POUNDS	KILOGRAMS
STRUCTURE	(94,260)	(42,748)
Wing	36,070	16,358
Fuselage	32,170	14,590
Horizontal Tail	5,870	2,662
Vertical Tail	3,070	1,392
Landing Gear	12,530	5,683
Nacelles	4,550	2,063
PROPULSION SYSTEM	(19,850)	(9,002)
Engines	17,420	7,900
Water Injection System	275	125
Fuel System	1,820	825
Engine Controls	195	88
Starting Systems	140	64
SYSTEMS AND EQUIPMENT	(42,080)	(19,084)
Surface Controls	3,650	1,656
Landing Gear Controls	1,445	656
Instruments	1,740	789
Hydraulics & Pneumatics	2,120	961
Electrical	3,217	1,459
Avionics	1,796	815
Furnishings	23,169	10,507
Air Conditioning	3,990	1,810
Auxiliary Gear	45	20
Auxiliary Power Unit	908	411
WEIGHT EMPTY	156,190	70,834
USEFUL LOAD	(7,364)	(3,340)
Crew	1,430	649
Unusable Fuel	354	161
Engine Oil	120	54
Passenger Service	5,460	2,476
OPERATING WEIGHT	163,554	74,174
PAYLOAD	40,000	18,140
ZERO FUEL WEIGHT	203,554	92,314
FUEL	100,281	45,479
WATER	965	438
GROSS WEIGHT	304,800	138,231

TABLE 14.1-3 ADVANCED TECHNOLOGY AIRCRAFT WEIGHT SUMMARY
MACH .90, ALUMINUM

(See Table 14.1-1 Columns 2 & 3 for Aircraft Description)

COMPONENTS	COLUMN 2 AIRCRAFT POUNDS	COLUMN 2 AIRCRAFT KILOGRAMS	COLUMN 3 AIRCRAFT POUNDS	COLUMN 3 AIRCRAFT KILOGRAMS
STRUCTURE	(88,510)	(40,140)	(81,670	(37,037)
Wing	33,390	15,143	28,130	12,757
Fuselage	32,170	14,590	31,330	14,209
Horizontal Tail	4,050	1,837	3,860	1,751
Vertical Tail	2,900	1,315	2,790	1,265
Landing Gear	11,750	5,329	11,390	5,166
Nacelles	4,250	1,926	4,170	1,891
PROPULSION SYSTEM	(18,326)	(8,311)	(17,780)	(8,063)
Engines	16,206	7,350	15,678	7,110
Water Injection System	260	118	252	114
Fuel System	1,525	691	1,515	687
Engine Controls	195	88	195	88
Starting Systems	140	64	140	64
SYSTEMS AND EQUIPMENT	(41,635)	(18,882)	(42,283)	(19,176)
Surface Controls	3,400	1542	4,153	1,884
Landing Gear Controls	1,370	622	1,315	597
Instruments	1,740	789	1,740	789
Hydraulics & Pneumatics	2,000	907	1,950	884
Electrical	3,217	1,459	3,217	1,459
Avionics	1,796	815	1,796	815
Furnishings	23,169	10,507	23,169	10,507
Air Conditioning	3,990	1,810	3,990	1,810
Auxiliary Gear	45	20	45	20
Auxiliary Power Unit	908	411	908	411
WEIGHT EMPTY	148,471	67,334	141,733	64,278
USEFUL LOAD	(7,364)	(3,340)	(7,364)	(3,340)
Crew	1,430	649	1,430	649
Unusable Fuel	354	161	354	161
Engine Oil	120	54	120	54
Passenger Service	5,460	2,476	5,460	2,476
OPERATING WEIGHT	155,835	70,674	149,097	67,618
PAYLOAD	40,000	18,140	40,000	18,140
ZERO FUEL WEIGHT	195,835	88,814	189,097	85,758
FUEL	88,995	40,361	86,956	39,436
WATER	910	413	895	406
GROSS WEIGHT	285,740	129,588	276,948	125,600

TABLE 14.1-4 ADVANCED TECHNOLOGY AIRCRAFT
WEIGHT SUMMARY:MACH .90
COMPOSITES

(See Table 41.1-1 Columns 4 & 5 for Aircraft Description)

COMPONENTS	COLUMN 4 AIRCRAFT POUNDS	KILOGRAMS	COLUMN 5 AIRCRAFT POUNDS	KILOGRAMS
STRUCTURE	(65,820)	(29,850)	(62,980)	(28,562)
Wing	22,320	10,122	20,070	9,102
Fuselage	25,210	11,433	24,870	11,279
Horizontal Tail	2,430	1,102	2,390	1,084
Vertical Tail	2,120	962	2,060	934
Landing Gear	10,280	4,662	10,180	4,617
Nacelles	3,460	1,569	3,410	1,546
PROPULSION SYSTEM	(16,255)	(7,372)	(15,933)	(7,226)
Engines	14,325	6,497	14,043	6,369
Water Injection System	235	106	230	105
Fuel System	1,360	617	1,325	600
Engine Controls	195	88	195	88
Starting Systems	140	64	140	64
SYSTEMS & EQUIPMENT	(40,936)	(18,565)	(41,658)	(18,893)
Surface Controls	3,080	1,397	3,830	1,738
Landing Gear Controls	1,216	552	1,213	550
Instruments	1,740	789	1,740	789
Hydraulics & Pneumatics	1,775	805	1,750	794
Electrical	3,217	1,459	3,217	1,459
Avionics	1,796	815	1,796	815
Furnishings	23,169	10,507	23,169	10,507
Air Conditioning	3,990	1,810	3,990	1,810
Auxiliary Gear	45	20	45	20
Auxiliary Power Unit	908	411	908	411
WEIGHT EMPTY	123,011	55,787	120,571	54,681
USEFUL LOAD	(7,364)	(3,340)	(7,364)	(3,340)
Crew	1,430	649	1,430	649
Unusable Fuel	354	161	354	161
Engine Oil	120	54	120	54
Passenger Service	5,460	2,476	5,460	2,476
OPERATING WEIGHT	130,375	59,127	127,935	58,021
PAYLOAD	40,000	18,140	40,000	18,140
ZERO FUEL WEIGHT	170,375	77,268	167,935	76,160
FUEL	78,749	35,714	78,687	35,686
WATER	820	372	810	367
GROSS WEIGHT	249,944	113,353	247,432	112,214

TABLE 14.1-5 ADVANCED TECHNOLOGY TRANSPORT
WEIGHT SUMMARY: MACH .98
ALUMINUM

(See Table 14.1-1 Columns 6 and 7 for Aircraft Description)

COMPONENTS	COLUMN 6 POUNDS	AIRCRAFT KILOGRAMS	COLUMN 7 POUNDS	AIRCRAFT KILOGRAMS
STRUCTURE	(110,200)	(49,977)	(99,790)	(45,256)
Wing	47,000	21,315	38,760	17,578
Fuselage	36,480	16,544	35,380	16,045
Horizontal Tail	4,580	2,077	4,280	1,940
Vertical Tail	3,280	1,488	3,200	1,451
Landing Gear	13,210	5,991	12,690	5,755
Nacelles	5,650	2,562	5,480	2,485
PROPULSION SYSTEM	(22,330)	(10,127)	(21,541)	(9,769)
Engines	19,725	8,945	19,056	8,642
Water Injection System	310	140	300	136
Fuel System	1,960	890	1,850	839
Engine Controls	195	88	195	88
Starting Systems	140	64	140	64
SYSTEMS & EQUIPMENT	(42,498)	(19,273)	(43,273)	(19,625)
Surface Controls	3,875	1,758	4,872	2,210
Landing Gear Controls	1,508	684	1,456	660
Instruments	1,740	789	1,740	789
Hydraulics & Pneumatics	2,250	1,020	2,080	994
Electrical	3,217	1,459	3,217	1,459
Avionics	1,796	815	1,796	815
Furnishings	23,169	10,507	23,169	10,507
Air Conditioning	3,990	1,810	3,990	1,810
Auxiliary Gear	45	20	45	20
Auxiliary Power Unit	908	411	908	411
WEIGHT EMPTY	175,028	79,377	164,604	74,650
USEFUL LOAD	(7,364)	(3,340)	(7,364)	(3,340)
Crew	1,430	649	1,430	649
Unusable Fuel	354	161	354	161
Engine Oil	120	54	120	54
Passenger Service	5,460	2,476	5,460	2,476
OPERATING WEIGHT	182,392	82,717	171,968	77,990
PAYLOAD	40,000	18,140	40,000	18,140
ZERO FUEL WEIGHT	222,392	100,857	211,968	96,130
FUEL	98,728	44,775	95,397	43,264
WATER	1,080	490	1,035	469
GROSS WEIGHT	322,200	146,122	308,400	139,863

TABLE 14.1-6 ADVANCED TECHNOLOGY TRANSPORT
WEIGHT SUMMARY: MACH .98
COMPOSITES

(See Table 14.1-1, Columns 8 and 9 for Aircraft Description)

COMPONENTS	COLUMN 8 AIRCRAFT POUNDS	COLUMN 8 AIRCRAFT KILOGRAMS	COLUMN 9 AIRCRAFT POUNDS	COLUMN 9 AIRCRAFT KILOGRAMS
STRUCTURE	(79,120)	(35,882)	(75,222)	(34,114)
Wing	29,400	13,333	26,300	11,927
Fuselage	28,450	12,902	28,075	12,732
Vertical Tail	2,720	1,234	2,650	1,202
Vertical Tail	2,580	1,170	2,500	1,134
Landing Gear	11,440	5,188	11,227	5,092
Nacelles	4,530	2,055	4,470	2,027
PROPULSION SYSTEM	(19,345)	(8,773)	(19,189)	(8,702)
Engines	17,175	7,789	17,064	7,738
Water Injection System	270	122	265	120
Fuel System	1,565	710	1,525	692
Engine Controls	195	88	195	88
Starting Systems	140	64	140	64
SYSTEMS AND EQUIPMENT	(41,545)	(18,841)	(42,353)	(19,208)
Surface Controls	3,350	1,520	4,210	1,910
Landing Gear Controls	1,330	603	1,318	598
Instruments	1,740	789	1,740	789
Hydraulics & Pneumatics	2,000	907	1,960	889
Electrical	3,217	1,459	3,217	1,459
Avionics	1,796	815	1,796	815
Furnishings	23,169	10,507	23,169	10,507
Air Conditioning	3,990	1,810	3,990	1,810
Auxiliary Gear	45	20	45	20
Auxiliary Power Unit	908	411	908	411
WEIGHT EMPTY	140,010	63,496	136,764	62,024
USEFUL LOAD	(7,364)	(3,340)	(7,364)	(3,340)
Crew	1,430	649	1,430	649
Unusuable Fuel	354	161	354	161
Engine Oil	120	54	120	54
Passenger Service	5,460	2,476	5,460	2,476
OPERATING WEIGHT	147,374	66,836	144,128	65,364
PAYLOAD	40,000	18,140	40,000	18,140
ZERO FUEL WEIGHT	187,374	84,976	184,128	83,504
FUEL	90,061	40,844	88,752	40,251
WATER	965	438	960	435
GROSS WEIGHT	278,400	126,258	273,840	124,190

component, the basic parameters and the approximate number of equations used in the statistical-analytical procedure for a total airframe light-alloy structural weight buildup. The stress/weight analyses performed to furnish data for refinement or conformation of weights calculated by the statistical/analytical procedures are summarized in Table 14.2-2. Although the final selected configuration wings and fuselages are sandwich construction, these analyses, performed before the decision to use sandwich, satisfactorily establish the desired confidence in the ability of the basic procedure to yield correct primary structural weight values.

The procedure defined above allows component structural weights to be calculated for light-alloy (aluminum) only. To obtain structural weights for these components when designed with composite materials, a ratio of composite weight to light-alloy weight was applied to the basic light-alloy component weight. These ratios were obtained from stress/weight analyses performed on both composites and light-alloys for the various structural components, some on advanced aircraft configurations and some on other comparable structural studies (B-1 and F-111). The ratios for the various components of the Phase II selected configurations are shown in Table 14.2-3. It should be noted that the composite ratios remain constant, by component, for both the Mach .90 and .98 configurations with the exception of the wings, which vary as a function of the ratio of the wing structural span to thickness. Tables 14.2-4 and -5 show the weight of composite material used and the percentage this weight is of the total component weight for the final selected advanced aircraft configurations. The component structural weights for these configurations are given in Section 14.1. (Tables 14.1-2 through 14.1-6)

The application of an active control system to the light-alloy- or composite-constructed airframe has been assumed to influence the structural weights of only the wings and fuselages. The structural weights of these components were determined by applying to the appropriate basic component weight (i.e., aluminum or composite), a ratio of the ACS component weight to the basic material component weight. These ratios were derived from the component stress/weight analyses and the stiffness requirements as determined by the DAEAC active control system studies. The ratios for these components and materials are also shown in Table 14.2-3.

WING W_{DES}, b', S_W t/c, λ, Λ, T, F_{TU} 15 Equations	+	**FUSELAGE** S_{WETT}, L_t, D, H, T, F_{TU}, Cutouts, Engines 29 Equations
+ **HORIZ. TAIL** F_H, b', S_{HT}, t/c, λ, Λ, T, F_{TU} 6 Equations	+	**VERT. TAIL** F_V, b', S_{VT} t/c, λ, Λ, T, F_{TU} 5 Equations
+ **LANDING GEAR** Percent of Gross Weight	+	**EXTERNAL NACELLE** S_N, S_{PYL}, W_{NC}, B_N, D_N, T, F_{TU} DC-10 Correlation + Engine Scaling

= TOTAL AIRFRAME

Table 14.2-1 Basic Parameters for Statistical-Analytical Weight Procedure

Table 14.2-2

SUMMARY OF STRESS/WEIGHT ANALYSES

Component	Type of Structure	Purpose
Wing	Multi-Spar Plate	• Statistical weight correlation • Stiffness data for flutter analysis • Member sizing & weight • Weight savings in expanded root • Vibration modes & frequencies
Wing	Multi-Spar Plate (alum) Multi-Spar Sandwich (composite) 3-Spar Plate-Stringer (alum & composite)	• 100% and reduced strength member sizes for active control system study
Wing	Multi-Spar Sandwich (composite) 3-Spar Plate-Stringer (alum & composite)	• Satisfy stiffness requirements and optimizing composite filament orientation
Wing	Skin Stringer	• 100% and reduced strength skin gages and stiffness for DAEAC active control system study
Fuselage	Sheet Stringer	• Confirm statistical weight & generate stiffness for active control system study
Horizontal Tail	Multi-Spar Sandwich (composite)	• Member sizes & stiffness for DAEAC active control system study
Horizontal Tail	Sandwich	• Member sizes & stiffness for DAEAC active control system study
Vertical Tail	Sandwich	• Stiffness for DAEAC active control system study

TABLE 14.2-3 STRUCTURAL WEIGHT RATIOS FOR COMPOSITE AND ACTIVE CONTROL SYSTEM EVALUATIONS

Mach No.	Component	Ratio		
		Composite Wt / Light-Alloy Wt	Light-Alloy ACS Wt / Light-Alloy Wt	Composite ACS Wt / Composite Wt
0.90	Wing	.746	.871	.912
	Fuselage	.801	.98	.99
	Horiz.Tail	.75	-	-
	Vert.Tail	.80	-	-
	Land.Gear	-	-	-
	Nac./Pyl.	.90	-	-
0.98	Wing	.717	.871	.912
	Fuselage	.801	.98	.99
	Horiz.Tail	.75	-	-
	Vert.Tail	.80	-	-
	Land.Gear	-	-	-
	Nac./Pyl.	.90	-	-

TABLE 14.2-4 SUMMARY OF COMPOSITE USAGE FOR MACH 0.90

SELECTED CONFIGURATIONS WITH SUPERCRITICAL WINGS

Configuration Description				
Active Control System	None	Full	Full	Full
Area-Ruled Fuselage	No	No	No	No
Engine Identification	P & W STF -429	P & W STF -429	P & W STF -433 15 db	P & W STF -433 max db
Engine Scale	0.565	0.560	0.568	0.724
S_W (Wing) ft^2 (m^2)	1990.0 (184.9)	1970.0 (183.0)	2005.0 (186.3)	2100.0 (195.1)
t/c ⊥ c/2 (Wing)	0.1415	0.1415	0.1415	0.1415
Λ c/2 (Wing) deg (rad)	36.0 (0.554)	36.0 (0.554)	36.0 (0.554)	36.0 (0.554)
AR (Wing)	9.0	9.0	9.0	9.0
W/S (Wing) lb/ft^2 (kg/m^2)	125.6 (613.2)	125.6 (613.2)	125.6 (613.2)	125.6 (613.2)

Composite Usage

Component	Weight of Composite Used lb (kg)	% of Component Weight	Weight of Composite Used lb (kg)	% of Component Weight	Weight of Composite Used lb (kg)	% of Component Weight	Weight of Composite Used lb (kg)	% of Component Weight
Wing	10180 (4620)	45.61	8110 (3680)	40.41	8290 (3760)	40.44	8710 (3950)	40.40
Fuselage	14270 (6470)	56.60	13980 (6340)	56.21	14020 (6360)	56.17	14280 (6480)	56.24
Horizontal Tail	1220 (550)	50.20	1190 (540)	49.79	1220 (550)	49.59	1310 (590)	49.81
Vertical Tail	790 (360)	37.26	770 (350)	37.38	790 (360)	37.26	1020 (460)	37.64
Landing Gear	- -	- -	- -	- -	- -	- -	- -	- -
Nacelles	380 (170)	10.98	380 (170)	11.14	390 (180)	11.27	500 (230)	11.11
Total	26840 (12170)	40.78	24430 (11080)	38.79	24710 (11210)	38.69	25820 (11710)	38.17

TABLE 14.2-5 SUMMARY OF COMPOSITE USAGE FOR MACH 0.98

SELECTED CONFIGURATIONS WITH SUPERCRITICAL WINGS

Configuration Description				
Active Control System	None	Full	Full	Full
Area-Ruled Fuselage	Yes	Yes	Yes	Yes
Engine Identification	P & W STF -429	P & W STF -429	P & W STF -433 15 db	P & W STF -433 max db
Engine Scale	0.669	0.662	0.670	0.786
S_W (Wing) ft^2 (m^2)	2320.0 (215.5)	2282.0 (212.0)	2325.0 (216.0)	2355.0 (218.8)
$t/c_{\perp}$ c/2 (Wing)	0.110	0.110	0.110	0.110
Λ c/2 (Wing) deg (rad)	40.0 (0.698)	40.0 (0.698)	40.0 (0.698)	40.0 (0.698)
AR (Wing)	8.0	8.0	8.0	8.0
W/S (Wing) lb/ft^2 (kg/m^2)	120.0 (585.8)	120.0 (585.8)	120.0 (585.8)	120.0 (585.8)

Composite Usage								
Component	Weight of Composite Used lb (kg)	% of Component Weight	Weight of Composite Used lb (kg)	% of Component Weight	Weight of Composite Used lb (kg)	% of Component Weight	Weight of Composite Used lb (kg)	% of Component Weight
Wing	15550 (7050)	52.89	12700 (5760)	48.29	12940 (5870)	48.28	13140 (5960)	48.31
Fuselage	16070 (7290)	56.48	15750 (7140)	56.11	15800 (7170)	56.09	15930 (7230)	56.27
Horizontal Tail	1340 (610)	49.26	1310 (590)	49.43	1340 (610)	49.26	1370 (620)	49.28
Vertical Tail	960 (430)	37.21	930 (420)	37.20	950 (430)	37.25	1060 (480)	37.32
Landing Gear	- -	- -	- -	- -	- -	- -	- -	- -
Nacelles	500 (230)	11.04	490 (220)	10.96	500 (230)	11.01	590 (270)	10.97
Total	34420 (15610)	43.50	31180 (14130)	41.4	31530 (14310)	41.34	32090 (14560)	41.02

14.3 PROPULSION

14.3.1 Power Plant

The Pratt and Whitney STF-429 engine was selected to provide the best overall propulsion subsystem for the advanced technology aircraft. The weights have been derived from scaling data supplied by the manufacturer. The basic installed engine weight of 7000 lb (3174.6 kg) includes the following items:

1. Fuel control system, including pump, filter, heater, speed control unit, etc.
2. Ignition system
3. Composite fan blades
4. Blade containment
5. Commercial design criteria (life, LCF, etc.)
6. Austerity gearbox
7. Oil tank, fuel/oil cooler
8. Airframe bleed provisions
9. Internal front mount.

The following items are not included:

1. Fan ducting
2. Acoustic treatment
3. Thrust reverser
4. Tailpipe or tailcone
5. Nose spinner
6. Provisions for water injection.

Engine installation layouts were made and surface areas obtained to develop weights for all of the equipment not supplied by Pratt and Whitney Aircraft.

For an engine scale of 1.0 the following weights were used for the STF 429 engine:

WEIGHT - pounds (kilograms)	
Basic Engine	7000 (3174.6)
Thrust Reverser	1060 (480.7)
Nozzle and Tailcone	218 (98.9)
Provisions for Water Injection	40 (18.1)
Nose Spinner	8 (3.6)
Total Basic Engine	8326 (3775.9)

A scaling data plot of relative engine size versus relative engine weight, supplied by Pratt and Whitney Aircraft, was used to establish weight for the above items. From engine installation drawings, scaling data for the inlet and fan ducting, including acoustic treatment, weights were developed. The values are as follows:

WEIGHT - pounds (kilograms)	
STF 429 Engine Scale = 1.0	
Inlet Duct and Splitters	415 (188.2)
Fan Ducts and Splitters	370 (167.8)
Total Ducts and Acoustic Treatment	785 (356)

14.3.2 Water Injection System

This system is required to reduce engine gaseous pollutants at takeoff thrust. Water for two minutes at a flow rate of 14,500 lb/hr (6,576 kg/hr) is required for the STF-429 scale 1.0 engine. Scaling data based on engine thrust and amount of water required for one takeoff was developed for the weight of this system. The water weight is an expendable item and is listed with fuel in the various weight summaries shown.

14.3.3 Fuel System

Weights for the fuel system are based on the following parameters, with a typical weight breakdown shown for an advanced technology aircraft:

		WEIGHT - pounds (kilograms)
1.	Integral tank bay sealing	250 (113.4)
2.	Booster and transfer pumps	265 (120.1)
3.	Distribution and transfer system	480 (217.7)
4.	Ground refueling	115 (52.2)
5.	Dump and drain	55 (25.0)
6.	Vent and pressurization	165 (74.8)
7.	Purging and miscellaneous	195 (88.4)
	Total	1525 (691.6)

14.3.4 Engine Controls

The weight analysis for the engine controls was established by the number and locations of engines and the airplane size. An estimate of 195 lb (88.4 kg) was used for all of the final configurations.

14.3.5 Starting Systems

Conventional air-turbine starters are used in this system. A weight study based on existing systems was made, and an estimate of 140 lb (63.5 kg) was calculated from engine size and location for all of the final configurations.

14.4 SYSTEMS AND EQUIPMENT

14.4.1 Surface Controls

The advanced (active) flight control system employs fly-by-wire techniques in the selected configurations. The availability of statistical data for this mode of control required that the weight analysis be made in two steps. Initially, conventional and existing aircraft designs were evaluated for a total system weight based on overall aircraft size and gross weight. Finally, surface control areas were derived from layouts, and the surface control weights were calculated. Additional equipment and controls are required for an active control system, and their weights were developed for increased operating velocities and pressure. The active control system design features were developed in systematic steps that involved weight penalties and reductions in the airframe structural weights. These features were evaluated for the best payoff in the total flight envelope, from flutter-free with maximum fuel to flutter-free with minimum fuel. The weight penalties for an active control system have been added to the surface control group, although a part of this weight should be coded into the hydraulic system group for the increased plumbing and fluid that will be required.

A typical weight breakdown for the surface control group as analyzed for the M .98 selected configuration is as follows:

	WEIGHT - pounds (kilograms)
Cockpit Controls	80 (36)
Autopilot	170 (77)
Primary Flight Controls	1936 (878)
Secondary Flight Controls	1064 (483)
Active Control System (Delta)	960 (435)
Total Group	4210 (1909)

14.4.2 Landing Gear Controls

A conventional gear control system has been used for all of the configurations, and the weights shown are for gear retraction, brake and steering operation, and emergency extension.

14.4.3 Instruments and Navigational Equipment

A constant value of 1740 lb (789 kg) has been used for the advanced technology aircraft. A functional weight breakdown for this group is as follows:

	WEIGHT - pounds (kilograms)
Flight Instruments	150 (68)
Flight Director and Warnings	190 (86)
Engine Instruments and Warnings	560 (254)
Surface Position Instruments	200 (91)
Cabin Warning and Controls	340 (154)
Emergency and Miscellaneous	300 (136)
Total Group	1740 (789)

14.4.4 Hydraulics and Pneumatics

The arrangement of systems and power sources for the hydraulic and pneumatic systems provides redundancy to accept the single-, dual-, and triple-hydraulic-system requirements for the powered flight controls. Multiple, independent power systems plus an auxiliary power source has been provided. A typical weight breakdown is shown below:

WEIGHT - pounds (kilograms)

Primary and Utility Pumps	250 (113)
Reservoirs and Accumulators	154 (70)
Valves and Controls	160 (73)
Plumbing	309 (140)
Fluid in System	375 (170)
Pneumatic Heat Exchanger and Ducts	662 (300)
Supports	50 (22)
Total Group	1960 (888)

A part of the active-control-system weight penalty in the surface control group is for additional hydraulic system weight.

14.4.5 Electrical Group

A constant value of 3217 lb (1459 kg) used for all of the configurations is based on the following analysis:

WEIGHT - pounds (kilograms)

AC Power Generating Equipment and Power Supply	675 (306)
DC Power Source and Conversion	165 (75)
AC Power Distribution	800 (363)
DC Power Distribution	95 (43)
Lights and Signals, etc.	1460 (662)
Miscellaneous	22 (10)
Total Group	3217 (1459)

14.4.6 Avionics Group

A constant weight of 1796 lb (815 kg) used for the avionics group for all of the advanced transports is based on the following analysis:

	WEIGHT - pounds (kilograms)
Communication and Radar Equipment	380 (173)
Installation	170 (77)
Navigation - Conventional Equipment	180 (82)
Installation	80 (36)
Navigation - International Equipment	230 (104)
Installation	104 (47)
Data Acquisition Equipment	97 (44)
Installation	44 (20)
P. A. System Equipment	239 (108)
Installation	100 (45)
Interphone - Service Equipment	70 (32)
Installation	30 (14)
Interphone - Flight Equipment	50 (23)
Installation	22 (10)
Total Group	1796 (815)

14.4.7 Furnishings

The furnishings group weight analysis is based on accommodations for personnel, furnishings equipment, and emergency equipment. A weight summary is shown for the

40,000-lb (18,140 kg) payload (195 passenger) airplanes with a four-man crew and five stewardesses:

	WEIGHT - pounds (kilograms)
Seats	7446 (3377)
Utility Trays	45 (20)
Lavatories and Water System	1319 (598)
Galleys and Water	3887 (1763)
Oxygen System	173 (78)
Instrument Panels and Consoles	255 (116)
Storage Provisions	184 (83)
Cargo Handling System	1137 (516)
Insulation and Floor Covering	2181 (989)
Coatrooms	676 (307)
Partitions, Window Shades, and Doors	830 (376)
Sidewall Paneling	802 (364)
Overhead Storage	1085 (492)
Ceiling	1214 (551)
Lining and Upholstery	133 (60)
Cargo Compartment Lining	1191 (540)
Firex System	390 (177)
Emergency Equipment	221 (100)
Total Group	23,169 (10,507)

14.4.8 Air Conditioning and Anti-Icing

The weight analysis for this group is based on the heating and cooling load for 195 passengers and 9 crew members. Anti-icing is provided for the windshields, nacelles, and wing and empennage leading edges, as required. The weight analysis made for each configuration is as follows:

WEIGHT - pounds (kilograms)

Pressurization System	265 (120)
Ventilation System	205 (93)
Cargo Compartment Heating	195 (88)
Cooling System (Includes Engine Bleed Ducts)	2690 (1220)
Ground Air Supply Provisions	35 (16)
Anti-Icing	600 (273)
Total Group	3990 (1810)

14.4.9 Auxiliary Gear

A handling gear weight allowance of 45 lb (20 kg) has been estimated for the advanced technology airplanes.

14.4.10 Auxiliary Power Unit

The installed auxiliary power unit weight used on all of the advanced technology airplanes is broken out as follows:

WEIGHT - pounds (kilograms)

Engine and Supports	305 (138)
Generator and Controls	120 (54)
Inlet and Exhaust Ducts	186 (84)

F

Starting System	30 (14)
Acoustic Treatment and Enclosure	188 (85)
Fuel System	34 (15)
Fire Detection and Extinguishers	45 (21)
Total Group	908 (411)

14.5 USEFUL LOAD

14.5.1 Crew

A four-man flight crew at 195 lb (88 kg) each and five cabin attendants at 130 lb (59 kg) each has been assumed for each of the advanced technology configurations.

14.5.2 Unusable Fuel

A weight estimate for 53 gallons (200 l) or 354 lb (161 kg) has been used for all of the advanced airplanes.

14.5.3 Engine Oil

An engine oil consumption rate of 1.5 lb/hr (.68 kg/hr) per engine has been indicated by the engine manufacturer. At this rate, an oil allowance for four flights or 30 hours of flight time has been assumed for all of the configurations. This is approximately 120 lb (54 kg) of engine oil.

14.5.4 Passenger Service

A weight of 28 lb (12.7 kg) per passenger has been used for all of the configurations shown. This weight is for food and food service, drinking water, blankets and pillows, magazines, toilet fluids, towels, paper supplies, and coat hangers.

14.6 P&WA STF433-1985 ENGINES

The 1979 technology STF 429 engine is designed to produce noise levels 10 EPNdB lower than the FAR Part 36 requirements at sideline, takeoff, and approach conditions, with acoustic treatment on the inlet and fan duct areas and their supporting structure. An additional engine, the STF 433, based on 1985 technology, was also considered. This engine will produce noise levels 15 EPNdB lower than the FAR Part 36 requirements. The weights for airplanes utilizing this engine are shown in Table 14.6-1. For maximum reduction of the noise level, an additional airplane was sized and is also shown in Table 14.6-1. This engine and airplane were sized for the same range and payload as the selected M .90 and M .98 advanced aircraft.

14.7 BALANCE AND INERTIA DATA

A weight, balance, and inertia study of the M .90 and M .98 advanced technology airplanes reveals that the center of gravity for both versions will stay within the required stability limits as specified in Section 9. A balance and inertia summary for the airplanes with takeoff and zero fuel conditions is presented in Table 14.7-1. A typical flight profile is discussed in Section 9 for the advanced transport, showing takeoff, inflight, and landing balance conditions.

TABLE 14.6-1 WEIGHT SUMMARY FOR STF433-1985 ENGINES

NOISE LEVEL REDUCTION	-15EPNdB	MAXIMUM	-15EPNdB	MAXIMUM
CRUISE MACH NUMBER	0.90	0.90	0.98	0.98
ENGINES	STF433	STF433	STF433	STF433
ENGINE SCALE	.568	.724	.670	.786
WING AREA-Ft^2(In^2)	2005 (186.3)	2105 (195.1)	2325 (216.0)	2355 (218.8)
WEIGHTS - LB(KG)				
STRUCTURAL WEIGHT	63,860 (28,961)	67,640 (30,676)	76,260 (34,585)	78,230 (35,478)
PROPULSION SYSTEM				
ENGINES	15,315 (6946)	20,445 (9272)	18,972 (8604)	22,257 (10,094)
SYSTEMS	1,950 (884)	2,100 (952)	2,225 (1009)	2,295 (1041)
EQUIPMENT	41,761 (18,939)	42,031 (19,062)	42,486 (19,268)	42,623 (19,330)
USEFUL LOAD	7,364 (3,340)	7,364 (3,340)	7,364 (3,340)	7,364 (3,340)
OPERATING WEIGHT	130,250 (59,070)	139,580 (63,302)	147,307 (66,806)	152,769 (69,283)
PAYLOAD	40,000 (18,140)	40,000 (18,140)	40,000 (18,140)	40,000 (18,140)
FUEL	80,710 (36,603)	83,080 (37,678)	90,673 (41,122)	88,641 (40,200)
WATER	870 (395)	1100 (499)	1020 (463)	1190 (540)
GROSS WEIGHT	251,830 (114,208)	263,760 (119,619)	279,000 (126,531)	282,600 (128,163)

TABLE 14.7-1 BALANCE AND INERTIA SUMMARY

(SELECTED MACH .90 AND .98 AIRPLANES)

CONDITION	PERCENT MAC	WEIGHT Lb. (Kg)	X LONG.	Y LAT. Inches (Centimeters)	Z VERTICAL	I_{xx} ROLL	I_{yy} PITCH Slug ft^2 (Kg $Meter^2$)	I_{xx} YAW	I_{xz} PRODUCT
MACH .90									
ZERO FUEL WEIGHT	13.5%	167,935 (76,160)	1098.5 (2790.2)	0	184.7 (469.1)	2,231,710 (3,025,975)	5,037,020 (6,829,695)	7,315,270 (9,918,775)	214,000 (290,163)
GROSS WEIGHT	20.8%	247,432 (112,214)	1112.5 (2825.8)	0	176.2 (447.5)	2,961,140 (4,015,010)	4,949,350 (6,710,823)	7,994,090 (10,839,187)	413,750 (561,004)
MACH .98									
ZERO FUEL WEIGHT	12.9%	184,128 (83,504)	1139.1 (2893.2)	0	186.6 (474.0)	2,445,620 (3,316,016)	5,341,770 (7,242,906)	7,622,000 (10,344,670)	216,000 (292,874)
GROSS WEIGHT	20.7%	273,840 (124,190)	1155.9 (2936.0)	0	178.3 (452.9)	3,407,250 (4,619,890)	5,197,420 (7,047,182)	8,649,240 (11,727,505)	417,800 (566,495)

SECTION 15

MATERIAL SELECTION ANALYSIS

The principal material selection decision for this aircraft configuration study was related to advanced composites materials. The question was whether or not advanced composite materials offer sufficient payoff for commercial transport aircraft to warrant their use. This question was resolved through a comparative design and cost study. One aircraft configuration was selected, and two independent designs were prepared in which the primary structural materials were varied. In one, light-alloy metals were used; in the other, advanced composites. Cost estimates were then made for these two designs to determine the relative costs of manufacturing commercial transport aircraft. As a result of this design and cost study, graphite-reinforced advanced composite materials were selected for extensive usage on the selected airplane configurations because of the cost savings realized. Study details are given in the following subsections.

15.1 BASIC GROUND RULES

The aircraft configuration selected for this study is shown in Figure 15.1-1. The airplane is similar to the $M_c = 0.98$ selected configuration. It has a 19.5-ft (5.9 m) maximum-diameter area-ruled fuselage approximately 180 ft (55 m) long, and a 2500-ft^2 (232 m^2), 40-deg (0.698 rad) swept-back wing at 6.4 aspect ratio and 0.110 thickness ratio (chord normal to the 50-percent chordline at the MAC). The design payload is 40,000 lb (18,140 kg), and the design gross weight is 300,000 lb (136,000 kg).

The engines, nacelles, landing gear, and empennage were neglected. The study was concerned with design of the wing and the fuselage between Station 200 and the aft pressure bulkhead. This portion of the fuselage is approximately 127 ft (39 m) long, is circular throughout except in the main wheel-well area, and has a diameter that varies between 14.5 ft (4.4 m) and 19.5 ft (5.9 m). The loads in this fuselage section result mainly from body bending and cabin pressure. The pressurized cabin loads criteria as presented in FAR 25, Section 25.365, were applicable with the exception of the modification to 25.365 as noted in Section 12.3 of this report. The maximum limit cabin pressure was 9.64 psi

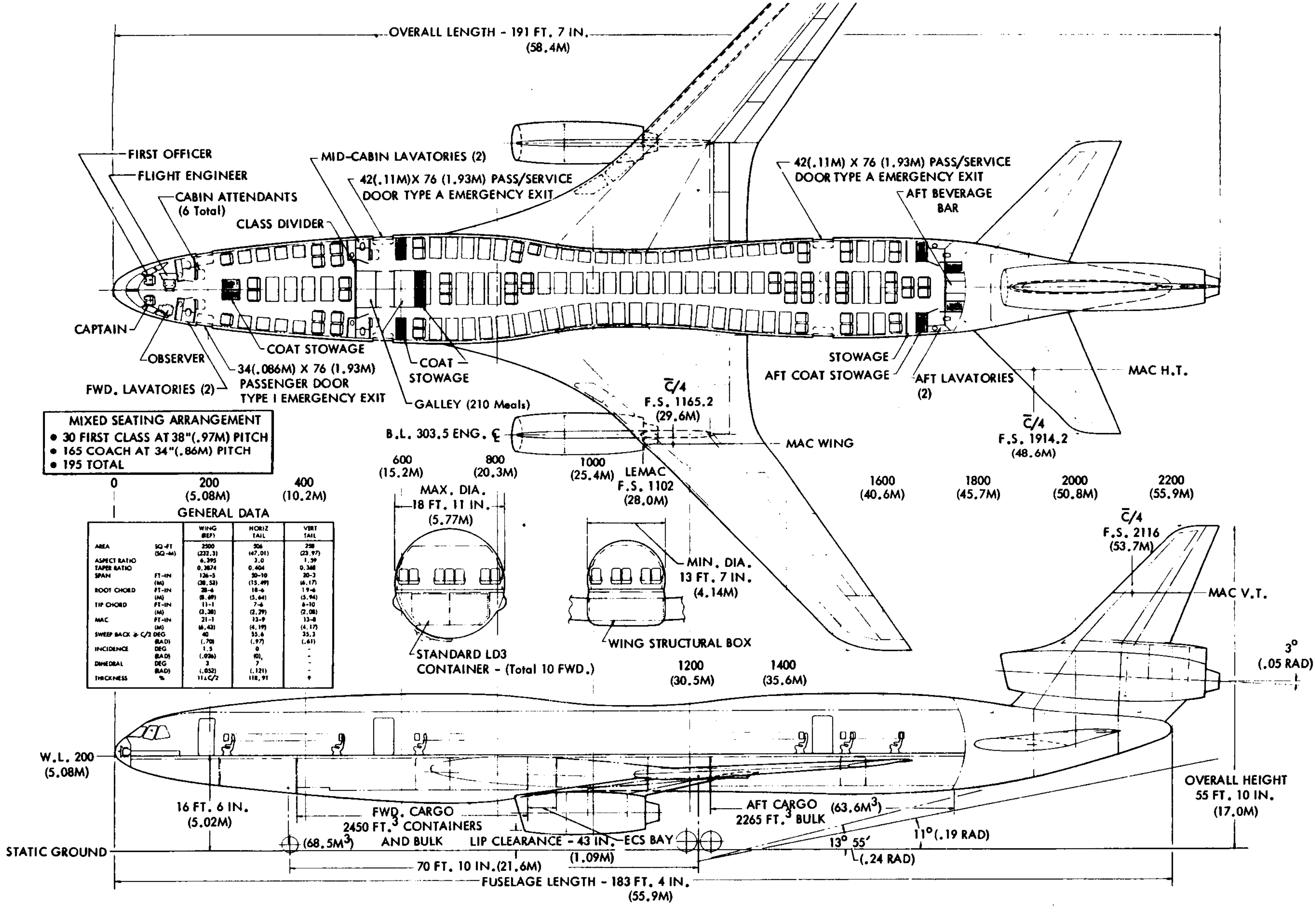

GENERAL DATA

		WING (REF)	HORIZ TAIL	VERT TAIL
AREA	SQ-FT	2500	506	258
	(SQ-M)	(232.3)	(47.01)	(23.97)
ASPECT RATIO		6.395	3.0	1.59
TAPER RATIO		0.3874	0.404	0.348
SPAN	FT-IN	126-5	50-10	20-3
	(M)	(38.53)	(15.49)	(6.17)
ROOT CHORD	FT-IN	28-6	18-6	19-6
	(M)	(8.69)	(5.64)	(5.94)
TIP CHORD	FT-IN	11-1	7-6	6-10
	(M)	(3.38)	(2.29)	(2.08)
MAC	FT-IN	21-1	13-9	13-8
	(M)	(6.43)	(4.19)	(4.17)
SWEEP BACK @ C/2	DEG	40	35.6	35.3
	(RAD)	(.70)	(.97)	(.61)
INCIDENCE	DEG	1.5	0	-
	(RAD)	(.026)	(0)	-
DIHEDRAL	DEG	3	7	-
	(RAD)	(.052)	(.121)	-
THICKNESS	%	11⊥C/2	11R, 9T	9

Figure 15.1-1 Material Selection Study Configuration

(66.5×10^3 N/m^2), which is based on maintaining a cabin internal pressure corresponding to ambient at 6000 ft (1820 m) of altitude while operating at from 25,700 ft (8120 m) to 45,000 ft (13,700 m).

The significant wing design loads resulted from the maximum 2.5-g limit load factor maneuver condition. The airloads were based on an elliptical distribution and were adjusted for inertia relief loads. The airload development methodology is discussed in Section 13.

The cost study was based on the production of 250 airframes. The assumed design go-ahead date was 1 January 1978, with certification on 1 January 1981. The maximum production rate was six aircraft per month, with deliveries complete in 1985. The RDT&E phase was assumed to be complete by design go-ahead, and no costs associated with this work were to be included in the airplane price.

15.2 MATERIALS SELECTED

The pertinent characteristics of the materials selected for the two airframe designs are discussed below.

15.2.1 Light Alloy

The light-alloy material selection was performed in a systematic manner. Typical comparison and evaluation sheets used to select the most applicable alloy are shown in Figures 15.2-1 and 15.2-2. The data are for the wing upper and lower skins in which three promising aluminum alloys are shown. This same format was used in alloy selection for other elements in both the wing and fuselage.

The 7475-T7351 material was selected for the wing lower skins because of its high fracture toughness, excellent exfoliation properties, and relatively good fatigue strength. For the wing upper surface, the 7475-T7651 material was selected over the 7075 material because the 7475 material has better fracture toughness and equivalent fatigue and exfoliation properties. It should be noted that the critical crack lengths noted on the evaluation sheets are based on using K_C values greater than K_{1C} values because, for the thicknesses involved, the plane stress rather than plane strain failure mode was considered applicable.

MATERIAL SELECTION CRITERIA

COMPONENT: WING SKINS - UPPER SURFACE

Temperature - Maximum: 100°

- Critical Condition: 3.75 g maneuver

Physical Constraints, (space, Curvature): Internal pressure

Structural Concept: Sheet stringer

Fuel Contact: Yes

MATERIAL FORM: (i.e., Plate, Sheet, Forging, Extrusion ....) Plate

NOTE: * items are estimated

MATERIAL COMPARISON CHART

MATERIAL		7475-T7651	7075-T651	7075-T7651
Thickness - in. - (Meters)		.25 → 1.0 (.00635 .0254)	.25 → 1.0 (.00635 - .0254)	.25 → 1.0 (.00635 .0254)
F_{tu} - F_{ty} - L psi (Room Temp.) (N/m^2)		69000 59000 (475.7×10^6) (406.8×10^6)	79000 69000 (544.7×10^6) (475.7×10^6)	71000 60000 (489.5×10^6) (413.7×10^6)
F_{tu} - F_{ty} - LT psi (Room Temp.) (N/m^2)		70000 59000 (475.7×10^6) (406.8×10^6)	77700 66000 (535.7×10^6) (455.45×10^6)	71000 60000 (489.5×10^6) (413.7×10^6)
Percent Elongation		8 6	8 6	8 6
K_C - K_{IC} - L ksi (N/m^2)		52* - 44 (358.5×10^6) (303.4×10^6)	35* - 29 (241.3×10^6) (193.4×10^6)	37* - 32.5 (255.1×10^6) (224.1×10^6)
K_C - K_{IC} - LT ksi (N/m^2)		49* - 42.5 (337.8×10^6) (293.0×10^6)	32* - 24 (220.6×10^6) (165.5×10^6)	34* - 26 (234.4×10^6) (179.3×10^6)
Fatigue Strength - S_{MAX} L& LT - ksi @ 10^6 cycles L& LT - (N/m^2 @ 10^6 cycles)		K_T = 3, 1 R = .5 23, 45 (158.6×10^6) (310.3×10^6)	K_T = 3, 1 R = .5 23, 45 (158.6×10^6) (310.3×10^6)	K_T = 3, 1 R = .5 23, 45 (158.6×10^6) (310.3×10^6)
Critical Crack Length @ Min. Yield psi - in (N/m^2 - Meters)		41350 = 1.00 (285.1×10^6 = .0254)	41350 = 1.00 (285.1×10^6 = .0254)	41350 = 1.00 (285.1×10^6 = .0254)
2 a. @ 2/3 Ult. L psi - in (N/m^2 - meters) LT psi - in (N/m^2 - meter)		46000 = .81 (317.2×10^6 = .0206) 47000 = .69 (324.0×10^6 = .0175)	52693 = .28 (363.3×10^6 = .06711) 51800 = .28 (357.1×10^6 = .0061)	47357 = .39 (326.5×10^6 = .0099) 27357 = .33 (288.6×10^6 = .00838)
Stress Corrosion - L, LT psi (Nm^2)		41300 , 35400 ($284.7\ 10^6$) (244.1×10^6)	48300 , 33000 (333.0×10^6) ($227.5\ 10^6$)	42000 , 36000 (288.6×10^6) (248.2×10^6)
Exfoliation		Good	Poor	Good
Etching		Good	Good	Good
Weld Sequence		No Fusion	No Fusion	No Fusion
Forming		W 51 Cond. only	W 51 Cond. only	W 51 Cond. only
Maching		Good	Good	Good
COST	Width = 48" = (1.219 Meters)	$0.58 per lb ($1.279 per Kg)	$0.53 per lb. ($1.168 per Kg)	$0.58 per lb. ($1.279 per Kg)
	Width = 60" = (1.524 meters)	$0.61 per lb ($1.345 per Kg)	$0.56 per lb ($1.234 per Kg)	$0.61 per lb. ($1.345 per Kg)
Experience	Industry	Some now	Extensive	Extensive
	G. D.	None	Yes	Yes
Selected Material and selection reasons		7475-T7651 - Has better fracture toughness and equivalent fatigue and exfoliation properties.		

FIGURE 15.2-1 LIGHT ALLOY CONFIGURATION MATERIAL EVALUATION AND SELECTION - WING SKINS - UPPER SURFACE

MATERIAL SELECTION CRITERIA

COMPONENT: WING SKINS - LOWER SURFACE
Temperature - Maximum: 100%
Critical Condition: 3.75 g maneuver
Physical Constraints, (Space, Curvature): Internal pressure
Structural Concept: Sheet - Stringer
Fuel Contact: Yes
MATERIAL FORM: (i.e., Plate, Sheet, Forging, Extrusion.....) Plate
NOTE: * items are estimated

MATERIAL COMPARISON CHART

MATERIAL		2024-T351	7075-T7351	7475-T7351
Thickness - in. - (Meters)		.5 ⟶ 1.0 .0127 .0254	.25 ⟶ .5 .00635 .0127	.25 ⟶ .5 .00635 .0127
F_{tu} - F_{ty} - L (Room Temperature)	psi (N/m^2)	62000 47000 (427.5×10^6) (324.0×10^6)	69000 57000 (475.7×10^6) (393.0×10^6)	66000 53000 (455.0×10^6) (365.4×10^6)
F_{tu} - F_{ty} - LT (Room Temperature)	psi (N/m^2)	62000 41000 (427.5×10^6) (282.7×10^6)	69000 57000 (475.7×10^6) (393.0×10^6)	66000 52000 (455.0×10^6) (358.5×10^6)
Percent Elongation		8	7	7
K_C - K_{IC} - L	ksi (N/m^2)	57* 50* (393.0×10^6) (344.7×10^6)	46* 37 (317.2×10^6) (255.1×10^6)	59* 48 (406.8×10^6) (330.9×10^6)
K_C - K_{IC} - LT	ksi (N/m^2)	54* 46* (372.3×10^6) (317.2×10^6)	37* 32 (255.1×10^6) (220.6×10^6)	56* 47.5 (386.1×10^6) (327.5×10^6)
Fatigue Strength - S_{MAX} L & LT - ksi @ 10^6 Cycles L & LT (N/m^2 @ 10^6 Cycles)		K_T = 3, 1 R = .5 24*, 45 (165.5×10^6) (310.0×10^6)	K_T = 3, 1 R = .5 23, 45 (158.6×10^6) (310.0×10^6)	K_T = 3, 1 R = .5 23, 45 (158.6×10^6) (310.0×10^6)
Critical Crack Length @ Min. Yield	psi - in. (N/m^2 - Meters)	41350 = 1.21 (285.0×10^6 = .0307)	41350 = .80 (285.0×10^6 = .0203)	41350 = 1.30 (285.0×10^6 = .0330)
2 a_c @ 2/3 Ult. - L	psi - in. (N/m^2 - Meters)	41350 = 1.21 (285.0×10^6 = .0307)	46000 = .64 (317.2×10^6 = .0163)	44000 = 1.14 (303.4×10^6 = .0290)
LT	psi - in. (N/m^2 - Meters)	41000 = 1.10 (282.7×10^6 = .0279)	46000 = .41 (317.2×10^6 = .0104)	44000 = 1.03 (303.4×10^6 = .0262)
Stress Corrosion - L, LT	psi (N/m^2)	32900, 20500 (226.8×10^6) ($141. \times 10^6$)	42750, 42750 (294.7×10^6) (294.7×10^6)	39750, 39000 (274.1×10^6) (268.9×10^6)
Exfoliation		Poor	Excellent	Excellent
Etching		Good	Good	Good
Weld Sequence		No Fusion	No Fusion	No Fusion
Forming		Fair	W51 Cond. only	W51 Cond. only
Maching		Good	Good	Good
Cost	Width = 48" = (1.219 Meters)	\$0.525 per lb (\$1.157 per kg.)	\$0.535 per lb. (\$1.179 per Kg.)	\$0.58 per lb. (\$1.279 per Kg.)
	Width = 60" = (1.524 Meters)	\$0.555 per lb. (\$1.224 per Kg.)	\$0.565 per lb. (\$1.246 per Kg.)	\$0.61 per lb. (\$1.34 per Kg.)
Experience	Industry	Extensive	Some	Some
	G.D.	Extensive	Some	Some
Selected material and selected reasons		7475-T7351 - Has high fracture toughness, excellent exfoliation properties and good fatigue strength.		

FIGURE 15.2-2 LIGHT ALLOY CONFIGURATION MATERIAL EVALUATION AND SELECTION - WING SKINS - LOWER SURFACE

Critical crack lengths for a given stress (σ_c) were calculated from the equation

$$\sigma_c = \frac{K_c}{\sqrt{\pi a_c}}$$

where a_c is one-half the surface length of a through crack and K_c is the plane stress intensity factor for the thickness applicable. K_c values for 0.25-in. (0.635 cm) to 0.5-in. (1.27 cm) thickness were conservatively estimated from preliminary Alcoa values at 0.090-in. (0.229 cm) thickness and constructed curves of K_{IC} and K_C vs thickness.

15.2.2 Advanced Composites

For this study, advanced composite materials refers to those materials reinforced with boron and graphite filaments. Advanced composite materials technology began development in the 1960's as the specific strength and specific modulus characteristics shown in Figure 15.2-3 began to be developed and recognized. Since January 1967, there have been several primary and secondary structure hardware demonstration components developed and flight tested, such as the F-111 horizontal stabilizer and secondary wing structure, F-4 rudder, C-5A wing leading-edge slat, and 707 wing foreflap. Today there are production advanced composite parts on the F-111 and F-14 and scheduled for the F-15.

The static strengths and moduli are shown in Figure 15.2-3 to be superior to most other candidate structural materials. Fatigue characteristics of the basic composite materials in useful structural orientations have also been shown to be superior to other structural materials. It is known that advanced composite materials require protection from lightning strike, erosion, and moisture absorption, but other aircraft environments have no adverse effect on the material, and no particular environmental problem has thus far been found with the articles that are currently in flight test or production use.

One of the interesting features of composite materials is the broad range of performance characteristics that can be realized with proper laminate design. One result of investigating this range of characteristics appears to be the possibility of arresting crack damage occurring in the laminates.

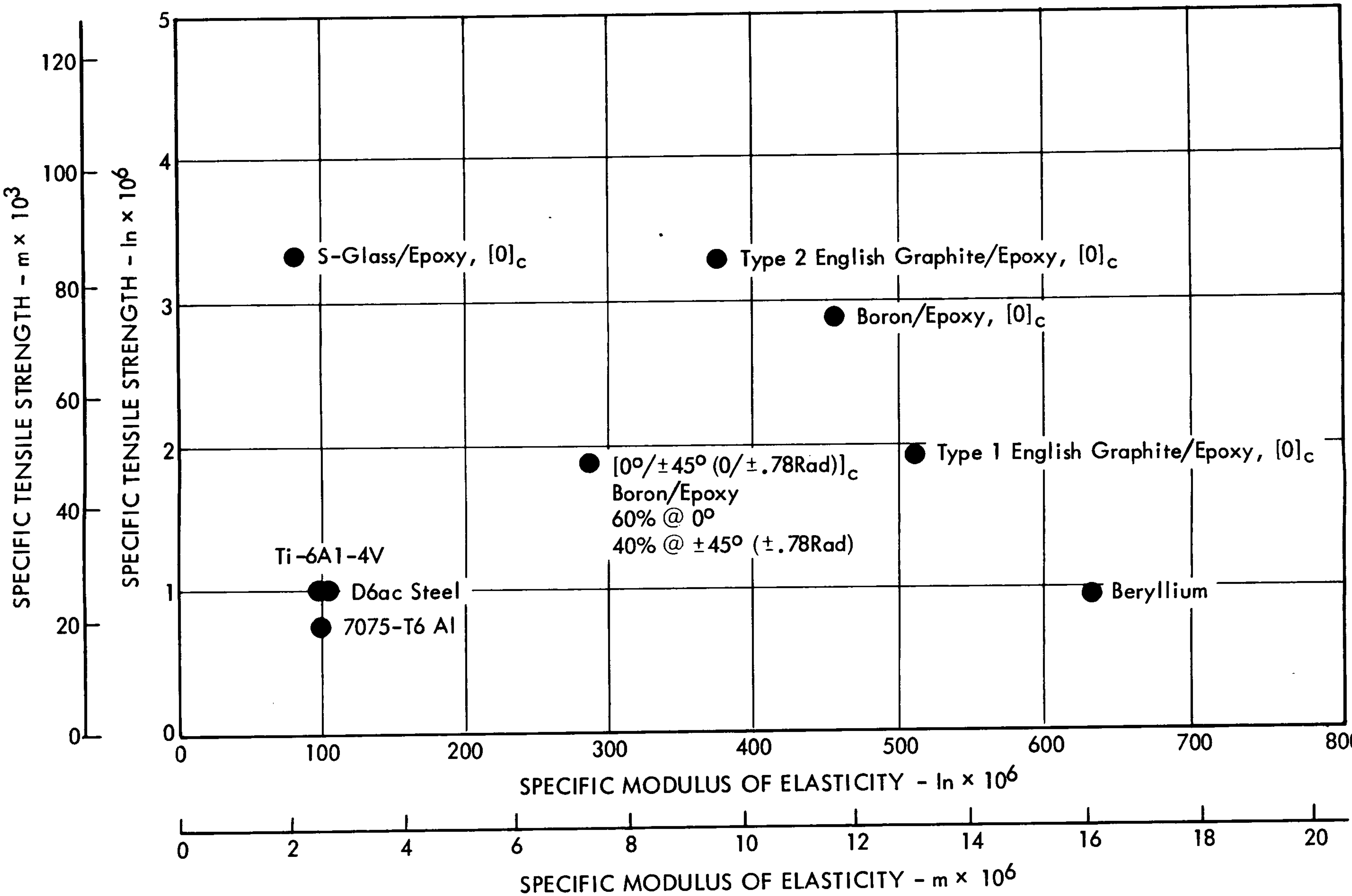

Figure 15.2-3 Specific Properties of Structural Materials

The technique of fabricating a laminate with crack-arresting capability is demonstrated by the model shown in Figure 15.2-4. A structural element carrying primarily axial tension in a high-modulus laminate contains low-modulus strips of width W_2 spaced W_1 apart. The residual strength of the primary laminate initially containing a slit of length 2L is predicted by

$$\sigma_{C_1} = \frac{K_{Q1}}{\sqrt{\pi L}}$$

where K_{Q1} is the critical stress intensity factor of the primary laminate and σ_{C_1} is the critical stress above which the flaw propagates as a fast crack, i.e., one which propagates at constant applied load as in a static test.

As the fast crack enters the low-modulus strips, the new value of critical stress is given by

$$\sigma_{C_2} = \frac{K_{Q2}}{\sqrt{\pi \frac{W_1}{2}}}$$

where K_{Q2} is the critical stress intensity factor of the low-modulus strips and σ_{C_2} is the critical stress above which the fast crack propagates in the low-modulus material.

If the stress, σ_2, in the low-modulus material is sufficiently below σ_{C_2}, the crack will arrest. The area of the remaining primary laminate is intact and capable of sustaining the required fail-safe load level.

The stresses in the high- and low-modulus areas are related by

$$\frac{\sigma_1}{\sigma_2} = \frac{E_1}{E_2}$$

where E_1 and E_2 are the extensional moduli of the two areas.

The criterion for attaining a fail-safe laminate containing a slit of length 2L becomes

$$\left(\frac{K_{Q_1}}{K_{Q_2}}\right)^2 \left(\frac{E_2}{E_1}\right)^2 \leqq \frac{L}{W_1 + 2W_2}$$

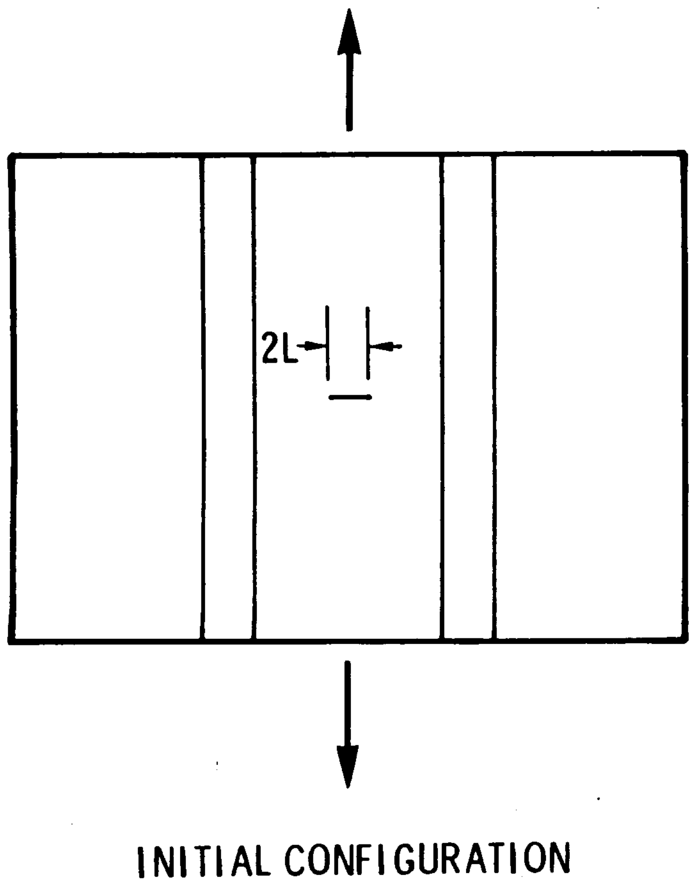

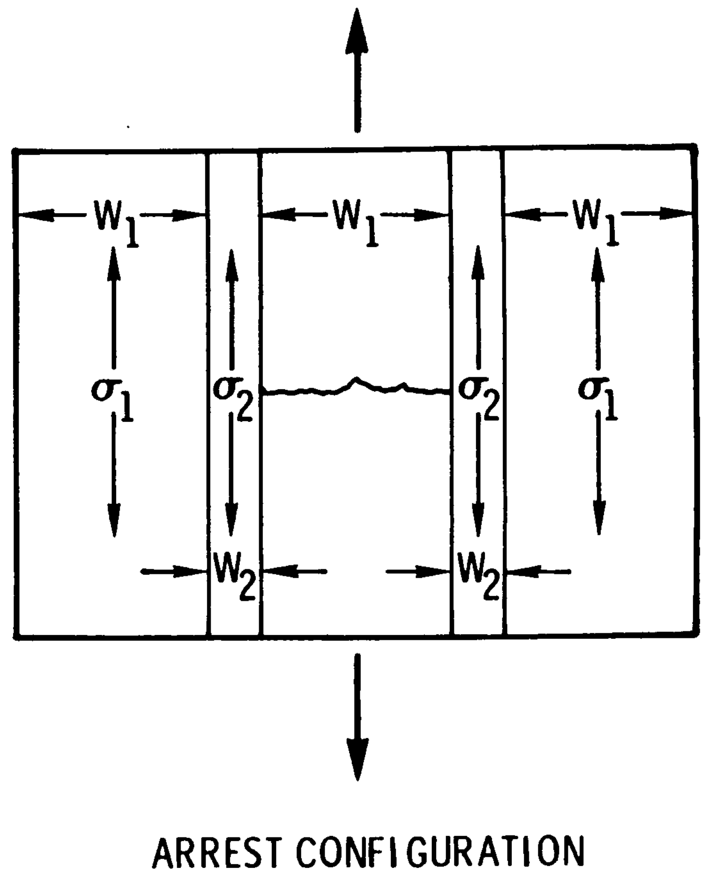

Figure 15.2-4 Fail - Safe Element

A similar development for a laminate containing a circular hole yields the following fail-safe criterion:

$$\left(\frac{K_{Q_1}}{K_{Q_2}}\right)^2 \left(\frac{E_2}{E_1}\right)^2 \leq \frac{a\left[f\left(\frac{a}{r}\right)\right]^2}{\frac{W_1}{2} + W_2}$$

Here (a) and $f(\frac{a}{r})$ define the behavior of a laminate containing a circular hole subject to uniaxial tension (Reference 15-1).

The feasibility of the arrestment concept has been demonstrated in static tests of tensile specimens configured as shown in Figure 15.2-4. The primary laminate was $[0/\pm45^\circ(\pm.78 \text{ rad})/90^\circ(1.57 \text{ rad})]_{2S}$ boron-epoxy with $[\pm45^\circ(\pm.78 \text{ rad})]_{4S}$ boron-epoxy low-modulus strips. The dimensions W_1 and W_2 were 2.0 in. (5.08 cm) and 1.0 in. (2.54 cm), respectively. Experimental results obtained to date are shown in Figure 15.2-5. These results are predictable by the above analysis techniques and have been duplicated in graphite-epoxy. One of the arrested fast cracks is shown in Figure 15.2-6.

Incorporating these approaches to structural design of fuselage and wing hardware with composites will enhance the safety and weight considerations of advanced composites applications. There are several elements of this particular phase of the technology in current development and research activities throughout the industry.

The composite material selected for evaluation of this design and cost study was a graphite-fiber-reinforced plastic. The plastic could be either epoxy or polyester. Graphite reinforcement was selected over boron because of an anticipated lower total aircraft system cost. Although boron preceded graphite in the technology development, many of the structural graphite-reinforced materials are already lower in cost than the boron, with even lower graphite costs predicted as sales volume continues to increase. A second source of lower total costs with graphite is in the manufacture of hardware. Graphite preimpregnated materials are more easily shaped to complex contours during lay-up and are less difficult to machine in cured shapes so that the manufacturing costs are lower than those resulting from use of boron-reinforced materials.

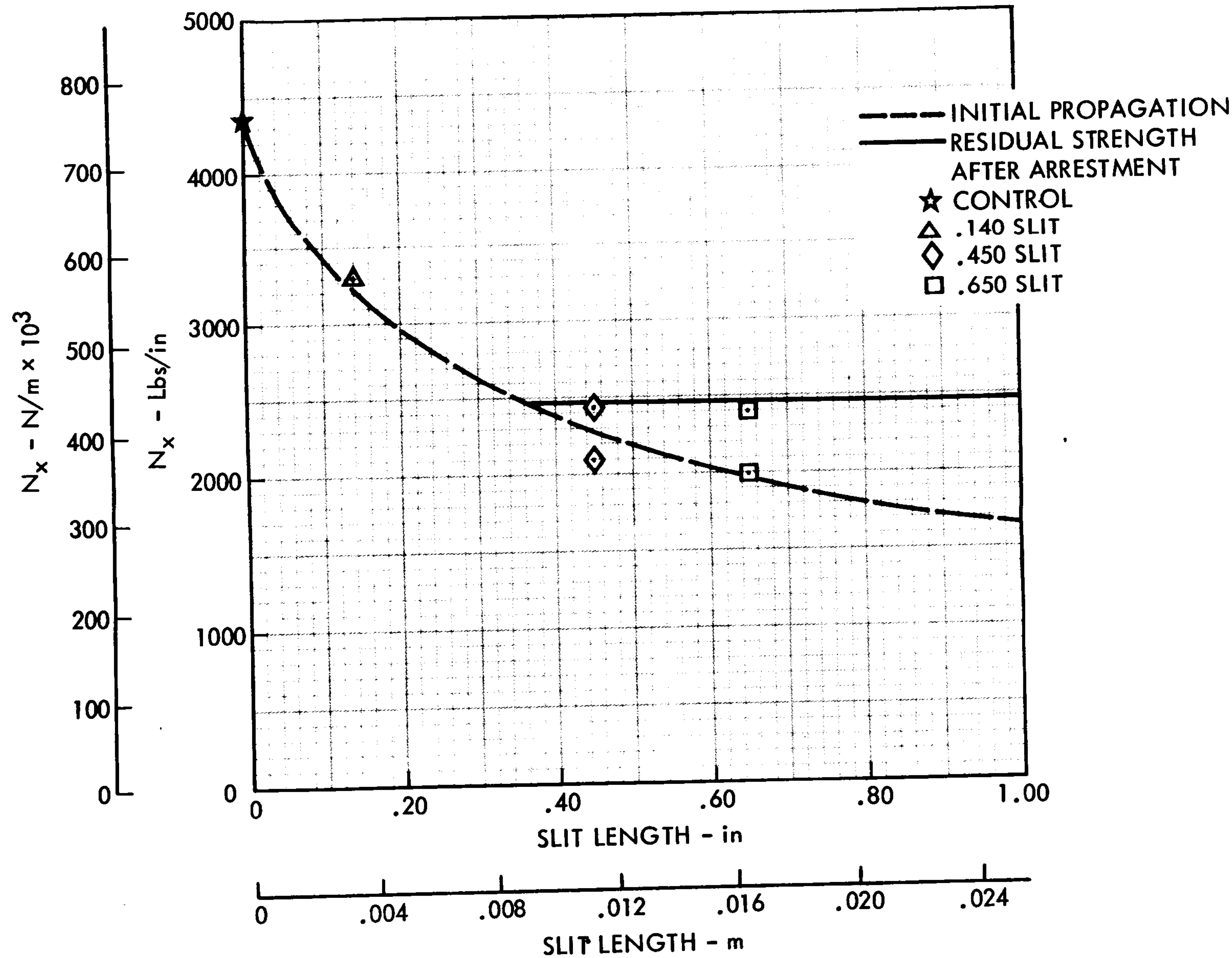

Figure 15.2-5 Arrest Specimen Behavior

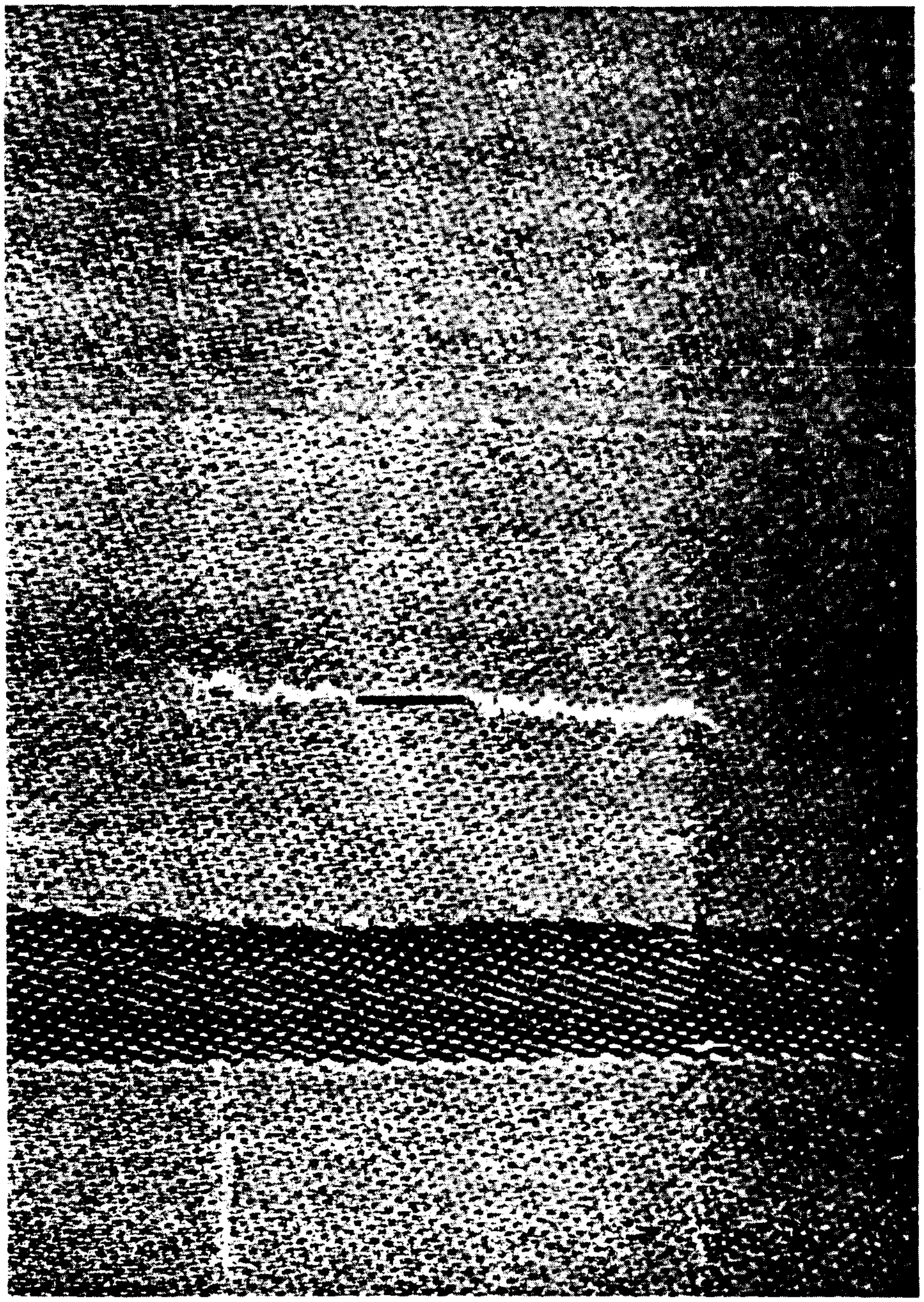

Figure 15.2-6 Arrested Crack

The graphite-fiber-reinforced preimpregnated material assumed available in this study will develop acceptable mechanical properties when cured at a temperature not exceeding 250°F (394°K) in a vacuum-bag environment and over a time span not exceeding 3 hr. The tape material for large parts such as wing and fuselage skins will be 24 in. (.61 m) wide, weighing approximately 165 lb (74.6 kg) in a roll 1320 ft (402 m) in length. The material will be delivered to the work area daily without having to undergo a low-temperature, extended storage stage.

15.3 COMPARATIVE DESIGNS

Particular designs were developed for light-alloy and advanced-composite fuselages and wings to serve as a basis for weight and cost comparisons.

15.3.1 Light-Alloy Design

15.3.1.1 Fuselage

The light-alloy fuselage structural arrangement shown in Figure 15.3-1 is typical of the latest light-alloy design concepts.

A material evaluation and selection process similar to that carried out for the wing and discussed in Subsection 15.2.1 was performed for the fuselage. The resulting list of materials for the fuselage is as follows.

Fuselage Element	Material-Condition
Upper Skin	7475-T761
Side Skin	7475-T761
Lower Skin	7475-T761
Upper Stringers	7475-T761
Lower Stringers	7075-T76
Upper Longerons	X7050-T73511
Lower Longerons	X7050-T73511
Frames (Formed)	7475-T761
Bulkheads (Machined)	7475-T7351 or X7050-T73651
Forgings	7075-T73 or X7050-T73 or 7175-T736 or 7049-T73
Crack Stoppers	6AL-4V (Titanium)

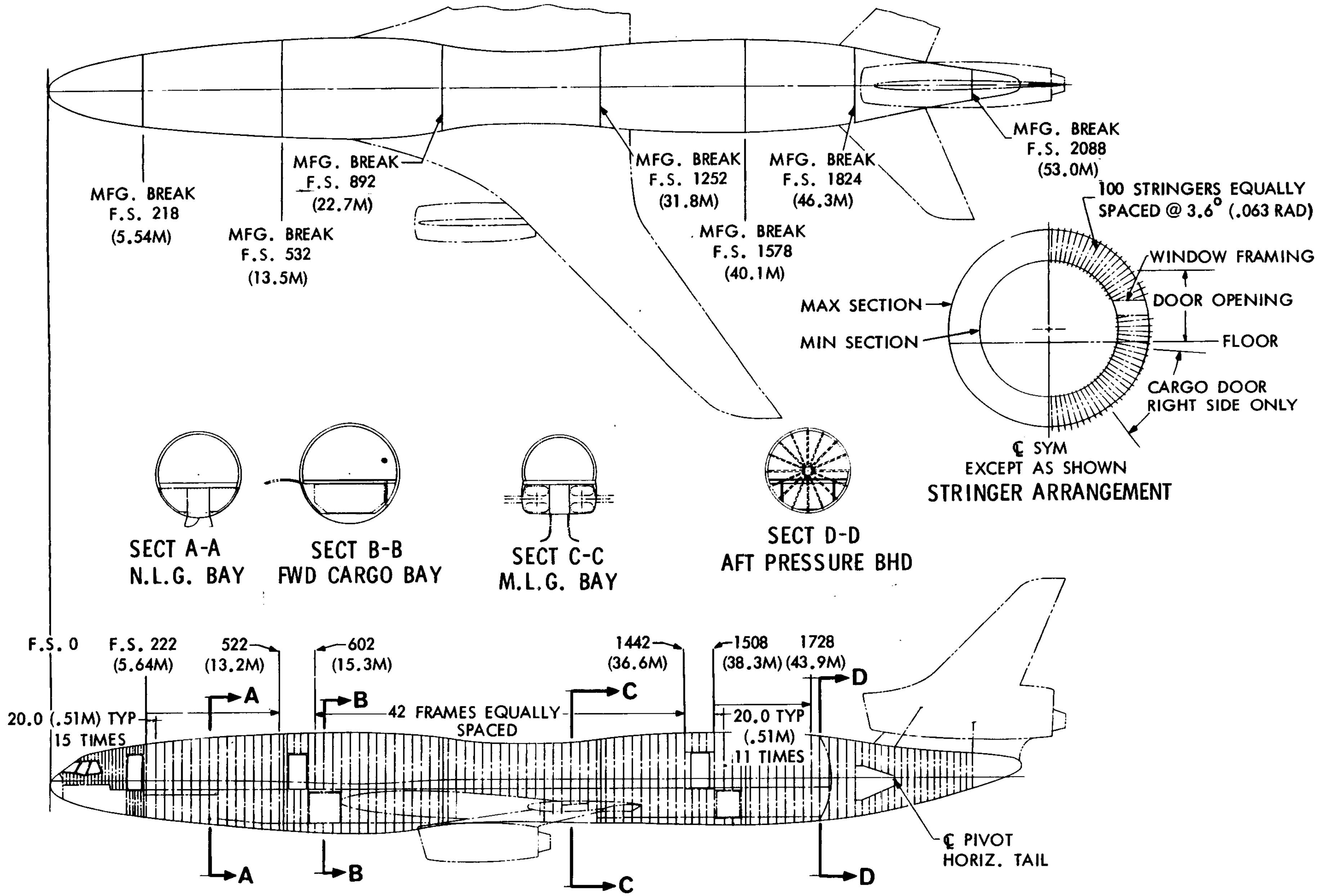

Figure 15.3-1 Light-Alloy - Fuselage Structural Arrangement

The 7475-T761 sheet material was selected over 2024-T3 material for skins and frames because of its better exfoliation resistance, critical crack length, and high tension ultimate.

For extrusions, the X7050 material strength is equivalent to 7075-T6511, and it has much better stress corrosion resistance and fracture toughness. Although 7075-T73 extrusions have slightly better stress corrosion resistance, the X7050 material is preferred because it has higher strength and equivalent fracture toughness and exfoliation resistance.

The forging selection is not quite so clear-cut. For forgings up to 3.0 in. (7.62 cm) maximum, the 7075-T73 is preferred over the 7175-T73 because of lower cost. The 7175-T736 heat-treat material is a single-source product. However, the 7175-T736 does have higher strength and higher fracture toughness. Both X7050-T73 and 7049-T73 are competitive with the 7075-T73 material in the thinner forgings. For hand and die forgings greater than 3 in. (7.62 cm), both X7050-T73 and 7049-T73 are acceptable, but the X7050 does have slightly higher strength and stress corrosion resistance.

15.3.1.2 Wing

The major emphasis of the wing analysis effort was applied to the primary structure box. The structural arrangement of the light-alloy wing is presented in Figure 15.3-2. The structural definition for this configuration was developed largely from a more detailed analysis performed on the original high-performance 0.98M configuration. A comparison between plate-stringer, thick-plate/multi-spar, and sandwich panel designs showed the plate-stringer design to be the more efficient from a weight and manufacturing standpoint. As was the case with the fuselage, the light-alloy design features the latest concepts of construction in the transport industry.

The wing-box materials selection, based on the type analysis described in Subsection 15.2.1, is as follows:

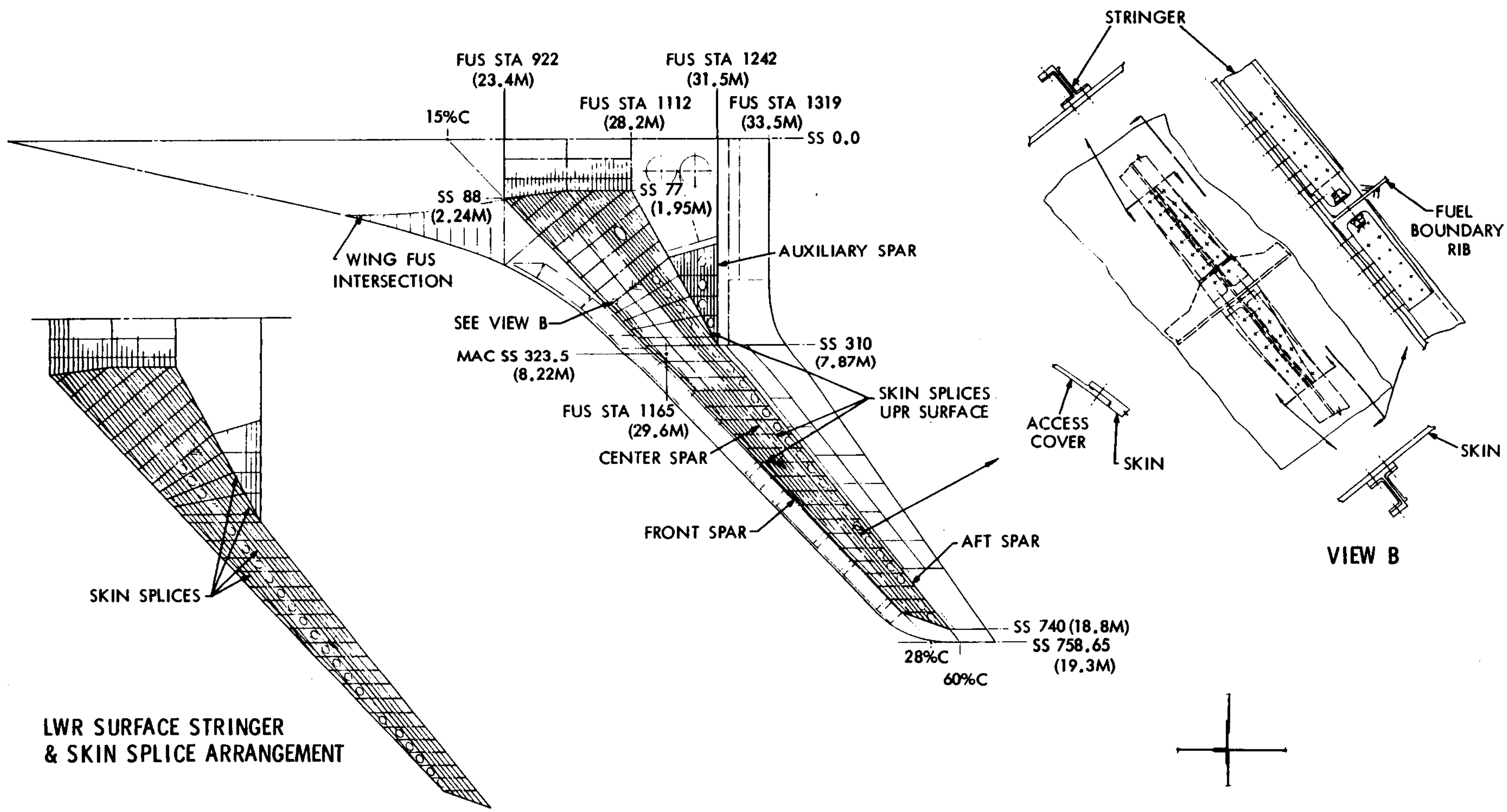

Figure 15.3-2 Light-Alloy - Wing Structural Arrangement

Wing Element	Material Condition
Upper Skin	7475-T7651
Lower Skin	7475-T7351
Upper Stringer	X7050-T73511
Lower Stringer	X7050-T73511
Spar Web-Built-Up	7475-T7651
Spar Caps-Extrusion	X7050-T73511
Rib Webs	7475-T7651
Rib Caps	X7050-T73511
Forgings	7075-T73 or X7050-T73 or 7175-T736 or 7049-T73

15.3.2 Composite Design

15.3.2.1 Fuselage

The composite fuselage structural arrangement is shown in Figure 15.3-3. The fuselage passenger cabin section is designed to be manufactured in three basic skin panels, each approximately 127 ft (39 m) long. A skin splice is located on the top centerline and one along each side at approximately the 120-deg (2.09 rad) point. The strength and weight studies dictated the lower panel to be of sandwich construction stabilized only with frames. The upper two panels were initially laminate skins with stiffeners and frames very similar to concepts employed with conventional light-alloy materials. Additional studies proved this method to be inefficient in composites from a manufacturing approach, and marginal in weight efficiency when compared to all sandwich panel construction. Therefore all three skin panels are finally of sandwich construction. The external and internal facings are graphite laminate with the orientation and thickness tailored to provide the required load-carrying capability (Figure 15.3-4). The core provides buckling stability for the skins and is filled with foam to provide thermal and acoustic insulation and maybe fire resistance.

Sandwich construction is acceptable for advanced composites but perhaps not for light-alloy applications in large structure because of the differences in manufacturing approaches. A co-cured bonding concept (described in Subsection 15.3.2.3) permits the fit of core and skins to be accomplished while the skin is uncured and still flexible. This procedure allows the skins and core to conform prior to

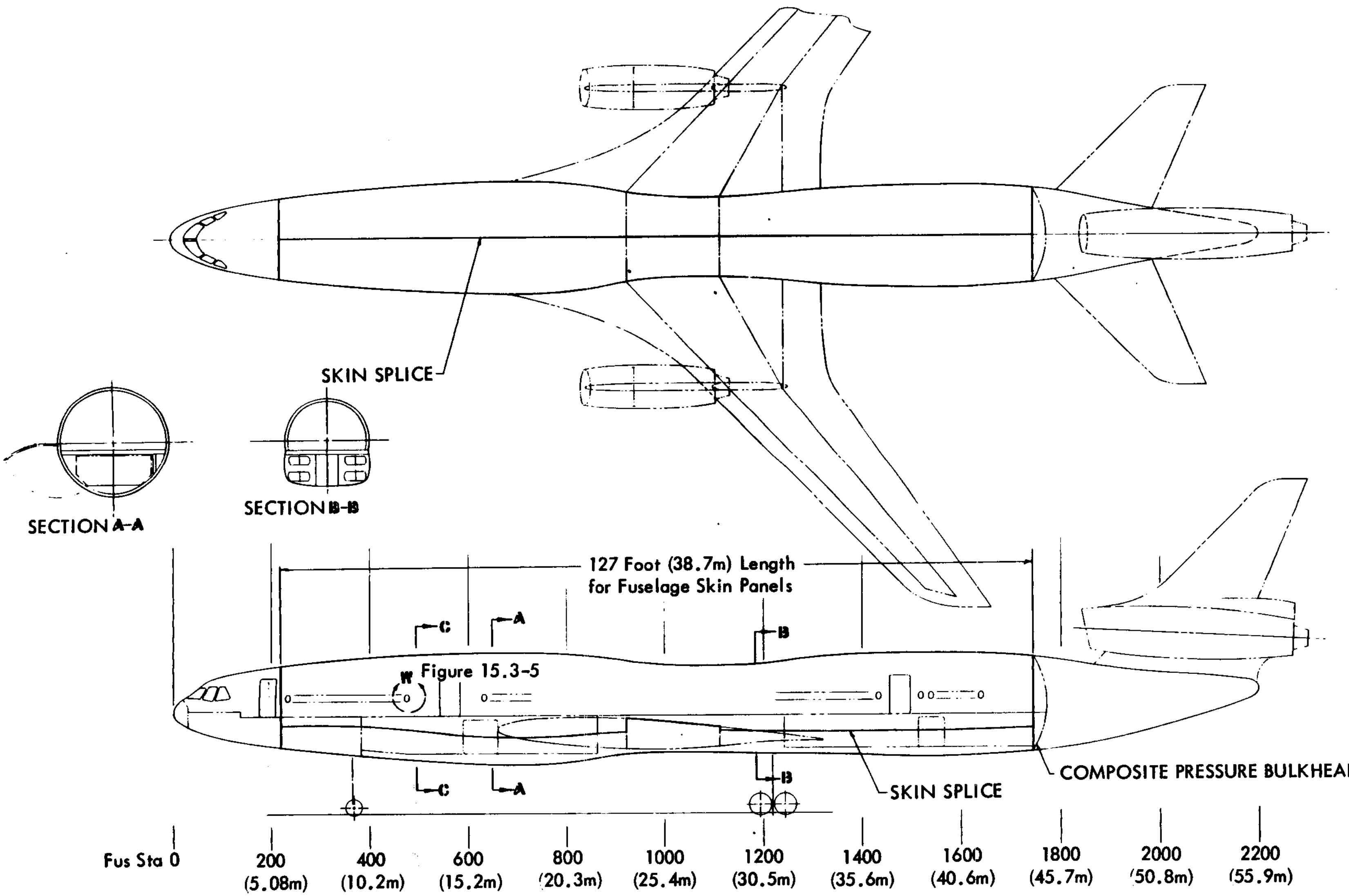

Figure 15.3-3 Composite - Fuselage Structural Arrangement - Planform

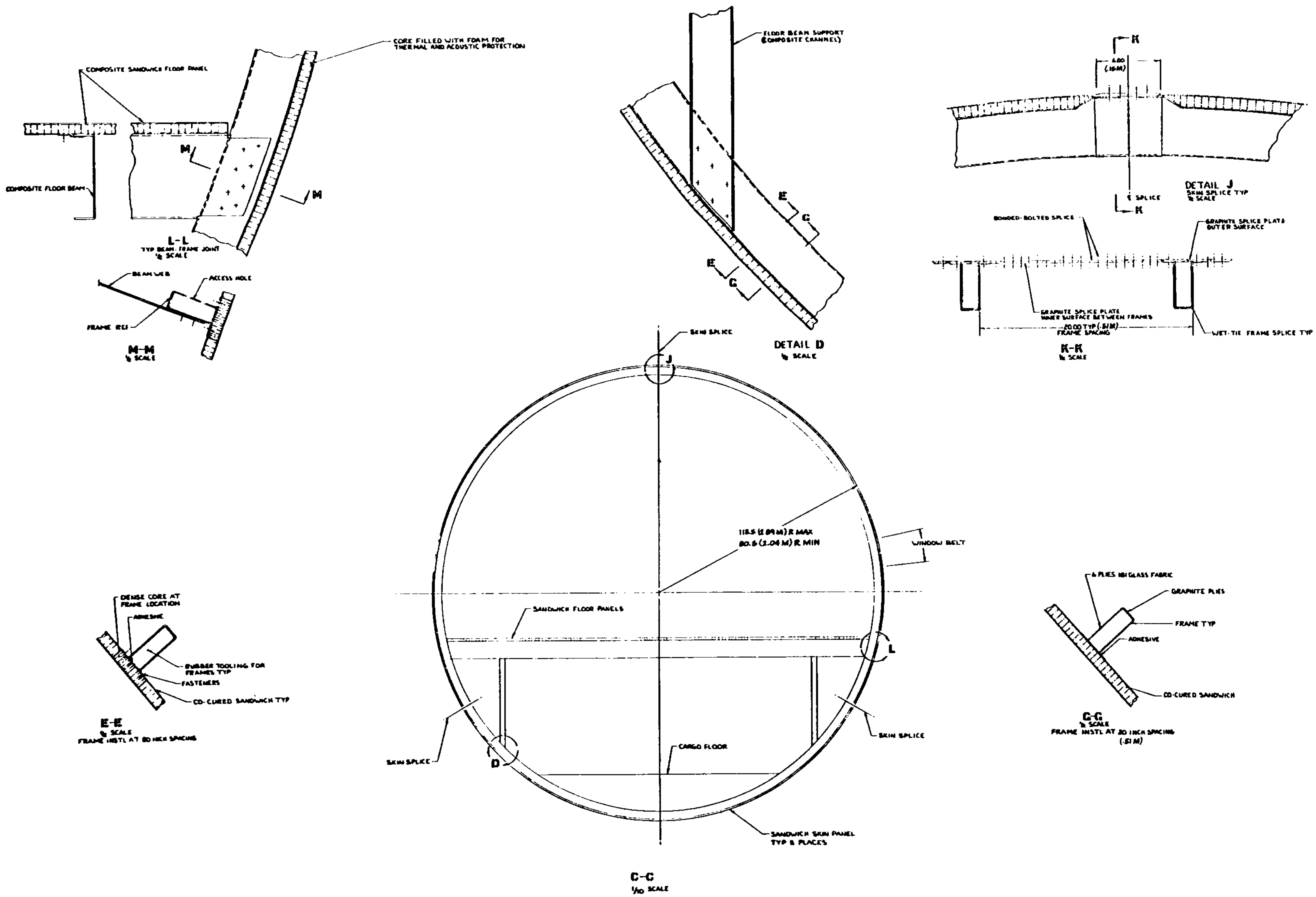

Figure 15.3-4 Composite - Fuselage Structural Detail

bonding and curing and produces good quality bonds. For sandwich bonding of the light alloy skins, great care must be taken to insure good fit between the core and the stiff skins or else areas of poor bonds or voids will result. These problems have prevented extensive use of sandwich construction with light alloy skins but should not be present in sandwich construction with co-cured advanced-composite skins.

Frames are located at approximately 20-in. (0.508 m) spacing to provide overall shell buckling stability. The frames are glass fabric with graphite reinforcing plies added to the cap. All frames are bonded to the skin panels. The bond attachment at approximately every fourth frame and in other local areas is reinforced with fasteners through the frame flange and inner skin face.

The basic shell structure is cut out at the wing box and main wheel well area. Addition of concentrated material in the form of longerons is necessary in this area to provide load-path continuity. The longerons are basically thick sections of longitudinally oriented (zero deg.) graphite plies in the basic skin lay-up.

Major bulkheads are required in the fuselage close to the forward and aft wing spar locations to distribute the concentrated loads into the basic skin panels. The feasibility of composite application to concentrated bulkhead load introductions of a similar type was firmly established in the Phase I Air Force Materials Laboratory fuselage program (Reference 15-2) wherein a bulkhead was successfully designed to introduce concentrated loads in the 120,000-lb (532×10^3 N) range through metallic-reinforced composite lugs.

The core in the upper two fuselage panels is omitted in the window belt area, as shown in Figure 15.3-5. Appreciably thicker basic skin laminate is required in this area because of the large number of window cutouts, thereby deleting the requirement for honeycomb core. The frame arrangement in this area is typical, with the frame inside radius remaining constant and the frame depth increasing slightly to accommodate the decreased skin panel thickness.

The main upper deck and lower cargo floor, both of composite sandwich panel design, employ existing manufacturing techniques in their fabrication and installation.

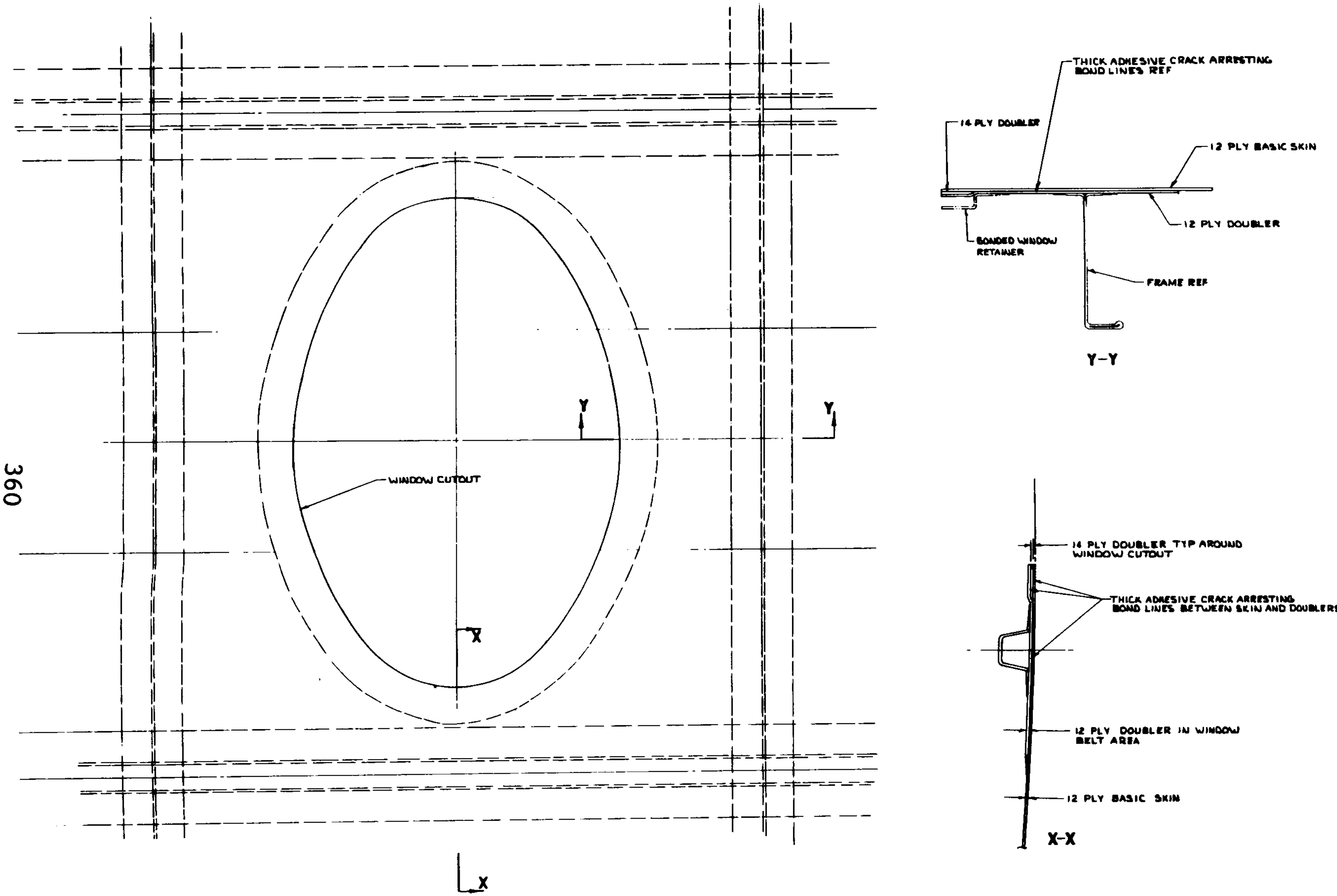

DETAIL W
VIEW LKG INBD AT WINDOW
(REF Figure 15.3-3)

Figure 15.3-5 Composite - Fuselage Window Details

15.3.2.2 Wing

The most efficient usage and, consequently, the greatest benefit which can be derived from the use of composite material in the wing is related to the unique tailoring of the material strength and stiffness characteristics Therefore, both strength and stiffness requirements were considered in the design. The stiffness requirements were derived from the detailed analysis work which was performed on the original high-performance 0.98 M_c configuration.

The philosophy applied in the wing design was to develop a producible, cost-effective concept that was structurally reliable. A driving factor was to take maximum advantage of the continuous property of composites by designing structural elements to be as large as possible. Manufacturing concepts are particularly oriented to the large-continuous-structure approach. Each competing design idea was evaluated to determine which was the most producible and cost effective from a manufacturing standpoint. The designs were revised as necessary to effect the best manufacturing producibility. This interaction between design and manufacturing developed a wing which met the goal of a structurally sound wing that was more producible and more cost effective than a conventional metal wing.

The wing is a continuous structure from tip to tip with one-piece skins, as shown in Figure 15.3-6. Spars are made in one piece from the wing-fuselage intersection to the tip.

The decision to utilize two spars from the wing box rather than three is based upon the desire to limit the number of holes to be placed in the wing skins. This approach simplifies the design procedure through elimination of stress concentrations and lowers the manufacturing costs through the reduction in attachment points. A third spar would complicate the manufacturing procedure through the introduction of aft-bay access holes, interfere with the flap drive mechanisms, and require many rib-to-spar and fuel-bulkhead-to-spar joints. All of these features would result in strength problems and their associated weight penalties.

The attachment of skins to front and rear spars by mechanical fasteners was necessitated by the high shear associated with these members. Since the graphite wing-skin laminates contains a high fraction of filaments in the primary load direction, the pressure of holes for mechanical fastening

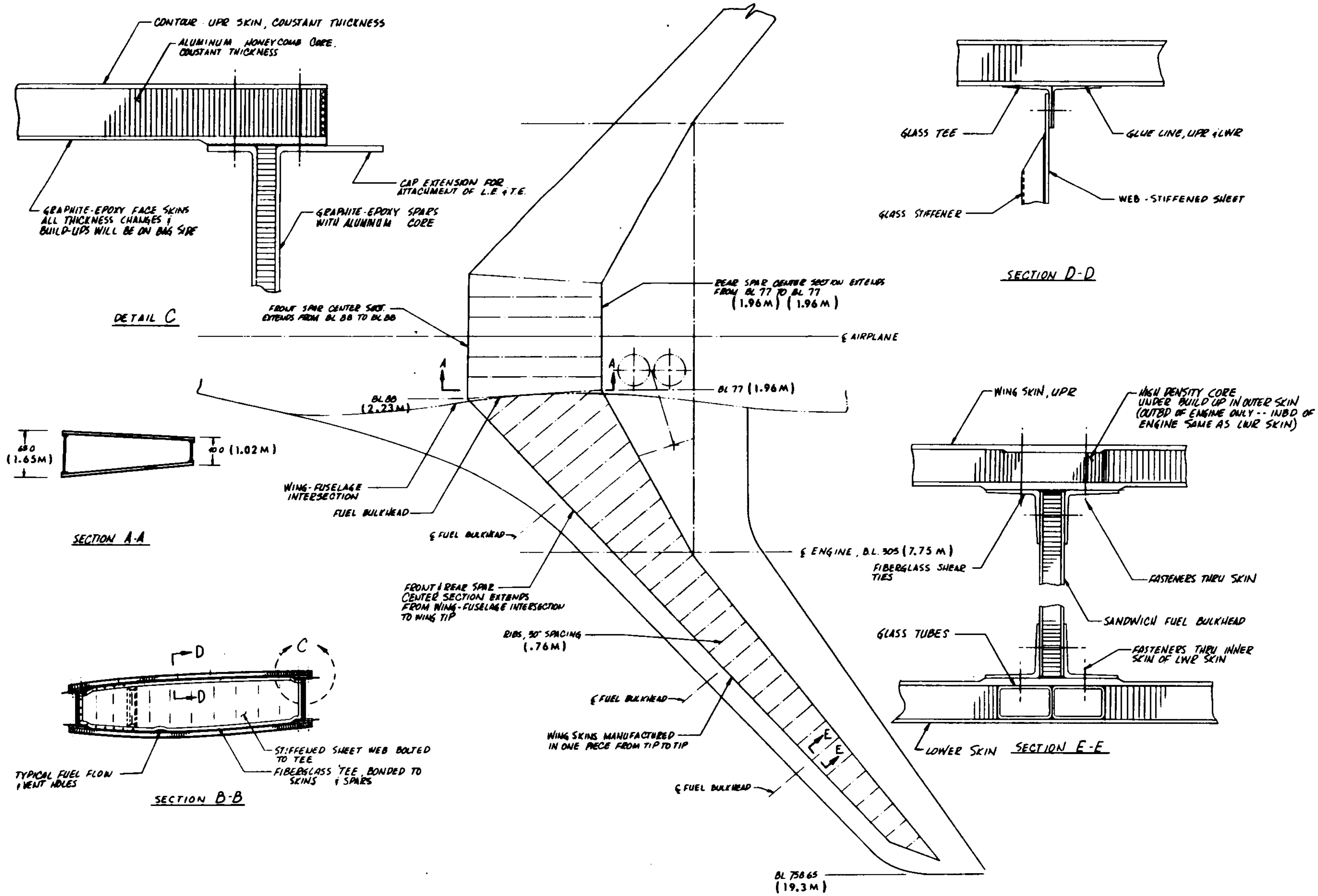

Figure 15.3-6 Composite - Wing Structural Arrangement

creates stress concentrations with a large reduction of tensile strength and low transverse strength, resulting in poor resistance to splitting and shear-out. Chordwise stress levels can be reduced on a gross basis by adding material, but the optimum solution to this problem is to provide strain-tolerant strips consisting of 100 percent of $\pm$ 45-deg ($\pm$.78 rad) plies locally along the bolt lines while retaining the primary structural laminate elsewhere. A discussion of the crack arresting capabilities of strain tolerant strips has been presented in Subsection 15.2.2.

This arrestment technique is particularly applicable to the proposed wing concept for two reasons, both of which serve to reduce the weight penalty incurred by inclusion of buffer strips. First, as shown in Reference 15-3 and 15-4, it is advantageous to include low-modulus strips in the wing skin at the spar locations. This has the effect of eliminating the stress concentration of mechanical fasteners. With slight modification, these strips could serve a dual purpose by acting as crack arresting buffer strips. Second, the majority of the wing skin is stiffness-critical rather than strength-critical. This reduces operating stresses, which allows wider spacing of the buffer strips than is possible in a strength-critical component.

The wing primary structure, i.e. wing-box skins, ribs, and spars are the same type design as described in Subsection 7.2.2; only dimensional differences exist. Several specific additional facts are pertinent to the detailed weight and cost study. They are summarized as follows:

1. At the wing fuselage intersection, the maximum aft spar shear is 18,350 lb/in. (3.19×10^6 N/m) and the maximum front spar shear is 6,240 lb/in. (1.085×10^6 N/m) limit.

2. The wing spar heights vary from 5 ft (1.52 m) at the inboard end to 1 ft (0.305 m) at the tip.

3. The internal fuel pressure requires more extensive sandwich and edge member support in the fuel pressure bulkheads. The usage of fasteners in the fuel-bulkhead-to-wing-skin attachments outboard of the engine-maintaining bulkheads requires inner-skin chordwise buildups to reduce working stresses.

C5

In the case of high-lift devices, three elements of the wing leading- and trailing-edge structure were selected for a cursory design and cost evaluation: the flaps, the vanes, and the Kruger slat nose (Figure 15.3-7). Design concepts are the same as described for these surfaces in Subsection 7.2.3. Other elements such as the spoilers, leading-edge skin, and air director doors can be readily made from advanced composites because parts similar to these have already been manufactured. Because of this, these elements were not treated in this design study.

15.3.2.3 Manufacturing Plan

The manufacturing plan for the composite airframe emphasizes fabrication and assembly of very large parts and utilizes automation in every phase, as shown in Figure 15.3-8. Also, the mass-production concept is emphasized, as demonstrated by the wing and fuselage support area in which very large solid laminate plates are manufactured from which smaller flat patterns are stamped for details. No part is completely fabricated in any one area.

The manufacturing sequence is separated into eight areas as follows:

- Area I - Fuselage and Wing Support
  - IA - Core Preparation
  - IB - Automated Solid-Laminate Layup
  - IC - Automated Sandwich-Panel Layup
- Area II - Sub-Component Fabrication
- Area III - Fuselage Shell Fabrication
- Area IV - Wing Skin Fabrication
- Area V - Wing Assembly
- Area VI - Primary Structure Assembly
- Area VII - High-Lift-Device Fabrication
- Area VIII - Final Assembly

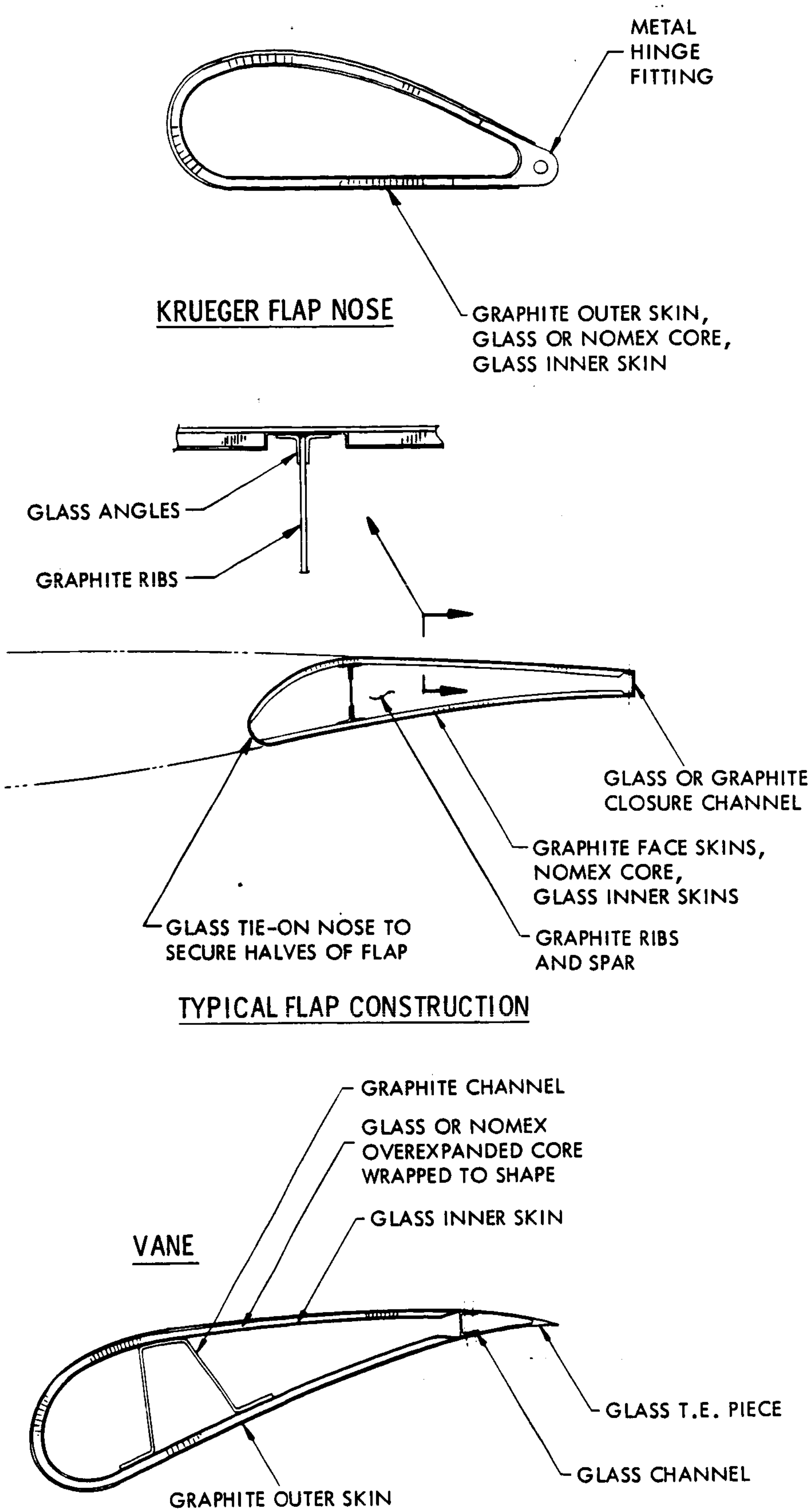

Figure 15.3-7 Composite - Wing High-Lift Devices

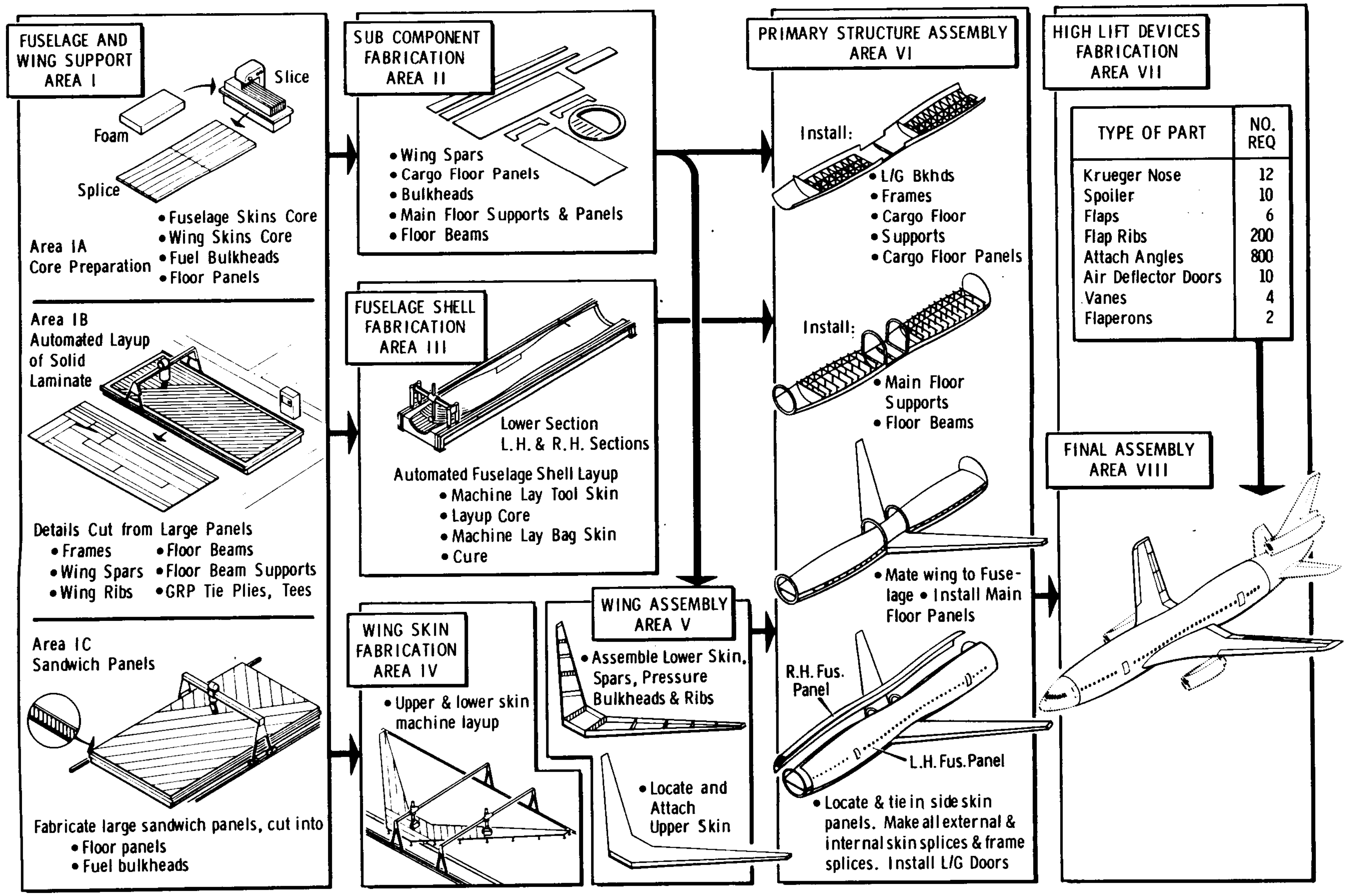

Figure 15.3-8 Composite Airframe Manufacturing Plan

A general description of each work area function is given below in sequence, although many of the functions occur simultaneously.

Area I - Fuselage and Wing Support. The functional setup of this area is based on the types of parts manufactured rather than on aircraft designation. The sub-areas function as follows:

IA - Core Preparation. Blocks of core are foamed (if for the fuselage shell), sliced in a gang saw into the required thickness, and spliced into large sections. From these sections, either smaller details are cut or the large sheets go to fuselage shell or wing skin work areas. All core preparation is accomplished in this work area.

IB - Automated Solid-Laminate Layup. This is an automated tape-laying-machine step in which continuous tape is made into large panels of the required size, thickness, and fiber orientation. Smaller details such as floor beams, supports, and fuselage frames are cut. Machines capable of utilizing several widths of tape are located in this area.

IC - Automated Sandwich-Panel Layup. In this last division of Area I, large, flat sandwich panels are fabricated and cured. The panels may have any required skin thickness, core thickness, and fiber orientation. The basic steps are: automatically lay up one skin, cover it with core, lay up a second skin over the core and cure. This sandwich panel is then cut into any of many sandwich parts such as fuel bulkheads and floor panels.

Area II - Sub-Component Fabrication. Components such as wing spars are fabricated as back-to-back channels with core between them. They are fabricated as follows:

1. Locate a spar skin layup (Area IB) on a male tool with the flange turned down and cure.

2. Locate a core section (Area IA) on the skin and cure.

3. Install side plates on the tool and locate a second spar skin over the core with the flange turned up along either edge and cure.

This process utilizes only one skin tool, requires no assembly fixture, and, since the second skin is bonded wet, requires no bond fixture. All spars are fabricated in the same manner. Similar simple procedures are used to fabricate other indicated components.

Area III - Fuselage Shell Fabrication. Three tools for each of the three basic fuselage-wing shell sections are required to meet the production rate of six aircraft per month. Each group of these tools is served by a simple automated layup machine. Only one tool typical of the nine required is shown. The layup sequence is as follows:

1. Lay up the outer (tool) skin.

2. Position the required sheets of core.

3. Lay up the inner (bag) skin.

4. Core.

5. Move to final assembly line.

Local buildups and window section buildups are fabricated as flat pattern details in Area IB and located in the shell as required. The outer skin is constant thickness.

Area IV - Wing Skin Fabrication. This area is much the same as Area III. Again, only one typical tool of six required is shown. The wing skin layup sequence is:

1. Lay up the outer (tool) skin.

2. Locate the core sheets.

3. Lay up the inner (bag) skin.

4. Cure.

5. Move to Wing Assembly Area V.

Area V - Wing Assembly. The lower wing skin is placed in an assembly fixture, and the front and rear spars are attached by bonding and mechanical fasteners. The ribs and pressure bulkheads are then located, bonded, and bolted in place with precured GRP tie plies. The upper-skin shear is fastened in place by bonding and bolting. The entire wing box is then oven cured.

Area VI - Primary Structure Assembly. The lower fuselage section is located in an assembly fixture and the frames and MLG bulkhead installed first. The cargo floor beams and support subassemblies are then installed along with the cargo floor panels. In the next stage, the main floor beams and support subassemblies are bonded. The wing box is mated to the fuselage, and the left- and right-hand fuselage sections along with skin splices (inner and outer) are installed. Main floor panels are fixed, frame splices are made, and the aft pressure bulkhead installed. Finally, the main landing gear doors are attached.

Area VII - High-Lift Device Fabrication. High-lift devices are manufactured from flat pattern skins from Area IB and from core from Area IA. The parts are cured and moved directly to final assembly. In one month, this area delivers 72 Kruger nose parts, 60 spoilers, 36 flaps, 1200 flap ribs, 4800 attach angles, 60 deflector doors, 24 vanes, and 12 flaperons.

Area VIII - Final Assembly. The high-lift devices from Area VII are added here to the primary structures assembly from Area VI.

15.4 WEIGHT COMPARISONS

The first step in the weight analysis was to establish a reference or baseline light-alloy-configuration weight distribution. The weight of the 2500-ft^2 (231 m^2) wing configuration shown in Figure 15.1-1 was calculated by the statistical/analytical procedure described in Section 14. The application of this procedure established the total configuration weight and permitted the allocation of weights to the individual major structural components: wing, fuselage, horizontal and vertical stabilizers, nacelles, and landing gear.

In the case of the composite component structural weights, the light-alloy weights were used as a reference for identification of non-optimum weight items, and calculated weight differences were subtracted from these reference weights. Results are listed in Table 15.4-1. It is emphasized that both the light-alloy and the composite weights apply to the same sized airplane. The calculated weight savings shown are:

Table 15.4-1

LIGHT-ALLOY/COMPOSITE MANUFACTURING COST STUDY -
WEIGHT BREAKDOWN SUMMARY

Structural Component	Light Alloy		Composite	
	lb	(kg)	lb	(kg)
Wing	41,100	(18,643)	30,900	(14,016)
Fuselage	32,700	(17,100)	26,200	(11,884)
Horizontal Tail	4,300	(1,950)	3,200	(1,452)
Vertical Tail	3,700	(1,678)	3,000	(1,361)
Nacelles	7,400	(3,357)	6,700	(3,039)
Landing Gear	12,300	(5,624)	12,300	(5,579)
Structural Wt. Total	101,500	(48,352)	82,300	(37,331)

Component	Percent Weight Saved
Wing	25
Fuselage	20
Horizontal Tail	26
Vertical Tail	19
Nacelles	10
Landing Gear	0
Total Airframe	19

In applying the results of this weights comparison to the development of the selected configurations, the cascading effect involved in resizing the aircraft as the structural weight decreases is apparent. The ratios of the weight of composites used to weight saved that are developed in Subsection 15.4.3 were employed in sizing the selected configurations. The cascading effect is well illustrated by comparing the .90M light-alloy, no-active-control-system airplane with the .90M all-composite, no-active-control-system airplane described in Tables 14.1-1, 14.1-3, and 14.1-4 presented in Section 14. The effect of composite applications on the resizing process is summarized as follows:

Component	Percent Weight Saved
Wing	33
Fuselage	21
Horizontal Tail	40
Vertical Tail	27
Nacelle	19
Landing Gear	13
Total Airframe	26

Weight area change = -12.5 percent

Engine scale change = - 9.8 percent

The development of fuselage and wing structural weights that were used in the manufacturing cost analysis is explained in the following subsections.

15.4.1 Fuselage Weight Breakdown

A summary of the fuselage weight breakdown is given in Table 15.4-2. For both the light-alloy and the composite designs, the listed elements of the cabin structure were further broken down for detailed geometrical definition and weight of individual items such as frames and bulkheads. This detail affords the best opportunity for a realistic cost comparison.

15.4.2 Wing Weight Breakdown

The light-alloy wing weight breakdown is shown in Table 15.4-3. As with the primary structure of the fuselage, additional detailed element definition and breakdown was developed for the cost analysis study. Individual rib web heights and widths were defined as well as individual rib weights. Secondary structure individual item weights were estimated on the basis of the weight distribution of similar items on current aircraft.

The weight breakdown for the composite material wing is shown in Table 15.4-4. The primary structural box weights were, in general, developed from stress analysis calculations at four selected section cuts. The weights for fixed items in the primary box such as fittings, seals, and miscellaneous were assumed to be the same as estimated for the light-alloy wing box. The secondary structure weights were obtained by using the light-alloy distribution as a reference baseline and estimating the weight of the individual items applicable to composite uage.

15.4.3 Composite-to-Light-Alloy Weight Ratios

Two types of ratios are necessary for a proper assessment of the impact of the use of composite materials in a modern transport. The first is the set of ratios of the individual composite component weight to the corresponding light-alloy component weight. It is necessary to establish

Table 15.4-2

LIGHT-ALLOY/COMPOSITE MANUFACTURING COST STUDY

FUSELAGE WEIGHT BREAKDOWN

Structural Element	Light Alloy Element Weights lb	Light Alloy Element Weights (kg)	Composite Element Weight lb	Composite Element Weight (kg)	% Savings
Primary Structure					
Skins-Stringer-Longerons	13,112	5,948	10,030	4,550	24.0
Frames	2,975	1,349	2,260	1.025	24.0
Bulkheads	1,282	582	1,282	582	0
Windown Framing	1,444	654	-	-	-
Misc.	1,854	841	1,854	841	0
Total	20,667	(9,374)	15,426	(6,998)	25.2
Secondary Structure					
Floors-Beams-Supports	4,349	(1,973)	4,010	1,819	7.5
Window Glass	944	(428)	944	428	0
NLG Door-Mech-Jamb	156	(71)	156	71	0
MLG Door-Mech-Jamb	709	(322)	609	276	14.0
Pass Door-Mech-Jamb	1,129	(512)	969	440	14.4
Cargo Door-Mech-Jamb	787	(357)	680	308	13.5
Large Fittings	540	(245)	540	245	0
Small Fittings	320	(145)	320	145	0
Misc.	307	(139)	307	139	0
Total	9,241	(4,192)	8,535	3,871	7.8
Total Weight-Fus. Sta. 222-1728	29,908	(13,566)	23,961	(10,869)	20.0
Other Weight (Not Applicable to Cost Study)	2,826	(1,282)	2,260	(1,025)	20.0
Total Fuselage Weight	32,734	(14,848)	26,221	(11,894)	20.0

Table 15.4-3

LIGHT-ALLOY/COMPOSITE MANUFACTURING COST STUDY - WING WEIGHT BREAKDOWN FOR LIGHT ALLOY

Structural Element	Leading Edge lb (kg)	Trailing Edge lb (kg)	Glove lb (kg)	L.E. Slats lb (kg)	Ailerons lb (kg)	Spoilers lb (kg)	Flaps lb (kg)	Basic Box lb (kg)	Secondary Structure lb (kg)	Total lb (kg)
Covers	606 (275)	440 (200)	235 (107)	1142 (518)	378 (171)	386 (175)	986 (447)	11119 (5044)	517 (235)	15789 (7162)
Stiffeners	62 (28)	100 (45)	26 (12)	128 (58)		230 (104)		6543 (2968)	196 (89)	7290 (3307)
Ribs (Webs, Caps & Stiffeners	481 (218)	40 (18)	187 (85)	239 (108)			456 (207)	1481 (672)	148 (67)	3032 (1375)
Spars (Webs, Caps & Stiffeners)	64 (29)	35 (16)	25 (11)	-	515 (234)		275 (125)	2227 (1010)	161 (73)	3302 (1498)
Joints & Fasteners & Splices	50 (23)	35 (16)	19 (9)	-				2054 (932)	97 (44)	2255 (1023)
Aerodynamic Seals	99 (45)	18 (8)	38 (17)	76 (34)				300 (136)	4 (2)	535 (243)
Small Fittings	141 (64)	-	55 (25)	616 (279)	234 (106)	62 (28)	56 (25)	757 (343)	23 (10)	1944 (882)
Large Fittings				303 (137)	102 (46)	88 (40)	2881 (1307)	728 (330)	354 (161)	4456 (2021)
Closure				168 (76)	32 (15)					200 (91)
Vanes or Wedges							582 (264)			582 (264)
Bushings & Bearings							303 (137)			303 (137)
Carriage							804 (364)			804 (365)
Miscellaneous				172 (78)	55 (25)			267 (121)		494 (224)
Finish & Sealant									150 (68)	150 (68)
Total	1503 (682	668 (287)	585 (266)	2844 (1290)	1316 (597)	766 (347)	6343 (2877)	25481 (11558)	1650 (749)	41136 (18659)

50% of small fittings are steel, 35% are aluminum and 15% are titanium
80% of large fittings are steel, 15% are aluminum and 5% are titanium
100% of bushings, bearings and carriages are steel
50% of joints & fasteners are steel, 25% are aluminum and 25% are titanium

Table 15.4-4

LIGHT-ALLOY/COMPOSITE MANUFACTURING COST STUDY - WING WEIGHT BREAKDOWN FOR COMPOSITES

Structural Element	Leading Edge lb (kg)	Trailing Edge lb (kg)	Glove lb (kg)	L.E. Slats lb (kg)	Ailerons lb (kg)	Spoilers lb (kg)	Flaps lb (kg)	Basic Box lb (kg)	Secondary Structure lb (kg)	Total lb (kg)
Skins (Sandwich)	534 (242)	432 (196)	183 (83)	1015 (460)	227 (103)	345 (156)	592 (269)	8520 (3865)	466 (211)	12314 (5586)
Ribs (56 + 11) = 67	433 (196)	36 (16)	168 (76)	215 (98)			342 (155)	1721 (781)	126 (57)	3041 (1379)
Spars	58 (26)	31 (14)	22 (10)		386 (175)	92 (42)	206 (93)	2019 (916)	124 (56)	2938 (1333)
Joints, Fasteners & Splices	75 (34)	53 (24)	28 (13)		52 (24)	62 (28)	98 (44)	2135 (968)	145 (66)	2648 (1201)
Aerodynamic Seals	99 (45)	18 (8)	38 (17)	76 (34)				300 (136)	4 (2)	535 (243)
Small Fittings	141 (64)		55 (25)	616 (279)	234 (106)	62 (28)	56 (25)	757 (343)	23 (10)	1944 (882)
Large Fittings				303 (137)	102 (46)	88 (40)	2881 (1307)	728 (330)	354 (161)	4456 (2021)
Closure				168 (76)	32 (15)					200 (91)
Vanes or Wedges							408 (185)			408 (185)
Bushings & Bearings							303 (137)			303 (137)
Carriage							804 (365)			804 (365)
Miscellaneous								1111 (504)		1111 (504)
Finish & Sealant									150 (68)	150 (68)
Total	1340 (607)	570 (258)	494 (224)	2393 (1084)	1033 (469)	649 (294)	5690 (2580)	17291 (7843)	1392 (631)	30852 (13927)
% Savings	10.8%	14.7%	15.6%	15.9%	21.5%	15.3%	10.3%	32.1%	14.6%	25%

50% of small fittings are steel, 35% aluminum and 15% titanium
80% of large fittings are steel, 15% aluminum and 5% titanium
100% of bushings, bearings and carriages are steel
50% of joints, fasteners are graphite, 20% steel, 25% titanium and 5% adhesive

these ratios at the component level rather than the total configuration level because there is sufficient variation in the component weight increments with component geometry variation (but with no gross weight variation) to affect the total configuration weight. The use of ratios of component composite to light-alloy geometry especially permits the optimum wing selection to be made by permitting weight and geometric variations to be traded off through configuration performance analyses. The ratio of composite to light-alloy weight for the wing varies with wing geometry. A relationship of this variation, established in Phase I, was used in establishing the composite wing structural weights for the Phase II matrix of configurations. This weight and cost analysis further verified that the relationship is reasonably valid by indicating a wing weight ratio of .75, which represents a 25-percent weight savings as shown on Table 15.4-4. A ratio of composite to light-alloy fuselage weight of .80 is indicated by the weight data of Table 15.4-2. This ratio has been used to determine the composite fuselage weights in the configuration selection analyses.

The second type of ratio needed for cost comparison studies is the ratio of the amount of composites used to the amount of weight saved. Table 15.4-5 shows the weights data generated by the weight analysis and the development of the ratio of composite weight used to weight saved for the fuselage. Similar data are shown in Table 15.4-6 for the wing. A ratio of weight used to weight saved of 1.5 is used for the horizontal and vertical stabilizers. This value is slightly conservative when compared to detailed analyses performed on other aircraft configurations. A ratio of 1.0 used for the nacelle is based on a nacelle analysis carried out in detail on a large military aircraft configuration.

In summary, the ratio of component composite to light-alloy weight is used in the configuration selection process to establish the composite-component weight from known (established by statistical/analytical method) light-alloy weights. The total configuration weight is then determinable for any combination of composite component usage and is available for performance analyses. The weight saved is obtained and is multiplied by the ratio of weight of composites used to the weight saved to establish a component composite weight-used value. The amount of composites used is then available for application to the cost analysis.

Table 15.4-5

COMPOSITE-FUSELAGE GRAPHITE USAGE

Structural Element	Element Weight lb	Element Weight (kg)	Graphite Weight lb	Graphite Weight (kg)
Primary Structure				
Skins-Stringers-Longerons	10,030	(4,550)	6,150	(2,790)
Frames	2,260	(1,025)	2,260	(1,025)
Bulkheads	1,282	(582)	-	-
Window Framing	-	-	-	-
Misc.	1,854	(841)	1,040	(472)
Secondary Structure				
Floors-Beams-Supports	4,010	(1,819)	2,990	(1,356)
Window Glass	944	(428)	-	-
NLG Door-Mech-Jamb	156	(71)	78	(35)
MLG Door-Mech-Jamb	609	(276)	153	(69)
Pass Door-Mech-Jamb	969	(440)	290	(132)
Cargo Door-Mech-Jamb	680	(308)	205	(93)
Large Fittings	540	(245)	-	-
Small Fittings	320	(145)	-	-
Misc.	307	(139)	150	(68)
Total Weight-Fus.Sta. 222-1728	23,961	(10,869)	13,316	(6,040)
Other Weight	2,260	(1,025)	1,600	(726)
Total Composite Fuselage Wt.	26,221	(11,894)	14,916	(6,766)

Total Light Alloy Fuselage Wt. 32,734# (14,848) kg

Total Weight Saved = 32,734 - 26,221 = 6,513# (1,340) kg

The Ratio of $\frac{\text{Weight of Composites Used}}{\text{Weight Saved}} = \frac{14916}{6513} = 2.29$

Table 15.4-6

COMPOSITE-WING GRAPHITE USAGE

Structural Element	Element Weight lb	(kg)	Graphite Weight lb	(kg)
Primary Structure Basic Box	17,291	(7,843)		
Wing Skins			5,840	(2,649
Spars - Rear			776	(352)
Front			720	(327)
Ribs			789	(358)
Joints			1,065	(483)
Secondary Structure				
Leading Edge	1,340	(608)		
Trailing Edge	570	(259)		
Glove	494	(224)		
L. E. High-Lift	2,393	(1,085)		
Ailerons	1,033	(469)		
Spoilers	649	(294)		
Flaps	5,690	(2,581)		
MLG Door	48	(22)		
Misc.	1,344	(610)		
Skins			2,950	(1,338)
Ribs			606	(275)
Spars			780	(354)
Joints, Fast.			255	(116)
TOTAL	30,852	(13,995)	13,781	(6,252)

Total Light Alloy Wing Wt. = 41,136# (18,659 kg)

Total Weight Saved = 41,136 - 30,852 = 10,284# (4,664 kg)

$$\text{The Ratio of } \frac{\text{Weight of Composites Used}}{\text{Weight Saved}} = \frac{13,781}{10,284} = 1.34$$

15.5 COST COMPARISONS

From the design study discussed above, the maximum amount of information could be provided to the cost estimators in the time period permitted. The final output of the cost study is in the form of comparative data between the manufacturing costs of the light-alloy and composite airframes. These data were then used in the economic analysis reported in Section 6. The data obtained are presented in Tables 15.5-1, -2, and -3. Because the goal of this study was to obtain a respectable comparison between the expected manufacturing costs of the composite design and those of light-alloy design, some discussion of the resulting data in light of that goal is warranted.

The most significant single result of the study is presented in Table 15.5-1, where the manufacturing costs of the light-alloy design exclusive of materials and engineering are seen to be 2.6 percent greater than those for the composite design of the same airframe configuration. On the basis of manufacturing departments, this difference in cost comes primarily from the less costly tooling associated with the composites manufacturing plan. On the basis of total costs of airframe components, the difference comes from the reduced costs of the composite wing box and fuselage.

The role of the factory operations in the manufacturing costs of both light-alloy and composite designs is shown in Table 15.5-2. The relationship of the fuselage to other component manufacturing costs is shown in Table 15.5-3.

As discussed in Subsection 15.3.2.1, in the original design of the composite fuselage, sheet-stiffened structure was used in two of the fuselage segments. But in the final design, sandwich structure was used exclusively. The data in Table 15.5-1 are based on the final design. For comparison, the cost data on the original composite fuselage design are presented in Table 15.5-4.

Table 15.5-1

RELATIVE MANUFACTURING COSTS OF LIGHT-ALLOY AND COMPOSITE AIRFRAMES

Component	Light Alloy Manhours/Composite Manhours			
	Tooling	Factory	Q.A.	Total
Fuselage				
Non-Recurring	1.506	-	1.461	1.505
Recurring	1.487	1.005	0.862	1.020
Total	1.496	1.005	0.867	1.053
Wing Box				
Non-Recurring	1.502	-	21.000	1.526
Recurring	1.518	1.453	1.379	1.444
Total	1.510	1.453	1.386	1.448
Wing Leading Edge*				
Non-Recurring	0.888	-	1.000	0.889
Recurring	0.983	0.513	0.493	0.536
Total	0.939	0.513	0.495	0.553
Wing Trailing Edge*				
Non-Recurring	1.268	-	1.273	1.268
Recurring	1.326	0.731	0.701	0.759
Total	1.299	0.731	0.704	0.784
Total	1.392	0.992	0.986	1.026

* These items have only been treated in a cursory manner, and more detailed analysis would be fruitful.

Table 15.5-2

RELATIVE MANUFACTURING COSTS OF FACTORY
AND OTHER DEPARTMENTS

Design	Factory Manhours/Other Department Manhours				
	Fuselage	Wing Box	Wing L.E.	Wing L.E.	Total
Light-Alloy Total	0.668	0.734	0.684	0.686	0.697
Composite Total	0.700	0.731	0.736	0.735	0.721

Table 15.5-3

RELATIVE MANUFACTURING COSTS OF FUSELAGE
TO OTHER COMPONENTS

Design	Fuselage Manhours/Other Component Manhours			
	Tooling	Factory	Q.A.	Total
Light-Alloy Total	0.474	0.357	0.336	0.372
Composite Total	0.441	0.352	0.355	0.363

Table 15.5-4

RELATIVE MANUFACTURING COSTS OF LIGHT-ALLOY
AND ORIGINAL COMPOSITE FUSELAGE

Costs	Light-Alloy Manhours/Composites Manhours			
	Tooling	Factory	Q.A.	Total
Non-Recurring	1.506	-	1.461	1.505
Recurring	1.487	0.849	0.599	0.841
Total	1.496	0.849	0.603	0.879

SECTION 16

MAINTENANCE

The maintenance features of the advanced aircraft configurations described in this report are basically the same as present day wide-body transport aircraft with the exception of the maintenance of composite structures and advanced flight control systems. The unique maintenance problems in these two areas are discussed in the following subsections. In addition, a description is given of the onboard data recording and equipment monitoring system, ground servicing, and engine maintenance.

16.1 COMPOSITE STRUCTURES MAINTENANCE

The structure in future aircraft built mostly from composite materials will be simpler to maintain than the conventional light-alloy structure used in today's aircraft. The aircraft constructed primarily from advanced composite materials will have much larger detail parts and therefore significantly fewer joints and riveted areas. The composite material is also more resistant to fatigue damage, resulting in increased service life and decreased inspection requirements.

16.1.1 Surfaces

Surface corrosion is not so severe with composite structures as with metal aircraft. Composite surfaces, however, do need protection from moisture absorbtion. This can best be achieved through the use of a surface coating. One of these, a polyurethane coating, is presently being evaluated on the F-111 boron-epoxy tail.

16.1.2 Joints

Permanent joints in composite structures do not present any significant maintenance problems. A real problem exists, however, in protecting part edges and fastener holes such as those around access doors. Solutions must be developed for the prevention of fastener erosion and moisture absorption into the exposed composite edge.

16.1.3 Electrical/Electromagnetic Interference

Since the composite is essentially a non-conductor, the surface must be provided with a conductor. Two systems are presently feasible: conductive coatings such as a silver filled paint or a wire mesh. Both systems are presently being evaluated in the F-111 boron tailplanes. The wire mesh is expensive and difficult to repair. The attractive approach, a sprayable, conductive coating, is recommended for further development.

16.1.4 Repairability

The composite aircraft can be repaired regardless of the extent of damage, although it might be economically desirable to install a new part in some cases. The fact that repairs can be made with parent materials and that the repaired component retains 100 percent of its design load carrying capability is a distinct advantage over metal aircraft.

Most damage to composite parts falls into one of three basic categories: surface (outer) skin; surface skin and core; or surface skin, core, and inner skin. All such types of damage are repairable, being different only in the time and material involved.

Outer skin - This type of damage requires the removal of damaged (delaminated) material and the replacement with new material and an adhesive. Such repairs can be accomplished in a vacuum bag and oven at temperatures not greater than 350^{o}F (449.7^{o}K).

Outer skin and core - This type of damage is repaired by removal of the skin in the damaged area and rework of the core. The core may be reworked by filling the damaged area flush with filler or removing the damaged core and replacing it with undamaged core. The skin repair is accomplished as in the repair above.

Outer skin, core, and inner skin - Damage to both skins and core is repaired by removal of a section of outer skin large enough to remove all damaged skin as follows:
(1) Remove the core in the damaged area to expose the inner skin; (2) Remove all of the damaged material in the inner skin; (3) Prepare a repair (replacement) panel as shown in Figure 16.1-1; (4) Locate the replacement panel in the

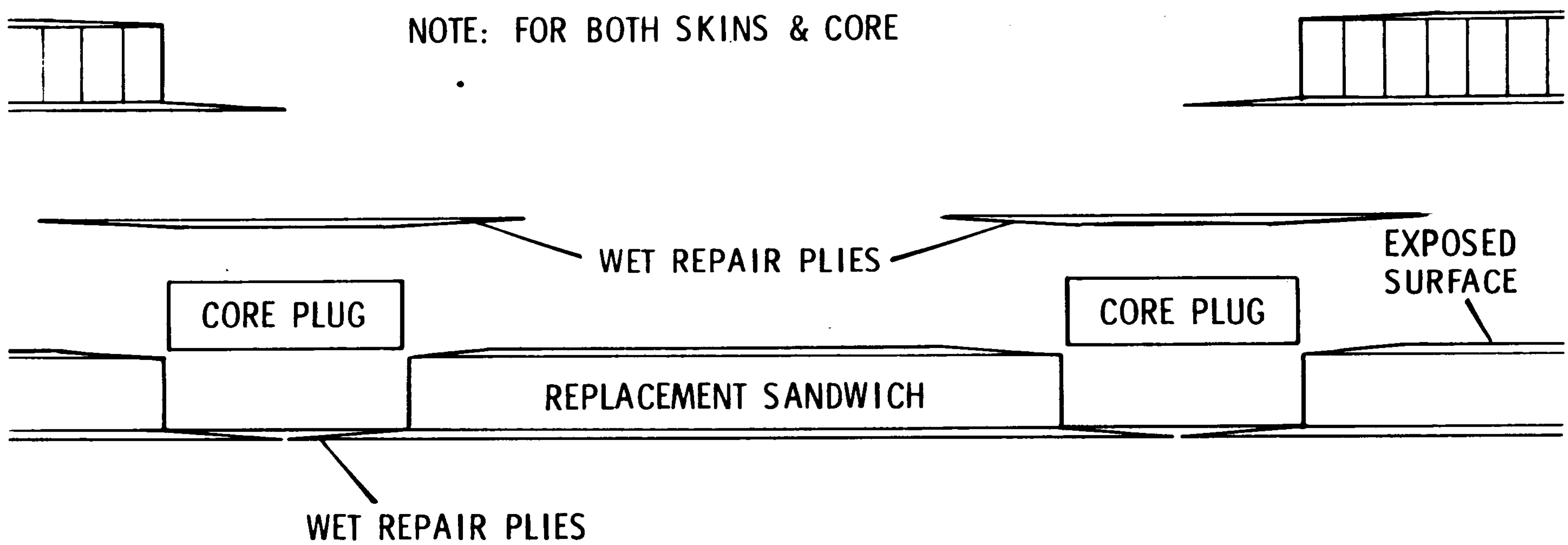

1. REMOVE ALL DAMAGED MATERIAL
2. TRIM BACK OUTER SKIN AND CORE-TAPER EXPOSED SKIN
3. FABRICATE NEW SANDWICH SECTION (ON TOOL) SLIGHTLY LARGER THAN PREPARED AREA. TRIM THIS REPAIR SECTION AS SHOWN. TAPER SKINS
4. MECHANICALLY FASTEN REPAIR SECTION IN PLACE AT INTERVALS OR SUPPORT FROM INNER SURFACE IF FEASIBLE
5. LAY UP WET TIE PLIES, CURE, BOND IN CORE PLUGS, SAND FLUSH
6. LAY UP WET REPAIR PLIES, CURE, SAND TO CONTOUR

Figure 16.1-1 Composite Skin & Core Repair Procedure prepared area and hold in place with clips or a support from the inner surface, if possible; (5) Bond the original inner skin and the replacement inner skin with parent material; (6) Bond in a core plug; (7) Sand flush with the original core; (8) Lay up and bond the original outer skin to the replacement outer skin with parent materials and an adhesive; (9) Sand to contour; (10) Finish.

16.2 ADVANCED FLIGHT CONTROL SYSTEM MAINTAINABILITY

The basic maintenance program envisioned for the advanced flight control system would be considerably abbreviated from current flight control system maintenance procedures. Scheduled maintenance for the electrical and electronic assemblies is minimized by the use of an on-board equipment monitoring system (see below, Subsection 16.3). The actuation systems for the primary and secondary controls would require maintenance procedures similar to those currently employed.

Significant features incorporated in an advanced flight control system that will result in improved maintainability are itemized below:

1. Elimination of the control cables, pulleys, tension regulators, etc., and replacement by fly-by-wire primary flight controls will reduce the maintenance time for rigging the flight control system.

2. Automatic failure detection and fault isolation by employment of a failure annuciator unit to indicate to maintenance personnel the status of all flight control system line replaceable units.

3. Utilization of multiplexing signal transmission techniques to reduce the numbers of electrical connectors and wires throughout the aircraft.

4. Design of line replaceable units for testing with automatic equipment and for repair with plug-in assemblies.

16.3 ONBOARD DATA RECORDING AND EQUIPMENT MONITORING SYSTEM

Incorporating onboard data recording and monitoring equipment into a commercial aircraft will enable the user airline to obtain expanded flight data to support long-term trend analysis for improved maintenance management, to identify and catalog inflight system performance and failures for use by ground maintenance crews, and to generate historical data files on aircraft crew performance. The potential cost savings in the maintenance areas are significant, since it has been estimated that a DC-10 type Aircraft Integrated Data System (AIDS), when integrated with an appropriate, ground-based information center, will reduce direct maintenance costs by 15 to 20 percent. At present, industry-wide annual outlays for direct maintenance are in excess of one billion dollars.

The single most important item in formulating a maintenance concept for commercial airlines is determining <u>when</u> to maintain. Many items and equipments will always be covered by scheduled maintenance, but the concept of condition monitoring will increase in importance. Condition monitoring is presently the fastest growing and largest item in the airline maintenance package. Condition monitoring relies on surveillance and analysis of operational performance to determine criteria for maintenance requirements rather than solely on time and condition standards. The onboard digital computer in conjunction with appropriate system monitor sensors comprises the recognized tool for maintenance condition monitoring and data manipulation. Variations in airline user preferences for onboard maintenance data recording system are generally dependent on fleet size, route structures, and maintenance concepts. Because of these variations, design of the onboard data monitoring system should be closely coordinated between the airline user and the aircraft manufacturer, beginning with the earliest engineering sketches and specifications of the airframe and its system.

Perhaps the most advanced data system presently in commercial service is the DC-10 Aircraft Integrated Data System (AIDS), which is designed to provide building-block data structured to meet the needs of any airline for flight data recording purposes. AIDS can be expanded to an onboard processor-oriented data system. The two cost-savings areas presently utilizing the capabilities of AIDS are engine trend analysis and aircraft crew performance. It is expected that the engine analysis will gradually change the engine maintenance concept from scheduled to on-condition maintenance and minimize major failures. The aircraft crew performance data will provide airline training departments with up-to-date information on their crews such that crew training can be concentrated in areas where it is most needed. Additional AIDS hardware includes data acquisition and signal conditioning systems for detection and recording of mechanical, pneumatic, hydraulic, electrical, and electronics systems malfunction and degradation.

16.4 GROUND SERVICING

Shown in Figure 16.4-1 is a typical arrangement of ground equipment around the ATT Mach .98 configuration. The accompanying table in the figure presents a turnaround schedule that compares with today's wide-body jets in turnaround capability. All ground equipment shown is the type presently in airline service.

16.5 ENGINE MAINTENANCE

Ease of maintenance of the engine/nacelle installation and all subsystem components is provided by built-in accessibility. Engine access doors, supported and hinged from the pylons, provide access to the entire engine and the accessories that may need inspection, maintenance, or servicing. These features are applicable to the wing-mounted and the tail-mounted arrangements. It should be noted that all access doors remain supported on the pylon during engine replacement.

Fan cowl doors provide access to the engine fan case section for engine service and engine removal.

Fan thrust reverser doors are integral with the core engine cowl, which contains the thrust reverser and its actuator mechanism, the fan duct and noise suppression splitters, fan duct walls (acoustic treated), and the core "cowl" wall constructed of firewall materials. When the two half-section doors are opened, the entire core section of the engine is exposed for inspection and servicing. All engine and airplane accessories are completely accessible as well as all engine routing, fire detectors, borescope holes, drains, engine mounts bleed ports and bleed manifolds, fuel inlet connections, and the engine-control quick dis-connects.

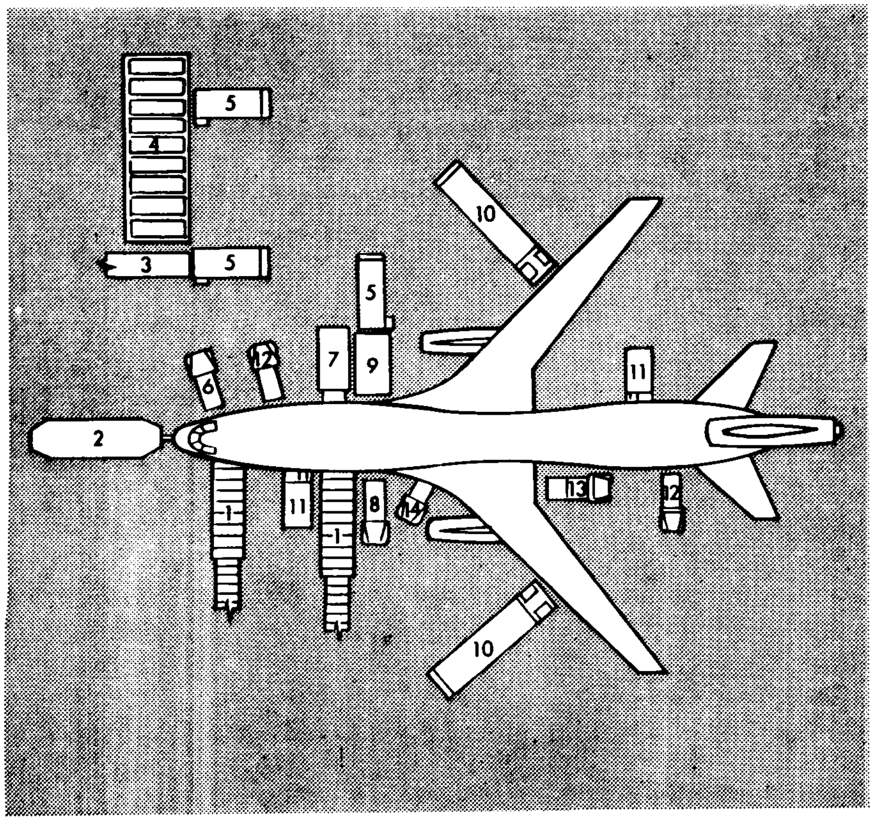

KEY
1 Passenger Loading Bridge
2 Tow Tractor
3 Terminating Baggage
4 Staging Rack
5 Transporter
6 Electrical Power Unit
7 Galley Service Vehicle
8 Potable Water
9 Loader
10 Refuel Truck
11 Bulk Cargo Loader
12 Toilet Service Vehicle
13 Air Starter Unit (If Reqd)
14 Air Conditioning Unit

TYPICAL TURNAROUND SCHEDULE

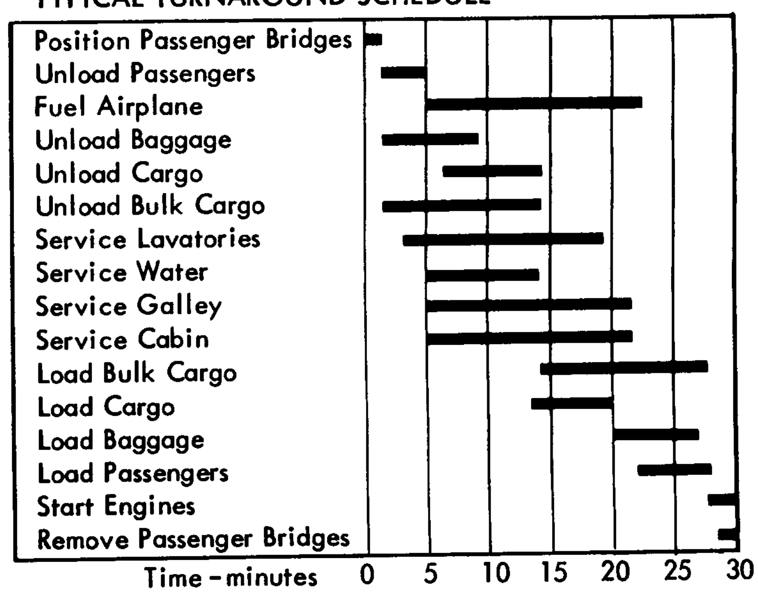

Figure 16.4-1 Ground Servicing Equipment and Turnaround Schedule

Nose cowls for both wing-mounted engine installations are interchangeable. They are supported by the pylon box structure and attached to the engine fan face with a quick attach-detach design.

In addition to its effective accessibility, the nacelle arrangement yields several additional benefits. The cost of the replacement engine buildup and the associated QEC kits is greatly reduced because the absence of the thrust reverser assemblies and, thus, the logistics of space is correspondingly improved. In addition the same engine buildup for all engine positions reduces the engine buildup QEC kit, which also improves spares logistics.

Wing engine maintainability is simple because the nacelle is only about 3 feet (.91 m) above ground level. However, the bottom of the tail-mounted nacelle is close to 25 feet (7.62 m) above ground level.

Tail-mounted engine maintainability is aided by built-in features of the fuselage tailcone. This built-in arrangement for engine accessibility and removal is illustrated in Figure 16.5-1. A telescoping ladder permits access to the fuselage tail cone and then to a work platform approximately 5 feet (1.52 m) below the accessories. At the work platform level the sides of the tailcone pivot open to provide space for movement as well as a guard against dropped tools or parts. This platform allows egress to inspection of the inlet duct, noise suppression splitters, fan rotors, and spinner. The built-in telescoping ladder also allows servicing the APU and the vertical/horizontal tail mechanism.

For heavy accessories such as the alternator, constant-speed drive, and starter, an accessory support cradle is supplied to hold and rotate these items for spline, quick attach-detach, and key-hole alignments. A hand-operated portable winch is used to lower and raise those items from the ground. Cutaway views of this operation are presented in Figure 16.5-2.

Rear-engine replacement is accomplished with a specially developed fork-lift type vehicle (Figure 16.5-3). A platform on the lift carries a cradle-type dolly capable of three-axis precision alignment. When an engine is to be replaced, the fuselage tail cone must first be pivoted downward and forward by hydraulic power. Initial positioning within several inches is accomplished by the lift operator as he aligns the lift with the pivoted fuselage tail cone.

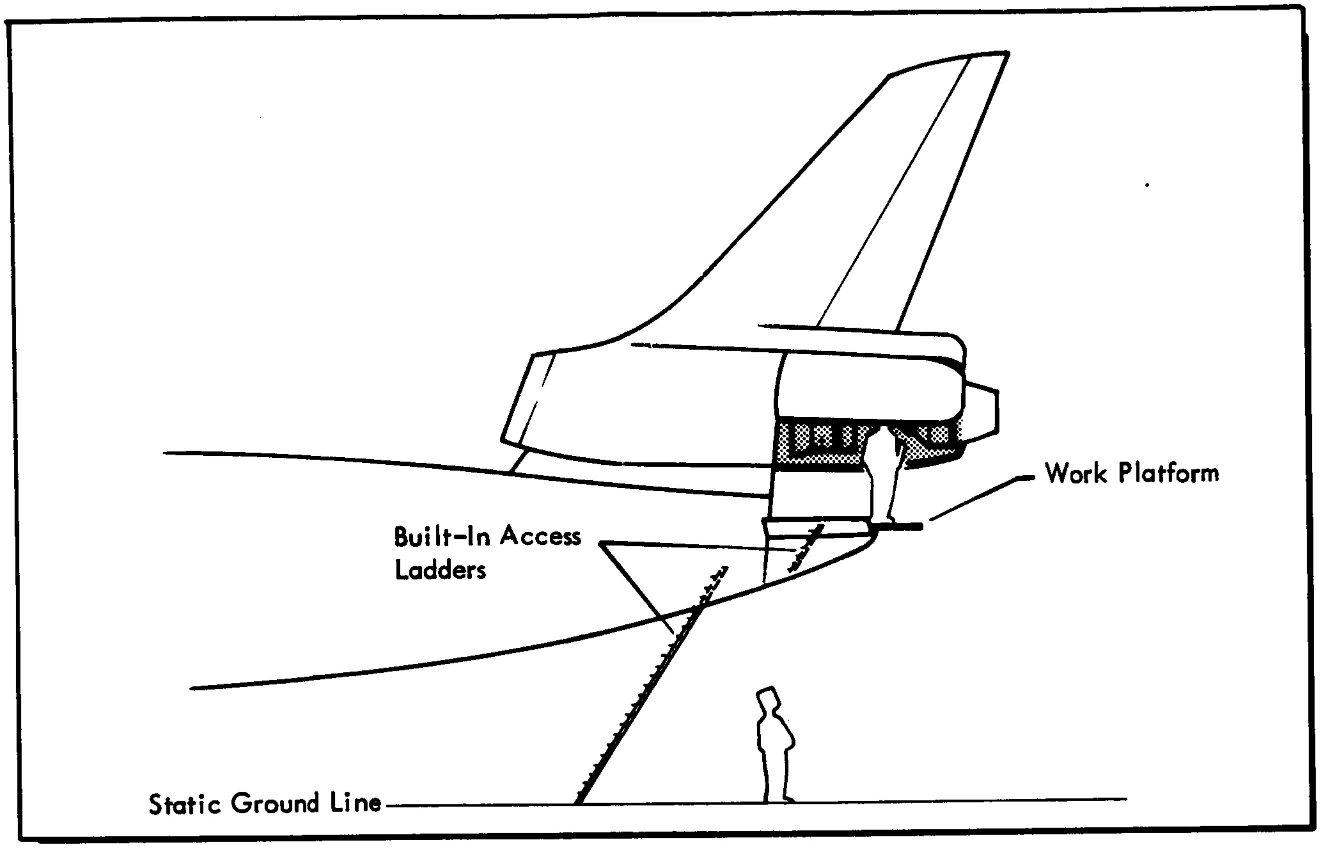

Figure 16.5-1 Tail-Cone Access

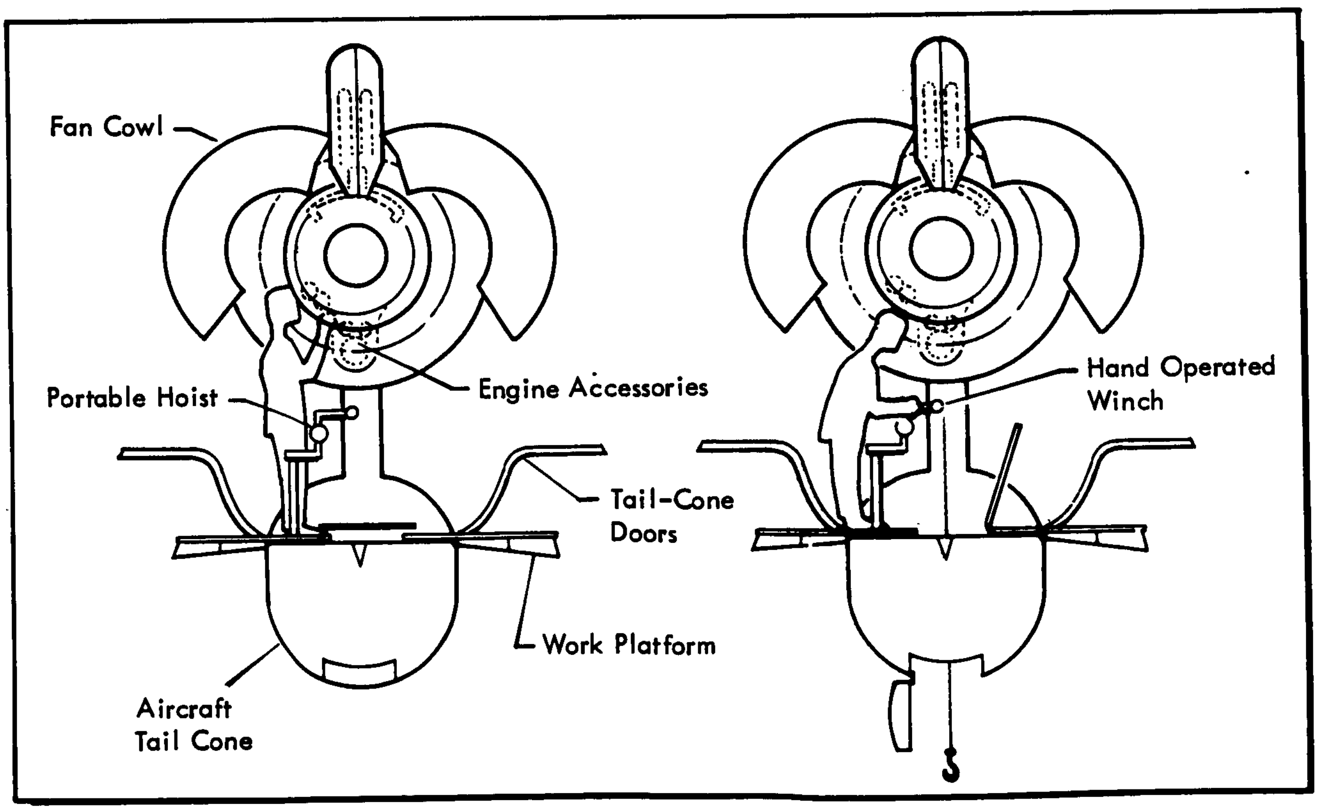

Figure 16.5-2 Engine Accessory Handling

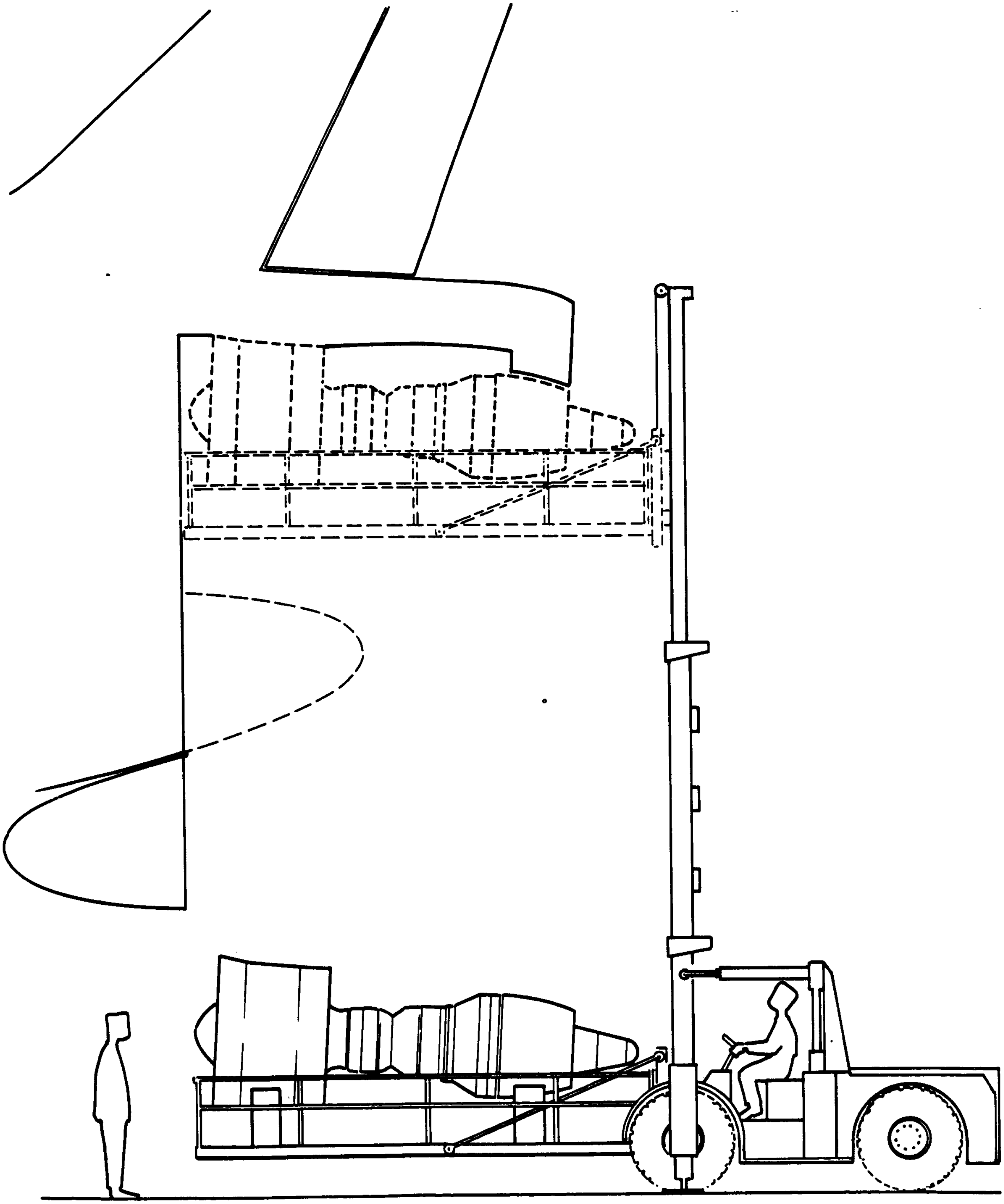

Figure 16.5-3 Tail-Mounted-Engine Removal

Replacement time of the wing-mounted and tail-mounted engines after ground crew familiarization is anticipated to be as follows:

Wing-mounted engine - 60 minutes or less

Tail-mounted engine - 90 minutes or less.

R E F E R E N C E S

3-1 Airport Paving, Federal Aviation Administration, AC150/5320-6A, 1 April 1970.

4-1 Handbook of Airline Statistics, Civil Aeronautics Board, 1968.

4-2 Official Airline Guide, International edition, March 1971.

4-3 Aviation Week, November 1, 1971.

4-4 Official Airline Guide, North American edition, Part One, July 1971.

6-1 Reid, R. J. and Knapton, W. E., Summary of Cost Estimating Procedures In Support of Early Aircraft Design Studies, GD Convair Aerospace Division Report GDC-EA-71-073, 1971.

6-2 Janes, All the Worlds Aircraft, 1970-1971.

6-3 Cooper, A. H., Economic Baseline for ATT Evaluation, GD Convair Aerospace Division Memo OR-7-005, 14 June 1971.

9-1 Nissim, E., Flutter Suppression Using Active Controls Based on the Concept of Aerodynamic Energy, NASA TN D-6199, March 1971.

9-2 Smith, L. R., Prillman, F. W., and Slingerland, R. D., "Direct Lift Control as a Landing Approach Aid," AIAA Paper No. 66-14, January 1966.

9-3 Stickle, J. W., Patton, J. M., and Henery, R. C., Flight Tests of a Direct Lift Control System during Approach and Landing, NASA TN D-4854, November 1968.

9-4 Rolls, L. S., Cook, A. M., and Innis, R. C., Flight-Determined Aerodynamic Properties of a Jet-Augmented Auxiliary Flaps/Direct Lift Control System, Including Correlation with Wind Tunnel Results, NASA TN D-5128, May 1969.

9-5 Aoyagi, K. Dickinson, S. O., and Soderman, P. T., Investigations of a 0.3-Scale Jet Transport Model Having a Jet-Augmented Boundary Layer Control Flap with Direct-Lift Control Capability, NASA TN D-5129, July 1969.

9-6 Boeing-80 Project and Staff Engineering Detail Design and Installation of a DLC Flap for the Boeing 367-80 Airplane, NASA CR 73292, 1969.

9-7 Taylor, C. R. Jr., Flight Results of a Trailing Edge Flap Designed for a Direct Lift Control, NASA CR-1426, October 1969.

9-8 Lee, J. A., and Johannes, R. P., "LAMS B-52 Flight Experiments in Direct Lift Control," SAE Paper 690406, April 1969.

9-9 Lorenzetti, R. C., and Nelsen, G. L., Direct Lift Control for the LAMS B-52, AFFDL-TR-134, October 1968.

9-10 Pinsker, W. J. G., The Control Characteristics of Aircraft Employing Direct-Lift Control, ARC R&M No. 3629, May 1968.

9-11 Hawkes, J. E., "Development Status of the L-1011 Tri Star," SAE Paper 710755, September 1971.

9-12 Technical Progress Narrative and Contract Progress Schedule, Study of the Application of Advanced Technologies to Long-Range Transport Aircraft, GD Convair Aerospace Division Report FPR-061-08, December 1971.

9-13 Task S-14c Fly-by-Wire FCS Study, Technical Report Phase I, GD Fort Worth Division Report FZM-6014, May 1969 (Secret Restricted Report).

9-14 Fenwick, C. A., "The Pilot Interface in Area Navigation" prepared for the Human Factors Society 14th Annual Meeting, San Francisco, California, 14-16 October 1970.

REFERENCES (Cont'd)

9-15 Aircraft Integrated Data System Software Capabilities, Technical Report 70-6383, Rev. 1, June 10, 1971 (Published by the Garrett/AiResearch Manufacturing Company).

9-16 Guidance for Aircraft Electrical Power Utilization and Transient Protection, ARINC Report No. 413, 1 July 1965.

9-17 Military Standard: Electric Power, Aircraft, Characteristics and Utilization of, MIL-STD-704, 6 October 1959.

9-18 Military Standard: Electric Power, Aircraft, Characteristics and Utilization of, MIL-STD-704A, 9 August 1966.

9-19 Electrical Interconnections for Fly-by-Wire Flight Control Systems, AFFDL-TR-70-134, October 1970.

10-1 Flechner, S. G., "Preliminary Wind-Tunnel Investigation of the Effects of Engine Nacelles on a Transport Configuration with High Lift-Drag Ratios to a Mach Number of 1.0," NASA Langley Working Paper No. LWP 939, February 1971.

10-2 McKinney, L. W., et al., "Installation Characteristics of Two Wing-Mounted Nacelles on a Near-Sonic Transport Configuration at Mach Numbers from 0.80 to 0.99," NASA Langley Working Paper No. LWP 1010, November 1971.

10-3 Pendley, R. E., et al., An Investigation of Three NACA 1-Series Nose Inlets at Subsonic and Transonic Speeds, NACA RM L52J23, 1953.

10-4 Goodmanson, L. T., and Schultz, W. H., "Installation and Integration of Transonic Transport Propulsion Systems," SAE Paper No. 710762, September 1971.

10-5 Kutney, J. T., "Airframe/Propulsion System Integration Analysis Using the Propulsion Simulator Technique," AGARD: Aerodynamic Interference, January 1971.

REFERENCES (Cont'd)

10-6 Magruder, W. M., "Development of Requirement, Configuration and Design for Lockheed 1011 Jet Transport," SAE Paper No. 680688, SAE Transactions, 1968.

15-1 Waddoups, M. E., Eisenmann, J. R., and Kaminski, B. E., "Macroscopic Fracture Mechanics of Advanced Composite Materials," Journal of Composite Materials, Vol. 5 (October 1971), 446.

15-2 "Advanced Composite Technology Fuselage Program," AFML Contract No. F33615-69-C-1494.

15-3 Studer, V. J., and Lee, B. D., Advanced Development of Graphite Composite Wing Structural Components, GD Convair Aerospace Division Report FZM-5648, 29 January 1971.

15-4 Leonhardt, J. L., Shockey, P. D., and Studer, V. J., Advanced Development of Boron Composite Wing Structural Components, AFML-TR-70-261, December 1970.